Théorie des liquides et verres en dimension infinie

Thibaud Maimbourg

THÈSE DE DOCTORAT

de l'Université de recherche Paris Sciences et Lettres
PSL Research University

**préparée au Laboratoire de Physique Théorique
de l'École Normale Supérieure**

Théorie des liquides et verres en dimension infinie

École doctorale de Physique
en Ile-de-France n°564

Spécialité : Physique

**Soutenue par Thibaud Maimbourg
le 5 octobre 2016**

**Dirigée par Francesco Zamponi
et Jorge Kurchan**

COMPOSITION DU JURY :

Giulio Biroli
ENS Paris & CEA Saclay
Examinateur

Bernard Derrida
Collège de France & ENS Paris
Examinateur

Jeppe Dyre
Université de Roskilde
Examinateur

Matthias Fuchs
Université de Constance
Rapporteur

Jorge Kurchan
ENS Paris
Codirecteur de thèse

Tommaso Rizzo
Université de Rome "La Sapienza"
Rapporteur

Frédéric van Wijland
Université Paris Diderot
Examinateur

Francesco Zamponi
ENS Paris
Directeur de thèse

ENS
ÉCOLE NORMALE SUPÉRIEURE

PSL
RESEARCH UNIVERSITY PARIS

THÈSE DE DOCTORAT
DE L'ÉCOLE NORMALE SUPÉRIEURE

Spécialité : Physique

École doctorale : Physique en Île-de-France

réalisée

au Laboratoire de Physique Théorique de l'ENS

présentée par

Thibaud MAIMBOURG

pour obtenir le grade de :

DOCTEUR DE L'ÉCOLE NORMALE SUPÉRIEURE

Sujet de la thèse :

Théorie des liquides et verres en dimension infinie

soutenue le 5 octobre 2016

devant le jury composé de :

M.	Giulio Biroli	Examinateur
M.	Bernard Derrida	Examinateur
M.	Jeppe Dyre	Examinateur
M.	Matthias Fuchs	Rapporteur
M.	Jorge Kurchan	Codirecteur de thèse
M.	Tommaso Rizzo	Rapporteur
M.	Frédéric van Wijland	Examinateur
M.	Francesco Zamponi	Directeur de thèse

Résumé

La dynamique des liquides, considérés comme des systèmes de particules classiques fortement couplées, reste un domaine où les descriptions théoriques sont limitées. Pour l'instant, il n'existe pas de théorie microscopique partant des premiers principes et recourant à des approximations contrôlées. Thermodynamiquement, les propriétés statiques d'équilibre sont bien comprises dans les liquides simples, *à condition* d'être loin du régime vitreux. Dans cette thèse, nous résolvons, en partant des équations microscopiques du mouvement, la dynamique des liquides et verres en exploitant la limite de dimension spatiale infinie, qui fournit une approximation de champ moyen bien définie. En parallèle, nous retrouvons leur thermodynamique à travers une analogie entre la dynamique et la statique. Cela donne un point de vue à la fois unificateur et cohérent du diagramme de phase de ces systèmes. Nous montrons que cette solution de champ moyen au problème de la transition vitreuse est un exemple du scénario de transition de premier ordre aléatoire (RFOT), comme conjecturé il y a maintenant trente ans, sur la base des solutions des modèles de verres de spin en champ moyen. Ces résultats nous permettent de montrer qu'une invariance d'échelle approchée du système, pertinente pour les expériences et les simulations en dimension finie, devient exacte dans cette limite.

Mots clés : Physique statistique des systèmes désordonnés, Théorie de champ moyen, Dynamique hors d'équilibre, Transition vitreuse, Théorie des liquides, Invariance d'échelle

ABSTRACT

The dynamics of liquids, regarded as strongly-interacting classical particle systems, remains a field where theoretical descriptions are limited. So far, there is no microscopic theory starting from first principles and using controlled approximations. At the thermodynamic level, static equilibrium properties are well understood in simple liquids *only* far from glassy regimes. Here we derive, from first principles, the dynamics of liquids and glasses using the limit of large spatial dimension, which provides a well-defined mean-field approximation with a clear small parameter. In parallel, we recover their thermodynamics through an analogy between dynamics and statics. This gives a unifying and consistent view of the phase diagram of these systems. We show that this mean-field solution to the structural glass problem is an example of the Random First-Order Transition scenario, as conjectured thirty years ago, based on the solution of mean-field spin glasses. These results allow to show that an approximate scale invariance of the system, relevant to finite-dimensional experiments and simulations, becomes exact in this limit.

Keywords: Statistical physics of disordered systems, Mean-field theory, Out-of-equilibrium dynamics, Glass transition, Liquid theory, Scale invariance

PREFACE

This thesis is based almost exclusively on published works by Jorge Kurchan, Francesco Zamponi and myself. The following chapters are largely inspired from them, with additional explanations and illustrations to clarify the ideas which may be more abrupt in articles intended to a specialized audience. The reciprocal links between chapters are emphasized to expose the coherence between the different works.

In this respect, chapters 1 and 2 attempt to make the present thesis self-contained, together with the appendices.

- Chapter 3 refers to [264].

- Chapter 4 and appendices B, E, F, G, H refer to [241].

- Chapter 5 refers to [263].

- Sections 3.10 and 5.7.3 contain unpublished results.

- Section 2.4.3 and appendix C present useful techniques in a self-contained way.

Chapter 0 is roughly a translation in French of some sections (1.1, 1.5 and 1.6) of the introductory chapter 1.

Le chapitre 0 est une traduction en français de certaines sections (1.1, 1.5 and 1.6) du chapitre d'introduction 1.

Cette thèse étant relativement spécialisée, il existe un article de vulgarisation en français sur les verres en dimension infinie rédigé par Berthier, Charbonneau et Zamponi dans la revue la Recherche [47], disponible ici.

REMERCIEMENTS

Mes remerciements vont tout d'abord à mes deux directeurs de thèse, Francesco et Jorge, pour m'avoir fait confiance dès le début. Ils ont su trouver le temps de discuter lorsque j'en avais besoin, malgré leurs nombreuses obligations, ainsi que la patience et la compréhension face à mes questions de novice. Je garde en tête leur volonté d'avancer, leur capacité technique à regarder droit dans les yeux les problèmes, leur créativité afin de se sortir de blocages sérieux qui n'étaient pas si loin de nous faire abandonner par moments, et surtout leur compréhension profonde de tant de sujets. Ils ont su m'aiguiller dans les choix à faire tant au niveau du travail quotidien de thèse ou d'enseignement que dans la poursuite en post-doctorat, et je leur en suis infiniment reconnaissant. Il va sans dire que rien de ce qui est présenté dans ma thèse n'aurait pu voir le jour sans eux.

Je tiens ensuite à exprimer ma profonde gratitude envers les rapporteurs, Matthias Fuchs et Tommaso Rizzo, d'avoir accepté cette tâche, ainsi que pour les nombreuses discussions que nous avons eues à propos de cette thèse pendant diverses conférences et par mail. Je remercie aussi les autres membres du jury d'en faire partie, mais pas seulement : Giulio Biroli pour les discussions sur ce sujet et pour ma poursuite en post-doc, Bernard Derrida pour son cours en M2 sur les systèmes désordonnés qui font l'objet de cette thèse, Jeppe Dyre pour venir exprès jusqu'à Paris et pour nos nombreux échanges à propos de ses travaux et du chapitre 5 de cette thèse, et enfin Frédéric van Wijland auprès de qui j'ai eu le plaisir plusieurs fois pendant mes études d'apprendre la physique statistique et à qui je dois beaucoup dans mes choix d'orientation ; à ce sujet je remercie aussi mes encadrants de M2, Christophe Coste et Michel Saint Jean.

Au chapitre des chercheurs dont l'aide a été précieuse, je tiens particulièrement à mentionner, en plus de ceux déjà cités, Camille Aron, Ludovic Berthier, Jean-Philippe Bouchaud, Patrick Charbonneau, Hugo Jacquin, Yuliang Jin, Theodore Kirkpatrick, Corrado Rainone, David Reichman, Rolf Schilling, Guilhem Semerjian, Grzegorz Szamel, Gilles Tarjus et Pierfrancesco Urbani, pour avoir judicieusement commenté ou critiqué nos travaux, ou pour leur aide précieuse sur certains sujets.

J'ai aussi eu la très grande chance de pouvoir enseigner en monitorat à l'ENS, parallèlement à la thèse, aux côtés de Lydéric Bocquet, Frédéric Chevy et Ken Sekimoto, qui m'ont fait découvrir de nouveaux sujets et ont rendu cette expérience enrichissante (et qui m'a donné le goût d'enseigner). Cela est dû aussi pour beaucoup aux élèves ; j'espère avoir été à la hauteur. Je remercie grandement celles et ceux qui s'occupent de l'enseignement à l'ENS (notamment Stephan Fauve, Guilhem Semerjian et les différents services administratifs) pour leur confiance.

La soutenance de thèse symbolisant l'achèvement des études, je tiens à exprimer ma reconnaissance envers celles et ceux qui m'ont instillé l'envie d'apprendre, notamment certain·e·s professeur·e·s que j'ai eu·e·s depuis tout petit. J'ai pu bénéficier de la gratuité du service public de l'éducation et de l'enseignement supérieur, et j'espère que beaucoup de générations pourront encore avoir cette chance. Par ailleurs, merci à la fondation CFM qui a permis le financement de cette thèse. Je remercie aussi Jean-François Allemand, et probablement d'autres, qui ont rendu possible des études extrêmement intéressantes et libres à l'ENS, à bien des égards.

En relisant, je me fais la remarque qu'on pourrait croire que je cite tant de grands chercheurs pour tromper sur la qualité de ce qui va suivre, comme dans les thèses des Bogdanov ; il n'en est évidemment rien.

"Pourquoi quand moi je plonge, lui passe sa thèse ?"
IAM, *Nés sous la même étoile*

Contents

0

LIQUIDES SURFONDUS ET TRANSITION VITREUSE

Outline

Le but de cette thèse étant de résoudre la dynamique des liquides et verres tout en établissant un pont avec la thermodynamique de ces systèmes, dans la limite de dimension spatiale d infinie, ce chapitre d'introduction présente tout d'abord les données expérimentales caractéristiques des liquides et verres du quotidien. La thermodynamique et la structure microscopique des liquides est relativement bien comprise théoriquement, tandis qu'un cadre théorique pour leur dynamique, qui partirait des équations du mouvement microscopiques et contrôlerait les approximations en vue de les raffiner systématiquement, est encore loin d'être établi.

Dans le régime de basse température proche de la vitrification, on observe expérimentalement un comportement différent des transitions de phase habituelles, ce qui motive l'étude de la transition vitreuse en soi, mais aussi pour ce qu'elle pourrait nous apprendre sur le champ encore en friches qu'est la physique hors d'équilibre. Le problème réside dans le fait que l'analyse exacte des liquides et verres en dimension $d = 2$ ou 3 est une tâche extrêmement ardue. C'est pourquoi les recherches théoriques se sont beaucoup concentrées sur des modèles de champ moyen pour comprendre la phénoménologie des verres, *en première approximation*. Cela dit, même à ce niveau, une théorie solide n'a pas encore émergé. Ainsi, l'idéologie champ moyen est pour beaucoup basée sur la résolution exacte de modèles de *verres de spin*, qui sont des alliages magnétiques désordonnés qui, de prime abord, paraissent être des systèmes physiques très éloignés des liquides et verres. Néanmoins, on retrouve de nombreux exemples de comportements universels en physique, et certaines caractéristiques expérimentales des verres de spin sont étrangement similaires avec celles des verres *structuraux* (le terme consacré pour les verres usuels, comme celui qui constitue les vitres des fenêtres). Les modèles champ moyen de verres de spin sont plus faciles à traiter et ont été résolus exactement. Leur solution a donné naissance, *par analogie*, à une théorie des verres structuraux dans les années 1980, la transition de premier ordre aléatoire (RFOT), qui est présentée dans la section 1.2.

Il semble dès lors naturel d'enquêter sur la limite de grande dimension des liquides et verres pour vérifier explicitement si ce scénario est valide *dans cette limite de champ moyen bien définie*. L'absence d'un petit paramètre perturbatif évident pour étudier les liquides et verres est alors compensé par l'introduction du *paramètre* $1/d$. En effet, contrairement à la matière condensée plus standard, il n'existe pas de traitement perturbatif canonique. Celui-ci nécessite un système de référence et un petit paramètre [404], comme pour le développement de basse densité autour du gaz parfait pour les gaz modérément denses, ou autour d'un réseau idéal périodique pour les cristaux (d'où provient la description en phonons via des vibrations harmoniques autour des positions d'équilibre) [85, 199, 17]. On rencontre une situation similaire dans les électrons fortement corrélés [179], la physique atomique [372], et la théorie des champs de jauge [134]. L'approche suivie dans tous ces cas fut celle d'un développement de dimension élevée. En résolvant le problème dans un espace de dimension infinie et en traitant ensuite $1/d$ comme un

petit paramètre, on peut ainsi espérer retrouver, en bonne approximation, le comportement de systèmes physiques en $d = 3$.

Concernant les liquides et verres, la thermodynamique de la phase de haute température (le liquide) a été étudiée exactement au milieu des années 1980 [162, 258, 164, 409, 163, 161]. Il fut compris il y a quelques années que tous les outils théoriques nécessaires à la construction d'une théorie exacte en $d \to \infty$ pour l'ensemble du diagramme des phases étaient à disposition. Cette observation déclencha l'effort de recherche actuel en ce sens, qui résulte en une confirmation du scénario RFOT en $d \to \infty$ (ainsi que de nouvelles prédictions, notamment en dimension finie). C'est la raison pour laquelle nous le présentons dans la section 1.2.

Le problème d'obtenir une théorie *dynamique* des liquides, en d'autres termes de systèmes macroscopiques de particules classiques dans un régime d'interactions fortes, qui est au cœur de cette thèse, est dépeint en §1.3. Ensuite, nous donnons une brève introduction à une invariance d'échelle récemment découverte dans le diagramme de phase des liquides, que nous étudierons dans un chapitre ultérieur comme corollaire de la dynamique et statique résolues. Des résultats antérieurs à ce travail sur la thermodynamique des systèmes de sphères dures denses en $d \to \infty$ sont résumés en §0.2. Enfin, nous énonçons le contenu du reste de la thèse.

Dans toute cette thèse, nous prenons la constante de Boltzmann comme unité, *i.e.* $k_{\mathrm{B}} = 1$. $\beta = 1/T$ est la température inverse. Des notations récurrentes sont tabulées dans l'annexe A.

0.1   Phénoménologie de base et diagramme des phases

Du point de vue théorique, un *liquide simple* est un système de N particules *classiques* interagissant via un potentiel de paires isotrope V. C'est certes une idéalisation mais certains aspects de la phénoménologie discutée dans ce chapitre peuvent être pertinents pour des systèmes différents, qu'ils soient anisotropes (*e.g.* les gels [341, 256, 416]), avec des interactions à plus de deux corps (*e.g.* les liquides métalliques [148, 269]) ou dans un régime quantique (verres quantiques [320, 250, 407, 391]). Dans le reste de cette section, nous nous concentrons sur des faits expérimentaux à propos de ce qui se passe lorsque l'on refroidit un liquide simple.

0.1.1   Fondus de liquides !

Intuitivement, à basse densité le système est un gaz tandis qu'à haute densité il devient un solide, dans le sens d'un corps compact et rigide. Inversement, les molécules s'affolent en raison de la chaleur [153, Chap. I] ; à cause de ces collisions thermiques, un solide à haute température va se dilater et devient de plus en plus fluide à mesure que la température monte, devenant liquide ou même gazeux à plus hautes températures. Commençons par cet état intermédiaire, le liquide. En le refroidissant, on s'attend à ce qu'il devienne plus compact.

En réalité, une transition du premier ordre vers une phase ordonnée survient, qui est un changement soudain et radical vers un arrangement périodique : le cristal. Les symétries (continues) de translation et de rotation sont brisées (devenant discrètes, dépendant du type de réseau cristallin). L'ergodicité est brisée à son tour : les configurations désordonnées (liquides) ne sont plus accessibles au système. Un mouvement collectif des particules est nécessaire pour que ce processus aboutisse. La température de transition est appelée *point de fusion* T_{m}. Cette *cristallisation* est une énigme pas encore tout-à-fait élucidée[1] en soi [217, 353, 387, 151, 35]. Le cristal est thermodynamiquement stable : il a une énergie libre plus basse que l'état liquide pour $T < T_{\mathrm{m}}$. Pourtant, cette transition peut être évitée et la branche d'équilibre du liquide peut être prolongée dans le diagramme des phases pour $T < T_{\mathrm{m}}$, comme illustré dans la figure 2. Le liquide est alors métastable et qualifié de *surfondu*: l'exemple pratique canonique étant l'eau minérale mise au congélateur. Elle peut ne pas cristalliser et une légère tape ou verser le contenu est suffisant pour la faire cristalliser, en facilitant la croissance de cristallites nucléés. Dans la *phase* surfondue, l'effet du refroidissement paraît être le plus naïf, bien que le moins bien compris : les

---

[1]Une description de champ moyen de cette transition est décrite dans [85, 199] à travers la théorie de la fonctionnelle de densité (DFT), qui se propose d'écrire une énergie libre approchée comme fonctionnelle du champ de densité locale, dans l'esprit d'un traitement à la Landau de la transition de phase [247, 248]. La théorie de champ moyen dans le cas de la vaporisation (transition liquide-gaz) est analogue au modèle d'Ising en champ moyen. Une transformation formelle existe entre le modèle d'Ising ferromagnétique et les gaz sur réseaux [412, 249].

molécules deviennent empilées de manière compacte, leur dynamique est plus lente et il n'y a aucun ordre spatial émergent contrairement au cristal [239]. Leur empilement est *amorphe*.

Cette phase métastable peut être ardue à obtenir. Expérimentalement, on utilise des matériaux qui sont notoirement connus pour être de bons *vitrificateurs*, *i.e.* qui ne cristallisent pas aisément, et en suivant un protocole de trempe suffisamment rapide pour éviter la nucléation et la croissance du cristal, mais pas trop[2] pour rester à l'équilibre au sens de la phase liquide. Ces précautions sont détaillées dans [83, Section III]. Une récente technique sophistiquée, la déposition par vapeur [310, 373, 360, 361, 261, 357], permet de former des liquides surfondus couche atomique par couche atomique, ce qui facilite l'équilibration en évitant la nécessité de relaxer la majeure partie du volume du système. On peut alors sonder des échelles de temps d'équilibration qui sont compliquées à atteindre autrement (*e.g.* 40 ans pour certains échantillons de [310, 373, 360, 361, 261, 357]), à moins de trouver par exemple du verre vieux de millions d'années dans la nature [420], bien que dans ce cas le protocole expérimental ne soit pas contrôlé et on étudie alors un régime hors de l'équilibre. Numériquement, on utilise habituellement des potentiels connus pour être de mauvais cristalliseurs et des systèmes polydisperses [8], en mettant ensemble différents composants avec différentes formes (*e.g.* des particules sphériques avec des diamètres différents, comme les mélanges binaires de Kob-Andersen [231, 229, 55]), ce qui prévient la cristallisation. Un échantillonnage de Monte-Carlo non local a été utilisé pour équilibrer à des densités ou températures inatteignables sinon [48].

0.1.2 Un peu de relaxation

Si l'on refroidit le liquide surfondu avec le soin requis pour rester à l'équilibre, à un moment donné le liquide devient énormément visqueux : si l'on appelle cette température typique $T_{\mathrm{g}} < T_{\mathrm{m}}$, la viscosité augmente de plusieurs ordres de grandeur dans un intervalle de température s'étendant sur une fraction seulement de T_{g}. Ce phénomène est surprenant en lui-même, mais aussi dans sa relative universalité : une large classe de systèmes se comportent ainsi, allant des liquides atomiques et moléculaires, suspensions colloïdales, milieux granulaires, aux alliage métalliques, polymères, gels, ... [136, 338].

La viscosité est une observable macroscopique facilement mesurable expérimentalement. Elle est reliée à une quantité microscopique, le temps de relaxation τ_{R} du système, via la relation de Maxwell [83, 82]

$$\eta = G_{\infty}\tau_{\mathrm{R}} \tag{1}$$

valide approximativement pour les liquides d'équilibre, où G_{∞} est le module de cisaillement de fréquence infinie, similaire au module d'Young des solides [245]. Cela signifie qu'au fur et à mesure que l'on s'approche de la *transition vitreuse expérimentale* à T_{g}, le temps de relaxation du système croît subitement et le fluide a de plus en plus de difficulté à s'écouler vu que la relaxation des particules qui le composent est gênée. T_{g} n'est pas bien défini et dépend du temps de l'expérience, *i.e.* du temps dont on est disposé à attendre; conventionnellement, un bon ordre de grandeur est 10^{12} Pa·s [83]. A titre de comparaison, l'eau est à $\sim 10^{-3}$ Pa·s et le miel autour de 10 Pa·s [323], et une tasse contenant un liquide proche de sa transition vitreuse mettrait environ 30 ans[3] à se vider sous l'action de la gravité [136, 418]. Dès lors que le temps de relaxation surpasse celui de l'expérience, ce qui est la définition de T_{g}, à toutes fins pratiques le liquide surfondu se comporte macroscopiquement comme un solide élastique ; sa réponse à une contrainte σ produit une déformation linéaire γ (qui mesure les déplacements relatifs de la structure microscopique) et est bien décrite par la loi de Hooke [245, 82], qui lui confère sa rigidité,

$$\sigma = G_{\infty}\gamma \tag{2}$$

alors que pour des temps plus grands que τ_{R} le module s'annule comme dans un liquide : c'est en effet une quantité dépendante du temps, *i.e.* $\sigma = G(t - t_0)\gamma$. Même un solide parfait (*e.g.* un cristal) s'écoule aux temps longs (mais finis dans la limite thermodynamique), bien que le mécanisme soit différent : la viscosité des solides parfaits diverge rapidement à contrainte nulle alors qu'elle reste finie pour un liquide newtonien à contrainte nulle [343].

La nette augmentation de la viscosité, ou du temps de relaxation, est très bien documentée expérimentalement et est résumée dans le graphique d'Angell [15, 14] du logarithme de la viscosité en fonction de T_{g}/T pour

---

[2]Typiquement 0,1 à 100 K/min [62].

[3]Un des expériences les plus longues à ce jour reliée à ce phénomène est l'expérience des gouttes de goudron [139] à Brisbane en Australie, où du goudron chaud avait été versé dans un bol troué en 1927 et a été redécouvert en 1961 après avoir été complètement oublié. La viscosité du goudron a été mesurée à $\sim 10^9$ Pa·s à 10°C et $\sim 10^6$ Pa·s à 30°C; tous les dix ans environ, une goutte tombe du bol.

de nombreux systèmes, tracé dans la figure 1. Les droites signifient qu'un comportement simple en loi d'Arrhénius

$$\tau_{\mathrm{R}} \propto \exp\left(\frac{\Delta}{T}\right) \tag{3}$$

rend compte de la relaxation, qui est dominée par la barrière d'énergie Δ à surmonter pour lancer le mécanisme d'activation. C'est en effet ce qui est attendu de manière générale pour des processus de relaxation simples [198]. Ces systèmes sont appelés des verres *forts* et quelques archétypes sont SiO_2 (verre de vitre) et GeO_2. Les systèmes correspondant aux lignes courbes au-dessous ont un comportement dit super-Arrhénius (qui diverge plus vite qu'Arrhénius) qui est intriguant. Ceux-ci sont appelés des verres *fragiles*, comme l'orthoterphényl et le toluène. Il faut toutefois prendre garde à ce genre de classification puisque la séparation entre les deux catégories peut être assez floue dans les données expérimentales. La terminologie *fort* et *fragile* n'est pas reliée aux propriétés mécaniques du verre mais à l'évolution de l'ordre à courte portée près de T_{g} : les structures localement favorisées (LFS) [338], *e.g.* l'ordre tétrahédrique, persistent aussi bien en-dessous qu'au-dessus de la transition vitreuse dans les verres forts tandis qu'elles disparaissent rapidement en chauffant les verres fragiles. Un temps de relaxation super-Arrhénius peut s'interpréter comme une élévation de la barrière effective d'énergie (libre) avec la température, qui laisse présager un phénomène collectif [239]. Ainsi, des ajustements populaires de courbes (η, T) différents de (3) semblent tout aussi plausibles, comme la loi Vogel-Fulcher-Tamman (VFT) [400, 167, 380]

$$\tau_{\mathrm{R}} \propto \exp\left(\frac{A}{T - T_0}\right) \tag{4}$$

ou la loi de Bässler [25]

$$\tau_{\mathrm{R}} \propto \exp\left[K\left(\frac{T^*}{T}\right)^2\right] \tag{5}$$
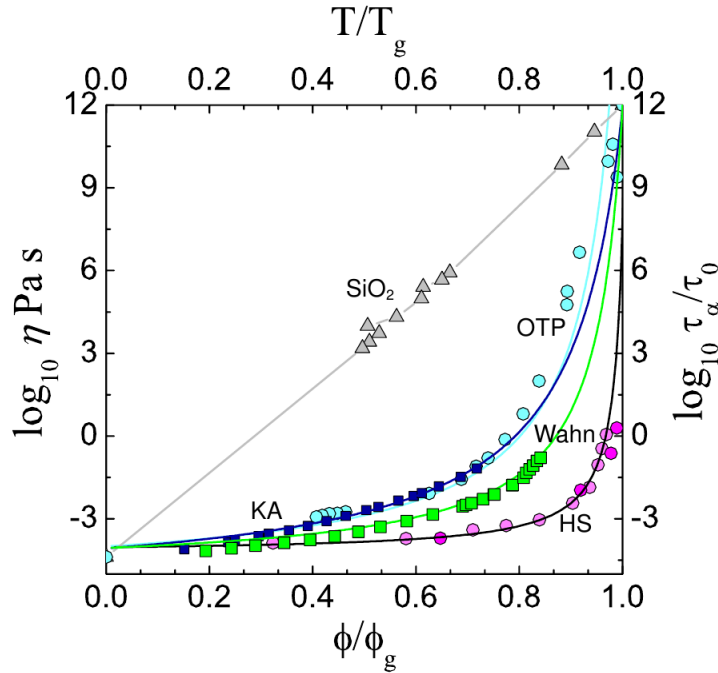
Figure 1: Le graphique d'Angell : représentation par rapport à la loi d'Arrhénius des viscosités de quelques liquides (ou de manière équivalente, de leur temps de relaxation, noté τ_α ici), en fonction de la température inverse rapportée à T_{g}. SiO_2 et l'orthoterphényl (OTP) sont des verres moléculaires standards [14, 53]. Les autres données concernent des systèmes modèles : KA abrège Kob-Andersen [231] et Wahn désigne un système binaire de particules de Lennard-Jones dû à Wahnström [254] tandis que HS signifie sphères dures où le paramètre de contrôle est la fraction volumique ϕ, notée φ dans cette thèse, *i.e.* le rapport entre le volume des sphères et le volume total du système. Dans ce cas τ_0 est ajusté pour permettre un alignement des données sur $T_{\mathrm{g}}/T = \varphi/\varphi_{\mathrm{g}}$. [*Repris de* [338]]

La loi VFT implique une divergence à une température finie non nulle T_0 (l'un de ses paramètres d'ajustement) et interpole entre les comportements fort ($T_0 = 0$) et fragile ($T_0 > 0$). Une telle divergence à $T_0 > 0$ signalerait un arrêt total de la dynamique, habituellement associé à une transition de phase. Par exemple, on pourrait imaginer voir ce ralentissement visqueux comme un ralentissement dynamique associé à un proche point critique thermodynamique [422]. L'existence d'une telle transition, dans un régime inaccessible aux expériences et simulations numériques, reste controversée [319, 201]. Par ailleurs, s'il n'y a pas de réelle transition de phase, le terme *crossover vitreux* serait plus approprié : en raison de l'activation thermique, le système doit relaxer si on est prêt à attendre suffisamment longtemps. Les expressions (4) et (5) ajustent correctement les données expérimentales (voir [367, 145] pour VFT) et sert de guide pour les expériences et théories. En fait, certains modèles théoriques, comme les modèles cinétiquement contraints (KCM, see §1.2.7), ont pu déduire ce type de lois. Cependant, il s'agit de garder en tête que ces ajustements sont heuristiques et ne pas accorder une confiance aveugle dans ce qu'ils supposent et impliquent.

Revenons à ce qui survient dans le diagramme des phases du système. Nous avons vu qu'en refroidissant encore plus le liquide surfondu, le temps de relaxation semble presque diverger. Il devient donc très difficile d'équilibrer l'échantillon, jusqu'à un certain point où la relaxation est tellement lente qu'il est *hors de l'équilibre* de manière effective, et suit une évolution dans le diagramme des phases qui dépend de l'histoire du système et ne peut pas être prédit par des calculs statiques d'équilibre. Ce diagramme des phases simplifié est résumé dans la figure 2.
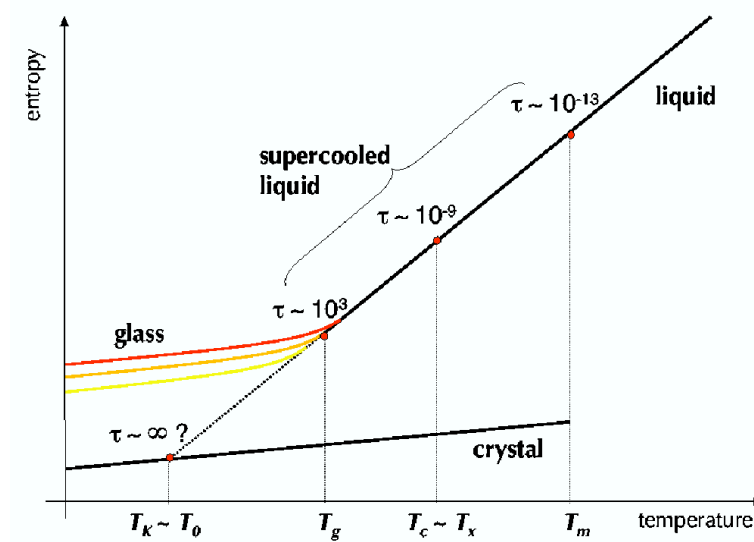
Figure 2: Diagramme de phase simplifié (entropie en fonction de la température) des liquides. Pour $T < T_m$ la branche liquide devient métastable (liquide surfondu). En s'approchant de T_g, le temps de relaxation croît jusqu'à ce que le système tombe hors de l'équilibre et suive une des branches vitreuses colorées dépendant de sa propre histoire (du protocole adopté). On remarque que le potentiel thermodynamique pertinent est l'énergie libre et non l'entropie. Le liquide étant bien plus désordonné que le cristal, il semble naturel que son entropie soit plus haute. [*Repris de* [83]]

0.1.3 Sonder la structure locale

Une surprenante caractéristique de ce phénomène dynamique est qu'au niveau microscopique, il semble qu'aucun changement apparent de la structure ne soit à noter. Les observables structurelles sont mesurées quotidiennement et bien décrites par la théorie des liquides [199], qui étudie la mécanique statistique des liquides simples à l'équilibre (et son application à des situations plus complexes comme des systèmes à plusieurs composants, liquides ioniques, degrés de liberté moléculaires, physique des interfaces et régimes hydrodynamiques) développée à partir des années 1950. Une des observables les plus simples est la fonction de distribution radiale

$$g(\mathbf{r}, \mathbf{r}') = \frac{\rho^{(2)}(\mathbf{r}, \mathbf{r}')}{\rho^2} = \frac{1}{\rho^2} \left\langle \sum_{i \neq j}^{1,N} \delta(\mathbf{r} - \mathbf{x}_i)\delta(\mathbf{r}' - \mathbf{x}_j) \right\rangle = \frac{1}{\rho N} \left\langle \sum_{i \neq j}^{1,N} \delta[\mathbf{r} - \mathbf{r}' - (\mathbf{x}_i - \mathbf{x}_j)] \right\rangle \qquad (6)$$

où ρ est la densité de particules d'un système homogène, $\rho^{(2)}$ est la fonction de distribution de paires et la moyenne porte sur l'ensemble canonique. Par isotropie c'est une fonction de la norme $|\mathbf{r} - \mathbf{r}'|$ seulement. La définition de $g(r)$ implique que le nombre moyen de particules à une distance comprise entre r et $r + \mathrm{d}r$ d'une particule de référence est $4\pi r^2 \rho g(r)\mathrm{d}r$ et les pics de $g(r)$ représente des *couches* de voisins autour de la particule de référence. Les propriétés thermodynamiques peuvent être exprimées en termes d'intégrales sur $g(r)$, ce qui en fait une quantité particulièrement recherchée. La fonction de distribution radiale est calculée précisément en théorie des liquides par une resommation soigneuse du développement du viriel décrite dans §2.1, menant à des équations intégrales autocohérentes comme les fermetures HNC [337, pp. 185-187] ou Percus-Yevick [313]. Celles-ci sont approchées car elles négligent des corrélations à trois corps, mais rendent très bien compte des données expérimentales et de simulations [199, 6]. Expérimentalement, cette quantité est accessible via la mesure du facteur de structure statique $S(q)$ par diffusion inélastique de neutrons [199] :

$$S(q) = \frac{1}{N} \left\langle \sum_{i,j}^{1,N} e^{i\mathbf{q}\cdot(\mathbf{x}_i - \mathbf{x}_j)} \right\rangle = 1 + \rho \int \mathrm{d}\mathbf{r}\, e^{i\mathbf{q}\cdot\mathbf{r}} g(r) \qquad (7)$$

qui est lié à la transformée de Fourier de la fonction de distribution radiale.

Ces observables sont de bons outils permettant de distinguer les différentes phases gaseuses, liquides ou solides : pour un gaz parfait on obtient $\forall r$, $g(r) = 1$, ce qui indique que le gaz est totalement décorrélé et n'a pas vraiment de structure locale, alors que pour un solide on observe des pics étroits à chaque pas du réseau, reflétant la structure périodique du cristal. Ces pics cristallins dans la fonction de distribution radiale sont dénommés, dans leur version réciproque *i.e.* dans le facteur de structure, pics de Bragg [17]. Dans le liquide il n'y a pas d'ordre à longue portée et les pics deviennent de plus en plus faibles avec la distance, voir la figure 3.

Cela dit, il n'y a pas de changement drastique repérable dans cette observable à deux corps durant le crossover.
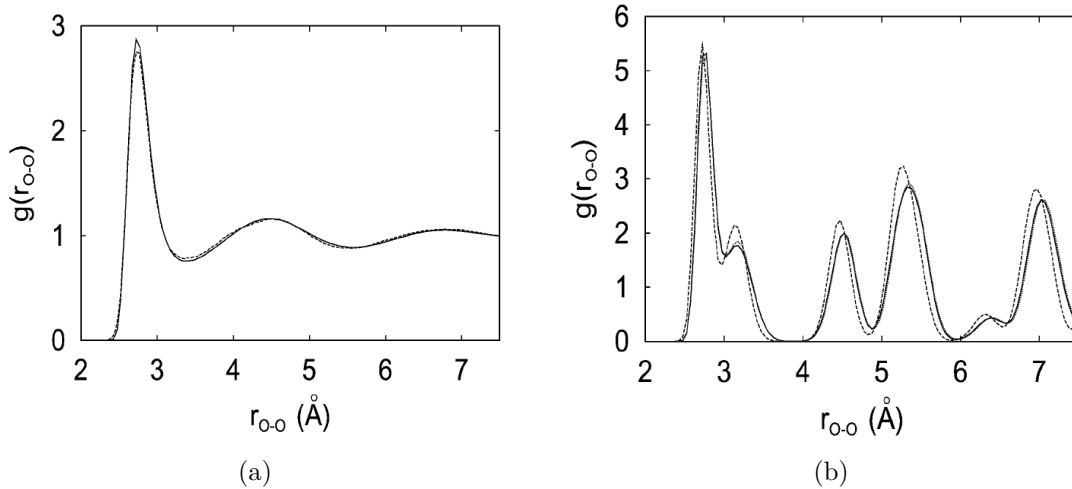
Figure 3: Fonctions de distribution radiale entre atomes d'oxygène pour : (a) L'eau à 298 K, 1 bar. La ligne continue est issue d'un modèle numérique tandis que la ligne pointillée est expérimentale. (b) La glace VII (un type de réseau cristallin particulier de la glace qui est cubique) à 300 K et 10^5 bar résultant de deux modèles numériques. [*Repris de* [398]]

0.1.4   L'effet de cage : relaxation en deux temps

La fonction de corrélation statique décrite ci-dessus est simple et suggère que la structure locale n'a rien de particulier, surtout lorsqu'on la compare aux phénomènes dynamiques relatés dans §0.1.2. Pourtant, il existe bien une signature du crossover vitreux, la relaxation en deux temps, mesurée par des fonctions de corrélation dynamiques. Si l'on mesure le déplacement quadratique moyen (MSD) d'une particule dans le liquide, voir la figure 5(b), on observe à des températures élevées le crossover habituel entre régime ballistique et régime diffusif, tandis que près de T_g un plateau émerge, impliquant que le mouvement d'une particule reste borné pendant un certain temps. Puisque la hauteur de ce plateau fournit une

distance petite comparée à la distance interparticulaire [232] (elle vaut environ un cinquième du diamètre d'une particule dans les suspensions colloïdales [401]), on l'interprète par le phénomène de *cage* : aux temps courts les particules se meuvent librement, mais pour des températures plus basses ou des densités suffisamment élevées, elles sont bloquées par leurs voisins, qui forment une sorte de cage autour de la particule en question. De temps en temps, en raison des collisions exacerbées par la température, la particule peut s'échapper de la cage, souvent pour retomber dans une autre (voir la figure 4), mais sur une échelle de temps comparable au temps de relaxation du système, le réseau de cages se réarrange pour permettre à la particule de diffuser librement. Ce réarrangement nécessite une coopération au sein du système.
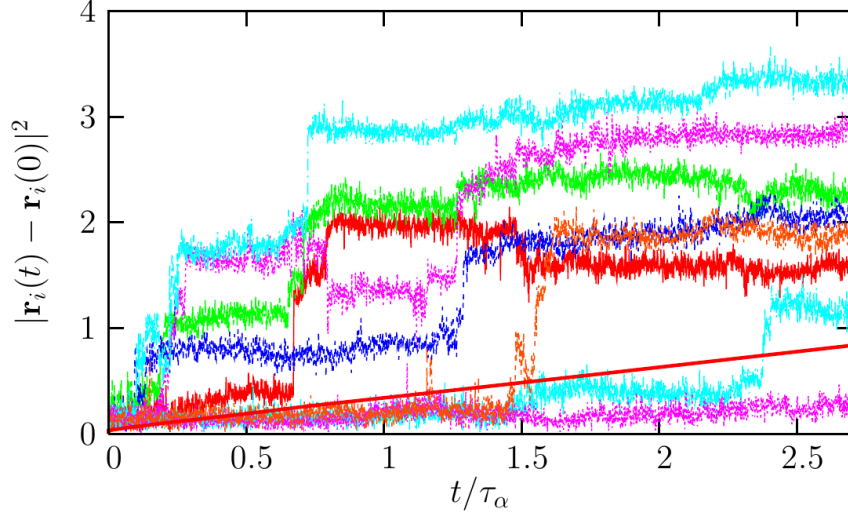
Figure 4: Déplacement de différents traceurs dans un liquide de Lennard-Jones surfondu en fonction du temps rapporté au temps de relaxation. La moyenne sur les trajectoires (ligne continue) produit un MSD régulier comme dans la figure 5(b) ; au niveau d'une particule unique cela montre que la dynamique est intermittente avec de brusques sauts et des vibrations durables dans une cage, ce qui souligne la pertinence des fluctuations dynamiques. [*Repris de* [45]]

Alternativement, on peut accéder dans les expériences de diffusion neutroniques aux *fonctions de corrélation intermédiaires de diffusion*

$$\phi_q(t,t') = \frac{\left\langle \sum_{i,j}^{1,N} e^{i\mathbf{q}\cdot[\mathbf{x}_i(t)-\mathbf{x}_j(t')]} \right\rangle}{NS(q)} \tag{8}$$

dont le dénominateur garantit que $\phi_q(t,t) = 1$ à l'équilibre. C'est une fonction de corrélation de la densité dans l'espace de Fourier, qui est tracée dans la figure 5(a). Pour des températures élevées, elle décroît typiquement exponentiellement :

$$\phi_q(t,t') \sim \exp\left(-\frac{|t-t'|}{\tau_R}\right) \tag{9}$$

Cependant, près du crossover vitreux elle développe aussi un plateau : on distingue une première relaxation exponentielle due aux modes collectifs rapides du système (via un transfert d'énergie par collisions aux temps courts), nommée relaxation β, puis un plateau et enfin une seconde relaxation plus lente (relaxation α) pour décroître vers zéro, afin que le système soit décorrélé à l'équilibre. Il y a donc deux échelles de temps de relaxation, et le temps de relaxation total est dominé par la relaxation α (comme le montre l'échelle logarithmique dans la figure 5). La relaxation en deux temps peut s'avérer plus complexe qu'une relaxation exponentielle due aux mouvements rapides suivie d'une relaxation exponentielle sur une échelle de temps plus longue, puisque la relaxation α est correctement ajustée par la loi exponentielle étendue de Kohlraush-Williams-Watts [235, 403] :

$$\phi_q(t,t') \sim \exp\left[-\left(\frac{|t-t'|}{\tau_R}\right)^{\beta'}\right], \quad \beta' < 1 \tag{10}$$

(a)   (b)
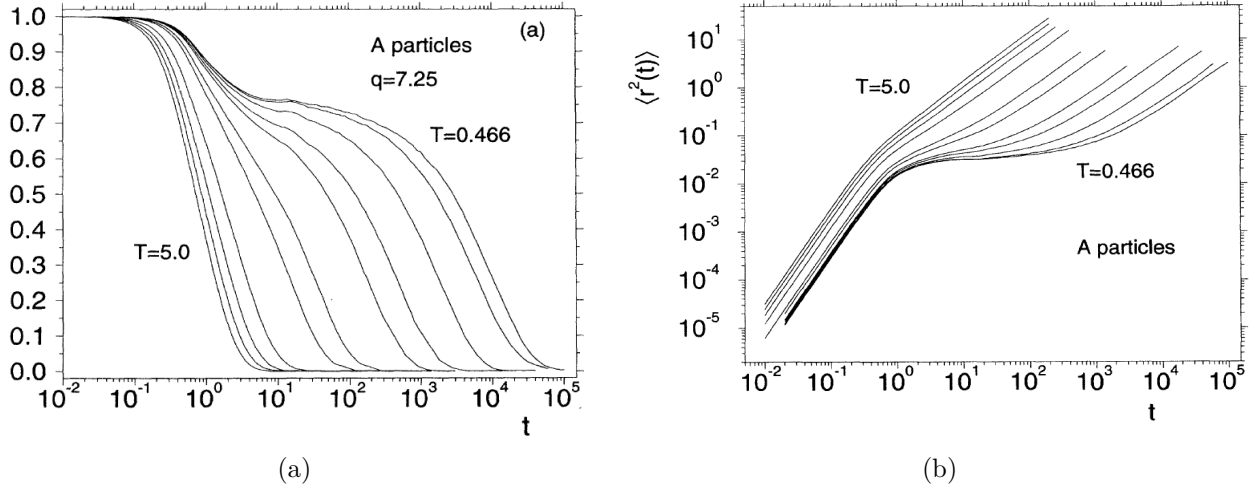
Figure 5: Différents tracés correspondent à différentes températures. (a) Fonction d'autocorrélation intermédiaire de diffusion pour une longueur d'onde fixée, impliquant seulement des processus à une particule, contrairement aux fonctions de diffusion cohérentes données dans l'équation (8): $\phi_q^{\mathrm{s}}(t) = \left\langle \sum_i e^{i\mathbf{q}\cdot[\mathbf{x}_i(t)-\mathbf{x}_i(0)]} \right\rangle /N$. Elles ont cependant des allures semblables. Le système considéré est un mélange binaire de particules de Lennard-Jones à la Kob-Andersen, et seulement les particules de la même espèce sont prises en compte. La dépendance en le vecteur d'onde influence très peu la forme globale de la fonction. (b) MSD en fonction du temps moyennés sur le nombre de ces particules. [*Repris de* [232, 233]]

Ces marqueurs dynamiques semblent provenir structurellement de l'effet de cage, montrant que la structure locale n'est pas si inintéressante, et peuvent être interprétés statiquement de manière plus complexe comme nous allons le voir ci-dessous.

0.1.5   Hétérogénéités dynamiques

L'existence des fluctuations dynamiques a déjà été rapportée à propos de l'effet de cage, où les sauts sont intermittents (figure 4), et sont à la base d'un phénomène supplémentaire, qui démontre encore une fois l'importance d'un point de vue en espace direct sur la structure, les *hétérogénéités dynamiques* : la relaxation s'effectue spatialement de manière hétérogène, certaines régions étant plus rapides que d'autres qui paraissent alors immobiles. La littérature sur ce sujet est extensive : on peut citer des compte-rendus à la fois expérimentaux [359, 140] et numériques [183], ainsi qu'un livre [37]. Un exemple visuel est donné en figure 6.

Pour caractériser les aspects importants des hétérogénéités dynamiques, concentrons-nous sur les corrélations en densité dans l'espace direct :

$$\mathcal{C}(\mathbf{x},t) = \delta\rho(\mathbf{x},0)\delta\rho(\mathbf{x},t) \qquad \text{with} \quad \delta\rho(\mathbf{x},t) = \sum_{i=1}^{N} \delta(\mathbf{x}-\mathbf{x}_i(t)) - \rho \qquad (11)$$

où $\delta\rho(\mathbf{x},t)$ est une fluctuation locale de la densité. A l'instar de sa version en espace réciproque, la fonction intermédiaire de diffusion (8), elles peuvent être utilisées pour examiner la relaxation dans une certaine région de l'espace. Si l'on souhaite étudier la coopérativité du système, *i.e.* comment la relaxation d'une région est corrélée avec celle d'une autre, on doit construire une fonction de corrélation connexe à quatre points[4] :

$$G_4(\mathbf{x},t;\mathbf{0},0) = \left\langle \mathcal{C}(\mathbf{x},t)\mathcal{C}(\mathbf{0},t) \right\rangle - \left\langle \mathcal{C}(\mathbf{x},t) \right\rangle \left\langle \mathcal{C}(\mathbf{0},t) \right\rangle \qquad (12)$$

qui encode les fluctuations dynamiques en deux points différents du système. En sommant sur le volume entier on obtient une susceptibilité dynamique, qui mesure ainsi le volume du système qui relaxe de manière coopérative avec l'origine :

$$\chi_4(t) = \int \mathrm{d}\mathbf{x}\, G_4(\mathbf{x},t;\mathbf{0},0) \qquad (13)$$

---

[4]L'idée de recourir à ce genre de fonctions de corrélation pour caractériser les fluctuations spatio-temporelles provient des études des verres de spin [43].
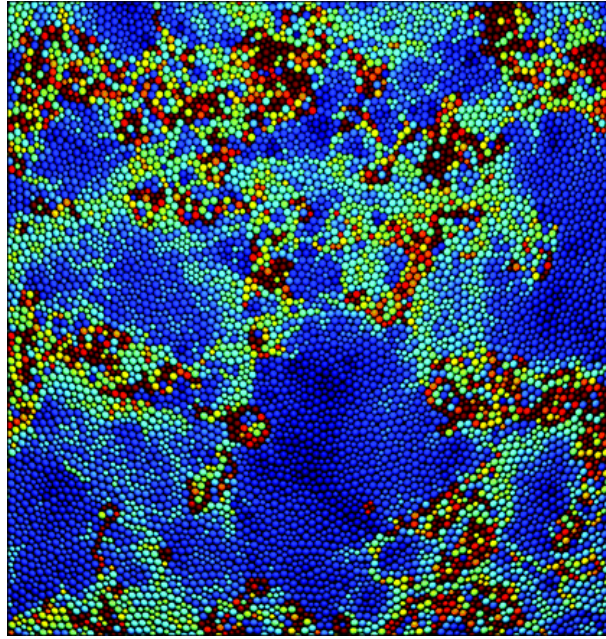
Figure 6: Rendu spatio-temporel de la dynamique d'équilibre d'un mélange bidimensionnel de 10000 particules à l'état de fluide surfondu après une fraction du temps de relaxation. Les particules sont colorées en fonction de leur recouvrement avec leur position initiale : une particule ayant bougé de plus d'un diamètre est en rouge sombre ; une particule qui n'a pas du tout bougé est en bleu marine ; toutes les couleurs intermédiaires du spectre visible coïncident avec des déplacements intermédiaires. La variabilité des couleurs illustre significativement la dynamique hétérogène. Néanmoins, l'arrangement spatial des particules à un temps donné semble parfaitement homogène si l'on moyenne localement sur un ou deux diamètres particuliers. La juxtaposition démontre que la dynamique du système est hautement corrélée, bien que la structure ne le soit pas du tout en apparence. [*Première de couverture de PNAS du 8 septembre 2009*]

A mesure que le temps file vers la relaxation, les régions coopératives grossissent et G_4 décroît plus lentement en espace, et donc χ_4 doit croître. Ceci a été confirmé dans les expériences [38] et simulations [158, 385], voir la figure 7. Cette fonction a un maximum qui coïncide avec le temps de relaxation α, ce qui nous indique qu'en effet la relaxation structurelle nécessite un pic de coopérativité.

La croissance du maximum de la susceptibilité dynamique, en abaissant T, suggère une croissance d'une certaine longueur dans les corrélations dynamiques. Puisqu'il existe une échelle de temps qui croît aussi dans le système (le temps de relaxation), une longueur croissante [38] fut activement recherchée, par analogie avec la théorie des transitions de phase critiques. Cependant, l'extraction d'une telle longueur à partir des fonctions de corrélation à quatre points est ardue et sujette à ambiguïtés [45].

Une autre échelle de longueur, la longueur *du point à l'ensemble*, a été introduite dans [69, 280]. L'idée maîtresse est de mesurer à quel point les conditions aux bords affectent le comportement du système, lui-même loin des bords. Les conditions aux limites dans le cas d'un ferromagnétique sont faciles à concevoir (tous les spins vers le haut ou tous les spins vers le bas) ; dans le cas des verres, on ne sait pas réellement comment imposer une condition au bord d'équilibre qui soit amorphe. Le mieux est encore de laisser le système choisir lui-même la condition aux limites : on laisse le système s'équilibrer, puis on fige toutes les particules à l'extérieur d'une cavité de taille donnée ξ, et enfin on étudie le système à l'intérieur de cette cavité qui (s')est donc soumis à une condition aux bords qui est une configuration d'équilibre typique. En se focalisant sur le recouvrement entre la configuration de référence (avant de figer les particules) et le sous-système rethermalisé au centre, *i.e.* en mesurant à quel point ces configurations sont semblables (correspondant au même état métastable, dans le point de vue thermodynamique développé dans les sections suivantes), on définit une fonction de corrélation statique du point à l'ensemble, qui, contrairement aux fonctions de corrélations statiques plus simples définies précédemment, possède un comportement non trivial près de la transition vitreuse. La longueur de corrélation, qui est la distance typique ξ_{PS} au-dessus de laquelle le recouvrement tombe à zéro, est une échelle de longueur dont la croissance est un net signal que le système est en train de développer un ordre statique à longue portée, et
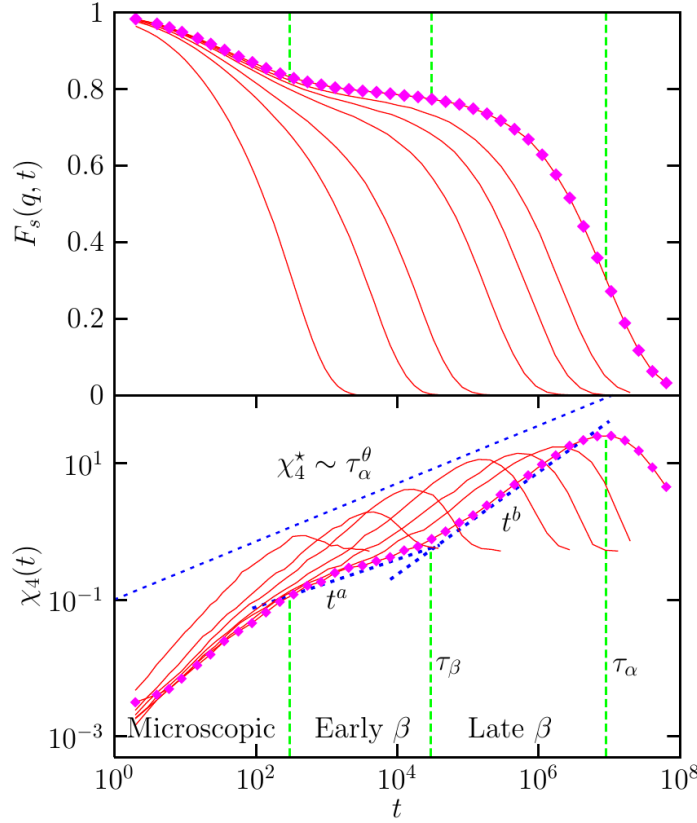
Figure 7: Dépendence temporelle de la fonction d'autocorrélation intermédiaire de diffusion $\phi^s \equiv F_s$ comme dans la figure 5(a) (haut), superposée à la susceptibilité dynamique (bas), pour différente températures décroissant de gauche à droite dans un liquide surfondu de Lennard-Jones simulé par un algorithme de Monte-Carlo. La température la plus basse est indiquée par des symboles. χ_4 admet un maximum χ_4^* près du temps de relaxation α, τ_α, se déplace vers des temps plus longs et a une valeur plus grande quand on refroidit le système qui est bien ajustée par une loi de puissance $\chi_4^* \sim \tau_\alpha^\theta$. Plusieurs régimes de relaxation distincts peuvent être inférés du tracé de la susceptibilité dynamique. [*Repris de* [45]]

dans le cas des verres, un ordre amorphe de longue portée. Il fut rigoureusement prouvé qu'elle doit croître s'il en va de même du temps de relaxation [289] et des simulations numériques de liquides surfondus l'ont effectivement montré [59]. Par conséquent, une question ouverte importante est de savoir si cette longueur du point à l'ensemble ξ_{PS} est une conséquence de corrélations statiques cachées ou si elle est totalement déconnectée de celles-ci. Nous renvoyons aux compte-rendus mentionnés précédemment [359, 140, 183, 37] pour de plus amples détails, puisque ce ne sera pas un sujet envisagé dans cette thèse.

0.1.6 Relation de Stokes-Einstein

Les hétérogénéités dynamiques sont supposées être à l'origine de la violation de la relation de Stokes-Einstein (SER) [83, 43] entre le coefficient de diffusion D, qui est donné par l'asymptote aux temps longs du MSD, et la viscosité (cinématique) des liquides surfondus :

$$D\eta = \frac{T}{\zeta} \tag{14}$$

où ζ est une constante (la friction de Stokes). Ce résultat a été obtenu par Einstein dans l'un de ses célèbres articles de 1905 [144], en considérant une particule brownienne immergée dans un fluide jouant le rôle d'un bain d'équilibre à température T. Le modèle brownien suppose un coefficient de dissipation qui peut être déduit, en principe, d'une modélisation microscopique du bain [424, 197]. Afin de garantir la compatibilité avec la loi de Stokes (1845) gouvernant la friction d'un fluide [370, 1, 246, 199], calculée à partir des équations de Navier-Stokes à petit nombre de Reynolds, en considérant le mouvement d'une

sphère dans un fluide visqueux, la dissipation doit être[5] $\zeta = 3\pi\sigma$ où σ est le diamètre du traceur. Bien que cette relation soit strictement valide pour un traceur bien plus gros que les molécules qui constituent le fluide, elle est en réalité étonnamment précise pour rendre compte du coefficient de diffusion d'une molécule entourée d'autres molécules de même taille dans les liquides à haute température, voir la figure 8. Cela dit, elle semble ne plus tenir dans certaines situations, typiquement lorsque le coefficient de diffusion demeure fini non nul alors que la viscosité est nulle (comme dans l'hélium superfluide) ou bien infinie (comme dans les cristaux élastiques). Cet écart surgit aussi dans les liquides surfondus près de leur transition vitreuse, où le coefficient de diffusion décroît plus doucement que le rapport T/η lorsque la température est abaissée, résultant en une disparité de plusieurs ordres de grandeur. Ceci a été vérifié expérimentalement dans *e.g.* [336, 166, 89, 100, 268, 411].
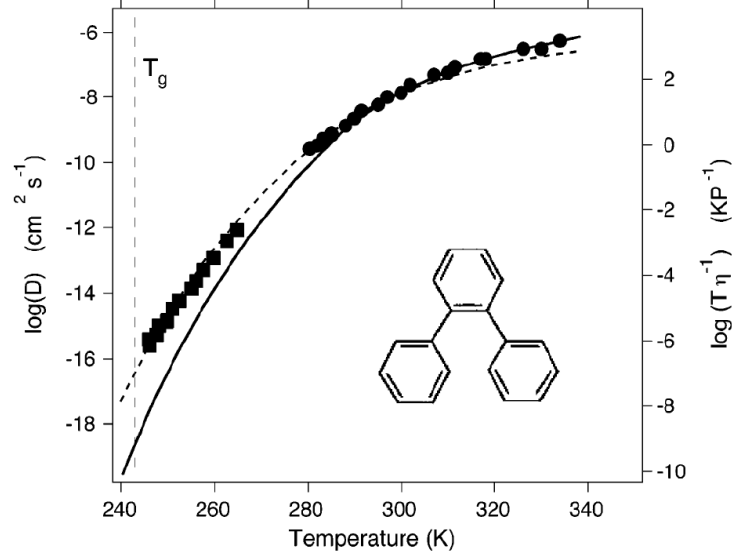
Figure 8: Découplage entre la viscosité et le coefficient de diffusion dans l'orthoterphényl surfondue. La ligne pointillée révèle un ajustement avec une SER fractionnaire, $D \sim (T/\eta)^{\#}$ où $\# \simeq 0.82$ au lieu de la valeur $\# = 1$ qui est valide à haute température, comme dans la SER usuelle (14). De telles lois fractionnaires ont aussi été annoncées dans *e.g.* [411]. [*Repris de* [268]]

L'*échec*[6] de la SER est une indication probante que différentes façons de mesurer les temps de relaxation, à travers la relation de Maxwell (1) ou à travers le MSD, mène à différentes réponses et constitue donc un indice significatif d'une large distribution d'échelles de temps de relaxation. Une explication à la fois simple et intuitive de cet effet a été trouvée par Cicerone et Ediger dans [100]. Le coefficient de diffusion est dominé par les régions les plus rapides, les contributions des domaines lents étant négligeables comparées aux rapides. Si $\tau_{\rm f}$ désigne une échelle de temps de relaxation, alors ce coefficient échelle grossièrement comme $D \sim \tau_{\rm f}$ (le préfacteur étant quelquechose comme le carré de la taille linéaire de la boîte contenant le système multiplié par le rapport entre les volumes des régions rapides et lentes). Inversement, le temps de relaxation est, lui, dominé par les régions les plus lentes (dont le temps de relaxation est $\tau_{\rm s}$), afin que la viscosité échelle comme $\eta \propto \tau_{\rm s}$ d'après la relation de Maxwell (1). Puisque $\tau_{\rm f} \ll \tau_{\rm s}$, on s'attend à ce que la diffusion soit supérieure à $T/\eta\zeta$. Cet argument est naïf et suppose une proportion comparable de régions rapides et lentes au sein du système, et dont les échelles de temps de relaxation sont clairement séparées, mais donne tout de même une bonne impression de ce qui se joue.

Un lien avec la décroissance non exponentielle des fonctions de corrélation dynamiques, la loi de Kohlraush-Williams-Watts law, a été établi dans [100] : l'exposant étendu β' dans (10) est d'autant plus petit que la déviation mesurée de la SER est grande. Ceci suggère un rôle central des hétérogénéités spatiales dans les caractéristiques non conventionnelles de la dynamique vitreuse.

---

[5]$\zeta = 3\pi\sigma$ vient d'une condition au bord de la sphère sans glissement due à la viscosité, tandis que d'autres expressions peuvent être obtenues dans d'autres situations, *e.g.* $\zeta = 2\pi\sigma$ pour l'approximation de glissement du champ de vitesse [1, 199].

[6]Comme dit précédemment, la SER n'a pas vocation à s'appliquer à toute une panoplie de situations, bien qu'elle ait trouvé une validité plus étendue que le cas originel d'un gros traceur dans un bain. Il est donc peu surprenant qu'elle ne tienne plus dans un régime *fortement couplé* (suggéré par l'effet de cage).

La violation de la SER a été analysée dans plusieurs cadres théoriques (assez différent conceptuellement) [382, 368, 214, 57]. Elle sera déduite dans le cas des liquides en dimension élevée dans §3.8.5.

0.1.7   Vieillissement

Conventionnellement, sous la transition vitreuse expérimentale, le liquide semble figé mais n'a pas encore atteint un état stationnaire : sa dynamique s'effectue hors de l'équilibre, en s'efforçant très lentement d'atteindre l'équilibre, ce que les expériences ne peuvent pas détecter en raison du temps de relaxation α déraisonnable. Néanmoins cette dynamique peut être étudiée et fournit une large variété d'effets intriguants. Les régimes hors de l'équilibre sont aussi d'importance capitale en physique puisqu'il n'y a, contrairement à la mécanique statistique d'équilibre, très peu de résultats génériques valides arbitrairement loin de l'équilibre, et ce domaine a trait à presque tous les phénomènes dont on a l'expérience quotidienne. Ces protocoles, dans le cas des verres, peuvent être de simples *trempes* vers un état vitreux. Un protocole plus élaboré est un *recuit* : par exemple on attend que l'échantillon s'équilibre dans un régime vitreux (de basse température) et on vient ensuite le perturber par une trempe à une température voulue.

Les verres hors de l'équilibre vieillissent : l'invariance par translation dans le temps (TTI) ne tient plus et l'évolution du système dépend de toute son histoire passée, notamment à travers le *temps d'attente* t_{w}, qui est le temps passé depuis sa préparation (par exemple après une trempe), aussi appelé son *âge*, et le temps d'observation t qui désigne le temps qui s'écoule durant l'expérience. Si l'on mesure pendant une durée t la fonction d'autocorrélation C d'une certaine observable (ainsi t est le temps passé entre la première mesure et la mesure en cours), elle dépendra des deux temps $C(t, t_{\mathrm{w}})$, contrairement à une situation d'équilibre où l'âge du système est vite oublié. La dépendance en t_{w} est le phénomène de vieillissement, voir la figure 9. Une multitude de protocoles alternatifs, exhibant d'intéressants effets de mémoire ou de rajeunissement, ont été réalisés expérimentalement (voir [40] pour un compte-rendu).

Expérimentalement, on observe une décomposition des corrélations (ou réponses) en une partie d'équilibre vérifiant TTI, et une partie de vieillissement présentant la *superposition en temps et âge*, *i.e.* qui dépend du rapport entre les deux échelles de temps :

$$C(t, t_{\mathrm{w}}) \simeq C_{\mathrm{eq}}(t - t_{\mathrm{w}}) + \mathcal{C}(t/t_{\mathrm{w}}) \tag{15}$$

Cette superposition est analogue à la *superposition en temps et température* découverte dans les données d'équilibre, qui, dans le processus de relaxation α, semble écheller selon le ratio $t/\tau_\alpha(T)$. La partie d'équilibre relaxe rapidement, et le temps de relaxation du système est donc directement proportionnel à l'âge en raison de la superposition en temps et âge, *i.e.* $\tau_\alpha \propto t_{\mathrm{w}}$, bien que certains liquides de polymères sont mieux ajustés par une loi sub-linéaire avec un certain exposant de vieillissement [371].

Des compte-rendus pédagogiques de ce comportement figurent dans [61, 112, 43]. Nous résumerons les résultats obtenus à propos de la dynamique hors d'équilibre des modèles de champ moyen dans §1.2.5.

0.2   Sphères dures amorphes en dimension infinie

Cette thèse poursuit une série d'articles par Charbonneau, Kurchan, Parisi, Urbani et Zamponi, qui analysent la physique statistique des systèmes de sphères dures (HS) en grande dimension spatiale [312, 243, 242, 96]. Un résumé récent, contenant une partie des résultats présentés dans cette thèse, reprend ses aspects clés [98].

Définissons tout d'abord le potentiel : il décrit des sphères dures de diamètre σ ayant une répulsion infinie par contact et n'interagissant pas au-delà de cette distance. En d'autres termes il s'agit d'une idéalisation des boules de billard :

$$V_{\mathrm{HS}}(r) = \begin{cases} \infty & \text{if } r < \sigma \\ 0 & \text{if } r > \sigma \end{cases} \quad \implies \quad e^{-\beta V_{\mathrm{HS}}(r)} - 1 = -\theta(\sigma - r) \tag{16}$$

qui peut être régularisé de plein de façons par un potentiel à cœur mou, en prenant la limite de répulsion infinie[7]. θ est la fonction théta d'Heaviside ; on voit dès à présent que la température n'a aucun impact sur

---

[7]Par exemple les sphères harmoniques $V_{\mathrm{SHS}}(r) = \kappa \left(1 - \frac{r}{\sigma}\right)^2 \theta(\sigma - r)$ avec $\kappa \to \infty$ pour retrouver les HS, ou la limite $n \to \infty$ des potentiels en loi de puissance inverse (IPL) $V_{\mathrm{IPL}}(r) = \epsilon \left(\frac{\sigma}{r}\right)^n$, ces derniers fournissant une régularisation C^∞ (pour tout n fini).
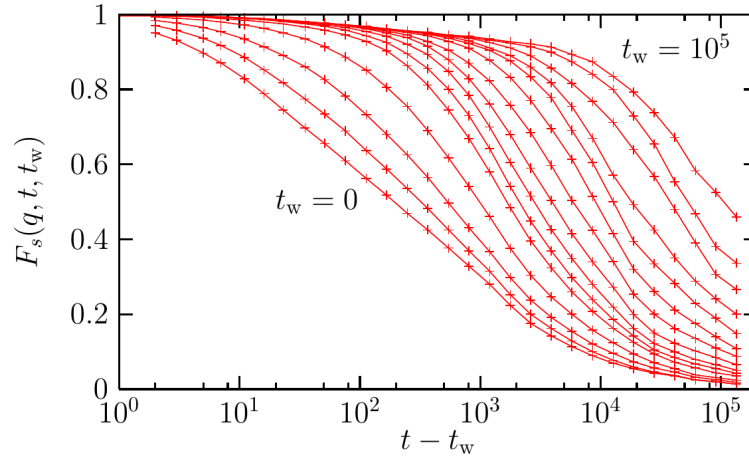
Figure 9: La fonction d'autocorrélation intermédiare de diffusion obtenue par une étude Monte-Carlo d'un liquide vitreux de Lennard-Jones à basse température. Le système subit une trempe au temps $t_w = 0$ vers des basses températures. Les mesures sont effectuées pour des temps d'attente croissant de gauche à droite. La relaxation devient d'autant plus lente que t_w croît, un effect typique du vieillissement. Aux temps d'attente courts, $t - t_w$ est l'échelle de temps pertinente alors qu'aux temps d'attente longs on doit sonder des temps plus longs pour observer une dépendance non triviale, ce qui illustre la superposition en temps et âge. [*Repris de* [43]]

la thermodynamique de ce système. Le diagramme de phases (T, ρ) est donc remplacé par un diagramme de phases unidimensionnel contrôlé par la seule densité ρ. Un paramètre de contrôle plus adapté, relié à la densité, est la fraction volumique $\varphi \in [0, 1]$ (rencontrée précédemment dans la figure 1), *i.e.* le rapport entre le volume occupé par les sphères et le volume total délimitant le système :

$$\varphi = \frac{N\mathcal{V}_d(\sigma/2)}{\mathcal{V}} = \frac{\rho\mathcal{V}_d(\sigma)}{2^d} \qquad (17)$$

La majeure partie de cette thèse généralise la thermodynamique de ce système à toute une classe de potentiels liquides qui peuvent être influencés par la température contrairement aux HS (chapitre 4) et analyse leur dynamique (chapitre 3). Nous mettons en évidence quelques résultats théoriques clés obtenus avant cette thèse :

- Le point de départ des études portant sur les liquides en grande dimension remonte en réalité au milieu des années 1980 avec le calcul de l'énergie libre de la phase liquide des HS par Frisch, Rivier et Wyler [162, 258, 164, 409, 163, 161] et leur équation d'état.

- Peu après, Kirkpatrick et Wolynes [225] proposèrent d'étudier la limite de dimension infinie des liquides et verres mais certains outils, comme la méthode des répliques pour des systèmes sans désordre explicite décrite brièvement dans §1.2.4.2, n'étaient pas disponibles à l'époque mais ont été développés dans les décennies qui suivirent.

- Parisi et Zamponi ont analysé le diagramme des phases en $d \to \infty$ (voir [312] pour un compte-rendu), en utilisant un ansatz gaussien pour la densité du liquide répliqué (la densité de *molécules*, *i.e.* de copies du système, à l'instar de §1.2.4.2).

- Dans la série d'articles [243, 242, 96], il fut montré que l'approximation gaussienne était exacte en $d \to \infty$, du moins pour calculer l'entropie, et le régime de haute densité a été étudié systématiquement, prouvant qu'une transition à la Kauzmann vers une phase de verre idéal existe et que, en comprimant plus avant, cette phase devenait instable et était remplacée par une phase de Gardner [325, 97], voir §4.4.

- Une conséquence majeure de la théorie est que ces résultats statiques fournissent un cadre pour étudier la *transition de blocage* (*jamming*). Celle-ci ne sera pas discutée dans cette thèse, mais est une prédiction cruciale de la théorie donc nous en soulignons quelques résultats[8]. Définissons le

---

[8] *And we hope you like jamming too.*

blocage de cette manière : prenons un empilement de HS dans une boîte, et compressons-les autant que possible, en augmentant la pression à travers des forces sur la boîte, ou en ajoutant de plus en plus de particules à l'intérieur, densifiant ainsi l'empilement. A un moment donné la pression atteinte est infinie (en raison de la répulsion infinie des HS ; un potentiel plus mou reste toujours compressible à température finie). Les particules sont alors *mécaniquement en contact* avec leurs voisines, et à cause de la contrainte de cœur dur, elles sont complètement bloquées par leurs voisines. L'empilement est alors qualifié de *bloqué* ; il a subi la transition de blocage d'un empilement assez lâche à un empilement très compact. Ceci est illustré dans la figure 10.
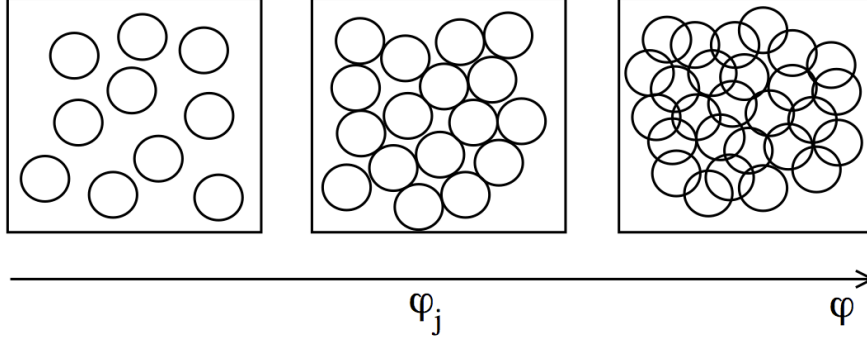
Figure 10: Configurations dans un régime liquide (gauche), pour un empilement bloqué à φ_j (milieu), et enfin pour des compressions plus fortes (droite) : si les sphères sont molles, elles doivent alors s'interpénétrer. [*Repris de* [206]]

Notons que cette forme de blocage est différente du blocage observé dans les verres. Dans l'état amorphe créé à la transition vitreuse, le blocage est dû à l'effet de cage et aux vibrations à l'intérieur de la cage, qui confèrent au liquide sa réponse similaire à un solide capable de supporter des charges. Cependant, le système reste compressible et la pression est finie. Dans le cas bloqué, la rigidité provient de la formation d'un réseau de contact mécanique entre les sphères qui a percolé ; si on suppose pouvoir modéliser ces sphères comme mécaniquement indéformables, le solide qui en résulte est incompressible et sa pression est infinie.

Un exemple typique d'empilement bloqué est un tas de sable : quand on fait tomber du sable d'un seau par terre, il s'écoule en l'air comme un liquide parce qu'il est alors dilué. Mais lorsqu'il atteint le sol, le sable qui s'amoncelle couche par couche fait croître petit à petit la densité de l'empilement sous l'effet de la gravité, qui agit comme une pression exercée sur le système. La couche la plus basse ne peut plus s'échapper à cause de la friction avec le sol, et lorsque tout le sable contenu dans le seau s'est déversé, après une réorganisation rapide et partielle des couches supérieures qui s'écoulent encore (*i.e.* qui sont encore dans un état liquide), ayant temporairement une densité locale plus faible, plus aucun mouvement local ne peut survenir dans le tas de sable : il est bloqué.

Le point de blocage atteint après une compression infinie se trouve dans la phase de Gardner de haute densité, et est caractérisée par sa fraction volumique φ_j (voir §10). Il dépend du protocole suivi, mais le comportement critique près de la transition de blocage est universel. Un certain nombre d'exposants critiques a été calculé [96, 97], décrivant *e.g.* la distribution des forces faibles au niveau des contacts (pour une version molle du potentiel HS) ou la distribution des vides entre les sphères. Ces deux distributions ont une dépendance en loi de puissance près de la transition. Ces lois d'échelle sont très différentes de celles attendues dans un verre normal ou un cristal.

L'existence de modes de vibration différents des phonons a aussi été déduite de la solution. Le nombre de contacts à la transition de blocage suit le critère d'isostaticité de Maxwell [273], s'élevant à $2d$ par particule en moyenne. Ceci est relié à la stabilité marginale de l'empilement, puisqu'il s'agit du nombre minimal de contacts requis pour qu'un empilement soit mécaniquement rigide. De cette seule propriété, des propriétés générales ont été déduites par Wyart [408, 53, 128] en dimension quelconque, indépendamment de la solution en $d \to \infty$, et ces prédictions en lois d'échelle sont compatibles avec celles découvertes dans cette limite. Les simulations numériques en $d \geqslant 2$ ont récemment montré [92] que la criticalité de la dimension infinie et la valeur des exposants sont

robustes pour toutes les dimensions, y compris les dimensions expérimentalement pertinentes $d = 2$ et 3.

Pour conclure, le système de HS en $d \to \infty$ fournit un cadre unificateur pour analyser toutes les phases du système quelque soit la densité : liquide, verre et bloqué. Un diagramme de phase est donné en figure 11, voir aussi figure 4.5.
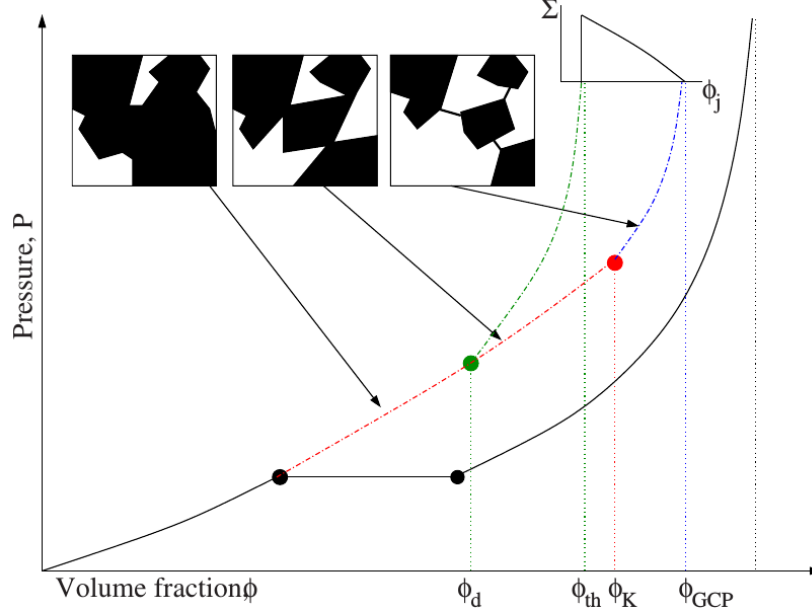
Figure 11: Pression en fonction de la fraction volumique pour les HS. La ligne noire continue représente la transition liquide-solide du premier ordre. Au-delà de la transition dynamique φ_d, le système se trouve dans un des états métastables exponentiellement nombreux. En comprimant plus avant il entre dans l'état vitreux idéal (à la transition de Kauzmann φ_K) et à pression infinie il acquiert une densité $\varphi_j \in [\varphi_{th}, \varphi_{GCP}]$ qui dépend du protocole et de l'état suivi. Les *minima du paysage d'entropie* les moins denses (les états purs les plus hauts) sont caractérisés par la fraction volumique de seuil φ_{th}. L'empilement le plus dense (GCP) a une densité φ_{GCP}. En cartouche la complexité est tracée. Les encarts illustrent une *vision d'artiste* de l'espace des phases à dN dimensions du système. Les configurations en noir sont accessibles tandis que les blanches sont interdites par la contrainte de cœur dur. Dans le régime surfondu l'espace des phases est connexe et ne l'est plus dans la phase vitreuse où les états purs sont bien définis. [*Repris de* [312]]

0.3 Aperçu et questions traitées dans cette thèse

Le reste de la thèse s'organise comme suit :

- Le chapitre 1 constitue l'introduction générale dont une partie est reprise ici en français. Elle introduit en outre le scénario champ moyen RFOT, les différentes théories de la dynamique des liquides, ainsi que l'invariance d'échelle (*isomorphes*) qui sera étudiée dans le chapitre 5.

- Dans le chapitre 2, on décrit un schéma d'approximation adapté à l'étude de la limite de dimension infinie des liquides, le développement du viriel, qui y sera appliqué dans le cas des HS. Ensuite on résout analytiquement à la fois la statique et la dynamique d'un modèle de verres de spins de champ moyen pour donner les outils et idées qui seront mis à profit dans le contexte des verres structuraux. Ce modèle est un exemple concret des idées de RFOT de la section 1.2. Nous espérons que ces sujets sont traités de manière pédagogique et qu'ils montrent de manière convaincante que la construction de la solution en $d \to \infty$ des chapitres suivants est, pour beaucoup, une répétition de ces quelques étapes.

- Dans le chapitre 3, on analyse la dynamique des liquides et verres en $d \to \infty$ à la fois à l'équilibre

et hors de l'équilibre. On explore ses implications pour la transition vitreuse et discute du lien avec la théorie de couplage de modes (MCT).

- Dans le chapitre 4, la thermodynamique de ce système est obtenue d'une manière complètement analogue à la dynamique. Ceci permet de prouver la cohérence entre la vision aux temps longs fournie par la dynamique et la vision statique.

- Dans le chapitre 5, en se basant sur les travaux des chapitres 3 et 4, on examine la notion d'isomorphes en $d \to \infty$ et l'on montre qu'elle devient exacte pour une large classe de potentiels de paires liquides.

- Dans le chapitre 6, on résume brièvement ce travail et donne une perspective sur les différents progrès et questions qui pourraient se déduire de nos résultats.

- Les annexes contiennent une table de notations et définitions employées tout au long de cette thèse, des points techniques qui ne sont pas strictement nécessaires dans le texte principal mais qui y sont reportés pour pouvoir s'y référer au besoin, ainsi qu'une présentation relativement complète et pédestre de la théorie des champs pour la dynamique des systèmes à plusieurs corps en interaction et en contact avec un bain thermique (formalisme de Martin-Siggia-Rose-De Dominicis-Janssen), qui est extensivement utilisé dans cette thèse.

SUPERCOOLED LIQUIDS AND THE GLASS TRANSITION

Outline

The present thesis being aimed at solving the dynamics of liquids and glasses while making contact with their thermodynamics, in the limit of high spatial dimension d, this introductory chapter first emphasizes experimental key features relevant to actual liquids and glasses. The thermodynamics and structure of liquids is quite well accounted for theoretically, whereas their dynamics lacks a theoretical framework starting from the microscopic equations and making controlled approximations which may be refined systematically.

In the low-temperature regime approaching glassiness, it is observed experimentally that they exhibit unusual behaviour compared to regular phase transition phenomena, which motivates the study of the glass transition in itself, but also for what it may teach us about the vast wilderness field of non-equilibrium physics. The issue is that studying exactly liquids and glasses is a tremendous task in $d = 2$ or 3. This is why theoretical research has focused quite a lot on mean-field models to understand the glassy phenomenology, *as a first approximation.* Yet, even at this level, there is no clear landmark. Indeed the mean-field ideology of the glass transition is mostly based on the exact study of *spin* glasses, which are disordered magnetic alloys that seem to have little in common at first sight with what happens in glass forging. Nevertheless, physics is full of examples of *universal* behaviour, and some experimental characteristics of spin glasses display a striking resemblance with *structural* glasses (which is the standard term for usual glasses, like windows). Mean-field spin-glass models are easier to deal with and were solved exactly. They gave birth *by analogy* to a theory of structural glasses in the 1980s, the Random First-Order Transition (RFOT) theory, which is presented in the second section.

It seems then natural to investigate the large-dimensional limit of liquids and glasses in order to check explicitly this scenario *in this well-defined mean-field limit.* The absence of an obvious small parameter to study liquids and glasses is then compensated for by $1/d$. Indeed, contrary to more standard condensed matter systems, there is no standard perturbative treatment necessitating a reference frame and a small parameter [404], like a low-density expansion around the ideal gas limit for moderately dense gases, or around an ideal periodic lattice for crystals (*e.g.* phonons via harmonic vibrations) [85, 199, 17]. A similar situation is encountered in strongly-correlated electrons [179], atomic physics [372], and gauge field theory [134]. These authors developed a dimensional expansion to tackle this issue. By solving the problem in infinite-dimensional space and treating $1/d$ as a small parameter, one may hope to recover, to a good approximation, the behavior of physical systems in $d = 3$.

As regards liquids and glasses, the high-temperature liquid phase's thermodynamics was exactly worked out in the mid-1980s [162, 258, 164, 409, 163, 161]. It was realized a few years ago that all the theoretical tools needed to construct an exact theory in $d \to \infty$ for the whole phase diagram were available. This observation triggered this current research effort, which results in a confirmation of the RFOT ideas in $d \to \infty$ (as well as novel predictions, notably in finite dimensions). This is the reason why we introduce it in §1.2.

The problem of obtaining a *dynamic* theory of liquids, in other words of large systems of classical particles in a strong-coupling regime, which is at the core of this thesis, is depicted in §1.3. We then review a scale invariance recently discovered in the phase diagram of liquids, that we will study in a later chapter as a by-product of the dynamics and statics derived. Prior results to this thesis about the thermodynamics of high-density hard-sphere systems in $d \to \infty$ are summarized in §1.5. Finally we give an outline of the rest of the thesis.

In the whole thesis, we set the Boltzmann constant $k_B = 1$. $\beta = 1/T$ is the inverse temperature. Recurrent notations are tabulated in appendix A.

1.1 Basic phenomenology and phase diagram

From the theoretical point of view, a *simple liquid* is a system of N *classical* particles interacting via an isotropic pair potential V. This is an idealization but some aspects of the phenomenology discussed in this chapter may also be relevant to different systems, be them anisotropic (*e.g.* gels [341, 256, 416]), with many-body interactions (*e.g.* liquid metals [148, 269]) or in a quantum regime (quantum glasses [320, 250, 407, 391]). In the following, we focus on experimental facts about what happens to simple liquids upon cooling.

1.1.1 Becoming supercool(ed)

Intuitively, at low density the system is a gas while at high density it becomes a solid, in the sense of a compact and rigid body. Conversely, molecules jiggle due to heat [153, Chap. I]; as a result, a solid at high temperature will expand owing to these thermal collisions and becomes more fluid as it gets hotter, becoming liquid-like or even gaseous for higher temperatures. Let us start from this intermediate regime, the liquid. When cooled down, we thus expect it to become more packed.

Actually, a first-order transition takes place to an ordered state, which is an abrupt change to a periodic arrangement: the crystal. The (continuous) translational and rotational symmetries are broken (becoming discrete, depending upon the type of crystal lattice). Ergodicity is broken as well: disordered (liquid) configurations are no longer accessible to the system. A collective motion of the particles is necessary to achieve this process. The transition temperature is called *melting point* T_m. This *freezing transition* is a process not entirely understood[1] in itself [217, 353, 387, 151, 35]. The crystal is thermodynamically stable: it has a lower free energy than the liquid state for $T < T_m$. Nevertheless, this transition can be avoided and the liquid equilibrium branch can be continued in the phase diagram to $T < T_m$, as shown in figure 1.2. The liquid is then metastable and is qualified as *supercooled*: the canonical practical example being mineral water put in the freezer. It may not freeze and a slight tap or pouring the water is enough to make it crystallize, assisting the growth of nucleated cristallites. In this supercooled liquid *phase*, the effect of cooling seems to be the most naive, although least understood: molecules become densely packed, their dynamics is slower and there is no spatial emergent ordering unlike in the crystal [239]. Their packing is *amorphous.*

This metastable phase may be tricky to obtain. Experimentally, one uses materials that are known to be good *glass formers*, *i.e.* that do not crystallize easily, and follows a quenching protocol which is fast enough to avoid nucleation and growth of the crystal, but not too fast[2] to remain equilibrated in the sense of the liquid phase. These precautions are detailed in [83, Section III]. A sophisticated recent technique, vapour deposition [310, 373, 360, 361, 261, 357], allows to form the supercooled liquid atomic layer by

---

[1] A mean-field description about the freezing transition is given in [85, 199] through Density-Functional Theory, which amounts to write an approximate free energy as a functional of the local density field, similarly to the Landau treatment of phase transitions [247, 248]. Mean-field theory in the case of the liquid-gas transition is analogous to the mean-field Ising model. Note also that a formal mapping exists between the ferromagnetic Ising model and lattice gases [412, 249].

[2] Typically 0.1 to 100 K/min [62].

atomic layer, easing equilibration by avoiding the necessity to relax the bulk of the system. It can probe equilibration timescales that are hard to reach otherwise (*e.g.* 40 years for some samples in [373]), unless resorting to find *e.g.* million years old glasses in Nature [420], although in this case the experimental protocol is uncontrolled and one necessarily studies out-of-equilibrium regimes. Numerically, one usually uses good glass-forming potentials and polydisperse systems [8], putting together different components with different shapes (*e.g.* spherical particles with different diameters, such as Kob-Andersen binary mixtures [231, 229, 55]), which hampers crystallization. Non-local Monte Carlo sampling has been used to achieve equilibration at densities or temperatures otherwise unreachable [48].

1.1.2 Relaxation matters

If one cools down the supercooled liquid carefully enough to stay equilibrated, at some point the liquid becomes dramatically viscous: if we note this typical temperature $T_g < T_m$, the viscosity increases by many orders of magnitude in a range of only a fraction of T_g. This phenomenon is striking in itself, and also in its relative universality: a wide class of systems exhibits this behaviour, ranging from atomic and molecular liquids, colloidal suspensions, granular media, to metallic alloys, polymeric melts, gels, ... [136, 338].

Viscosity is a macroscopic quantity easily measurable experimentally. It is related to a microscopic quantity, the relaxation time τ_R of the system, through Maxwell's relation [83, 82]

$$\eta = G_\infty \tau_R \tag{1.1}$$

approximately valid for equilibrium liquids, with G_∞ the infinite-frequency shear modulus, similar to Young's modulus in solids [245]. This means that as we go towards this *experimental glass transition* at T_g, the relaxation time of the system has a sudden growth and the fluid experiences more and more difficulty to flow since its composing particles' relaxation is hindered. T_g is not well defined and depends on the experimental time one accepts to wait; conventionally, a good order of magnitude is 10^{12} Pa·s [83]. For comparison, water is $\sim 10^{-3}$ Pa·s and honey is around 10 Pa·s [323], and a mug containing a liquid close to its glass transition would take approximately 30 years[3] to empty under the action of gravity [136, 418]. Then, when the relaxation time becomes larger than the experimental time, which is the definition of T_g, for practical purposes the supercooled liquids behaves macroscopically as an elastic solid; its response to a shear stress σ gives a linear strain γ (measuring the relative displacement of the microscopic structure) is as in Hooke's law [245, 82], which confers its rigidity,

$$\sigma = G_\infty \gamma \tag{1.2}$$

while for times larger than τ_R the modulus vanishes as in a liquid: it is indeed a time-dependent quantity, *i.e.* $\sigma = G(t - t_0)\gamma$. Even a perfect solid (*e.g.* a crystal) flows for large times (but still finite in the thermodynamic limit), although the mechanism is different: viscosity of perfect solids quickly diverges at zero stress while it stays finite for a Newtonian liquid at zero stress [343].

The sharp rise of the viscosity, or relaxation time, is well documented experimentally and is summarized in Angell's plot [15, 14] of the logarithm of the viscosity versus T_g/T for various systems, shown in figure 1.1. Straight lines means that a simple Arrhenius behaviour

$$\tau_R \propto \exp\left(\frac{\Delta}{T}\right) \tag{1.3}$$

accounts for the relaxation, which is dominated by the energy barrier Δ to cross in order to trigger the activation mechanism. This is indeed what is generally expected for simple relaxation processes [198]. These systems are termed *strong* glass formers and archetypical examples are SiO_2 (window glass) and GeO_2. Systems corresponding to curved lines below display a super-Arrhenius behaviour which is intriguing. These are called *fragile* glasses, such as orthoterphenyl and toluene. One has to be careful with such classifications since the separation is not clear cut in experimental data. The terminology *strong* and *fragile* is not related to the mechanical properties of the glass but to the evolution of the short-range order close to T_g: locally favoured structures (LFS) [338], *e.g.* tetrahedric order, persist both below and

---

[3]One of the longest related experiment to date is the pitch-drop experiment [139] in Brisbane, Australia, where hot tar had been poured into a cup in 1927 and was rediscovered in 1961 after being completely forgotten. The tar's viscosity has been measured to be $\sim 10^9$ Pa·s at 10°C and $\sim 10^6$ Pa·s at 30°C; every 10 years or so, one drop falls off the cup.

above the glass transition in strong glasses while they disappear quickly upon heating fragile glasses. Super-Arrhenius behaviour can be seen as an increase of the effective energy (or free energy) barrier with temperature, which hints at a collective phenomenon [239]. Indeed, popular fits different from (1.3) give reasonable results on (η, T) curves, such as the Vogel-Fulcher-Tamman law (VFT) [400, 167, 380]

$$\tau_{\rm R} \propto \exp\left(\frac{A}{T - T_0}\right) \tag{1.4}$$

or the Bässler law [25]

$$\tau_{\rm R} \propto \exp\left[K\left(\frac{T^*}{T}\right)^2\right] \tag{1.5}$$
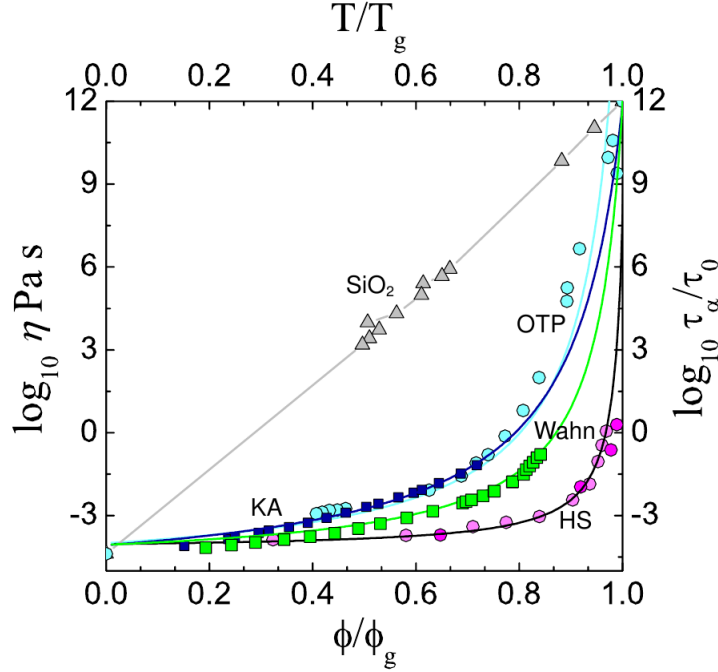
Figure 1.1: Angell's plot: Arrhenius representation of liquid viscosities (or equivalently relaxation times, noted τ_α here), with inverse temperature scaled by $T_{\rm g}$. SiO_2 and orthoterphenyl (OTP) are standard molecular glasses [14, 53]. The other data concern model systems: KA denotes Kob-Andersen [231] and Wahn denotes Wahnström binary Lennard-Jones systems [254] while HS denotes Hard Spheres where the control parameter is the volume fraction ϕ, but noted φ in this thesis, *i.e.* the ratio between the volume of the spheres and the total volume enclosing the system. In this case, τ_0 is scaled to enable data collapse at $T_{\rm g}/T = \varphi/\varphi_{\rm g}$. [*Reprinted from* [338]]

The VFT law implies a divergence at a finite temperature T_0 (one of its fitting parameters) and interpolates between strong ($T_0 = 0$) and fragile ($T_0 > 0$) behaviours. Such a divergence at $T_0 > 0$ would signal a complete dynamical arrest, usually associated with a phase transition. For example one could imagine to interpret the viscous slowdown as a critical slowing down associated to some thermodynamic critical point [422]. The existence of such a transition, in a regime unaccessible to experiments or simulations, remains a controversy [319, 201]. As a result, if there is no true phase transition, the term glass *crossover* might be more appropriate: due to thermal activation the system should relax if we are prepared to wait long enough. The expressions (1.4) and (1.5) fit reasonably well experimental data (see [367, 145] for the VFT law) and serve as a guide for experiments and theories. As a matter of fact, some theoretical models, such as Kinetically Constrained Models (see §1.2.7), have indeed found such laws to hold. Nevertheless one should be aware that they are heuristic fits and not be too confident in what they assume and imply.

Let us go back to what happens in the phase diagram of the system. We have just seen that upon cooling further the supercooled liquid, the relaxation time almost diverges. This means that it becomes very difficult to equilibrate the sample, and at some point relaxation becomes so slow that it is effectively

out of equilibrium and follows a history-dependent route in the phase diagram that cannot be predicted by equilibrium static computations. This simplified phase diagram is summarized by figure 1.2.
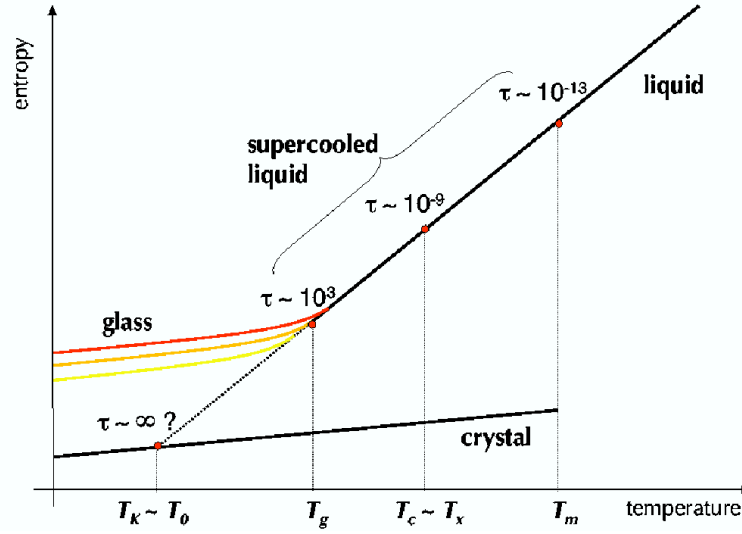
Figure 1.2: Simplified phase diagram (entropy versus temperature) of liquids. For $T < T_\mathrm{m}$ the liquid branch becomes metastable (supercooled liquid). Approaching T_g the relaxation time increases until the system falls off-equilibrium and drives itself into one of the colored glassy branches depending on the history of the system (the protocol used). Note that here the relevant thermodynamic potential is the free energy not the entropy. The liquid being more disordered than the ordered crystal, it seems natural that its entropy is higher. [*Reprinted from* [83]]

1.1.3   Probing the local structure

A surprising feature of this dynamic phenomenon is that there seems to be no apparent structural changes related to it. Structural observables are routinely measured and are well described by liquid theory [199], which studies the statistical mechanics of simple equilibrium liquids (and its application to more complex situations such as multicomponent systems, ionic liquids, molecular degrees of freedom, interfacial phenomena and hydrodynamic regimes) developed starting from the 1950s. One of the simplest observables is the radial distribution function

$$g(\mathbf{r}, \mathbf{r}') = \frac{\rho^{(2)}(\mathbf{r}, \mathbf{r}')}{\rho^2} = \frac{1}{\rho^2} \left\langle \sum_{i \neq j}^{1,N} \delta(\mathbf{r} - \mathbf{x}_i)\delta(\mathbf{r}' - \mathbf{x}_j) \right\rangle = \frac{1}{\rho N} \left\langle \sum_{i \neq j}^{1,N} \delta[\mathbf{r} - \mathbf{r}' - (\mathbf{x}_i - \mathbf{x}_j)] \right\rangle \tag{1.6}$$

where ρ is the particle density of a homogeneous system, $\rho^{(2)}$ is the pair distribution function and the mean is the canonical average. By isotropy it is only a function of the norm $|\mathbf{r} - \mathbf{r}'|$. The definition of $g(r)$ implies that on average the number of particles lying within the range r to $r + \mathrm{d}r$ from a reference particle is $4\pi r^2 \rho g(r)\mathrm{d}r$ and the peaks in $g(r)$ represent *shells* of neighbours around the reference particle. Thermodynamic properties can be expressed in terms of integrals over $g(r)$, which makes it a much needed quantity. Computing the radial distribution function is done with quantitative accuracy within liquid theory by careful resummations of the virial expansion described in §2.1, leading to self-consistent integral equations such as the Hypernetted Chain [337, pp. 185-187] or Percus-Yevick [313] closures. These are however approximate since they somehow neglect three-body correlations, but compare very well with experiments and simulations [199, 6]. Experimentally this quantity is accessed through inelastic neutron scattering measuring the static structure factor [199]

$$S(q) = \frac{1}{N} \left\langle \sum_{i,j}^{1,N} e^{i\mathbf{q}\cdot(\mathbf{x}_i - \mathbf{x}_j)} \right\rangle = 1 + \rho \int \mathrm{d}\mathbf{r}\, e^{i\mathbf{q}\cdot\mathbf{r}} g(r) \tag{1.7}$$

which is related to the Fourier transform of the radial distribution function.

These quantities are good ways to distinguish between gas, liquid and solid phases: for an ideal gas one has $\forall r,\ g(r) = 1$, indicating the gas is totally uncorrelated and has no structure whatsoever, while for

a solid there is a sharp peak at each lattice spacing corresponding to the periodic structure of the crystal. The crystalline peaks in the radial distribution function are Bragg peaks [17] in the structure factor. In the liquid there is no long-ranged order so that the peaks get weaker with distance, see figure 1.3.

However, there is no drastic change in this two-body observable accross the glass crossover.

(a)   (b)
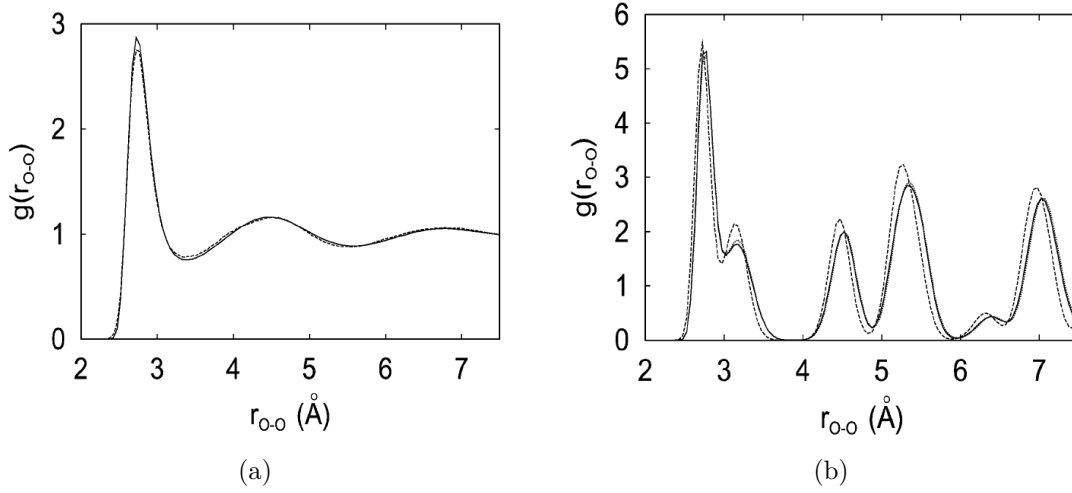
Figure 1.3: Radial Oxygen-Oxygen distribution functions for: (a) Water at 298 K, 1 bar. The solid line is a numerical model while the dashed line is experimental. (b) Ice VII (a cubic crystalline form of ice) at 300 K and 10^5 bar for two numerical models. [*Reprinted from* [398]]

1.1.4   The caging effect: two-step relaxation

The above simple static correlation function seems to tell us local structure is uninteresting, especially compared to the dynamical phenomena described in §3.7.4. Still, a related hallmark of the glass crossover is the two-step relaxation, measured by dynamic correlation functions. If one measures the mean-squared displacement (MSD) of a particle in the liquid, see figure 1.5(b), at high temperatures the usual crossover from ballistic to diffusive regime is observed while close to T_g there appears a plateau, meaning that the particle motion seem to be bounded for a while. Since the height of this plateau gives a distance that is small compared to the interparticle distance [232] (it is about one-fifth of a particle diameter in colloids [401]), this is interpreted as the *caging* phenomenon: at short times particles follow a free dynamics, and for low enough temperatures or high enough densities they are blocked by their neighbours, forming a cage. From time to time, due to collisions activated by temperature, the particle can hop from the cage, usually falling in another cage (see figure 1.4), but on timescales comparable to the relaxation time the network of cages rearranges and make way for the particle to diffuse. This rearrangement necessitates a cooperative behaviour.

Alternatively, one has access in scattering experiments to the *intermediate scattering function*

$$\phi_q(t,t') = \frac{\left\langle \sum_{i,j}^{1,N} e^{i\mathbf{q}\cdot[\mathbf{x}_i(t)-\mathbf{x}_j(t')]} \right\rangle}{NS(q)} \tag{1.8}$$

whose denominator ensures $\phi_q(t,t) = 1$ at equilibrium. It is a density-density correlation function in Fourier space, and is plotted in figure 1.5(a). For high temperatures, it has the typical exponential relaxation of correlation functions:

$$\phi_q(t,t') \sim \exp\left(-\frac{|t-t'|}{\tau_{\mathrm{R}}}\right) \tag{1.9}$$

Yet, close to the glass crossover it also develops a plateau: there is a first exponential relaxation due to fast collective modes of the system (energy-transferring collisions at short times), called β-relaxation, then the plateau regime and a long relaxation (α-relaxation) to decay to zero, so that the system decorrelates at equilibrium. There are thus two relaxational timescales, and the relaxation time is dominated by the α-relaxation (as shown by the logarithmic scale in figure 1.5). The two-step relaxation may be more complex than just an exponential relaxation due to fast motion and then an exponential relaxation with a
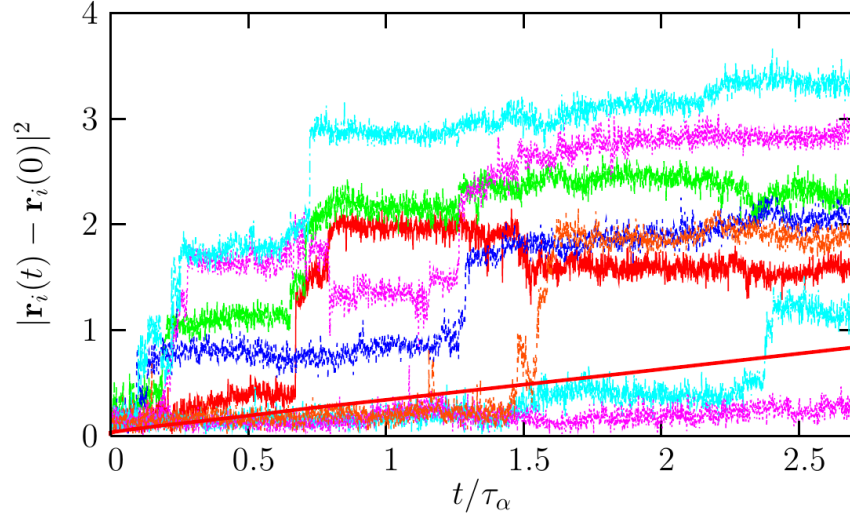
Figure 1.4: Displacement of different tagged particles in a supercooled Lennard-Jones liquid as a function of time rescaled by the relaxation time. Average over all trajectories (solid line) gives a smooth MSD as in figure 1.5(b); at the single-particle level this shows that the dynamics is intermittent with fast jumps and long vibrations inside a cage, and emphasizes the relevance of dynamical fluctuations. [*Reprinted from* [45]]

longer timescale, since the α-relaxation is well-fitted by Kohlraush-Williams-Watts stretched exponential law [235, 403]:

$$\phi_q(t,t') \sim \exp\left[-\left(\frac{|t-t'|}{\tau_R}\right)^{\beta'}\right], \quad \beta' < 1 \tag{1.10}$$
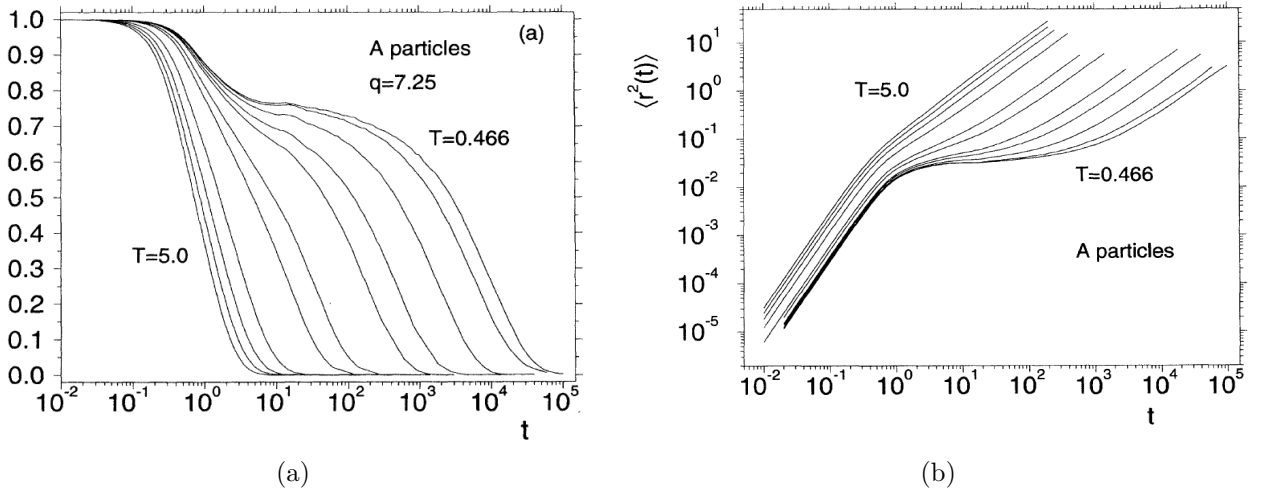
Figure 1.5: Different curves are displayed for various temperatures. (a) Self-intermediate scattering function at a fixed wavevector, involving only one particle, contrary to the coherent scattering function (1.8): $\phi_q^s(t) = \left\langle \sum_i e^{i\mathbf{q}\cdot[\mathbf{x}_i(t)-\mathbf{x}_i(0)]}\right\rangle/N$. It has however a very similar shape. The system considered is a Kob-Andersen binary mixture of Lennard-Jones particles, and only same-species particles are taken into account. The wavevector dependence influences very little the global shape of the function. (b) MSD as a function of time averaged over these particles. [*Reprinted from* [232, 233]]

These dynamic fingerprints seem to have a structural origin in caging, so that local structure is not that uninteresting, and may have more complex static interpretations as we shall see below.

1.1.5   Heterogeneous dynamics

Dynamical fluctuations have already been emphasized about the caging process, where jumps are intermittent (figure 1.4), and have been stressed by yet another phenomenon, showing again the importance of a real-space viewpoint on the structure, *dynamical heterogeneities*: relaxation is spatially heterogeneous, some regions being faster than others that can appear almost immobile. The literature on this subject is extensive: we can mention both experimental [359, 140] and numerical [183] reviews as well as a book [37]. A visual example is in figure 1.6.
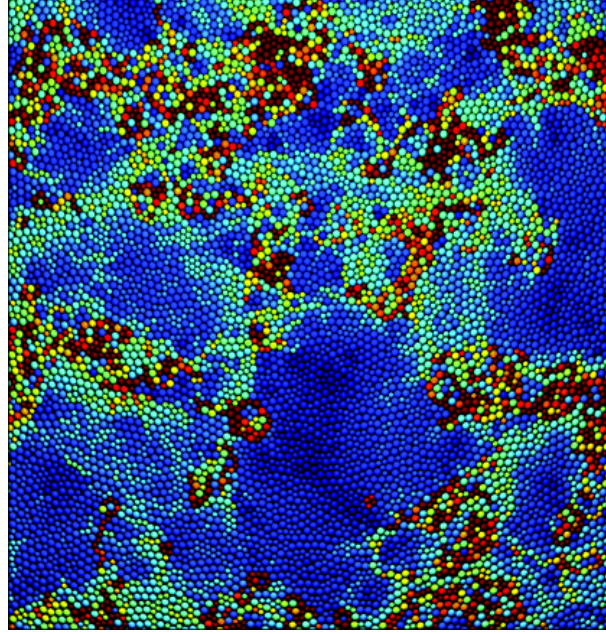
Figure 1.6: Spacetime rendering of the equilibrium dynamics of a two-dimensional supercooled fluid mixture of 10000 particles after a fraction of the structural relaxation time. Particles are colored according to their overlap with their initial positions: a particle that is displaced by more than one particle diameter is dark red; a particle that has no displacement is dark blue; intermediate colors in the visible spectrum coincide with intermediate displacements. The color variation illustrates significant dynamic heterogeneity. Yet the spatial arrangement of particles at a given time seems perfectly homogeneous when coarse grained over only one of two particle diameters. The juxtaposition shows that the dynamics of this system are highly correlated, but the structure is seemingly not. [*Front cover of PNAS, September 8, 2009*]

To characterize important aspects of dynamical heterogeneities, we focus on real space density correlations:

$$\mathcal{C}(\mathbf{x},t) = \delta\rho(\mathbf{x},0)\delta\rho(\mathbf{x},t) \qquad \text{with} \quad \delta\rho(\mathbf{x},t) = \sum_{i=1}^{N} \delta(\mathbf{x}-\mathbf{x}_i(t)) - \rho \qquad (1.11)$$

where $\delta\rho(\mathbf{x},t)$ is a local density fluctuation. As in its reciprocal space version, the intermediate scattering function (1.8), it can be used to assess the relaxation in a certain region of space. If we wish to study the cooperativity of the system, *i.e.* how a region's relaxation is correlated with another's, we must then build a four-point[4] connected correlation function:

$$G_4(\mathbf{x},t;\mathbf{0},0) = \left\langle \mathcal{C}(\mathbf{x},t)\mathcal{C}(\mathbf{0},t) \right\rangle - \left\langle \mathcal{C}(\mathbf{x},t) \right\rangle \left\langle \mathcal{C}(\mathbf{0},t) \right\rangle \qquad (1.12)$$

which encodes dynamical fluctuations in two different points of the system. By summing over the whole volume one gets the dynamical susceptibility, which thus measures the volume of the system that relaxes cooperatively with respect to the origin:

$$\chi_4(t) = \int \mathrm{d}\mathbf{x}\, G_4(\mathbf{x},t;\mathbf{0},0) \qquad (1.13)$$

---

[4]The insight that such four-point correlation functions would give useful characterization of spatio-temporal fluctuations comes from spin glass studies [43].

As time goes by towards relaxation, cooperative regions get wider and G_4 decays more slowly in space, therefore χ_4 must increase. This has been confirmed in experiments [38] and simulations [158, 385], see figure 1.7. This function has a maximum coinciding with the α-relaxation time, which tells us that indeed the structural relaxation necessitates a peak in cooperativity.
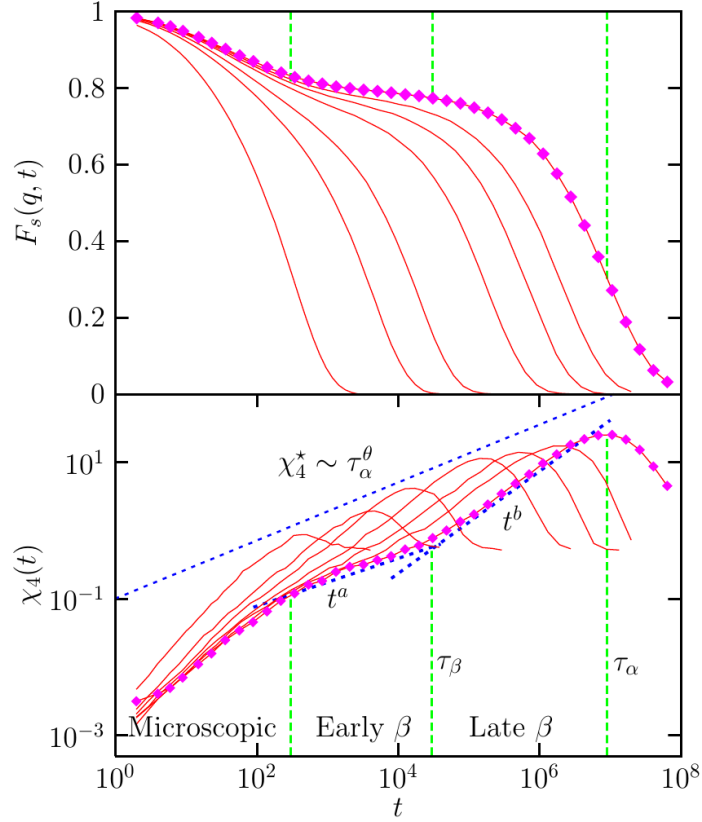
Figure 1.7: Time dependence of the self-intermediate scattering function $\phi^s \equiv F_s$ as in figure 1.5(a) (top), and the superimposed dynamical susceptibility (bottom), for different temperatures decreasing from left to right in a Lennard-Jones supercooled liquid in Monte Carlo simulations. The lowest temperature is highlighted with symbols. χ_4 has a maximum χ_4^* near the α-relaxation time τ_α, shifts to larger times and has a larger value when cooling the system as an approximate power law $\chi_4^* \sim \tau_\alpha^\theta$. Several distinct relaxation regimes can be inferred from the plot of the dynamic susceptibility. [*Reprinted from* [45]]

The growth of the maximum in the dynamical susceptibility, lowering T, indicates a growth of some lengthscale in the dynamical correlations. Since there is a growing timescale (the relaxation time) in the system, a growing lengthscale [38] has been sought after, by analogy with the theory of critical phase transitions. However, the extraction of such a lengthscale from four-point correlation functions is difficult and subject to ambiguities [45].

Another lengthscale, the *point-to-set* length, was introduced in [69, 280]. The basic idea is to measure how much boundary conditions affect the behaviour of the system, far away from the boundaries themselves. Boundary conditions in the case of a ferromagnet are easy to devise (all up spins or all down spins); in the case of glasses, it is not clear what an amorphous equilibrium boundary solution should be. The way out is to let the system itself choose the boundary conditions: let the system equilibrate, then freeze all particles outside a cavity of a given size ξ, and then study the subsystem inside the cavity which is thus subjected to a typical equilibrium boundary condition. Focusing on the overlap between the reference configuration (before freezing the particles) and the newly thermalized subsystem at the center, *i.e.* measuring how these configurations are similar (corresponding to the same metastable state, in the thermodynamic picture developed in the next sections), defines a static point-to-set correlation function, which, contrary to simpler static correlation functions previously defined, has a non-trivial behaviour close to the glass transition. The correlation length, which is the typical distance ξ_{PS} above which the overlap drops to zero, is a lengthscale whose increase is a clear signal that the system is developing long-ranged static order, and in the case of glasses, amorphous long-ranged order. It was proved rigorously that it

must increase if the relaxation time does so [289] and has been shown to grow in numerical simulations of supercooled liquids [59]. Therefore, an important open question is whether this point-to-set lengthscale ξ_{PS} is just a consequence of hidden static correlations or if it is instead quite unrelated to them. We refer to the above-mentioned reviews [359, 140, 183, 37] for more details, since this will not be a subject investigated in this thesis.

1.1.6 Stokes-Einstein relation

Heterogeneous dynamics is believed to be at the basis of the violation of Stokes-Einstein relation (SER) [83, 43] between translational diffusion coefficient D, which is given by the long-time asymptote of the MSD, and (shear) viscosity in supercooled liquids:

$$D\eta = \frac{T}{\zeta} \tag{1.14}$$

where ζ is a constant (Stokes drag). This result has been first derived by Einstein in one of his famous 1905 papers [144], considering a Brownian particle immersed in a fluid acting as an equilibrium bath at temperature T. The Brownian description assumes a phenomenological friction coefficient that can be derived, in principle, from microscopic modelling of the bath [424, 197]. To ensure consistency with the Stokes law (1845) of friction in a fluid [370, 1, 246, 199], computed from the Navier-Stokes equations at low Reynolds number, considering the motion of a sphere in a viscous flow, the drag must be[5] $\zeta = 3\pi\sigma$ with σ the diameter of the tracer. Although this relation strictly holds only for a diffusing sphere much larger than the molecules comprising the fluid, it is in fact surprisingly accurate in describing the self-diffusion coefficient of a molecule surrounded by other molecules of equal size in high-temperature liquids, see figure 1.8. Yet, it appears to fail in some situations, typically when the diffusion coefficient remains finite while the viscosity is either zero (as in superfluid helium), or infinite (as in elastic crystals). This failure happens as well in supercooled liquids close to the glass transition, where the diffusion coefficient decreases less steeply than T/η when decreasing temperature, resulting in a disparity of several orders of magnitude. This has been checked experimentally in *e.g.* [336, 166, 89, 100, 268, 411].
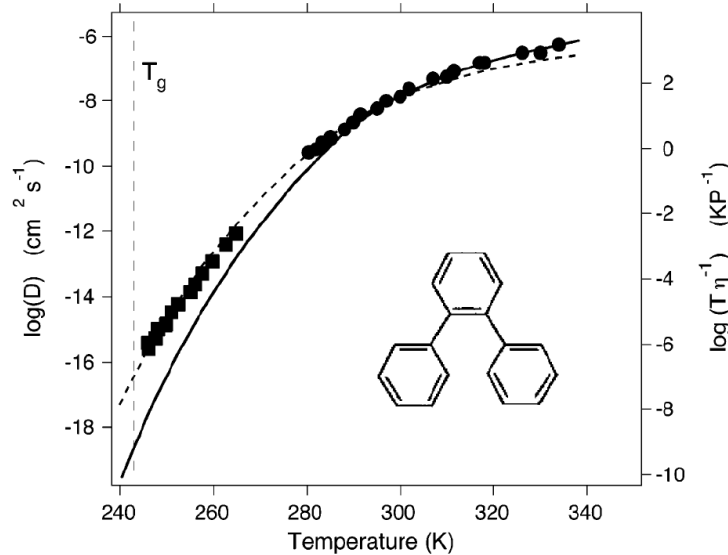
Figure 1.8: Decoupling between viscosity and self-diffusion coefficient in supercooled orthoterphenyl. The dashed line shows a fit with a *fractional* SER, $D \sim (T/\eta)^{\#}$ with $\# \simeq 0.82$ instead of the value $\# = 1$ which holds at high temperatures, as in the usual SER (1.14). Such fractional scalings have also been reported in *e.g.* [411]. [*Reprinted from* [268]]

The SER *breakdown*[6] is a significant indication that different ways to measure relaxation times, via

---

[5]$\zeta = 3\pi\sigma$ comes from no-slip boundary conditions on the sphere due to viscosity, while other expressions can be given, *e.g.* $\zeta = 2\pi\sigma$ for the slip approximation of the velocity field [1, 199].

[6]As emphasized earlier, the SER was not meant to apply to a broad range of situations, although it has found wider applicability than the original case of a large tracer in a bath. It is therefore quite natural that it may not hold in a *strongly-interacting* regime (think of the cage effect).

Maxwell's relation (1.1) or via the MSD, lead to different answers and therefore is a strong hint of the existence of a broad distribution of relaxation timescales. A simple and intuitive explanation of this effect has been given by Cicerone and Ediger in [100]. The diffusion coefficient is dominated by the fastest regions, contributions from the slow domains are negligible compared to the fast ones. If $\tau_{\rm f}$ is a relaxation timescale, then this coefficient will scale roughly as $D \sim \tau_{\rm f}$ (the prefactor being something like the squared linear size of the box enclosing the system times the ratio between fast and slow regions' volumes). On the contrary, the relaxation time is dominated by the slowest regions (whose relaxation time is $\tau_{\rm s}$), so that the viscosity will scale as $\eta \propto \tau_{\rm s}$ from Maxwell's relation (1.1). Since $\tau_{\rm f} \ll \tau_{\rm s}$, we may expect that the diffusion will be much larger than $T/\eta\zeta$. This argument is oversimplified and assumes a comparable proportion of fast and slow regions with well-separated timescales, but still gives a useful viewpoint on what may be going on.

A connection with the non-exponential decay of dynamic correlation functions, the Kohlraush-Williams-Watts law, has been unveiled in [100]: the stretched exponent β' in (1.10) is smaller the larger the measured deviation from SER. This suggests a pivotal role of spatial heterogeneities in the unconventional features of glassy dynamics.

The SER violation has been investigated in several (quite conceptually different) theoretical frameworks [382, 368, 214, 57]. It will be derived for high-dimensional liquids in §3.8.5.

1.1.7 Aging

Conventionnally below the experimental glass transition, the liquid seems frozen but actually has not attained a steady state: its dynamics proceeds in a non-equilibrated way, trying very slowly to reach an equilibrium that experiments usually cannot probe owing to the large α-relaxation time. Nevertheless this dynamics can be studied and displays a variety of interesting effects. Out-of-equilibrium regimes are also of primary importance in physics since there are, unlike equilibrium statistical mechanics, very few generic results valid arbitrarily far from equilibrium, and this field is relevant to almost all phenomena we experience daily, which are intrinsically off-equilibrium. One has to rely on the protocol-dependent dynamics of the system. These protocols, in the case of glasses, can be a simple rapid *quench* down to some glassy regime. A more complicated protocol is an *annealing*: for example one waits to equilibrate the sample in some glassy (low-temperature) regime and then perturb it by a quench to a desired temperature.

Out-of-equilibrium glasses display aging: time-translational invariance (TTI) does not hold and the evolution of the system depends upon its full previous history, notably through the *waiting time* $t_{\rm w}$, the time it has spent since preparation (for example after quenching), also called its *age*, and the observation time t which labels the time spent during the experiment. If we measure during a time t an autocorrelation function C of some observable (t is then the time spent between the first measurement and the current one), it will thus depend upon both times $C(t, t_{\rm w})$, unlike the situation at equilibrium where the age of the system is forgotten. This dependence upon $t_{\rm w}$ is the aging phenomenon, see figure 1.9. Plenty of alternate protocols, displaying intriguing memory or rejuvenation effects, have been realized experimentally (see [40] for a review).

Experimentally, one observes a decomposition of correlations (or responses) in an equilibrium part verifying TTI, and an aging part displaying *time-aging time superposition*, *i.e.* depending upon the ratio of the two timescales:

$$C(t, t_{\rm w}) \simeq C_{\rm eq}(t - t_{\rm w}) + \mathcal{C}(t/t_{\rm w}) \tag{1.15}$$

This superposition is analogous to the *time-temperature superposition* found in equilibrium data, which in the α-relaxation process seem to scale according to the ratio $t/\tau_\alpha(T)$. The fast equilibrium part relaxing quickly, the relaxation time of the system is thus directly proportional to the age due to the time-aging time superposition, *i.e.* $\tau_\alpha \propto t_{\rm w}$, although some polymeric liquids are better fitted with a sublinear law with an aging exponent [371].

Pedagogical reviews of this behaviour can be found in [61, 112, 43]. We will describe a brief outcome of the out-of-equilibrium dynamics of mean-field models in §1.2.5.
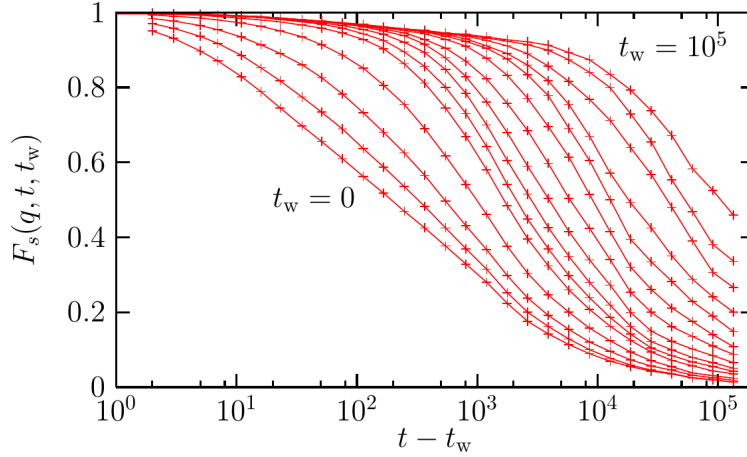
Figure 1.9: The self-intermediate scattering function in a Monte Carlo study of a Lennard-Jones glass-forming liquid at low temperature. The system is quenched at time $t_w = 0$ to a low temperature. Measures are performed for increasing waiting times from left to right. The relaxation becomes slower as t_w increases, a typical aging effect. At small waiting times $t - t_w$ is a relevant timescale while at large waiting time one has to probe longer times to observe a non-trivial dependence, illustrating the time-aging time superposition. [*Reprinted from* [43]]

1.2 A mean-field theoretical viewpoint: the Random First-Order Transition scenario

Here we present a theoretical scenario for the glass transition, the Random First-Order Transition (RFOT) scenario, which is strongly rooted in mean-field concepts. This thesis is a part of a research attempt to get an exact theory of liquids and structural glasses in the limit of large spatial dimension, which, as a very important corollary, gives a mean-field description of what is going on in the thermodynamics and dynamics of the system. As such it is relevant to compare it to the basic assumptions of RFOT, since it is predicted by its founders to hold exactly for high dimensions [225].

RFOT has emerged from the early insights of Adam-Gibbs-Di Marzio's theory (AGDM) [154, 180, 181, 2] and Goldstein's energy landscape interpretation [185], the dynamical input from the liquid community with Mode-Coupling Theory [252, 33, 187] and some arguments from liquid theory (*e.g.* Density Functional Theory) [199], spin glass theory [279] and the mosaic scaling picture [224, 69]. It was formulated as a sort of *patchwork* [43] relating these ideas in a series of papers by Kirkpatrick, Thirumalai and Wolynes in the late 1980s [220, 225, 226, 221, 222, 223, 224].

1.2.1 Dynamics within Mode-Coupling Theory

First let us introduce a dynamic theory of the onset of the slowdown in the supercooled liquid phase, the Mode-Coupling Theory (MCT), a first-principle approach to get closed dynamical equations on correlation functions that has been successful in reproducing some of the above-mentioned aspects, which also compares well to experiments in the supercooled regime and serves as a dynamic justification for the whole RFOT approach. Work on this topic, in order to apply MCT to different systems or regimes, or to find better extensions, has been impressive since the first results in the mid-1980s. Furthermore, once one makes the central (although somewhat crude and unjustified) approximation, the whole theory has enjoyed a rigorous treatment, followed by crucial numerical [232, 233, 295, 352, 234] and experimental tests [188, 116].

We quickly review here its outcomes, relevant for this thesis. We will not go into all details of the derivation since there are great reviews on this point, using the projection operator formalism [229, 199, Chap.9], or comparing it with diagrammatic techniques [326] first established in [71, 72]. MCT is fully detailed in Götze's book [187] while the essence of it is reviewed in [186].

1.2.1.1 The MCT equation

MCT starts by projecting the Hamiltonian dynamics using the Mori-Zwanzig formalism [423, 292, 291] onto slow degrees of freedom of the system equilibrated at time $t = 0$. This is done by writing, for a relevant quantity we wish to study, its classical evolution with the Liouville operator [244] and performing a partial average over the slow degrees of freedom of the equilibrium initial conditions. The remaining fast modes' contributions result in a fluctuating force. Integrating out the fast modes leads to a memory kernel in the dynamical equation ruling the slow (projected) part of the quantity under study, which is related to the autocorrelation of the fluctuating force. These slow modes may be the density in reciprocal space $\rho_q(t) = \sum_i e^{i\mathbf{q}\cdot\mathbf{x}_i(t)}$ and density currents, proportional to its time derivative. They are indeed slowly varying at small q (large lengthscales).

Another way is a diagrammatic approach [71, 72]. One starts from the microscopic dynamics of the system containing some disorder (such as a Brownian noise), *e.g.* for the particle density, Dean's equation for Brownian dynamics [127] or the nonlinear fluctuating hydrodynamics of Das, Mazenko, Ramaswamy and Toner [120] for Newtonian dynamics. Then an expansion in the potential strength is performed, giving rise to a dynamical equation for the correlation and response of the considered field similar to the Schwinger-Dyson equation of quantum field theory [315, 422, 112] with a self-energy representing a memory kernel.

With this one gets exact equilibrium equations (TTI holds, see §2.5.3) for the coherent intermediate scattering function (1.8):

$$\ddot{\phi}_q(t) + \Omega_q^2\phi_q(t) + \int_0^t \mathrm{d}t'\, \mathcal{M}_q(t - t')\dot{\phi}_q(t') = 0 \tag{1.16}$$

with $\Omega_q = q/\sqrt{\beta m S(q)}$. $\mathcal{M}$ is a memory kernel which encodes all the dynamics, and can be seen as the autocorrelation of some fluctuating force of the system in the Mori-Zwanzig viewpoint, or as the resummation of a certain class of diagrams in the diagrammatic approach.

Owing to the glassy phenomenology where a separation between fast transient liquid-like relaxation and slow rearrangement emerges, the memory kernel is splitted into two contributions, respectively:

$$\mathcal{M}_q(t) = M_q^{\mathrm{reg}}(t) + \Omega_q^2 M_q(t) \tag{1.17}$$

The regular part linked to fast modes is usually neglected close to the glass transition. For now this is just a sort of *change of variables* from describing the dynamics by $\phi_q(t)$ to $M_q(t)$. Using a factorization ansatz for the kernel yields the Mode-Coupling approximation:

$$\begin{aligned} M_q(t) &= \mathcal{F}_q(\{\phi_k(t)\}) \\ \mathcal{F}_q(\{f_k\}) &= \sum_{\mathbf{k}+\mathbf{p}=\mathbf{q}} \widetilde{V}(\mathbf{q},\mathbf{k},\mathbf{p}) f_k f_p \\ \widetilde{V}(\mathbf{q},\mathbf{k},\mathbf{p}) &= \rho S(q)S(k)S(p)\frac{\{\mathbf{p}\cdot[\mathbf{k}c(k) + \mathbf{p}c(p)]\}^2}{2q^4} \end{aligned} \tag{1.18}$$

where $c(k)$ is a direct correlation function related to the structure factor by the Ornstein-Zernicke equation [199] similar to (1.7): $S(k) = 1/[1 - \rho c(k)]$.

At this stage one already sees that the whole dynamics is determined by the sole input of the structure factor, a static quantity. Besides, the memory kernel is local in time since it is a second order polynomial of ϕ_k for several wavevectors at the same time.

1.2.1.2 The dynamical transition

Then MCT proceeds with mathematical implications of the above equations (1.16),(1.17),(1.18). The long-time limit $f_q = \lim_{t\to\infty} \phi_q(t) \in [0, 1]$, called Debye-Waller factor or non-ergodic parameter in the liquid literature [199, 187], or Edwards-Anderson parameter in the spin glass literature [141, 142], changes discontinuously from 0 to $f_q^c > 0$, the critical form factor, at the dynamical transition temperature T_d (or density if one follows a isothermal protocol). Indeed, at long times, equation (1.16) gives (see *e.g.* §2.5.5)

$$\frac{f_q}{1 - f_q} = \mathcal{F}_q(\{f_k\}) \tag{1.19}$$

where a saddle-node bifurcation of solutions occurs at T_d, which does not depend upon any wavevector. Charaterizing the distance to the singularity by $\epsilon = (T_d - T)/T_d$ or $\epsilon = (\rho - \rho_d)/\rho_d$, one has the usual square-root approach to the bifurcation

$$f_q = f_q^c + h_q \sqrt{\frac{C\epsilon}{1-\lambda}} + O(\epsilon) \tag{1.20}$$

where C is a constant and $\lambda \in \left[\frac{1}{2}, 1\right]$ is the so-called MCT parameter. This bifurcation means that at T_d the plateau becomes infinite, resulting in a breaking of ergodicity. In the pictorial view of the cage, the particles do not escape anymore and the structure does not relax, *even at long times*. This can be interpreted as a spurious effect of the Mode-Coupling approximation since in reality the real system must relax and avoid the ergodicity breaking, whatever time it takes, *e.g.* by an activation mechanism as emphasized earlier. The MCT transition may be seen as an idealized version of the glassy crossover. Indeed, as an example, it can be rigorously proven [300] that the self-diffusion coefficient cannot go continuously to zero at thermal equilibrium and finite temperature and pressure.

Above the dynamical temperature, the intermediate scattering function develops a plateau (or becomes exponentially damped at higher temperatures), observed in simulations and experiments, as in figure 1.5(a). This points out that MCT may contain some of the right ingredients to describe the glass crossover, in spite of a spurious sharp transition.

1.2.1.3   MCT scaling laws

From studying the previous MCT equations, a number of scaling laws in several well-identified relaxation regime are recovered [186, 187]. They are valid close to the dynamical transition (small $\epsilon > 0$), where the plateau is well formed and the α-relaxation still occurs at long times.

We denote by t_0 a transient time scale. Upon approaching the plateau close to the dynamic transition, *i.e.* in the β-relaxation window, a scaling law holds with $\hat{t} = t/t_0$:

$$\phi_q(\hat{t}t_0) = f_q^c + h_q \hat{t}^{-a} + O(\hat{t}^{-2a}) \tag{1.21}$$

This is valid for times $t_0 \ll t \ll \tau_\beta$ with $\tau_\beta = t_0/(C|\epsilon|)^{1/2a}$. The latter timescale represents the β-relaxation timescale, which diverges at the transition.

Similarly, upon leaving the plateau (for small negative ϵ), the so-called von Schweidler's scaling law is obtained for $t > \tau_\beta$ with $\tilde{t} = t/\tau_\alpha$:

$$\phi_q(\tilde{t}\tau_\alpha) = f_q^c - h_q \tilde{t}^b + O(\tilde{t}^{2b}) \tag{1.22}$$

where τ_α can be defined by $\phi_q(\tau_\alpha) = f_q^c/2$ up to an ϵ-independent factor. We shall call it in the same way as the α-relaxation time since it can be viewed as a practical definition of it. The scaling with τ_α is reminiscent of the time-temperature superposition of §1.1.7.

One can prove that both MCT exponents $a \in \left]0, \frac{1}{2}\right]$, $b \in]0, 1]$ are given by the MCT parameter and thus related by:

$$\lambda = \frac{\Gamma(1-a)^2}{\Gamma(1-2a)} = \frac{\Gamma(1+b)^2}{\Gamma(1+2b)} \tag{1.23}$$

Finally for larger times $\tau_q = (f_q/h_q)^{1/b}\tau_\alpha$, Fuchs [165] has shown that during the α-relaxation process one retrieves Kohlraush-Williams-Watts' stretched exponential law [235, 403] for large wavevectors, as in (1.10) with the exponent $\beta' = b$:

$$\lim_{q\to\infty} \phi_q(t^*\tau_q) = f_q^c \exp\left(-t^{*b}\right) \tag{1.24}$$

For a generic wavevector, one can try such an ansatz but then the exponent depends upon the wavevector. It has been put forward to explain why spectra generically do not follow Kohlraush-Williams-Watts' law precisely.

For a generic observable A coupled to density fluctuations, the same laws hold for its correlation replacing f_q and h_q by similar quantities f_A and h_A [186, 187]. λ (hence the exponents), t_0 and τ_α remain the same. As a result, (1.21) and von Schweidler's law (1.22) emphasize a remarkable property of MCT (from which they are actually derived), the so-called *factorization property*, which states that close to the plateau (in the β-relaxation window), the fluctuations of correlations from the plateau value

(*e.g.* $\phi_q(t) - f_q^{\mathrm{c}}$) factorize into a wavevector-dependent (or space, by inverting the Fourier transform) function only (*e.g.* h_q) times a time-dependent function only. This is a stringent test of MCT in simulations [232, 233].

The diffusion coefficient can be computed from the MCT approach. Note that, as an example, the MSD $\mathsf{D}(t, t') = \left\langle [x(t) - x(t')]^2 \right\rangle$ is provided by the incoherent or self-intermediate scattering function for which a similar MCT equation can be obtained. One gets, due to isotropy,

$$\phi_q^{\mathrm{s}}(t, t') = \frac{1}{N} \left\langle \sum_{i=1}^{N} e^{i\mathbf{q}\cdot[\mathbf{x}_i(t) - \mathbf{x}_i(t')]} \right\rangle \underset{q\to 0}{=} 1 - \frac{q^2}{2d} \mathsf{D}(t, t') + O(q^4) \tag{1.25}$$

The second timescale τ_α verifies

$$\tau_\alpha \propto \frac{t_0}{(C\epsilon)^\gamma} \sim \epsilon^{-\gamma}, \qquad \gamma = \frac{1}{2a} + \frac{1}{2b} \tag{1.26}$$

From (1.16) and (1.25), when the plateau diverges one has

$$\mathsf{D}(t) = 2dDt \quad \text{with} \quad D \propto \tau_\alpha^{-1} \sim \epsilon^\gamma \tag{1.27}$$

The relaxation time diverges and the diffusion vanishes as a power law at the transition, whose exponent is determined by the MCT parameter λ.

1.2.1.4   MCT and the *p*-spin model

Standard MCT, as briefly described above, gives predictions about the dynamics of a liquid if we input the static structure factor $S(q)$. Since these equations are quite cumbersome in the general case, simplified models have been first studied, which reproduces all behaviours shown above. This is the *schematic* MCT, and the first such equation studied by Leutheusser [252] and Bengtzelius-Götze-Sjölander [33] consisted in keeping only the dominant first peak q_0 of the structure factor, thus getting rid of all wavevector dependence, the memory kernel becoming a simple quadratic function of $\phi(t) = \phi_{q_0}(t)$. The schematic MCT equation can be written as

$$\ddot{\phi}(t) + \nu\dot{\phi}(t) + \Omega^2\phi(t) + \Psi \int_0^t \mathrm{d}t' \, \phi^2(t - t')\dot{\phi}(t') = 0 \tag{1.28}$$

This is the same equation, dropping the inertial term irrelevant for large-time dynamics, as the one ruling the exact dynamics of the *p*-spin spherical model [107, 81, 417] for $p = 3$, a spherical model of spin glasses first introduced for Ising spins by Derrida [129, 130, 192, 109] analyzed in chapter 2, see (2.164). Spin-glass theory was developed starting from the 1970s, initially to describe the strange behaviour of disordered magnetic alloys [56]. This compelling parallelism was noticed by Kirkpatrick and Thirumalai [220], and is one of the reasons that make this mean-field spin glass model a paradigm for the structural glass transition. This also hints at MCT being some kind of mean-field theory for the dynamics of supercooled liquids, as was argued by Andreanov, Biroli and Bouchaud [11]. The fact that T_{d} is in experiments greater than T_{g} may be seen as another (slight) evidence, since mean-field effects are known to increase free energy barriers (see next sections concerning this interpretation). In experiments, adjustments of T_{d} and λ must then be made, which is tricky especially when dealing with the difficulty of obtaining accurate measurements at very long times. Some experiments have claimed that the MCT prediction for the relaxation time was not fullfilled close to the crossover in colloidal HS [74, 272]. The power-law prediction is indeed very different from VFT-like fits shown in §3.7.4. Another serious concern is the work of Berthier and Tarjus [50, 51, 52], where they used a model of glass former where the attractive part of the interaction between particles can be switched on and off in such a way that the static structure factor is left unchanged, and is determined accurately numerically. The resulting dynamics is seen to change radically between the two systems (the one with attraction being much slower than the one without), even in the weakly supercooled regime, undermining the MCT basic tenet that static pair correlations determine the dynamics. Currently lots of works are aimed at understanding the MCT foundations and improving it [73], see the short review in §1.3.

1.2.2   Thouless-Anderson-Palmer free energy

To develop a static mean-field interpretation, let us analyze first the case of the mean-field Ising model in zero external field. In its Curie-Weiss or Bragg-Williams treatment, one gets the free energy as a function of the order parameter, as in Landau theory of phase transitions [247, 248], the *global* magnetization m. For $T < T_c$ the up-down (Z_2) symmetry is spontaneously broken and the system becomes non-ergodic: there are two minima with either positive or negative magnetization $\pm m^*(T)$, and since the barrier between the two *basins* of the free energy diverges with the system size, the system in the thermodynamic limit is trapped in one of these two *pure states* [279, 308, 81, 339]. These pure states are disjoint sets of configurations having either positive or negative global magnetization m. They can be selected by imposing a vanishing external field with either sign on the system, which plays a similar role in choosing the state of the system to boundary conditions in physical systems. Both pure states are related by the Z_2 symmetry. The partition function can be decomposed into a sum of partition functions restricted to either pure state. When the system falls in one of the basins, then only the corresponding restricted partition function is relevant to compute its thermodynamic properties: it will explore ergodically all configurations inside this state as time goes by, but will never encounter one of the configurations of the other pure state.

For disordered magnetic systems, a similar procedure has been followed by Thouless, Anderson and Palmer (TAP) in 1977 [384]: they considered a mean-field (fully connected) disordered model of a magnet, the Sherrington-Kirkpatrick (SK) model [358], where the coupling between pairs of spins is a random variable, giving rise to amorphous configurations of spins at low temperature (a spin glass). They computed its free energy as a function of *local* magnetizations m_i. Minimizing the free energy with respect to the local magnetization gives the TAP states, which are an operational definition of pure states in the disordered case. Each TAP state is identified by its set of local magnetizations $\{m_i\}$ and gathers all spin configurations that have these magnetizations. The free energy landscape is obtained by scanning the values of the free energy over all possible sets of local magnetizations. As usual in mean-field, the free energy barrier between these states are infinite and the system can be trapped metastable states (local but not absolute minima of the free energy landscape) as well as it may in equilibrium (lowest-lying) states.

In the case of liquids and glasses, in principle this procedure may be repeated. One can think of it as a coarse-graining [85] of the system, or by using a lattice gas model [43]. Consider a thermodynamic potential of a lattice gas defined by occupation number[7] $n_i \geqslant 0$ on site i (number of particles whose center falls into the volume occupied by site i), Hamiltonian H and local chemical potentials μ_i (on each site i, acting as external fields):

$$\Omega(\{\mu_i\}) = -\frac{1}{\beta} \ln \sum_{\{n_i\}} \exp\left(-\beta H(\{n_i\}) + \beta \sum_i \mu_i n_i\right) \tag{1.29}$$

One has

$$\frac{\partial \Omega}{\partial \mu_i} = -\langle n_i \rangle \equiv -\rho_i \tag{1.30}$$

where the average is generated by the partition function $e^{-\beta\Omega}$.

We may put ourselves in a situation where one fixes the average particle number of site i rather than imposing local chemical potentials. We may achieve this by performing the Legendre transform $\mu_i \leftrightarrow \rho_i$:

$$\begin{cases} F(\{\rho_i\}) = \Omega(\{\mu_i^*\}) + \sum_i \mu_i^* \rho_i \\ \mu_i^*(\{\rho_j\}) \text{ defined by } \quad \left.\frac{\partial \Omega}{\partial \mu_i}\right|_{\mu_i = \mu_i^*} = -\rho_i \end{cases} \tag{1.31}$$

From these definitions, using the sum rule, one has

$$\frac{\partial F}{\partial \rho_i} = \mu_i^* \tag{1.32}$$

---

[7]Note that for the hard core case $n_i \in \{0,1\}$ with homogeneous chemical potential there is a mapping to the Ising ferromagnet [412, 249], which can be obtained by a coarse-graining process.

so that when no external field is present the profiles $\{\rho_i\}$ are determined as stationary points of the free energy, as for the TAP computation. In the next sections, we will generalize this thanks to liquid theory to a continuum [199], expressing the free energy as a *functional* of the local particle density $\rho(x)$. Defining the fluctuation $\delta\rho(x) = \rho(x) - \rho$ where $\rho = N/\mathcal{V}$ is the global particle density of the liquid, we see that the situation is comparable to the TAP case. In the homogeneous liquid phase, $\delta\rho = 0$ which is analogous to the high temperature paramagnet. At low T, the amorphous glassy phases can be described by a space-dependent $\delta\rho(x)$ as for a spin glass phase. Crystalline states would not be homogeneous but would have a periodic $\delta\rho(x)$, similarly to the anti-ferromagnet [323], even if the analogy does not go much further: the mean-field paramagnetic/antiferromagnetic transition is very different from the freezing transition.

1.2.3 Goldstein's energy landscape picture

An interpretation of the dynamical facts presented above in terms of static (free) energy landscape has been formulated in a very influential paper by Goldstein in 1969 [185]. The argument is reviewed in detail in [83, Sec. V.]. He imagined what the trajectory of the system would be in the potential energy landscape, its position given by the coordinates of all particles and the value of the whole potential energy at this phase space point. This multi-dimensional landscape can be seen as a very rugged one, like hills separated by narrow valleys [112, 323], see figure 1.10. Local minima of the potential energy landscape are called *inherent structures* in the literature [369, 83]. They enjoy the property of being mathematically well defined, but are not necessarily thermodynamically relevant. Therefore, it is more correct to talk about the *free* energy landscape in this way, whose shape changes according to temperature and density, and denote the basins as pure TAP states rather than inherent structures; the main drawback of the former compared to the latter is that pure (metastable) states are not well defined in non-mean field models, though attempts building on the *effective* separation of timescales have been suggested by *e.g.* Biroli and Kurchan [63], based on the works of Gaveau and Schulman [175, 176, 177, 174], defining metastable states as eigenvectors of the *ground states* of a Fokker-Planck operator of the system.

In some fully connected models such as SK or the p-spin TAP states and inherent structures are equivalent [108] as well as for other analytical approaches of liquids in the RFOT spirit [284, 283, 103], which adds to the confusion [60].

The deepest minima, which are very few compared to the total number of local minima, represent crystalline configurations. They are very narrow and thus hard to find but separated by very high energy barriers to the rest of the valleys so that nucleation of liquid-like configuration is heavily suppressed for $T < T_{\mathrm{m}}$. At low T, such that energy barriers are greater than T, the system is stuck in some local minimum and the passage from a valley to another can be done only through an activated event [198]. These events represent *local* rearrangement of the structure, like hopping from a cage. The time spent in a basin, visiting configurations within this basin may give an interpretation of the β-relaxation process while the activated jumps allow for broader relaxations allowing *in fine* to visit the whole phase space, recovering ergodicity, as in the α-process. When the temperature is very high, there is no need to cross barriers since the activated energy scale T is greater: the relaxation proceeds by following simple paths from a point to another, climbing valleys and descending saddles which have unstable directions. The nature of the relaxation is very different. These two mechanisms separate two temperature regions, and one may think that this occurs at some definite temperature T_{x}. By analogy with MCT one may identify the two temperatures

$$T_{\mathrm{x}} \simeq T_{\mathrm{d}} \tag{1.33}$$

giving a connection between statics and dynamics. Simulations [349] and experiments [364] have shown it to be consistent.

The topology of the potential energy landscape of mean-field spin glass models, such as the p-spin, has been explored since they are amenable to an analytic treatment [81, 82, 237]. It was shown that for $E < E_{\mathrm{th}}$ that the extrema of the Hamiltonian are dominated by minima, which means that the eigenvalues of the Hessian at these points are strictly positive, while at $E = E_{\mathrm{th}}$ marginal directions (with zero eigenvalues) appear, and for $E < E_{\mathrm{th}}$ the extrema are dominated by saddles having a nonzero fraction of the eigenvalues negative [84]. Besides, the energy $E(T)$ of the typical minima trapping the system for $T < T_{\mathrm{d}}$ can be computed and grows with temperature, meaning that the system is trapped by higher energy minima the higher the temperature. In addition, one finds

$$E(T_{\mathrm{d}}) = E_{\mathrm{th}} \tag{1.34}$$
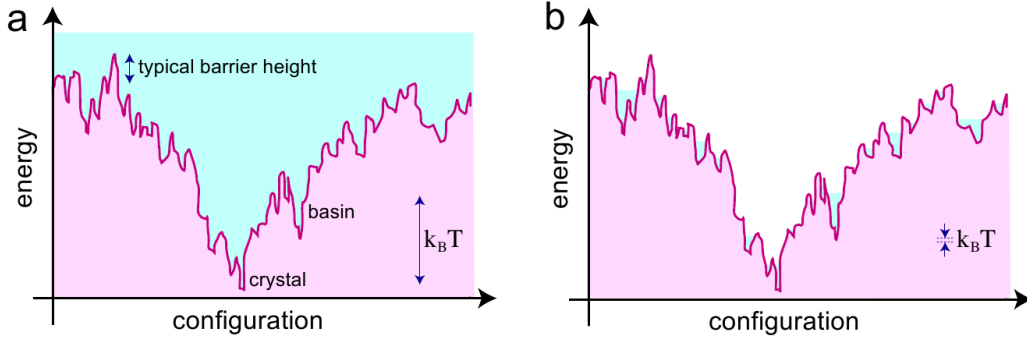
Figure 1.10: A schematic illustration of the potential energy landscape. The longitudinal axis represents configurations of all *dN* coordinates. (a) High temperature liquid, the typical barrier height is less than the thermal energy, and all configurations can be accessed as indicated in blue. (b) Low temperature glass. The barrier height between basins is now much higher than T. [*Reprinted from* [338]]

confirming the guess (1.33). The *p*-spin model realizes exactly Goldstein's scenario. Pure states appearing at this crossover from saddles to minima are called *threshold states*. The fact that for $T > T_d$ the plateau is already well formed *before* the dynamical transition can be interpreted in light of these results: the system first relaxes exponentially along the many stable directions that constitutes the vast majority of the spectrum of the Hessian of a typical extremum of the potential energy landscape, resulting in the β-relaxation and the emergence of the plateau. Later, the system finds its way through the few almost marginal unstable directions, and leaves the saddle. This triggers the α-relaxation which is here of a non-activated nature. Nevertheless, for $T < T_d$, since only minima with stable directions are present, the α-relaxation must proceed through an activated event, while the β-relaxation is a similar process of visiting stable directions. The *p*-spin is rather peculiar and one may question the applicability of the concepts derived from it to real glass former where analytical computations are much harder, but numerical studies seem to confirm this picture (see *e.g.* [13, 77, 191]).

1.2.4 Low temperature thermodynamics of glasses

1.2.4.1 Configurational entropy and Kauzmann's paradox

The above static interpretation of the two-step relaxation process has been turned into an operative scheme to analyze the thermodynamics of the system. The picture of a temporary relaxation inside *metastable* states followed by cooperative rearrangements leading to an ergodic sampling of the phase space is translated at the level of the entropy of the system. The β-relaxation process leads to a *restricted equilibrium* defined by the time window $\tau_\beta \ll t \ll \tau_\alpha$, to which we can associate an entropy, the *vibrational entropy*, counting logarithmically the number of configurations visited in a typical *basin*, corresponding to vibrational motion inside cages. The α-relaxation aims at visiting disconnected basins and we count the number of these in the so-called *configurational entropy*. We may write the total entropy of the (supercooled) liquid as

$$S_{\text{liq}}(T) = S_{\text{vib}}(T) + S_c(T) \tag{1.35}$$

This equation assumes a sharp definition of metastable states and independence of the two relaxational processes. The basins *trapping* the dynamics are somewhat considered as equivalently populated in terms of configurations (or their distribution has a meaningful typical value, *i.e.* is not fat-tailed), which is only approximate in real glass formers, and better holds the lower the temperature, similarly to Goldstein's scenario. A way to compute the configurational entropy is to regard the vibrational motion and its associated set of configurations as similar to the one observed in crystals, where harmonic modes perturb the lattice equilibrium positions for small non-zero temperature. These are not exactly the same as in crystals but it seems a reasonable approximation. Then we identify the vibrational entropy and the crystal entropy at the same temperature $S_{\text{vib}}(T) \simeq S_{\text{cry}}(T)$, and using the definition of the specific heat $C(T) = T\partial S/\partial T|_{N,\mathcal{V}}$, one obtains

$$S_c(T) = S_{\text{liq}}(T) - S_{\text{cry}}(T) = \Delta S_m - \int_T^{T_m} \frac{dT'}{T'}[C_{\text{liq}}(T') - C_{\text{cry}}(T')] \tag{1.36}$$

where ΔS_{m} is the entropy difference between the liquid and the crystal at the melting point.

Substance	OTP	2-MTHF	n-prop	3-BP	12 PD
T_{g}	246	91	97	108	172
T_0	202.4	69.6	70.2	82.9	114
T_{K}	204.2	69.3	72.2	82.5	127
T_{K}/T_0	1.009	0.996	1.028	0.995	1.11

(d)
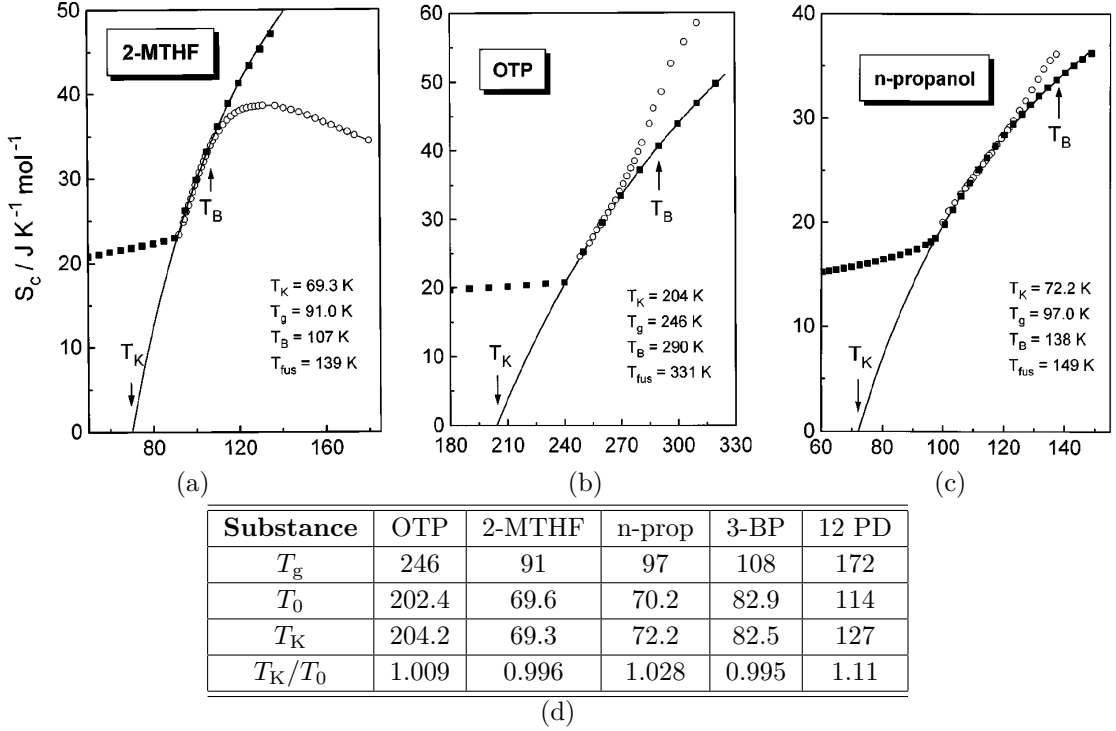
Figure 1.11: (Top) The configurational entropy $S_{\mathrm{c}}(T)$ measured for three different fragile glass-forming liquids: (a) 2-MTHF (2-methyltetra-hydrofuran), (b) OTP (o-terphenyl), (c) n-propanol. The black squares come from the calorimetric measurements while the white circles are from dielectric relaxation. At the glass transition point T_{g} each system fall off equilibrium and the black line shows the extrapolation of the measurements for temperatures below this point. (d) Table of values of glass transition temperature, VFT singularity and Kauzmann temperatures for these three supercooled liquids and two others: 3-bromopentane, 1-2 prop-diol. [*From* [328]]

The configurational entropy for some substances is shown in figure 1.11 from experimental measurements. Upon cooling down the configurational entropy tends to decrease up to the glass transition point where the system falls out of equilibrium and the structural relaxation is frozen, as in figure 1.2. Then one measures only a sort of off-equilibrium vibrational entropy. If one extrapolates the data to lower temperatures, one finds a point T_{K} at which the configurational entropy vanishes. This would mean that if somehow we were able to equilibrate the system below the experimental glass transition temperature we would observe that at some point the entropy of the supercooled liquid becomes lower to the one of the crystal. This is the Kauzmann paradox [215]; this seems rather weird since we are used to think of a liquid as very disordered and thus expect its entropy to be larger than the ordered crystal. Kauzmann suggested that above T_{K} there should be a *kinetic spinodal*, meaning that the relaxation time becomes larger than the time to nucleate the crystal and thus such extrapolations have no meaning, since the supercooled liquid cannot exist anymore near T_{K}. Then, AGDM proposed that T_{K} must be associated with a phase transition to an *ideal glass state*, where ergodicity is broken, the system being trapped in the lowest-lying states that are a few (subexponential) since $S_{\mathrm{c}} = 0$ [83, 154, 180, 181, 2], inducing a downward jump of the specific heat. This was actually verified in some mean-field spin glass models, such as the spherical p-spin [109, 81, 417, 279], see §2.3. However, some spin-glass models do not exhibit such transitions, such as finite-dimensional spin plaquette models [205]. The experimental evidence (see figure 1.11) that the extrapolated Kauzmann transition point and the VFT divergence point seem to coincide, $T_{\mathrm{K}} \simeq T_0$, gives an interpretation of the dynamic slowdown as a critical slowing down linked to a true thermodynamic phase transition towards the ideal glass, hence the search of a diverging correlation length. These temperature regions being out-of-reach experimentally and numerically, at least for now, only such speculations relying on theoretical hypothesis can be put forward.

1.2.4.2   The replica method

The number of stationary points (minima for low temperatures) of the free energy, *i.e.* the number of TAP states $\mathcal{N}$, is given by the configurational entropy, also called *complexity* $\Sigma = S_c$ in the spin glass context. In mean-field models they are shown to scale exponentially with the system size [81, 417]:

$$\mathcal{N}(f, T, N) \sim e^{N\Sigma(f,T)} \tag{1.37}$$

with the free energy per particle $f = F/N$. The fact that the number of metastable states is exponential in the system size leads to a unusual thermodynamics and makes this entropic contribution compete with the free energy restricted to these states. When computing the partition function one gets, assuming a clear-cut separation in states indexed by α

$$Z(T, \mathcal{V}, N) = \sum_{\mathcal{C}} e^{-\beta H(\mathcal{C})} \sim \sum_{\alpha} \sum_{\mathcal{C} \in \alpha} e^{-\beta H(\mathcal{C})} = \sum_{\alpha} e^{-\beta N f_{\alpha}} = \sum_{f_{\alpha}} \mathcal{N}(f_{\alpha}, T, N) e^{-\beta N f_{\alpha}} \tag{1.38}$$

Shifting from a discrete view of the free energy *levels* to a continuous one in the thermodynamic limit, we may use a saddle-point approximation:

$$Z(T, \mathcal{V}, N) \sim \int_{f_{\min}}^{f_{\max}} \mathrm{d}f \, e^{N[\Sigma(f,T) - \beta f]}$$
$$F(T, \mathcal{V}, N) = -T \ln Z \sim f^*(T) - T\Sigma(f^*(T), T) \tag{1.39}$$

where $f^*(T)$ is a solution of the following saddle-point equation

$$\frac{1}{T} = \left. \frac{\partial \Sigma(f, T)}{\partial f} \right|_{f = f^*(T)} \tag{1.40}$$

At the dynamical point T_d the solution of this equation is $f^*(T_d) = f_{\max}(T_d)$ while when the temperature is lowered the solution is between $f_{\min}(T)$ and $f_{\max}(T)$. At some point T_K the solution to this equation becomes $f^*(T_K) = f_{\min}(T_K)$. The thermodynamics is then dominated by the states that have zero complexity, *i.e.* states that are in subexponential number compared to the size of the system. This is nothing but the Kauzmann temperature at which the ideal glass transition takes place. For $T < T_K$ the thermodynamics is dominated by the same states that have zero complexity.
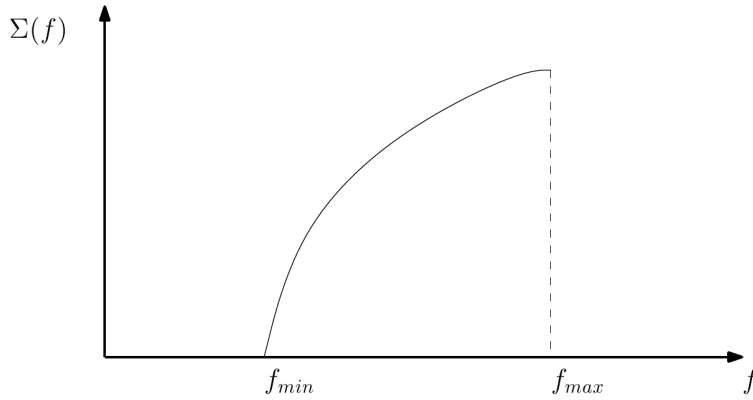
Figure 1.12: The complexity curve in the mean-field treatment of structural glasses. [*Reprinted from* [389]]

We observe that in order to characterize statically the system we must find a way to compute the complexity. This is provided by the real replica method, developed by Monasson, Mézard and Parisi [288, 277, 283, 284, 276, 285, 278]. The idea is to introduce m replicas (or *clones*) of the system, and introduce an attraction coupling of vanishing strength ϵ. This coupling, here put by hand, can be seen as emerging from imposing an external disordered field on the system, that will pin it into an amorphous configuration we wish to study [288]. As is usual with explicit disorder, this introduction can be analyzed through the use of replicas, see §2.3 for a detailed example. The Mari-Kurchan model [270] studied in chapter 4 can be seen as a practical realization. Another way is to take a clone of the system, let it equilibrate and couple the system to it: the clone then provides the pinning to an amorphous configuration, similarly to

the spirit of the point-to-set pinning in §1.1.5. This is a second equivalent procedure, the Franz-Parisi potential method [156]. These are answers to the difficult problem of pinning the system in a given pure state when there is no obvious symmetry breaking occuring and no explicit description of this pure state. Indeed, in the simple example of the ferromagnetic Ising model where the Z_2 symmetry allows to compute easily restricted equilibrium measures in one of the two ferromagnetic pure states at $T < T_c$.

When the strength of the coupling $\epsilon \to 0$, for $T > T_d$ the coupling has no effect, the m systems are independent ergodic liquids, since states do not have yet an influence on the thermodynamics of the system. For $T < T_d$ the coupling is effective, there is a first-order transition to a phase where the m systems have the same free energy: they are trapped by the same metastable state [277, 283, 284, 276, 285, 278]. The m clones of a particle composing the system condense in the same *cage*, forming a kind of *molecule* of m atoms.

Then the replicated partition function, through a similar calculation than the one above, reads

$$Z_m = e^{-\beta N \psi(m,T)} \sim \sum_\alpha e^{-\beta N f_\alpha} \sim \int_{f_{\min}}^{f_{\max}} \mathrm{d}f\, e^{N[\Sigma(f,T)-\beta m f]}$$

$$\psi(m,T) \sim m f^*(m,T) - T\Sigma(f^*(m,T),T)$$

(1.41)

where

$$\frac{m}{T} = \left.\frac{\partial \Sigma(f,T)}{\partial f}\right|_{f=f^*(m,T)}$$

(1.42)

m is thus a parameter conjugated to the free energy of the metastable states, which, through a Legendre transform, gives access to the replicated free energy of the system $\psi(m,T)$. From this one infers

$$f^*(m,T) = \frac{\partial \psi}{\partial m}(m,T)$$

$$\Sigma(m,T) \equiv \Sigma(f^*(m,T),T) = m^2 \frac{\partial}{\partial m}[\beta \psi(m,T)/m]$$

(1.43)

If we are able to compute the free-energy of the replicated system and perform its analytic continuation to real values of m, the real replica method enables us to compute the free energy $f^*(m,T)$ of the equilibrium states fixed by (1.42) and their complexity $\Sigma(m,T)$. The full complexity function can be then computed by inverting (1.42) to get $m(f^*,T)$, and, plugging it into the m-dependent complexity (1.43) to get $\Sigma(f^*,T)$ [417].
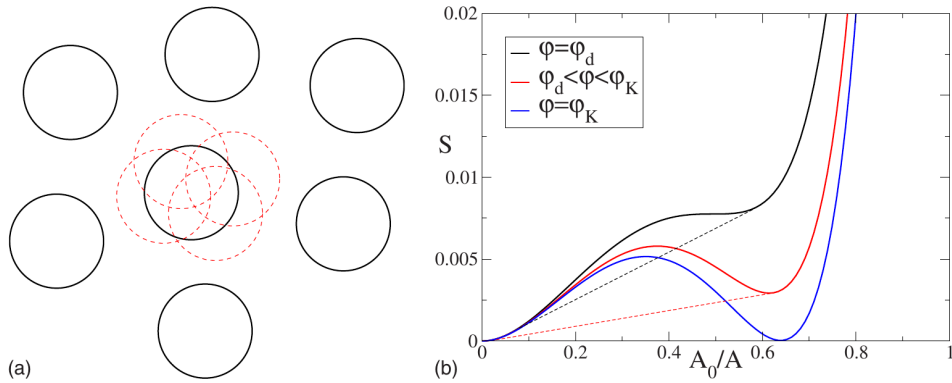
Figure 1.13: (a) A molecule of the replicated liquid: each particle (sphere) of the original liquid is replicated m times (dashed spheres), and the m copies vibrate around a reference one. (b) Replicated Legendre transform of the free energy (noted ψ in the text) as a function of the order parameter A_0/A where A represents the size of the cage, *i.e.* the plateau value of the MSD, for $m < 1$. A_0 is some reference value. The full line is the mean-field curve, while the dashed line takes into account the finite-dimensional nature of the system via a Maxwell construction [86]. Here the system considered is Hard Spheres: the control parameter is the packing fraction φ instead of the temperature, the correspondence is roughly $\varphi \leftrightarrow 1/T$. The $A = \infty$ minimum represents the ergodic liquid phase, while the secondary minimum appearing at φ_d and taking over at φ_K has $A < +\infty$ and stands for an ideal glass solution. [*Reprinted from* [312]]

The passage from a phase where the m replicas are independent, as particles within a liquid, to a phase where molecular clusters of replicas emerge, echoing the disconnected ergodicity-breaking clusters in phase space, dynamically signalled at T_d and thermodynamically at T_K, is known as a *replica-symmetry breaking* (RSB). This phenomenon will be emphasized in §2.3.

From (1.42), we notice that choosing a different m selects a different group of metastable states (described by f^*), which are different from the equilibrium states of the system unless $m = 1$, comparing with (1.40): the presence of the parameter m allows us to choose f^*, thereby probe different groups of states according to our needs. Within this formalism, choosing a dynamical protocol corresponds to a choice of a function $m(T)$. Comparing (1.40) and (1.42), we may define an effective temperature

$$\frac{1}{T_{\text{eff}}} = \frac{m}{T} = \frac{\partial \Sigma(f, T)}{\partial f}\bigg|_{f=f^*(m,T)} \tag{1.44}$$

which means that the states we select by choosing m at temperature T are effectively those that would be equilibrated at $T = T_{\text{eff}}$.

Summarizing:

- At high temperature, the system is in an ergodic liquid phase and the minimization of the TAP free energy yields the homogeneous solution $\forall i$, $\rho_i = \rho$, $F(\{\rho_i\}) = F_{\text{liq}}$.

- At T_d, $f = f_{\text{max}}$. The free energy is analytic at T_d, it is only a dynamic ergodicity-breaking transition.

- At moderate temperatures $T \in [T_K, T_d]$: pure states are well formed with $f > F_{\text{liq}}/N \equiv f_{\text{liq}}$, hence these states are metastable but they compensate with their entropic complexity contribution, catching up the liquid free energy and thus becoming thermoynamically relevant states: $f^* - T\Sigma(f^*, T) = f_{\text{liq}}(T)$.

- At T_K, the equilibrium TAP states verify $f = f_{\text{min}}$ and the complexity vanishes; the number of states has decreased up to this point where they become subexponential in N. The relation $f_{\text{min}} - T_K \Sigma(f_{\text{min}}) = f_{\text{liq}}(T_K)$ still holds. The total entropy is continuous but its first derivative, the specific heat, has a jump, leading to the Kauzmann transition to an ideal stable glass phase.

- For $T < T_K$, the thermodynamic properties of the ideal glass phase can still be computed with the real replica method [417, 43, 283, 206].

1.2.5   Out-of-equilibrium dynamics

Likewise the statics, the theoretical viewpoint on off-equilibrium regimes (see §1.1.7) is based on spin-glass models. Coming back to the spherical p-spin model where the Mode-Coupling approximation becomes exact (§1.2.1.4), its dynamical equations without assuming equilibrium features like TTI or FDT is a set of closed equations for the spin autocorrelation and response (to a space-time dependent external field $h_i(t)$) functions:

$$C(t, t') = \frac{1}{N} \sum_{i=1}^{N} \langle \sigma_i(t) \sigma_i(t') \rangle, \qquad R(t, t') = \frac{1}{N} \sum_{i=1}^{N} \frac{\delta \langle \sigma_i(t) \rangle}{\delta h_i(t')} \tag{1.45}$$

where the mean is taken over the dynamical process. This set of equations read [107, 81, 112]:

$$\frac{\partial C(t, t_w)}{\partial t} = 2TR(t_w, t) - \mu(t)C(t, t_w) + \frac{p(p-1)}{2} \int_{-\infty}^{t} dt'\, R(t, t')C^{p-2}(t, t')R(t', t_w)$$

$$+ \frac{p}{2} \int_{-\infty}^{t_w} dt'\, R(t_w, t')C^{p-1}(t, t')$$

$$\frac{\partial R(t, t_w)}{\partial t} = \delta(t - t_w) - \mu(t)R(t, t_w) + \frac{p(p-1)}{2} \int_{t_w}^{t} dt'\, R(t, t')C^{p-2}(t, t')C(t', t_w) \tag{1.46}$$

$$\mu(t) = \frac{p^2}{2} \int_{-\infty}^{t} dt'\, R(t, t')C^{p-1}(t, t') + T$$

This result was proven rigorously by Ben Arous, Dembo and Guionnet [32]. Similar equations for the spherical soft-spin SK model were also proved by these authors [31].

The solution to these equations have been first obtained by Cugliandolo and Kurchan for a fixed initial condition in [110], and is reviewed in [112]. Generically one can show that two-time correlation functions take the form:

$$C(t, t') \simeq C_{\text{eq}}(t - t') + \mathcal{C}\left(\frac{f(t)}{f(t')}\right) \tag{1.47}$$

where the function f can take different forms according to the model [112]. The solution exhibits a similar behaviour than the one displayed in figure 1.9. Models with a full-RSB (see §2.3) have a more complicated form involving a continuous hierarchy of aging timescales.

The solution has shown a link between correlation and response, a generalized FDT:

$$R(t, t_{\text{w}}) = \frac{X(t, t_{\text{w}})}{T} \frac{\partial C(t, t_{\text{w}})}{\partial t_{\text{w}}} \tag{1.48}$$

For large times $t_{\text{w}} \to \infty$, in mean-field spin glass models the so-called fluctuation-dissipation ratio is directly function of the correlations *i.e.*

$$X(t, t_{\text{w}}) \simeq x[C(t, t_{\text{w}})] \tag{1.49}$$

Then at short time differences, $X \sim 1$ and standard FDT holds; for large-time differences, the correlation reaches the plateau and the ratio correspondingly shifts $X \sim X_\infty$. Again for full-RSB phases the ratio is a continuous function of a hierarchy of plateaus $X \sim x(C)$, establishing a connection between the statics and dynamics.

One defines an *effective temperature*:

$$T_{\text{eff}} = \frac{T}{X_\infty} \tag{1.50}$$

which is analogous to its static counterpart (1.44). This effective temperature has the properties of a standard one: it can be measured by a suitable thermometer, like a harmonic oscillator of fixed frequency coupled linearly to the system. Such a heat bath description will be used in §3.7.3. At high frequency the fluctuations of the oscillator measure the actual temperature T while at low frequency it measures T_{eff}. This has been realized in computer simulations by using a tracer particle as a thermometer and tuning its frequency by modifying its mass. Likewise, its kinetic energy was controlled by the actual temperature for light tracers whereas it was related to the effective one for heavy tracers [42]. It also controls the direction of heat flows [113]. The fact that it depends clearly about the two-step behaviour of the correlations is interpreted as follows: the fast modes equilibrate on a timescale τ_β with the bath at temperature T while the slow degrees of freedom do not equilibrate (in mean field) and may be seen as quasi-equilibrated at the temperature T_{eff}. A thermodynamics based on the concept of effective temperatures is the subject of a whole book [253].

Besides, the non-equilibrium aging dynamics in mean-field spin glasses turns out to describe the slow descent of the system in an energy landscape which becomes more and more flat as the age increases [240], which accounts for slowing down with the age of the system. After a quench, due to the ergodicity breaking, the system is then stuck in the threshold states of the free-energy landscape. To access metastable states, one must consider an equilibrium initial condition of the system in a low temperature $T < T_{\text{d}}$. This has also been realized for the *p*-spin model [24]. In real liquids, a static approach to this problem is the *state-following construction* [325, 323]. The out-of-equilibrium dynamics for a structural glass in $d \to \infty$ will be derived in §3.10.

Note that, as already underlined, the mean-field approach misses activation events which leads to negative effective temperatures in alternative theories or experiments [43].

1.2.6 Scaling arguments beyond mean-field

We have seen that the theoretical viewpoint above, inherited from mean-field models, claims that the glassy slowdown comes from trapping the system in an exponential number of metastable states, which have a static origin, their large entropy contribution helping them compete in the free energy landscape with stable states. The very definition of pure states is blurred in finite dimension, and one may reject such a scenario on the basis of its over-reliance on mean-field concepts. This is where the *mosaic theory* of RFOT [224, 69, 260, 58, 405] tries to complete the picture: it aims at providing a finite-dimensional scaling theory of amorphous liquids based on these mean-field observations. The mosaic picture comes

from AGDM's scenario [154, 180, 181, 2] that takes into account the configurational entropy to explain the dynamic slowdown, which was later rewritten by Kirkpatrick, Thirumalai and Wolynes [224] incorporating nucleation theory and then put on a firmer basis by Biroli and Bouchaud introducing the point-to-set procedure [69].

In mean-field the system falls into one out of many TAP states. We know that for stability reasons in finite dimension the free energy must be convex, the TAP states are ill-defined and we may resort to a Maxwell construction [86]. Two thermodynamically stable states with different free energies cannot coexist, the one with smallest free energy would nucleate and expand locally. If several thermodynamically stable state with same free energy per particle f^* are present, what happens is that the system is then in a mixture -a mosaic- of these states: they are nucleated locally. AGDM called these states, which are defined locally both in space and time (in contrast to mean-field pure states), *cooperatively rearranged regions* (CRR). Between T_d and T_K, we have seen that the free energy difference between the metastable states and the liquid state is $f^* - f_{\text{liq}} = T\Sigma(T)$ where $\Sigma(T) = \Sigma(f^*(T), T)$. The nucleation of the metastable state comes therefore with a volumic free energy cost $T\Sigma(T)\Omega_d R^d/d$ with $\Omega_d R^d/d \equiv \mathcal{V}_d(R)$ the volume of a d-dimensional ball of radius R, but an interfacial gain term $\Upsilon(T)R^\theta$, where θ is a generalized surface exponent $\theta \leqslant d - 1$, as in some models the interface can have a more complicated shape [83], especially here since we do not know what an interface between CRR may look like. The free energy gain of the nucleating droplet is then

$$\Delta F(R) = -T\Sigma(T)\frac{\Omega_d}{d}R^d + \Upsilon(T)R^\theta \tag{1.51}$$

whose maximum value is obtained at $R = \xi$:

$$\xi(T) = \left[\frac{\theta\Upsilon(T)}{T\Sigma(T)\Omega_d}\right]^{\frac{1}{d-\theta}} \tag{1.52}$$

where the free energy barrier scales as (forgetting about constant factors in temperature, assuming θ is one of them)

$$\Delta \sim \frac{\Upsilon(T)^{\frac{d}{d-\theta}}}{[T\Sigma(T)]^{\frac{\theta}{d-\theta}}} \tag{1.53}$$

How does the nucleation proceed? To answer this question, Biroli and Bouchaud [69] proceeded with the point-to-set framework. Suppose we are able to select a given metastable state α. Then we take a cavity of radius R inside the system and we freeze all the degrees of freedom outside the cavity, and we let the interior of the cavity relax. We assume the surface tension is the same for all states, which is a strong hypothesis, see [83] for a discussion. The partition function of the cavity in contact with a *bath* in state α, with R as a unusual control parameter, reads

$$Z_{\text{cav}} \sim Z_{\text{in}} + Z_{\text{out}} = \exp\left(-\beta f_\alpha \frac{\Omega_d}{d}R^d\right) + \sum_{\gamma \neq \alpha} \exp\left(-\beta f_\alpha \frac{\Omega_d}{d}R^d - \beta\Upsilon(T)R^\theta\right)$$

$$\sim \exp\left(-\beta f_\alpha \frac{\Omega_d}{d}R^d\right) + \int_{f_{\text{min}}}^{f_{\text{max}}} df \, \exp\left([\Sigma(f, T) - \beta f]\frac{\Omega_d}{d}R^d - \beta\Upsilon(T)R^\theta\right) \tag{1.54}$$

$$\sim \exp\left(-\beta f^* \frac{\Omega_d}{d}R^d\right) + \left([\Sigma(f^*, T) - \beta f^*]\frac{\Omega_d}{d}R^d - \beta\Upsilon(T)R^\theta\right)$$

where we have made a similar decomposition as in (1.38). Here quantities are defined in a volumic way, the difference with the previous ones is just a density ρ factor. Since the *bath* is already in state α there is no surface energy cost associated to it, unlike the other states, that thus are less probable the higher the price of the interface. The integral has been computed approximately for large enough R^d. The saddle-point values f^* are still defined by (1.40). State α is one of the many metastable states dominating the total partition function of the system, and thus also its free energy is equal to f^*: the rearrangement of the sphere does not, on average, bring the system to a lower free-energy level.

Then the probability that the cavity relaxes to the state α, p_{in}, or that it shifts to another state, p_{out},

is given respectively by:

$$p_{\text{in}} = \frac{Z_{\text{in}}}{Z_{\text{cav}}} \sim \frac{\exp\left(\beta\Upsilon(T)R^\theta\right)}{\exp\left(\beta\Upsilon(T)R^\theta\right) + \exp\left(\Sigma(T)\frac{\Omega_d}{d}R^d\right)}$$

$$p_{\text{out}} = \frac{Z_{\text{out}}}{Z_{\text{cav}}} \sim \frac{\exp\left(\Sigma(T)\frac{\Omega_d}{d}R^d\right)}{\exp\left(\beta\Upsilon(T)R^\theta\right) + \exp\left(\Sigma(T)\frac{\Omega_d}{d}R^d\right)}$$

$$(1.55)$$

The surface tension tends to keep the cavity in the surrounding state, while the complexity is trying to force it in another one. The probabilities balance for $R = \xi$ defined in (1.52), up to an irrelevant factor $(\theta/d)^{1/(d-\theta)}$. Due to the rapid decay of exponentials, if $R < \xi$, p_{in} is close to 1, and close to 0 if $R < \xi$.

Thus if the droplet's size is $R < \xi$, the surrounding state is recovered by shrinking of the droplet to zero, and otherwise it goes into one of the many others. This means that metastable states can only be defined up to a scale ξ. Beyond this size, the droplet is unstable. Note that if, classically, the surface tension $\Upsilon(T) = \Omega_d\gamma(T)$ and $\theta = d - 1$, then this length scales as $\xi \sim d$ and diverges in the large-dimensional limit, giving back the mean-field notion of a homogeneous pure state, not a mosaic one.

A typical relaxation time can be estimated by an Arrhenius laws with the barrier given by (1.53):

$$\tau_{\text{R}} \propto \exp\left(\frac{\Delta}{T}\right) \sim \exp\left(\frac{\Upsilon(T)^{\frac{d}{d-\theta}}}{[T\Sigma(T)]^{\frac{\theta}{d-\theta}}}\right) \tag{1.56}$$

The vanishing of the configurational entropy induces a divergent timescale. This gives back a VFT-like law with an exponent $\theta/(d-\theta)$ if one assumes for example that the specific heat difference ΔC in (1.36) is constant with respect to temperature:

$$\frac{\mathrm{d}\Sigma}{\mathrm{d}T} = \frac{\Delta C}{T} \quad\Longrightarrow\quad \Sigma(T) \underset{T\to T_{\text{K}}^+}{\sim} \frac{\Delta C}{T_{\text{K}}}(T - T_{\text{K}}) \tag{1.57}$$

We have then seen that CRR are limited both in space and time. The configuration provided by the mosaic picture of many droplets constantly rearranging produces a typical equilibrium configuration and equilibrium dynamics of the whole system [83]. This theoretical viewpoint provides a way to understand the empirical correspondence between the raise of the relaxation time and the drop of the complexity. Barriers increase when lowering the temperature because larger and larger regions of the systems must be rearranged in order to restore ergodicity, and because the size of the barrier scales as some power of the size of the CRR (see (1.52) and (1.53)), which is similar to the point-to-set lengthscale defined in §1.1.5. This growth provides a mechanism for the super-Arrhenius increase of the relaxation time in fragile liquids.

1.2.7 Alternative theories

In this section we briefly reviewed the mean-field RFOT scenario since it gives the correct picture of what happens for structural glasses in the limit of infinite dimension: a part of this statement is one of the main outcomes of this thesis, which investigates in a unified framework both dynamics and statics of such systems.

Nevertheless, we stress here that alternative scenarios exist, aiming at describing what happens in *finite* dimensions in a different manner than the RFOT-based mosaic approach of §1.2.6. Some of them seem antagonistic with RFOT since they are based on a purely dynamical viewpoint while their statics is trifling, so that no reference to an underlying free energy landscape interpretation à la Goldstein can be made. An example of such analysis is the Dynamical Facilitation Theory [87, 172]. Still, some models share features of both theories [205]. Others, *e.g.* Frustration Limited Domains [383], are focused on the local structure and its influence on the slowing down of the dynamics, due to the incompatibility (*frustration*) between extension of the locally preferred order and tiling of the whole space, which is not necessarily contradictory with the mosaic picture, but sheds light on aspects overlooked by RFOT, or at least hidden in the somewhat abstract notion of states. Many other scenarios have been proposed during the last decades, as well as specific models of one of the many features of supercooled liquids (such as aging [70, 290]).

Brief reviews of some of them are provided by [83, Sec. VIII], [43, Sec. IV] and [126, 136, 381, 338].

1.3   Dynamical theories of structural liquids and glasses

As stressed previously, solving the dynamics of liquids from first principles is a notably difficult task, since the finite-dimensional coupled equations of motion cannot be solved exactly, and in writing equations for dynamical quantities one has to resort to a closure scheme to be able to solve them. A case amenable to an analytic treatment is the one in which a small parameter is clearly identified so that a self-consistent reliable approximation may be performed without modifying the *qualitative* behaviour of the solution (as is the case of the spurious nonergodic dynamical transition in §1.2.1). It then may provide very good *quantitative* results as well, where the precision is directly set by the small parameter, and may be improved systematically, as in any perturbative strategy. The issue is that for liquids such a small parameter is found missing.

We mention here a few theories of the dynamics, ranked according to their domain of validity. This is not at all an exhaustive list.

1.3.1   In the low-density liquid phase

- The first attempts at a complete theory of dynamics of liquids originate from the classical kinetic theory [327, 199], which was successful in gases. One of its main outcomes is Boltzmann's equation which describes the time evolution of the one-particle phase space density function[8], approximating the so-called collision term. The linearized version of it allows to recover the laws of hydrodynamics [1, 246] for small wavevectors and frequencies, giving microscopic expressions for macroscopic variables such as the transport coefficients (shear viscosity, thermal conductivity, sound velocity...) [327, 199]. Indeed, the hydrodynamic equations come from coarse-grained conservation laws and linearization of the inter-particle forces. The specific case of the HS potential has been tackled by Enskog [147] in 1922 to derive a refined Boltzmann equation of this system, which now bears his name. Yet, this kind of equations break down at high density or outside linear response regimes. It includes only short-range uncorrelated binary collisions of the constituent particles. Typical fluctuations from equilibrium decay exponentially in time, which clearly fails at high enough densities.

- More specifically in relation with infinite-dimensional systems, Elskens and Frisch [146], soon after the finding of the HS equation of state in the liquid phase reviewed in §2.2, made use of an expansion in the number of collisions of the particles to solve the dynamics in $d \to \infty$. The equation obtained is a modified Enskog equation for the evolution of the one-particle distribution function; the latter was first derived by van Beijeren and Ernst [393, 392] to improve Enskog's equation dealing with HS [327, 199]. In fact, in the glassy regime there are multiple collisions between a particle and its nearest neighbours, which makes a collision expansion ineffective. Besides, such an approach is restricted to HS, since for soft potentials the notion of collision is not well defined.

1.3.2   Liquids to supercooled liquids

- We already described in §1.2.1 the Mode-Coupling Theory, which starts from an exact dynamical equation for the intermediate scattering functions and approximates quadratically the memory kernel. However, refined approximation schemes have been proposed over the years. The strategy is to include higher-order corrections to the memory kernel, ideally in a systematic way. This was started by Szamel in 2003 [374] and triggered a vast number of works [406, 350, 275, 99, 54, 375, 377]. It was recently improved to potentially include all orders by Janssen, Mayer and Reichman [211, 213, 212]. In these *generalized MCT*, the exact time evolution of the four-point correlations is governed by six-point correlations, which in turn are controlled by eight-point correlations, and so on. This leads to a hierarchy of coupled equations that makes it possible to delay the uncontrolled factorization approximation to a later stage, which has been shown to systematically improve the predictions with respect to MCT [374, 406]. It takes only static structural information as input. Including all orders rounds off the sharp MCT transition and gives back a crossover. Besides, it

---

[8]If it is denoted by f, $f(\boldsymbol{p}, \boldsymbol{r}, t)\mathrm{d}\boldsymbol{p}\mathrm{d}\boldsymbol{r}$ is the number of particles that lie at time t in the region of small volume $\mathrm{d}\boldsymbol{p}\mathrm{d}\boldsymbol{r}$ centered around the phase space point $(\boldsymbol{p}, \boldsymbol{r})$, *i.e.* in its neighbourhood.

makes the distinction between fragile (super-Arrhenius) and strong (Arrhenius) liquids, a feature that is missed by MCT. This is analytically tractable for schematic versions, and a concern is that including wavevector dependence as in standard MCT is very difficult to deal with computationally; nonetheless a fourth-level account of quasi-HS has been performed in [213], displaying a crossover and good quantitative results, despite some further approximations. Another issue is the question of the convergence of this scheme, which is not clear a priori. Encouraging results demonstrates at the schematic level that low-level truncations uniformly converge to the infinite-order solution as the closure level increases [211, 213, 212], in this sense resembling to a perturbative expansion although there is no small parameter.

- As for the hydrodynamic regimes of §1.3.1, a coarse-grained theory was developed by Das, Mazenko and collaborators [120, 117, 118, 119]. The first version showed that one recovers a dynamic transition at high enough density. Then they unveiled that coupling density modes to currents would keep the equations clear of this spurious transition. By definition this theory is general and does not account for microscopic details, such as those of the underlying interaction potential between the constituents of the system. It was noticed that the equations were not consistent with microscopic reversibility [287].

  Similar coupling to currents were considered within MCT by Götze and Sjögren [187] to avoid the non-ergodic transition.

- Jacquin and van Wijland [207] developped a diagrammatic expansion of Dean's [127] dynamic equation for density-density correlations by taking the strength of the interaction potential as a perturbative parameter. This is well-defined but fails *e.g.* for HS systems and may be quite involved to give quantitative predictions in a deeply supercooled (strongly-coupled) regime. Nevertheless it gives comparable results to MCT for higher temperatures. A serious issue is the breaking of a symmetry of the system by the perturbative scheme [206]. An approach which preserves the symmetries of the system is the one by Kim and Kawasaki [219] (see also Andreanov, Biroli and Lefèvre [12]), although one has to systematically compute higher orders in a loop expansion (which is cumbersome) and it is not straightforward to generalize their approach for many-body correlation functions.

1.3.3 Theory of the glass crossover

An interesting approach is the development of a dynamical Landau theory[9] of the glass crossover by Rizzo [329, 332, 330, 331]. The starting point is the observation of a regime in supercooled liquids well described by MCT, which is a mean-field dynamical theory with a well-defined critical point at $T_{\rm d}$. Then one may define an effective Hamiltonian by expanding around the mean-field dynamical action, *e.g.* as provided by the $d \to \infty$ solution in §3.3.5. This expansion à la Landau [247, 248] is done via general symmetry arguments. One ends up with a dynamical field theory which enjoys a mapping to a stochastic one with quenched disorder. The latter may be studied non-perturbatively and leads to a crossover instead of a sharp transition. The next step is to explore and compare the predictions to experimental data, a task which has been initiated by Rizzo and Voigtmann in [332].

1.4 Invariant curves in the phase diagram of liquids

We introduce here the notion of *isomorphs* used in chapter 5, where a study of the following approximate scale invariance is done in the high-dimensional limit. For a recent and pedagogical review, see [138].

1.4.1 Static and dynamic scalings

In an early experiment, Rosenfeld [335] revealed that a single static quantity, the excess entropy (the entropy minus the entropy of the ideal gas) seemed to control a dynamic observable, the diffusion constant. More recently, a number of studies displayed striking similarities in structure and dynamics of some model liquids [195, 346, 255]. In the early 2000s, Alba-Simionesco, Tarjus and coworkers [4, 3, 5] proposed a scaling of the α-relaxation time by a function of a single parameter $h(\rho)/T$, where $h(\rho)$ is some function

---

[9]This is reminiscent of the above-mentioned work [11].

of the liquid density. These observations were confirmed by other groups in supercooled liquids and polymers [133, 79, 334, 155]. In a series of recent papers [19, 20, 21, 347, 184, 348], the Roskilde group of Dyre, Schrøder and coworkers have rationalized this idea with their isomorph theory: roughly speaking, an isomorph is a curve in the (T, ρ) phase diagram where static and dynamic quantities are invariant when expressed in reduced units. We quickly outline some of their main defining arguments.

1.4.2   Isomorph theory

Let us consider a simple liquid in d-dimensional space at temperature T and number density ρ. Two state points (T_1, ρ_1) and (T_2, ρ_2) are *isomorphic* if there is a rescaling of the coordinates of all particles $\mathbf{r}_i^{(2)} = (\rho_1/\rho_2)^{1/d}\mathbf{r}_i^{(1)}$ that makes their Boltzmann factors proportional

$$e^{-U(\mathbf{r}_1^{(1)}, \cdots, \mathbf{r}_N^{(1)})/T_1} = C_{12}\, e^{-U(\mathbf{r}_1^{(2)}, \cdots, \mathbf{r}_N^{(2)})/T_2} \tag{1.58}$$

where C_{12} depends only upon the state points 1 and 2, not on the microscopic configurations. This means that both potential energies in reduced units $\tilde{\mathbf{r}} = \rho^{1/d}\mathbf{r}$ divided by temperature are the same up to an additive constant depending on the state points. In the following we note $\mathbf{R} = (\mathbf{r}_1, \ldots, \mathbf{r}_N)$.

Note that there is an alternative (and more complete) basic definition of this isomorph correspondence, see [138, Sec. 6.2.]. For the purpose of this brief introduction we will stick to this one.

Inverse-Power Law (IPL) potentials $V_{\mathrm{IPL}}(r) \propto r^{-n}$ are the only potentials for which the isomorphic property exactly holds, for all points lying on curves given by $\rho^{n/d}/T = \mathrm{const}$, which define an invariant curves *i.e.* isomorphs. It is instead only an approximation for all the other potentials, and yet, surprisingly enough, it turns out [19, 20, 21, 347, 184, 348] that there is a wide class of situations in which it is a very good one. Indeed, these authors have related (see *e.g.* [184, Appendix A]) the existence of isomorphs to the *strongly correlating* property of the system, measured by the virial-potential energy correlation coefficient $R \in [-1, 1]$:

$$R = \frac{\langle \Delta W \Delta U \rangle}{\sqrt{\langle (\Delta W)^2 \rangle \langle (\Delta U)^2 \rangle}} \tag{1.59}$$

where $\Delta W = W - \langle W \rangle$ and brackets denote canonical equilibrium averages. U is the potential energy of the system and W is the so-called virial function [199]

$$\begin{aligned} U &= \sum_{i<j} V(|\mathbf{r}_i - \mathbf{r}_j|) \\ W &= -\frac{1}{d}\sum_i \mathbf{r}_i \cdot \nabla_{\mathbf{r}_i} U \end{aligned} \tag{1.60}$$

IPL potentials have strict proportionality between their energy and virial function. For all the other potentials it is an approximation, which however can be considered as a very good one if *e.g.* $R > 0.9$, which is a conventional threshold in practice. Many widely used potentials define strongly-correlating liquids, as studied in [20, 21, 348].

Defining the excess free energy in a virial sense, *i.e.* with respect to the ideal gas, and the associated canonical probability by

$$\begin{aligned} Z(\rho, T) &= e^{-F_{\mathrm{ex}}/T} = \int_{\mathcal{V}^N} d\mathbf{R}\, e^{-\beta U(\mathbf{R})} \\ P(\mathbf{r}_1, \ldots, \mathbf{r}_N) &= e^{-\beta[U(\mathbf{r}_1, \ldots, \mathbf{r}_N) - F_{\mathrm{ex}}]} \end{aligned} \tag{1.61}$$

$\mathcal{V} = N/\rho$ is the volume of the system. In reduced units it may be written as

$$\begin{aligned} \int_{(\rho\mathcal{V})^N} d\tilde{\mathbf{R}}\, \widetilde{P}(\tilde{\mathbf{r}}_1, \ldots, \tilde{\mathbf{r}}_N; \rho, T) &= 1 \\ \text{with} \quad \widetilde{P}(\tilde{\mathbf{R}}; \rho, T) &= \frac{e^{-\beta U(\rho^{-1/d}\tilde{\mathbf{R}})}}{\rho^N Z(\rho, T)} \end{aligned} \tag{1.62}$$

One can easily check that condition (1.58) tells us that the reduced-coordinate canonical probability, $\widetilde{P}(\tilde{\mathbf{R}}; \rho, T)$, is an isomorph invariant. The constant C_{12} in (1.58) is therefore allowed since it does not contribute to the probability due to normalization. This means that rescaled (excess) static quantities which can be expressed in terms of $\widetilde{P}$ are invariant along an isomorph.

In [137], Dyre showed that, for a strongly-correlating liquid, there exists two functions of the density, h and g, such that

$$U(\mathbf{r}_1, \ldots, \mathbf{r}_N) = h(\rho)\widetilde{\Phi}(\widetilde{\mathbf{R}}) + g(\rho) \tag{1.63}$$

where $\widetilde{\Phi}$ is a dimensionless, state-point independent function of the reduced coordinates. In fact, h and g are responsible for the non-invariance of quantities which directly depend upon them. This implies that the equation of the isomorphs is given by

$$\frac{h(\rho)}{T} = \text{constant} \tag{1.64}$$

Dynamically, if the reduced-units force is given by

$$\widetilde{\mathbf{F}} = -\beta\widetilde{\nabla}U(\mathbf{r}_1, \ldots, \mathbf{r}_N) = -C\widetilde{\nabla}\widetilde{\Phi}(\tilde{\mathbf{r}}_1, \ldots, \tilde{\mathbf{r}}_N) \tag{1.65}$$

where C is the constant defining a particular isomorph in (1.64), then since the equations of motion are, in reduced units,

$$\frac{\mathrm{d}^2\widetilde{\mathbf{R}}}{\mathrm{d}\tilde{t}^2} = \widetilde{\mathbf{F}} \tag{1.66}$$

with $\tilde{t} = t\rho^{1/d}/\sqrt{\beta m}$ a reduced time (m is the mass of the particles), the dynamics is also invariant along an isomorph. This holds as well for Brownian dynamics, changing the scaling of time involving the dissipation.

1.4.3 Exploiting the invariance

The isomorph property can be checked numerically or experimentally, in a direct fashion by showing that *e.g.* the radial pair distribution or the MSD for different state points collapse into a master curve (see examples in §5.9.1). Indirectly, it can be checked by computing the WU coefficient R for different state points. It means that if one knows an invariant quantity, be it static or dynamic in nature, in one point of the phase diagram, then doing simple rescalings of the units one may compute it *along the whole isomorph*.

This quasi-universality led to a number of *a posteriori* explanations and interpretations of facts that had been previously observed [19, 184, 348], such as phenomenological rules along freezing or melting lines [388, 218, 10, 200, 26], or observations that a single static quantity controls dynamic properties [335, 321, 415, 187]. It can also be used to rule out theories that are incompatible with these invariances [184], or make novel predictions [410, 251]. Equilibrium properties but also off-equilibrium regimes (aging) [184] have been investigated in light of this invariance, aas well as similar inferences in crystals or quantum liquids [137].

As an example related to this introduction, the MCT basic idea that statics determines the dynamics is consistent with the existence of isomorphs: for any strongly correlating liquid, if two state points have the same reduced radial pair distribution, they are isomorphic. This means that they have the same reduced dynamics, so in this sense the pair correlation function *determines* the dynamics. From the isomorph perspective MCT may be expected to work best for strongly correlating liquids.

1.5 Amorphous Hard Spheres in high dimension

The present thesis follows a previous series of works by Charbonneau, Kurchan, Parisi, Urbani and Zamponi analyzing the statistical physics of Hard Spheres (HS) in large space dimension [312, 243, 242, 96]. A recent review, containing part of the results presented in this thesis, summarizes its key aspects [98].

First let us define this potential: it describes hard-core spheres of diameter σ with infinite repulsion at contact and is non interacting away from this distance. In other words, this is an idealization of billiard balls:

$$V_{\mathrm{HS}}(r) = \begin{cases} \infty & \text{if } r < \sigma \\ 0 & \text{if } r > \sigma \end{cases} \quad \implies \quad e^{-\beta V_{\mathrm{HS}}(r)} - 1 = -\theta(\sigma - r) \tag{1.67}$$

which can be regularized as a soft-core potential in various ways, taking the limit of infinite repulsion[10]. θ is the Heaviside theta function; one already sees that temperature has no effect on the thermodynamics

---

[10]For instance Soft Harmonic Spheres $V_{\mathrm{SHS}}(r) = \kappa\left(1 - \frac{r}{\sigma}\right)^2 \theta(\sigma - r)$ with $\kappa \to \infty$ to recover HS, or the limit $n \to \infty$ of IPL potentials $V_{\mathrm{IPL}}(r) = \epsilon\left(\frac{\sigma}{r}\right)^n$, the latter being an example of a smooth regularization (for all finite n).

of the system. The (T, ρ) phase diagram is thus replaced by a one-dimensional phase diagram controlled by the density ρ. A better control parameter, related to density, is the packing fraction $\varphi \in [0, 1]$ (first encountered in figure 1.1), *i.e.* the ratio between the volume of the spheres and the total volume enclosing the system:

$$\varphi = \frac{N\mathcal{V}_d(\sigma/2)}{\mathcal{V}} = \frac{\rho\mathcal{V}_d(\sigma)}{2^d} \tag{1.68}$$

The main part of this thesis generalizes the thermodynamics of this system to a broad range of liquid potentials that can be influenced by temperature contrary to HS (chapter 4), and analyzes their dynamics (chapter 3). We highlight a few key theoretical results obtained prior to the present thesis:

- The starting point of the studies of liquids in large dimension actually dates back to the mid-1980s with the derivation of the free energy of the HS liquid phase by Frisch, Rivier and Wyler [162, 258, 164, 409, 163, 161] and its equation of state.

- Soon after, Kirkpatrick and Wolynes [225] proposed to study the high-dimensional limit of liquids and glasses but some tools, such as the replica method for systems without explicit disorder described briefly in §1.2.4.2, were lacking at the time, but were developed in the following decades.

- Parisi and Zamponi analyzed the HS phase diagram in $d \to \infty$ (see [312] for a review), using a Gaussian ansatz for the replicated liquid density (the density of *molecules*, *i.e.* copies of the system, as in §1.2.4.2).

- In the series of works [243, 242, 96], it was shown that this Gaussian approximation is actually exact for $d \to \infty$, as far as the entropy is concerned, and the high density regime in the entropy was systematically studied, proving that a Kauzmann transition to an ideal glass phase takes place and that, on further compression, this phase is unstable and is replaced by a Gardner phase [325, 97], see §4.4.

- A major outcome of these static results is that they provide a framework to investigate the *jamming* transition. This will not be discussed in this thesis, but is a crucial prediction of the theory so we just emphasize a few results[11]. Let us define jamming in this way: take a HS packing in a box, and compress it as much as you can, by increasing the pressure via forces at the boundaries, or by putting more and more particles in it, increasing density. At some point the pressure reached is infinite (owing to the infinite repulsion of HS; a soft-core potential remains compressible at finite temperature). What happens is that particles are now *mechanically in contact* with their neighbours, and due to the hard-core constraint, they are truly blocked by these neighbours. The packing is then said to be *jammed*; it has undergone the jamming transition from a rather loose packing to a very tight one. This is depicted in figure 1.14.
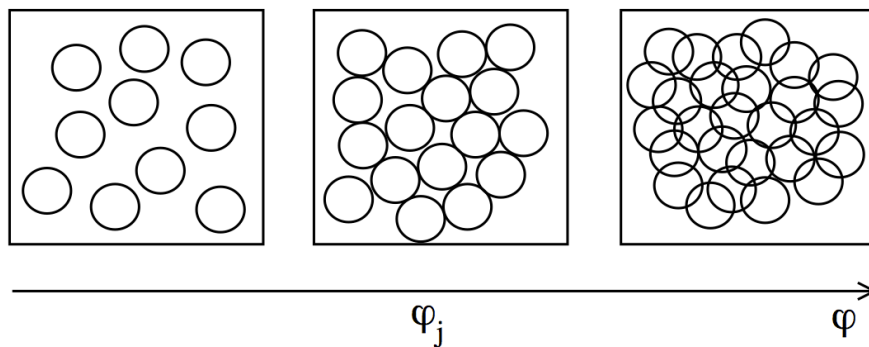
Figure 1.14: Configurations for a liquid regime (left), for a jammed packing at φ_j (middle), and finally for further compression (right): if the spheres are soft, they must overlap. [*Reprinted from* [206]]

Note that this form of blocking is different from the blocking observed in glasses. In the amorphous state created at the glass transition, blocking is due to caging and vibrations inside the cage, which make it respond like a solid capable of bearing loads. Yet, the system is still compressible and

---

[11]*And we hope you like jamming too.*

pressure is finite. In the jammed case, the rigidity comes from the formation of a network of mechanical contacts between the spheres which has percolated; if we assume we can model these spheres as mechanically undeformable, the resulting solid is incompressible and its pressure infinite.

A typical example of jammed packings is sandpiles: when one drops sand from a bucket onto the ground, it flows in the air like a liquid because it is then diluted. But when it touches the ground, the sand which gets added layer by layer increases gradually the density of the packing due to gravity, which acts as the exerted pressure on the system. The bottom layer does not escape due to friction on the ground, and when all the sand in the bucket has been poured, after a quick reorganization of the still flowing (*i.e.* still liquid-like) top layers, having a temporary lower local density, local motion no longer takes place in the sandpile: it is jammed.

The jamming point reached through infinite compression lies in the high-density Gardner phase, and is characterized by its packing fraction φ_j (see §1.14). It is protocol dependent, but critical behaviour near jamming is universal. A certain number of critical exponents has been computed [96, 97], describing *e.g.* the distribution of weak forces applied on the contacts (for a soft-core realization of the HS potential) as well as the distribution of small gaps between spheres. Both enjoy a power-law scaling close to the transition point. These scalings are very different from what one expects in a normal glass or in a crystal.

The existence of vibrational modes different from phonons has also been worked out from the solution. The number of force-bearing contacts at jamming follows Maxwell's criterion of isostaticity [273], being $2d$ on average per particle. This is related to the marginal mechanical stability of the packing, since it is the minimal number of contacts required for a packing to be mechanically rigid. From this sole assumption, general properties have been derived by Wyart [408, 53, 128] in any dimension, independently from the $d \to \infty$ solution, and its scaling predictions are fully consistent with the ones discovered in this limit. Numerical simulations in $d \geqslant 2$ have recently shown [92] that the $d \to \infty$ criticality and the value of the exponents are robust for all dimensions, including the experimentally relevant ones $d = 2$ and 3.

In conclusion, the HS system in $d \to \infty$ thus provides a nice unifying framework to investigate all phases of the system for all densities: liquid, glass and jamming. A phase diagram is displayed in figure 1.15, see also figure 4.5.

1.6   Outline and questions addressed in this thesis

The rest of the thesis is organized as follows:

- In chapter 2, we introduce an approximation scheme well suited for the high-dimensional limit of liquids, the virial expansion, which we apply to the HS system. Then we solve both statics and dynamics of a mean-field spin-glass model to give the tools and ideas that will be identically pursued in the context of structural glasses. This illustrates in a concrete example the RFOT ideas of §1.2. We hope both subjects are treated in a pedagogical manner and that one sees in a convincing way that the construction of the $d \to \infty$ solution in the next chapters is mostly a repetition of these steps.

- In chapter 3, we derive the dynamics of liquids and glasses in $d \to \infty$ both in and out of equilibrium. We explore its implications for the glass transition and discuss the link with MCT.

- In chapter 4, the thermodynamics of the system is derived in a way which is explicitly analogous to the dynamics. This allows to prove the consistency of the long-time limit dynamical picture and the static one.

- In chapter 5, building upon the dynamics and statics of 3 and 4, we examine the notion of isomorphs in $d \to \infty$ and prove that it becomes exact for a general class of liquid pair potentials.

- In chapter 6, we summarize briefly this work and give an outlook of further progresses and questions that may be investigated in direct connection with these results.
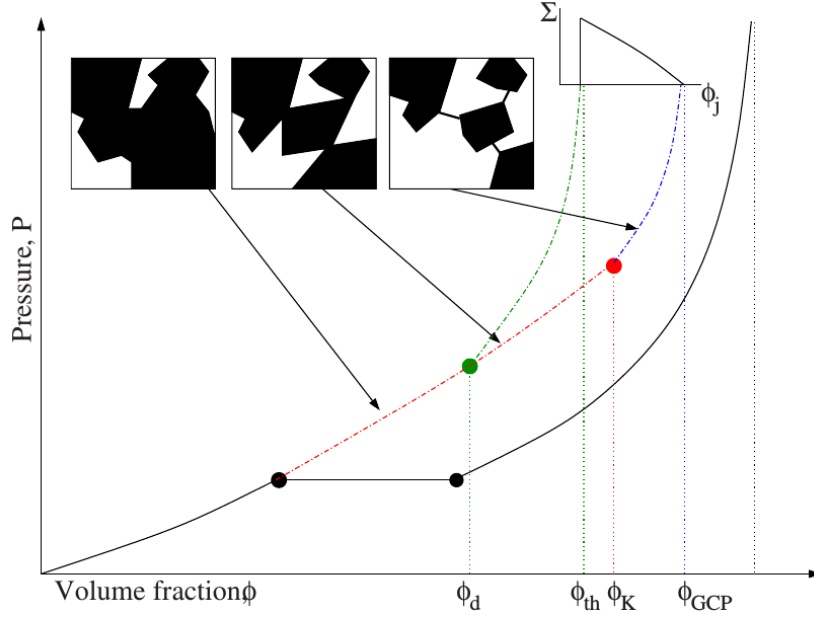
Figure 1.15: Pressure versus packing fraction diagram for HS. The full black line represents the first-order liquid-solid transition. Above the dynamical transition φ_d, the system is in one out of exponentially many pure states. Upon further compression it enters the ideal glass state (Kauzmann transition φ_K) and at infinite pressure it goes to a density $\varphi_\mathrm{j} \in [\varphi_\mathrm{th}, \varphi_\mathrm{GCP}]$ depending on the protocol and the state it follows. The least dense *bottoms of the entropy landscape* (highest pure states) are characterized by the threshold packing fraction φ_th. The densest packing is dubbed greatest close packing (GCP) with density φ_GCP. In inset the complexity is plotted. The boxes display an *artist's impression* of the dN-dimensional phase space of the system. Black configurations are allowed whereas white ones are forbidden by the hard-core constraint. In the supercooled liquid regime the phase space is connected and it is disconnected in the glass phase where pure states are defined. [*Reprinted from* [312]]

- The appendices contain a summary of notations and definitions employed throughout the thesis, technical points that are not strictly necessary in the main text but reported there for completeness, as well as a quite complete and pedestrian introduction to the field-theoretical expression of the dynamics of many-body interacting systems in contact with a heat bath (Martin-Siggia-Rose-De Dominicis-Janssen formalism), which is widely put to work in this thesis.

2

FORMALISM OF MANY-BODY DISORDERED SYSTEMS

Outline

We have seen that *static* equilibrium properties of liquids are well understood far from the glassy regime of high densities, thanks to the development of liquid theory. To get an exact mean-field theory of liquids and glasses in all regimes we need a well-defined approximation scheme with a small parameter, which will be given by the limit $d \to \infty$. The approximation scheme will be borrowed to liquid theory where a diagrammatic expansion of the grand potential has been designed, and is well suited to our needs since one term dominates the series in the large-dimensional limit. In the first half of this chapter we will thus discuss this virial expansion and its application to Hard-Sphere (HS) liquids in infinite dimension discovered by Frisch, Rivier and Wyler in the mid-1980s, which will be the starting point of the next chapters. Note that one can circumvent the use of such a technique by introducing an irrelevant quenched disorder, in the spirit of the similar mean-field spin-glass models. This will be put to use in the statics in chapter §4 for completeness, and shown to lead to the exact same results, making a bridge between *quenched disordered* models (such as *spin* glasses) and models with *self-generated disorder* (such as *structural* glasses). In the second half we will illustrate RFOT ideas in the case of the spherical p-spin model, both statically -using the replica method- and dynamically -using the supersymmetric formalism (SUSY)-, introducing the superspace notation and a convenient way of doing practical calculations with it through a formal analogy between superfields and two-by-two block matrices. We will display the analogy between the static replica formalism and the dynamic SUSY formalism explicitly in this case, which will be of a great help to derive the statics and dynamics in the more complex case of structural glasses.

2.1   The virial expansion in liquid theory

2.1.1   The grand potential

The virial expansion is a standard tool of liquid theory and is reviewed in [199, 293, 206]. We will mostly follow these reviews here.

Let us consider generically the grand-canonical partition function of a one-component system with

interaction potential V and submitted to an external field ψ; its Hamiltonian reads

$$H(\{p_i, r_i\}) = \sum_{i=1}^{N} \frac{p_i^2}{2m} + \sum_{i=1}^{N} \psi(r_i) + \sum_{i<j}^{1,N} V(r_i, r_j) \tag{2.1}$$

and the grand-canonical partition function is

$$\Xi = \sum_{N=0}^{\infty} \frac{1}{N!} \int_{1,\ldots,N} \prod_{i=1}^{N} z(i) \prod_{i<j}^{1,N} [1 + f(i,j)]$$

$$z(i) = \left(\frac{2\pi m}{\beta h^2}\right)^{d/2} e^{\beta\mu - \beta\psi(i)}, \qquad f(i,j) = e^{-\beta V(i,j)} - 1 \tag{2.2}$$

We consider an inhomogeneous system as it will prove useful for the next chapters. The external field is put here for a later generalization to the dynamics in §3.2.2. To simplify the notation, in this section we use $i \equiv r_i$ and $\int_i \equiv \int \mathrm{d}r_i$. μ is the chemical potential and the de Broglie thermal length prefactor $\Lambda = \sqrt{\beta h^2/2\pi m}$ in the (generalized) activity z comes from integration over the momenta, which are irrelevant here. Let us comment the choice of this expression. In the following the grand-canonical formalism is used because it is better suited to the resummations we are going to use. z gathers all single-particle terms. The Mayer function f is a good choice for an expansion since it decays to zero at large distances, which will be a crucial property; it is also zero in the ideal gas limit which is the reference situation here, and it is well-defined even for the singular model of HS in which it admits a very simple expression: $f_{\mathrm{HS}}(r) = -\theta(\sigma - r)$, without resorting to any regularization or limit of any kind.

To compute the grand-canonical partition function giving access to equilibrium quantities, we expand the product over pairs of particle and express it more easily with a diagrammatic representation. Expanding the product at fixed N we have to choose which pairs (i,j) enter into account in the term we write, as they give a $f(i,j)$ factor each and the *non-chosen* pairs do not produce any factor since they give a factor 1. We write such a term as a cluster graph with z vertices coming from the single-particle product and f links[1]. Black vertices are summed over the position labeled with the particle index. As an example the $N = 3$ terms are given by the prefactor $1/3!$ and the sum of Mayer diagrams

$$\{N = 3\} = \frac{1}{3!}\left(\vcenter{\hbox{\includegraphics{d1}}} + \vcenter{\hbox{\includegraphics{d2}}} + \vcenter{\hbox{\includegraphics{d3}}} + \vcenter{\hbox{\includegraphics{d4}}} + \vcenter{\hbox{\includegraphics{d5}}} + \vcenter{\hbox{\includegraphics{d6}}} + \vcenter{\hbox{\includegraphics{d7}}} + \vcenter{\hbox{\includegraphics{d8}}} \right)$$

$$= \frac{1}{3!}\vcenter{\hbox{\includegraphics{e1}}} + \frac{3}{3!}\vcenter{\hbox{\includegraphics{e2}}} + \frac{3}{3!}\vcenter{\hbox{\includegraphics{e3}}} + \frac{1}{3!}\vcenter{\hbox{\includegraphics{e4}}} \tag{2.3}$$

where for example

$$\vcenter{\hbox{\includegraphics{f1}}} = \int_{1,2,3} z(1)z(2)z(3)f(1,2)f(2,3) \tag{2.4}$$

The counting of diagrams has to be made with great care, and in the second line of (2.3) we noted that a number of terms in the first line have the same value. These diagrams have a prefactor $T/N! = 1/S$ where T is a degeneracy number (the order of the subgroup of *link* permutations that leave the value of the diagram unaltered) and S is the *symmetry number* which here is the order of the subgroup of *black nodes* permutations that leave the value of the labeled diagram unaltered (*i.e.* the set of connections $f(i,j) = f(j,i)$ preserved). Indeed the $1/N!$ prefactor takes care of all possible relabelings of the nodes but among them, some diagrams do not appear in the expansion due to the fact that the links are directed by the $i < j$ condition.

We group the *topologically equivalent* (*i.e.* having the same set of connections, hence the same value) labeled diagrams in a single unlabeled diagram, including the prefactor, with the convention:

$$\text{unlabeled diagram} = \frac{1}{S} \times \text{the value of the same diagram labeled in an arbitrary way}$$

---

[1]Similarly to propagators in Feynman diagrams (note however that Mayer cluster graphs have been designed much earlier [274]).

In this way (2.3) writes:

$$\{N = 3\} = \text{} \quad (2.5)$$

Now, equation (2.2) can be written in a diagrammatic form:

$$(2.6)$$

The *disconnected* diagrams can be removed by taking the logarithm of this expansion[2] [422]. Indeed, we define the following subset of diagrams appearing in Ξ: $\mathcal{E} = \{\text{connected diagrams}\} \cup \{\bullet\}$. Any diagram Γ in Ξ is composed of the product of $\mathcal{N}$ subdiagrams in the subset $\mathcal{E}$, and is uniquely characterized by the number of times n_i each subdiagram $\gamma_i \in \mathcal{E}$ appears (we identify the diagrams and their value). Its value is thus a function $\Gamma(n_1, \ldots, n_{\mathcal{N}})$. To evaluate it, we need its symmetry number: it is given by the symmetry numbers of the subdiagrams that composes it and the number of permutations of each subdiagram. Therefore

$$S_\Gamma = \prod_{i=1}^{\mathcal{N}} \left[n_i! (S_{\gamma_i})^{n_i} \right]$$

$$\Gamma(n_1, \ldots, n_{\mathcal{N}}) = \frac{\prod_{i=1}^{\mathcal{N}} \gamma_i^{n_i}}{\prod_{i=1}^{\mathcal{N}} n_i!} \quad (2.7)$$

To recover all the diagrams in the expansion (2.6) we need to sum over all possible sets of integers and get:

$$\Xi = \exp\left(\sum_{\gamma_i \in \mathcal{E}} \gamma_i \right) \quad (2.8)$$

Hence

$$\ln \Xi = \text{} + O(z^5) \quad (2.9)$$

2.1.2   Legendre transform

The partition function gives the one- and two-particle distribution functions [199], used in the following chapters:

$$\rho(r) = \left\langle \sum_{i=1}^{N} \delta(r - r_i) \right\rangle_\Xi = z(r) \frac{\delta \ln \Xi}{\delta z(r)}$$

$$\rho^{(2)}(r, r') = \left\langle \sum_{i \neq j}^{1, N} \delta(r - r_i) \delta(r' - r_j) \right\rangle_\Xi = -2 \frac{\ln \Xi}{\beta V(r, r')} \quad (2.10)$$

where $\langle \bullet \rangle_\Xi$ are grand-canonical averages using (2.2). For now $\ln \Xi$ is a functional of the activity and the potential through the Mayer function. The first line of (2.10) shows[3] that we can express it in terms of the local particle density $\rho(r)$ instead of $\ln z(r)$ through a Legendre transform[4] $\ln z \leftrightarrow \rho$:

$$\begin{cases} \ln Z[\rho, f] = \ln \Xi[\ln z^*[\rho], f] - \displaystyle\int_1 \rho(1) \ln z^*[\rho](1) \\[2mm] z^*[\rho] \text{ defined by} \quad \left. \dfrac{\delta \ln \Xi[\ln z, f]}{\delta \ln z(r)} \right|_{z=z^*[\rho]} = \rho(r) \end{cases} \quad (2.11)$$

---

[2]This is an instance of the *linked-cluster theorem.*

[3]Together with convexity properties of the grand potential, so that there is a one-to-one correspondence between $\ln z$ and the *slope* ρ [421].

[4]The Legendre transform is called $\ln Z$ because it is exactly [86, 132] the same Legendre transform to go from the grand-canonical ensemble to the canonical one in homogeneous systems, with $\ln \Xi = \ln Z - \beta \mu N$.

Let us perform the Legendre transform by functionally deriving (2.9) with respect to z. This step will have the effect of resumming an infinite class of diagrams. In the following, we explicitly do this for the Mayer series up to diagrams with three links f and then generalize the result:

$$\ln \Xi = \bullet + \bullet\!-\!\bullet + \diagram + \diagram + \diagram + \diagram + O(f^4) \qquad (2.12)$$

The functional derivative $\delta \ln \Xi / \delta z(1)$ amounts to derive with respect to the vertices, and has the effect of generating, through the product rule, each diagram in (2.12) with a white dot[5] representing the factor 1 instead of any one of the black dots z. This white dot means no factor but imposes the value of the position 1 at this link, *i.e.* $f(1, \bullet)$. For the single circle, the value is just the number $\int_2 \delta z(2)/\delta z(1) = \int_2 \delta(1-2) = 1$. Therefore from (2.10):

$$\frac{\rho(1)}{z(1)} = 1 + \diagram + \diagram + \diagram + \diagram + \diagram + \diagram + \diagram + \diagram + O(f^4) \quad (2.13)$$

We multiply each side by $z(1)$ to get

$$z(1) = \rho(1) - \diagram - \diagram - \diagram - \diagram - \diagram - \diagram - \diagram - \diagram + O(f^4) \quad (2.14)$$

where $\textcircled{z}$ means a $z(1)$ vertex. Inverting this expression will help us replacing the z vertices by ρ vertices.

By definition of the Legendre transform (2.11),

$$\frac{\delta \ln Z[\rho, f]}{\delta \rho(r)} = \frac{\delta \ln \Xi[z^*[\rho], f]}{\delta \rho(r)} - \int_1 \rho(1) \frac{\delta \ln z^*[\rho](1)}{\delta \rho(r)} - \ln z^*[\rho](r)$$

$$= \int_1 \frac{\delta \ln z^*[\rho](1)}{\delta \rho(r)} \frac{\delta \ln \Xi[z, f]}{\delta \ln z(1)} \bigg|_{z=z^*[\rho]} - \int_1 \rho(1) \frac{\delta \ln z^*[\rho](1)}{\delta \rho(r)} - \ln z^*[\rho](r) \qquad (2.15)$$

$$\Leftrightarrow \frac{\delta \ln Z[\rho, f]}{\delta \rho(r)} = - \ln z^*[\rho](r)$$

we wish to find the expansion of $\ln z$ and then integrate it with respect to ρ to get the functional $\ln Z[\rho, f]$. Taking the logarithm of (2.13) has a similar effect to suppressing the disconnected diagrams in §2.1.1. Indeed, all diagrams in the expansion (2.13) in which the white dot is an *articulation circle*, *i.e.* a vertex which disconnects the diagram upon removal, are products of subdiagrams of the series. With the same argument than in §2.1.1, taking the logarithm[6] suppresses these diagrams in which the white dot is an articulation circle. Hence

$$- \ln z(1) = - \ln \rho(1) + \diagram + \diagram + \diagram + \diagram + \diagram + O(f^4) \qquad (2.17)$$

Then one uses (2.14) to replace, order by order in f, the z vertices by ρ ones in (2.17). In doing so one sees that the diagrams with articulation circles, be them black or white, are suppressed[7], so that:

$$- \ln z(1) = - \ln \rho(1) + \diagram + \diagram + O(f^4) \qquad (2.18)$$

The diagrams appearing in (2.18) are all the connected diagrams with one white vertex $\textcircled{1}$, black (*i.e.* summed over) ρ vertices and bonds f, which have no articulation circles.

---

[5] The symmetry factor keeps the same definition; for example it is $S = 3!$ for $\diagram$ but $S = 2$ for $\diagram$ since it only affects the black dots, enabling for the factor 3 due to deriving with the product rule.

[6] One can also see it in this way, with this *small f* expansion: the formula

$$\ln(1 + x) = \sum_{p=1}^{\infty} \frac{(-1)^p}{p} x^p \qquad (2.16)$$

cancels, order by order in f, the diagrams that are products of others. The factors $1/p$ take care of the symmetry factor discrepancies between the product of subdiagrams and the diagram suppressed.

[7] A diagrammatic proof of this is in [199, 293].

Finally, evaluating (2.18) in the *extremum* $z = z^*[\rho]$ defining uniquely the Legendre transform, using (2.15) and integrating it with respect to $\rho(1)$, which has the inverse effect on diagrams than derivation (as in (2.12)→(2.13)), *i.e.* replacing the white 1 dots by black dots, we find:

$$
\begin{aligned}
\ln Z[\rho, f] &= \ln \Xi[z^*[\rho], f] - \int_1 \rho(1) \ln z^*[\rho](1) \\
&= \int_1 \rho(1)[1 - \ln \rho(1)] + \text{⬤—⬤} + \text{△} + \text{▢} + \text{◩} + \text{⊠} + \dots
\end{aligned}
\tag{2.19}
$$

The integration constant is fixed with the ideal gas case where $f = 0$. From (2.2) one has the usual ideal gas value of the grand-canonical partition function:

$$
\Xi[z, f = 0] = \exp\left(\int_1 z(1) \right)
\tag{2.20}
$$

then (2.18) gives $z^*[\rho] = \rho$ in the ideal gas case. Therefore, by definition of the Legendre transform (2.11)

$$
\ln Z[\rho, f = 0] = \int_1 \rho(1)[1 - \ln \rho(1)]
\tag{2.21}
$$

which tells us that the integration constant is zero.

Equation (2.19) is the so-called virial expansion. The series is composed of all the connected diagrams with ρ (full) vertices and f bonds that contain no articulation circle[8], *i.e.* that do not disconnect upon removal of a vertex.

2.2 The virial expansion of Hard-Sphere liquids in high dimension

Having introduced the virial series in (2.19), we now summarize the arguments of Frisch, Percus, Rivier and Wyler in [162, 258, 164, 409, 163, 161] who have extensively studied the virial series of the HS system in high dimension, and shown that in this limit the series is dominated by its first term, in a wide range of (scaled) densities. The Mayer function for HS of diameter σ is translation and rotation invariant and reads

$$
f_{\text{HS}}(x, y) \equiv f_{\text{HS}}(x - y) = -\theta(\sigma - |x - y|)
\tag{2.22}
$$

with θ the Heaviside step function. We drop the HS label in this section.

The reason why one expects the limit $d \to \infty$ to become simple is common to many other fields of physics, *e.g.* ferromagnetic systems [178] or strongly correlated electrons [179]. Consider a particle 1 interacting with, amongst others, two particles 2 and 3; what can we say about the interaction between 2 and 3? In order that 2 and 3 interact, if the forces have finite range, we need 1,2,3 in *contact* (defined by the range of interaction, here the particle diameter σ, but a generalization is done in §5.2) with each other, forming a closed chain ①②③ . This is the meaning of the one-loop *triangle* diagram with three ρ nodes △ : it is proportional to the probability that 3 given spheres overlap[9] and computes the number of triplet of particles that overlaps (if the centers are thrown randomly with a flat distribution) in the thermodynamic limit. Now, the number of configurations for which 2–1–3 form an open chain ②①③ in $d = \infty$ is overwhelmingly larger than those in which 2–1–3 close a chain: we conclude that in $d \to \infty$, 2 and 3 may be considered non-interacting. Again, this closed chain is the analog of the *tree diagram* ⋀ and has a similar probabilistic interpretation (two spheres among three overlap). The probability of such a configuration is dominated in $d \to \infty$ by the ones where 2–1–3 are orthogonal:

---

[8]In the context of quantum field theory for example, these connected diagrams are called *one-particle irreducible diagrams*.

[9]This probability is

$$
\frac{(-1)^3 \int_{123} f_{\text{HS}}(1, 2) f_{\text{HS}}(2, 3) f_{\text{HS}}(1, 3)}{\mathcal{V}^3}
\tag{2.23}
$$

$\overset{\textcircled{2}}{\underset{\textcircled{1}\textcircled{3}}{}}$, which can be seen easily from the fact that the hyperspherical measure defined below (2.26) is in this case dominated by putting 3 at the *equator* of the axis 1–2. The high-dimensional limit therefore corresponds to a mean-field approximation in the sense that the network of interactions is tree-like. This simple observation led to the exact solution of liquid equilibrium in $d \to \infty$ [162, 409, 161].

We introduce first some notations: the d-dimensional volume of a ball of radius R is

$$\mathcal{V}_d(R) = \frac{\Omega_d}{d} R^d = \frac{\pi^{d/2}}{\Gamma(1 + d/2)} R^d \tag{2.24}$$

where Γ is the Euler gamma function and Ω_d is the d-dimensional solid angle, needed for isotropic integrands. Indeed, we will sometimes resort to hyperspherical coordinates. In d dimensions, if $x = (x^1, \ldots, x^d)$ denotes usual Cartesian coordinates, they are defined by the change of variables $x = (r, \theta_1, \ldots, \theta_{d-1})$ where

$$\begin{cases} r = |x| = \sqrt{(x^1)^2 + \cdots + (x^d)^2} \\ x^1 = r \cos \theta_1 \\ x^2 = r \sin \theta_1 \cos \theta_2 \\ \quad \vdots \\ x^d = r \sin \theta_1 \cdots \sin \theta_{d-2} \cos \theta_{d-1} \end{cases} \tag{2.25}$$

with the Euler angles $\theta_{d-1} \in [0, 2\pi[$, $\theta_{\mu \neq d-1} \in [0, \pi]$. The measure is

$$\mathrm{d}x \equiv \prod_{\mu=1}^{d} \mathrm{d}x^\mu = r^{d-1} \sin^{d-2} \theta_1 \sin^{d-3} \theta_2 \cdots \sin \theta_{d-2} \, \mathrm{d}r \prod_{\mu=1}^{d-1} \mathrm{d}\theta_\mu \tag{2.26}$$

If we integrate the position of a vector x with respect to a fixed reference vector y, due to isotropy we only need to describe x by its norm r and the angle θ_1 between x and y (the other angles may be integrated away). From (2.26), we remark that when $d \to \infty$ the direction of x concentrates on the *equator* with $\theta_1 = \pi/2$ since other angles give vanishingly small contributions. This observation will be applied many times in the rest of this thesis.

Note that by definition[10]

$$\Omega_d \equiv 2\pi \int_{[0,\pi]^{d-2}} \mathrm{d}\theta_1 \ldots \mathrm{d}\theta_{d-2} \, \sin^{d-2} \theta_1 \sin^{d-3} \theta_2 \cdots \sin \theta_{d-2} \tag{2.27}$$

which is given in appendix A.

In the spirit of [409], we focus on the first two terms with two and three vertices. In the equilibrium liquid phase, due to translation invariance the density is uniform *i.e.*

$$\rho(r) = \rho = \frac{N}{\mathcal{V}} \tag{2.28}$$

These first two diagrams are thus:

$$\begin{aligned} \bullet\!\!-\!\!\bullet &= \frac{\rho^2}{2} \int \mathrm{d}x \mathrm{d}y \, f(x - y) = \frac{N\rho}{2} \int \mathrm{d}r f(r) = -\frac{N}{2} \rho \mathcal{V}_d(\sigma) \\ \triangle &= \frac{\rho^3}{3!} \int \mathrm{d}x \mathrm{d}y \mathrm{d}z \, f(x-y) f(y-z) f(x-z) = \frac{N\rho^2}{3!} \int \mathrm{d}r_1 \, f(r_1) \int \mathrm{d}r_2 \, f(r_2) f(r_1 - r_2) \\ &= -\frac{N\rho^2}{3!} \int_{B(0,\sigma)} \mathrm{d}r_1 \int_{B(0,\sigma) \cap B(r_1,\sigma)} \mathrm{d}r \end{aligned} \tag{2.29}$$

with $B(x, \sigma)$ the ball of center located at x and radius σ. For the triangle term we have to compute the the volume of the intersection of two balls of radius σ in high d. This intersection is composed of the volume of two identical *hyperspherical caps*, see figure 2.1. To compute the volume of the hyperspherical cap, we have to sum, for all angles θ from θ_m to zero with $\cos \theta_m = r_1/2\sigma$, the infinitesimal volume made of a basis which is a $d - 1$-dimensional hypersphere of radius $\sigma \sin \theta$ with a height element $\mathrm{d}(\sigma \cos \theta)$,

$$\frac{1}{2} \int_{B(0,\sigma) \cap B(r_1,\sigma)} \mathrm{d}r = \int_{\theta_m}^{0} \mathrm{d}(\sigma \cos \theta) \mathcal{V}_{d-1}(\sigma \sin \theta) = \mathcal{V}_{d-1}(\sigma) \sigma \int_{0}^{\theta_m} \mathrm{d}\theta \, \sin^d \theta \tag{2.30}$$

---

[10]We frequently make use of $\int_{\mathbb{R}} \mathrm{d}x \, \bullet = \Omega_d \int_{0}^{\infty} \mathrm{d}r \, r^{d-1} \bullet$ for an isotropic integrand.
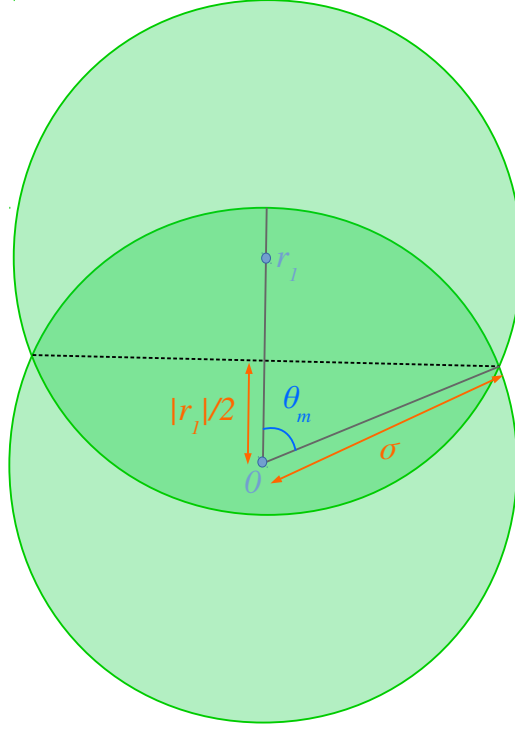
Figure 2.1: Notations for the computation of the overlap between two hyperspheres $B(0, \sigma) \cap B(r_1, \sigma)$.

Coming back to (2.29):

$$
\begin{aligned}
\vcenter{\hbox{\includegraphics{triangle}}} &= \frac{N\rho^2}{3!} \mathcal{V}_{d-1}(\sigma)\sigma \int_0^\sigma \mathrm{d}s\, \Omega_d s^{d-1} \int_0^{\arccos(s/2\sigma)} \mathrm{d}\theta\, \sin^d\theta \\
&\underset{\cos\alpha \equiv s/2\sigma}{=} \frac{N\rho^2}{3!} \mathcal{V}_{d-1}(\sigma)\sigma^{d+1} 2^d \Omega_d \int_{\frac{\pi}{3}}^{\frac{\pi}{2}} \mathrm{d}\alpha\, \sin\alpha \cos^{d-1}\alpha \int_0^\alpha \mathrm{d}\theta\, \sin^d\theta \\
&= \frac{N\rho^2}{3!} \mathcal{V}_{d-1}(\sigma)\sigma^{d+1} 2^d \frac{\Omega_d}{d} \left(-\left[\cos^d\alpha \int_0^\alpha \mathrm{d}\theta\, \sin^d\theta\right]_{\frac{\pi}{3}}^{\frac{\pi}{2}} + \int_{\frac{\pi}{3}}^{\frac{\pi}{2}} \mathrm{d}\alpha\, \cos^d\alpha \sin^d\alpha \right) \\
&= \frac{N\rho^2}{3!} \mathcal{V}_d(\sigma)\mathcal{V}_{d-1}(\sigma)\sigma \left[\int_0^{\frac{\pi}{3}} \mathrm{d}\theta\, \sin^d\theta + \int_{\frac{\pi}{3}}^{\frac{\pi}{2}} \mathrm{d}\theta\, 2^d \cos^d\theta \sin^d\theta \right]
\end{aligned}
\tag{2.31}
$$

The last integral can be written as

$$
\int_{\frac{\pi}{3}}^{\frac{\pi}{2}} \mathrm{d}\theta\, \sin^d(2\theta) \underset{2\theta \equiv \pi - \alpha}{=} \frac{1}{2} \int_0^{\frac{\pi}{3}} \mathrm{d}\alpha\, \sin^d\alpha
\tag{2.32}
$$

so that

$$
\vcenter{\hbox{\includegraphics{triangle}}} = \frac{N\rho^2}{3!} \mathcal{V}_d(\sigma)\mathcal{V}_{d-1}(\sigma) \frac{3\sigma}{2} \int_0^{\frac{\pi}{3}} \mathrm{d}\theta\, \sin^d\theta
\tag{2.33}
$$

Note that the last integral is bounded by
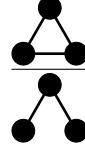
$$
\int_0^{\frac{\pi}{3}} \mathrm{d}\theta\, \sin^d\theta \leqslant \frac{\pi}{3} \left(\frac{\sqrt{3}}{2} \right)^d
\tag{2.34}
$$

Comparing with the tree diagram of same order

$$
\vcenter{\hbox{\includegraphics{tree}}} = \frac{1}{2} N [\rho \mathcal{V}_d(\sigma)]^2
\tag{2.35}
$$

we thus have an exponentially decreasing factor α^d with $\alpha < 1$ (here $\alpha = \sin(\pi/3)$) due to the value of the angle $\pi/3$ and the Wallis-like integral in (2.33) (here we give the exact value computed in [409], but

the bound (2.34) will be enough in the following argument):
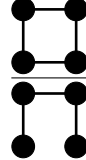
$$\underset{d\to\infty}{\sim} \frac{3}{4}\sqrt{\frac{3e}{2\pi d}}\left(\frac{\sqrt{3}}{2}\right)^{d} \tag{2.36}$$

Similarly, with diagrams of order 4, where the tree diagram

$$= N[\rho\mathcal{V}_d(\sigma)]^3 \tag{2.37}$$

one has [409, Appendix B]:

$$< \kappa d^{3/2}\left(\frac{4}{3^{3/2}}\right)^d\left[1+O\left(\frac{1}{d}\right)\right] \tag{2.38}$$

where κ is a numerical constant of order 1. Once again there is an exponential damping factor α^d where α is smaller than the third order diagram one in (2.36); indeed note that $\sqrt{3}/2 \simeq 0.87$ and $4/3^{3/2} \simeq 0.77$. If we look to the other diagrams of order 4 in (2.19), they have more bonds hence necessarily more constraints which means that they are bounded by this *ring diagram*: for example the simplest two-loop diagram verifies

$$< \tag{2.39}$$

but it remains of the same exponential order $\sim (4/3^{3/2})^d$ [409, Appendix C].

We can state a generalization of this fact: each diagram of order n (*i.e.* with n vertices) scales roughly as the prefactor $N[\rho\mathcal{V}_d(\sigma)]^{n-1}$ where N is a consequence of extensivity, times an exponential damping factor α^d with $\alpha < 1$, the higher the order n the smaller α, as if the *effective angle* (which is $\pi/3$ for $n = 3$) was decreased. An obvious bound for a closed loop diagram with n vertices (other than the prefactor $N[\rho\mathcal{V}_d(\sigma)]^{n-1}$), writing it as we did for $n = 3$ in (2.29), is $d^k(\sqrt{3}/2)^{d\lfloor n/2\rfloor}$ with $k = O(1)$ because the integration over alternating variables in the analog of (2.29) involves $\lfloor n/2\rfloor$ hyperspherical overlaps, each of which is bounded by $\theta_m \sin^d \theta_m$ (see (2.30) and (2.31)). The subexponential factor comes from the hyperspherical basis in dimension less than d (compared to the d-dimensional factor $\mathcal{V}_d(\sigma)$) [409]. Note also, for a general diagram, that an overlap (approximately spherical for simplicity) with a radius R smaller than another one has an exponentially damped volume in comparison due to dimension (*i.e.* due to the factor R^d).

Let us now recap. Defining the packing fraction φ of HS of diameter σ:

$$\varphi = \frac{N\mathcal{V}_d(\sigma/2)}{\mathcal{V}} \tag{2.40}$$

we saw that

$$\rho\mathcal{V}_d(\sigma) = 2^d\varphi = \widetilde{\varphi} \tag{2.41}$$

is the natural parameter of the HS virial expansion. If $\widetilde{\varphi}$ scales such that it tends to zero for $d \to \infty$ the expansion is trivially dominated by the ideal gas term. This means that densities or packing fraction that are weaker than the corresponding scaling describe an ideal gas regime. Note that due to the peculiarity of the spherical geometry in high dimension where the volume of a hypersphere is exponentially small[11], if $\widetilde{\varphi} = O(1)$ (or $\varphi = O(1)$) the density is already exponentially high. This is why in the following chapters we will scale the densities as
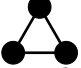
$$\rho(x) \sim e^{d\Omega(x)} \tag{2.42}$$

---

[11] This fact does not correspond to our usual low-dimensional thinking. On the one hand the definition of spheres implies that all pairs of points within it are closer than a certain distance, which corresponds to an intuition of *proximity* and might be suitable for defining volumes, but in high d their volume *with respect to hypercubes* is ridiculously small; on the other hand, our usual definition of volumes relies on hypercubic objects that are simple to manipulate (and tile space easily) but their geometry have *pathologies* with respect to our low-dimensional idea of volume. Indeed between two *diagonal* points of a unit hypercube, say $(0,\dots,0)$ and $(1,\dots,1)$, the distance is $\sqrt{d}$ which diverges in $d \to \infty$, and thus this volume does not enjoy this intuition of *proximity*.

The meaning of the x dependence will be precised in chapters 3 and 4.

From (2.21) at uniform density, the ideal gas free energy is[12] $\beta F_{\mathrm{IG}}/N = 1 - \ln\rho$. For ideal gas regimes such that (2.42) holds, the free energy is of order $O(d)$. Therefore the first virial correction to the ideal gas regime comes when its first term ●—● is $O(d)$, meaning that

$$\varphi = \frac{d}{2^d}\widehat{\varphi} \tag{2.43}$$

with $\widehat{\varphi} = O(1)$. This is the scaling that we will focus on in the following where non-trivial liquid or even glassy behaviour may appear. Note that, although in this regime the parameter $\widetilde{\varphi} = O(d)$, the virial expansion is dominated by its first interaction term ●—● due to the α^d ($\alpha < 1$) prefactors of the other terms. One needs to go to exponentially high $\widetilde{\varphi}$ to feel the effect of the triangle term ◭ and so on.

This argument holds only if one can interchange the limit $d \to \infty$ and the sum of the virial series, that is, if the number of diagrams at order n in (2.19) do not grow too fast with n. This is the case and one can show [161] that this truncation holds at least up to densities such that $\widetilde{\varphi} \sim (e/2)^{d/2}$, which is exponentially denser than what we will consider in the following.

Note that the density scaling (2.41) had already been obtained by Kirkpatrick and Wolynes [225] through a phenomenological study of the glass transition of HS liquids in high dimension aiming at making a connection between MCT and Dynamical Field Theory, using a Gaussian approximation for the local particle density, in a spirit similar to [243, 242]. It has then been proved in the glassy statics of infinite-dimensional HS in [243, Eq. (65)], see §3.3.2 for a discussion.

We conclude that, in these ranges of density, the HS liquid free-energy is given by

$$\ln Z = \int_1 \rho(1)[1 - \ln\rho(1)] + \frac{1}{2}\int_{12} \rho(1)\rho(2)f(1,2)$$
$$\Longleftrightarrow \frac{\ln Z_{\mathrm{HS}}}{N} = 1 - \ln\rho - \frac{\rho\mathcal{V}_d(\sigma)}{2} \tag{2.44}$$

For future needs, we rewrite it in this way and derive the equilibrium reduced pressure [162, 161]

$$\frac{\beta F}{N} = \ln\rho - 1 - \frac{\rho}{2}\int dr\left(e^{-\beta V(r)} - 1\right)$$
$$\frac{\beta P}{\rho} = \rho\frac{\partial(\beta F/N)}{\partial\rho}\Big|_T = 1 - \frac{\rho}{2}\int dr\left(e^{-\beta V(r)} - 1\right) \tag{2.45}$$

Specializing to HS unaffected by temperature, one has

$$\frac{\beta F_{\mathrm{HS}}}{N} = \ln\rho - 1 + \frac{\rho}{2}\mathcal{V}_d(\sigma)$$
$$\frac{\beta P_{\mathrm{HS}}}{\rho} = 1 + \frac{\rho}{2}\mathcal{V}_d(\sigma) \tag{2.46}$$

In this case where the only parameter is the density, the volumic free energy is thus $-\ln Z_{\mathrm{HS}}/\mathcal{V} = \rho\ln\rho - \rho + \rho^2\mathcal{V}_d(\sigma)/2$. This free energy has a single minimum directly set by the volume of the spheres. There is no sign of a phase transition:

- to a gas phase. Indeed, for HS the liquid and gas phases are equivalent, there is just a dilute or dense system according to the value of the packing fraction. One needs to study another potential with an attractive tail to observe the usual first-order liquid-gas phase transition (such as the Lennard-Jones potential). This potential would be affected by temperature.

- to a crystal phase, which is perfectly fine since one assumes from the start a homogeneous phase, not suitable to investigate the emergence of a crystalline order.

- to a possible ideal glass phase, presented in §1.2.4. Here again the homogeneity assumption is the reason why one cannot observe it from (2.46). It would correspond to a high-temperature *paramagnetic* phase in the Curie-Weiss model. From §1.2.2, one concludes that *e.g.* a TAP-like computation [7] for a non-homogeneous system is required in order to detect a glassy phase. This

---

[12]The usual additional factor $\ln(\Lambda^d)$ is not there because we stored it in the activity (2.2), hence in the chemical potential that is substracted here by Legendre transform.

might be also inferred by minimizing the free energy in the first equation of (2.44) for an inhomogeneous density profile. The similar strategy of benefiting from replica theory (see §1.2.4.2 and §2.3) will be put to work to this end in chapter 4.

As a final remark, one may study deviations to the uniform liquid phase with $\rho(x) = \rho$ by performing a linear stability analysis of (2.44). Unstable modes develop at high enough packing fraction [163], leading to the Kirkwood instability [228, 270]. We will not be concerned by this issue since it lies well beyond the density regime we will focus on in the following chapters.

2.3 Statics and the replica method: example of the spherical p-spin glass model

The derivation of static and dynamic properties of liquids and *structural* glasses being generally more involved than the corresponding computations for their quenched disordered cousins, the *spin* glasses, we here compute the static free energy of the p-spin spherical model, one of the simplest spin glass models. Note that the even simpler Random Energy Model introduced by Derrida in [129, 130] is also very instructive. This allows to introduce the replica method and the replica-symmetry-breaking phases. This computation is instructive and we will only repeat similar steps in the next chapters. We here follow a similar presentation to the very pedagogical reviews [81, 417].

The p-spin spherical model ($p \geqslant 3$) is defined by the Hamiltonian of N interacting *real* continuous spins $\sigma = (\sigma_1, \ldots, \sigma_N)$

$$H_J[\sigma] = - \sum_{i_1 < \cdots < i_p}^{1,N} J_{i_1,\ldots,i_p} \sigma_{i_1} \ldots \sigma_{i_p} \tag{2.47}$$

with the spherical constraint [109]

$$\sigma \cdot \sigma = \sum_{i=1}^{N} \sigma_i^2 = N \tag{2.48}$$

We denote by $\sigma \cdot \tau = \sum_i \sigma_i \tau_i$. These spins are different from the usual Ising-like spins taking discrete values [129, 130, 192], and the reason of their introduction, together with the spherical constraint, is the simplicity of computations[13]. The couplings $J_{i_1,\ldots,i_p}$ are independent identically distributed Gaussian random variables with zero mean and variance

$$\overline{J^2} = \frac{p!}{2N^{p-1}} \tag{2.49}$$

needed to ensure an extensive $O(N)$ Hamiltonian. We note its measure $\mathcal{D}J$. The physical justification of such a quenched disorder is that some variables of the system, here the couplings[14], evolve on a much longer timescale than the variables we are interested in here (the spins). This model is mean-field because it is *fully connected*: each spin interacts with every other spin, thus with a great number of them, justifying usual mean-field assumptions.

The partition function of the system reads

$$Z[J] = \int \mathrm{D}\sigma \, e^{-\frac{\beta\mu}{2}(\sigma\cdot\sigma - N) - \beta H_J[\sigma]} \tag{2.50}$$

where μ is a Lagrange multiplier enforcing the spherical constraint (2.48). The free energy of the model is a *self-averaging* quantity[15], meaning that in the thermodynamic limit it is independent of the particular realization of the quenched disorder [81, 279]. We thus can average over the disorder, which simplifies the computation, to get the physical value of an observable.

---

[13]See also the spherical $O(N)$ model as an example [34, 28, 294].

[14]Modelling *e.g.* interactions with impurities.

[15]In finite-dimensional systems this is a consequence of short-ranged interactions and the central limit theorem, dividing the system in many independent subsystems.

2.3.1 Replicated partition function

In order to average the free energy, we make use of the *replica trick* [279, 81]:

$$\overline{\ln Z} = \lim_{n \to 0} \partial_n \overline{Z^n} \tag{2.51}$$

since, for integer n, averaging a product reduces to average directly the partition function of n independent systems, *i.e.* we just have to study the *moments* of Z. Then we assume an analytic continuation to 0 [279]. We call the n systems *replicas* of the original system.

The replicated partition function is, introducing nN spins $\bar{\sigma} = (\sigma^1, \dots, \sigma^n)$:

$$\overline{Z^n} = \int D\bar{\sigma} \, e^{-\frac{\beta\mu}{2} \sum_a (\sigma^a \cdot \sigma^a - N)} \overline{e^{-\beta \sum_a H[\sigma^a]}}$$

$$= \int D\bar{\sigma} \, e^{-\frac{\beta\mu}{2} \sum_a (\sigma^a \cdot \sigma^a - N)} \prod_{i_1 < \dots < i_p}^{1,N} \int DJ_{i_1,\dots,i_p} \exp \left[-J_{i_1,\dots,i_p}^2 \frac{N^{p-1}}{p!} + \beta J_{i_1,\dots,i_p} \sum_{a=1}^n \sigma_{i_1}^a \dots \sigma_{i_p}^a \right]$$

$$= \int D\bar{\sigma} \, e^{-\frac{\beta\mu}{2} \sum_a (\sigma^a \cdot \sigma^a - N)} \prod_{i_1 < \dots < i_p}^{1,N} \exp \left[\frac{\beta^2 p!}{4N^{p-1}} \sum_{a,b}^{1,n} \sigma_{i_1}^a \sigma_{i_1}^b \dots \sigma_{i_p}^a \sigma_{i_p}^b \right]$$

$$= \int D\bar{\sigma} \, \exp \left[-\frac{N\beta\mu}{2} \sum_{a=1}^n (Q_{aa} - 1) + \frac{\beta^2 N}{4} \sum_{a,b}^{1,n} (Q_{ab})^p \right] \tag{2.52}$$

where we used $p! \sum_{i_1 < \dots < i_p} = \sum_{i_1,\dots,i_p}$ in the thermodynamic limit and defined the *overlap matrix*, which measures how much configurations in two different replicas are similar [81, 417, 279]:

$$Q_{ab} = \frac{\sigma^a \cdot \sigma^b}{N} \tag{2.53}$$

We see that the integrand is a function of $\hat{Q}$ exclusively; we thus change variables $\bar{\sigma} \longleftrightarrow \hat{Q}$ with the identity[16]

$$1 = \int d\hat{Q} \prod_{a,b}^{1,n} \delta(NQ_{ab} - \sigma^a \cdot \sigma^b) = \int d\hat{Q} d\hat{\lambda} \, e^{\sum_{a,b} N\lambda_{ab} Q_{ab} - \lambda_{ab} \sigma^a \cdot \sigma^b} \tag{2.54}$$

The variables λ_{ab} lie on the imaginary axis. Inserting (2.54) in (2.52), the sites are decoupled and performing the Gaussian integration over $\bar{\sigma}$ we get

$$\overline{Z^n} = \int d\hat{Q} d\hat{\lambda} \, e^{NX(\hat{Q},\hat{\lambda})}$$

$$\text{with} \quad X(\hat{Q}, \hat{\lambda}) = \sum_{a,b}^{1,n} \left(\frac{\beta^2}{4} (Q_{ab})^p + \lambda_{ab} Q_{ab} \right) - \frac{1}{2} \ln \det(2\hat{\lambda}) - \frac{\beta\mu}{2} \sum_{a=1}^n (Q_{aa} - 1) \tag{2.55}$$

however now the replicas are coupled. The Gaussian integration brings additive constants (not depending upon $\hat{Q}, \hat{\lambda}$) to X (neglecting the $\sqrt{\det \hat{\lambda}}$ subdominant in N prefactor), which we do not write because they are irrelevant for our current purpose. Thanks to the fully-connected aspect of the model, we have a N factor in the exponent and can resort to a saddle-point evaluation of the integral, computing the maximum of the exponent. Doing so, we are exchanging the limits $N \to \infty$ and $n \to 0$, which may be problematic [81, 358]. The saddle-point equation for $\hat{\lambda}$ is $2\hat{\lambda} = \hat{Q}^{-1}$, therefore, neglecting irrelevant constants once more,

$$\overline{Z^n} = \int d\hat{Q} \, e^{N\mathcal{S}(\hat{Q})}$$

$$\frac{\overline{F}}{N} = -\frac{1}{\beta} \lim_{n \to 0} \partial_n \mathcal{S}(\hat{Q}^{\text{sp}})$$

$$\text{with} \quad \mathcal{S}(\hat{Q}) = \frac{\beta^2}{4} \sum_{a,b}^{1,n} (Q_{ab})^p + \frac{1}{2} \ln \det \hat{Q} - \frac{\beta\mu}{2} \sum_{a=1}^n (Q_{aa} - 1) \tag{2.56}$$

---

[16]This is similar to a Faddeev-Popov method in quantum field theory [149, 315, 422] and is a widely use method of changing variables [294, 365, 112, 81].

The saddle-point equation for $\hat{Q}$ is then

$$\frac{\beta^2}{2}p(Q_{ab})^{p-1} + Q_{ab}^{-1} - \beta\mu\delta_{ab} = 0 \qquad \Longleftrightarrow \qquad \beta\mu Q_{ab} = \delta_{ab} + \frac{\beta^2}{2}p\sum_{c=1}^{n}(Q_{ac})^{p-1}Q_{cb} \qquad (2.57)$$

Note that the last equation is similar to a MCT equation written in static terms (see (1.16)), with a memory kernal $(p/2)Q_{ab}^{p-1}$. This fact will be used to develop a dynamic-static analogy.

2.3.2 Replica-symmetric solution

A natural assumption is to think that replicas are indistinguishable and that $Q_{a\neq b}$ must not depend upon the replica indices. This is the *replica-symmetric* (RS) ansatz first proposed by Sherrington and Kirkpatrick (SK) in another spin glass model [358]:

$$Q_{ab}^{\mathrm{RS}} = (1-q_0)\delta_{ab} + q_0 \, , \qquad (Q^{\mathrm{RS}})_{ab}^{-1} = \frac{1}{1-q_0}\left(\delta_{ab} - \frac{q_0}{1+(n-1)q_0}\right) \qquad (2.58)$$

Putting it into (2.57) provides on the off-diagonal and diagonal elements respectively the Lagrange multiplier and the parameter q_0, for $n \to 0$:

$$\beta\mu = \frac{\beta^2 p}{2} + \frac{1-2q_0}{(1-q_0)^2}$$

$$\frac{\beta^2 p}{2}q_0^{p-1} - \frac{q_0}{(1-q_0)^2} = 0 \quad \Leftrightarrow \quad q_0 = 0 \quad \text{or} \quad q_0^{p-2}(1-q_0)^2 = \frac{2T^2}{p} \qquad (2.59)$$

The RS solution $q_0 = 0$ is always a solution and corresponds to the paramagnetic solution $Q_{ab} = \delta_{ab}$ where different replicas are totally uncorrelated, hence their overlap is zero. The free energy[17] is $\overline{F_{\mathrm{PM}}}/N = -\beta/4$. It is the only solution at high temperature and is always stable [109]: remember that we must select solutions that are local maxima of $\mathcal{S}(\hat{Q})$ and here we have only applied the saddle point $\mathrm{d}\mathcal{S}/\mathrm{d}\hat{Q} = \hat{0}$ condition. Lowering the temperature two non-trivial solution appears $0 < q_0 < 1$ (and an extra negative one if p is even), and among them only one that decreases with T as one would expect, see figure 2.2. The free energy in this case can be easily calculated from (2.56). The determinant term can be computed using the formula[18], for an invertible matrix $\hat{\mathcal{M}}$:

$$\ln\det(\hat{\mathcal{M}} + \alpha\hat{I}^n) = \ln\det\hat{\mathcal{M}} + \ln\left(1 + \alpha\sum_{a,b}^{1,n}\mathcal{M}_{ab}^{-1}\right) \qquad (2.60)$$

with $\hat{I}^n$ the $n \times n$ matrix of all ones. The free energy is then

$$\frac{\overline{F_{\mathrm{RS}}}}{N} = -\frac{\beta}{4} + \frac{\beta}{4}q_0^p - \frac{1}{2\beta}\ln(1-q_0) - \frac{1}{2\beta}\frac{q_0}{1-q_0} \qquad (2.61)$$

For low temperatures this free energy is lower than the paramagnetic one if $q_0 < 0$ or in some intervals only for $q_0 > 0$, potentially signalling a (discontinuous) phase transition from the paramagnetic phase to a *spin glass* phase. *Yet*, these non-paramagnetic solutions are unstable [109, 121]. This hints to the fact that the low-temperature phase could be described by a *replica-symmetry-breaking* (RSB) ansatz.

2.3.3 One-step replica-symmetry-breaking solution

Several ways of breaking the replica permutation symmetry have been first proposed in the context of the SK model [358] by Bray and Moore [75], De Dominicis and Garel [123] and Blandin [66, 67] and but the correct one, mathematically proven twenty years afterwards by Talagrand [378], was given by

---

[17]The high-temperature case is called an *annealed* case because the disorder is irrelevant -one has $\overline{\ln Z} = \ln\overline{Z}$ and does not need to introduce replicas- and may be considered as a thermalized variable like the rest of the system, unlike a quenched disorder which evolves on different timescales [279, 81].

[18]A proof in the similar case of SUSY operators is in §2.4.5.3.
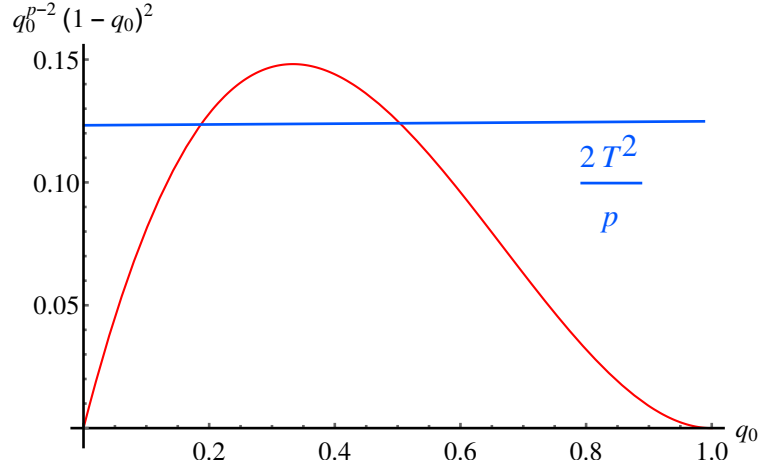
Figure 2.2: The non-trivial RS solutions for $p = 3$.

Parisi [303, 306, 307, 304, 305, 301] with the hierarchical ansatz:

$$
\hat{Q}^{1-\text{RSB}} =
\begin{pmatrix}
\begin{pmatrix} 1 & q_1 & q_1 \\ q_1 & 1 & q_1 \\ q_1 & q_1 & 1 \end{pmatrix} & & q_0 \\
& \ddots & \\
q_0 & & \begin{pmatrix} 1 & q_1 & q_1 \\ q_1 & 1 & q_1 \\ q_1 & q_1 & 1 \end{pmatrix}
\end{pmatrix}
\tag{2.62}
$$

where replicas are grouped in n/m *clusters* (blocks) of m replicas (in (2.62) we set $m = 3$); m and q_1 are additional parameters allowing to break the symmetry[19]. This ansatz can be described using the algebra of $n \times n$ hierarchical matrices: define a $n \times n$ matrix $\hat{I}^m$ which has elements $I^m_{ab} = 1$ in blocks of size m around the diagonal, and $I^m_{ab} = 0$ otherwise. Note that $\hat{I}^1$ is the identity matrix with $I^1_{ab} = \delta_{ab}$, and $\hat{I}^n$ is the matrix of all ones. Assuming that m_1 is a multiple of m_2 (hence $m_1 \geqslant m_2$), with $(m_1, m_2) \in [\![1, n]\!]^2$ we have

$$
\hat{I}^{m_1} \hat{I}^{m_2} = m_2 \hat{I}^{m_1}
\tag{2.63}
$$

The 1-RSB ansatz reads:

$$
\hat{Q}^{1-\text{RSB}} = q_0 \hat{I}^n + (q_1 - q_0) \hat{I}^m + (1 - q_1) \hat{I}^1
\tag{2.64}
$$

Let us compute the 1-RSB free energy with (2.56). The determinant is obtained through the formula (2.60) applied recursively on the blocks then on the whole matrix, and using the algebra (2.63) together with the definition of the inverse of the matrix (2.64) for inverting the blocks. We get

$$
\ln \det \hat{Q}^{1-\text{RSB}} = \frac{n(m-1)}{m} \ln(1 - q_1) + \frac{n}{m} \ln[1 - q_1 + m(q_1 - q_0)] + \ln \left[1 + n \frac{q_0}{1 - q_1 + m(q_1 - q_0)} \right]
$$

$$
\sum_{a,b}^{1,n} (Q^{1-\text{RSB}}_{ab})^p = n(n - m) q_0^p + n(m - 1) q_1^p + n
$$

$$
\tag{2.65}
$$

from which we derive the 1-RSB free energy:

$$
\frac{\overline{F_{1-\text{RSB}}}}{N} = -\frac{\beta}{4}[1 - q_1^p + m(q_1^p - q_0^p)] + \frac{1-m}{2\beta m} \ln(1 - q_1) - \frac{1}{2\beta m} \ln[1 - q_1 + m(q_1 - q_0)] - \frac{1}{2\beta} \frac{q_0}{1 - q_1 + m(q_1 - q_0)}
\tag{2.66}
$$

Note that the RS solution (2.61) is recovered when either $q_1 \to q_0$ or $m \to 1$. When $n \to 0$, the parameter m has also to be analytically continued, and a consistency check about the positivity of the probability distribution of overlaps gives $0 \leqslant m \leqslant 1$, *i.e.* the reversed of the original inequality $1 \leqslant m \leqslant n$ [279, 81].

---

[19]m is the same parameter as in the real replica method of §1.2.4.2.

Resorting to the Parisi ansatz amounts to apply a variational method to determine the solution of the problem: here we thus minimize the free energy, hoping the solution is within the *subspace* of solutions generated by the 1-RSB ansatz. We extremize (2.66): the equation $\partial_{q_0}\overline{F_{1-\mathrm{RSB}}} = 0$ admits $q_0 = 0$ as a natural solution in absence of a magnetic field, as in the RS case. The two other variational equations $\partial_{q_1}\overline{F_{1-\mathrm{RSB}}} = 0$ and $\partial_m\overline{F_{1-\mathrm{RSB}}} = 0$ are:

$$(1-m)\left(\frac{\beta^2 p}{2}q_1^{p-1} - \frac{q_1}{(1-q_1)[1+(m-1)q_1]}\right) = 0$$

$$\frac{\beta^2}{2}q_1^p + \frac{1}{m^2}\ln\left[\frac{1-q_1}{1-(1-m)q_1}\right] + \frac{q_1}{m[1-(1-m)q_1]} = 0$$

(2.67)

These equations can be solved numerically, but for the present discussion we look at a particular case only. Indeed, $m = 1$ solves the first equation, and then the other one reads

$$\frac{\beta^2}{2}q_1^p + \ln(1-q_1) + q_1 \equiv g(q_1) = 0$$

(2.68)

The situation is shown in figure 2.3. For $q_1 < 0$, $g(q_1) < 0$; $g(0) = 0$ while $q(1) \to -\infty$. At high temperatures only the RS solution $q_1 = 0$ is possible. At lower temperatures, the function develops a maximum which becomes zero at a temperature T_s, different from the one of the alleged RS transition in (2.59) or figure 2.2, and touches the horizontal axis at some $q_s > 0$. T_s is obtained from the study of the function g and reads [109, 237, 23]

$$T_s = y^*\sqrt{\frac{p(1-y^*)^{p-2}}{2y^*}}$$

with y^* defined by $\quad \dfrac{2}{p} = -2y^*\dfrac{1-y^*+\ln y^*}{(1-y^*)^2}$

(2.69)

Then this positive maximum increases with decreasing temperature, and the curve hits again the horizontal axis at some $q_1 \in]q_s, 1[$. $T = T_s$ is a thermodynamic transition temperature to a new *spin glass*
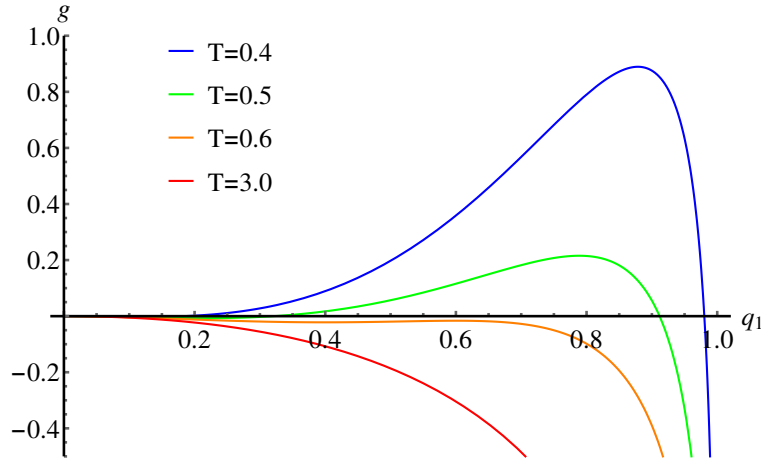
Figure 2.3: The function $g(q_1)$ for $p = 3$ and $T = 0.4, 0.5, 0.6, 3.0$.

phase with overlap q_s and $m = 1$. The transition is discontinuous because at T_s the overlap goes from 0 to a nonzero value q_s. Below T_s, m decreases and q_1 increases. It *is* a phase transition because the resulting phase is stable, unlike in the RS case, and the free energy becomes lower than the paramagnetic one [109]. The 1-RSB ansatz in this case is enough to find the exact solution, as it has been proven rigorously [378].

The meaning of this 1-RSB ansatz is the same as in §1.2.4.2: metastable states are well formed before the static transition, and this is detected by a stronger overlap between some replicas, that belong to the same state identified by being in the same block. They become true thermodynamically stable states at T_s. In the paramagnetic phase replicas are totally uncorrelated, there is no overlap between them, as in the RS solution.

As a final remark in the 1-RSB phase, we can compute *statically* the value of the *plateau* q_{EA} (or *Edwards-Anderson parameter* [141, 142] in the spin glass literature), with the help of *e.g.* the saddle-point equation (2.57), as we will do in §4.5.4. We need the inverse of the 1-RSB matrix; noting $(\hat{Q}^{1-RSB})^{-1} = a\hat{I}^n + b\hat{I}^m + c\hat{I}^1$, from the definition of the inverse $\hat{Q}\hat{Q}^{-1} = \hat{I}^1$ and using the algebra of 1-RSB matrices (2.63), we find

$$
\begin{aligned}
c &= \frac{1}{1-q_1} \\
b &= \frac{q_0 - q_1}{(1-q_1)[1 - q_1 + m(q_1 - q_0)]} \\
a &= -q_0 \frac{C + Bm}{1 + q_1(m-1) + q_0(n-m)} = -\frac{q_0}{1-q_1} \frac{1 + (m-2)q_1 + (1-m)q_0}{[1 + q_1(m-1) + q_0(n-m)][1 - q_1 + m(q_1 - q_0)]}
\end{aligned}
\tag{2.70}
$$

Then the first equation of (2.57) gives, for the outermost indices, an equation admitting $q_0 = 0$ as a solution, which we retain as before. The diagonal elements give the value of the Lagrange multiplier

$$
\beta\mu = \frac{\beta^2 p}{2} + a + b + c
\tag{2.71}
$$

and finally the values within a block give for $q_0 = 0$ and $m = 1$

$$
\frac{\beta^2 p}{2} q_1^{p-1} + a + b = 0 \qquad \underset{\substack{q_0 = 0 \\ q_1 \neq 0,1}}{\Leftrightarrow} \qquad q_1^{p-2}(1 - q_1) = \frac{2T^2}{p}
\tag{2.72}
$$

This equation gives the plateau value $q_1 = q_{EA}$ and the dynamical transition temperature (which is the highest-temperature point where the equation has a solution) as we shall see in the dynamical calculation from the MCT equation.

Note that this equation is of course very similar to the first one of (2.67), $\partial_{q_1} \overline{F_{1-RSB}} = 0$. However, the saddle-point equation (2.57) contains less information than the variational equations above, since it assumes that the optimization is made on the elements of the matrix but not on its size, which is (and must be) considered by the variational equations; in other words, the equation $\partial_m \overline{F_{1-RSB}} = 0$ is missing from this saddle-point equation.

2.3.4 Full replica-symmetry breaking

The spherical p-spin model exhibits a low-temperature 1-RSB phase, corresponding to states that are all equivalent, with a self-overlap q_1 *which is the same for all replicas in the same state*, and zero mutual overlap ($q_0 = 0$), which amounts to say that they are randomly distributed in phase space. However, in several spin-glass models, the low-temperature properties of the phase space are more complex, the states are not equivalent and can have non-zero overlaps. This is the case *e.g.* of the SK model [358, 417, 125, 279]. In this model, the same permutation-symmetry-breaking arises, the RS ansatz giving non-physical results such as a negative entropy and being unstable in a region of phase space [121, 56, 279, 125]. Although these issues are improved by plugging a 1-RSB ansatz instead, the entropy becoming less negative and the unstable mode of the stability matrix becoming smaller [125], they are not resolved. Then Parisi's solution consists in repeating iteratively this construction to get k-RSB ansätzes. One starts from the 1-RSB matrix and iterates this construction on the blocks, getting a 2RSB matrix, and so on. Thus a k-RSB matrix $\hat{Q}^{kRSB}$ is defined by its values $(q_0, \ldots, q_k)$ and the diagonal q_d, as well as the sequence of $k + 2$ integer parameters $1 \equiv m_k \leqslant m_{k-1} \leqslant \cdots \leqslant m_0 \equiv m \leqslant n$ which are multiples. For example at the 3RSB level we have n/m blocks of m replicas, each divided in m/m_1 blocks of m_1 replicas, themselves divided in m_1/m_2 blocks of m_2 replicas; from outermost to innermost the values are q_0, q_1, q_2, q_3 and finally q_d on the diagonal. The k-RSB matrices form a closed algebra from (2.63), generated by $\{\hat{I}^1, \hat{I}^{m_{k-1}}, \ldots, \hat{I}^{m_0}, \hat{I}^n\}$ and they read

$$
\hat{Q}^{kRSB} = \sum_{i=0}^{k} q_i(\hat{I}^{m_{i-1}} - \hat{I}^{m_i}) + q_d\hat{I}^1
\tag{2.73}
$$

where $m_{-1} \equiv n$. The matrices are left invariant by permutations of the indices belonging to a corresponding subgroup of the permutation group of n elements, as usual in spontaneous symmetry breaking [279]. A 3RSB matrix is shown in figure 2.4.
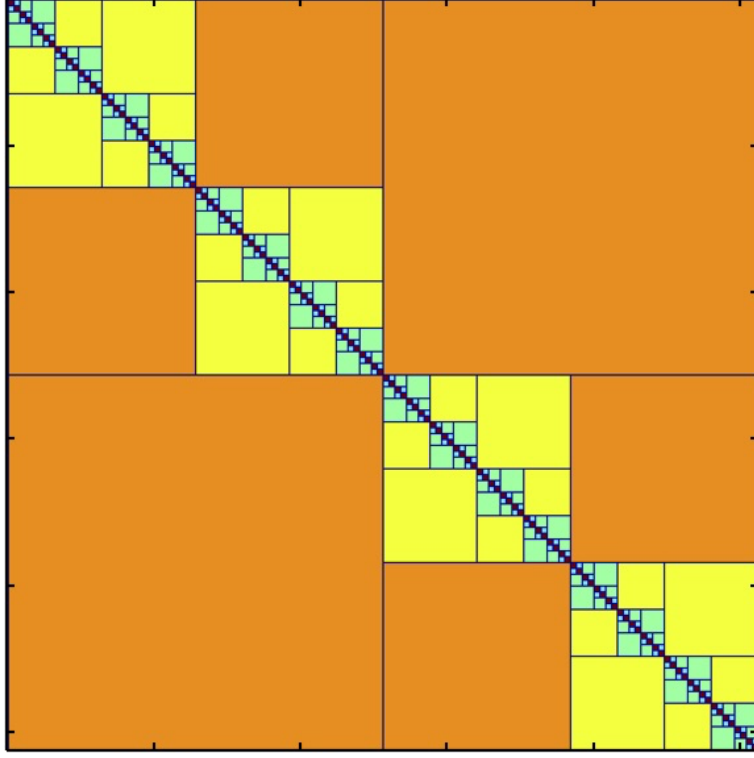
Figure 2.4: A 3RSB 128×128 matrix with $m_2 = 2$, $m_1 = 8$ and $m = 32$. The colors stand for the values of q_0, q_1, q_2, q_3 and q_d. [*From Harvard's mathematics department's website*]

The physical interpretation is the following: the pure states have an overlap q_k but are arranged in clusters of states that have a mutual overlap q_{k-1}, which themselves are arranged in superclusters of mutual overlap q_{k-2}, and so on. In the limit $k \to \infty$ the organization of the states becomes quite complex. An example of such a phase will be provided by large-dimensional structural glasses in §4.4.3; we refer to this section for a physical interpretation.

A further discussion of the structure of the states, called *ultrametric* in the related context of metric spaces, is found in [279].

This k-RSB scheme can be implemented through the introduction of a piecewise constant function that takes $\forall i \in [\![0, k]\!]$ the values q_i in the interval $]m_i, m_{i-1}[$. Then one has to give an analytic continuation of this function for $n \to 0$: similarly to the 1-RSB case, it appears that the inequalities between the m_i are reversed [279]: $0 \leqslant m = m_0 \leqslant \ldots m_{k-1} \leqslant 1$. The solution to finding the low-temperature phase of the SK model is obtained when iterating to infinity the k-RSB scheme, in which the piecewise constant function becomes any *reasonable* function (*e.g.* piecewise continuous) on the interval $[0,1]$: the hierarchical *matrix* is represented by $\{q_d, q(x)\}$ where $x \in [0, 1]$, q is the continuum limit of the piecewise constant function, and q_d is the diagonal value, missing in the values of the function [279]. This function now takes $\forall i \in [\![0, k]\!]$ the value q_i on the interval $]m_{i-1}, m_i[$. An example of such a function will be given in §4.4.3, and some aspects of the algebra of k-RSB matrices with zero diagonal are studied in §B.
Parisi's solution of the SK model has been checked numerically and was proven mathematically in 2006 by Guerra and Talagrand [194, 379].

For future needs, we give here some algebraic results about the construction of the continuum-limit function $q(x)$. Indeed the free energy must be written in terms of $\{q_d, q(x)\}$ and therefore one must write the continuum limit of its terms in the limit $n \to 0$. A very simple example is the following, where f is any continuous function $[-1, 1] \to \mathbb{R}$:

$$\frac{1}{n} \sum_{ab}^{1,n} f(Q_{ab}) = f(q_d) + \sum_{i=0}^{k-1} f(q_i)(m_{i-1} - m_i) \xrightarrow[\substack{n \to 0 \\ k \to \infty}]{} f(q_d) - \int_0^1 \mathrm{d}x \, f[q(x)] \tag{2.74}$$

the minus sign being due to the reversal of the inequalities, with which we defined the function q, with respect to the standard finite k k-RSB matrix.

The sum and product operations defining the ∞-RSB algebra are obtained in the same way. If $C = A + B$ with the *matrix C* represented by $\{c_d, c(x)\}$, $A \leftrightarrow \{a_d, a(x)\}$ and $B \leftrightarrow \{b_d, b(x)\}$, one has trivially

$$\begin{cases} c_d = a_d + b_d \\ c(x) = a(x) + b(x) \end{cases} \tag{2.75}$$

The diagonal parameter of the product $C = AB$ is:

$$\sum_{c=1}^{n} A_{ac} B_{ca} = a_d b_d + \sum_{i=0}^{k-1} a_i b_i (m_{i-1} - m_i) \xrightarrow[\substack{n \to 0 \\ k \to \infty}]{} a_d b_d - \int_0^1 \mathrm{d}x\, a(x) b(x) = a_d b_d - \langle ab \rangle \tag{2.76}$$

where $\langle a \rangle = \int_0^1 \mathrm{d}x\, a(x)$, and with a similar computation for $C_{ab} = \sum_{c=1}^{n} A_{ac} B_{cb}$, separating the cases in each sub-block, we get [304]

$$c(x) = a(x)(b_d - \langle b \rangle) + b(x)(a_d - \langle a \rangle) + \int_0^x \mathrm{d}y\, [a(x) - a(y)][b(x) - b(y)] \tag{2.77}$$

2.4 Dynamics: the supersymmetric formalism

2.4.1 Introduction

In this section we introduce the supersymmetric (SUSY) notation for our dynamical fields. The path integral formulation of the dynamics presented in next section employs an auxiliary field $\hat{\sigma}_i(t)$ for each spin $\sigma_i(t)$. One can encode both of them in a superfield

$$\boldsymbol{\sigma}_i(a) = \sigma_i(t) + \bar{\theta}\theta i \hat{\sigma}_i(t) \tag{2.78}$$

where $a = (t, \theta, \bar{\theta})$ and $(\theta, \bar{\theta})$ are Grassmann variables which are anticommuting. A Grassmann algebra is generated by the unit 1 and a number of anticommuting variables θ_i, *i.e.* $\forall(i,j)$, $\{\theta_i, \theta_j\} = 0$. This implies in particular that $\theta_i^2 = 0$ and all elements in the algebra are first degree polynomials in the generators θ_i. One can define a linear map, called derivation $\partial/\partial\theta$ or integration $\int \mathrm{d}\theta$, by selecting the θ coefficient (defined by convention, due to the anticommuting property, as being on the right of the variable θ) in this first degree polynomial, *i.e.* writing any element of the algebra uniquely as $(a + \theta b)$ where a and b are also elements of the algebra *that do not contain θ*, $\partial/\partial\theta(a + \theta b) = \int \mathrm{d}\theta(a + \theta b) = b$. A more detailed presentation is made *e.g.* in [422].

The formal technique of introducing superfields outside of high-energy physics [173] has received interest in condensed matter physics[20], *e.g.* in disordered metals and quantum chaotic systems [143]. In classical disordered systems, the SUSY formulation of the dynamics [302, 311] allows one to view equilibrium relations such as time-translation invariance or the fluctuation-dissipation theorem as consequence of a formal supersymmetry of the system [189, 236, 190, 112, 16, 422], which is broken in off-equilibrium regimes. This is emphasized in §2.5.3. It also simplifies a lot the derivations or diagrammatic expansions [71] and makes a bridge between the replica static approach and the dynamics of the system through a very helpful analogy that identifies formally replica indices (when $n \to 0$) to time [236, 238]. Hence one can study first the statics through the replica method and then follow a similar derivation to solve the dynamics, which is usually more cumbersome than static computations. The statics is used as a guide to the dynamic derivation and this is what we have employed here.

As a remark, the usual formulation of a superfield such as $\boldsymbol{\sigma}_i$ makes use of additional terms linear in the Grassmann variables:

$$\boldsymbol{\sigma}_i(a) = \sigma_i(t) + \bar{c}(t)\theta + \bar{\theta}c(t) + \bar{\theta}\theta i \hat{\sigma}_i(t) \tag{2.79}$$

where $(c, \bar{c})$ are also *fermionic* variables (*i.e.* Grassmann variables) which are *ghosts* used to exponentiate the Jacobian [315, 422] in the dynamical path integral presented in §2.5 and §C. However for our purposes we do not need to resort to these since we can interprete the Langevin equation in the Itô sense, implying the Jacobian is one. Any other discretization scheme can be equivalently considered by adding two such ghosts. We will thus ignore these, setting $c = \bar{c} = 0$, to lighten the presentation. Then it is not needed

---

[20]SUSY has also applications outside of high-energy physics in other fields such as photonic optics [286, 202] through supersymmetric quantum mechanics [104], but this has less common characteristics with the disordered systems supersymmetric approach.

to consider two Grassmann variables $\bar{\theta}\theta$ in (2.78), we could have instead introduced a single commuting variable Θ such that $\Theta^2 = 0$ and define similar derivation and integration rules; nevertheless we stick with the usual definition.

We generalize some useful formulas for superfields in this self-contained section, and develop an analogy with 2×2 block matrices to ease the computations.

2.4.2   Superfields and the superspace notation

We will consider (one-component) superfields and define them as $\boldsymbol{h}(a) = h(t) + \bar{\theta}_1\theta_1\hat{h}(t)$. We will also use operator (two components) superfields analogous to the replica case, such as $\boldsymbol{q}(a,b) = \boldsymbol{x}(a) \cdot \boldsymbol{x}(b)$. Similarly, an operator superfield $\boldsymbol{r}$ can be cast in the canonical expression with Grassmann variables and real scalar fields:

$$\boldsymbol{r}(a,b) = r_1(t,t') + \bar{\theta}_1\theta_1\hat{r}_1(t,t') + \bar{\theta}_2\theta_2\hat{r}_2(t,t') + \bar{\theta}_1\theta_1\bar{\theta}_2\theta_2 r_2(t,t') \tag{2.80}$$

2.4.2.1   Dirac deltas

For superfields, they are functionally defined as $\delta(\boldsymbol{h}(a)) = \delta(h(t))\delta(\hat{h}(t))$. For operator superfields, they are simply functionally defined as a product of the functional deltas of their components appearing in notation (2.80). If the superfield is symmetric we need to introduce deltas only on the independent part, which is the case for $\boldsymbol{q}$.

2.4.2.2   Path integral measure

We clarify here the path integral measure for future needs; for a d-dimensional trajectory of a particle the path integral measure is given by

$$\mathrm{D}x = \prod_{n=1}^{M} \frac{\mathrm{d}x^n}{(2\pi)^{\frac{d}{2}}} \tag{2.81}$$

when discretizing the trajectory $x(t)$ in M time steps. This is the MSRDDJ path integral measure used in §2.5 and §3.2.1, see §C. For a general superfield $\boldsymbol{r}$, the path integral measure is defined as $\mathrm{D}\boldsymbol{r} = \mathrm{D}r_1\mathrm{D}\hat{r}_1\mathrm{D}\hat{r}_2\mathrm{D}r_2$. For symmetric superfields such as $\boldsymbol{q}$, we will only sum on the symmetric components of it, and call it $\mathrm{D}^s\boldsymbol{q} = \mathrm{D}^sq_1\mathrm{D}\hat{q}_1\mathrm{D}^sq_2$ with $\mathrm{D}^sq_1 = \mathrm{D}q_1\prod_{t>t'}\delta(q_1(t,t') - q_1(t',t))$ in a discretized point of view. Therefore $\boldsymbol{q}(a,b)$ with '$a > b$' (loosely speaking) will appear in the path integral, the previous Dirac deltas imposing them to be $\boldsymbol{q}(b,a)$, so that we can use all components and introduce $\boldsymbol{q}$ as a symmetric superfield in the path integral as it should be from its definition[21].

2.4.2.3   Product of superfields

We define the product of two superfields $\boldsymbol{r} = \boldsymbol{pq}$ as the generalization of the operator product

$$\boldsymbol{r}(a,b) = \int \mathrm{d}c\, \boldsymbol{p}(a,c)\boldsymbol{q}(c,b) \tag{2.82}$$

2.4.2.4   Identity

We define the identity for superfields according to the usual definition:

$$\int \mathrm{d}b\, \mathbf{1}(a,b)\boldsymbol{h}(b) = \boldsymbol{h}(a) \tag{2.83}$$

A direct calculation provides $\mathbf{1}(a,b) = \bar{\theta}_1\theta_1\delta(t - t') + \bar{\theta}_2\theta_2\delta(t - t')$.

---

[21]We will come back to this convention in section 2.4.3.5 and show that it is useful.

2.4.3 Matricial representation: analogy with 2×2 block matrices

In subsections 2.4.4 and 2.4.5, we will put superfields into a matricial form in order to simplify calculations and use standard linear algebra calculus[22]. Indeed the above-defined superfields bear analogies with 2×2 block matrices and similar supermatrices of supersymmetric models in particle physics [160, 173].

2.4.3.1 *Supermatrix*

We now define an operator M on superfields, which gives a matricial representation, from definition (2.80):

$$\mathsf{M}(\boldsymbol{r}) = \begin{pmatrix} r_1 & \hat{r}_2 \\ \hat{r}_1 & r_2 \end{pmatrix} \tag{2.84}$$

which is in a way similar to the definition of SUSY supermatrices[23] [160, 173, 143]. This definition have some drawbacks, for example the superfield product is not a usual matrix product. It can be turned into a matrix product if we multiply (in the usual matricial sense) supermatrices first on the left by $\begin{pmatrix} 0 & \mathbb{1} \\ \mathbb{1} & 0 \end{pmatrix}$. The identity reads $\mathsf{M}(\boldsymbol{1}) = \begin{pmatrix} 0 & \mathbb{1} \\ \mathbb{1} & 0 \end{pmatrix}$, with $\mathbb{1}$ being the identity operator, *i.e.* $\mathbb{1}(t,t') = \delta(t-t')$. If a superfield is symmetric, *i.e.* $\boldsymbol{q}(a,b)^{\mathrm{T}} = \boldsymbol{q}(a,b)$ with $\boldsymbol{q}(a,b)^{\mathrm{T}} = \boldsymbol{q}(b,a)$, then we directly have that $\begin{pmatrix} q_1 & \hat{q}_2 \\ \hat{q}_1 & q_2 \end{pmatrix}$ is symmetric in the matrix sense, *i.e.* $\begin{pmatrix} q_1 & \hat{q}_2 \\ \hat{q}_1 & q_2 \end{pmatrix} = \begin{pmatrix} q_1^{\mathrm{T}} & \hat{q}_1^{\mathrm{T}} \\ \hat{q}_2^{\mathrm{T}} & q_2^{\mathrm{T}} \end{pmatrix}$.
The superfield product is then transcribed with operator products by:

$$\mathsf{M}(\boldsymbol{qp}) = \mathsf{M}(\boldsymbol{q}) \begin{pmatrix} 0 & \mathbb{1} \\ \mathbb{1} & 0 \end{pmatrix} \mathsf{M}(\boldsymbol{p}) \tag{2.85}$$

The map M is thus an isomorphism between superfields and these 'supermatrices' defined with such a product, and is convenient to prove some algebraic results on superfields.

2.4.3.2 Inverse

The definition of the inverse $\boldsymbol{r}\boldsymbol{r}^{-1} = \boldsymbol{1}$ in the superfield sense reads for matrices:

$$\mathsf{M}(\boldsymbol{r}) \begin{pmatrix} 0 & \mathbb{1} \\ \mathbb{1} & 0 \end{pmatrix} \mathsf{M}(\boldsymbol{r}^{-1}) = \begin{pmatrix} 0 & \mathbb{1} \\ \mathbb{1} & 0 \end{pmatrix} \tag{2.86}$$

which gives directly $\mathsf{M}(\boldsymbol{r}^{-1}) = \begin{pmatrix} 0 & \mathbb{1} \\ \mathbb{1} & 0 \end{pmatrix} \mathsf{M}(\boldsymbol{r})^{-1} \begin{pmatrix} 0 & \mathbb{1} \\ \mathbb{1} & 0 \end{pmatrix}$. Using the inverse of a 2 by 2 block matrix[24] we get:

$$\mathsf{M}(\boldsymbol{r}^{-1}) = \begin{pmatrix} \beta & \gamma\beta \\ \beta\alpha & \gamma\beta\alpha + r_1^{-1} \end{pmatrix} \tag{2.87}$$

with $\beta = (r_2 - \hat{r}_1 r_1^{-1} \hat{r}_2)^{-1}$, $\gamma = -r_1^{-1}\hat{r}_2$ and $\alpha = -\hat{r}_1 r_1^{-1}$. This defines the inverse of a superfield. Hence a superfield has an inverse if and only if its matrix representation is non singular.

2.4.3.3 Superdeterminant

We will therefore define a *superdeterminant*[25] for superfields as

$$\mathrm{sdet}(\boldsymbol{r}) = \det(\mathsf{M}(\boldsymbol{r})) = \det(r_1)\det(r_2 - \hat{r}_1 r_1^{-1} \hat{r}_2) \tag{2.88}$$

---

[22]Formulating the problem in terms of superfields is the right formalism to draw an analogy as clear as possible with replicas (see §2.5), as a guide throughout the derivation. Nevertheless, for calculations, it is often easier to go back and forth with a matricial representation, as lots of useful formulas are well known for matrix calculus.

[23]There are main differences between the definitions here and the usual ones in supersymmmetry. SUSY supermatrices are also 2 by 2 block matrices, but the off-diagonal blocks are zero in our case since our superfield have no fermionic part.

[24]The inverse is $\begin{pmatrix} A & B \\ C & D \end{pmatrix}^{-1} = \begin{pmatrix} A^{-1} + A^{-1}B(D - CA^{-1}B)^{-1}CA^{-1} & -A^{-1}B(D - CA^{-1}B)^{-1} \\ -(D - CA^{-1}B)^{-1}CA^{-1} & (D - CA^{-1}B)^{-1} \end{pmatrix}$.
There is another symmetric expression exchanging the roles of $A \leftrightarrow D$ and $B \leftrightarrow C$, and a more compact expression combining the two, which may be useful [36, page 117].

[25]The determinant for a 2 by 2 block matrix is $\det \begin{pmatrix} A & B \\ C & D \end{pmatrix} = \det(A)\det(D - CA^{-1}B) = \det(D)\det(A - BD^{-1}C)$ [36].

and other symmetric expressions[26]. Taking the determinant of equation (2.85) we see that it has the usual morphism property up to a ± 1 depending on the parity of the dimension of the blocks:

$$\text{sdet}(\boldsymbol{q})\text{sdet}(\boldsymbol{p}) = (-1)^M \text{sdet}(\boldsymbol{qp}) \tag{2.90}$$

This makes sense if we see operators as a discretized version where trajectories are divided in M time steps; if not one needs to define properly $\text{sdet}\begin{pmatrix} 0 & \mathbb{1} \\ \mathbb{1} & 0 \end{pmatrix}$.

For example, from $\boldsymbol{qq}^{-1} = \mathbf{1}$ we get:

$$\text{sdet}(\boldsymbol{q})\det\begin{pmatrix} 0 & \mathbb{1} \\ \mathbb{1} & 0 \end{pmatrix}\text{sdet}(\boldsymbol{q}^{-1}) = \text{sdet}\mathbf{1} = \det\begin{pmatrix} 0 & \mathbb{1} \\ \mathbb{1} & 0 \end{pmatrix} \tag{2.91}$$

thus $\text{sdet}(\boldsymbol{q}^{-1}) = 1/\text{sdet}(\boldsymbol{q})$.

2.4.3.4 Supertrace

In this matricial representation, the *supertrace* defined by $\text{str}(\boldsymbol{r}) = \int \mathrm{d}a\, \boldsymbol{r}(a,a) = \int \mathrm{d}t\, (\hat{r}_1 + \hat{r}_2)(t,t)$ reads

$$\text{str}(\boldsymbol{r}) = \text{Tr}\left(\begin{pmatrix} 0 & \mathbb{1} \\ \mathbb{1} & 0 \end{pmatrix} \mathsf{M}(\boldsymbol{r})\right) \tag{2.92}$$

2.4.3.5 Integral representation of Dirac deltas for superfields

Noticing that

$$\int \mathrm{d}\theta_1 \mathrm{d}\bar{\theta}_1 \mathrm{d}\theta_2 \mathrm{d}\bar{\theta}_2\, \boldsymbol{p}(a,b)\boldsymbol{q}(b,a) = p_1(t,t')q_2(t',t) + p_2(t,t')q_1(t',t) + \hat{p}_1(t,t')\hat{q}_1(t',t) + \hat{p}_2(t,t')\hat{q}_2(t',t) \tag{2.93}$$

an integral representation is expressed as:

$$\begin{aligned}
\delta(\boldsymbol{q}) &= \int \mathrm{D}\boldsymbol{p}\, e^{i\int \mathrm{d}a\mathrm{d}b\, \boldsymbol{p}(a,b)\boldsymbol{q}(b,a)} = \int \mathrm{D}\boldsymbol{p}\, e^{i\text{str}(\boldsymbol{pq})} \quad \text{for a superfield operator} \\
\delta(\boldsymbol{h}) &= \int \mathrm{D}\boldsymbol{g}\, e^{i\int \mathrm{d}a\, \boldsymbol{g}(a)\boldsymbol{h}(a)} \quad \text{similarly for a one-component superfield}
\end{aligned} \tag{2.94}$$

For a symmetric superfield such as $\boldsymbol{q}(a,b) = \boldsymbol{x}(a) \cdot \boldsymbol{x}(b)$, we only need to introduce the independent part of it, that is, taking the additional superfield $\boldsymbol{p}$ to be also symmetric, we only have to sum in the exponential over half of $\int \mathrm{d}a\mathrm{d}b\, \boldsymbol{p}(a,b)\boldsymbol{q}(a,b)$. Rescaling $\boldsymbol{p}$ with the factor $\frac{1}{2}$, the formula above is unchanged[27] provided that the measure is understood as $\mathrm{D}^{\text{s}}\boldsymbol{p}$ since $\boldsymbol{p}$ is symmetric.

2.4.3.6 Gaussian integration on superfields

Formula We will have to compute Gaussian integrals such as:

$$I = \int \mathrm{D}\boldsymbol{x}\, e^{-\frac{1}{2}\int \mathrm{d}a\mathrm{d}b\, \boldsymbol{q}(a,b)\boldsymbol{x}(a)\boldsymbol{x}(b) + \int \mathrm{d}a\, \boldsymbol{h}(a)\boldsymbol{x}(a)} \tag{2.95}$$

$\boldsymbol{h}$ and $\boldsymbol{x}$ being here scalar fields for the sake of clarity (*i.e.* $d = 1$). Without loss of generality, $\boldsymbol{q}$ can be assumed symmetric, so $\mathsf{M}(\boldsymbol{q}) = \begin{pmatrix} q_1 & \hat{q}_1^{\text{T}} \\ \hat{q}_1 & q_2 \end{pmatrix}$ with q_1 and q_2 symmetric operators.

A direct calculation with components shows that the Gaussian integral can be cast in the familiar form:

$$I = \text{sdet}^{-\frac{1}{2}}(\boldsymbol{q})e^{\frac{1}{2}\int \mathrm{d}a\mathrm{d}b\, \boldsymbol{q}^{-1}(a,b)\boldsymbol{h}(a)\boldsymbol{h}(b)} \tag{2.96}$$

The Gaussian integrations require that $\mathsf{M}(\boldsymbol{q})$ is positive definite, *i.e.* q_1 (respectively q_2) and $q_2 - \hat{q}_1 q_1^{-1}\hat{q}_2$ (respectively $q_1 - \hat{q}_2 q_2^{-1}\hat{q}_1$) are positive definite.

---

[26]The symmetry in these expressions can be shown by Sylvester's theorem $\det(\mathbb{1} + AB) = \det(\mathbb{1} + BA)$ [36], giving a symmetric form

$$\text{sdet}(\boldsymbol{r}) = \det(r_1)\det(r_2 - \hat{r}_1 r_1^{-1}\hat{r}_2) = \det(r_2)\det(r_1 - \hat{r}_2 r_2^{-1}\hat{r}_1) = \det(r_1 r_2)\det(\mathbb{1} - r_2^{-1}\hat{r}_1 r_1^{-1}\hat{r}_2) \tag{2.89}$$

[27]All numerical constants, such as this one coming from the rescaling in the measure, will be omitted in chapter 3 as we will eventually calculate all such proportionality constants in another way, see §3.3.3 and §3.3.4.2.

Derivation   Writing $\hat{h}^{\mathrm{T}} M h = \int \mathrm{d}t \mathrm{d}t' \, \hat{h}(t) M(t,t') h(t')$, with components of $\boldsymbol{q}$ we expand the superintegral [28]

$$I = \int \mathrm{D}x \mathrm{D}\hat{x} \, e^{-\frac{1}{2}(\hat{x}^{\mathrm{T}} q_1 \hat{x} + 2x^{\mathrm{T}} \hat{q}_1 \hat{x} + x^{\mathrm{T}} q_2 x) + x^{\mathrm{T}} \hat{h} + \hat{x}^{\mathrm{T}} h} = \det(q_1)^{-\frac{1}{2}} \int \mathrm{D}x \, e^{-\frac{1}{2} x^{\mathrm{T}} q_2 x + x^{\mathrm{T}} \hat{h} + \frac{1}{2} H^{\mathrm{T}} q_1^{-1} H} \quad (2.97)$$

with $H = -\hat{q}_1^{\mathrm{T}} x + h$, we now write this in a Gaussian form:

$$\frac{1}{2} H^{\mathrm{T}} q_1^{-1} H = \frac{1}{2} h^{\mathrm{T}} q_1^{-1} h + \frac{1}{2} x^{\mathrm{T}} \hat{q}_1 q_1^{-1} \hat{q}_1^{\mathrm{T}} x + h^{\mathrm{T}} \alpha^{\mathrm{T}} x \quad \text{with} \quad \alpha = -\hat{q}_1 q_1^{-1} \quad (2.98)$$

so that

$$I = \det(q_1)^{-\frac{1}{2}} \int \mathrm{D}x \, e^{-\frac{1}{2} x^{\mathrm{T}} \beta^{-1} x + (\alpha h + \hat{h})^{\mathrm{T}} x + \frac{1}{2} h^{\mathrm{T}} q_1^{-1} h} \quad \text{with} \quad \beta = (q_2 - \hat{q}_1 q_1^{-1} \hat{q}_1^{\mathrm{T}})^{-1} \quad (2.99)$$

ending up with

$$I = \det(q_1)^{-\frac{1}{2}} \det(\beta^{-1})^{-\frac{1}{2}} e^{\frac{1}{2}[h^{\mathrm{T}}(\alpha^{\mathrm{T}} \beta \alpha + q_1^{-1})h + 2\hat{h}^{\mathrm{T}} \beta \alpha h + \hat{h}^{\mathrm{T}} \beta \hat{h}]} \quad (2.100)$$

which gives the final expression (2.96). Exchanging the order of integration on x and $\hat{x}$ gives the symmetric expression for determinant and inverse.

2.4.4 Derivation of a scalar field with respect to a superfield

2.4.4.1 Derivation using the matrix representation

For future saddle-point equations, we will need to derive the exponent with respect to each component of a superfield $\boldsymbol{r}$ *i.e.* r_1, $\hat{r}_1$, $\hat{r}_2$ and r_2, as in equation (2.80). For convenience we will put this in a matricial (or superfield) form to treat the equations as a whole. Indeed, for a scalar $s(\boldsymbol{r})$, let us define

$$\frac{\delta s}{\delta \boldsymbol{r}} = \begin{pmatrix} \frac{\delta s}{\delta r_1} & \frac{\delta s}{\delta \hat{r}_2} \\ \frac{\delta s}{\delta \hat{r}_1} & \frac{\delta s}{\delta r_2} \end{pmatrix} \quad (2.101)$$

Using, for an operator A [36],

$$\frac{\partial \ln\det(A)}{\partial x} = \mathrm{Tr}\left(A^{-1} \frac{\partial A}{\partial x}\right) \quad (2.102)$$

we obtain for a symmetric superfield $\boldsymbol{Q}$[29] and any independent symmetric superfield $\boldsymbol{p}$,

$$\frac{\delta \ln\det(\boldsymbol{Q})}{\delta \boldsymbol{Q}} = 2 \begin{pmatrix} 0 & \mathbb{1} \\ \mathbb{1} & 0 \end{pmatrix} \mathsf{M}(\boldsymbol{Q}^{-1}) \begin{pmatrix} 0 & \mathbb{1} \\ \mathbb{1} & 0 \end{pmatrix} \quad \text{(which is } 2\,\mathsf{M}(\boldsymbol{Q})^{-1}\text{)}$$

$$\frac{\delta \mathrm{str}(\boldsymbol{p}\boldsymbol{Q})}{\delta \boldsymbol{Q}} = 2 \begin{pmatrix} 0 & \mathbb{1} \\ \mathbb{1} & 0 \end{pmatrix} \mathsf{M}(\boldsymbol{p}) \begin{pmatrix} 0 & \mathbb{1} \\ \mathbb{1} & 0 \end{pmatrix} \quad (2.103)$$

The presence of $\mathsf{M}(\mathbf{1})$ on the right and left amounts to an exchange between diagonal (respectively off-diagonal) blocks. This can be removed using the redefinition of the derivative in §2.4.4.2.

For the next expression, we apply the following formula [36] for a scalar function s of an operator A,

$$\frac{\partial s}{\partial A} = -A^{-\mathrm{T}} \frac{\partial s}{\partial (A^{-1})} A^{-\mathrm{T}} \quad (2.104)$$

This helps us compute the derivative of the trace $\mathrm{str}(\boldsymbol{Q}^{-1} \boldsymbol{p})$, noticing that:

$$\mathrm{str}(\boldsymbol{Q}^{-1} \boldsymbol{p}) = \mathrm{Tr}\left[\begin{pmatrix} 0 & \mathbb{1} \\ \mathbb{1} & 0 \end{pmatrix} \mathsf{M}(\boldsymbol{Q}^{-1} \boldsymbol{p})\right] = \mathrm{Tr}\left[\begin{pmatrix} 0 & \mathbb{1} \\ \mathbb{1} & 0 \end{pmatrix} \mathsf{M}(\boldsymbol{Q}^{-1}) \begin{pmatrix} 0 & \mathbb{1} \\ \mathbb{1} & 0 \end{pmatrix} \mathsf{M}(\boldsymbol{p})\right] = -\mathrm{Tr}[\mathsf{M}(\boldsymbol{Q})^{-1} \mathsf{M}(\boldsymbol{p})]$$

$$(2.105)$$

---

[28]There are no $\sqrt{2\pi}$ constants coming from Gaussian integrations since these factors cancel with the one contained in the MSRdDJ path integral measure.

[29]We must pay attention while deriving that $\boldsymbol{Q}$ is symmetric, hence the factors 2.

hence we can work directly on block matrices:

$$
\begin{aligned}
\frac{\delta}{\delta \boldsymbol{Q}} \mathrm{Tr}[\mathsf{M}(\boldsymbol{Q})^{-1}\,\mathsf{M}(\boldsymbol{p})] &= \frac{\delta}{\delta\,\mathsf{M}(\boldsymbol{Q})} \mathrm{Tr}[\mathsf{M}(\boldsymbol{Q})^{-1}\,\mathsf{M}(\boldsymbol{p})] \\
&= -\,\mathsf{M}(\boldsymbol{Q})^{-1}.\frac{\delta\mathrm{Tr}[\mathsf{M}(\boldsymbol{Q})^{-1}\,\mathsf{M}(\boldsymbol{p})]}{\delta\,\mathsf{M}(\boldsymbol{Q})^{-1}}.\mathsf{M}(\boldsymbol{Q})^{-1} \\
&= -2\,\mathsf{M}(\boldsymbol{Q})^{-1}\,\mathsf{M}(\boldsymbol{p})\,\mathsf{M}(\boldsymbol{Q})^{-1} \quad \text{since } \mathsf{M}(\boldsymbol{Q})^{-1} \text{ is symmetric} \\
&= -2 \begin{pmatrix} 0 & \mathbb{1} \\ \mathbb{1} & 0 \end{pmatrix} \mathsf{M}(\boldsymbol{Q}^{-1}) \begin{pmatrix} 0 & \mathbb{1} \\ \mathbb{1} & 0 \end{pmatrix} \mathsf{M}(\boldsymbol{p}) \begin{pmatrix} 0 & \mathbb{1} \\ \mathbb{1} & 0 \end{pmatrix} \mathsf{M}(\boldsymbol{Q}^{-1}) \begin{pmatrix} 0 & \mathbb{1} \\ \mathbb{1} & 0 \end{pmatrix} \\
&= -2 \begin{pmatrix} 0 & \mathbb{1} \\ \mathbb{1} & 0 \end{pmatrix} \mathsf{M}(\boldsymbol{Q}^{-1}\boldsymbol{p}\boldsymbol{Q}^{-1}) \begin{pmatrix} 0 & \mathbb{1} \\ \mathbb{1} & 0 \end{pmatrix}
\end{aligned}
\tag{2.106}
$$

As a final remark, these equations for a symmetric superfield hold only on the 'off-diagonal $a \neq b$' terms of the superfields (loosely speaking), whence the factors 2. This will be the case in §3 since the saddle point equations will only affect these independent parts ('$a < b$').

2.4.4.2　Summary

From the results derived above we can see that, equivalently, one can work directly on superfields, redefining the derivative with respect to a superfield in a way similar to functional differentiation, using the convention for functional derivation:

$$
\begin{aligned}
\frac{\delta \boldsymbol{x}(a)}{\delta \boldsymbol{x}(b)} &= \mathbf{1}(a,b) \\
\frac{\delta \boldsymbol{r}(a,b)}{\delta \boldsymbol{r}(c,d)} &= \mathbf{1}(a,c)\mathbf{1}(b,d)
\end{aligned}
\tag{2.107}
$$

where $\mathbf{1}$ is the equivalent of the Dirac delta for superfields (see subsection 2.4.2.4). Similarly for a symmetric superfield $\boldsymbol{Q}$ we get

$$
\frac{\delta \boldsymbol{Q}(a,b)}{\delta \boldsymbol{Q}(c,d)} = \mathbf{1}(a,c)\mathbf{1}(b,d) + \mathbf{1}(a,d)\mathbf{1}(b,c)
\tag{2.108}
$$

which gives the factors 2. We will thus use the formulas

$$
\begin{aligned}
\frac{\delta \mathrm{lndet}(\boldsymbol{Q})}{\delta \boldsymbol{Q}} &= 2\boldsymbol{Q}^{-1} \\
\frac{\delta \mathrm{str}(\boldsymbol{p}\boldsymbol{Q})}{\delta \boldsymbol{Q}} &= 2\boldsymbol{p} \\
\frac{\delta}{\delta \boldsymbol{Q}} \mathrm{str}(\boldsymbol{Q}^{-1}\boldsymbol{p}) &= -2\boldsymbol{Q}^{-1}\boldsymbol{p}\boldsymbol{Q}^{-1}
\end{aligned}
\tag{2.109}
$$

2.4.4.3　Gaussian moments

Moments of a Gaussian random variable in SUSY notation enjoy similar properties than discrete Gaussian random variables. As an example, we can compute the following variance:

$$
\begin{aligned}
\sqrt{\mathrm{sdet}(\boldsymbol{q})} \int \mathrm{D}\boldsymbol{x}\, \boldsymbol{x}(a)\boldsymbol{x}(b) e^{-\frac{1}{2}\int \mathrm{d}a\mathrm{d}b\, \boldsymbol{q}(a,b)\boldsymbol{x}(a)\boldsymbol{x}(b)} &= \frac{\delta^2}{\delta \boldsymbol{h}(a)\delta \boldsymbol{h}(b)} \int \mathrm{D}\boldsymbol{x}\, e^{-\frac{1}{2}\int \mathrm{d}a\mathrm{d}b\, \boldsymbol{q}(a,b)\boldsymbol{x}(a)\boldsymbol{x}(b) + \int \mathrm{d}a\, \boldsymbol{h}(a)\boldsymbol{x}(a)} \bigg|_{\boldsymbol{h}=0} \\
&= \frac{\delta^2}{\delta \boldsymbol{h}(a)\delta \boldsymbol{h}(b)} e^{\frac{1}{2}\int \mathrm{d}a\mathrm{d}b\, \boldsymbol{q}^{-1}(a,b)\boldsymbol{h}(a)\boldsymbol{h}(b)} \bigg|_{\boldsymbol{h}=0} = \boldsymbol{q}^{-1}(a,b)
\end{aligned}
\tag{2.110}
$$

2.4.5　Other useful identities

Here we prove the following relations, for any superfields $\boldsymbol{A}$ and $\boldsymbol{B}$ such that the series converge:

$$
\ln \mathrm{sdet}(\boldsymbol{A}+\boldsymbol{B}) = \ln \mathrm{sdet}\boldsymbol{A} + \mathrm{str} \sum_{n \geqslant 1} \frac{(-1)^{n-1}}{n}(\boldsymbol{A}^{-1}\boldsymbol{B})^n = \ln \mathrm{sdet}\boldsymbol{A} + \mathrm{str} \sum_{n \geqslant 1} \frac{(-1)^{n-1}}{n}(\boldsymbol{B}\boldsymbol{A}^{-1})^n
\tag{2.111}
$$

$$
(\boldsymbol{A}+\boldsymbol{B})^{-1} = \left(\sum_{n \geqslant 0}(-1)^n(\boldsymbol{A}^{-1}\boldsymbol{B})^n \right) \boldsymbol{A}^{-1} = \boldsymbol{A}^{-1} \sum_{n \geqslant 0}(-1)^n(\boldsymbol{B}\boldsymbol{A}^{-1})^n
$$

These formulas are just generalizations of power series to superfields. The radius of convergence of the series used is 1.

2.4.5.1 Proof of the first relation

From the definition of the superdeterminant in (2.88),

$$\ln\mathrm{sdet}(\boldsymbol{A}+\boldsymbol{B}) = \ln\det(\mathsf{M}(\boldsymbol{A})+\mathsf{M}(\boldsymbol{B})) = \ln\mathrm{sdet}\,\boldsymbol{A} + \ln\det(\mathbb{1}+\mathsf{M}(\boldsymbol{A})^{-1}\,\mathsf{M}(\boldsymbol{B}))$$

$$= \ln\mathrm{sdet}\,\boldsymbol{A} + \mathrm{Tr}\sum_{n\geqslant 1}\frac{(-1)^{n-1}}{n}(\mathsf{M}(\boldsymbol{A})^{-1}\,\mathsf{M}(\boldsymbol{B}))^n \qquad (2.112)$$

We have, using definitions of this section,

$$(\mathsf{M}(\boldsymbol{A})^{-1}\,\mathsf{M}(\boldsymbol{B}))^n = \left[\begin{pmatrix}0 & \mathbb{1}\\ \mathbb{1} & 0\end{pmatrix}\mathsf{M}(\boldsymbol{A}^{-1})\begin{pmatrix}0 & \mathbb{1}\\ \mathbb{1} & 0\end{pmatrix}\mathsf{M}(\boldsymbol{B})\right]^n = \begin{pmatrix}0 & \mathbb{1}\\ \mathbb{1} & 0\end{pmatrix}\mathsf{M}((\boldsymbol{A}^{-1}\boldsymbol{B})^n) \qquad (2.113)$$

which leads to:

$$\ln\mathrm{sdet}(\boldsymbol{A}+\boldsymbol{B}) = \ln\mathrm{sdet}\,\boldsymbol{A} + \mathrm{Tr}\left[\begin{pmatrix}0 & \mathbb{1}\\ \mathbb{1} & 0\end{pmatrix}\mathsf{M}\left(\sum_{n\geqslant 1}\frac{(-1)^{n-1}}{n}(\boldsymbol{A}^{-1}\boldsymbol{B})^n\right)\right] \qquad (2.114)$$

providing the result owing to the definition of the supertrace in 2.4.3.4. The second part of (2.111) comes from reversing the order of $\mathsf{M}(\boldsymbol{A})^{-1}\,\mathsf{M}(\boldsymbol{B})$ in the first line of the proof.

2.4.5.2 Proof of the second relation

From the definition of the inverse in 2.4.3.2,

$$\mathsf{M}((\boldsymbol{A}+\boldsymbol{B})^{-1}) = \begin{pmatrix}0 & \mathbb{1}\\ \mathbb{1} & 0\end{pmatrix}(\mathsf{M}(\boldsymbol{A})+\mathsf{M}(\boldsymbol{B}))^{-1}\begin{pmatrix}0 & \mathbb{1}\\ \mathbb{1} & 0\end{pmatrix} = \begin{pmatrix}0 & \mathbb{1}\\ \mathbb{1} & 0\end{pmatrix}(\mathbb{1}+\mathsf{M}(\boldsymbol{A})^{-1}\,\mathsf{M}(\boldsymbol{B}))^{-1}\,\mathsf{M}(\boldsymbol{A})^{-1}\begin{pmatrix}0 & \mathbb{1}\\ \mathbb{1} & 0\end{pmatrix}$$

$$= \begin{pmatrix}0 & \mathbb{1}\\ \mathbb{1} & 0\end{pmatrix}(\mathbb{1}+\mathsf{M}(\boldsymbol{A})^{-1}\,\mathsf{M}(\boldsymbol{B}))^{-1}\,\mathsf{M}(\boldsymbol{A})^{-1}\begin{pmatrix}0 & \mathbb{1}\\ \mathbb{1} & 0\end{pmatrix}$$

$$= \begin{pmatrix}0 & \mathbb{1}\\ \mathbb{1} & 0\end{pmatrix}\left[\sum_{n\geqslant 0}(-1)^n(\mathsf{M}(\boldsymbol{A})^{-1}\,\mathsf{M}(\boldsymbol{B}))^n\right]\begin{pmatrix}0 & \mathbb{1}\\ \mathbb{1} & 0\end{pmatrix}\mathsf{M}(\boldsymbol{A}^{-1})$$

$$(2.115)$$

Using again (2.113),

$$\mathsf{M}((\boldsymbol{A}+\boldsymbol{B})^{-1}) = \left[\sum_{n\geqslant 0}(-1)^n\,\mathsf{M}((\boldsymbol{A}^{-1}\boldsymbol{B})^n)\right]\begin{pmatrix}0 & \mathbb{1}\\ \mathbb{1} & 0\end{pmatrix}\mathsf{M}(\boldsymbol{A}^{-1}) = \mathsf{M}\left(\left[\sum_{n\geqslant 0}(-1)^n(\boldsymbol{A}^{-1}\boldsymbol{B})^n\right]\boldsymbol{A}^{-1}\right)$$

$$(2.116)$$

The result follows from the equality of the matricial representation. The second part of (2.111) comes from reversing the order of $\mathsf{M}(\boldsymbol{A})^{-1}\,\mathsf{M}(\boldsymbol{B})$ in the first line of the proof.

2.4.5.3 The projector

We define a superfield $\boldsymbol{P}(a,b)=1$ and λ a scalar. We have, from (2.111):

$$\ln\mathrm{sdet}(\lambda\boldsymbol{P}+\boldsymbol{B}) = \ln\mathrm{sdet}(\boldsymbol{B}) + \mathrm{str}\sum_{n\geqslant 1}\frac{(-1)^{n-1}\lambda^n}{n}(\boldsymbol{P}\boldsymbol{B}^{-1})^n \qquad (2.117)$$

It can be further simplified (with $n\geqslant 1$):

$$\mathrm{str}((\boldsymbol{P}\boldsymbol{B}^{-1})^n) = \int \mathrm{d}a_1\,(\boldsymbol{P}\boldsymbol{B}^{-1})^n(a_1,a_1)$$

$$= \int \mathrm{d}a_1\cdots\mathrm{d}a_n\mathrm{d}b_1\cdots\mathrm{d}b_n\,\boldsymbol{B}^{-1}(b_1,a_2)\boldsymbol{B}^{-1}(b_2,a_3)\cdots\boldsymbol{B}^{-1}(b_{n-1},a_n)\boldsymbol{B}^{-1}(b_n,a_1) \qquad (2.118)$$

$$= \left(\int \mathrm{d}a\mathrm{d}b\,\boldsymbol{B}^{-1}(a,b)\right)^n = [\mathrm{str}(\boldsymbol{P}\boldsymbol{B}^{-1})]^n$$

We thus get the following important formula:

$$\ln \text{sdet}(\lambda \boldsymbol{P} + \boldsymbol{B}) = \ln \text{sdet}(\boldsymbol{B}) + \ln \left[1 + \lambda \text{str}(\boldsymbol{P}\boldsymbol{B}^{-1}) \right] \tag{2.119}$$

Similarly, from (2.111):

$$(\lambda \boldsymbol{P} + \boldsymbol{B})^{-1} = \boldsymbol{B}^{-1} \sum_{n \geqslant 0} (-1)^n \lambda^n (\boldsymbol{P}\boldsymbol{B}^{-1})^n \tag{2.120}$$

We can simplify, for $n \geqslant 1$:

$$(\boldsymbol{P}\boldsymbol{B}^{-1})^n(a, b) = \int \mathrm{d}a_1 \cdots \mathrm{d}a_{n-1} \, (\boldsymbol{P}\boldsymbol{B}^{-1})(a, a_1)(\boldsymbol{P}\boldsymbol{B}^{-1})(a_1, a_2) \cdots (\boldsymbol{P}\boldsymbol{B}^{-1})(a_{n-1}, b)$$

$$= \int \mathrm{d}a_1 \cdots \mathrm{d}a_{n-1} \mathrm{d}b_1 \cdots \mathrm{d}b_n \, \boldsymbol{B}^{-1}(b_1, a_1)\boldsymbol{B}^{-1}(b_2, a_2) \cdots \boldsymbol{B}^{-1}(b_{n-1}, a_{n-1})\boldsymbol{B}^{-1}(b_n, b)$$

$$= \left(\int \mathrm{d}a \mathrm{d}b \, \boldsymbol{B}^{-1}(a, b) \right)^{n-1} \int \mathrm{d}b_n \, \boldsymbol{B}^{-1}(b_n, b) = \left(\int \mathrm{d}a \mathrm{d}b \, \boldsymbol{B}^{-1}(a, b) \right)^{n-1} (\boldsymbol{P}\boldsymbol{B}^{-1})(a, b) \tag{2.121}$$

Inserting it in equation (2.120):

$$(\lambda \boldsymbol{P} + \boldsymbol{B})^{-1} = \boldsymbol{B}^{-1} \left[1 - \lambda \boldsymbol{P}\boldsymbol{B}^{-1} \sum_{n=0}^{\infty} (-1)^n \lambda^n \left(\int \mathrm{d}a \mathrm{d}b \, \boldsymbol{B}^{-1}(a, b) \right)^n \right] \tag{2.122}$$

we get

$$(\lambda \boldsymbol{P} + \boldsymbol{B})^{-1} = \boldsymbol{B}^{-1} \left[1 - \frac{\lambda}{1 + \lambda \text{str}(\boldsymbol{P}\boldsymbol{B}^{-1})} \boldsymbol{P}\boldsymbol{B}^{-1} \right] \tag{2.123}$$

Both formulas (2.119) and (2.123) require $\left| \text{str}(\boldsymbol{P}\boldsymbol{B}^{-1}) \right| < 1/|\lambda|$.

2.5 Analogy with static replica computations: application in the p-spin spherical model

We consider a Langevin dynamics of the p-spin spherical model with a Gaussian centered thermal noise,

$$\gamma \dot{\sigma}_i(t) = -\mu(t)\sigma_i(t) - \frac{\partial H_J}{\partial \sigma_i} + \eta_i(t) \qquad \langle \eta_i(t)\eta_j(t') \rangle = 2T\gamma \delta_{ij}\delta(t - t') \tag{2.124}$$

$\mu(t)$ is a Lagrange multiplier to impose the spherical constraint at each time, equivalent to adding a term $\frac{1}{2}\mu(t)(\sigma \cdot \sigma - N)$ in the Hamiltonian (2.47).

We will solve the dynamics of this model using the SUSY formalism which renders the derivation formally similar to the static one in §2.3.

2.5.1 The Lagrange multiplier

Let us start by computing the Lagrange multiplier. We can discretize (in the Itô sense)

$$\sigma_i(t + dt) = \sigma_i(t) - \frac{1}{\gamma}\mu(t)\sigma_i(t)\mathrm{d}t - \frac{1}{\gamma}\frac{\partial H_J}{\partial \sigma_i}\mathrm{d}t + \frac{1}{\gamma}\eta_i \qquad \langle \eta_i\eta_j \rangle = 2T\gamma \mathrm{d}t\delta_{ij} \tag{2.125}$$

We enforce the spherical constraint. At order $\mathrm{d}t$:

$$N = \sigma(t + dt) \cdot \sigma(t + dt) = \sigma(t) \cdot \sigma(t) - \frac{2\mathrm{d}t}{\gamma}\sigma(t) \cdot \left[\mu(t)\sigma(t) + \frac{\partial H_J}{\partial \sigma}(t) \right] + \frac{1}{\gamma^2}\sum_{i=1}^{N}\eta_i^2 \tag{2.126}$$

Hence we get, applying the central limit theorem in the thermodynamic limit $\sum_{i=1}^{N}\eta_i^2 \underset{N \to \infty}{\longrightarrow} N\langle \eta_i^2 \rangle = 2NT\gamma \mathrm{d}t$:

$$0 = -\mu(t) - \frac{1}{N}\sigma(t) \cdot \frac{\partial H_J}{\partial \sigma}(t) + T = -\mu(t) - \frac{p}{N}H_J(t) + T \tag{2.127}$$

and we obtain

$$\mu(t) = -\frac{p}{N}H_J(t) + T \tag{2.128}$$

At equilibrium in the paramagnetic phase, we can compute

$$\overline{\langle H_J \rangle} = \frac{\partial(\beta \overline{F_{\mathrm{PM}}})}{\partial \beta} \tag{2.129}$$

with $\overline{F_{\mathrm{PM}}}/N = -\beta/4$ (see §2.3.2), and get

$$\frac{\overline{\langle H_J \rangle}}{N} = -\frac{\beta}{2} \quad \Longrightarrow \quad \mu = \frac{\beta p}{2} + T \tag{2.130}$$

since from time-translation invariance $\mu(t) = \mu$ and therefore we have recovered (2.59) with $q_0 = 0$.

2.5.2 Field-theoretical formulation of the dynamics in SUSY notation

The Langevin dynamics (2.124) can be equivalently formulated as a field theory for the time evolution of the spins with a generating path integral, through the Martin-Siggia-Rose-De Dominicis-Janssen (MSRDDJ) formalism [112, 81] presented in appendix C, allowing one to use the standard field theoretical tools.

The dynamical averages over the whole history of the thermal noises $\eta_i(t)$ in (2.124) are equivalently realized with the generating path integral

$$\overline{Z[J]} = \int \mathrm{D}\sigma \mathrm{D}\hat{\sigma} \,\overline{e^{-\mathcal{A}[\sigma, \hat{\sigma}, J]}} = \int \mathrm{D}[\sigma, \hat{\sigma}] \exp\left[-\int \mathrm{d}t \left(T\gamma\hat{\sigma} \cdot \hat{\sigma} + i\hat{\sigma} \cdot \gamma\dot{\sigma} + i\hat{\sigma} \cdot \mu\sigma \right) \right] \overline{\exp\left[-\int \mathrm{d}t \, i\hat{\sigma} \cdot \frac{\partial H_J}{\partial \sigma} \right]} \tag{2.131}$$

where the measures are $\mathrm{D}\sigma = \prod_{i=1}^{N} \mathrm{D}\sigma_i = \prod_{i=1}^{N} \prod_{m=1}^{M} \left(\mathrm{d}\sigma_i^m/\sqrt{2\pi} \right)$ (interpreting the trajectory $\sigma_i(t)$ as a discrete stochastic process with M time steps) and $\hat{\sigma}(t)$ is an additional *response* field which generates the response of the system to an external field. The advantage of this dynamical formulation is that we do not have to resort to the mathematically risky machinery of replicas [122] to average over the disorder since conservation of probability implies that $Z = 1$ (it is the sum of all the probability weights of the paths that can be taken by the system in phase space in a given time interval, see §C). If we note $Z[J] = \int \mathrm{D}[\sigma, \hat{\sigma}] e^{-\mathcal{A}[\sigma, \hat{\sigma}]}$, averages over the thermal history are directly $\langle \bullet \rangle = \int \mathrm{D}[\sigma, \hat{\sigma}] \bullet e^{-\mathcal{A}[\sigma, \hat{\sigma}, J]}$ and therefore one does not need to introduce replicas as if one could try when averaging

$$\overline{e^{-\mathcal{A}[\sigma, \hat{\sigma}, J]}/Z[J]} = \lim_{n \to 0} \overline{e^{-\sum_{a=1}^{n} \mathcal{A}[\sigma^a, \hat{\sigma}^a, J]} Z[J]^{n-1}} \tag{2.132}$$

with a non-trivial $Z[J]$.

Here we assume we start in a some configuration at time $t = -\infty$, hence all integrals over t extend from $-\infty$ to ∞ (or whatever latest time used in a given correlation function since we sum over all final *states* of the spins; by causality all transition probabilities to later times, encoded in $\mathcal{A}$, add up to one, see §C).

We introduce the superspace notation with:

$$\boldsymbol{\sigma}(a) = \sigma(t) + i\hat{\sigma}(t)\bar{\theta}\theta$$

$$\int \mathrm{d}a \, f[\boldsymbol{\sigma}(a)] = \int \mathrm{d}t \mathrm{d}\theta \mathrm{d}\bar{\theta} \, f[\sigma(t) + i\hat{\sigma}(t)\bar{\theta}\theta] = \int \mathrm{d}t \, i\hat{\sigma}(t) \cdot \nabla_\sigma f[\sigma(t)]$$

$$\mathcal{D}_a = 2T\gamma \frac{\partial^2}{\partial\bar{\theta}\partial\theta} + 2\gamma\frac{\partial}{\partial t} - 2\gamma\bar{\theta}\frac{\partial^2}{\partial\bar{\theta}\partial t} \tag{2.133}$$

$$\frac{1}{2}\int \mathrm{d}a \, \boldsymbol{\sigma}(a) \cdot \mathcal{D}_a \boldsymbol{\sigma}(a) = \int \mathrm{d}t \, [T\gamma\hat{\sigma}(t) \cdot \hat{\sigma}(t) + i\hat{\sigma}(t) \cdot \gamma\dot{\sigma}(t)]$$

in such a way that

$$\overline{Z[J]} = \int \mathrm{D}\boldsymbol{\sigma} \, e^{-\frac{1}{2}\int \mathrm{d}a \, \boldsymbol{\sigma}(a) \cdot [\mathcal{D}_a + \mu]\boldsymbol{\sigma}(a)} \overline{e^{-\int \mathrm{d}a \, H[\boldsymbol{\sigma}(a)]}} \tag{2.134}$$

The analogy with the static replicated partition function (2.52), except for the so-called *kinetic term* including $\mathcal{D}_a$ which is just an additional quantity to the exponent and needs no averaging, is striking, and we may then perform the exact same steps in the computation of this (path) integral. This formal analogy is exactly realized in the so-called *fast motion limit* ($\gamma \to 0$ here) which ignores transient dynamics and suppresses the kinetic term [236, 238, 309]. This SUSY algebra has formal connections with the algebra of hierarchical matrices *with the limit $n \to 0$ already taken*, even though a rigorous connection has not

been established yet [236, 238, 112]. For example a summation over a replica index $\sum_{a=1}^{n}$ for $n \to 0$ translates into an integral $\int \mathrm{d}a$. The fact that the dynamics in the fast motion limit is analogous to the replica approach points at the static replica method as probing the long-time regimes of the system *e.g.* for the equilibrium relaxation or the relaxation within the plateau which is a long-lived metastable state. This is emphasized in figure 4.2 in chapter 4. Doing so we get

$$
\overline{Z[J]} = \int \mathrm{D}^s \boldsymbol{Q}(a,b)\, e^{N\mathcal{S}(\boldsymbol{Q})}
$$
$$
\mathcal{S}(\boldsymbol{Q}) = -\frac{1}{2}\mathrm{str}(\boldsymbol{\mathcal{K}Q}) + \frac{1}{4}\int \mathrm{d}a\mathrm{d}b [\boldsymbol{Q}(a,b)]^p + \frac{1}{2}\ln \mathrm{sdet}\boldsymbol{Q}
$$
(2.135)

where

$$
\boldsymbol{Q}(a,b) = \frac{\boldsymbol{\sigma}(a)\cdot\boldsymbol{\sigma}(b)}{N}
$$
$$
\boldsymbol{\mathcal{K}}(a,b) = [\mathcal{D}_a + \mu]\boldsymbol{1}(a,b)
$$
$$
\mathrm{str}(\boldsymbol{\mathcal{K}Q}) = \int \mathrm{d}a\, \boldsymbol{\sigma}(a)\cdot[\mathcal{D}_a + \mu]\boldsymbol{\sigma}(a)
$$
(2.136)

The saddle-point equation is therefore

$$
-\boldsymbol{\mathcal{K}}(a,b) + \frac{p}{2}[\boldsymbol{Q}(a,b)]^{p-1} + \boldsymbol{Q}^{-1}(a,b) = 0 \quad \Leftrightarrow \quad [\mathcal{D}_a + \mu]\boldsymbol{Q}(a,b) = \frac{p}{2}\int \mathrm{d}c\, [\boldsymbol{Q}(a,c)]^{p-1}\boldsymbol{Q}(c,b) + \boldsymbol{1}(a,b)
$$
(2.137)

This equation has the form of a Schwinger-Dyson equation [315, 422, 112, 71] with self-energy $\boldsymbol{\Sigma}(a,b) = (p/2)[\boldsymbol{Q}(a,c)]^{p-1}$ or in the context of liquids, a MCT equation with $\boldsymbol{\Sigma}$ as a memory kernel [187], and is formally very similar to the static one (2.57).

This dynamical equation is general, starting from some fixed configuration at an initial time and letting the system evolve. Various dynamical regimes can be probed by making assumptions on the correlator $\boldsymbol{Q}$ and modifying the initial condition, such as the equilibrium regime or a long-time aging one.

2.5.3   (Super)symmetries and equilibrium relations

2.5.3.1   Equilibrium relations as Ward-Takahashi identities

Here we emphasize physical consequences of some symmetries of the dynamical action which are simple in the SUSY notation. More details are given in [189, 236, 190, 112, 16, 266].

Let us consider the generating functional (2.134). We call the average generated by it $\langle \bullet \rangle_{\overline{Z}}$. We define the correlation and response functions

$$
C(t,t') = \frac{1}{N}\left\langle \sigma(t)\cdot\sigma(t') \right\rangle_{\overline{Z}}
$$
$$
R_i(t,t') = \left.\frac{\delta\left\langle \sigma_i(t) \right\rangle_{\overline{Z}}}{\delta f_i(t')}\right|_{f_i=0}, \qquad R(t,t') = \frac{1}{N}\sum_{i=1}^{N} R_i(t,t')
$$
(2.138)

by adding an external field $f_i(t)$ in the right-hand side of the Langevin equation (2.124). R is the response function which arises when computing the linear response of an observable with respect to an external field imposed on the whole system [322]. This amounts to shift the exponent $-\mathcal{A}$ giving the dynamical action in (2.131) by a term $\sum_i \int \mathrm{d}t\, i\hat{\sigma}_i(t)f_i(t)$. Therefore by a direct functional derivation of $\langle \sigma_i(t) \rangle_{\overline{Z}}$ we see that

$$
R(t,t') = \frac{1}{N}\left\langle \sigma(t)\cdot i\hat{\sigma}(t') \right\rangle_{\overline{Z}}
$$
(2.139)

which is the classical Kubo formula. Note that causality implies $R(t,t') = 0$ for $t < t'$, and

$$
\left\langle i\hat{\sigma}_j(t) \right\rangle_{\overline{Z}} = \left.\frac{\delta\left\langle 1 \right\rangle_{\overline{Z}}}{\delta f_j(t)}\right|_{f_j=0} = 0
$$
$$
\left\langle i\hat{\sigma}_j(t)i\hat{\sigma}_j(t') \right\rangle_{\overline{Z}} = \left.\frac{\delta^2\left\langle 1 \right\rangle_{\overline{Z}}}{\delta f_j(t)\delta f_j(t')}\right|_{f_j=0} = 0
$$
(2.140)

We now focus on one of the symmetries of the system at equilibrium. A preliminary remark: if some field ψ is described by an action $S[\psi]$, generating averages of the form

$$\left\langle A[\psi]\right\rangle_S = \int \mathrm{D}\psi\, A[\psi]e^{-S[\psi]} \tag{2.141}$$

If $\mathcal{T}$ is a symmetry of the system i.e. $S[\mathcal{T}\psi] = S[\psi]$ and the measure and integration domain are invariant under this symmetry, we then have

$$\left\langle A[\psi]\right\rangle_S = \int \mathrm{D}\psi\, A[\psi]e^{-S[\psi]} = \int \mathrm{D}[\mathcal{T}\psi]\, A[\mathcal{T}\psi]e^{-S[\mathcal{T}\psi]} = \int \mathrm{D}\psi\, A[\mathcal{T}\psi]e^{-S[\psi]} = \left\langle A[\mathcal{T}\psi]\right\rangle_S \tag{2.142}$$

Let us consider a system equilibrated at the initial time, and for simplicity the time window is $[-\tau, \tau]$ with an arbitrary τ. This means that the initial condition $\sigma(-\tau)$ in the MSRDDJ path integral, which is fixed in its presentation in appendix C, is now averaged with the probability $P_{\mathrm{eq}} = e^{-\beta H}/\mathcal{Z}$ where

$$H[\sigma] = H_J + \frac{\mu}{2}\sum_{i=1}^{N}\sigma_i^2\,, \qquad \mathcal{Z} = \int \mathrm{d}\sigma\, e^{-\beta H[\sigma]} \tag{2.143}$$

The action we consider is thus

$$S_{\mathrm{eq}}[\sigma, \hat{\sigma}, J] = \mathcal{A}[\sigma, \hat{\sigma}, J] + \beta H[\sigma(-\tau)] + \ln \mathcal{Z} \tag{2.144}$$

The following symmetry

$$\mathcal{T}_{\mathrm{eq}} : \begin{cases} \sigma(t) \longrightarrow \sigma(-t) \\ i\hat{\sigma}(t) \longrightarrow i\hat{\sigma}(-t) + \beta\partial_t\sigma(-t) \end{cases} \tag{2.145}$$

leaves the system invariant. Indeed, its Jacobian is one and since the integration domain does not change on all trajectories during $[-\tau, \tau]$, $\mathrm{D}[\mathcal{T}_{\mathrm{eq}}\sigma, \mathcal{T}_{\mathrm{eq}}\hat{\sigma}] = \mathrm{D}[\sigma, \hat{\sigma}]$. The response field $\hat{\sigma}(t)$, under $\mathcal{T}_{\mathrm{eq}}$, is shifted by an imaginary number $-i\beta\partial_t\sigma(-t)$ but the contour can be closed at both infinities since there is a Gaussian damping factor $e^{-T\gamma\hat{\sigma}\cdot\hat{\sigma}}$ coming from $\mathcal{A}$, and since there are no poles we can go back to a real axis integration. The action S_{eq} is invariant since, from (2.131),

$$\mathcal{A}[\mathcal{T}_{\mathrm{eq}}\sigma, \mathcal{T}_{\mathrm{eq}}\hat{\sigma}, J] = -T\gamma\int_{-\tau}^{\tau}\mathrm{d}t\,[i\hat{\sigma}(-t) + \beta\partial_t\sigma(-t)]^2 + \int_{-\tau}^{\tau}\mathrm{d}t\,[i\hat{\sigma}(-t) + \beta\partial_t\sigma(-t)]\cdot\left[\frac{\partial H}{\partial\sigma}[\sigma(-t)] + \gamma\partial_t\sigma(-t)\right]$$

$$\underset{\{t\to-t\}}{=}\int_{-\tau}^{\tau}\mathrm{d}t\,\left(T\gamma\hat{\sigma}(t)\cdot\hat{\sigma}(t) + i\hat{\sigma}(t)\cdot\frac{\partial H}{\partial\sigma}[\sigma(t)]\right) - T\gamma\int_{-\tau}^{\tau}\mathrm{d}t\,\left[\beta^2(\partial_t\sigma(t))^2 - 2\beta i\hat{\sigma}(t)\cdot\dot{\sigma}(t)\right]$$

$$- \beta\int_{-\tau}^{\tau}\mathrm{d}t\,\dot{\sigma}(t)\cdot\left[\frac{\partial H}{\partial\sigma}[\sigma(t)] - \gamma\dot{\sigma}(t)\right] - \gamma\int_{-\tau}^{\tau}\mathrm{d}t\,i\hat{\sigma}(t)\cdot\dot{\sigma}(t)$$

$$=\mathcal{A}[\sigma, \hat{\sigma}, J] - \beta\int_{-\tau}^{\tau}\mathrm{d}t\,\dot{\sigma}(t)\cdot\frac{\partial H}{\partial\sigma}[\sigma(t)] = \mathcal{A}[\sigma, \hat{\sigma}, J] - \beta\int_{-\tau}^{\tau}\mathrm{d}t\,\frac{\mathrm{d}}{\mathrm{d}t}H[\sigma(t)]$$

$$=\mathcal{A}[\sigma, \hat{\sigma}, J] - \beta\left(H[\sigma(\tau)] - H[\sigma(-\tau)]\right) \tag{2.146}$$

where we performed the change of variables $t \to -t$ in all integrals in the second line. The additional term $-\beta H[\sigma(\tau)]$ given by the transform of $\mathcal{A}$ under $\mathcal{T}_{\mathrm{eq}}$ is compensated by the transform of the term coming from the equilibrium probability P_{eq} at initial time in (2.144).

This equilibrium symmetry can be written in the compact SUSY notation:

$$\mathcal{T}_{\mathrm{eq}}\boldsymbol{\sigma}(t, \theta, \bar{\theta}) \equiv \boldsymbol{\sigma}(-t - \beta\bar{\theta}\theta, -\bar{\theta}, \theta) \tag{2.147}$$

We can now apply (2.142):

$$\left\langle \boldsymbol{\sigma}(a)\right\rangle_{\overline{Z}} = \left\langle \mathcal{T}_{\mathrm{eq}}\boldsymbol{\sigma}(a)\right\rangle_{\overline{Z}} \qquad \Longleftrightarrow \qquad \begin{cases} \left\langle \sigma(t)\right\rangle_{\overline{Z}} = \left\langle \sigma(-t)\right\rangle_{\overline{Z}} \\ \left\langle i\hat{\sigma}(t)\right\rangle_{\overline{Z}} = \left\langle i\hat{\sigma}(-t)\right\rangle_{\overline{Z}} + \beta\partial_t\left\langle \sigma(-t)\right\rangle_{\overline{Z}} \end{cases} \tag{2.148}$$

The first line expresses microreversibility and is redundant here since, from (2.140), the second line implies

$$\frac{\mathrm{d}}{\mathrm{d}t}\left\langle \sigma(t)\right\rangle_{\overline{Z}} = 0 \tag{2.149}$$

which is stationarity. This expresses time-translational invariance (TTI). More generally, using the same symmetry and generalized Kubo formulas similar to (2.139) one can prove this for a general function $A(\sigma)$ [16]. Similarly, two-time functions are then function of a single variable, the time difference.

Now employing the same procedure for the two-point correlation function

$$\langle \boldsymbol{\sigma}(a)\boldsymbol{\sigma}(b)\rangle_{\overline{Z}} = \langle \mathcal{T}_{\mathrm{eq}}\boldsymbol{\sigma}(a)\mathcal{T}_{\mathrm{eq}}\boldsymbol{\sigma}(b)\rangle_{\overline{Z}} \tag{2.150}$$

we get from the scalar and $\bar{\theta}_1\theta_1$ components, respectively,

$$\langle \sigma(t)\sigma(t')\rangle_{\overline{Z}} = \langle \sigma(-t)\sigma(-t')\rangle_{\overline{Z}} \quad \Leftrightarrow \quad C(t,t') = C(-t,-t')$$
$$\langle \sigma(t)i\hat{\sigma}(t')\rangle_{\overline{Z}} = \langle \sigma(-t)i\hat{\sigma}(-t')\rangle_{\overline{Z}} + \beta\langle \sigma(-t)\partial_{t'}\sigma(-t')\rangle_{\overline{Z}} \tag{2.151}$$
$$\Leftrightarrow \quad R(t,t') = R(-t,-t') + \beta\partial_{t'}C(-t,-t')$$

Combining these two equations provides the fluctuation-dissipation theorem (FDT)

$$R(t,t') - R(-t,-t') = \beta\partial_{t'}C(t,t') \tag{2.152}$$

Note that, setting $t' = 0$ and due to TTI, multiplying the latter equation by $\theta(t)$ and using causality of the response,

$$R(t) = -\beta\theta(t)\dot{C}(t) \tag{2.153}$$

We mention that, if we had included fermionic terms (ghosts) in the action to exponentiate the MSRDDJ Jacobian, additional symmetries can be noticed. The measure, kinetic term and Hamiltonian term are invariant in the following supersymmetries[30]:

$$\boldsymbol{\sigma}(t,\theta,\bar{\theta}) \longrightarrow \boldsymbol{\sigma}(t,\theta,\bar{\theta}+\bar{\epsilon}) = e^{\bar{\epsilon}D}\boldsymbol{\sigma}(t,\theta,\bar{\theta})$$
$$\boldsymbol{\sigma}(t,\theta,\bar{\theta}) \longrightarrow \boldsymbol{\sigma}(t+\epsilon\bar{\theta},\theta+\epsilon,\bar{\theta}) = e^{\epsilon\bar{D}}\boldsymbol{\sigma}(t,\theta,\bar{\theta}) \tag{2.154}$$
$$D = \frac{\partial}{\partial\bar{\theta}}, \qquad \bar{D} = \frac{\partial}{\partial\theta} + \bar{\theta}\frac{\partial}{\partial t}$$

which are then symmetries of the action, generated respectively by D and $\bar{D}$. ϵ and $\bar{\epsilon}$ are fermionic (Grassmann) numbers. This is still true here but since the ghosts are not introduced they do not correspond to a transform on the fields σ, $\hat{\sigma}$ and one cannot use them as we did with $\mathcal{T}_{\mathrm{eq}}$. They are called *supersymmetries* because their action on the bosonic superfield $\boldsymbol{\sigma}$ gives a fermionic variable (and vice-versa):

$$D\boldsymbol{\sigma} = i\hat{\sigma}\theta, \qquad \bar{D}\boldsymbol{\sigma} = \bar{\theta}(\dot{\sigma} - i\hat{\sigma}) \tag{2.155}$$

The symmetry generated by D is called BRS symmetry [30, 29, 16] and generically arises when a system has a dynamical constraint (here the spins obey the Langevin equation of motion). One can recover for example FDT from these supersymmetries, as well as relations between bosonic and fermionic correlation functions [16].

We have thus obtained the general equilibrium relations as Ward-Takahashi identities [315, 422, 16] of (super)symmetries of the system, which are very easy to prove in this formalism. Other equilibrium relations can be obtained in this way [16, 266], such as reciprocity relations [298, 299, 80, 322] or the equipartition theorem. An out-of-equilibrium regime is signalled by a spontaneous supersymmetry breaking due to the initial conditions (similarly to a spatial symmetry breaking due to boundary conditions in *e.g.* mechanical systems or a ferromagnet), that here were explicitly chosen to be equilibrated. When the out-of-equilibrium regime is due to a forcing of the system, the forcing terms break supersymmetry explicitly [112]. Therefore some of the above Ward-Takahashi identities do not hold, such as TTI and FDT. However, a breaking of symmetry can leave invariant a symmetry subgroup, and then give some relations such as non-equilibrium fluctuation theorems [16, 266] valid in these regimes.

We make a final comment on the equilibrium regime. If the initial condition is a fixed one, thus breaking the equilibrium symmetry, in the equilibrium ergodic phase ($T > T_{\mathrm{d}}$) this induces a transient non-equilibrium regime but for later times equilibrium is recovered. This is similar to spatial symmetries where the boundary conditions matter very close to the boundary but do not affect the *bulk*. On the contrary, in a non-ergodic regime ($T < T_{\mathrm{d}}$), the system remains non-equilibrated at all times (*the boundary conditions' order propagates through the bulk*).

---

[30]For the second line using the generator $\bar{D}$ note that $\left[\partial_\theta, \bar{\theta}\partial_t\right] = 0$ so that $e^{\epsilon\bar{D}}$ is the product of the exponentials of the two preceding operators.

2.5.3.2 Equilibrium hypothesis

The saddle-point equation (2.137) is general, but we now wish to write it for the simplest case of an equilibrium situation satisfying TTI and FDT. From the results in the preceding subsection:

$$
\begin{aligned}
C(t - t') &= \frac{\langle \sigma(t) \cdot \sigma(t') \rangle}{N} \\
R(t - t') &= \frac{\langle \sigma(t) \cdot i\hat{\sigma}(t') \rangle}{N} \\
0 &= \frac{\langle i\hat{\sigma}(t) \cdot i\hat{\sigma}(t') \rangle}{N} \\
R(t) &= -\beta\theta(t)\dot{C}(t)
\end{aligned}
\tag{2.156}
$$

we derive the equilibrium form of the dynamical overlap

$$
\boldsymbol{Q}(a, b) = C(t - t') + \bar{\theta}_1\theta_1 R(t' - t) + \bar{\theta}_2\theta_2 R(t - t') \ .
\tag{2.157}
$$

2.5.4 The Mode-Coupling equation

Since the only independent function is $C(t)$, we can obtain an equation for $C(t)$ by considering the term without any Grassmann variable in equation (2.137). Furthermore we consider $t > t'$.

The contribution of the kinetic term is

$$
[\mathcal{D}_a + \mu]\boldsymbol{Q}(a, b) = \gamma\dot{C}(t - t') - 2\gamma T R(t' - t) + \mu C(t - t')
\tag{2.158}
$$

and the response term is zero by causality because $t > t'$. The kernel gives

$$
\int \mathrm{d}c\, \boldsymbol{Q}(a, c)^{p-1}\boldsymbol{Q}(c, b) = \int \mathrm{d}t'' \left[C(t - t'')^{p-1}R(t' - t'') + (p - 1)C(t - t'')^{p-2}R(t - t'')C(t'' - t') \right]
\tag{2.159}
$$

Finally, the identity gives no contribution (see (2.4.2.4)). We therefore obtain, setting $t' = 0$:

$$
\gamma\dot{C}(t) = -\mu C(t) + \frac{p}{2}\int_{-\infty}^{\infty} \mathrm{d}s\, [C(t - s)^{p-1}R(-s) + (p - 1)C(t - s)^{p-2}R(t - s)C(s)]
\tag{2.160}
$$

Using FDT a somewhat miraculous (but expected) cancellation happens: we do not have to consider times outside of the interval $[0, t]$. This is due to causality (for the upper boundary) and the fact that being at equilibrium *resums* all the past history (for the lower boundary), see §3.7.3. Indeed we get, using $R(-s) = -\beta\theta(-s)\dot{C}(-s) = \beta\theta(-s)\dot{C}(s)$,

$$
\gamma\dot{C}(t) = -\mu C(t) + \frac{\beta p}{2}\int_{-\infty}^{0} \mathrm{d}s\, C(t - s)^{p-1}\dot{C}(s) - \frac{\beta p}{2}\int_{-\infty}^{t} \mathrm{d}s\, \left[-\frac{\partial}{\partial s}C(t - s)^{p-1} \right]C(s)
\tag{2.161}
$$

and integrating by parts the last term

$$
\gamma\dot{C}(t) = -\left(\mu - \frac{\beta p}{2}\right)C(t) + \frac{\beta p}{2}\int_{-\infty}^{0} \mathrm{d}s\, C(t - s)^{p-1}\dot{C}(s) - \frac{\beta p}{2}\int_{-\infty}^{t} \mathrm{d}s\, C(t - s)^{p-1}\dot{C}(s)
\tag{2.162}
$$

so the contributions coming from $s \in]-\infty, 0[$ cancel and we have

$$
\gamma\dot{C}(t) = -\left(\mu - \frac{\beta p}{2}\right)C(t) - \frac{\beta p}{2}\int_{0}^{t} \mathrm{d}s\, C(t - s)^{p-1}\dot{C}(s)
\tag{2.163}
$$

Using equation (2.130) we obtain the final result which coincides with [81, Eq. (143)] which was first obtained by Crisanti, Horner and Sommers [107], following the method of Sompolinsky and Zippelius [365]:

$$
\gamma\dot{C}(t) = -TC(t) - \frac{\beta p}{2}\int_{0}^{t} \mathrm{d}s\, C(t - s)^{p-1}\dot{C}(s)
\tag{2.164}
$$

The numerical solution of this equation displayed in figure 2.5 exhibits a fast transient relaxation and, only at low temperatures, the formation of a plateau in the correlation, which diverges at some temperature. This equation was obtained in the a priori very far field of liquid dynamics for density correlators by Leutheusser [252] and Bengtzelius-Götze-Sjölander [33] as a schematic MCT equation, see §1.2.1.4.
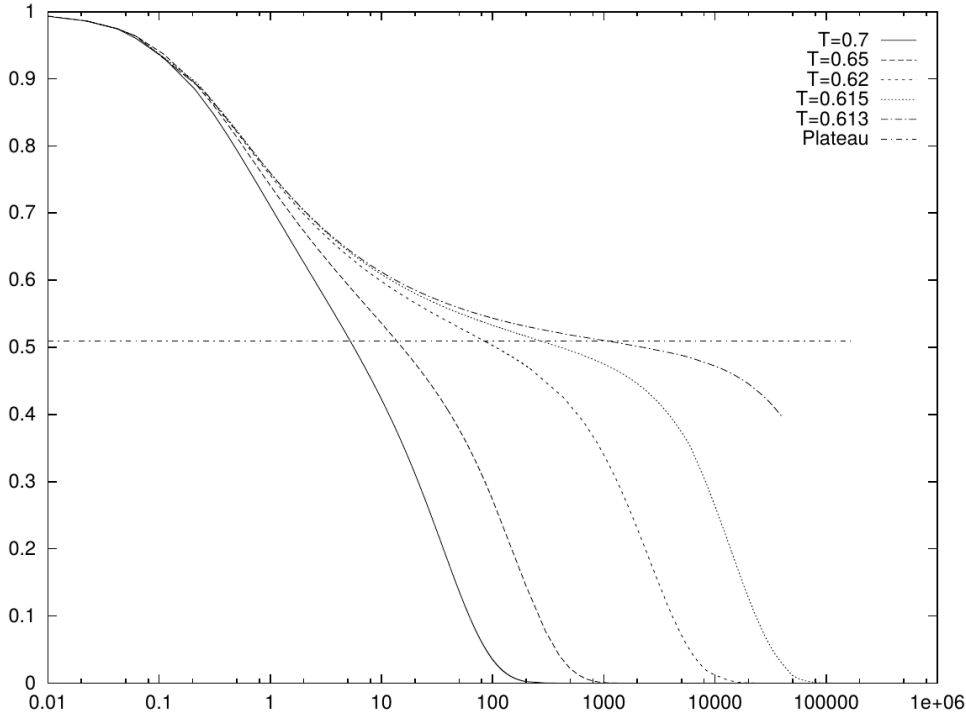
Figure 2.5: Numerical solution of (2.164) for $p = 3$ and $\gamma = 1$, for several temperatures $T = 0.7, 0.65, 0.62, 0.615, 0.613$; here $T_{\mathrm{d}} \simeq 0.612372$. The horizontal dashed line is the limiting value of the plateau $C(\infty) = q_{\mathrm{EA}}$. [*Reprinted from* [23]]

From (2.163) we can also obtain μ with the following reasoning. We compute it at $t = 0$ and we obtain

$$0 = -\gamma \dot{C}(0^+) - \mu + \frac{\beta p}{2} = T\gamma R(0^+) - \mu + \frac{\beta p}{2} \tag{2.165}$$

where in the second step we used FDT. The correlation and response functions at very short times $t \to 0^+$ do not depend on the interaction, only the type of dynamics, and can be computed using non-interacting dynamics (see §3.10.1 for a similar discussion), *i.e.* the potential does not have the time to influence the dynamics at short delays. In that case we have $\mu = T$ in (2.124) and $\gamma \dot{\sigma} = -T\sigma + \eta$ which gives $C(t) = \exp[-(T/\gamma)\,t]$ and $\gamma \dot{C}(0) = -T$. This gives the correct result (2.130) for μ.

2.5.5   Dynamical transition

We look for a plateau in the relaxational dynamics of $C(t)$: we set $C(t) \equiv C(\infty) + \delta C(t)$ where $\delta C(t)$ is small for large times and $C(\infty) = \lim_{t \to \infty} C(t)$. By consistency we should find that $C(\infty) = 0$ is a possible solution, since for temperatures above the dynamical transition we expect ergodicity to hold and therefore the correlation must relax to zero. Remember that in the last section we used that $C(\infty) = 0$ and we try to see if this is always satisified by the MCT equation. Expanding the time integral in (2.164) we have[31]:

$$\gamma \dot{C}(t) = -TC(t) - \frac{\beta p}{2} C(\infty)^{p-1}[C(t) - 1] - \frac{\beta p}{2} C(\infty)^{p-2}(p-1) \int_0^t \mathrm{d}s \, \delta C(t-s)\dot{C}(s) \tag{2.166}$$

At large times the left-hand side vanishes. If the dynamics is relaxational then in the integrand $\delta C(t-s) \geqslant 0$ and $\dot{C}(s) \leqslant 0$, thus the whole integral is negative and neglecting first order deviations that are small in the large-time limit, we then get the inequality, valid for large times:

$$C(t)^{p-2}[1 - C(t)] \leqslant \frac{2T^2}{p} \tag{2.167}$$

The function $\mathcal{G}(C) = C^{p-2}(1 - C)$ is very similar to the one plotted in figure 2.2: it is positive, $\mathcal{G}(0) = \mathcal{G}(1) = 0$ and thus has a maximum whose position $C = q_{\mathrm{EA}}$ is given by

$$q_{\mathrm{EA}} = \frac{p-2}{p-1} \tag{2.168}$$

---

[31]Note that $C(0) = C(t,t) = 1$ due to the spherical constraint.

When the temperature is high, the inequality (2.167) is always fulfilled since $\mathcal{G}(q_{\text{EA}}) \ll 2T^2/p$. Indeed, in the high-temperature paramagnetic phase the dynamics is ergodic and we expect $C(\infty) = 0 = q_0$ as in the statics, §2.3.2. When the temperature is lowered, the difference between the two sides of the inequality is lowered and is controlled by $\int_0^t \mathrm{d}s\, \delta C(t-s)\dot{C}(s)$, shown in figure 2.6.
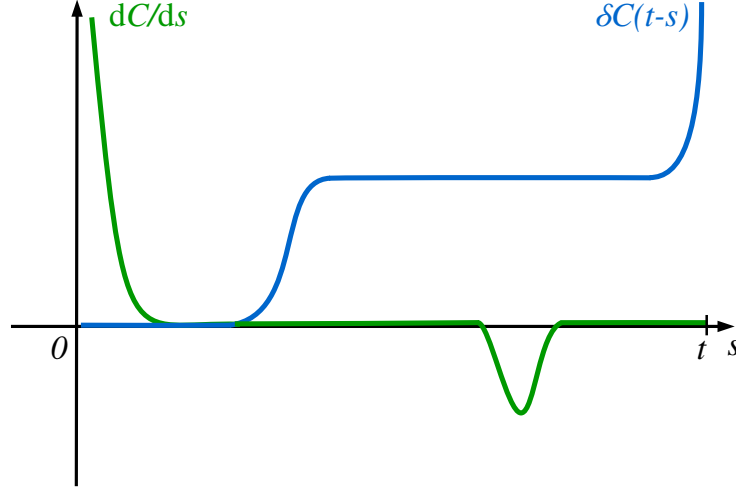
Figure 2.6: In the ergodic regime where $C(\infty) = 0$, the relaxation of the plateau induces a bump in the derivative of the correlation which gives the dominant (negative) contribution to the integral $\int_0^t \mathrm{d}s\, \delta C(t-s)\dot{C}(s)$. At the dynamical transition the plateau diverges and the integral becomes zero due to the vanishing of the bump and the separation of timescales.

At the temperature saturating the bound (2.167), $\int_0^t \mathrm{d}s\, \delta C(t-s)\dot{C}(s)$ must become zero *i.e.* the plateau diverges (see figure 2.6). This temperature is $2T_{\text{d}}^2/p = \mathcal{G}(q_{\text{EA}})$ *i.e.* , from (2.168),

$$T_{\text{d}} = \sqrt{\frac{p(p-2)^{p-2}}{2(p-1)^{p-1}}} \tag{2.169}$$

This is the dynamical transition: the correlation has an infinite plateau and the system does not relax anymore, it is trapped in some metastable state since, as $T_{\text{s}} < T_{\text{d}}$, the system is still in the paramagnetic phase thermodynamically speaking. Below T_{d} our equilibrium assumptions break down and $C(\infty) = q_{\text{EA}}$. Note that

$$q_{\text{EA}}^{p-2}(1 - q_{\text{EA}}) = \frac{2T^2}{p} \tag{2.170}$$

which defines T_{d}, is exactly the same equation we got with the static 1-RSB saddle-point equation at $m = 1$ (2.72). This is to be expected: the 1-RSB ansatz becomes the RS one in this limit $m \to 1$. The former describes an infinite plateau regime of size q_1 in the dynamics whereas the latter is correct for the high-temperature phase. The plateau value at the transition is thus obtained for $m \to 1$ where q_1 becomes q_{EA}. In the replica method presented in §1.2.4.2, the conjugated parameter m is the same as the one of the 1-RSB Parisi ansatz here. Indeed, m replicas are constrained to fall in the same state, which is represented by the block of size m. Note that $m \to 1$ describes the non-replicated system, *i.e.* the high-temperature phase in this framework, see (1.38), (1.39) and (1.41). This coincides with what we have just remarked for the passage from 1-RSB to RS matrices in the limit $m \to 1$.

3

DYNAMICS OF LIQUIDS AND GLASSES IN THE LARGE-DIMENSIONAL LIMIT

Outline

In this chapter we derive the dynamical equations ruling the evolution of a system of particles interacting via a liquid pair potential which is general and is precised below, in the thermodynamic limit and in the limit of infinite space dimension d (taken after the thermodynamic limit). To achieve this, we generalize the virial expansion to the dynamics. The problem simplifies in $d \to \infty$ since, as in the HS statics in §2.2, this expansion reduces to a few terms that we compute. We could have equivalently employed a quenched-disorder model which is inherently mean field in all dimensions and is equivalent in $d \to \infty$, the Mari-Kurchan model [270]. This is discussed below and in appendix D. It will be instead put to use for the thermodynamics of the system in chapter 4, where it will also be shown that, conversely, solving the normal model without disorder gives the same results. We get that the system is equivalently described by the effective one-dimensional dynamics of the interparticle gap. We derive a closed set of equations for the autocorrelation and the response of the system. First, we test these equations in the ideal-gas limit of vanishing density to show that they coincide with the one given by a free motion of independent particles. We then specialize them to an equilibrium situation. The dynamical equation in this regime is akin to a Mode-Coupling one, but is not the same as the one predicted by MCT. As a result, the asymptotic scaling for some quantities differ from MCT. However the phenomenology is the same, and some properties and relations derived within MCT remain valid in $d \to \infty$. It is shown that the system relaxes at long times in the liquid phase, corresponding to a diffusive behaviour. We connect the diffusion coefficient to the shear viscosity and make a prediction for the Stokes-Einstein relation. Nonetheless, an ergodicity-breaking transition takes place at sufficiently low temperature or high density, as expected in mean field. We give MCT-like exponents that describe the behaviour of the MSD close to the plateau and the vanishing of the diffusion coefficient at the dynamical transition. The dynamical equations are then compared to the MCT ones, studying intermediate scattering functions and discussing some of their properties. Finally we abandon the equilibrium hypothesis and provide the closed set of equations deter-

mining the dynamic quantities for an off-equilibrium protocol of a non-stationary temperature or density evolution.

3.1   Introduction

3.1.1   Definition of the model

We consider an assembly of N spheres of mass m interacting through a pair potential $V(r)$. The interaction Hamiltonian is then

$$H = \sum_{i<j} V(x_i - x_j) \tag{3.1}$$

with $x_i(t)$ the positions of the particles. In order to have a proper limit $d \to \infty$, we consider inter-particle potentials such that the particles are *rather hard*: there is a strong repulsion at short distances and a negligible interaction at large distances. The relevant range of density where the behaviour is liquid or glass-like will be found when neighbouring particles are at a distance falling into the crossover region between the forbidden distances due to strong repulsion and the almost non-interacting range. For the potentials we will consider, this region becomes more narrow as the dimension is increased.

More precisely, we consider potentials such that their Mayer function $f = e^{-\beta V} - 1$ is exponentially (in d) close to -1 below a distance σ, which will be denoted as the effective diameter of the spheres: this is the forbidden region due to strong repulsion. Then f is of $O(1)$ in a crossover region and finally is exponentially small at larger distances, practically non-interacting. Such a Mayer function satisfies the requirements for the truncation of the virial series in §2.2. We refer to such potentials as being rather hard since they are HS-like *when we look with our three-dimensional eyes* at *e.g.* the Mayer function at $O(1)$ distances, *i.e.* without any rescaling with dimension (see figures 5.1 and 5.5). However note that in the crucial region where the Mayer function is $O(1)$, which is of size $O(1/d)$ in the potentials we will consider, the potential may behave like any known liquid potential (*e.g.* Lennard-Jones), and its behaviour can be analyzed by setting the temperature in order to impose the value of the below-defined effective diameter σ to fall in this region, see equation (3.3). This is also discussed in chapter 5.

A class of potentials which fits these requirements is the *exponential potentials*

$$V(r) = e^{-dA(r)} \tag{3.2}$$

with A a differentiable function of order one, such that $\forall r > \sigma$, $[\ln r - A(r)]_r^\sigma > 0$, where σ is by definition in the crossover region where

$$\beta V(\sigma) = O(1) \tag{3.3}$$

which defines σ up to $O(1/d)$, and such that $\forall r < \sigma$, $\lim_{d\to\infty} f(r) = -1$. This is clearly provided by the analysis of chapter 5. σ is an effective particle diameter.

These exponential potentials are not the only ones to which the following derivation applies: for instance a sum of them is suitable, as well as the HS potential. Potentials with a discontinuous exponent $A(r)$ may be analyzed as long as the above properties of the Mayer function are met: the latter sum of exponential potentials can be expressed in this way (see the case of the Lennard-Jones potential in §5.8). For all the potentials we will consider, the crucial crossover regime will be shown to lie in a range of distance of size $O(1/d)$. A crucial scaling property of the potential is thus

$$\lim_{d\to\infty} \beta V(r) = \bar{V}(h) \ , \qquad h = d(r - \sigma)/\sigma \ , \qquad r = \sigma(1 + h/d) \ , \tag{3.4}$$

where $\bar{V}(h)$ is a finite function of h. This is automatically verified for the exponential potentials with differentiable exponent defined in (3.2). The scaling $r = \sigma(1 + h/d)$ is physically related to the fact that interactions are dominated by neighbouring particles that are typically almost touching and whose positions are fluctuating with amplitude $O(1/d)$, see §5.2.3. This means[1], together with the scaling of density given by the packing fraction $\varphi = O(d/2^d)$ (see §2.2), as shown below, that a particle interacts

---

[1]An interesting geometrical feature of infinite dimension is here at play. When $d \to \infty$, the volume of a very small *crust* of a sphere of size $1/d$, given by $\mathcal{V}_d(\sigma) - \mathcal{V}_d(\sigma(1 - 1/d))$, is 63% $(1 - 1/e)$ of the total volume of the sphere $\mathcal{V}_d(\sigma)$. This illustrates the fact that in $d \to \infty$, *everything lies at the boundaries* due to the power d at which lengths (or radiuses) are

with $\sim \rho[\mathcal{V}_d(\sigma(1 + h_{\max}/d)) - \mathcal{V}_d(\sigma)] = 2^d\varphi(e^{h_{\max}} - 1) = O(d)$ neighbours[2], for times shorter than the relaxation time. This is consistent with the general picture of mean-field behaviour [178].

A concrete example of an *exponential potential* is an IPL potential with $\alpha < 1$

$$\beta V_{\text{IPL}}(r) = \epsilon \left(\frac{\sigma}{r}\right)^{d/\alpha} \xrightarrow[d\to\infty]{} \epsilon e^{-h/\alpha} = \bar{V}(h) \tag{3.5}$$

Explicit examples of other important potentials that can be treated here as well but do not belong to the *exponential potentials* class are:

- HS with $e^{-\beta V_{\text{HS}}(r)} = \theta(r - \sigma) = \theta(h) = e^{-\beta \bar{V}_{\text{HS}}(h)}$.

- Soft Harmonic Spheres with $\beta V_{\text{SHS}}(r) = \epsilon d^2 (r/\sigma - 1)^2 \theta(\sigma - r) = \epsilon h^2 \theta(-h) = \bar{V}_{\text{SHS}}(h)$.

- Lennard-Jones with $\beta V_{\text{LJ}}(r) = \epsilon \left[(\sigma/r)^{4d} - (\sigma/r)^{2d}\right] \xrightarrow[d\to\infty]{} \epsilon[e^{-4h} - e^{-2h}] = \bar{V}_{\text{LJ}}(h)$.

- Weeks-Anderson-Chandler [402, 88] with $\beta V_{\text{WCA}}(r) = \epsilon \left[(\sigma/r)^{4d} - (\sigma/r)^{2d} + 1/4\right] \theta(2^{1/2d} - r/\sigma) \xrightarrow[d\to\infty]{}$ $\epsilon[e^{-4h} - e^{-2h} + 1/4]\theta(\ln 2/2 - h) = \bar{V}_{\text{WCA}}(h)$.

Note that this is the natural generalisation of potentials such as the Lennard-Jones one to $d > 3$, because in any case one has to impose $V(r) \ll r^{-d}$ at large r to keep the interaction short ranged and a finite second virial coefficient. In many cases we will specialize to the HS potential for concreteness, but all the main results we obtain apply to a generic potential described above.
We note $\bar{V}(\mu) = V(\sigma(1 + \mu/d))$ and the rescaled force $F(\mu) = -\bar{V}'(\mu)$.

3.1.2 Crystal cleared

What about crystalline states? As mentioned in §1.1.1, we shall focus on liquid and amorphous states in all regimes considered, not on the thermodynamically stable crystal for temperatures below the melting transition. It will be ruled out by restricting ourselves to local density profiles $\rho(x)$, or dynamically speaking, density of trajectories $\rho[\{x_i(t)\}]$ defined below, that satisfy *statistical* continuous invariances such as translation symmetry $\forall\lambda, \rho[\{x_i(t)\}] = \rho[\{x_i(t) + \lambda\}]$ and rotational symmetry $\forall\mathcal{R}, \rho[\{x_i(t)\}] = \rho[\{\mathcal{R}x_i(t)\}]$ where $\mathcal{R}$ is a d-dimensional rotation. The crystal phase is only invariant under *discrete* rotations and translations and is therefore *a priori* an unreachable solution. This exclusion is justified by our will to study the liquid phase and the metastable amorphous configurations, as well as by numerical studies in high dimension that show that the crystal becomes harder to nucleate as dimension increases [363, 396, 395, 386].

Note that the (ideal) gas phase has the same symmetries as the liquid and is obtained in the limit of vanishing density ($\rho \to 0$ or $\varphi \to 0$), which is shown in §3.6.

3.1.3 The convenience of the spherical model

The derivation is easier if one considers a spherical model. From section 3.2.3 on, we will constrain the particles to live on the surface of a $(d + 1)$-dimensional hypersphere of radius R (which we call $\mathbb{S}_d(R)$), hence each particle is a point $x_i \in \mathbb{R}^{d+1}$ with the constraint $x_i^2 = R^2$. The *volume* of this d-dimensional curved space is

$$\mathcal{V} = \Omega_{d+1} R^d \tag{3.6}$$

where Ω_d is volume of the unit d-dimensional sphere expressed in appendix A. For $R \to \infty$ we recover a system defined on a flat (Euclidean) and infinite space $\mathbb{R}^d$. The thermodynamic limit corresponds to $R \to \infty$ with constant density.

The reasons which make this choice very convenient are the following:

---

raised. Now if one takes a crust whose finite size *is not scaled with d*, be it arbitrarily small, one then gets that the crust contains 100% of the volume and the rest of the sphere contains 0%, which is very counter-intuitive to our three-dimensional thinking. In other words, in infinite dimension, a pumpkin is just made of skin : Halloween is saved, but there is nothing to eat...

[2]This leaves the -actually verified- possibility of an isostatic number of contacts at jamming [273, 97], equal to $2d$ per particle (see §1.5).

- At finite R, the global rotational invariance in $\mathbb{R}^{d+1}$ encodes both the rotational and translational symmetries of the d-dimensional Euclidean problem. These symmetries play a central role in the derivation. The rotational invariance is exploited in a field-theoretical formulation in §3.3, and thus both symmetries are handled together in this way.

  The translational symmetry is much less obvious to deal with. In the previous derivation of the glassy statics of the HS system [243, 242], an origin was fixed by the center of mass of the system (actually, of the replicated system, *i.e.* of the molecules) which was integrated on the whole space to recover homogeneity. Technically, this means the order parameter, the overlap between particles $q_{ab} = u_a \cdot u_b$, where $u_a = x_a - X$ is the fluctuation of a particle x_a in a replica of the system around its center of mass X, acquires a zero mode. Indeed, by definition the center of mass of m replicas is $X = (1/m) \sum_{a=1}^{m} x_a$, so that $\sum_{a=1}^{m} u_a = 0$, and therefore $\sum_{a=1}^{m} q_{ab} = 0$. This gives rise to a number of expressions that needed to be restrained to the subspace orthogonal to the zero mode direction, and thus use mathematical object exploiting this *discrete* property of finite-dimensional matrices. With the SUSY formalism, by analogy one would construct a dynamical field theory for a similar dynamical overlap $\boldsymbol{q}(a, b)$ (which is what will be done, as in §2.5). However this singularity is not easy to treat in a *continuous* field-theoretical formulation.

- In the statics in chapter 4, it gives a unambiguous meaning to the order parameter in the liquid phase, which is not the case in the molecular replica formulation of [312, 243, 242]. In this phase, the replicas of a given particle are unconstrained and thus independent, they will typically be far away from each other in real space. At finite R and large space dimension, a replica x_b lies on the equator with respect to replica x_a (*i.e.* they are orthogonal vectors). This is due to the fact that the measure is peaked at $\theta = \pi/2$ if θ is the angle between x_a and x_b, see the comment of (2.26) in §2.2. Then we must find that the MSD is $\mathsf{D}_{ab} = (x_a - x_b)^2 = 2R^2$ by Pythagoras' theorem, which will be the case in §4.4.1.

- It corresponds to a choice of *periodic boundary conditions* for particles enclosed in a finite volume V.

- As a general statement, spherical models in statistical physics are usually simpler to analyze, as in the p-spin case in chapter 2.

3.1.4 Outline of the derivation

The derivation of the general dynamical equations occupies three sections §3.2, §3.3, §3.4. We summarize the main idea here.

The microscopic dynamics is expressed in a field-theoretical language through the MSRDDJ formalism already encountered in §2.5.2 and presented in appendix C. This transcription into a field-theoretical language allows one to use the standard field theoretical tools. The MSRDDJ path integral is analogous to a canonical partition function. One can create a grand-canonical partition function by varying the number of particles N and then expand it as a virial series as in §2.1. One observes that in $d \to \infty$, as in §2.2, this expansion is well adapted since it reduces to an ideal gas term (without interactions) and only one interaction term, the first of the virial series. We then express both of them, via the rotation and translation symmetries of the system, in terms of two-point functions, the MSD or the autocorrelation function, and the response function. Using the appropriate scalings to recover a finite limit in $d \to \infty$, we finally observe that these two terms can be computed through a saddle-point evaluation exact in the $d \to \infty$ limit. The saddle-point equations show that these two-point functions are non fluctuating in the large-dimensional limit, and determines them. An effective single-particle dynamics naturally emerges from the computation, and is related to the dynamics of the interparticle gap. The correlation and response functions of the microscopic model can be viewed as correlation and response functions of the effective particle, *i.e.* averages over its dynamical evolution.

3.2 Formulation of the dynamics

3.2.1 The dynamical action

A possible choice of the dynamics of the particles in the d-dimensional space is the following Langevin process:

$$m\ddot{x}_i + \gamma\dot{x}_i = -\sum_{j\neq i}\nabla V(x_i - x_j) + \xi_i \tag{3.7}$$

$\xi_i(t)$ being a centered white Gaussian noise with $\langle \xi_i^\mu(t)\xi_j^\nu(t')\rangle = 2\gamma T\delta_{ij}\delta_{\mu\nu}\delta(t - t')$. In the following, we will consider the overdamped[3] case where $m = 0$. Given a set of initial conditions, the MSRDDJ generating path integral (appendix C) reads, with Itô convention:

$$Z_N = \int \prod_{i=1}^N \mathrm{D}x_i \mathrm{D}\hat{x}_i \, e^{-\mathcal{A}[\{x_i,\hat{x}_i\}]} \tag{3.8}$$

where the action is:

$$\mathcal{A}[\{x_i,\hat{x}_i\}] = \sum_{i=1}^N \Phi[x_i,\hat{x}_i] + \sum_{i<j}^{1,N} W[x_i,\hat{x}_i,x_j,\hat{x}_j] \tag{3.9}$$

$$\Phi[x,\hat{x}] = \gamma\int \mathrm{d}t \left(T\hat{x}^2 + i\hat{x}\cdot\dot{x} \right), \quad W[x,\hat{x},y,\hat{y}] = i\int \mathrm{d}t\,(\hat{x} - \hat{y})\cdot\nabla V(x - y) = W[x - y,\hat{x} - \hat{y}]$$

The sum in Z_N is done over all possible trajectories, with the measure given by $\mathrm{D}x_i = \prod_{n=1}^M \frac{\mathrm{d}x_i^n}{(2\pi)^{\frac{d}{2}}}$ when discretizing the trajectory $x_i(t)$ in M time steps. Time integrals are taken over an interval noted $[t_\mathrm{p}, t_1]$ in section 3.7 where the $\{x_i(t_\mathrm{p})\}$ are fixed (initial conditions, which would correspond to $n = 0$ in the latter discretization) and the $\{x_i(t_1)\}$ are summed over (which would correspond to $n = M$). In section 3.7 we will need averages of the type $\langle x_i(t_0)x_i(t_1)\rangle$ with $t_0 \in [t_\mathrm{p}, t_1]$, and it is not needed to consider times larger than t_1 in the action owing to causality, as they will give no contribution to the average by probability conservation (*i.e.* for the same reason as $Z_N = 1$).

The action $\mathcal{A}$ is rotation invariant (for both position and response fields using the same global rotation) and translation invariant along positions[4]. Because of the so-called kinetic term Φ, it is not translation invariant along the response fields (which are already centered at the origin owing to the white noise), though the interaction term is.

3.2.2 Derivation of the generating functional using a virial expansion

We derive the dynamic generating functional $\ln Z_N$, which is the dynamical equivalent of the free energy in the statics in chapter 4. In order to do this, a *dynamic virial* similar to the static virial expansion in §2.2 is a reliable method where we can exploit the truncation of the series in $d \to \infty$, as in the statics. Another way is to consider the mean-field Mari-Kurchan (MK) model [270] where the truncation appears more naturally, and which is equivalent to the normal model This is discussed in chapter 4, together with the equivalence between the normal model and MK in §4.1, §4.2 and appendix H. It is the way used in the statics (chapter 4), and the argument is very similar in the dynamical case. For completeness it is reproduced in appendix §D where one sees the clear analogy with the static calculation (see also §2.5.2 in the p-spin and §4.6).

3.2.2.1 Dynamic virial

We define $\Xi = \sum_{N=0}^{+\infty} \frac{1}{N!}Z_N$ in order to use the Mayer expansion[5] as in liquid theory [199]. The goal here is to generalize the static argument of Frisch, Percus, Rivier and Wyler for *trajectories* of particles (see §2.2). This *grand canonical* form is handy as a generating functional, but note that we assume there

---

[3]Either Newtonian ($\gamma = 0$, no noise nor dissipation) or Brownian ($m = 0$) dynamics can be treated by changing the kernel associated to Φ in the following sections. This is discussed in §3.7.5.

[4]The invariances for response fields follow if one studies the system modulo *rigid* rotations and translations of the entire system.

[5]This is why W is cast in a symmetric form so that links in the product $\prod_{i<j}$ are not directed.

is *no* exchange of particles with a reservoir; $\ln \Xi$ and $\ln Z_N$ are related by a Legendre transform and virial expansions are more fruitful with the former. We have:

$$\Xi = \sum_{N=0}^{+\infty} \frac{1}{N!} \prod_{i=1}^{N} \int D[x_i, \hat{x}_i]\, z[x_i, \hat{x}_i] \prod_{i<j} \left(1 + f[x_i, \hat{x}_i, x_j, \hat{x}_j]\right) \tag{3.10}$$

with a generalized fugacity $z = e^{-\Phi}$ and a Mayer function $f = e^{-W} - 1$. We Legendre transform $\ln \Xi$ with respect to $N \ln z$ since one has

$$\frac{\delta \ln \Xi}{\delta z[x, \tilde{x}]} = \frac{1}{\Xi} \sum_{N=0}^{+\infty} \frac{1}{N!} \int \prod_{i=1}^{N} D[x_i, \tilde{x}_i] \prod_{i<j} \left(1 + f[x_i, \tilde{x}_i, x_j, \tilde{x}_j]\right) \frac{\delta}{\delta z[x, \tilde{x}]} \prod_{i=1}^{N} z[x_i, \tilde{x}_i]$$

$$= \frac{1}{\Xi} \sum_{N=0}^{+\infty} \frac{1}{N!} \int \prod_{i=1}^{N} D[x_i, \tilde{x}_i] \prod_{i<j} \left(1 + f[x_i, \tilde{x}_i, x_j, \tilde{x}_j]\right) \left[\sum_{i=1}^{N} \delta(x - x_i)\delta(\tilde{x} - \tilde{x}_i) \frac{1}{z[x_i, \tilde{x}_i]}\right] \prod_{j=1}^{N} z[x_j, \tilde{x}_j]$$

$$= \frac{1}{z[x, \tilde{x}]} \frac{1}{\Xi} \sum_{N=0}^{+\infty} \frac{1}{N!} \int \prod_{i=1}^{N} D[x_i, \tilde{x}_i] \left[\sum_{i=1}^{N} \delta(x - x_i)\delta(\tilde{x} - \tilde{x}_i)\right] \prod_{i<j} \left(1 + f[x_i, \tilde{x}_i, x_j, \tilde{x}_j]\right) \prod_{j=1}^{N} z[x_j, \tilde{x}_j]$$

$$\Leftrightarrow \frac{\delta \ln \Xi}{\delta(N \ln z[x, \tilde{x}])} = \left\langle \frac{1}{N} \sum_{i=1}^{N} \delta(x - x_i)\delta(\tilde{x} - \tilde{x}_i) \right\rangle_{\Xi} \equiv \rho[x, \tilde{x}]$$

$$\tag{3.11}$$

where the mean is generated by the functional Ξ. Next, due to the formal analogy of (2.2) with (2.2), the usual Mayer expansion can be carried out in this dynamical case, and inverting the Legendre transform, $\ln \Xi$ can be written as an ideal gas contribution and the sum of all connected 1-irreducible Mayer diagrams (see §2.2) with $N\rho[x, \hat{x}]$ nodes and $f[x - y, \hat{x} - \hat{y}]$ bonds (see §2.2):

$$\ln \Xi = -N \int D[x, \hat{x}]\, \rho[x, \hat{x}](\Phi[x, \hat{x}] + \ln \rho[x, \hat{x}]) + \bullet\!\!-\!\!\bullet + \triangle + \boxtimes + \boxtimes + \boxtimes + \dots \tag{3.12}$$

In infinite dimension, the Mayer expansion reduces to its first term. However, this is strictly true if we assume that we are in a regime where the trajectories have the time to wander away only a finite fraction of the box. Because we expect (and confirm) that all interesting dynamics (namely, the β relaxation with the formation of a plateau in correlations and the onset of a relaxation towards equilibrium - α relaxation -) occur on such scales, where the fluctuations around the initial position is of amplitude $O(1/d)$, see §3.3.2. We will show that one even gets the diffusive behaviour which is already decided at the $1/d$ scale (see figure 3.1).

To justify this truncation, let us consider for example the second term of this expansion (one-loop triangle diagram):

$$\triangle = \frac{N^3}{3!} \int D[x, \hat{x}] D[y, \hat{y}] D[z, \hat{z}]\, \rho[x, \hat{x}]\rho[y, \hat{y}]\rho[z, \hat{z}]\, f[x - y, \hat{x} - \hat{y}] f[y - z, \hat{y} - \hat{z}] f[z - x, \hat{z} - \hat{x}] \tag{3.13}$$

For a finite-support[6] potential V, $\nabla V(x - y) \propto \theta(\sigma - |x - y|)$, hence

$$f[x - y, \hat{x} - \hat{y}] = \begin{cases} 0 & \text{if } \forall t,\; \left|x(t) - y(t)\right| > \sigma \\ \tau[x - y, \hat{x} - \hat{y}] & \text{if } \exists t,\; \left|x(t) - y(t)\right| < \sigma \end{cases} = [\theta(|x - y| - \sigma) - 1]\tau[x - y, \hat{x} - \hat{y}] \tag{3.14}$$

Essentially, τ is just a numerical value depending on the short-distance details of V (with $|\tau| \leqslant 2$) and the physical content of f lies in its finite support, *i.e.*

$$f[x - y, \hat{x} - \hat{y}] \simeq \theta(|x - y| - \sigma) - 1 = -1 + \prod_{n=1}^{M} \theta(|x^n - y^n| - \sigma) \tag{3.15}$$

For finite times, a trajectory stays in a bounded region of space, represented as a ball of diameter the typical size $\propto \sigma/d$ of the trajectory in figure 1(b). The Mayer functions require that each couple

---

[6]The *rather hard* potentials we consider are in this regard very similar to HS since when $d \to \infty$ the Mayer function is exponentially damped at distances larger than σ, making the potential practically short-ranged.

of trajectories gets closer than σ at some time. To each set of three trajectories one can associate a corresponding static diagram with three overlapping balls (figure 1(b)). One can see this static diagram as the equivalence class of all dynamic diagrams with trajectories contained inside these balls. Actually there are lots of trajectories contained by these bounding balls that do not contribute because they do not get close enough. Then the sum over trajectories of the value of the integrand is at most of the same order of the static diagram value due to the normalization $\int D[x,\hat{x}]\,\rho[x,\hat{x}] = 1$ which accounts for the huge number of equivalent dynamic diagrams compared to the static one. The same program applies to all terms in the expansion. We conclude, from [409], that the first term dominates the series[7] in the $d \to \infty$ limit. A more careful but maybe less intuitive argument is given in 3.2.2.2. The result is then[8]

$$\mathcal{S} \equiv \frac{\ln\Xi}{N} = -\int D[x,\hat{x}]\,\rho[x,\hat{x}](\Phi[x,\hat{x}]+\ln\rho[x,\hat{x}]) + \frac{N}{2}\int D[x,\hat{x}]D[y,\hat{y}]\,\rho[x,\hat{x}]\rho[y,\hat{y}]f[x-y,\hat{x}-\hat{y}] \quad (3.16)$$

with $\delta\mathcal{S}/\delta\rho[x,\hat{x}] = 0$ from the Legendre transform and the normalization $\int D[x,\hat{x}]\,\rho[x,\hat{x}] = 1$. We neglected purely additive constants irrelevant for the dynamics.

3.2.2.2 The Mayer expansion in infinite dimension

We discuss here the truncation of the Mayer expansion when $d \to \infty$ in a more pedestrian way. As in 3.2.2.1, we focus on the triangle diagram in (3.13) with the Mayer function given by (3.15).
Consider two typical trajectories $x(t)$ and $y(t)$ which we expect from the static case to dominate the dynamics at large d, and let us focus on the positions x^1 and y^1 (any other couple would do). These typical trajectories scale as follows: the other positions of the trajectory $\{x^n\}_{n\neq 1}$ (respectively $\{y^n\}_{n\neq 1}$) fluctuate around x^1 (respectively y^1) over a neighborhood of size $O(1/d)$, see figures 1(a),(b). Besides, the typical distance between the two trajectories is the diameter σ (plus $O(1/d)$ fluctuations). Then essentially $\prod_{n=1}^{M}\theta(|x^n-y^n|-\sigma) \simeq \theta(|x^1-y^1|-\sigma)$ except in the neighborhood $|x^1-y^1| \in [\sigma(1-\frac{\mu}{d}),\sigma(1+\frac{\mu}{d})]$ where these fluctuations of order $1/d$ matter (μ is of order 1). However this neighborhood has to be accounted for since its volume $\mathcal{V}_d(\sigma)[(1+\frac{\mu}{d})^d - (1-\frac{\mu}{d})^d] \underset{d\to\infty}{\sim} \mathcal{V}_d(\sigma)(e^\mu - e^{-\mu})$, is comparable to the volume $\mathcal{V}_d(\sigma)e^{-\mu}$ of $|x^1-y^1| \in [0,\sigma(1-\frac{\mu}{d})]$ where the contribution of $f[x-y,\hat{x}-\hat{y}]$ (3.15) is also non zero (for $|x^1-y^1| > \sigma(1+\frac{\mu}{d})$, $f[x-y,\hat{x}-\hat{y}]$ is zero).
Hence $f[x-y,\hat{x}-\hat{y}] \simeq f^*(x^1-y^1)$ with $f^*(x)$ being -1 for $|x| \in [0,\sigma(1-\frac{\mu}{d})]$, of order 1 for $|x| \in [\sigma(1-\frac{\mu}{d}),\sigma(1+\frac{\mu}{d})]$ and 0 further. What counts for the truncation done in [409] is that $\int_{[0,\alpha]^d} f^* \underset{d\to\infty}{\propto} \mathcal{V}_d(\sigma)$ with α around[9] σ and f^* is zero elsewhere. This is the case here since

$$\int_{[0,\sigma(1+\frac{\mu}{d})]^d} f^* \underset{d\to\infty}{\sim} -\mathcal{V}_d(\sigma)e^{-\mu} + \underbrace{\int_{[\sigma(1-\frac{\mu}{d}),\sigma(1+\frac{\mu}{d})]^d} f^*}_{\propto \mathcal{V}_d(\sigma)(e^\mu - e^{-\mu})} \quad (3.17)$$

Thus we will replace $f[x-y,\hat{x}-\hat{y}] \simeq f_{\text{HS}}(x^1-y^1) = -1 + \theta(|x^1-y^1|-\sigma)$, where f_{HS} is the usual static Mayer function of hard spheres, since it does not change the scalings given by f^* up to an irrelevant proportional constant. The term in equation (3.13) reduces to

 $\simeq \dfrac{N^3}{3!}\int D[x,\hat{x}]D[y,\hat{y}]D[z,\hat{z}]\,\rho[x,\hat{x}]\rho[y,\hat{y}]\rho[z,\hat{z}]f_{\text{HS}}(x^1-y^1)f_{\text{HS}}(y^1-z^1)f_{\text{HS}}(z^1-x^1)$ (3.18)

We can integrate on all variables except x^1, y^1 and z^1 because

$$\int \frac{dx^2}{(2\pi)^{\frac{d}{2}}}\cdots\frac{dx^M}{(2\pi)^{\frac{d}{2}}}D\hat{x}\,\rho(x^1,\ldots,x^M,\hat{x}) = \rho(x^1) = \text{constant} = \frac{(2\pi)^{\frac{d}{2}}}{\mathcal{V}} \quad (3.19)$$

since $\rho(x^1) = \left\langle \frac{1}{N}\sum_{i=1}^{N}\delta(x^1-x_i^1)\right\rangle_\Xi$ must be a translation-invariant function of x^1 *i.e.* a constant. $\mathcal{V}$ is the volume of the liquid. So the second term in the expansion is actually approximated for large

---

[7]The critical packing fraction later found in (3.141) is of order $O(d/2^d)$ where it is known that the virial series does not converge anymore; nevertheless, Frisch & Percus [161] have shown that in high d the truncation used here is valid largely above this bound (see §2.2).
[8]In the thermodynamic limit $\ln\Xi/N = \ln Z_N/N$ (as if *formally* the chemical potential was zero in the static partition functions analogy).
[9]More generally bounded by a finite and independent of d quantity (for example here it is bounded by 2σ for large enough d).
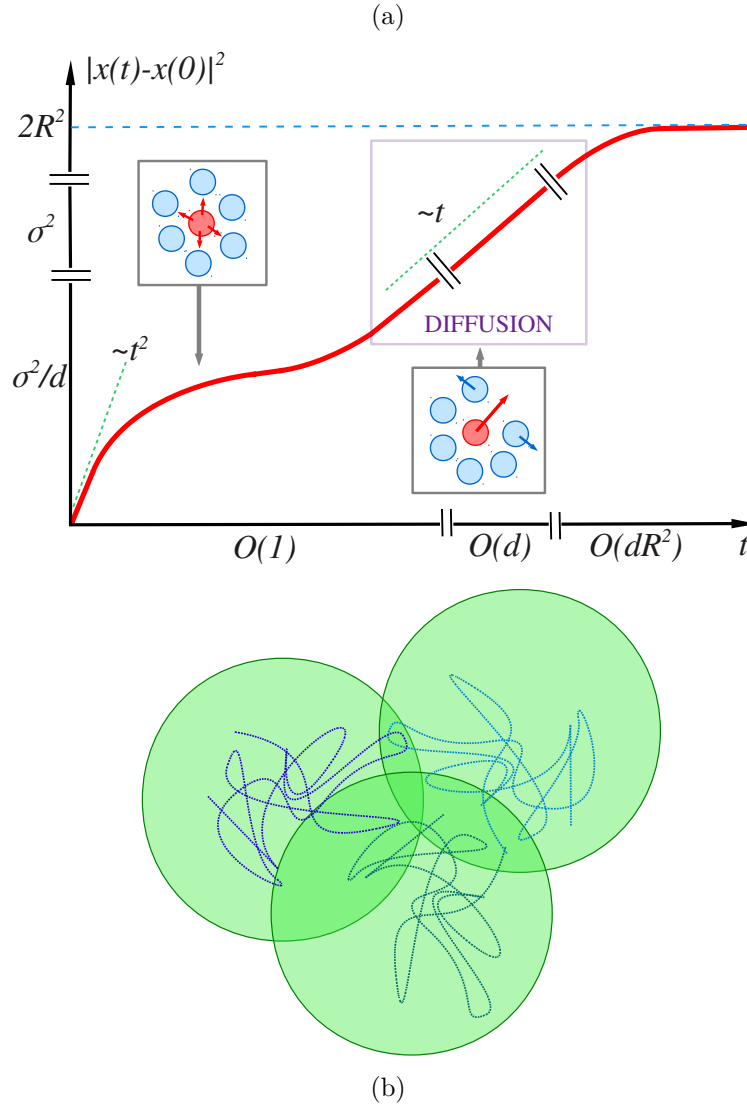
Figure 3.1: (a) The different dynamical regimes, described by equation (3.102): most of the dynamics is determined at the cage size scaling $1/d$. We assume that the diffusive regime found already at this scale extends trivially at longer times. Concerning the slope at very short times, the mean-squared displacement is $\propto t^2$ if inertia is not neglected; for purely overdamped motions it is $\propto t$. Finally, the particles feel the *box* for distances of order R, hence a saturation at this scale. (b) The dynamic triangle diagram with three trajectories.

dimension by

$$\vcenter{\hbox{\includegraphics{triangle}}} \simeq \frac{\rho^3}{3!} \int \mathrm{d}x\mathrm{d}y\mathrm{d}z\, f_{\mathrm{HS}}(x-y) f_{\mathrm{HS}}(y-z) f_{\mathrm{HS}}(z-x) \tag{3.20}$$

where $\rho = N/\mathcal{V}$ is the average particle density. We recognize the same term as in the usual static Mayer expansion of HS and can conclude as in 3.2.2.1 from [409].

3.2.3 Spherical setup

From now on, we constrain the particles to live on the surface of a sphere of radius R embedded in $d+1$ dimensional space, $\mathbb{S}_d(R)$, see section 3.1.3. The field $x(t)$ is promoted to $x : \mathbb{R} \longrightarrow \mathbb{R}^{d+1}$ and $\forall t,\ x(t)^2 = R^2$ must be verified. Concerning the response field $\hat{x}(t)$, we will rather constrain it to be orthogonal to the position field: $\forall t,\ x(t) \cdot \hat{x}(t) = 0$, thus living at each time in the hyperplane tangential to the sphere at $x(t)$, cf. figure 2. This way we ensure that we will recover rotation and translation invariances for position fields and only rotation invariance for response fields once $R \to \infty$ is taken[10]. There are many possible ways to enforce these constraints, which are eventually equivalent:

1. One strategy is to use Lagrange multipliers via a term $-\nu_i(t)x_i(t)$ in the right-hand side of (3.7), promoted to $d+1$ dimensions, which ensures that the trajectory does not get out of the sphere due to interactions or thermal noise [81]. This what we did in the p-spin model in §2.5.1, and we make a similar analysis here.

In $d \to \infty$, the value of $\nu_i \sim \nu$ is non-fluctuating and is obtained by discretizing (3.7) as follows (in the Itô sense):

$$x_i(t+\mathrm{d}t) = x_i(t) - \frac{1}{\gamma}\nu_i(t)x_i(t)\mathrm{d}t - \frac{1}{\gamma}\nabla_{x_i}H\mathrm{d}t + \frac{1}{\gamma}\eta_i\ , \qquad \langle \eta_i^\mu \eta_j^\nu \rangle = 2\gamma T\mathrm{d}t\delta_{ij}\delta_{\mu\nu} \tag{3.21}$$

At order $\mathrm{d}t$, using that for large d one has $B \cdot \eta_i \to 0$ (for any vector B uncorrelated with η_i in the Itô sense) and $\eta_i \cdot \eta_i \sim 2dT\gamma\mathrm{d}t$ due to the central limit theorem, we impose the constraint

$$R^2 = x_i(t+\mathrm{d}t) \cdot x_i(t+\mathrm{d}t) = x_i(t) \cdot x_i(t) - \frac{2\mathrm{d}t}{\gamma}x_i(t) \cdot \left[\nu_i(t)x_i(t) + \nabla_{x_i}H\right] + \frac{2dT\mathrm{d}t}{\gamma} \tag{3.22}$$

and therefore

$$\nu_i(t) = -\frac{1}{R^2}x_i \cdot \nabla_{x_i}H + \frac{dT}{R^2} \tag{3.23}$$

We have a general relation [199, Eq.(2.2.10)] (virial equation) for the reduced pressure, which is shown in §5.7.1:

$$\frac{\beta P}{\rho} = 1 - \frac{\beta}{dN}\left\langle \sum_i x_i \cdot \nabla_{x_i}H \right\rangle \tag{3.24}$$

For $d \to \infty$ the fluctuations vanish because we average over d dimensions, we thus have

$$\frac{1}{N}\sum_i x_i \cdot \nabla_{x_i}H \sim \frac{1}{N}\left\langle \sum_i x_i \cdot \nabla_{x_i}H \right\rangle = dT\left(1 - \frac{\beta P}{\rho}\right) \tag{3.25}$$

and plugging this in Eq. (3.23) we obtain that all $\nu_i(t)$ are equal and constant in time, given by

$$\nu_i(t) \sim \nu = \frac{dP}{\rho R^2} \tag{3.26}$$

From the liquid entropy in $d \to \infty$ [162, 409, 161, 312, 270] (see (2.45)):

$$\frac{\beta P}{\rho} = 1 - \frac{\rho}{2}\int \mathrm{d}\mathbf{r}\left(e^{-\beta V(r)} - 1\right) \tag{3.27}$$

For example, $\beta P/\rho = 1 + d\widehat{\varphi}/2$ in the HS liquid phase, where $\widehat{\varphi}$ is the rescaled packing fraction $\widehat{\varphi} = 2^d\varphi/d = \rho\mathcal{V}_d(\sigma)/d$ and the number density $\rho = N/V$.

This choice results in an additional term $\int \mathrm{d}t\, \nu\hat{x} \cdot x$ in the definition of Φ (3.9), and the summation of

---

[10]Another way to see it is that the spherical constraint implies $\dot{x}_i \cdot x_i = 0$ and only tangential fields $\hat{x}_i$ are needed to exponentiate the Langevin equation in the MSRDDJ path integral.

paths in (3.16) is over the sphere $\mathbb{S}_d(R)$ for positions and the tangential hyperplane. In practice, we will integrate on the whole $d+1$ dimensional space and enforce the constraint through Dirac deltas. Note that, with x (respectively $\hat{x}$) representing the position (respectively response) field at some time and $E = \text{Span}(x)$,

$$\int_{\mathbb{R}^{d+1}} \mathrm{d}x\, \delta(x^2 - R^2) = \Omega_{d+1} \int_0^\infty \mathrm{d}r\, r^d \delta(r^2 - R^2) = \Omega_{d+1} \frac{R^d}{2R} = \frac{\mathcal{V}}{2R} = \frac{1}{2R} \int_{\mathcal{V}} \mathrm{d}x$$

$$\int_{\mathbb{R}^{d+1}} \mathrm{d}\hat{x}\, \delta(2x \cdot \hat{x}) = \int_{E \times E^\perp} \mathrm{d}\hat{x}_\parallel \mathrm{d}\hat{x}_\perp\, \delta(2|x|\,\hat{x}_\parallel) = \int_{E \times E^\perp} \mathrm{d}\hat{x}_\parallel \mathrm{d}\hat{x}_\perp\, \delta(2R\hat{x}_\parallel) = \frac{1}{2R} \int_{E^\perp} \mathrm{d}\hat{x}_\perp$$

(3.28)

These choices rescale the path integral measures with respect to the ones on $\mathbb{R}^d$, which does not affect the dynamics. In the thermodynamic limit of infinite radius R (with $\rho = N/\mathcal{V}$ fixed), we recover the original d-dimensional space.

2. In the previous method, we would exponentiate the Dirac delta functions, giving additional terms in the exponent $\int \mathrm{d}t\, \mu x \cdot \hat{x}$ and $\int \mathrm{d}t\, \hat{\mu}(x^2 - R^2)$. We see that the Lagrange multiplier would just shift μ. Hence, another technique is directly (and somewhat physically blindly) to promote the path integrals in (3.16) to $d+1$ dimensions and use Dirac deltas to constrain the x, $\hat{x}$ fields. This is what we are going to follow with fields ν, $\hat{\nu}$ but note that *it is not exactly the Lagrange multiplier*, even if it plays a similar role.

3. We might as well add a soft constraint $A \sum_i (x_i^2 - R^2)^2$ in the Hamiltonian. It would add a single-particle term $2A \int \mathrm{d}t\, i\hat{x} \cdot x(x^2 - R^2)$ to Φ. Then we can write (still at a given time)

$$e^{-2Ai\hat{x} \cdot x(x^2 - R^2)} \propto \int_{\mathbb{R}^{d+1}} \mathrm{d}\hat{\nu}\, \delta\left(\frac{\hat{\nu}}{2A} - \hat{x} \cdot x\right) e^{-i\hat{\nu}(x^2 - R^2)} \propto \int_{\mathbb{R}^{d+1}} \mathrm{d}\nu \mathrm{d}\hat{\nu}\, e^{i\nu\hat{\nu}/A - 2i\nu x \cdot \hat{x} - i\hat{\nu}(x^2 - R^2)}$$

(3.29)

and in the hard limit $A \to \infty$ this is the same as enforcing the constraints through $\delta(x^2 - R^2)$, $\delta(2x \cdot \hat{x})$.

3.2.4 Translation of the dynamics into superfield language

As a compact way to write dynamical equations, we will use superspace notation, introduced in §2.4. At any step, one can unfold this notation to recover the standard dynamical variables. $\{\theta_i, \bar{\theta}_i\}$ are Grassmann variables[11]. Let us define $\tilde{x} = i\hat{x}$ for convenience. We encode the position and response fields $[x, \hat{x}]$ in a superfield $\boldsymbol{x}(a) = x(t) + \bar{\theta}_1 \theta_1 \tilde{x}(t)$, where arguments are denoted by $a = (\theta_1, \bar{\theta}_1, t)$. The Mayer function and the kinetic part can be explicitly written:

$$f(\boldsymbol{x}) = e^{-\int \mathrm{d}a\, V(\boldsymbol{x})} - 1 \quad \text{with} \quad \int \mathrm{d}a = \int \mathrm{d}\theta_1 \mathrm{d}\bar{\theta}_1 \mathrm{d}t$$

$$\Phi(\boldsymbol{x}) = \gamma \int \mathrm{d}a\, \frac{\partial \boldsymbol{x}}{\partial \theta_1} \cdot \left(T \frac{\partial \boldsymbol{x}}{\partial \bar{\theta}_1} - \theta_1 \frac{\partial \boldsymbol{x}}{\partial t}\right)$$

(3.30)

$\boldsymbol{x}(a)^2 = x(t)^2 + 2\bar{\theta}_1 \theta_1 x(t) \cdot \tilde{x}(t)$ implies for the constraints that $\delta(x(t)^2 - R^2)\delta(2x(t) \cdot \hat{x}(t)) = \delta(\boldsymbol{x}(a)^2 - R^2)$. The measure $\mathrm{D}[x, \hat{x}]$ is replaced by $\mathrm{D}\boldsymbol{x} = \mathrm{D}[x, \hat{x}]$ where integration over $\hat{x}$ is on the *imaginary axis* $i\mathbb{R}^{d+1}$. Then the action can be written in the form:

$$\mathcal{S} = -\int \mathrm{D}\boldsymbol{x}\, \delta(\boldsymbol{x}(a)^2 - R^2)\rho(\boldsymbol{x})(\ln\rho(\boldsymbol{x}) + \Phi(\boldsymbol{x})) + \frac{N}{2} \int \mathrm{D}\boldsymbol{x} \mathrm{D}\boldsymbol{y}\, \delta(\boldsymbol{x}(a)^2 - R^2)\delta(\boldsymbol{y}(b)^2 - R^2)\rho(\boldsymbol{x})\rho(\boldsymbol{y})f(\boldsymbol{x} - \boldsymbol{y})$$

(3.31)

still with $\delta\mathcal{S}/\delta\rho(\boldsymbol{x}) = 0$ and $\int \mathrm{D}\boldsymbol{x}\, \delta(\boldsymbol{x}(a)^2 - R^2)\rho(\boldsymbol{x}) = 1$.

3.3 Translational and rotational invariances

We now take into account rotational and translational invariances and take the limit $d \to \infty$. In some cases the order of the two limits is irrelevant, but when relevant, we should take the $R \to \infty$ limit first. In other words, we should consider for example that R/d is a large quantity.

---

[11]Let us emphasize here that this is only a compact notation, but we note by way of excuse that the computation is prohibitively complicated proceeding otherwise.

3.3.1 *Functional spherical coordinates*: invariances using the mean-squared displacement

As emphasized in section 3.1, the aim of the introduction of $\mathbb{S}_d(R)$ is to take into account both translation and rotation invariances on Euclidean d-dimensional space by only rotation invariance on a sphere of a $d + 1$ dimensional space, which is actually easier to handle in the viewpoint of the dynamics. Indeed, the MSRDDJ action $\mathcal{A}$ in (3.9), now promoted to $d + 1$ dimensional fields, and the constraints in (3.31) are invariant by the same rotation $\mathcal{R}$ for both fields *i.e.* $(x, \hat{x}) \to (\mathcal{R}x, \mathcal{R}\hat{x})$, which is transposed to superfields as a global rotation[12] $\boldsymbol{x} \to \mathcal{R}\boldsymbol{x}$.

Now considering expression (3.31), we define a superfield

$$\boldsymbol{q}(a, b) = \boldsymbol{x}(a) \cdot \boldsymbol{x}(b) \tag{3.32}$$

We assume that the $d+1$-dimensional liquid is invariant by rotation *i.e.* $\rho(\boldsymbol{x}) = \rho(\{\boldsymbol{x}(a) \cdot \boldsymbol{x}(b)\}_{a,b}) = \rho(\boldsymbol{q})$. This way we will remove all irrelevant variables and be able to use a saddle point method.

Eventually, as regards the $R \to \infty$ limit, it is more convenient to consider the mean-squared displacement (MSD)

$$\boldsymbol{D}(a, b) = (\boldsymbol{x}(a) - \boldsymbol{x}(b))^2 \tag{3.33}$$

since it is a finite quantity as long as the difference $t - t'$ is finite, at equilibrium. Before the dynamical transition is met, $\boldsymbol{D}$ is of order R^2 when $t - t' \to \infty$. We thus expect an artificial second plateau of order R^2 due to finite size effects, that will be removed when $R \to \infty$, giving back diffusion at long times (see figure 3.1). One can check explicitly that in this limit the original d-dimensional MSD is recovered and that it is translation and rotation invariant for the position and rotation invariant for the response field, writing

$$\boldsymbol{D}(a, b) = (x(t) - x(t'))^2 + 2\bar{\theta}_1\theta_1(x(t) - x(t')) \cdot \hat{x}(t') + 2\bar{\theta}_2\theta_2(x(t') - x(t)) \cdot \hat{x}(t) - 2\bar{\theta}_1\theta_1\bar{\theta}_2\theta_2\hat{x}(t) \cdot \hat{x}(t') \tag{3.34}$$

Fixing a unit vector $\hat{u} = x(t_0)/R$ from the center of the sphere pointing towards a point on its surface, the origin of the trajectory at time t_0, we can write

$$\begin{aligned} x(t) &= R\hat{u} + x_0(t) \\ \hat{x}(t) &= \hat{x}_0(t) \end{aligned} \tag{3.35}$$

where $x_0(t)$ is along a chord and $\hat{x}_0(t)$ points to the hyperplane tangential to $x(t)$ from the sphere. When $R \to \infty$, they both are in this hyperplane which is the original d-dimensional Euclidean space; they represent the original position and response fields. We immediately have, from the constraints on the fields, for finite times $t > t_0$ such that $(x(t) - x(t_0))^2 \ll R^2$,

$$\begin{aligned} x_0(t) \cdot \hat{u} &= -\frac{x_0(t)^2}{2R} \xrightarrow[R\to\infty]{} 0 \\ \hat{x}_0(t) \cdot \hat{u} &= -\frac{x_0(t) \cdot \hat{x}_0(t)}{2R} \xrightarrow[R\to\infty]{} 0 \end{aligned} \tag{3.36}$$

ensuring that when $R \to \infty$, trajectories x_0 and $\hat{x}_0$ live in the same d-dimensional Euclidean space and that $\boldsymbol{D}$ reduces to the one we would have written in the original d-dimensional space (putting the 0 subscripts everywhere in (3.34) and taking the limit of infinite radius). It has the right invariances described above (d-dimensional rotation on both fields and translation on positions only) for the original position and response fields $\lim_{R\to\infty} x_0$ and $\lim_{R\to\infty} \hat{x}_0$.

3.3.2 Scalings in the infinite d limit

To use the saddle point method, we need to specify how the quantities defined here scale with dimension. As in the statics in [312], if we define $u = x - X$ where X denotes the translational degree of freedom of a particle so that u characterizes motion around an average position, u scales as $1/d$. This fact will be easily seen in the liquid phase in §5.2 and has been also shown by studying the scaling of the cage in [312, 243, 242, 225].

---

[12]See subsection 3.2.3 and footnote 4.
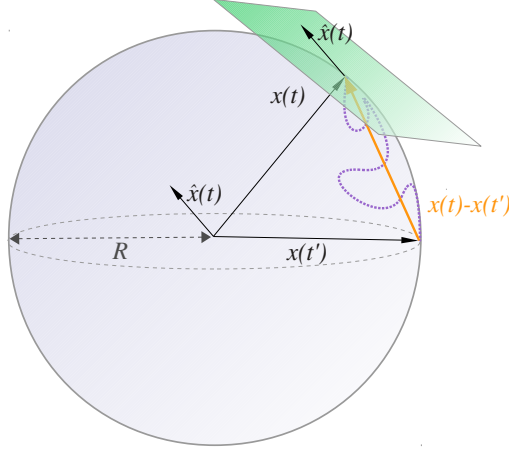
Figure 3.2: Notations on the sphere for x, $\hat{x}$. The vector $x(t) - x(t')$ is along a chord and when $R \to \infty$, it lives in the same d-dimensional space as $\hat{x}$.

As Φ is translation invariant along x,

$$\Phi[x, \tilde{x}] = \Phi[u, \tilde{u} \equiv \tilde{x}] = \gamma \int \mathrm{d}t \left(-T\tilde{u}^2 + \tilde{u} \cdot \dot{u} \right) \tag{3.37}$$

$\dot{u} \sim 1/d$ implies that, for the action to describe the Langevin process above ((3.7)), we need the two terms in the integral to scale identically in the limit $d \to \infty$. Thus $\tilde{u} \sim 1/d$ as well. This implies that

$$\boldsymbol{D} = \frac{\sigma^2}{d} \boldsymbol{\Delta} \tag{3.38}$$

where $\boldsymbol{\Delta}$ is of order 1. Hence, for convenience, noticing that $\boldsymbol{D} = 2R^2 - 2\boldsymbol{q}$, we define the rescaled quantities

$$\Delta_{\mathrm{liq}} = \frac{2dR^2}{\sigma^2}, \qquad \boldsymbol{Q} = \Delta_{\mathrm{liq}} - \boldsymbol{\Delta} = \frac{2d}{\sigma^2} \boldsymbol{q} \tag{3.39}$$

Δ_{liq} corresponds to a typical MSD between particles (in the liquid phase) on the sphere $\mathbb{S}_d(R)$. $\boldsymbol{Q}(a, a) = \Delta_{\mathrm{liq}}$ is the spherical constraint.
We then choose

$$\gamma = \frac{2d^2}{\sigma^2} \widehat{\gamma} \quad \text{in order to write} \quad \Phi = d\widehat{\Phi} \tag{3.40}$$

with $\widehat{\gamma}$ and $\widehat{\Phi}$ of order 1 so that $\Phi(\boldsymbol{x})$ scales like $\ln\rho(\boldsymbol{x})$, otherwise the infinite d limit would not be well defined.
Indeed, from the consideration of the $d \to \infty$ virial expansion in §2.2 and specifically (2.42), we will assume that ρ is exponential in d, that is

$$\rho(\boldsymbol{q}) = \Lambda(\boldsymbol{Q})e^{d\Omega(\boldsymbol{Q})} \quad \textit{i.e.} \quad \ln\rho(\boldsymbol{q}) \underset{d \to \infty}{\sim} d\Omega(\boldsymbol{Q}) \tag{3.41}$$

with Ω of order 1 and Λ a subdominant factor (*i.e.* non-exponential in d).
This is discussed in §2.2 and has been proven in the statics in [243, Eq. (65)], see the argument in §4.3 that can be transposed to dynamics.

3.3.3 Ideal gas term

We write equation (3.31) as $\mathcal{S} = \mathcal{S}_{\mathrm{IG}} + \mathcal{S}_{\mathrm{int}}$ and focus on the ideal gas term $\mathcal{S}_{\mathrm{IG}}$. Exploiting the invariances, we apply the program mentioned in 3.3.1:

$$\begin{aligned}
\mathcal{S}_{\mathrm{IG}} &\propto \int \mathrm{D}\boldsymbol{x}\, \delta(\boldsymbol{x}(a)^2 - R^2)\rho(\boldsymbol{x})(\ln\rho(\boldsymbol{x}) + \Phi(\boldsymbol{x})) \\
&= \int \mathrm{D}\boldsymbol{x}\mathrm{D}^{\mathrm{s}}\boldsymbol{q}\, \delta(\boldsymbol{q}(a, b) - \boldsymbol{x}(a) \cdot \boldsymbol{x}(b))\delta(\boldsymbol{q}(a, a) - R^2)\rho(\boldsymbol{q})(\ln\rho(\boldsymbol{q}) + \Phi(\boldsymbol{q})) \\
&= \int \mathrm{D}\boldsymbol{x}\mathrm{D}^{\mathrm{s}}\boldsymbol{q}\mathrm{D}^{\mathrm{s}}\boldsymbol{q}'\, \delta(\boldsymbol{q}(a, a) - R^2)e^{i\mathrm{str}(\boldsymbol{q}\boldsymbol{q}') - i \int \mathrm{d}a\mathrm{d}b\, \boldsymbol{q}'(a, b)\boldsymbol{x}(a) \cdot \boldsymbol{x}(b)}\rho(\boldsymbol{q})(\ln\rho(\boldsymbol{q}) + \Phi(\boldsymbol{q})) \\
&= \int \mathrm{D}^{\mathrm{s}}\boldsymbol{q}\mathrm{D}^{\mathrm{s}}\boldsymbol{q}'\, \delta(\boldsymbol{q}(a, a) - R^2)e^{i\mathrm{str}(\boldsymbol{q}\boldsymbol{q}') - \frac{d+1}{2} \ln \mathrm{sdet}(2i\boldsymbol{q}')}\rho(\boldsymbol{q})(\ln\rho(\boldsymbol{q}) + \Phi(\boldsymbol{q}))
\end{aligned} \tag{3.42}$$

The explicit expression of $\Phi(\boldsymbol{q})$ will be computed in 3.4.1. The integral over $\boldsymbol{q'}$ is evaluated through a saddle point method for $d \to \infty$. As in §2.3.1, the saddle-point equation is $2i\boldsymbol{q} = (d+1)\boldsymbol{q'}^{-1}|_{\text{sp}}$. We introduce the rescaled variable $\boldsymbol{Q}$ and neglect subdominant terms which will be calculated in subsection 3.3.3. For convenience with respect to the saddle-point equation in section 3.4, we exponentiate the resulting spherical constraint $\boldsymbol{Q}(a,a) - \Delta_{\text{liq}}$,

$$\mathcal{S}_{\text{IG}} \propto \int \mathrm{D}[\boldsymbol{Q},\boldsymbol{\nu}]e^{\frac{d}{2}\ln\text{sdet}\,\boldsymbol{Q}-\frac{d}{2}\int \mathrm{d}a\,\boldsymbol{\nu}(a)(\boldsymbol{Q}(a,a)-\Delta_{\text{liq}})}\rho(\boldsymbol{Q})(\ln\rho(\boldsymbol{Q}) + \Phi(\boldsymbol{Q})) \tag{3.43}$$

In the limit $d \to \infty$ we apply a saddle point method, thanks to the scalings provided in 3.3.2. We can get rid of proportionality constants using the normalization of the density:

$$\mathcal{S}_{\text{IG}} = \frac{\mathcal{S}_{\text{IG}}}{\int \mathrm{D}\boldsymbol{x}\,\delta(\boldsymbol{x}(a)^2 - R^2)\rho(\boldsymbol{x})} = -\frac{\int \mathrm{D}[\boldsymbol{Q},\boldsymbol{\nu}]\mathcal{C}(\boldsymbol{Q})e^{\frac{d}{2}\Gamma(\boldsymbol{Q},\boldsymbol{\nu})}(\ln\rho(\boldsymbol{Q}) + \Phi(\boldsymbol{Q}))}{\int \mathrm{D}[\boldsymbol{Q},\boldsymbol{\nu}]\mathcal{C}(\boldsymbol{Q})e^{\frac{d}{2}\Gamma(\boldsymbol{Q},\boldsymbol{\nu})}} \tag{3.44}$$

where $\mathcal{C}(\boldsymbol{Q})$ accounts for forgotten subdominant contributions to the integral, and

$$\Gamma(\boldsymbol{Q},\boldsymbol{\nu}) = \ln\text{sdet}\,\boldsymbol{Q} - \int \mathrm{d}a\,\boldsymbol{\nu}(a)\left(\boldsymbol{Q}(a,a) - \Delta_{\text{liq}}\right) + 2\Omega(\boldsymbol{Q}) \tag{3.45}$$

is the saddle point function. In $d \to \infty$ we maximize Γ, in particular

$$\left.\frac{\delta\Gamma}{\delta\boldsymbol{Q}}\right|_{\text{sp}} = \boldsymbol{0} \qquad \text{and} \qquad \left.\frac{\delta\Gamma}{\delta\boldsymbol{\nu}}\right|_{\text{sp}} = \boldsymbol{0} \Leftrightarrow \boldsymbol{Q}(a,a) = \Delta_{\text{liq}} \tag{3.46}$$

giving the result

$$\mathcal{S}_{\text{IG}} \underset{d\to\infty}{=} -d[\Omega(\boldsymbol{Q}^{\text{sp}}) + \widehat{\Phi}(\boldsymbol{Q}^{\text{sp}})] \tag{3.47}$$

This can be expressed explicitly using once again the normalization condition

$$\int \mathrm{D}[\boldsymbol{Q},\boldsymbol{\nu}]\mathcal{C}(\boldsymbol{Q})e^{\frac{d}{2}\Gamma(\boldsymbol{Q},\boldsymbol{\nu})} = 1 \tag{3.48}$$

Evaluating it for $d \to \infty$ and taking the logarithm of the resulting equation at dominant order $O(d)$ provides $\Gamma(\boldsymbol{Q}^{\text{sp}},\boldsymbol{\nu}^{\text{sp}}) = 0$ up to irrelevant additive constants[13], from which we get

$$\mathcal{S}_{\text{IG}} \underset{d\to\infty}{=} \frac{d}{2}\ln\text{sdet}\,\boldsymbol{Q}^{\text{sp}} - \frac{d}{2}\int \mathrm{d}a\,\boldsymbol{\nu}^{\text{sp}}(a)\left(\boldsymbol{Q}^{\text{sp}}(a,a) - \Delta_{\text{liq}}\right) - d\widehat{\Phi}(\boldsymbol{Q}^{\text{sp}}) \tag{3.49}$$

3.3.4 Interaction term

3.3.4.1 Changes of variables to *functional spherical coordinates*

Now focusing on $\mathcal{S}_{\text{int}}$, we introduce the superfields $\boldsymbol{q}(a,b) = \boldsymbol{x}(a) \cdot \boldsymbol{x}(b)$, $\boldsymbol{p}(a,b) = \boldsymbol{y}(a) \cdot \boldsymbol{y}(b)$ (through a symmetric measure D^{s}) and the interaction superfield $\boldsymbol{\omega}(a) = (\boldsymbol{x}(a) - \boldsymbol{y}(a))^2$, a one component variable since the Mayer function $f[x - y, \hat{x} - \hat{y}]$ in (3.30) needs only scalar products between its variables at equal times.

$$\begin{aligned}
\mathcal{S}_{\text{int}} &\propto \int \mathrm{D}[\boldsymbol{x},\boldsymbol{y}]\delta(\boldsymbol{x}(a)^2 - R^2)\delta(\boldsymbol{y}(b)^2 - R^2)\rho(\boldsymbol{x})\rho(\boldsymbol{y})f(\boldsymbol{x} - \boldsymbol{y}) \\
&= \int \mathrm{D}[\boldsymbol{x},\boldsymbol{y},\boldsymbol{q},\boldsymbol{q'},\boldsymbol{p},\boldsymbol{p'},\boldsymbol{\omega},\boldsymbol{\omega'}]\delta(\boldsymbol{q}(a,a) - R^2)\delta(\boldsymbol{p}(a,a) - R^2)e^{i\text{str}(\boldsymbol{qq'}+\boldsymbol{pp'})}\rho(\boldsymbol{q})\rho(\boldsymbol{p})f(\sqrt{\boldsymbol{\omega}}) \\
&\qquad \times e^{-i\int \mathrm{d}a\mathrm{d}b\,[\boldsymbol{q'}(a,b)\boldsymbol{x}(a)\cdot\boldsymbol{x}(b)+\boldsymbol{p'}(a,b)\boldsymbol{y}(a)\cdot\boldsymbol{y}(b)]-i\int \mathrm{d}a\,\boldsymbol{\omega'}(a)[(\boldsymbol{x}(a)-\boldsymbol{y}(a))^2-\boldsymbol{\omega}(a)]} \\
&= \int \mathrm{D}[\boldsymbol{q},\boldsymbol{q'},\boldsymbol{p},\boldsymbol{p'},\boldsymbol{\omega},\boldsymbol{\omega'}]\delta(\boldsymbol{q}(a,a) - R^2)\delta(\boldsymbol{p}(a,a) - R^2)\rho(\boldsymbol{q})\rho(\boldsymbol{p})f(\sqrt{\boldsymbol{\omega}}) \\
&\qquad \times \exp\left(i\text{str}(\boldsymbol{qq'} + \boldsymbol{pp'}) + i\int \mathrm{d}a\,\boldsymbol{\omega'}(a)\boldsymbol{\omega}(a) - \frac{d+1}{2}\ln\det\begin{pmatrix} \boldsymbol{q'}+\bar{\boldsymbol{\omega}} & -\bar{\boldsymbol{\omega}} \\ -\bar{\boldsymbol{\omega}} & \boldsymbol{p'}+\bar{\boldsymbol{\omega}} \end{pmatrix}\right)
\end{aligned} \tag{3.50}$$

The last line is obtained by Gaussian integration on superfields $\boldsymbol{x}$ and $\boldsymbol{y}$, introducing the superfield $\bar{\boldsymbol{\omega}}(a,b) = \boldsymbol{\omega'}(a)\mathbf{1}(a,b)$, and det means the determinant of the 2×2 block matrix consisting of superfields. We now change variables to exploit the $\boldsymbol{x} \leftrightarrow \boldsymbol{y}$ symmetry in (3.50),

$$\boldsymbol{q}_{\pm} = \frac{\boldsymbol{q} \pm \boldsymbol{p}}{2} \qquad \text{and} \qquad \boldsymbol{q'}_{\pm} = \frac{\boldsymbol{q'} \pm \boldsymbol{p'}}{2} \tag{3.51}$$

---

[13]These constants were hidden in $\mathcal{C}(\boldsymbol{Q}^{\text{sp}})$ and do not depend upon $\boldsymbol{Q}^{\text{sp}}$, therefore having no influence on the dynamics.

whose Jacobian is subdominant. The 2×2 block matrix can be transformed through a (Weyl) rotation which does not affect the determinant:

$$\frac{1}{\sqrt{2}}\begin{pmatrix} \mathbb{1} & -\mathbb{1} \\ \mathbb{1} & \mathbb{1} \end{pmatrix}\begin{pmatrix} q'+\bar{\omega} & -\bar{\omega} \\ -\bar{\omega} & p'+\bar{\omega} \end{pmatrix}\frac{1}{\sqrt{2}}\begin{pmatrix} \mathbb{1} & \mathbb{1} \\ -\mathbb{1} & \mathbb{1} \end{pmatrix} = \begin{pmatrix} q'_+ + 2\bar{\omega} & q'_- \\ q'_- & q'_+ \end{pmatrix} \tag{3.52}$$

In $d \to \infty$, owing to the $\boldsymbol{x} \leftrightarrow \boldsymbol{y}$ or $\boldsymbol{q} \leftrightarrow \boldsymbol{p}$ (respectively $\boldsymbol{q}' \leftrightarrow \boldsymbol{p}'$) symmetry in (3.50), the saddle-point value of $\boldsymbol{q}_-$ (respectively $\boldsymbol{q}'_-$) is zero. Dropping the $+$ index for the two other superfields[14], we get

$$\mathcal{S}_{\text{int}} \propto \int \mathrm{D}[\boldsymbol{q}, \boldsymbol{q}', \boldsymbol{\omega}, \boldsymbol{\omega}']\delta(\boldsymbol{q}(a,a) - R^2)e^{2i\mathrm{str}(\boldsymbol{q}\boldsymbol{q}')+i\int \mathrm{d}a\,\boldsymbol{\omega}'(a)\boldsymbol{\omega}(a)-\frac{d+1}{2}\ln\mathrm{sdet}\boldsymbol{q}'-\frac{d+1}{2}\ln\mathrm{sdet}(\boldsymbol{q}'+2\bar{\omega})}\rho(\boldsymbol{q})^2 f(\sqrt{\boldsymbol{\omega}}) \tag{3.53}$$

To simplify the last term in the exponential, we make the following change of variables:

$$\boldsymbol{q} = R^2\boldsymbol{P} - \frac{1}{2}\boldsymbol{D} \qquad \text{and} \qquad \boldsymbol{q}' = \frac{d+1}{2i}\left(R^2\boldsymbol{P} - \frac{1}{2}\boldsymbol{D}'\right)^{-1} \tag{3.54}$$

The Jacobian is subdominant ; all such subdominant terms will be calculated in subsection 3.3.4.2. The aim is to recover the same saddle point function Γ at $O(d)$ in the exponential in $\mathcal{S}_{\text{int}}$ as in the ideal gas term. Let us focus on the last term in the exponential, neglecting irrelevant constants:

$$\begin{aligned}\ln\mathrm{sdet}(\boldsymbol{q}'+2\bar{\omega}) &= -\ln\mathrm{sdet}\left(R^2\boldsymbol{P} - \frac{\boldsymbol{D}'}{2}\right) + \ln\mathrm{sdet}\left(\mathbb{1} - \frac{2i}{d+1}\bar{\omega}\boldsymbol{D}'\right) \\ &\quad + \ln\left(\mathbb{1} + \frac{2R^2}{d+1}\mathrm{str}\left[\boldsymbol{P}\left(\frac{\bar{\omega}^{-1}}{2i} - \frac{\boldsymbol{D}'}{d+1}\right)^{-1}\right]\right) \\ &= -\ln\mathrm{sdet}\left(R^2\boldsymbol{P} - \frac{\boldsymbol{D}'}{2}\right) + \ln\mathrm{sdet}\left(\mathbb{1} - \frac{2i}{d+1}\bar{\omega}\boldsymbol{D}'\right) + \ln\mathrm{str}\left[\boldsymbol{P}\left(\frac{\bar{\omega}^{-1}}{2i} - \frac{\boldsymbol{D}'}{d+1}\right)^{-1}\right]\end{aligned} \tag{3.55}$$

We used (2.119) and expanded using the limit $R \to \infty$ before $d \to \infty$ in the last line as emphasized in the introduction to this section, which is valid if $\mathrm{str}\left[\boldsymbol{P}\left(\frac{\bar{\omega}^{-1}}{2i} - \frac{\boldsymbol{D}'}{d+1}\right)^{-1}\right]$ is not zero.

We expect the same scalings for $\boldsymbol{D}$ and $\boldsymbol{D}'$, so let us assume $\boldsymbol{D}' = \sigma^2\boldsymbol{\Delta}'/d$ and $\boldsymbol{\omega}' = d\boldsymbol{\mu}'/\sigma^2$, hence $\bar{\omega}\boldsymbol{D}' = \bar{\mu}\boldsymbol{\Delta}' = O(d^0)$. Using (2.111), we can use expansions:

$$\begin{aligned}\ln\mathrm{sdet}\left(\mathbb{1} - \frac{2i}{d+1}\bar{\omega}\boldsymbol{D}'\right) &\underset{d\to\infty}{=} -\frac{2i}{d+1}\mathrm{str}(\bar{\mu}\boldsymbol{\Delta}') + O\left(\frac{1}{d^2}\right) \\ \ln\mathrm{str}\left[\boldsymbol{P}\left(\frac{\bar{\omega}^{-1}}{2i} - \frac{\boldsymbol{D}'}{d+1}\right)^{-1}\right] &\underset{d\to\infty}{=} \ln\mathrm{str}(\boldsymbol{P}\bar{\mu}) + \frac{2i}{d+1}\frac{\mathrm{str}(\boldsymbol{P}\bar{\mu}\boldsymbol{\Delta}'\bar{\mu})}{\mathrm{str}(\boldsymbol{P}\bar{\mu})} + O\left(\frac{1}{d^2}\right)\end{aligned} \tag{3.56}$$

Summarizing,

$$\begin{aligned}\mathcal{S}_{\text{int}} \propto \int \mathrm{D}[\boldsymbol{D}, \boldsymbol{D}']\delta(\boldsymbol{D}(a,a))&e^{2i\mathrm{str}\left[\left(R^2\boldsymbol{P}-\frac{1}{2}\boldsymbol{D}\right)\frac{d+1}{2i}\left(R^2\boldsymbol{P}-\frac{1}{2}\boldsymbol{D}'\right)^{-1}\right]-(d+1)\ln\mathrm{sdet}\left(R^2\boldsymbol{P}-\frac{\boldsymbol{D}'}{2}\right)}\rho(\boldsymbol{D})^2 \\ &\times \int \mathrm{D}[\boldsymbol{\omega}, \boldsymbol{\mu}']e^{id\int \mathrm{d}a\,\boldsymbol{\mu}'(a)\boldsymbol{\omega}(a)+i\mathrm{str}(\bar{\mu}\boldsymbol{\Delta}')-\frac{d+1}{2}\ln\mathrm{str}(\boldsymbol{P}\bar{\mu})-i\mathrm{str}(\boldsymbol{P}\bar{\mu}\boldsymbol{\Delta}'\bar{\mu})/\mathrm{str}(\boldsymbol{P}\bar{\mu})}f(\sqrt{\boldsymbol{\omega}})\end{aligned} \tag{3.57}$$

At order $O(d)$ in the exponential in $\mathcal{S}_{\text{int}}$, we get (twice) the same terms that we had in (3.42); therefore in the last line, all dependence in $\boldsymbol{D}'$ is of $O(d^0)$. We now go back to the original variables $\boldsymbol{q}$ and $\boldsymbol{q}'$ by making again the change of variables (3.54). The terms in the exponent that must be kept for the saddle point in d becomes

$$2i\mathrm{str}(\boldsymbol{q}\boldsymbol{q}') - (d+1)\ln\mathrm{sdet}(2i\boldsymbol{q}') + 2\ln\rho(\boldsymbol{q}) \tag{3.58}$$

which is exactly twice what we had for $\mathcal{S}_{\text{IG}}$. Hence, $2i\boldsymbol{q} = (d+1)\boldsymbol{q}'|_{\text{sp}}^{-1}$ i.e. $\boldsymbol{D}'|_{\text{sp}} = \boldsymbol{D}$.
Then the term $\mathrm{str}(\bar{\mu}\boldsymbol{\Delta}) = \int \mathrm{d}a\,\boldsymbol{\mu}'(a)\boldsymbol{\Delta}(a,a) = 0$ because of the constraint. We also note that

$$\boldsymbol{\omega}(a) = (\boldsymbol{x}(a) - \boldsymbol{y}(a))^2 = (x(t) - y(t))^2 + 2\bar{\theta}_1\theta_1(x(t) - y(t))\cdot(\tilde{x}(t) - \tilde{y}(t)) \tag{3.59}$$

---

[14]The symmetry also implies that the saddle-point value of $\boldsymbol{q}_+$ is the same than $\boldsymbol{q}$ or equivalently $\boldsymbol{p}$ (same for the primes).

As we expect $(x(t) - y(t))^2 = \sigma^2(1 + O(1/d))$ (see §3.3.2), we define

$$\boldsymbol{\omega}(a) = \sigma^2 \left(1 + \frac{2}{d}\boldsymbol{\mu}(a)\right) \tag{3.60}$$

We set $\lambda = \int \mathrm{d}a \, \boldsymbol{\mu}'(a) = \mathrm{str}(\boldsymbol{P}\bar{\boldsymbol{\mu}})$ with a Dirac delta and exponentiate it with a conjugated λ' as usual. The interaction term[15] now reads, once again exponentiating the constraint $\delta(\boldsymbol{Q}(a, a) - \Delta_{\mathrm{liq}})$ through a superfield $\boldsymbol{\nu}$,

$$\mathcal{S}_{\mathrm{int}} \propto \int \mathrm{D}[\boldsymbol{Q}, \boldsymbol{\nu}] e^{d\Gamma(\boldsymbol{Q},\boldsymbol{\nu})} \mathcal{F}(\boldsymbol{Q}), \text{ with } \mathcal{F} \text{ defined by:}$$

$$\mathcal{F}(\boldsymbol{Q}) \propto \int \mathrm{D}[\boldsymbol{\mu}, \boldsymbol{\mu}'] \mathrm{d}\lambda \mathrm{d}\lambda' \exp\left(i\lambda\lambda' + id\lambda - \frac{d+1}{2}\ln\lambda + 2i\int \mathrm{d}a \, \boldsymbol{\mu}'(a)(\boldsymbol{\mu}(a) - \lambda'/2)\right) \tag{3.61}$$

$$\times \exp\left(-i\lambda\Delta_{\mathrm{liq}} + i\mathrm{str}(\boldsymbol{P}\bar{\boldsymbol{\mu}}\boldsymbol{Q}\bar{\boldsymbol{\mu}})/\lambda\right) f\left(\sqrt{1 + \frac{2\boldsymbol{\mu}}{d}}\right)$$

We used the simplification $\mathrm{str}(\boldsymbol{P}\bar{\boldsymbol{\mu}}\boldsymbol{P}\bar{\boldsymbol{\mu}}) = \lambda^2$. The integral over λ can be performed in the infinite d limit: the saddle-point equation gives $\lambda|_{\mathrm{sp}} = 1/2i$. Performing the following steps:

1. In the Mayer function f, expand the square root $\sqrt{1 + 2\boldsymbol{\mu}(a)/d}$ in the limit $d \to \infty$

2. Rescale $\boldsymbol{\mu}(a) - \lambda'/2 \longrightarrow \boldsymbol{\mu}(a)$, still calling the new superfield $\boldsymbol{\mu}$

3. Rescale $\lambda'/2 \longrightarrow \lambda$, dropping the prime for convenience

4. Perform the Gaussian integration on $\boldsymbol{\mu}'$

we obtain[16]

$$\mathcal{F}(\boldsymbol{Q}) \propto \frac{e^{-\Delta_{\mathrm{liq}}/2}}{\sqrt{\mathrm{sdet}\,\boldsymbol{Q}}} \int \mathrm{d}\lambda \mathrm{D}\boldsymbol{\mu} \, e^{\lambda - \frac{1}{2}\int \mathrm{d}a\mathrm{d}b \, \boldsymbol{\mu}(a)\boldsymbol{Q}^{-1}(a,b)\boldsymbol{\mu}(b)} f\left(1 + \frac{\boldsymbol{\mu} + \lambda}{d}\right) \tag{3.62}$$

3.3.4.2 Normalization

Note that all the non-exponential in d dependences overlooked during the procedures of the different changes of variables does not depend upon the choice of the Mayer function f. Here we benefit from this to give the explicit expression of $\mathcal{S}_{\mathrm{int}}$.

In the MSRDDJ action $\mathcal{A}$ (3.9) we sum on times belonging to an interval $[t_{\mathrm{p}}, t_1]$, where initial conditions are fixed at t_{p}. t_1 labels the final state, and if we sum on all positions at t_1, we have $Z_N = 1$ in (3.8). Let us pick $s \in]t_{\mathrm{p}}, t_1[$ and define a test function $f_0[x, \hat{x}] = \theta(\sigma - |x(s)|)$. Note that the choice of the test function is not completely arbitrary: as seen in 3.2.2, it should satisfy the properties of the true Mayer function f that we used to derive $\mathcal{S}$, as it must reject all trajectories that do not get close at some time. Making a choice that does not respect these properties would lead to absurd results. We obtain, using first the expression of $\mathcal{S}_{\mathrm{int}}$ in (3.16) and setting $y = u + x$ and $\hat{y} = \hat{u}$:

$$\mathcal{S}_{\mathrm{int}}[f_0] = \frac{N}{2}\int \mathrm{D}[x, \hat{x}]\mathrm{D}[u, \hat{u}]\rho[x, \hat{x}]\rho[u + x, \hat{u}]\theta(\sigma - |u(s)|)$$

$$= \frac{N}{2}\int \frac{\mathrm{d}x^{n_s}}{(2\pi)^{\frac{d}{2}}} \frac{\mathrm{d}u^{n_s}}{(2\pi)^{\frac{d}{2}}} \rho(x^{n_s})\rho(x^{n_s} + u^{n_s})\theta(\sigma - |u^{n_s}|) \tag{3.63}$$

$$= \frac{N}{2}\left(\frac{(2\pi)^{\frac{d}{2}}}{\mathcal{V}}\right)^2 \frac{\mathcal{V}}{(2\pi)^{\frac{d}{2}}} \int \frac{\mathrm{d}u^{n_s}}{(2\pi)^{\frac{d}{2}}}\theta(\sigma - |u^{n_s}|) = \frac{\rho\mathcal{V}_d(\sigma)}{2}$$

As in 3.2.2.2, we discretized the trajectories and used that translation invariance and the normalization $\int \mathrm{D}[x, \hat{x}]\rho[x, \hat{x}] = 1$ imply

$$\int \mathrm{D}\hat{x} \prod_{n \neq n_s}^{1,M} \frac{\mathrm{d}x^n}{(2\pi)^{\frac{d}{2}}} \rho[\{x^1, \cdots, x^M\}, \hat{x}] = \text{constant} = \frac{(2\pi)^{\frac{d}{2}}}{\mathcal{V}} \tag{3.64}$$

---

[15]For now we put all subexponential dependence in $\mathcal{F}$; explicit expressions will be given in 3.3.4.2.

[16]Note that $f\left(1 + \frac{\boldsymbol{\mu}+\lambda}{d}\right)$ is a shorthand for $f\left(\sigma\left[1 + \frac{\boldsymbol{\mu}+\lambda}{d}\right]\right)$.

n_s labels the time s, i.e. $s = t_{\mathrm{p}} + n_s(t_1 - t_{\mathrm{p}})/M$. We define $\mathcal{C}'(\boldsymbol{Q}, \Delta_{\mathrm{liq}})$ accounting for all the overlooked terms. We have, taking the saddle point over $\boldsymbol{Q}$,

$$
\begin{aligned}
\frac{\mathcal{S}_{\mathrm{int}}[f]}{\mathcal{S}_{\mathrm{int}}[f_0]} &= \frac{\mathcal{S}_{\mathrm{int}}[f]}{\rho \mathcal{V}_d(\sigma)/2} \\
&= \frac{e^{-\Delta_{\mathrm{liq}}/2} \int \mathrm{d}\lambda \mathrm{D}[\boldsymbol{Q}, \boldsymbol{\nu}, \boldsymbol{\mu}] \mathcal{C}'(\boldsymbol{Q}, \Delta_{\mathrm{liq}}) e^{d\Gamma(\boldsymbol{Q}, \boldsymbol{\nu})} e^{\lambda - \frac{1}{2} \int \mathrm{d}a \mathrm{d}b\, \boldsymbol{\mu}(a) \boldsymbol{Q}^{-1}(a,b) \boldsymbol{\mu}(b)} f\left(1 + \frac{\boldsymbol{\mu} + \lambda}{d}\right)}{e^{-\Delta_{\mathrm{liq}}/2} \int \mathrm{d}\lambda \mathrm{D}[\boldsymbol{Q}, \boldsymbol{\nu}, \boldsymbol{\mu}] \mathcal{C}'(\boldsymbol{Q}, \Delta_{\mathrm{liq}}) e^{d\Gamma(\boldsymbol{Q}, \boldsymbol{\nu})} e^{\lambda - \frac{1}{2} \int \mathrm{d}a \mathrm{d}b\, \boldsymbol{\mu}(a) \boldsymbol{Q}^{-1}(a,b) \boldsymbol{\mu}(b)} f_0\left(1 + \frac{\boldsymbol{\mu} + \lambda}{d}\right)} \quad (3.65) \\
&= \frac{1}{\mathcal{C}''(\boldsymbol{Q}^{\mathrm{sp}}, \Delta_{\mathrm{liq}})} \int \mathrm{D}\boldsymbol{\mu} \mathrm{d}\lambda\, e^{\lambda - \frac{1}{2} \int \mathrm{d}a \mathrm{d}b\, \boldsymbol{\mu}(a) \boldsymbol{Q}^{-1}|_{\mathrm{sp}}(a,b) \boldsymbol{\mu}(b)} f\left(1 + \frac{\boldsymbol{\mu} + \lambda}{d}\right)
\end{aligned}
$$

$\mathcal{C}''$ is given by

$$
\begin{aligned}
\mathcal{C}''(\boldsymbol{Q}^{\mathrm{sp}}, \Delta_{\mathrm{liq}}) &= \int \mathrm{D}\boldsymbol{\mu} \mathrm{d}\lambda\, e^{\lambda - \frac{1}{2} \int \mathrm{d}a \mathrm{d}b\, \boldsymbol{\mu}(a) \boldsymbol{Q}^{-1}|_{\mathrm{sp}}(a,b) \boldsymbol{\mu}(b)} \theta\left(-\frac{\mu(s) + \lambda}{d}\right) \\
&= \int \mathrm{D}\boldsymbol{\mu}\, e^{\int \mathrm{d}a\, \boldsymbol{\mu}(a) \boldsymbol{g}(a) - \frac{1}{2} \int \mathrm{d}a \mathrm{d}b\, \boldsymbol{\mu}(a) \boldsymbol{Q}^{-1}|_{\mathrm{sp}}(a,b) \boldsymbol{\mu}(b)} = e^{\Delta_{\mathrm{liq}}/2} \sqrt{\mathrm{sdet}\, \boldsymbol{Q}^{\mathrm{sp}}}
\end{aligned} \quad (3.66)
$$

where we introduced the superfield $\boldsymbol{g}(a) = -\bar{\theta}_1 \theta_1 \delta(t - s)$ to integrate the Gaussian. We also used the constraint $\boldsymbol{Q}^{\mathrm{sp}}(a,a) = \Delta_{\mathrm{liq}}$. Now we can conclude[17]:

$$
\begin{aligned}
\mathcal{S}_{\mathrm{int}} &\underset{d\to\infty}{=} -\frac{\rho \mathcal{V}_d(\sigma)}{2} \mathcal{F}(\boldsymbol{Q}^{\mathrm{sp}}) \\
\text{where} \quad \mathcal{F}(\boldsymbol{Q}) &= -\frac{e^{-\Delta_{\mathrm{liq}}/2}}{\sqrt{\mathrm{sdet}\, \boldsymbol{Q}}} \int \mathrm{D}\boldsymbol{\mu} \mathrm{d}\lambda\, e^{\lambda - \frac{1}{2} \int \mathrm{d}a \mathrm{d}b\, \boldsymbol{\mu}(a) \boldsymbol{Q}^{-1}(a,b) \boldsymbol{\mu}(b)} f\left(1 + \frac{\boldsymbol{\mu} + \lambda}{d}\right)
\end{aligned} \quad (3.67)
$$

3.3.5 Final result in the limit $d \to \infty$

Collecting the results from the last two subsections, and using (2.119), we obtain the final result in the infinite dimension limit:

$$
\mathcal{S} \underset{d\to\infty}{=} \frac{d}{2} \ln \mathrm{sdet}\, \boldsymbol{Q} - \frac{d}{2} \int \mathrm{d}a\, \boldsymbol{\nu}(a) \left(\boldsymbol{Q}(a,a) - \Delta_{\mathrm{liq}}\right) - d\widehat{\Phi}(\boldsymbol{Q}) - \left.\frac{d\widehat{\varphi}}{2} \mathcal{F}(\boldsymbol{Q})\right|_{\mathrm{sp}} \quad (3.68)
$$

up to irrelevant additive constants (cf. 3.3.3), with $\mathcal{F}$ defined in (3.67).

3.4 Saddle-point equation

3.4.1 Explicit form of the kinetic term

We now make explicit the $\boldsymbol{Q}$ dependence of Φ using $\widehat{\Phi}$ justified in subsection 3.3.2. From (3.9), it is Gaussian in x and $\tilde{x}$,

$$
\widehat{\Phi}(\boldsymbol{x}) = \frac{1}{d} \Phi(\boldsymbol{x}) = \frac{\widehat{\gamma} d}{\sigma^2} \int \mathrm{d}t \left(\tilde{x} \cdot \dot{x} - T\tilde{x}^2\right) = \frac{2d}{\sigma^2} \left[\int \mathrm{d}t \mathrm{d}t'\, \tilde{x}(t) k(t,t') \tilde{x}(t') + 2 \int \mathrm{d}t \mathrm{d}t'\, \tilde{x}(t) \hat{k}(t,t') x(t')\right]
$$

$$
\text{with } k(t,t') = -\widehat{\gamma} T \delta(t - t') \text{ and } \hat{k}(t,t') = \frac{\widehat{\gamma}}{2} \frac{\partial}{\partial t} \delta(t - t')
$$

$\quad (3.69)$

The kernel k is symmetric while $\hat{k}$ is antisymmetric. Let us define a symmetric superfield:

$$
\boldsymbol{k}(a,b) = k(t,t') - \bar{\theta}_1 \theta_1 \hat{k}(t,t') + \bar{\theta}_2 \theta_2 \hat{k}(t,t') \quad (3.70)
$$

One can check that $\widehat{\Phi}(\boldsymbol{Q}) = \mathrm{str}(\boldsymbol{k}\boldsymbol{Q})$ gives back expression (3.69).

3.4.2 Saddle-point equation for the dynamic correlations

From subsection 3.2.3, the probability density of trajectories ρ is given by the saddle-point equation $\delta\mathcal{S}/\delta\rho(\boldsymbol{x}) = \delta\mathcal{S}/\delta\rho(\boldsymbol{Q}) = 0$. In the infinite d limit, $\mathcal{S}$ depends on ρ, or equivalently on its logarithm Ω, only through its saddle-point value $\Omega(\boldsymbol{Q}^{\mathrm{sp}})$. From the relation $\Gamma(\boldsymbol{Q}^{\mathrm{sp}}, \boldsymbol{\nu}^{\mathrm{sp}}) = 0$ derived in 3.3.3 thanks to the normalization of ρ, $\Omega(\boldsymbol{Q}^{\mathrm{sp}})$ is explicitly determined by the saddle-point values $\boldsymbol{Q}^{\mathrm{sp}}$ and $\boldsymbol{\nu}^{\mathrm{sp}}$. Hence the saddle point condition is equivalent[18] to $\delta\mathcal{S}/\delta\boldsymbol{Q}|_{\mathrm{sp}} = 0$ in (3.68), and is, as a consequence, equivalent

---

[17] The minus sign in the definition of $\mathcal{F}$ is just a convention for closer contact with previous static works.

[18] The condition $\delta\mathcal{S}/\delta\boldsymbol{\nu}|_{\mathrm{sp}} = 0$ is once again the spherical constraint $\boldsymbol{Q}^{\mathrm{sp}}(a,a) = \Delta_{\mathrm{liq}}$.

to the saddle point condition used in the virial terms for $d \to \infty$,

$$\left.\frac{\delta \mathcal{S}}{\delta \boldsymbol{Q}}\right|_{\mathrm{sp}} = 0 \Leftrightarrow -\boldsymbol{Q}^{-1} - \boldsymbol{\nu}\boldsymbol{1} + 2\boldsymbol{k} - \frac{\widehat{\varphi}}{2}\left.\frac{\delta \mathcal{F}}{\delta \boldsymbol{Q}}\right|_{\mathrm{sp}} = 0 \tag{3.71}$$

The derivative of $\mathcal{F}$ is

$$\frac{\delta \mathcal{F}}{\delta \boldsymbol{Q}(a,b)} = \mathcal{F}(\boldsymbol{\Delta})\boldsymbol{Q}^{-1}(a,b) + \int \mathrm{d}a'\mathrm{d}b'\,\boldsymbol{Q}^{-1}(a,a') \int \mathrm{d}\lambda\, e^{\lambda-\Delta_{\mathrm{liq}}/2} \int \mathcal{D}\boldsymbol{\mu}\,\boldsymbol{\mu}(a')\boldsymbol{\mu}(b')f\left(1 + \frac{\boldsymbol{\mu}+\lambda}{d}\right)\boldsymbol{Q}^{-1}(b',b)$$

with the Gaussian measure $\displaystyle\int \mathcal{D}\boldsymbol{\mu}\,\bullet = \frac{1}{\sqrt{\mathrm{sdet}\,\boldsymbol{Q}}} \int \mathrm{D}\boldsymbol{\mu}\,\bullet\, e^{-\frac{1}{2}\int \mathrm{d}a\mathrm{d}b\,\boldsymbol{\mu}(a)\boldsymbol{Q}^{-1}(a,b)\boldsymbol{\mu}(b)}$

$$\tag{3.72}$$

Hence the saddle-point equation, $\forall(a,b)$,

$$\left.\left(1 + \frac{\widehat{\varphi}\mathcal{F}(\boldsymbol{Q})}{2}\right)\boldsymbol{Q}^{-1}(a,b) - 2\boldsymbol{k}(a,b) - \boldsymbol{\nu}(a)\boldsymbol{1}(a,b)\right|_{\mathrm{sp}}$$
$$\left.\left.+ \frac{\widehat{\varphi}}{2}\boldsymbol{Q}^{-1}\int \mathrm{d}\lambda\, e^{\lambda-\Delta_{\mathrm{liq}}/2}\int \mathcal{D}\boldsymbol{\mu}\,\boldsymbol{\mu}\boldsymbol{\mu}\,f\left(1 + \frac{\boldsymbol{\mu}+\lambda}{d}\right)\boldsymbol{Q}^{-1}\right|_{(a,b)} = 0\right|_{\mathrm{sp}} \tag{3.73}$$

Together with the spherical constraint $\boldsymbol{Q}^{\mathrm{sp}} = \Delta_{\mathrm{liq}}$ which shall provide $\boldsymbol{\nu}^{\mathrm{sp}}$, this determines $\boldsymbol{Q}^{\mathrm{sp}}$.

3.4.3 Simplification of the saddle-point equation

3.4.3.1 Exploiting Ward-Takahashi-like identities

Here we drop the labels 'sp' for convenience. Generically, derivatives of $\mathcal{S}$ are needed for example to compute the MCT exponents. They can be simplified using Ward-Takahashi-like identities [315, 422]. From the definition of the Mayer function f (3.30), a quantity like $\int \mathcal{D}\boldsymbol{\mu}\,\bullet\,f$ is a difference between two averages, one with potential V and the other without. Let us focus on the non-Gaussian part, with potential:

$$\int \mathcal{D}\boldsymbol{\mu}\,e^{-\int \mathrm{d}a\,\bar{V}(\boldsymbol{\mu}(a)+\lambda)} \equiv \langle 1 \rangle_V \tag{3.74}$$

Let us shift $\boldsymbol{\mu}(a) \longrightarrow \boldsymbol{\mu}(a) + \boldsymbol{\epsilon}(a)$ in the above expression. Each order in $\boldsymbol{\epsilon}$ must be zero except the zeroth one, which gives back the original expression (3.74). Doing so we get

At linear order: $\quad \left\langle \boldsymbol{Q}^{-1}\boldsymbol{\mu} \right\rangle_V = \left\langle F(\boldsymbol{\mu}+\lambda) \right\rangle_V$

At second order: $\quad \boldsymbol{Q}^{-1}\left.\langle \boldsymbol{\mu}\boldsymbol{\mu} \rangle_V\, \boldsymbol{Q}^{-1}\right|_{(a,b)} - \boldsymbol{Q}^{-1}(a,b)$

$$= -\left\langle F(\boldsymbol{\mu}(a)+\lambda)F(\boldsymbol{\mu}(b)+\lambda) \right\rangle_V - \boldsymbol{1}(a,b)\left\langle F'(\boldsymbol{\mu}(a)+\lambda) \right\rangle_V + 2\left\langle [\boldsymbol{Q}^{-1}\boldsymbol{\mu}](a)F(\boldsymbol{\mu}(b)+\lambda) \right\rangle_V$$
$$\tag{3.75}$$

where we have defined the force $F(x) = -\bar{V}'(x)$. The left-hand side in the second order equation is precisely the term containing the Mayer function f in the saddle-point equation.

It can be further simplified if we repeat this procedure with $\left\langle F(\boldsymbol{\mu}(b)+\lambda) \right\rangle_V$, demanding that the linear order in $\boldsymbol{\epsilon}$ is zero:

$$\left\langle F(\boldsymbol{\mu}(a)+\lambda)F(\boldsymbol{\mu}(b)+\lambda) \right\rangle_V + \boldsymbol{1}(a,b)\left\langle F'(\boldsymbol{\mu}(a)+\lambda) \right\rangle_V = \left\langle [\boldsymbol{Q}^{-1}\boldsymbol{\mu}](a)F(\boldsymbol{\mu}(b)+\lambda) \right\rangle_V \tag{3.76}$$

We thus get the simple identity, $\forall(a,b)$:

$$\boldsymbol{Q}^{-1}\left.\langle \boldsymbol{\mu}\boldsymbol{\mu} \rangle_V\, \boldsymbol{Q}^{-1}\right|_{(a,b)} - \boldsymbol{Q}^{-1}(a,b) = \left\langle F(\boldsymbol{\mu}(a)+\lambda)F(\boldsymbol{\mu}(b)+\lambda) \right\rangle_V + \boldsymbol{1}(a,b)\left\langle F'(\boldsymbol{\mu}(a)+\lambda) \right\rangle_V \tag{3.77}$$

A more compact way to get moments of $\boldsymbol{Q}\boldsymbol{\mu}$ is to write, $\forall(a,b)$,

$$\boldsymbol{Q}^{-1}\left.\langle \boldsymbol{\mu}\boldsymbol{\mu} \rangle_V\, \boldsymbol{Q}^{-1}\right|_{(a,b)} = \frac{1}{\sqrt{\mathrm{sdet}\,\boldsymbol{Q}}}\int \mathrm{D}\boldsymbol{\mu}\,e^{-\int \mathrm{d}c\,\bar{V}(\boldsymbol{\mu}(c)+\lambda)}\left[\frac{\delta^2}{\delta\boldsymbol{\mu}(a)\delta\boldsymbol{\mu}(b)} + \boldsymbol{Q}^{-1}(a,b)\right]e^{-\frac{1}{2}\int \mathrm{d}c\mathrm{d}e\,\boldsymbol{\mu}(c)\boldsymbol{Q}^{-1}(c,e)\boldsymbol{\mu}(e)}$$

$$= \boldsymbol{Q}^{-1}(a,b) + \int \mathcal{D}\boldsymbol{\mu}\,\frac{\delta^2}{\delta\boldsymbol{\mu}(a)\delta\boldsymbol{\mu}(b)}e^{-\int \mathrm{d}c\,\bar{V}(\boldsymbol{\mu}(c)+\lambda)}$$

$$= \boldsymbol{Q}^{-1}(a,b) + \left\langle F(\boldsymbol{\mu}(a)+\lambda)F(\boldsymbol{\mu}(b)+\lambda) \right\rangle_V + \left\langle F'(\boldsymbol{\mu}(a)+\lambda) \right\rangle_V\, \boldsymbol{1}(a,b)$$
$$\tag{3.78}$$

where we integrated by parts twice. These methods can be easily generalized to higher moments.

3.4.3.2 The saddle-point value of $\mathcal{F}$

The measure in (3.74) can be interpreted as an average over a Langevin process with potential V. Provided we sum over all possible trajectories of $\boldsymbol{\mu}$, equation (3.74) is actually the conservation of probability $\langle 1 \rangle_V = 1$.

Similarly $\mathcal{F}(\boldsymbol{Q})$ can be interpreted as a difference between averages over two dynamical processes, one with potential V and the other free,

$$
\begin{aligned}
\mathcal{F}(\boldsymbol{Q}) &= -\int \mathrm{d}\lambda\, e^{\lambda - \Delta_{\mathrm{liq}}/2} \int \mathcal{D}\boldsymbol{\mu}\, f\left(1 + \frac{\boldsymbol{\mu} + \lambda}{d}\right) = -\int \mathrm{d}\lambda\, e^{\lambda - \Delta_{\mathrm{liq}}/2} \left[\int \mathcal{D}\boldsymbol{\mu}\, e^{-\int \mathrm{d}a\, \bar{V}(\boldsymbol{\mu}(a) + \lambda)} - \int \mathcal{D}\boldsymbol{\mu}\, 1\right] \\
&= -\int \mathrm{d}\lambda\, e^{\lambda - \Delta_{\mathrm{liq}}/2} \left[\langle 1 \rangle_V - \langle 1 \rangle_0\right] \Leftrightarrow \mathcal{F}(\boldsymbol{Q}) = 0
\end{aligned}
$$

(3.79)

Hence $\mathcal{F}$ is zero for all acceptable dynamical propagators (positive definite, as we expect $\boldsymbol{Q}$ is, at least at its saddle-point value dominating the dynamics) due to normalization.

3.4.3.3 Definition of the memory kernel

From equations (3.73), (3.77) and (3.79), the saddle-point equation is simplified as:

$$
\boldsymbol{Q}^{-1}(a,b) = 2\boldsymbol{k}(a,b) - \boldsymbol{M}(a,b) + (\boldsymbol{\nu}(a) + \boldsymbol{\delta\nu}(a))\mathbf{1}(a,b) \tag{3.80}
$$

where

$$
\begin{aligned}
\boldsymbol{M}(a,b) &= \frac{\widehat{\varphi}}{2} \int \mathrm{d}\lambda\, e^{\lambda - \Delta_{\mathrm{liq}}/2} \left\langle F(\boldsymbol{\mu}(a) + \lambda) F(\boldsymbol{\mu}(b) + \lambda) \right\rangle_V \\
\boldsymbol{\delta\nu}(a) &= -\frac{\widehat{\varphi}}{2} \int \mathrm{d}\lambda\, e^{\lambda - \Delta_{\mathrm{liq}}/2} \left\langle F'(\boldsymbol{\mu}(a) + \lambda) \right\rangle_V
\end{aligned}
$$

(3.81)

In our study of the dynamics of the system, $\boldsymbol{M}$ will play the role of the analog of the MCT kernel.

3.5 Equilibrium hypothesis

In the following we will unfold the SUSY notation to get rid of it, coming back to the standard dynamical variables, as in §2.5.4.

We focus on the equilibrium dynamics of the system, assuming that time-translation invariance (TTI) as well as causality hold, and consequently fluctuation-dissipation theorem (FDT): we assume we start in the remote past (time t_{p}, formally sent to $-\infty$), so that the system is at equilibrium when a finite t_0 is reached. Equilibrium properties have been studied generally in §2.5.3.
$\boldsymbol{Q} = 2d\boldsymbol{q}/\sigma^2$ (equivalently $\boldsymbol{\Delta}$) takes its equilibrium form and so does $\boldsymbol{M}$:

$$
\begin{aligned}
\boldsymbol{Q}(a,b) &= C(t - t') + \bar{\theta}_1\theta_1 R(t' - t) + \bar{\theta}_2\theta_2 R(t - t') \\
\boldsymbol{M}(a,b) &= M(t - t') + \bar{\theta}_1\theta_1 \widehat{M}(t' - t) + \bar{\theta}_2\theta_2 \widehat{M}(t - t')
\end{aligned}
$$

(3.82)

This is given by §2.5.3.2.

Along with TTI and (3.80), it implies that $\boldsymbol{\nu}(a) = \nu$ and $\boldsymbol{\delta\nu}(a) = \delta\nu$ are constant and real quantities. From this the inverse $\boldsymbol{Q}^{-1}$ reads from §2.4.3.2:

$$
\boldsymbol{Q}^{-1}(a,b) = \widetilde{C}(t - t') + \bar{\theta}_1\theta_1 \widetilde{R}(t' - t) + \bar{\theta}_2\theta_2 \widetilde{R}(t - t') \quad \text{with} \quad \widetilde{C} = -R^{-\mathrm{T}} C R^{-1} \quad \text{and} \quad \widetilde{R} = R^{-1} \tag{3.83}
$$

C and R satisfying fluctuation-dissipation theorem, one can check that $\widetilde{C}$ and $\widetilde{R}$ also do. This is done in appendix I.
Similarly, we can verify directly with (3.69) that $\boldsymbol{k}$ and $\mathbf{1}$ verify the latter relation. We conclude, from (3.80), that $\boldsymbol{M}$ also satisfies FDT (which was suggested by (3.81)).

3.6 Free dynamics

Here we check the dynamical equations obtained above in the simpler case where the density or the interactions are negligible, which is solvable. We do this for a dissipative dynamics and show they are the same as the ones found for independent free Brownian particles on the sphere. We mention the Hamiltonian dynamics case afterwards.

3.6.1   Saddle-point equation

Without interactions, *i.e.* $V = 0$ (or $\varphi = 0$), we have an ideal gas and the saddle-point equation reads:

$$\mathbf{1}(a,b) = 2\boldsymbol{k}\boldsymbol{Q}(a,b) + \boldsymbol{\nu}(a)\boldsymbol{Q}(a,b) \tag{3.84}$$

We know from §2.5.3 that

$$\mathsf{M}(\boldsymbol{Q}) = \begin{pmatrix} C(t,t') & R(t,t') \\ R(t',t) & 0 \end{pmatrix} \tag{3.85}$$

from which we deduce

$$\mathsf{M}(\boldsymbol{k}\boldsymbol{Q}) = \begin{pmatrix} \hat{k}C + kR^{\mathrm{T}} & \hat{k}R \\ -\hat{k}R^{\mathrm{T}} & 0 \end{pmatrix} \tag{3.86}$$

From (3.84), we get, as a result of causality, that $\tilde{\nu}(t) = 0$ *i.e.* $\boldsymbol{\nu}(a) = \nu(t)$. Writing the two independent components of (3.84) leads to the coupled dynamical equations:

$$\begin{cases} \widehat{\gamma}\dfrac{\partial C}{\partial t}(t,t') = 2\widehat{\gamma}TR(t',t) - \nu(t)C(t,t') \\ \widehat{\gamma}\dfrac{\partial R}{\partial t}(t,t') = \delta(t - t') - \nu(t)R(t,t') \end{cases} \tag{3.87}$$

3.6.2   Brownian diffusion on the sphere $\mathbb{S}_d(R)$

3.6.2.1   Equivalence of the dynamics

We consider the free diffusion of an overdamped particle on the sphere described by $x = (x^1, \cdots, x^{d+1}) \in \mathbb{S}_d(R)$. Its dynamics is ruled by:

$$\gamma\dot{x}^\mu(t) = -\frac{2d^2}{\sigma^2}\nu(t)x^\mu(t) + \xi^\mu(t) \tag{3.88}$$

where $\nu(t)$ is a Lagrange multiplier for the constraint $\forall t, \ \sum_{\mu=1}^{d+1}(x^\mu)^2(t) = R^2$. We have

$$\gamma\sum_{\mu=1}^{d+1}x^\mu(t')\dot{x}^\mu(t) = -\frac{2d^2}{\sigma^2}\nu(t)\sum_{i=1}^{d+1}x^\mu(t)x^\mu(t') + \sum_{\mu=1}^{d+1}x^\mu(t')\xi^\mu(t) \tag{3.89}$$

For a Gaussian noise [81],

$$\begin{aligned} \left\langle x^\mu(t)\xi^\mu(t')\right\rangle &= \int \mathrm{d}t''\, G^\mu(t',t'')R^\mu(t,t'') \\ \text{where} \quad G^\mu(t',t'') &= \left\langle \xi^\mu(t')\xi^\mu(t'')\right\rangle = 2\gamma T\delta(t'-t'') \\ \text{and} \quad R^\mu(t,t'') &= \left\langle x^\mu(t)\tilde{x}^\mu(t'')\right\rangle \end{aligned} \tag{3.90}$$

therefore, defining[19] $C(t,t') = \left\langle x(t)\cdot x(t')\right\rangle = \sum_{\mu=1}^{d+1}\left\langle x^\mu(t)x^\mu(t')\right\rangle$ and $R(t,t') = \left\langle x(t)\cdot\tilde{x}(t')\right\rangle = \sum_{\mu=1}^{d+1}R^\mu(t,t')$, and recalling that $\gamma = 2\widehat{\gamma}d^2/\sigma^2$,

$$\widehat{\gamma}\frac{\partial C}{\partial t}(t,t') = 2\widehat{\gamma}TR(t',t) - \nu(t)C(t,t') \tag{3.91}$$

which is the same equation as in (3.87). This provides the interpretation of $\boldsymbol{\nu}$ as a Lagrange multiplier implementing the spherical constraint.

3.6.2.2   Equilibrium dynamics: Ornstein-Uhlenbeck process

Let us consider the equilibrium dynamics of (3.88), in which $\nu(t) = \nu$ is an equilibrium constant. This defines an Ornstein-Uhlenbeck process for each $x^\mu(t)$, $\mu \in [\![1, d+1]\!]$.
Equation (3.88) can be directly integrated. Defining:

$$C(t,t') = \left\langle x(t)\cdot x(t')\right\rangle = \sum_{\mu=1}^{d+1}\left\langle x^\mu(t)x^\mu(t')\right\rangle \quad \text{and} \quad R(t,t') = \sum_{\mu=1}^{d+1}R^\mu(t,t') = \sum_{\mu=1}^{d+1}\frac{\delta\left\langle x^\mu(t)\right\rangle}{\delta h^\mu(t')} \tag{3.92}$$

---

[19]They are the same as the ones appearing in $\boldsymbol{Q}$ up to the rescaling $2d/\sigma^2$, which has no effect on the linear equation (3.91).

where h^μ is an external field on x^μ switched on for the response, we get

$$C(t,t') = \frac{T(d+1)\sigma^2}{2d^2\nu}e^{-\nu|t-t'|/\widehat{\gamma}\sigma^2} + \left(R^2 - \frac{T(d+1)\sigma^2}{2d^2\nu}\right)e^{-\nu(t+t')/\widehat{\gamma}\sigma^2}$$

$$R(t,t') = \sigma^2\frac{d+1}{2\widehat{\gamma}d^2}e^{-\nu(t-t')/\widehat{\gamma}\sigma^2}\theta(t-t'),\quad R(t,t)\text{ depends upon the discretization}$$

(3.93)

They verify equations (3.87) for large d. At equilibrium, time-translation invariance requires

$$\nu = \frac{T(d+1)\sigma^2}{2d^2R^2} \underset{d\to\infty}{\sim} \frac{T}{\Delta_{\text{liq}}}$$

(3.94)

which can be seen in many ways, *e.g.* using the spherical constraint with equation (3.91) or simply with the equipartition theorem $\left\langle \frac{d^2}{\sigma^2}\nu(x^\mu)^2 \right\rangle = T/2$.

From this we get, setting $\tau = t - t'$,

$$C(\tau) \underset{d\to\infty}{\sim} R^2 e^{-2Td|\tau|/\gamma R^2}$$

$$R(\tau) \underset{d\to\infty}{\sim} \frac{d}{\gamma}e^{-2Td|\tau|/\gamma R^2}\theta(\tau)$$

$$\beta\dot{C}(\tau) = R(-\tau) - R(\tau)\ \ (\text{FDT})$$

(3.95)

C decreases exponentially on a typical time $\propto R^2$, a diffusive scaling which means that a distance of order R on the sphere is needed to decorrelate from the initial position. C is not a relevant quantity to discuss diffusion on the sphere $\mathbb{S}_d(R)$ once R has been sent to infinity, which can be seen by $C(\tau) \underset{R\to\infty}{\sim} R^2$, because for any finite time difference $\tau = t - t'$, $x(t)$ and $x(t')$ are almost aligned when R is large. As emphasized in subsection 3.3.1, we need to consider the MSD

$$\left\langle \left(x(t) - x(t')\right)^2 \right\rangle = 2R^2 - 2C(t,t') = 2R^2 - 2R^2 e^{-2Td|\tau|/\gamma R^2} \underset{R\to\infty}{\sim} \frac{2Td}{\gamma}\tau$$

(3.96)

which is indeed the correct one for d-dimensional Brownian diffusion, as in equation (3.7) for $V = 0$.

3.6.3   Newtonian dynamics

The Newtonian case is similar, so we will be brief and it is better explained in words.

One has to restore the inertia term and set $\gamma = 0$, the dynamics of each (independent) particle is a ballistic one with a Lagrange multiplier, *i.e.* the one of a harmonic oscillator. Its frequency is directly set by the ratio between the Lagrange multiplier and the mass. Conservation of energy, which is the sum of the kinetic energy and the harmonic energy straightforwardly given by the spherical constraint, tells us that the value of the Lagrange multiplier, hence the frequency, is set by the initial velocity (or equivalently by the constant total energy of the particle). Indeed, the particles undergo a free motion (*i.e.* with constant velocity) on the sphere without seeing each other, thus oscillate on a circle depending on the initial velocity.

Multiplying the Newton equation by the position at an initial time, the exact same terms arise in the equation for the correlation. It is the same as the saddle-point equation, up to a rescaling of the mass and the Lagrange multiplier. The correlation therefore becomes also oscillating at the same frequency determined by the initial velocity, due to periodic return to the starting point after traveling one perimeter distance $2\pi R$.

3.7   Equation for the equilibrium dynamic correlations

In this section we derive the self-consistent equations for the saddle-point quantities dominating the dynamics at equilibrium. They can be computed through an effective single particle process, in analogy with the mean-field soft-spin case for instance [71, 365, 114, 220, 221], where the dynamics reduces to an effective single spin evolution.

3.7.1 Mode-coupling form of the saddle-point equation and the effective stiffness

We can cast the saddle-point equation into a mode-coupling form by multiplying (3.80) by Q on the right. The scalar component of the equation obtained reads at (t', t):

$$
\begin{aligned}
0 = & -2(\hat{k}C + kR^{\mathrm{T}}) - \widehat{M}C - MR^{\mathrm{T}} + (\nu + \delta\nu)C \\
= & \widehat{\gamma}\partial_{t'}C(t' - t) - 2\widehat{\gamma}TR(t - t') + (\nu + \delta\nu)C(t - t') - \beta \int_{-\infty}^{t'} \mathrm{d}u \left(\partial_u M(t' - u)\right) C(u - t) \\
& - \beta \int_{-\infty}^{t} \mathrm{d}u\, M(t' - u)\partial_u C(t - u)
\end{aligned}
\tag{3.97}
$$

We can assume, for instance, that $t > t'$, and use FDT:

$$
0 = \widehat{\gamma}\dot{C}(t - t') + (\nu + \delta\nu)C(t - t') - \beta \int_{t'}^{t} \mathrm{d}u\, M(t' - u)\partial_u C(t - u) - \beta \int_{-\infty}^{t'} \mathrm{d}u\, \partial_u \left[M(t' - u)C(t - u)\right] \tag{3.98}
$$

Using the relaxation for long times and making the substitution $v = t + t' - u$,

$$
\begin{aligned}
\widehat{\gamma}\dot{C}(t - t') = & -\left(\nu + \delta\nu - \beta M(0)\right)C(t - t') - \beta \int_{t'}^{t} \mathrm{d}v\, M(t - v)\dot{C}(v - t') \\
& t' \to t^- \text{ gives } \quad \nu + \delta\nu - \beta M(0) = -\frac{\widehat{\gamma}\dot{C}(0)}{\Delta_{\mathrm{liq}}}
\end{aligned}
\tag{3.99}
$$

$\dot{C}(0) = -TR(0^+)$ represents the immediate response to a perturbation. At such very short times the potential is not relevant, particles follow a free dynamics. We can use the results of §3.6.2.2: we solve the associated Ornstein-Uhlenbeck process and compute as in (3.95) $C(t) = \Delta_{\mathrm{liq}} \exp(-dTt/\gamma R^2)$, giving $-\widehat{\gamma}\dot{C}(0) = T$, hence

$$
\nu + \delta\nu - \beta M(0) = \frac{T}{\Delta_{\mathrm{liq}}} \tag{3.100}
$$

We conclude that the mode-coupling-like equation for C is, for $t > t'$:

$$
\widehat{\gamma}\dot{C}(t - t') = -\frac{T}{\Delta_{\mathrm{liq}}}C(t - t') - \beta \int_{t'}^{t} \mathrm{d}v\, M(t - v)\dot{C}(v - t') \tag{3.101}
$$

or equivalently for the MSD $\Delta = d\mathsf{D} = \Delta_{\mathrm{liq}} - C$ at $t > t'$:

$$
\widehat{\gamma}\dot{\Delta}(t - t') = T - \frac{T}{\Delta_{\mathrm{liq}}}\Delta(t - t') - \beta \int_{t'}^{t} \mathrm{d}v\, M(t - v)\dot{\Delta}(v - t') \tag{3.102}
$$

3.7.2 Effective Langevin process

The aim is to compute M, the mode-coupling-like kernel, as a function of Q^{sp} to solve the saddle-point equation for Q^{sp}, providing correlation and response of the system. To do this, we must calculate correlations of the force F at two times t_0 and $t_1 \geqslant t_0$. To achieve this program, we will interpret, as mentioned in 3.4.3.2, the average defining M as two-point correlation functions of a Langevin dynamics with potential V. We drop the notation V in averages since we will be refering only to this process from now on. To this end, let us unfold the MSRDDJ path integral in SUSY notation (3.74) using the saddle-point equation (3.80), where $\boldsymbol{\mu}(a) = \mu(t) + \bar{\theta}_1\theta_1\tilde{\mu}(t)$:

$$
\begin{aligned}
\langle 1 \rangle &\equiv \frac{1}{\sqrt{\mathrm{sdet}\, Q}} \int \mathrm{D}\boldsymbol{\mu}\, e^{-\frac{1}{2}\int \mathrm{d}a\mathrm{d}b\, \boldsymbol{\mu}(a)Q^{-1}(a,b)\boldsymbol{\mu}(b) - \int \mathrm{d}a\, \bar{V}(\boldsymbol{\mu}(a) + \lambda)} \\
&= \frac{1}{\sqrt{\mathrm{sdet}\, Q}} \int \mathrm{D}\boldsymbol{\mu}\, e^{-\frac{1}{2}\int \mathrm{d}a\mathrm{d}b\, \boldsymbol{\mu}(a)\left[(\boldsymbol{\nu}+\boldsymbol{\delta\nu})\mathbf{1} + 2\boldsymbol{k} - \boldsymbol{M}\right](a,b)\boldsymbol{\mu}(b) - \int \mathrm{d}a\, \bar{V}(\boldsymbol{\mu}(a) + \lambda)}
\end{aligned}
\tag{3.103}
$$

$\sqrt{\mathrm{sdet}\, Q}$ plays the role of normalization[20]. The corresponding Langevin process with potential V, depending on λ, is:

$$
\widehat{\gamma}\dot{\mu}(t) = -(\nu + \delta\nu)\mu(t) + \int_{t_{\mathrm{p}}}^{t} \mathrm{d}t'\, \widehat{M}(t - t')\mu(t') + F(\mu(t) + \lambda) + \zeta(t) \tag{3.104}
$$

$$
\text{with } \langle \zeta(t) \rangle = 0 \text{ and } \langle \zeta(t)\zeta(t') \rangle = 2\widehat{\gamma}T\delta(t - t') + M(t - t')
$$

---

[20]Note that $\mathrm{sdet}\, Q$ = numerical constant depending only on the response at equal times at the saddle-point level if the system is causal. Indeed, it is easily expressed in terms of $\det R$, which is a causal operator, see (3.85).

We used that $\widehat{M}$ is causal and consider times $t \in [t_0, t_1]$. M (and $\widehat{M}$ by FDT) can be computed self-consistently with force correlation functions of this process through its definition (3.81):

$$M(t - t') = \frac{\widehat{\varphi}}{2} \int d\lambda \, e^{\lambda - \Delta_{\text{liq}}/2} \left\langle F(\mu(t) + \lambda) F(\mu(t') + \lambda) \right\rangle \tag{3.105}$$

Using FDT for $\boldsymbol{M}$, an integration by part with the fact that $t - t_{\text{p}} > t_0 - t_{\text{p}} \gg \tau_\alpha$ the relaxation time of the system, above which correlations vanish, and (3.100), we get the generalized Langevin equation equivalent to (3.104):

$$\widehat{\gamma}\dot{\mu}(t) = -\frac{T}{\Delta_{\text{liq}}}\mu(t) - \beta \int_{t_{\text{p}}}^{t} dt' \, M(t - t')\dot{\mu}(t') + F(\mu(t) + \lambda) + \zeta(t) \tag{3.106}$$

Note that so far in this section we have used equilibrium properties for all observables. It is either because we considered them at a time $t \geqslant t_0$ where equilibrium is reached, or in the case of convolution products with $\boldsymbol{M}$ where the integral extends to the remote past, because we expect that $\widehat{M}$ (respectively M) vanishes quickly (respectively vanishes on a finite time scale τ_α). Then for finite times where they do not vanish, the system has equilibrated from the initial condition in the remote past t_{p}, and we can consider their equilibrium properties.

3.7.3 Memory kernel in equilibrium: resumming trajectories from the remote past

As emphasized before, dynamical two points functions at (t_0, t_1) should be function of a single argument, the time difference $t_1 - t_0$, as we assume that equilibrium is reached. But equilibrium properties hold *only* if we consider times $t \geqslant t_0$. Therefore, we wish to use t_0 as our initial time, *but in the understanding that at this time the system is at equilibrium*. Similarly, we are not interested in what happens after t_1, as it should be irrelevant due to causality, as stressed in section 3.2.1 (see also figure 3). However one expects the Langevin equation (3.106) to describe a non-Markovian process in which the memory kernel persists for a duration of the order of τ_α. How are we going to ignore the times $t < t_0$ if the kernel M extends to the remote past?

A similar discussion for the special case of simpler kernels, such as exponentially decaying or with a simple explicit dependence on correlations $M[C]$, can be found respectively in §E and §2.5.4, but here we detail the case of a general memory kernel.

An equation like (3.106) may be thought of as having originated in a system coupled linearly to a bath of harmonic oscillators, à la Zwanzig [424, 197]. Let us consider the Hamiltonian evolution of this system, described by coordinates denoted collectively by $\Gamma = \{\mu, p_\alpha, q_\alpha\}$, according to the Hamiltonian[21]:

$$H_{\text{tot}}(\Gamma) = \underbrace{\frac{T}{2\Delta_{\text{liq}}}\mu^2 + \bar{V}(\mu + \lambda)}_{H_0(\mu)} + \underbrace{\sum_\alpha \left[\frac{p_\alpha^2}{2m_\alpha} + \frac{m_\alpha \omega_\alpha^2}{2}\left(q_\alpha - \frac{c_\alpha}{m_\alpha \omega_\alpha^2}\mu\right)^2 \right]}_{H_{\text{B}}(\Gamma)} \tag{3.107}$$

$\{c_\alpha, \omega_\alpha, m_\alpha\}$ are chosen suitably to reproduce dissipation and noise terms in (3.106). As before, assume we start in the remote past t_{p} at a point in phase space Γ_{p} and let us distinguish two times t_0 and t_1, such that $t_1 > t_0 \gg t_{\text{p}}$. We can rewrite averages over the effective Langevin process as averages over the Markovian process $\Gamma(t)$, by defining the transition probabilities, for fixed Γ_{p} and Γ_1,

$$P_V(\Gamma_1, t_1 | \Gamma_{\text{p}}, t_{\text{p}}) = \int_{\Gamma_{\text{p}}, t_{\text{p}}}^{\Gamma_1, t_1} D[\Gamma] \, \rho_V[\Gamma(t) | \Gamma_{\text{p}}, t_{\text{p}}] \tag{3.108}$$

where ρ_V is the transition probability density of the whole system {effective particle} ∪ {bath}. The marginal of $\rho_V[\Gamma(t)|\Gamma_{\text{p}}, t_{\text{p}}]$ over all trajectories of the bath degrees of freedom $\{p_\alpha, q_\alpha\}$ is the marginal of $\rho_V[\mu, \tilde{\mu}|\mu_{\text{p}}, t_{\text{p}}]$ over trajectories of the response field $\tilde{\mu}$ of the MSRDDJ probability density in (3.103), namely in compact SUSY notation with fixed initial conditions at t_{p}:

$$D\boldsymbol{\mu} \, e^{-\frac{1}{2}\int_{t_{\text{p}}}^{t_1}\int_{t_{\text{p}}}^{t_1} dadb \, \boldsymbol{\mu}(a)\boldsymbol{Q}^{-1}(a,b)\boldsymbol{\mu}(b) - \int_{t_{\text{p}}}^{t_1} da \, \bar{V}(\boldsymbol{\mu}(a) + \lambda)} = D[\mu, \tilde{\mu}]\rho_V[\mu, \tilde{\mu}|\mu_{\text{p}}, t_{\text{p}}] \tag{3.109}$$

---

[21] If we restore the inertia term in the dynamics, we would add to Γ one more coordinate p_μ, momentum of the particle of position $\mu(t)$. Similarly, H_Γ would have one more term $p_\mu^2/2m$.

We can now write, using Markovianity:

$$P_V(\Gamma_1, t_1 | \Gamma_{\rm p}, t_{\rm p}) = \int {\rm d}\Gamma_0 \, P_V(\Gamma_1, t_1 | \Gamma_0, t_0) P_V(\Gamma_0, t_0 | \Gamma_{\rm p}, t_{\rm p}) \tag{3.110}$$

where[22] ${\rm d}\Gamma = \frac{{\rm d}\mu}{\sqrt{2\pi}} \prod_\alpha {\rm d}p_\alpha {\rm d}q_\alpha$. For $t_0 - t_{\rm p} \gg \tau_\alpha$ the system relaxes, *i.e.* we may assume that $P_V(\Gamma_0, t_0 | \Gamma_{\rm p}, t_{\rm p}) = P_V^{\rm eq}(\Gamma_0)$, the equilibrium distribution in the phase space of the whole system:

$$P_V^{\rm eq}(\Gamma_0) = \frac{e^{-\beta H_{\rm tot}(\Gamma_0)}}{\mathcal{Z}_0 \mathcal{Z}_{\rm B}} = P_V^{\rm eq}(\mu_0) P_{\rm B}^{\rm eq}(\Gamma_0) \tag{3.111}$$

with the marginals describing respectively the effective particle

$$P_V^{\rm eq}(\mu_0) = \frac{e^{-\beta H_0(\mu_0)}}{\mathcal{Z}_0} = \frac{e^{-\mu_0^2/2\Delta_{\rm liq} - \beta \bar{V}(\mu_0 + \lambda)}}{\mathcal{Z}_0} \tag{3.112}$$

and the bath

$$P_{\rm B}^{\rm eq}(\Gamma_0) = \frac{e^{-\beta H_{\rm B}(\Gamma_0)}}{\mathcal{Z}_{\rm B}} \quad \text{with} \quad \mathcal{Z}_{\rm B} = \int \prod_\alpha {\rm d}p_\alpha {\rm d}q_\alpha \, e^{-\beta H_{\rm B}(\Gamma_0)} = \prod_\alpha \frac{2\pi}{\beta \omega_\alpha} \tag{3.113}$$

We may now get rid of the bath degrees of freedom as in Zwanzig's calculation, here integrating them out:

$$P_V(\Gamma_1, t_1 | \Gamma_{\rm p}, t_{\rm p}) = \int \frac{{\rm d}\mu_0}{\sqrt{2\pi}} P_V^{\rm eq}(\mu_0) \underbrace{\int \prod_\alpha {\rm d}p_\alpha^0 {\rm d}q_\alpha^0 \, P_{\rm B}^{\rm eq}(\Gamma_0) \int_{\Gamma_0, t_0}^{\Gamma_1, t_1} {\rm D}[\Gamma] \, \rho_V[\Gamma(t) | \Gamma_0, t_0]} \tag{3.114}$$

Following Hänggi [197], the last term (underbraced) can be interpreted as the transition probability of a Langevin process, with full equilibrium at t_0 between the harmonic oscillators and the effective particle, given by $H_{\rm B}$, *i.e.* not neglecting the coupling to the particle. This generating functional reads, using again MSRDDJ:

$$1 = \int {\rm d}\Gamma_1 \, P_V(\Gamma_1, t_1 | \Gamma_{\rm p}, t_{\rm p}) = \int \frac{{\rm d}\mu_0}{\sqrt{2\pi}} P_V^{\rm eq}(\mu_0) \int {\rm D}[\mu, \tilde{\mu}] \, \rho_V[\mu, \tilde{\mu} | \mu_0, t_0] \tag{3.115}$$

where now the effective Langevin process ruling the dynamics is:

$$\widehat{\gamma}\dot{\mu}(t) = -\frac{T}{\Delta_{\rm liq}}\mu(t) - \beta \int_{t_0}^t {\rm d}t' \, M(t - t')\dot{\mu}(t') + F(\mu(t) + \lambda) + \zeta(t)$$
$$\text{with} \quad \langle \zeta(t) \rangle = 0 \quad \text{and} \quad \langle \zeta(t)\zeta(t') \rangle = 2\widehat{\gamma}T\delta(t - t') + M(t - t') \tag{3.116}$$
$$\mu(t_0) = \mu_0 \text{ is picked with the equilibrium measure } P_V^{\rm eq}(\mu_0)$$

Notice the lower limit of the friction kernel and the fact that there is no extra term, called *initial slip* in [197], due to the somewhat unusual *conditional average* over the perturbed bath, given by $H_{\rm B}$.

3.7.4 Relaxation at long times in the liquid phase

From now on we will be able to compute physically relevant observables, and with this in mind we will use standard MCT methodology [187, 186]. At long time difference $t - t' \to \infty$, if we assume that the correlation and the memory kernel tend to a limiting value $C(\infty)$ and $M(\infty)$ respectively, equation (3.101) gives

$$0 = -\frac{T}{\Delta_{\rm liq}}C(\infty) - \beta M(\infty)[C(\infty) - \Delta_{\rm liq}] \; \Rightarrow \; C(\infty) = \frac{\Delta_{\rm liq}^2 \beta^2 M(\infty)}{1 + \Delta_{\rm liq}\beta^2 M(\infty)}$$
$$\Leftrightarrow \; \beta^2 M(\infty) = \frac{1}{\Delta_{\rm liq}} \frac{C(\infty)}{\Delta_{\rm liq} - C(\infty)} \tag{3.117}$$

In the long time limit, decorrelation occurs *if we assume ergodicity* (which will be questioned at the dynamical transition, see 3.8.1), the average in (3.105) splits and by TTI we actually have to compute equilibrium averages:

$$M(\infty) = \frac{\widehat{\varphi}}{2} \int {\rm d}\lambda \, e^{\lambda - \Delta_{\rm liq}/2} \left\langle F(\mu_0 + \lambda) \right\rangle^2 \tag{3.118}$$

---

[22]Constants are arbitrary here, they can be absorbed in the normalizations.
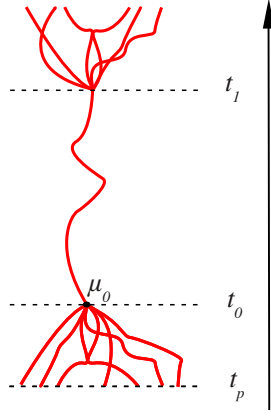
Figure 3.3: The procedure can be more intuitively interpreted as a resummation before t_0 of all possible trajectories starting from a fixed initial position at t_{p} (thanks to the relaxation towards equilibrium) and after t_1 (owing to causality), leaving us with finite times motions in the interval $[t_0, t_1]$.

Using the procedure of the last subsection, $\langle F(\mu_0 + \lambda) \rangle = \int \frac{\mathrm{d}\mu_0}{\sqrt{2\pi}} P_V^{\mathrm{eq}}(\mu_0) F(\mu_0 + \lambda)$. Note that in equilibrium we can show through an integration by parts that, for any observable $O(\mu_0)$,

$$T \left\langle \frac{\mathrm{d}O}{\mathrm{d}\mu_0} \right\rangle = \frac{T}{\Delta_{\mathrm{liq}}} \langle \mu_0 O \rangle - \langle F(\mu_0 + \lambda) O \rangle \tag{3.119}$$

In particular by choosing $O = 1$ we obtain

$$\langle F(\mu_0 + \lambda) \rangle = \frac{T}{\Delta_{\mathrm{liq}}} \langle \mu_0 \rangle \tag{3.120}$$

For simplicity we focus here on HS. For this potential the normalization reads:

$$\mathcal{Z}_0 = \int_{-\lambda}^{\infty} \frac{\mathrm{d}\mu_0}{\sqrt{2\pi}} e^{-\mu_0^2/2\Delta_{\mathrm{liq}}} = \sqrt{\Delta_{\mathrm{liq}}} \, \Theta(\lambda/\sqrt{2\Delta_{\mathrm{liq}}}) \quad \text{with} \quad \Theta(x) = \frac{1 + \mathrm{erf}(x)}{2} \tag{3.121}$$

Given that

$$\langle \mu_0 \rangle = \frac{\int_{-\lambda}^{\infty} \frac{\mathrm{d}\mu_0}{\sqrt{2\pi}} e^{-\mu_0^2/2\Delta_{\mathrm{liq}}} \mu_0}{\sqrt{\Delta_{\mathrm{liq}}} \, \Theta(\lambda/\sqrt{2\Delta_{\mathrm{liq}}})} = \sqrt{\frac{\Delta_{\mathrm{liq}}}{2\pi}} \frac{e^{-\lambda^2/2\Delta_{\mathrm{liq}}}}{\Theta(\lambda/\sqrt{2\Delta_{\mathrm{liq}}})} \tag{3.122}$$

after a short computation we find in the limit $R \to \infty$:

$$\beta^2 M(\infty) \underset{\Delta_{\mathrm{liq}} \to \infty}{\sim} \frac{\widehat{\varphi}}{4\sqrt{\pi}} \frac{e^{-\Delta_{\mathrm{liq}}/4}}{\sqrt{\Delta_{\mathrm{liq}}}} \tag{3.123}$$

which shows with (3.117) that both $M(\infty)$ and $C(\infty)$ go exponentially to zero for $\Delta_{\mathrm{liq}} \to \infty$, as one would expect in the liquid phase.

3.7.5   Getting rid of the sphere $\mathbb{S}_d(R)$: infinite radius limit

Applying the method in 3.7.3, the equation for the memory kernel (3.105) reads

$$M(t - t') = \frac{\widehat{\varphi}}{2} \int \mathrm{d}\lambda \, e^{\lambda - \Delta_{\mathrm{liq}}/2} \int \frac{\mathrm{d}\mu_0}{\sqrt{2\pi}} P_V^{\mathrm{eq}}(\mu_0) \left\langle F(\mu(t) + \lambda) F(\mu(t') + \lambda) \right\rangle \tag{3.124}$$

where the average is computed over the Langevin process (3.198). Fixing λ, we make the change of variables $h(t) = \mu(t) + \lambda$ centered at the *wall*: $h < 0$ is where the effective hard core repulsion of the potential takes place, see figure 3.7.5. The normalization of P_V^{eq} is unchanged and

$$P_V^{\mathrm{eq}}(h_0) = \frac{e^{-(h_0 - \lambda)^2/2\Delta_{\mathrm{liq}} - \beta \bar{V}(h_0)}}{\mathcal{Z}_0} \tag{3.125}$$

We can simplify the expression of M through a saddle-point method[23] for $\Delta_{\text{liq}} \to \infty$, setting $\alpha = \lambda/\Delta_{\text{liq}}$:

$$M(t - t') = \frac{\widehat{\varphi}}{2} \sqrt{\Delta_{\text{liq}}} \int \frac{\mathrm{d}h_0}{\sqrt{2\pi}} \mathrm{d}\alpha \, e^{-\beta \bar{V}(h_0) - \frac{h_0^2}{2\Delta_{\text{liq}}} - \frac{\Delta_{\text{liq}}}{2}(\alpha - 1)^2 + h_0 \alpha} \left\langle F(h(t))F(h(t')) \right\rangle$$

$$\Rightarrow M(t - t') \underset{\Delta_{\text{liq}} \to \infty}{\sim} \frac{\widehat{\varphi}}{2} \int \mathrm{d}h_0 \, e^{-\beta w(h_0)} \left\langle F(h(t))F(h(t')) \right\rangle \quad \text{with} \quad w(h) = \bar{V}(h) - Th + \underbrace{\frac{T}{2\Delta_{\text{liq}}} h^2}$$

$$\tag{3.126}$$

since $\alpha = 1$ at the saddle point. We replaced the normalization by

$$\mathcal{Z}_0 = \int \frac{\mathrm{d}\mu_0}{\sqrt{2\pi}} \, e^{-\mu_0^2/2\Delta_{\text{liq}} - \beta \bar{V}(\mu_0 + \alpha \Delta_{\text{liq}})} \underset{\Delta_{\text{liq}} \to \infty}{\sim} \sqrt{\Delta_{\text{liq}}} \tag{3.127}$$

since the potential goes to zero at long distances[24]. The Langevin equation is affected by the change of variables only with an additional term $T\alpha \simeq T$:

$$\widehat{\gamma} \dot{h}(t) = T - \underbrace{\frac{T}{\Delta_{\text{liq}}} h(t)} - \beta \int_{t_0}^{t} \mathrm{d}t' \, M(t - t')\dot{h}(t') + F(h(t)) + \zeta(t)$$

$$\text{with} \quad \left\langle \zeta(t) \right\rangle = 0 \quad \text{and} \quad \left\langle \zeta(t)\zeta(t') \right\rangle = 2\widehat{\gamma}T\delta(t - t') + M(t - t') \tag{3.128}$$

$$h(t_0) = h_0 \text{ is picked with the equilibrium measure} \propto e^{-\beta w(h_0)}$$

Our problem is mapped onto a one-dimensional diffusion with colored noise (as usual in mean field [81]) and a harmonic effective potential $w(h)$ perturbed by the spheres' repulsion (cf. figure 4). The linear part of the potential is interpreted in §5.4. The underbraced terms -the harmonic potential well- are negligible for finite times, but necessary to confine the system: they represent the *box*.

Equations (3.101), (3.102), (3.126) and (3.128) are our final expressions for the dynamical equations, valid for finite times.

A numerical procedure (*i.e.* the logical steps) to solve the problem obtaining the memory kernel (or equivalently the MSD or correlation function) could be

- Start with a guess for $M(t)$

- Solve the process in (3.128) to compute the force-force correlation that appears in (3.126).

- Use (3.126) to obtain a new guess for $M(t)$

- Iterate until convergence

- Use (3.102) or (3.101) to obtain $\Delta(t)$ or $C(t)$ from the memory kernel.

A possible interpretation of these equations is the following. Due to the infinite-dimensional limit and the virial argument of §3.2.2 implying the independence between neighbours of a given particle (*i.e.* a tree-like interaction network as in the Mari-Kurchan model [270] presented in chapter 4), the dynamics of the system can be expressed as the dynamics of a tagged particle with its interacting neighbours, and more precisely with one *typical* neighbour: this is a two-body problem in presence of the *bath* constituted by the other neighbours. Indeed, if we consider $h(t)$ as representing the $O(1/d)$ fluctuation of the gap between neighbours, its dynamics in (3.128) is governed by the original potential, which tends to forbid overlaps between the two particles ($h < 0$), and an entropic term due to isotropy (see §5.4) which tends to separate the neighbours and make them diffuse away. This motion is done in presence of a bath which mixes the original heat bath *and* has another component coming from the self-induced disorder of the system (all other particles that are also interacting with the tagged particle).

To conclude this section, let us note that an interesting alternative self-consistent equation for $M(t)$ is obtained from (3.126) if we choose $t > t'$ and $t' = t_0$, which is possible because the dynamics starts in

---

[23]From the Langevin equation, the bracketed term $\left\langle F(h(t))F(h(t')) \right\rangle$ depends upon α but it cannot be exponential in Δ_{liq} and as a consequence gives no contribution to the saddle-point equation.

[24]Note that in Eq. (3.126) $\left\langle \bar{V}'(h(t))\bar{V}'(h(t')) \right\rangle$ is small if h_0 is large, because the potential falls quickly to zero for positive h_0, hence the integral over h_0 is convergent.
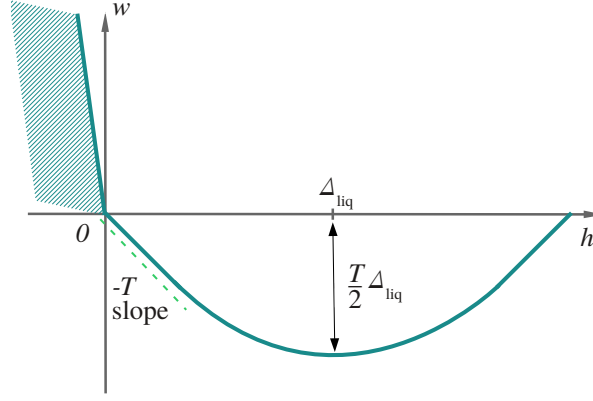
Figure 3.4: Effective potential landscape. If V is hard, there is an infinite wall at $h = 0$ prohibiting any motion in the $h < 0$ half line. If the constraint is softer, as drawn here, motion is possible for $h < 0$ but is rather unlikely. The entropic term tends to make h diffuse away to the limits set by the box containing the system.

equilibrium. Let us also assume that $\bar{V}(h) = 0$ for $h \geqslant 0$. We obtain

$$
\begin{aligned}
M(t) &= \frac{\widehat{\varphi}}{2} \int_{-\infty}^{0} \mathrm{d}h_0 \, e^{-\beta \bar{V}(h_0) + h_0} F(h_0) \langle F(h(t)) \rangle \\
&= -\frac{\widehat{\varphi}T}{2} \left\{ \left[e^{-\beta \bar{V}(h_0) + h_0} \langle F(h(t)) \rangle \right]_{-\infty}^{0} - \int_{-\infty}^{0} \mathrm{d}h_0 \, e^{-\beta \bar{V}(h_0)} \frac{\partial}{\partial h_0} \left[e^{h_0} \langle F(h(t)) \rangle \right] \right\} \\
&= -\frac{\widehat{\varphi}T}{2} \left\{ \langle F(h(t)) \rangle_{h_0 = 0} - \int_{-\infty}^{0} \mathrm{d}h_0 \, e^{-\beta \bar{V}(h_0)} \frac{\partial}{\partial h_0} \left[e^{h_0} \langle F(h(t)) \rangle \right] \right\}
\end{aligned}
\tag{3.129}
$$

For HS we have $\bar{V}(h) \to \infty$ for $h < 0$ and the second term in the last line can be neglected, so we obtain a very simple expression:

$$
M(t) = -\frac{\widehat{\varphi}T}{2} \langle F(h(t)) \rangle_{h_0 = 0}
\tag{3.130}
$$

where the dynamics starts at time t_0 from a fixed initial condition $h_0 = 0$. Note that $\langle F(h(t)) \rangle$ is then not independent of time, firstly because the dynamics in equation (3.128) has a drift term proportional to T, and secondly because if we impose a fixed initial condition $h_0 = 0$ and consider finite times the system is not in a stationary state anyway.

This gives a possible strategy to determine the memory kernel. The problem to solve is thus a sort of *return-to-the-origin* problem of a diffusive tracer (owing to the hard constraint at $h = 0$) which moves on the half-line $h > 0$ in presence of a colored noise and an additional drift T (see (3.128)).

3.7.6 The *Lagrange multiplier*

Plugging in (3.100) the value at equal times[25] $M(0)$, which can be computed at equilibrium using TTI, we have

$$
\nu - \frac{T}{\Delta_{\text{liq}}} = -\delta\nu + \beta M(0) = \frac{\widehat{\varphi}}{2} \int_{-\infty}^{0} \mathrm{d}h_0 \, e^{h_0 - \beta \bar{V}(h_0)} F'(h_0) + \beta \frac{\widehat{\varphi}}{2} \int_{-\infty}^{0} \mathrm{d}h_0 \, e^{h_0 - \beta \bar{V}(h_0)} F(h_0)^2
\tag{3.131}
$$

since $\bar{V}(h_0) = 0$ for $h_0 > 0$. We will focus in the following on hard spheres and assume a regularization of the potential which is of class C^1, *e.g.* soft spheres[26] $\beta \bar{V}_{\text{SS}}(h) = \kappa r^2 \theta(-h)$. We have, with integrations

---

[25] $M(0)$ diverges in the HS limit, which is natural given its interpretation as a force-force correlation.

[26] It is actually valid for a linear regularization $\beta \bar{V}_{\text{lin}}(h) = -\kappa h \theta(-h)$ too. Indeed we get $\delta\nu = \frac{\widehat{\varphi}}{2} T \kappa$ and $\beta M(0) = \frac{\widehat{\varphi}}{2} T(\kappa - 1) + O(1/\kappa)$.

by parts, due to the continuity of $\bar{V}$ and F in 0,

$$
\begin{aligned}
\nu - \frac{T}{\Delta_{\text{liq}}} =& \frac{\widehat{\varphi}}{2} \left\{ \left[e^{h_0 - \beta \bar{V}(h_0)} F(h_0) \right]_{-\infty}^0 - \int_{-\infty}^0 dh_0 \, e^{h_0 - \beta \bar{V}(h_0)} F(h_0) \left(1 + \beta F(h_0) \right) \right\} \\
& + \frac{\widehat{\varphi}}{2} \beta \int_{-\infty}^0 dh_0 \, e^{h_0 - \beta \bar{V}(h_0)} F(h_0)^2 \\
=& \frac{\widehat{\varphi}}{2} \left\{ \left[e^{h_0 - \beta \bar{V}(h_0)} \left(F(h_0) - T \right) \right]_{-\infty}^0 + T \int_{-\infty}^0 dh_0 \, e^{h_0 - \beta \bar{V}(h_0)} \right\}
\end{aligned}
\tag{3.132}
$$

The last integral being zero for HS, we conclude that the Lagrange multiplier[27] is (up to exponentially small corrections in $\Delta_{\text{liq}} \to \infty$ due to $M(0)$ and $\delta\nu$):

$$
\beta\nu = -\frac{\widehat{\varphi}}{2} + \frac{1}{\Delta_{\text{liq}}}
\tag{3.133}
$$

3.7.7 Choice of the dynamics

Note that in the dynamical equations (3.126) and (3.128), we have considered the overdamped case $m = 0$, which could be restored at any time by changing the kernel associated to the kinetic term Φ in §3.4.1.

Another possible strategy is to keep the inertial term, let the system equilibrate, and then remove the friction and noise terms. One may do so directly assuming the Gibbs-Boltzmann distribution for the initial condition, as in §3.7.3. Remarkably enough, nothing dramatic happens with the equations and their solution in the limit $\gamma \to 0$. The external noise is absent, but the one induced on a particle by the others is still here, just as the induced friction term. It is tempting to think that we have thus *proven* chaoticity for a particle system, but a caveat is in order. Our path integrals are defined for finite noise level, which we are taking to zero *after* the limit of large particle number and of large dimension. Thus, we are *proving chaos* with some level of coarse-graining, which we are taking to zero after all other parameters have gone to infinity.

The choice of the dynamical rules has been studied in [182, 376] and revealed no significant differences in terms of averaged dynamical quantities, except obviously at short times. This holds even for Monte Carlo dynamics not considered here [49, 41], and might be interpreted in terms slow modes of the system that dominates the dynamics. The results found here for all values of the mass m or the friction γ confirms these results in mean field. Yet, as a final remark, important differences were found concerning long-time fluctuations of correlators [39, 44].

3.8 Physical consequences of the equilibrium dynamical equations

Here we study some implications of the above-derived equilibrium equations. A dynamical transition with the persistence of a plateau appears in the correlations or the MSD. We compute the diffusion coefficient of the liquid, as well as its viscosity, and find a relation akin to the Stokes-Einstein one. We provide microscopic expressions of the memory kernel and the saddle-point functions Δ and C.

3.8.1 Plateau and dynamical transition

3.8.1.1 Metastable glassy states: plateau value

We now look for a plateau in the dynamics: we assume a strong separation between a fast and a slow motion. We can split the correlations (and similarly the memory kernel) into a vibrational short-lived contribution and a slowly decaying function:

$$
C(t - t') = C^f(t - t') + C^s(t - t'), \quad M(t - t') = M^f(t - t') + M^s(t - t')
\tag{3.134}
$$

each decaying on timescales $\tau_f \ll \tau_s$, respectively. Let us look at intermediate times $\tau_f \ll t - t' \ll \tau_s$. The slowly varying functions are approximately constant at this scale, equal to the plateau value noted

---

[27]As noted in 3.2.3, ν is not the actual Lagrange multiplier, but is related to it.

C_{EA} (respectively M_{EA}). We have $C_{\mathrm{EA}} = \Delta_{\mathrm{liq}} - \Delta_{\mathrm{EA}}$ where Δ_{EA} is the plateau of the MSD. Similarly to (3.117), we get from (3.101) the relation between M_{EA} and Δ_{EA}:

$$\beta^2 M_{\mathrm{EA}} = \frac{1}{\Delta_{\mathrm{liq}}} \frac{C_{\mathrm{EA}}}{\Delta_{\mathrm{liq}} - C_{\mathrm{EA}}} = \frac{1}{\Delta_{\mathrm{EA}}} - \frac{1}{\Delta_{\mathrm{liq}}} \tag{3.135}$$

From (3.134), we can consider the Langevin noise as the sum of two independent centered Gaussian noises, a slowly varying one $\bar{\zeta}$ and a fast one ζ^f. In this limit, the Langevin equation (3.128) reads, using (3.135),

$$\widehat{\gamma}\dot{h}(t) = s - \frac{T}{\Delta_{\mathrm{EA}}}h(t) - \beta\int_{t_0}^{t} \mathrm{d}t'\, M^f(t-t')\dot{h}(t') + F(h(t)) + \zeta^f(t)$$

$$\text{with } s \equiv \bar{\zeta} + \beta M_{\mathrm{EA}}h_0 + T\,,\ \ \left\langle \zeta^f(t)\zeta^f(t')\right\rangle = 2\widehat{\gamma}T\delta(t-t') + M^f(t-t')\,, \tag{3.136}$$

$$\left\langle\bar{\zeta}(t)\bar{\zeta}(t')\right\rangle = M^s(t-t')\ \ \text{and for } \tau_f \ll t-t' \ll \tau_s\,,\ \ \left\langle\bar{\zeta}^2\right\rangle \simeq M_{\mathrm{EA}}$$

Following [111, Sec. 4.], s acts as a quasistatic field: for times $t - t' \ll \tau_s$, $(\bar{\zeta}, h_0)$ or equivalently s can be considered as quenched variables, picked with probability $P_{\mathrm{slow}}(s)$. For $t - t' \gg \tau_f$, the process relaxes to an *equilibrium* state selected by s, which is the actual metastable glassy state, with probability[28]

$$P_1(h|s) = \frac{e^{-\beta H_1(h,s)}}{Z_1(s)}\ \ \text{with}\ \ H_1(h,s) = \frac{T}{2\Delta_{\mathrm{EA}}}h^2 - sh + \bar{V}(h)$$

$$P_{\mathrm{slow}}(s) = \int \frac{\mathrm{d}h_0}{\sqrt{2\pi}}\mathrm{d}\bar{\zeta}\, P_V^{\mathrm{eq}}(h_0)\frac{e^{-\bar{\zeta}^2/2M_{\mathrm{EA}}}}{\sqrt{2\pi M_{\mathrm{EA}}}}\delta(s - \bar{\zeta} - \beta M_{\mathrm{EA}}h_0 - T) \tag{3.137}$$

$$= \int \frac{\mathrm{d}h_0}{\sqrt{2\pi}}e^{-\beta w(h_0)}\frac{e^{-\frac{\beta^2 M_{\mathrm{EA}}}{2}\left(h_0 - \frac{T}{M_{\mathrm{EA}}}(s-T)\right)^2}}{\sqrt{2\pi M_{\mathrm{EA}}}} \times \frac{e^{\Delta_{\mathrm{liq}}/2 - \lambda + h_0(\alpha-1) - \Delta_{\mathrm{liq}}(\alpha-1)^2/2}}{\mathcal{Z}_0}$$

with $\alpha = \lambda/\Delta_{\mathrm{liq}}$. Taking $\Delta_{\mathrm{liq}} \to \infty$ as in (3.126) provides the plateau value:

$$\sqrt{M_{\mathrm{EA}}} = \frac{\widehat{\varphi}}{2}\int \mathrm{d}s\, e^{-(s-T)^2/2M_{\mathrm{EA}}}Z_1(s)\left\langle F(h)\right\rangle_1^2 \tag{3.138}$$

As an example, we restrict ourselves to the HS case. Then, with an integration by parts,

$$\left\langle F(h)\right\rangle_1 = \int \frac{\mathrm{d}h}{\sqrt{2\pi}}P_1(h|s)F(h) = \frac{T}{Z_1(s)\sqrt{2\pi}}$$

$$\text{with}\ \ \ Z_1(s) = \int \frac{\mathrm{d}h}{\sqrt{2\pi}}e^{\beta sh - h^2/2\Delta_{\mathrm{EA}} - \beta\bar{V}(h)} = \sqrt{\Delta_{\mathrm{EA}}}\,\Theta\left(s\beta\sqrt{\Delta_{\mathrm{EA}}/2}\right)e^{\beta^2 s^2\Delta_{\mathrm{EA}}/2} \tag{3.139}$$

setting $u = \sqrt{\Delta_{\mathrm{EA}}}(\beta s - 1)$ finally gives

$$\frac{1}{\sqrt{\Delta_{\mathrm{EA}}}} = \widehat{\varphi}\int \frac{\mathrm{d}u}{4\pi}\frac{e^{-u^2/2 - (u+\sqrt{\Delta_{\mathrm{EA}}})^2/2}}{\Theta\left(\frac{u+\sqrt{\Delta_{\mathrm{EA}}}}{\sqrt{2}}\right)} \tag{3.140}$$

This plateau value coincides with the one found in the statics, see §4.6.

Note that in the glassy regime, both the plateau solution M_{EA} and the solution $M(\infty)$ discussed formally exist as solutions for the long-time limit of $M(t)$; however, the dynamics always selects the solution with the largest value of M, which is M_{EA} (see *e.g.* the discussion in [81] or [187]).

3.8.1.2 Dynamical transition

Plotting the function $\widehat{\varphi}$ versus Δ_{EA} using (3.140) (see figure 3.5), we get a minimum at the critical packing fraction (see figure 3.8.1.2)

$$\varphi_{\mathrm{d}} \simeq 4.80678\frac{d}{2^d} \tag{3.141}$$

where the plateau is $\Delta_{\mathrm{EA}}(\widehat{\varphi}_{\mathrm{d}}) \simeq 1.15336$. This is the minimal packing fraction at which a plateau value occurs, which signals the dynamical transition where the system does not relax anymore and is trapped in a metastable state.

---

[28]One has to be careful here with the limit $\Delta_{\mathrm{liq}} \to \infty$: we cannot use directly equation (3.126), this is why we have to compute P_{slow} on the sphere and take the infinite radius limit. In principle we would also do it for $P_1(h|s)$ but it is subdominant (as in footnote 23), so that we can compute it directly with (3.136), where $\Delta_{\mathrm{liq}} \to \infty$ has already been taken.
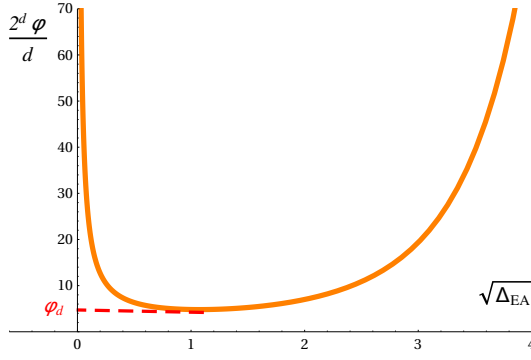
Figure 3.5: Plateau value and critical packing fraction

3.8.2 Relation with rigorous lower bounds for sphere packings in high dimensions

The packing fraction (3.141) is larger than the best known lower bound for the existence of sphere packings $\widehat{\varphi} \geqslant 6/e$ [397]. It took nearly 20 years to improve the previous best lower bound $\widehat{\varphi} \geqslant 2$ [22] by a small factor $3/e$, see figure 3.6. This means that a HS system may be prepared in equilibrium up to these densities in times that do not scale exponentially with the size of the box, and they can be constructed easily through a sufficiently slow compression of the liquid [257, 289]. In other words, packings as good as this are easy to obtain, and we conclude that this would be a constructive improvement on the best bound known in high d. It would require the present derivation to be turned into a rigorous proof, which seems feasible along the lines of [31, 32] since our calculation, though a bit tedious, is quite elementary.

Another outcome of this section is that we can get the dynamical transition curve in the (T, ρ) plane for a more general potential than HS, see (3.135) and (3.138). For instance, one can imagine to maximize the dynamic packing fraction over a HS-like potential which would be infinite below some diameter but arbitrary in the $O(1/d)$ regime around the diameter. This would still be a generic HS packing easy to construct, and would be denser than $\widehat{\varphi} = 4.8$. A first step in this direction has been achieved by Sellitto and Zamponi [356, 355], using a truncated LJ-like potential, *i.e.* an HS with a small attractive step (*sticky sphere*), which promotes the critical packing fraction to $\widehat{\varphi} = 6.5$, *i.e.* a factor 3 higher than the best rigorous lower bound of Vance. Further progress is under way.

Note that the densest sphere packings are mathematically known in dimensions $d = 1$, 2 (triangular lattice), 3 (face-centered cubic) and very recently in $d = 8$ and $d = 24$ by Viazovska and coworkers [399, 102], see [386] for a review of the packing problem.

3.8.3 Diffusion at long times

From (3.102) we obtain an expression for the diffusion coefficient for times larger than the relaxation time but still $\Delta \ll \Delta_{\text{liq}}$. In this regime, the mode-coupling-like equation for the MSD reduces to

$$\gamma \dot{\mathsf{D}}(t - t') = 2dT - \frac{2d^2}{\sigma^2} \beta \int_{t'}^{t} \mathrm{d}v \, M(t - v) \dot{\mathsf{D}}(v - t') \tag{3.142}$$

where $\mathsf{D} = \Delta/d$ is the non-rescaled MSD, that is, the MSD of the original system of particles (see §3.8.4.1). Using Laplace transform and the fact that $\mathsf{D}(0) = 0$ we have

$$\widetilde{\mathsf{D}}(p) = \frac{1}{p^2} \frac{2dT}{\gamma + \frac{2d^2}{\sigma^2} \beta \widetilde{M}(p)} \underset{p \to 0}{\sim} \frac{1}{p^2} \frac{2dT}{\gamma + \frac{2d^2}{\sigma^2} \beta \widetilde{M}(0)} \tag{3.143}$$

By definition $\widetilde{M}(0) = \int_0^\infty \mathrm{d}t \, M(t)$. A Tauberian theorem then gives the long-time diffusive behaviour of the MSD from the small p behaviour of its Laplace transform [150]:

$$\mathsf{D}(t) \sim 2dDt \qquad \text{with} \qquad D = \frac{T}{\gamma + \frac{2d^2}{\sigma^2} \beta \int_0^\infty M} = \frac{D_0}{1 + \frac{\beta}{\gamma} \int_0^\infty M} \tag{3.144}$$

where $D_0 = T/\gamma$. At low density $M \simeq 0$ and we recover the usual diffusion coefficient D_0 of the free dynamics, as in (3.96). Upon increasing density, M increases and the diffusion coefficient decreases. At
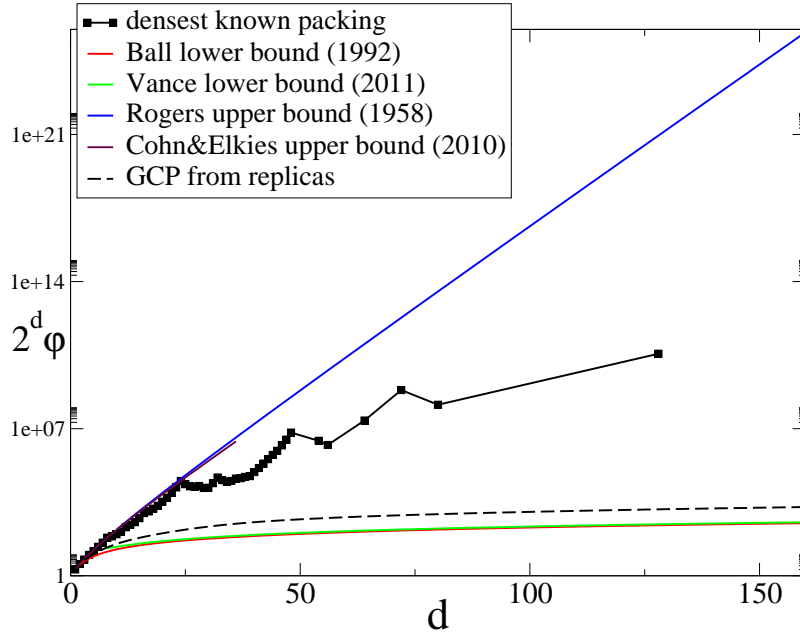
Figure 3.6: Ball's 1992 lower bound [22] was refined by Vance in 2011 [397]. Rogers gave an upper bound in 1958 [333]. Cohn and Elkies provided upper bounds for $d \leqslant 36$ [101]. The squares are numerical results. The greatest close packing (GCP) has been obtained (non-rigorously) for infinite-pressure HS by Parisi and Zamponi [312], and scales as $\widehat{\varphi} \sim \ln d$.

the dynamical transition, M displays a persistence of a plateau, the relaxation time $\tau_\alpha \propto \int_0^\infty M$ diverges and the diffusion coefficient vanishes. One usually defines an exponent γ such that, for $\varphi \to \varphi_{\mathrm{d}}^-$,

$$\tau_\alpha \sim \left(\frac{\varphi_{\mathrm{d}} - \varphi}{\varphi_{\mathrm{d}}} \right)^{-\gamma} \quad \text{and} \quad D \sim \left(\frac{\varphi_{\mathrm{d}} - \varphi}{\varphi_{\mathrm{d}}} \right)^{\gamma} \tag{3.145}$$

γ is one of the so-called MCT exponents [186, 187], see §1.2.1.3.

Restoring the inertial term does not affect (3.144): we have $\dot{\mathsf{D}}(0) = 0$ if $m \neq 0$ and the second derivative gives a p^2 contribution, which is subdominant in the $p \to 0$ limit compared to the friction term.

This diffusive behaviour is consistent with HS simulations by Charbonneau's group [91], as displayed in figure 3.7, see also §3.8.5.

3.8.4 Connections with the microscopic model

In this section we make close contact between the quantities appearing in the *single-particle* effective dynamics and the microscopic ones defined for the Langevin process of the N particles (3.7). We prove that the saddle-point values of the MSD or correlation and responses, that can be obtained by solving the set of self-consistent dynamical equations in §3.7.5, correspond to the same microscopic quantities. We establish a connection between the memory kernel and microscopic force-force correlations as well as microscopic stress-stress correlations, and use it to derive a relation between the diffusion coefficient and the shear viscosity of the liquid.

3.8.4.1 Correlation, response and mean-squared displacement

We wish to establish a connection between microscopic quantities and their counterpart at the saddle-point level in $d \to \infty$. Let us look at the MSD, but a similar reasoning can be done for correlations and responses (which are related to it). Let us look at the microscopic MSD for a particle i

$$\left\langle \left(x_i(t) - x_i(t') \right)^2 \right\rangle_{Z_N} = \frac{1}{N} \left\langle \sum_{i=1}^{N} \left(x_i(t) - x_i(t') \right)^2 \right\rangle_{Z_N} = \frac{\delta \left(\ln Z_N[h]/N[h] \right)}{\delta h(t, t')} \bigg|_{h=0} \tag{3.146}$$
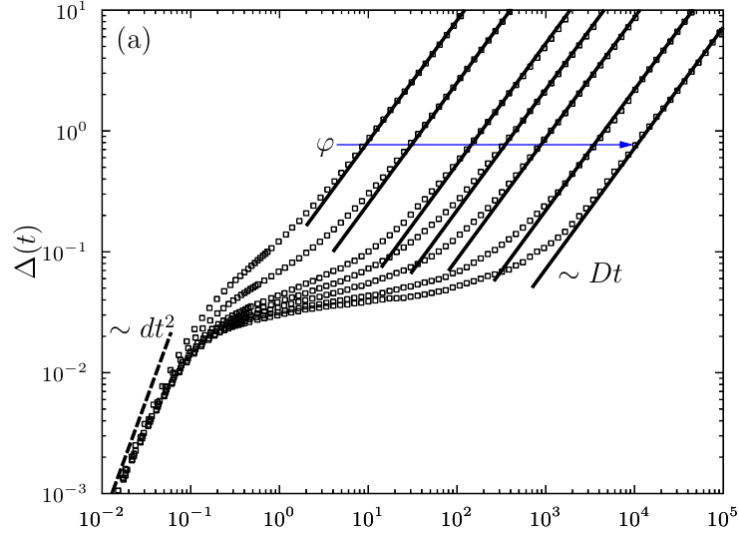
Figure 3.7: The MSD in $d = 6$ HS for increasing $\varphi \in [0.1453, 0.1720]$ illustrates the developing caging regime (dashed line), intermediate between the ballistic (thick line) and the diffusive (solid line) regimes. This figure echoes figure 3.1(a). [*Reprinted from* [91, 98]]

since $Z_N[h = 0] = 1$, with $Z_N[h]$ (or $\Xi[h]$) obtained by adding to the dynamical action a coupling to a generating field $h(t, t')$,

$$\mathcal{A}[\{x_i, \hat{x}_i\}, h] = \mathcal{A}[\{x_i, \hat{x}_i\}] - \sum_{i=1}^{N} \int \mathrm{d}t\mathrm{d}t' \left(x_i(t) - x_i(t')\right)^2 h(t, t') \tag{3.147}$$

This is a single-particle term, which amounts to shift the kinetic term in the following way:

$$\Phi[x, \hat{x}, h] = \Phi[x, \hat{x}] - \int \mathrm{d}t\mathrm{d}t' \left(x(t) - x(t')\right)^2 h(t, t') \tag{3.148}$$

Then we use the above-derived $d \to \infty$ limit of $\ln Z_N/N \underset{N\to\infty}{\sim} \ln \Xi/N = \mathcal{S}$ with $\mathcal{S}[h] = \mathcal{S}_{\mathrm{IG}}[h] + \mathcal{S}_{\mathrm{int}}$, where only the ideal gas term depends on h: $\mathcal{S}_{\mathrm{IG}} = - \int \mathsf{D}[x, \hat{x}]\rho[x, \hat{x}](\Phi[x, \hat{x}, h] + \ln\rho[x, \hat{x}])$. Consequently, going to generalized spherical coordinates,

$$\begin{aligned}
\left\langle \left(x_i(t) - x_i(t')\right)^2 \right\rangle_{Z_N} &= \left.\frac{\delta \mathcal{S}_{\mathrm{IG}}[h]}{\delta h(t, t')}\right|_{h=0} \underset{d\to\infty}{=} -\left.\frac{\delta \Phi(\boldsymbol{Q}^{\mathrm{sp}}, h)}{\delta h(t, t')}\right|_{h=0} \\
&= \left.\frac{\delta}{\delta h(t, t')} \int \mathrm{d}u\mathrm{d}u' \, \mathsf{D}(u, u')h(u, u')\right|_{h=0} = \mathsf{D}(t, t')
\end{aligned} \tag{3.149}$$

We deduce that the adimensional rescaled correlation functions

$$\frac{2d}{\sigma^2 N} \sum_i x_i(t) \cdot x_i(t') \underset{d\to\infty}{\sim} C(t, t'), \qquad \frac{2d}{\sigma^2 N} \sum_{i,\mu} \frac{\delta x_i^\mu(t)}{\delta \bar{h}_i^\mu(t')} \underset{d\to\infty}{\sim} R(t, t') ,$$

$$\frac{d}{\sigma^2 N} \sum_i |x_i(t) - x_i(t')|^2 \underset{d\to\infty}{\sim} \Delta(t, t') \tag{3.150}$$

(with external fields $\bar{h}_i$) are non-fluctuating, imposed by their saddle-point value.

3.8.4.2   Force-force correlation and its relation to the memory kernel

Here we establish a connection between a microscopic force-force correlation $\left\langle \sum_{i<j} F_{ij}(t) \cdot F_{ij}(t') \right\rangle_{Z_N}$, where $F_{ij} = -\nabla V(x_i - x_j)$, and the memory kernel M. To generate such terms we will use a random shift similar to the MK model [270] studied in chapter 4, and once again resort to the SUSY notation for compactness. We will thus consider a shift of vector $A_{ij}\boldsymbol{g}(a)$ for each pair of particles, where A_{ij} are Gaussian centered random vectors in d dimensions, of variance Σ_A^2, independent and identically

distributed. We will note

$$\mathcal{D}A = \prod_{\mu=1}^{d} \mathrm{d}A^{\mu} e^{-(A^{\mu})^2/2\Sigma_A^2}/\sqrt{2\pi\Sigma_A^2} \tag{3.151}$$

their common measure. $\boldsymbol{g}$ is a scalar time-dependent external field that will be sent to zero in the end, in order to recover the original model. Again for compactness, we will note averages over the A_{ij} by an overbar, i.e. $\overline{A_{ij}^{\mu}} = 0$ and $\overline{A_{ij}^{\mu}A_{kl}^{\nu}} = \Sigma_A^2 \delta_{ik}\delta_{jl}\delta^{\mu\nu}$. The dynamical action becomes

$$\mathcal{A}[\{\boldsymbol{x}_i\}, \{A_{ij}\}, \boldsymbol{g}] = \sum_{i=1}^{N} \Phi(\boldsymbol{x}_i) + \sum_{i<j}^{1,N} \int \mathrm{d}a\, V(\boldsymbol{x}_i(a) - \boldsymbol{x}_j(a) + A_{ij}\boldsymbol{g}(a)) \tag{3.152}$$

We still note $\boldsymbol{F}_{ij}^{\mu}(a) = -\nabla^{\mu}V(\boldsymbol{x}_i(a) - \boldsymbol{x}_j(a) + A_{ij}\boldsymbol{g}(a))$, knowing that we recover the previously defined force by $F_{ij}^{\mu}(t) = \boldsymbol{F}_{ij}^{\mu}(a)\big|_0$ where the 0 stands for $\boldsymbol{g}$ and all Grassmann variables being sent to zero. Let us compute the second derivative of the generating dynamic functional $Z_N[\boldsymbol{g}]$:

$$\frac{\delta Z_N[\boldsymbol{g}]}{\delta\boldsymbol{g}(a)} = \int \prod_{i=1}^{N} \mathrm{D}\boldsymbol{x}_i\, e^{-\mathcal{A}[\{\boldsymbol{x}_i\}, \{A_{ij}\}, \boldsymbol{g}]} \sum_{i<j} A_{ij}^{\mu}\boldsymbol{F}_{ij}^{\mu}(a)$$

$$\frac{\delta^2 Z_N[\boldsymbol{g}]}{\delta\boldsymbol{g}(a)\delta\boldsymbol{g}(b)} = \int \prod_{i=1}^{N} \mathrm{D}\boldsymbol{x}_i\, e^{-\mathcal{A}[\{\boldsymbol{x}_i\}, \{A_{ij}\}, \boldsymbol{g}]} \left[\sum_{\substack{i<j \\ k<l}} A_{ij}^{\mu}A_{kl}^{\nu}\boldsymbol{F}_{ij}^{\mu}(a)\boldsymbol{F}_{kl}^{\nu}(b) + \boldsymbol{\delta}(a,b)\sum_{i<j} A_{ij}^{\mu}A_{ij}^{\nu}\nabla^{\nu}\boldsymbol{F}_{ij}^{\mu}(a) \right] \tag{3.153}$$

where repeated Greek indices are summed over. Sending the external field to zero and averaging over the random shifts directly give $\delta\overline{Z_N}[\boldsymbol{g}]/\delta\boldsymbol{g}(a) = \boldsymbol{0}$ and

$$\frac{\delta^2 \overline{Z_N}[\boldsymbol{g}]}{\delta\boldsymbol{g}(a)\delta\boldsymbol{g}(b)}\bigg|_0 = \Sigma_A^2 \left\langle \sum_{i<j} F_{ij}(t)\cdot F_{ij}(t') \right\rangle_{Z_N} \tag{3.154}$$

which is the original force-force correlation looked for. As in [270], one can compute the average $\overline{Z_N}[\boldsymbol{g}]$ introducing an averaged Mayer function

$$\overline{f_{ij}}[\boldsymbol{g}] = \int \mathcal{D}A\, f(\boldsymbol{x}_i(a) - \boldsymbol{x}_j(a) + A\boldsymbol{g}(a)) = \int \mathcal{D}A \left[e^{-\int \mathrm{d}a\, V(\boldsymbol{x}_i(a) - \boldsymbol{x}_j(a) + A\boldsymbol{g}(a))} - 1 \right] \tag{3.155}$$

For a non-zero $\boldsymbol{g}(a)$ and large enough Σ_A, we still have the same crucial fact that $\overline{f_{ij}}[\boldsymbol{g}] = 1 + O(\mathcal{V}_d(\Gamma)/\mathcal{V})$ where Γ is a typical length of a trajectory (for finite times), due to the requirement that two trajectories overlap to feel the effect of the potential. As a consequence, we can repeat the MK computation and obtain in the thermodynamic limit $\overline{Z_N}[\boldsymbol{g}] = e^{N\mathcal{S}[\boldsymbol{g}]}$ with the action

$$\mathcal{S} = -\int \mathrm{D}\boldsymbol{x}\, \rho(\boldsymbol{x})(\ln\rho(\boldsymbol{x}) + \Phi(\boldsymbol{x})) + \frac{N}{2} \int \mathrm{D}[\boldsymbol{x}, \boldsymbol{y}]\, \rho(\boldsymbol{x})\rho(\boldsymbol{y}) \int \mathcal{D}A\, f(\boldsymbol{x} - \boldsymbol{y} + A\boldsymbol{g}(a)) \tag{3.156}$$

The difference here is that we cannot simplify further by translation invariance since the shift is time-dependent. Nevertheless, we can still compute derivatives of $\overline{Z_N}[\boldsymbol{g}]$, reminding that due to probability conservation $\overline{Z_N}[\boldsymbol{g}] = 1$:

$$\frac{\delta\overline{Z_N}}{\delta\boldsymbol{g}(a)}\bigg|_0 = N\frac{\delta\mathcal{S}}{\delta\boldsymbol{g}(a)}\bigg|_0 = 0$$

$$\frac{\delta^2\overline{Z_N}}{\delta\boldsymbol{g}(a)\delta\boldsymbol{g}(b)}\bigg|_0 = N\frac{\delta^2\mathcal{S}}{\delta\boldsymbol{g}(a)\delta\boldsymbol{g}(b)}\bigg|_0 + N^2\frac{\delta\mathcal{S}}{\delta\boldsymbol{g}(a)}\bigg|_0\frac{\delta\mathcal{S}}{\delta\boldsymbol{g}(b)}\bigg|_0 = N\frac{\delta^2\mathcal{S}}{\delta\boldsymbol{g}(a)\delta\boldsymbol{g}(b)}\bigg|_0 \tag{3.157}$$

We will use, as in 3.3.4, the $d \to \infty$ limit to compute $\mathcal{S}$. We know in this limit that the trajectory density $\rho(\boldsymbol{x})$ is determined, at leading order, by a saddle-point equation implying only the Jacobian of the change to generalized spherical coordinates, hence it is independent of the external field at this order. Thus we can overlook this dependence and compute derivatives of the Mayer function, leading to, after averaging:

$$\frac{\delta^2\mathcal{S}}{\delta\boldsymbol{g}(a)\delta\boldsymbol{g}(b)}\bigg|_{\boldsymbol{g}=0} = \Sigma_A^2 \frac{N}{2} \int \mathrm{D}[\boldsymbol{x}, \boldsymbol{y}]\, \rho(\boldsymbol{x})\rho(\boldsymbol{y}) e^{-\int \mathrm{d}a\, V(\boldsymbol{x}-\boldsymbol{y})(a)}$$
$$\times \left[\boldsymbol{F}(\boldsymbol{x}-\boldsymbol{y})(a)\cdot\boldsymbol{F}(\boldsymbol{x}-\boldsymbol{y})(b) + \boldsymbol{\delta}(a,b)\nabla\cdot\boldsymbol{F}(\boldsymbol{x}-\boldsymbol{y})(a) \right] \tag{3.158}$$

We are interested in the *boson-boson* part, so we can focus on the first term only, which reads

$$\boldsymbol{F}(\boldsymbol{x} - \boldsymbol{y})(a) \cdot \boldsymbol{F}(\boldsymbol{x} - \boldsymbol{y})(b)|_0 = \frac{(x-y)(t) \cdot (x-y)(t')}{|x-y|(t)|x-y|(t')} V'\left(|x-y|(t)\right) V'\left(|x-y|(t')\right) \tag{3.159}$$

The content of subsection 3.3.2 is that the trajectory of $(x - y)(t) \sim X$ plus a correction that is in $1/d$. For any finite time, the vector X can be considered to be constant, with $|X| = \sigma$ and on average $(X^\mu)^2 \sim \sigma^2/d$. This is because particles do not move by $O(1)$ in a finite time. The correction term has zero average and $|(x - y)(t)| = \sigma(1 + h(t)/d)$. Recalling the definitions $\bar{V}(h) = V(\sigma(1 + h/d))$ and $F(h) = -\bar{V}'(h)$, we have $F(h) = -V'(\sigma(1 + h/d))\sigma/d$. Using this and the same analysis[29] of this two-body term as in 3.3.4, we get, at leading order in $d \to \infty$:

$$\frac{\delta^2 \overline{Z_N}[\boldsymbol{g}]}{\delta \boldsymbol{g}(a)\delta \boldsymbol{g}(b)}\bigg|_0 = \Sigma_A^2 \frac{Nd^3 \widehat{\varphi}}{2\sigma^2} \int \mathrm{d}h_0 \, e^{-\beta w(h_0)} \left\langle F\left(h(t)\right) F\left(h(t')\right) \right\rangle = \Sigma_A^2 \frac{Nd^3}{\sigma^2} M(t, t') \tag{3.160}$$

We conclude from (3.154)

$$M(t, t') = \frac{\sigma^2}{Nd^3} \sum_{i<j} \left\langle F_{ij}(t) \cdot F_{ij}(t') \right\rangle_{Z_N} \tag{3.161}$$

We make a final comment about two-body correlations that have the same structure as the interaction term. The truncated virial expansion in $d \to \infty$ tells us that the two-body density of trajectories, which is the average of $\tilde{\rho}^{(2)}$ defined in (5.52), is simply given by[30] [293, 342]

$$\rho^{(2)}[x, y, \hat{x}, \hat{y}] = \left\langle \tilde{\rho}^{(2)}[x, y, \hat{x}, \hat{y}] \right\rangle_{Z_N} = N^2 \rho[x, \hat{x}]\rho[y, \hat{y}] \left(1 + f[x - y, \hat{x} - \hat{y}]\right) = N^2 \rho(\boldsymbol{x})\rho(\boldsymbol{y})e^{-\int \mathrm{d}a \, V(\boldsymbol{x}-\boldsymbol{y})(a)} \tag{3.162}$$

We obtain the relation, for a function $\mathcal{O}$,

$$\frac{1}{N} \sum_{i \neq j} \left\langle \mathcal{O}\left(x_{ij}(t)\right) \mathcal{O}\left(x_{ij}(0)\right) \right\rangle = \frac{1}{N} \int \mathrm{D}[x, \hat{x}]\mathrm{D}[y, \hat{y}]\rho^{(2)}[x, y, \hat{x}, \hat{y}]\mathcal{O}\left(x(t) - y(t)\right) \mathcal{O}\left(x(0) - y(0)\right)$$

$$\sim N \int \mathrm{D}[x, \hat{x}]\mathrm{D}[y, \hat{y}]\rho[x, \hat{x}]\rho[y, \hat{y}] \left(1 + f[x - y, \hat{x} - \hat{y}]\right) \mathcal{O}\left(x(t) - y(t)\right) \mathcal{O}\left(x(0) - y(0)\right) \tag{3.163}$$

To this kind of function we can apply the same reasoning as in subsection 3.3.4, with the replacement $f \to (1 + f)\mathcal{O}(t)\mathcal{O}(0)$, if $\mathcal{O}$ rejects trajectories that do not get close enough[31], as was the Mayer function's role, now replaced by $1 + f = e^{-W}$ (which is 1 for most trajectories), giving an average over the effective dynamics with potential. This argument gives more directly Eq. (3.161). However one has to be careful for correlations of a higher number of particles, as in the next subsection.

3.8.4.3   Stress-stress correlation and its relation to the memory kernel

Here we repeat the former procedure to obtain the link between the correlation of the off-diagonal ($\mu \neq \nu$) components of the stress tensor, which reads [199, 413]

$$\sigma_{\mu\nu} = \sum_{i<j}(x_i - x_j)^\mu \nabla^\nu V(x_i - x_j) \tag{3.164}$$

Once again, we use external random fields to generate the correlation function. This amounts to turn the dynamical action into

$$\mathcal{A}[\{\boldsymbol{x}_i\}, \{A_{ij}, B_{ij}\}, \boldsymbol{g}_1, \boldsymbol{g}_2, \boldsymbol{h}_1, \boldsymbol{h}_2] = \sum_{i=1}^N \Phi(\boldsymbol{x}_i) - \sum_{i<j}^{1,N} \int \mathrm{d}a \, \left[A_{ij}\boldsymbol{g}_1(a) + B_{ij}\boldsymbol{g}_2(a)\right] \cdot (\boldsymbol{x}_i - \boldsymbol{x}_j)(a)$$

$$+ \frac{1}{2} \sum_{i<j}^{1,N} \int \mathrm{d}a \, \left[V\left(\boldsymbol{x}_i - \boldsymbol{x}_j + A_{ij}\boldsymbol{h}_1\right)(a) + V\left(\boldsymbol{x}_i - \boldsymbol{x}_j + B_{ij}\boldsymbol{h}_2\right)(a)\right] \tag{3.165}$$

---

[29] The normalization, giving a factor proportional to the packing fraction as in 3.3.4.2, follows from a similar analysis since, though the Mayer function $f(\boldsymbol{x} - \boldsymbol{y})$ constraining the trajectories to be close is not there anymore (it is replaced by $1 + f$), $\boldsymbol{F}(\boldsymbol{x} - \boldsymbol{y})$ has the same role.

[30] The N^2 factor only comes from the choice of a different normalization of $\rho[x, \hat{x}]$ its definition (3.11), with respect to the one used in liquid theory.

[31] This is important for *e.g.* the normalization as in 3.3.4.2.

where $\boldsymbol{g}_1, \boldsymbol{g}_2, \boldsymbol{h}_1, \boldsymbol{h}_2$ are external d-dimensional fields and $\{A_{ij}, B_{ij}\}$ are one-dimensional independent identically distributed centered Gaussian random variables of variance Σ_A^2 and Σ_B^2, respectively. Note that when the external fields are zero, we recover the original model. Using the shorthand notation $\partial_{1234} \equiv \delta^4 / \delta \boldsymbol{g}_1^\mu(a) \delta \boldsymbol{g}_2^\mu(b) \delta \boldsymbol{h}_1^\nu(a) \delta \boldsymbol{h}_2^\nu(b)$, we have, microscopically,

$$\partial_{1234}\overline{Z_N}\big|_{\boldsymbol{g}_i = \boldsymbol{h}_i = \boldsymbol{0}} = \int \prod_{i=1}^N \mathrm{D}\boldsymbol{x}_i \, e^{-\mathcal{A}[\{\boldsymbol{x}_i\}]} \sum_{\substack{i<j \\ k<l \\ m<n \\ p<q}} \frac{1}{4} \overline{A_{ij}(\boldsymbol{x}_i - \boldsymbol{x}_j)^\mu(a) B_{kl}(\boldsymbol{x}_k - \boldsymbol{x}_l)^\nu(b) A_{mn}\boldsymbol{F}_{mn}^\mu(a) B_{pq}\boldsymbol{F}_{pq}^\nu(b)}$$

$$= \frac{\Sigma_A^2 \Sigma_B^2}{4} \left\langle \sum_{\substack{i<j \\ k<l}} (\boldsymbol{x}_i - \boldsymbol{x}_j)^\mu(a)(\boldsymbol{x}_k - \boldsymbol{x}_l)^\nu(b) \boldsymbol{F}_{ij}^\mu(a) \boldsymbol{F}_{kl}^\nu(b) \right\rangle = \frac{\Sigma_A^2 \Sigma_B^2}{4} \left\langle \boldsymbol{\sigma}_{\mu\nu}(a) \boldsymbol{\sigma}_{\mu\nu}(b) \right\rangle_{Z_N}$$

$$(3.166)$$

$\ln \overline{Z_N}$ generates the connected correlation functions (cumulants), so that, using another shorthand notation ∂^n relative to any n^{th} derivative with respect to the fields involved in ∂_{1234}:

$$\partial_{1234} \ln \overline{Z_N} = \partial^4 \ln \overline{Z_N} = \frac{1}{\overline{Z_N}} \underbrace{\partial^4 \overline{Z_N}}_{1 \text{ term}} - \frac{1}{\overline{Z_N}^2} \underbrace{\partial^1 \overline{Z_N} \partial^3 \overline{Z_N}}_{4 \text{ terms}} - \frac{1}{\overline{Z_N}^2} \underbrace{\partial^2 \overline{Z_N} \partial^2 \overline{Z_N}}_{3 \text{ terms}} + \frac{2}{\overline{Z_N}^3} \underbrace{\partial^1 \overline{Z_N} \partial^1 \overline{Z_N} \partial^2 \overline{Z_N}}_{6 \text{ terms}}$$

$$- \frac{6}{\overline{Z_N}^4} \underbrace{\partial^1 \overline{Z_N} \partial^1 \overline{Z_N} \partial^1 \overline{Z_N} \partial^1 \overline{Z_N}}_{1 \text{ term}}$$

$$(3.167)$$

By isotropy (or average over the disorder), when evaluated at zero external field, all terms containing a first derivative are zero. Furthermore, second derivative terms are also zero, either due to $\overline{AB} = 0$ for terms involving different times, or by isotropy for terms involving different indices[32] $\mu \neq \nu$. We are thus left with only one term, which is $\partial_{1234}\overline{Z_N}$ since $\overline{Z_N} = 1$. Once again as in [270], one can compute $\ln \overline{Z_N}[\boldsymbol{g}_1, \boldsymbol{g}_2, \boldsymbol{h}_1, \boldsymbol{h}_2]$ introducing an averaged Mayer function

$$\overline{f_{ij}}[\boldsymbol{g}_1, \boldsymbol{g}_2, \boldsymbol{h}_1, \boldsymbol{h}_2] = \int \mathcal{D}A\mathcal{D}B \, f(\boldsymbol{x}_i(a) - \boldsymbol{x}_j(a), \boldsymbol{g}_1, \boldsymbol{g}_2, \boldsymbol{h}_1, \boldsymbol{h}_2)$$

$$= \int \mathcal{D}A\mathcal{D}B \left[e^{\int \mathrm{d}a \left[(A\boldsymbol{g}_1(a) + B\boldsymbol{g}_2(a)) \cdot (\boldsymbol{x}_i - \boldsymbol{x}_j)(a) - \frac{1}{2} V(\boldsymbol{x}_i - \boldsymbol{x}_j + A\boldsymbol{h}_1)(a) - \frac{1}{2} V(\boldsymbol{x}_i - \boldsymbol{x}_j + B\boldsymbol{h}_2)(a) \right]} - 1 \right]$$

$$(3.168)$$

Note that, for finite times, $e^{-\frac{1}{2} \int \mathrm{d}a \, V(\boldsymbol{x}_i - \boldsymbol{x}_j + A\boldsymbol{h}_1)(a)} - 1$ is zero except if h_1 is for some time approximately in the same direction as $x_i - x_j$, and in that case it is of order $O(\Gamma/L)$ where once again Γ is the typical length of a trajectory and $L^d \sim \mathcal{V}$, for large enough Σ_A. This implies, for fixed non-zero $\boldsymbol{h}_1$ and small $\boldsymbol{g}_1 = \varepsilon \tilde{\boldsymbol{g}}_1 / \Sigma_A$ with $\tilde{\boldsymbol{g}}_1$ of order one,

$$\int \mathcal{D}A \, e^{\int \mathrm{d}a \, A\boldsymbol{g}_1(a) \cdot (\boldsymbol{x}_i - \boldsymbol{x}_j)(a) - \frac{1}{2} \int \mathrm{d}a \, V(\boldsymbol{x}_i - \boldsymbol{x}_j + A\boldsymbol{h}_1)(a)} \simeq \int \mathcal{D}A \, e^{\int \mathrm{d}a \, A\boldsymbol{g}_1(a) \cdot (\boldsymbol{x}_i - \boldsymbol{x}_j)(a)} + O(\Gamma/L)$$

$$= e^{\Sigma_A^2 \left[\int \mathrm{d}a \, A\boldsymbol{g}_1(a) \cdot (\boldsymbol{x}_i - \boldsymbol{x}_j)(a) \right]^2 / 2} + O(\Gamma/L) \qquad (3.169)$$

$$= 1 + O(\varepsilon^2) + O(\Gamma/L)$$

One must be careful with the order of limits, the reasoning is the following here:

1. we fix $\boldsymbol{h}_1$ (non-zero)

2. we fix $\boldsymbol{g}_1 = \varepsilon \tilde{\boldsymbol{g}}_1 / \Sigma_A$ with $\tilde{\boldsymbol{g}}_1$ of order one

3. we take large Σ_A so that Ah_1 covers the whole line spanned by h_1, and $\mathcal{D}A \sim \mathrm{d}A/L$

4. we then take $\varepsilon \to 0$. In the end we will set all external fields to zero so defining them only in the neighborhood of 0 is enough[33].

---

[32]These are averages of an expression proportional to $(\boldsymbol{x} - \boldsymbol{y})^\mu (\boldsymbol{x} - \boldsymbol{y})^\nu$ which is its own opposite when rotating by an angle $\pi/2$ in the (μ, ν) plane.

[33]We can choose $\varepsilon = 1/\Sigma_A$ if we do not wish to introduce an additional parameter.

The same holds for the terms involving $\boldsymbol{g}_2$ and $\boldsymbol{h}_2$, with B instead of A. This way, $\overline{f_{ij}} = O(\varepsilon^2) + O(\Gamma/L)$ is small and we may repeat the same steps as in [270], so that $\ln \overline{Z_N} = N\mathcal{S}$, where

$$\mathcal{S} = -\int \mathrm{D}\boldsymbol{x}\, \rho(\boldsymbol{x})(\ln\rho(\boldsymbol{x}) + \Phi(\boldsymbol{x})) + \frac{N}{2}\int \mathrm{D}[\boldsymbol{x},\boldsymbol{y}]\, \rho(\boldsymbol{x})\rho(\boldsymbol{y}) \int \mathcal{D}A\mathcal{D}B\, f(\boldsymbol{x} - \boldsymbol{y}, \boldsymbol{g}_1, \boldsymbol{g}_2, \boldsymbol{h}_1, \boldsymbol{h}_2) \quad (3.170)$$

We only need to compute, to leading order[34]

$$
\begin{aligned}
\partial_{1234}\mathcal{S}|_{\boldsymbol{g}_i=\boldsymbol{h}_i=\boldsymbol{0}} =& \frac{N}{2}\int \mathrm{D}[\boldsymbol{x},\boldsymbol{y}]\, \rho(\boldsymbol{x})\rho(\boldsymbol{y})e^{-\int \mathrm{d}a V(\boldsymbol{x}-\boldsymbol{y})(a)} \\
&\times \frac{1}{4}\overline{A(\boldsymbol{x}-\boldsymbol{y})^\mu(a)B(\boldsymbol{x}-\boldsymbol{y})^\mu(b)A\boldsymbol{F}^\nu(\boldsymbol{x}-\boldsymbol{y})(a)B\boldsymbol{F}^\nu(\boldsymbol{x}-\boldsymbol{y})(b)} \\
=& \frac{N}{8}\Sigma_A^2\Sigma_B^2\int \mathrm{D}[\boldsymbol{x},\boldsymbol{y}]\, \rho(\boldsymbol{x})\rho(\boldsymbol{y})e^{-\int \mathrm{d}a V(\boldsymbol{x}-\boldsymbol{y})(a)} \\
&\times (\boldsymbol{x}-\boldsymbol{y})^\mu(a)(\boldsymbol{x}-\boldsymbol{y})^\mu(b)\boldsymbol{F}^\nu(\boldsymbol{x}-\boldsymbol{y})(a)\boldsymbol{F}^\nu(\boldsymbol{x}-\boldsymbol{y})(b)
\end{aligned}
\quad (3.171)
$$

Likewise (3.159), we have for $d \to \infty$

$$
\begin{aligned}
(\boldsymbol{x}-\boldsymbol{y})^\mu(a)&(\boldsymbol{x}-\boldsymbol{y})^\mu(b)\boldsymbol{F}^\nu(\boldsymbol{x}-\boldsymbol{y})(a)\boldsymbol{F}^\nu(\boldsymbol{x}-\boldsymbol{y})(b)|_0 \\
&= \frac{\left[(x-y)^\mu\right]^2(t)\left[(x-y)^\mu\right]^2(t')}{|x-y|(t)|x-y|(t')}V'\left(|x-y|(t)\right)V'\left(|x-y|(t')\right) \\
&\sim \frac{(X^\mu)^2(X^\nu)^2}{|X|^2}V'\left(|x-y|(t)\right)V'\left(|x-y|(t')\right) \\
&\sim F\left(h(t)\right)F\left(h(t')\right)
\end{aligned}
\quad (3.172)
$$

We deduce, as in the last subsection,

$$\left.\frac{\delta^4 \ln \overline{Z_N}}{\delta\boldsymbol{g}_1^\mu(a)\delta\boldsymbol{g}_2^\mu(b)\delta\boldsymbol{h}_1^\nu(a)\delta\boldsymbol{h}_2^\nu(b)}\right|_0 = \Sigma_A^2\Sigma_B^2\frac{Nd\widehat{\varphi}}{8}\int \mathrm{d}h_0\, e^{-\beta w(h_0)}\left\langle F\left(h(t)\right)F\left(h(t')\right)\right\rangle = \frac{\Sigma_A^2\Sigma_B^2}{4}dNM(t,t') \quad (3.173)$$

and from (3.166) and (3.167)

$$M(t,t') = \frac{1}{Nd}\left\langle \sigma_{\mu\nu}(t)\sigma_{\mu\nu}(t')\right\rangle_{Z_N} \quad (3.174)$$

We conclude that the memory function coincides with the force-force and stress-stress correlations.

3.8.5   Stokes-Einstein relation

Within linear response theory, the viscosity of the liquid can be deduced from the auto-correlation function of the stress [199]. From (3.174), this quantity actually coincides with the memory kernel in $d \to \infty$. Here we follow the conventions of [413], hence we neglect the kinetic term of the stress tensor (i.e. we neglect the contribution of the ideal gas, which is irrelevant in the glassy regime) and define a viscosity η as follows[35]:

$$\eta = \beta \int_0^\infty \mathrm{d}t\, N\left\langle \sigma_{\mu\nu}(t)\sigma_{\mu\nu}(0)\right\rangle = d\beta \int_0^\infty \mathrm{d}t\, M(t) \quad (3.175)$$

where $\mu \neq \nu$ are two arbitrary components of the stress tensor $\sigma_{\mu\nu}$.
Putting together Eq. (3.144) and Eq. (3.175) we obtain

$$D = \frac{T}{\gamma + \frac{2d}{\sigma^2}\eta} \quad (3.176)$$

This relation shows that for $\widehat{\varphi} \to \widehat{\varphi}_\mathrm{d}^-$, $\eta \propto 1/D \sim (\widehat{\varphi}_\mathrm{d} - \widehat{\varphi})^{-\gamma}$, as it is found in MCT.
At low densities, $\eta \to 0$ while $D \to T/\gamma$. Upon approaching the glass transition, $D \to 0$ and $\eta \to \infty$ with constant $D\eta$:

$$D\eta \simeq \frac{T\sigma^2}{2d} = \frac{T}{\zeta} \quad (3.177)$$

---

[34]As in 3.8.4.2, for $d \to \infty$ we can ignore the external fields dependence of the trajectory density ρ.
[35]Following the convention of [413], here η is the mass times the kinematic viscosity, $\eta = m\eta_K$, or the shear viscosity divided by the number density, $\eta = \eta_S/\rho$; i.e. it has units of kg m^2/s.

Hence, the Stokes-Einstein relation is satisfied with an apparent Stokes drag $\zeta = \sigma^2/(2d)$. A general discussion about SER in glasses is in §1.1.6. Note that expressing the SER in terms of the shear viscosity $\eta_S = \rho\eta$ we obtain

$$D\eta_S = \frac{T\sigma^2\rho}{2d} = \frac{T}{\zeta_S} \ , \qquad \zeta_S = \frac{2d}{\rho\sigma^2} = \frac{\sigma^{d-2}}{\widehat{\varphi}}\frac{2\pi^{d/2}}{\Gamma(d/2+1)} \ . \tag{3.178}$$

This scaling of the Stokes drag is very close to the hydrodynamic one [90]. Also, the prediction that $D\eta_S \propto \rho$ is well satisfied by the numerical data of Charbonneau's group investigating HS fluids [90] and the MK model [95] for high densities and $d \geqslant 3$, see figure 3.8. They inferred from data that the approximate validity of the SER in $d = 3$ at intermediate densities is somehow accidental, since SER violations occur in all regimes of density and spatial dimensions.
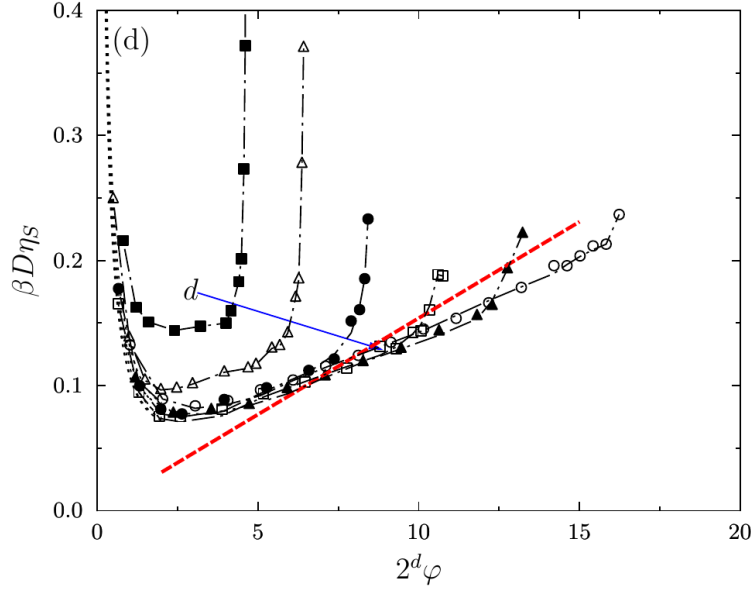
Figure 3.8: Computation of the variation of the ratio $\beta D\eta_{\mathrm{S}}$ as a function of density in simulated HS fluids for $d \in [\![3, 8]\!]$. The low-density behaviour seems to be adequately captured by the Enskog kinetic theory prediction (dashed line), as expected [90]. At intermediate densities in $d = 3$ the ratio is indeed a constant as in the SER. Yet one sees that this is a specificity of three-dimensional systems, which is violated for high enough densities even in these systems. As the dimension is increased, this ratio develops a non-trivial density dependence that qualitatively follows the high-dimensional prediction (3.178) (red dashed line). [*Reprinted from* [90, 98]]

3.9 Relation to the standard density formulation of Mode-Coupling Theory

Here we discuss the relations between the dynamical equations obtained here and Mode-Coupling Theory. Indeed, it has been a long-standing question whether MCT becomes exact in infinite dimension [225, 230, 345, 203, 207, 93]. HS liquids for large d have been specifically studied within the MCT framework in [345, 203, 344, 204].

First we give the MCT-like exponents a, b and γ that describe the behaviour of the MSD close to the plateau and the divergence of the relaxation time, or equivalently the vanishing of the diffusion coefficient, see §1.2.1.3. Then we prove a relation between the self-intermediate scattering functions and the MSD, which allows to make a direct connection. Finally we comment on the possible similarities and divergences.

3.9.1 MCT exponents

Starting from equations (3.101),(3.102), one can compute the different MCT exponents related to the approach to the plateau $\Delta_{EA} - \Delta(t) \sim t^{-a}$ or the departure from it $\Delta(t) - \Delta_{EA} \sim t^b$, by expanding

around the plateau value Δ_{EA} [187, 186, 326]. We do not report here the full dynamical computation since this expansion has been done *from the static free energy* in the HS case in [242, Sec. VI], using the argument of Parisi and Rizzo [309]. Let us briefly review this argument, which has been applied to various spin-glass models [78, 157, 309, 159] and is general.

The dynamical SUSY saddle-point equation for $\boldsymbol{Q}(a,b)$ is cast in a Mode-Coupling form by multiplying (3.80) by $\boldsymbol{Q}$ on the right. If one expands this equation around the plateau value, one gets at the lowest order terms up to second order in $\boldsymbol{\delta Q}(a,b)$ and for times close to the plateau one can get rid of the kinetic term which has no influence on the critical properties of the transition. One gets a *quadratic* equation (whatever the memory kernel) which is of the same type as Götze's equation in the β-relaxation regime [187]. The latter equation is the one used to get the critical exponents through the coefficients whose combination define the parameter λ. Then the coefficients of this expansion may be directly read from the same expansion at the level of the dynamical action without the kinetic term Φ, which is *formally similar to the static one* (see §2.5.2 and chapter 4). One concludes that these coefficients can be extracted directly through an expansion of the static free energy, given by (4.37), around the 1-RSB solution describing the plateau regime. Indeed it has the same symmetries as the dynamical action and thus the same terms in this Landau-like expansion. As a consequence, one finds that the general MCT critical properties are valid with coefficients that are not necessarily the same as the MCT ones since they depend explicitly upon the details of the dynamical action (or similarly the 1-RSB static coefficients). This means that, in particular, the exponents are controlled by the exponent parameter λ *through the same relations as in MCT* [187, 186, 326, 78] (see §1.2.1.3):

$$\frac{\Gamma(1-a)^2}{\Gamma(1-2a)} = \frac{\Gamma(1+b)^2}{\Gamma(1+2b)} = \lambda, \qquad \gamma = \frac{1}{2a} + \frac{1}{2b} \tag{3.179}$$

For HS, the expansion of the free energy is a bit tedious but feasible and one obtains [242, Sec. VI] $\lambda \simeq 0.70698$ which implies $a \simeq 0.324016$, $b \simeq 0.629148$ and $\gamma \simeq 2.33786$. We emphasize that the value of γ is consistent with numerical results obtained in [95], see figure 3.9.

(a)   (b)
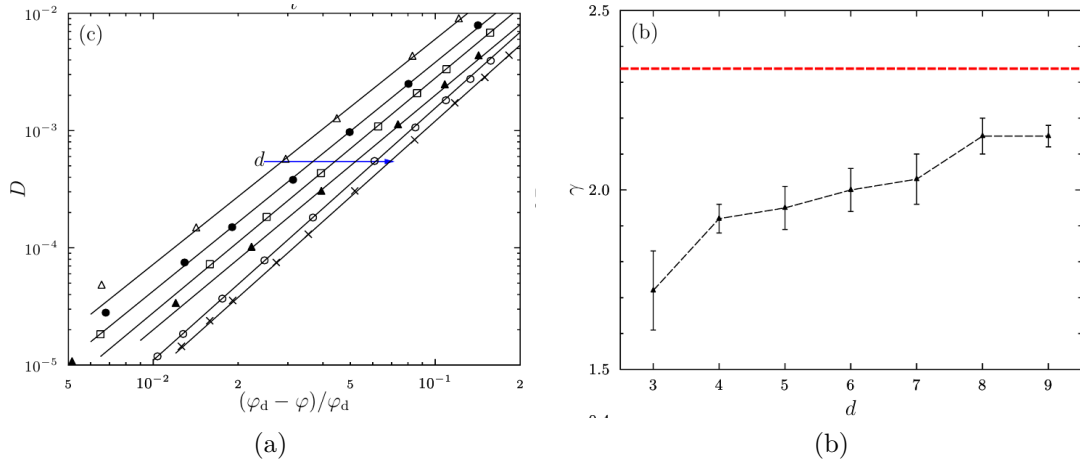
Figure 3.9: (a) The decay of the diffusivity with density grows increasingly power-law-like as dimension increases, at least in the dynamical regime accessible in simulations of HS [91]. (b) The critical MCT-like exponent γ, extracted from simulations of the MK model steadily approaches the prediction for $d \to \infty$ (red horizontal line) as d increases [95]. [*Reprinted from* [98]]

We may clarify here some short-time dependences. The scalings of the large-dimensional solution are summarized in figure 3.2.2.1 (a). In particular, in the caging regime, times are of order $O(1)$ with dimension. As an example the short-time ballistic regime may be computed through the equation without interactions, *e.g.* the d-dimensional Brownian[36] one $\gamma \dot{x} = \xi$. By solving it and extracting the MSD $\langle [x(t) - x(0)]^2 \rangle = \sigma^2 \Delta(t)/d$, one gets $\Delta(t) = Tt/\widehat{\gamma}$. Thus the short times are $O(1)$ with $O(1/d)$ motions, and well beyond the relaxation time when the MSD becomes $O(1)$, the diffusive scaling displayed by (3.144) shows that times are such that, forgetting about all but dimensional dependences,

---

[36]For Hamiltonian dynamics, the ballistic regime would be described by a free-flight $\Delta(t)/d \propto v_0^2 t^2$. As a typical value of the initial velocity, one can compare to a typical energy given by a heat bath -even if there is none here-, provided by the equipartition theorem: $v_0^2 \propto Td/m \propto T/d\widehat{m}$. We here care only about dimensionality dependence. The two latter equations then mean that here again, the dimensional dependence of short times is $O(1)$.

$t \propto 1/dD_0 \propto d$. If one considers a finite but large box whose volume is here set by R, one thus gets that the diffusion hits the boundaries when the MSD is of order R^2 which means times of order $O(dR^2)$. Coming back to the caging regime, as argued above, the general properties of MCT-like equations imply the validity of scaling laws found in §1.2.1.3, *e.g.* the connection of the transient timescale t_0 (which here is thus $O(1)$) to the other timescales of the β and α relaxations:

$$\tau_\beta \propto \frac{t_0}{\epsilon^{1/2a}}, \qquad \tau_\alpha \propto \frac{t_0}{\epsilon^\gamma}, \qquad \epsilon = \frac{\varphi_d - \varphi}{\varphi_d} \tag{3.180}$$

where ϵ is the parameter describing the approach to the dynamic transition, here expressed in terms of the packing fraction (*e.g.* for HS). One concludes that the separation of timescales is not due to any dimensional scaling (apart from the fact that it necessitates a true dynamic transition only valid for large d), but rather, as in MCT, to the intrinsic mechanism of timescales separation typical of mean-field glassy behaviour. As a matter of fact, from (3.180) the separation comes from the vicinity of the dynamic transition although all the timescales t_0, τ_β and τ_α are $O(1)$ for what concerns dimensionality (and decided at the caging regime of $O(1/d)$ fluctuation of trajectories).

3.9.2 Intermediate scattering functions

In its standard formulation, MCT provides equations for density correlators between time t and the origin $\phi_q(t) = \langle \rho_q(t)^* \rho_q \rangle / \langle |\rho_q|^2 \rangle$, where $\langle \bullet \rangle$ is a canonical average over initial conditions, and $\rho_q = \sum_{i=1}^N e^{iq \cdot x_i}$ is the Fourier transform of the particle density [187, 186], see (1.8) and §1.2.1. This correlator thus reads

$$\phi_q(t) \propto \left\langle \sum_{ij} e^{iq \cdot [x_i(t) - x_j(0)]} \right\rangle, \qquad \phi_q(0) = 1 \tag{3.181}$$

We can define, as in 3.2.2.1 and similarly to standard liquid theory [199] (see §1.1.3 and (2.10)), the (non-averaged) local densities of trajectories

$$\tilde{\rho}^{(1)}[x, \hat{x}] = \sum_i \delta(x - x_i)\delta(\hat{x} - \hat{x}_i), \qquad \tilde{\rho}^{(2)}[x, y, \hat{x}, \hat{y}] = \sum_{i \neq j} \delta(x - x_i)\delta(\hat{x} - \hat{x}_i)\delta(y - x_j)\delta(\hat{y} - \hat{x}_j) \tag{3.182}$$

so that the intermediate scattering functions can be written as

$$\phi_q(t) = \phi_q^s(t) + \phi_q^d(t) \propto \left\langle \int D[x, \hat{x}]\, \tilde{\rho}^{(1)}[x, \hat{x}]e^{iq \cdot [x(t) - x(0)]} + \int D[x, y, \hat{x}, \hat{y}]\, \tilde{\rho}^{(2)}[x, y, \hat{x}, \hat{y}]e^{iq \cdot [x(t) - y(0)]} \right\rangle \tag{3.183}$$

where the self ($i = j$) and distinct ($i \neq j$) parts are defined. Both parts can then be expressed as a function of $\Delta(t)$ through the saddle point evaluation of the integrals. In the following for simplicity we discuss only the self part.

3.9.3 The self part in infinite dimension

In $d \to \infty$, the self part is simply expressed in terms of the MSD. Using rotation invariance of $\left\langle \tilde{\rho}^{(1)} \right\rangle$ and the measure to average over $d + 1$-dimensional random rotations[37] $\mathcal{R}$:

$$\phi_q^s(t) \propto \left\langle \int D[x, \hat{x}]\, \tilde{\rho}^{(1)}[x, \hat{x}]e^{iq \cdot [x(t) - x(0)]} \right\rangle = \int d\mathcal{R} \left\langle \int D[\mathcal{R}x, \mathcal{R}\hat{x}]\, \tilde{\rho}^{(1)}[\mathcal{R}x, \mathcal{R}\hat{x}]e^{iq \cdot \mathcal{R}[x(t) - x(0)]} \right\rangle$$

$$= \int d\mathcal{R} \int D[\mathcal{R}x, \mathcal{R}\hat{x}] \left\langle \tilde{\rho}^{(1)}[\mathcal{R}x, \mathcal{R}\hat{x}] \right\rangle e^{iq \cdot \mathcal{R}[x(t) - x(0)]} = \int D[x, \hat{x}] \left\langle \tilde{\rho}^{(1)}[x, \hat{x}] \right\rangle \int d\mathcal{R}\, e^{iq \cdot \mathcal{R}[x(t) - x(0)]}$$

$$\propto \int D[x, \hat{x}] \left\langle \tilde{\rho}^{(1)}[x, \hat{x}] \right\rangle \int_0^\pi d\theta\, \sin^{d-1}\theta\, e^{i|q||x(t) - x(0)|\cos\theta} \tag{3.184}$$

where θ denotes the angle between q and $\mathcal{R}[x(t) - x(0)]$ and we used hyperspherical coordinates defined in §2.2, which give the parametrization of the rotation $\mathcal{R}$ in terms of the Euler angles. Now we can proceed as in 3.3.3 and express the dynamical variables in terms of $\boldsymbol{Q}$, using $\left\langle \tilde{\rho}^{(1)}[x, \hat{x}] \right\rangle \propto \rho(\boldsymbol{Q})$:

$$\phi_q^s(t) \propto \int D[\boldsymbol{Q}, \boldsymbol{\nu}]\, e^{\frac{d}{2}\Gamma(\boldsymbol{Q}, \boldsymbol{\nu})} \int_0^\pi d\theta\, \sin^{d-1}\theta\, e^{i|q|\sigma\sqrt{\Delta(t)/d}\cos\theta} \tag{3.185}$$

---

[37]The same can be done in the usual d-dimensional space, but here we keep the same notations as in the spherical setup.

The last integral can be evaluated through a saddle-point method in $d \to \infty$. Provided $|q|\sigma\sqrt{\Delta(t)}/d^{3/2} \ll 1$, the q-dependent term is irrelevant for the saddle-point evaluation[38] on $\mathbf{Q}$. The saddle-point value of θ is imposed at the equator $\pi/2$,

$$\int_0^\pi \mathrm{d}\theta \, \sin^{d-1}\theta \, e^{i|q|\sigma\sqrt{\Delta(t)/d}\cos\theta} \underset{\theta=\pi/2+\epsilon}{=} \int_0^\pi \mathrm{d}\epsilon \, e^{(d-1)\ln\cos\epsilon - i|q|\sigma\sqrt{\Delta(t)/d}\sin\epsilon}$$

$$\underset{d\to\infty}{\sim} \int_\mathbb{R} \mathrm{d}\epsilon \, e^{-(d-1)\epsilon^2/2 - i|q|\sigma\sqrt{\Delta(t)/d}\epsilon} \propto e^{-q^2\sigma^2\Delta(t)/2d^2} \tag{3.186}$$

The remaining integral over $\mathbf{Q}$ and $\boldsymbol{\nu}$ is dealt with as in 3.3.3 and is normalized to 1, since the saddle point is not affected by the last term in (3.185) as long as $(q\sigma)^2\Delta(t)/d^3 \ll 1$. Together with the normalization $\phi_q^{\mathrm{s}}(0) = 1$, we finally conclude for all wavevectors satisfying the latter condition,

$$\phi_q^{\mathrm{s}}(t) \underset{d\to\infty}{=} \exp\left(-\frac{q^2\sigma^2}{2d^2}\Delta(t)\right) \tag{3.187}$$

Note that the small q behaviour gives back (1.25), valid in any dimension.

3.9.4 The factorization property

A crucial outcome of MCT is the so-called factorization property [187, 186], which allows to get MCT scaling laws (see §1.2.1.3). It states that, in the β-relaxation window (*i.e.* close to the plateau), the difference between the value of the intermediate scattering functions and their value at the plateau can be factorized into a product of a function of the wavector *only* and a function of time *only*:

$$\delta\phi_q^{\mathrm{s}}(t) \equiv \phi_q^{\mathrm{s}}(t) - \phi_{q,\mathrm{EA}}^{\mathrm{s}} \simeq H(q)G(t) \tag{3.188}$$

This property is a stringent test of MCT in simulations [232, 233]. In $d \to \infty$, the self intermediate scattering functions for all wavevectors are governed by a single quantity, the MSD. Close to the plateau, $\delta\Delta(t) = \Delta(t) - \Delta_{\mathrm{EA}}$ is small and from equation (3.187),

$$\delta\phi_q^{\mathrm{s}}(t) \simeq -\frac{q^2\sigma^2}{2d^2}\phi_{q,\mathrm{EA}}^{\mathrm{s}}\delta\Delta(t) \tag{3.189}$$

We conclude that the factorization property holds in the infinite d limit. Besides, equation (3.187) is more general since it provides all orders in $\delta\Delta$ and is valid even far from the plateau.

3.9.5 Comparison with MCT

We now use the previous results to compare both theories. We emphasize some of its aspects although much more details could be studied to make an exhaustive comparison, and possibly infer how to refine such approximations.

The MCT-like equations (3.101) or (3.102) show that the memory kernel is a *functional* of the auto-correlation function or the MSD. If the memory kernel were a simple *function* of C, $M = \mathsf{F}(C)$, then the latter equations would be in the *schematic MCT* form, see §1.2.1. Schematic MCT is obtained as the exact dynamics of a system of spherical spins $\sum_i s_i^2 = N$ with p-spin random interactions [220, 221, 72, 112, 81], for which we have obtained in §2.5.4 the following memory kernel

$$M = \mathsf{F}(C) = \frac{p}{2}C^{p-1} \ . \tag{3.190}$$

However, as soon as one considers non-spherical variables, e.g. soft-spins with a potential $V(s) = a(s^2 - 1)^2$, one obtains an equation like (3.104) with this $V(s)$ [71, 365, 114, 220, 221]:

$$\dot{s}(t) = -V'(s) - \beta\int_{t_0}^t \mathrm{d}u \, M(t-u)\dot{s}(u) + \zeta(t) \ . \tag{3.191}$$

Here again, Eq. (3.190) holds and the system is closed by $C(t-t') = \langle s(t)s(t')\rangle$. Within the liquid phase, this more general form of dynamic equation has essentially the same phenomenology as schematic MCT.

---

[38]If $q = O(d^{3/2})$, which, a priori, does not represent any physical distance (much less than the typical zone spanned by vibrations inside a cage $q = O(d)$), the saddle-point values of θ are different, although also simple; however the q-dependent term now contributes to the saddle-point equation on $\boldsymbol{\Delta}$, changing its value and the formula (3.187) does not hold anymore.

Our system of equations belongs to this more general class, and they thus show exactly the same MCT phenomenology for what concerns *universal* quantities that are independent of details of the memory kernel:

- We find the usual emergence of a plateau and divergence at a critical point signalling a sharp dynamical transition, which is a purely mean-field concept.

- At this dynamical transition, the diffusivity vanishes, the relaxation time and the viscosity diverges. These are purely dynamical quantities that could not be obtained from a static framework so far; neither can the full time dependency of the MSD or correlations and responses given by solving the self-consistent equations.

- The factorization property is valid close to the plateau, at least as far as the self part is concerned.

- We have found that the relations between critical exponents (3.179) controlled by the single parameter λ hold. The dynamical scaling forms of quantities like the MSD or auto-correlation functions are the same (power laws) [11, 326].

However, important *quantitative* differences are observed with respect to applying the MCT approximation to the intermediate scattering functions, which leads to the *standard* formulation of MCT for liquids [186, 187], see §1.2.1.1. Standard MCT has the same qualitative structure as schematic MCT, but also provides quantitative results for the self and collective scattering functions in all dimensions, in particular in $d = 3$ [232, 233]; its $d \to \infty$ limit was discussed in [203, 345, 344, 204]. Our result in $d \to \infty$ is formulated in terms of the MSD, and most of the other natural observables are functionals of it. A clear relationship between the self part and the MSD is given by (3.187). First, we note that the self correlator is Gaussian in $d \to \infty$, in contrast to what is found in [345, 203]. In these articles, the MCT equations for the plateau value (the so-called Debye-Waller factor or non-ergodic parameter, which reads here $\phi^{\rm s}_{q,{\rm EA}} = e^{-q^2 \Delta_{\rm EA}/2d^2}$) are solved numerically for the HS system up to $d = 800$, and its shape is found to be non-Gaussian. Besides, the self van Hove function [199, 187], which is the inverse Fourier transform of the self-intermediate scattering function, *i.e.* a direct space density-density autocorrelation function, exhibits unphysical negative dips within MCT in high d [203, 204]. By Fourier transform of the Gaussian in (3.187), we find that the self van Hove function is also Gaussian and there is no contradiction with the fact that it must remain positive by definition.

Note that this expression is also exact for any dimension both in the free-particle regime (lengths and time small compared to mean free path and collision time respectively) and hydrodynamic limit (lengths and time large compared to mean free path and collision time respectively) [199], see also §1.3.

(3.187) implies, by substitution in (3.102), equations for the $\phi^{\rm s}_q$, with noticeable qualitative differences with respect to MCT equations (such as a non-local memory kernel M). One could then write our equations in terms of $\phi^{\rm s}_q$. The result, however, is different from standard MCT and in particular our kernel M is not an analytic function of the variable $\phi^{\rm s}_q$, in the sense that it depends upon $\phi^{\rm s}_q(t)$ at different times t (which is what we mean by *non-local*).

It is less clear if there is a relationship between the collective intermediate scattering functions and the MSD, and we do not have a definite answer from studying it in the same way as in §3.9.3. It is not surprising that the self part is in a one-to-one correspondence with the MSD, since it is concerned by the evolution of a single particle governed by a single two-point function $\Delta(t, t')$ at the saddle-point level. The collective intermediate scattering functions are concerned with the time evolution of the distance between two particles. Saddle-point arguments would lead to a relation with Δ; however for wavevectors of order d the factor $\exp[iq \cdot (x(t) - y(0))]$ could modify the saddle point.

The functional dependence of the self intermediate scattering function upon the wavevector is an example, discussed above, of a quantitative difference. The gap scaling of $O(\sigma/d)$ strongly suggests that the wavevectors that matter for this transition are not the ones associated with the first-neighbour distance $1/\sigma$, but rather the much larger ones d/σ corresponding to the cage size.

Another one regards the scalings of key quantities with dimension. In [345, 203] the dynamical transition point for HS is computed within MCT: $\varphi^{\rm MCT}_d \simeq 0.22 \, d^2/2^d$, at variance with our result $\varphi_d \simeq 4.80678 \, d/2^d$. The exponents can be computed from the parameter λ. Schmid and Schilling in [345] have computed it within MCT for d up to 1000 but the result fails to converge to a definite value. It appears however for $d > 100$ to lie in the interval $[0.8, 0.9]$; here we find its $d \to \infty$ value to be $\lambda \simeq 0.70698$.

In summary, our equations fall in the same universality class as schematic MCT, but provide different quantitative results with respect to standard MCT in $d \to \infty$.

3.10 Out-of-equilibrium dynamics

In the last sections we focused on equilibrium dynamics of the particles, using TTI and FDT. Nevertheless, the dynamical equation (3.80) is general and one can extract from it the out-of-equilibrium dynamics of the system. Here, as an example, we derive these equations in the case of a protocol starting from an equilibrated liquid at $T_0 = T(0)$ followed by a time-dependent temperature evolution $T(t)$ for $t > 0$. Examples of such protocols are a quench, or a periodic temperature drive, both of which are of considerable interest in the literature [40]. We also give the nonequilibrium equations in the case of a protocol driven by density changes created by modifying the particles' volume, in the spirit of the Lubachevsky-Stillinger algorithm [257] for HS packings.

3.10.1 From the SUSY equations to the dynamical equations in an off-equilibrium regime

We write the dynamical equations assuming only causality. In SUSY language the dynamical equation (3.80) is

$$\boldsymbol{Q}^{-1}(a,b) = 2\boldsymbol{k}(a,b) - \boldsymbol{M}(a,b) + (\boldsymbol{\nu}(a) + \boldsymbol{\delta\nu}(a))\mathbf{1}(a,b) \tag{3.192}$$

with $\boldsymbol{\nu}(a)$ some Lagrange multiplier enforcing $\boldsymbol{Q}(a,a) = \Delta_{\text{liq}}$, and (see (3.81))

$$\begin{aligned}
\boldsymbol{M}(a,b) &= \frac{\widehat{\varphi}}{2} \int \mathrm{d}\lambda \, e^{\lambda - \Delta_{\text{liq}}/2} \left\langle F(\boldsymbol{\mu}(a) + \lambda) F(\boldsymbol{\mu}(b) + \lambda) \right\rangle_V \\
\boldsymbol{\delta\nu}(a) &= -\frac{\widehat{\varphi}}{2} \int \mathrm{d}\lambda \, e^{\lambda - \Delta_{\text{liq}}/2} \left\langle F'(\boldsymbol{\mu}(a) + \lambda) \right\rangle_V \\
\langle \bullet \rangle_V &\equiv \int \mathcal{D}\boldsymbol{\mu} \, e^{-\int \mathrm{d}a \, \bar{V}(\boldsymbol{\mu}(a) + \lambda)} \bullet, \quad \mathcal{D}\boldsymbol{\mu} = \mathrm{D}\boldsymbol{\mu} \frac{e^{-\frac{1}{2}\int \mathrm{d}a\mathrm{d}b \, \boldsymbol{\mu}(a)\boldsymbol{Q}^{-1}(a,b)\boldsymbol{\mu}(b)}}{\sqrt{\mathrm{sdet}\boldsymbol{Q}}}
\end{aligned} \tag{3.193}$$

In components, we have (see §3.4.1 and §3.5)

$$\begin{aligned}
\boldsymbol{Q}(a,b) &= C(t,t') + \bar{\theta}_1\theta_1 R(t',t) + \bar{\theta}_2\theta_2 R(t,t') \\
\boldsymbol{\Delta}(a,b) &= \Delta(t,t') + \bar{\theta}_1\theta_1 \widehat{\Delta}(t',t) + \bar{\theta}_2\theta_2 \widehat{\Delta}(t,t') \\
\boldsymbol{M}(a,b) &= M(t,t') + \bar{\theta}_1\theta_1 \widehat{M}(t',t) + \bar{\theta}_2\theta_2 \widehat{M}(t,t') \\
\boldsymbol{k}(a,b) &= k(t,t') - \bar{\theta}_1\theta_1 \hat{k}(t,t') + \bar{\theta}_2\theta_2 \hat{k}(t,t') \\
k(t,t') &= -\widehat{\gamma} T\delta(t-t'), \quad \hat{k}(t,t') = \frac{\widehat{\gamma}}{2}\frac{\partial}{\partial t}\delta(t-t')
\end{aligned} \tag{3.194}$$

We can rewrite (3.192) as

$$\mathbf{1}(a,b) = 2\int \mathrm{d}c \, \boldsymbol{k}(a,c)\boldsymbol{Q}(c,b) - \int \mathrm{d}c \, \boldsymbol{M}(a,c)\boldsymbol{Q}(c,b) + (\boldsymbol{\nu}(a) + \boldsymbol{\delta\nu}(a))\boldsymbol{Q}(a,b) \tag{3.195}$$

From this we get, first looking at the $\bar{\theta}_1\theta_1\bar{\theta}_2\theta_2$ component of the dynamical equation, that necessarily $\forall t, \ \hat{\nu}(t) + \delta\hat{\nu}(t) = 0$. Then we get the coupled equations $\forall(t,t')$

$$\begin{aligned}
\widehat{\gamma}\frac{\partial C}{\partial t}(t,t') &= 2\widehat{\gamma} T(t)R(t',t) - (\nu + \delta\nu)(t)C(t,t') + \int_{t_{\text{p}}}^{t'} \mathrm{d}u \, M(t,u)R(t',u) + \int_{t_{\text{p}}}^{t} \mathrm{d}u \, \widehat{M}(t,u)C(u,t') \\
\widehat{\gamma}\frac{\partial R}{\partial t}(t,t') &= \delta(t-t') - (\nu + \delta\nu)(t)R(t,t') + \int_{t'}^{t} \mathrm{d}u \, \widehat{M}(t,u)R(u,t')
\end{aligned}$$

$$\tag{3.196}$$

t_{p} is the initial time. In terms of $\boldsymbol{\Delta} = \Delta_{\mathrm{liq}} - \boldsymbol{Q}$, they read:

$$
\begin{aligned}
\widehat{\gamma}\frac{\partial \Delta}{\partial t}(t,t') =& 2\widehat{\gamma}T(t)\widehat{\Delta}(t',t) - (\nu + \delta\nu)(t)\Delta(t,t') - \left[\int_{t_{\mathrm{p}}}^t \mathrm{d}u\, \widehat{M}(t,u) - (\nu + \delta\nu)(t)\right]\Delta_{\mathrm{liq}} \\
& + \int_{t_{\mathrm{p}}}^{t'} \mathrm{d}u\, M(t,u)\widehat{\Delta}(t',u) + \int_{t_{\mathrm{p}}}^t \mathrm{d}u\, \widehat{M}(t,u)\Delta(u,t')
\end{aligned}
\tag{3.197}
$$

$$
\widehat{\gamma}\frac{\partial \widehat{\Delta}}{\partial t}(t,t') = -\delta(t-t') - (\nu + \delta\nu)(t)\widehat{\Delta}(t,t') + \int_{t'}^t \mathrm{d}u\, \widehat{M}(t,u)\widehat{\Delta}(u,t')
$$

The dynamical process is, as in (3.104),

$$
\begin{aligned}
\widehat{\gamma}\dot{\mu}(t) &= -(\nu + \delta\nu)(t)\mu(t) + \int_{t_{\mathrm{p}}}^t \mathrm{d}t'\, \widehat{M}(t,t')\mu(t') + F(\mu(t) + \lambda) + \zeta(t) \\
&\text{with} \quad \langle \zeta(t)\rangle = 0 \quad \text{and} \quad \langle \zeta(t)\zeta(t')\rangle = 2\widehat{\gamma}T(t)\delta(t-t') + M(t,t')
\end{aligned}
\tag{3.198}
$$

Multiplying (3.192) by $\boldsymbol{Q}$ on the left and taking the real component, we also get

$$
\widehat{\gamma}\frac{\partial C}{\partial t'}(t,t') = 2\widehat{\gamma}T(t)R(t,t') - (\nu + \delta\nu)(t)C(t,t') + \int_{t_{\mathrm{p}}}^{t'} \mathrm{d}u\, C(t,u)\widehat{M}(t',u) + \int_{t_{\mathrm{p}}}^t \mathrm{d}u\, R(t,u)M(u,t')
\tag{3.199}
$$

We now get rid of the Lagrange multiplier $\nu(t) + \delta\nu(t)$. Since $C(t,t) = \Delta_{\mathrm{liq}}$, we have

$$
\frac{\mathrm{d}}{\mathrm{d}t}C(t,t) = 0 = \frac{\partial C}{\partial t} + \frac{\partial C}{\partial t'}\Big|_{t=t'}
\tag{3.200}
$$

Then we can sum the first equation of (3.196) and (3.199) for $t' \to t^-$:

$$
0 = \widehat{\gamma}T(t)R(t,t^-) - (\nu + \delta\nu)(t)\Delta_{\mathrm{liq}} + \int_{t_{\mathrm{p}}}^t \mathrm{d}u\, C(t,u)\widehat{M}(t,u) + \int_{t_{\mathrm{p}}}^t \mathrm{d}u\, R(t,u)M(u,t)
\tag{3.201}
$$

One needs to evaluate $R(t,t^-)$. As in §3.7.1, for very short time differences, potentials and memory effects do not matter, only the type of dynamics considered, *e.g.* Newtonian or Brownian, is relevant. Thus we can consider $V = 0$; if so, the dynamics is purely Gaussian and one has $\langle \boldsymbol{\mu}(a)\boldsymbol{\mu}(b)\rangle_{V=0} = \boldsymbol{Q}(a,b)$, so one can compute R using the effective single-particle dynamics (called hereafter the *0 process*), which reads, neglecting memory effects,

$$
\begin{aligned}
\widehat{\gamma}\dot{\mu}(t) &= -(\nu + \delta\nu)(t)\mu(t) + \zeta(t) + h(t) \\
&\text{with} \quad \langle \zeta(t)\rangle_0 = 0 \quad \text{and} \quad \langle \zeta(t)\zeta(t')\rangle_0 = 2\widehat{\gamma}T\delta(t-t')
\end{aligned}
\tag{3.202}
$$

h is an external force used to compute the response to a field. We included the noise ζ and the Lagrange multiplier term; as argued above, we do not really need them but to illustrate the idea that they are irrelevant, we keep them since it is easy to solve. We now repeat the argument of §3.6.2.2 in this time-dependent case. The solution to equation (3.202) reads

$$
\mu(t) = \mu(t_{\mathrm{p}})e^{-\int_{t_{\mathrm{p}}}^t (\nu+\delta\nu)/\widehat{\gamma}} + \frac{1}{\widehat{\gamma}}\int_{t_{\mathrm{p}}}^t \mathrm{d}u\, (\zeta(u) + h(u))e^{-\int_u^t (\nu+\delta\nu)/\widehat{\gamma}}
\tag{3.203}
$$

Then

$$
R_0(t,t') = \frac{\delta \langle \mu(t)\rangle_0}{\delta h(t')} = \frac{1}{\widehat{\gamma}}\theta(t-t')e^{-\int_{t'}^t (\nu+\delta\nu)/\widehat{\gamma}} \quad \Rightarrow \quad R(t,t^-) = \frac{1}{\widehat{\gamma}}
\tag{3.204}
$$

We conclude that the Lagrange multiplier reads

$$
\begin{aligned}
(\nu + \delta\nu)(t) =& \frac{1}{\Delta_{\mathrm{liq}}}\left[T(t) + \int_{t_{\mathrm{p}}}^t \mathrm{d}u\, C(t,u)\widehat{M}(t,u) + \int_{t_{\mathrm{p}}}^t \mathrm{d}u\, R(t,u)M(u,t)\right] \\
\Leftrightarrow (\nu + \delta\nu)(t) =& -\frac{1}{\Delta_{\mathrm{liq}}}\left[\int_{t_{\mathrm{p}}}^t \mathrm{d}u\, \Delta(t,u)\widehat{M}(t,u) + \int_{t_{\mathrm{p}}}^t \mathrm{d}u\, \widehat{\Delta}(t,u)M(u,t) - T(t)\right] + \int_{t_{\mathrm{p}}}^t \mathrm{d}u\, \widehat{M}(t,u)
\end{aligned}
\tag{3.205}
$$

Plugging it into equations (3.196) and (3.197), and using the fact that responses are causal:

$$\widehat{\gamma}\frac{\partial C}{\partial t}(t,t') = 2\widehat{\gamma}T(t)R(t',t) - (\nu + \delta\nu)(t)C(t,t') + \int_{t_{\mathrm{p}}}^{t'} \mathrm{d}u\, M(t,u)R(t',u) + \int_{t_{\mathrm{p}}}^{t} \mathrm{d}u\, \widehat{M}(t,u)C(u,t')$$

$$\widehat{\gamma}\frac{\partial R}{\partial t}(t,t') = \delta(t-t') - (\nu + \delta\nu)(t)R(t,t') + \int_{t'}^{t} \mathrm{d}u\, \widehat{M}(t,u)R(u,t')$$

$$\widehat{\gamma}\frac{\partial \Delta}{\partial t}(t,t') = 2\widehat{\gamma}T(t)\widehat{\Delta}(t',t) + T(t) - (\nu + \delta\nu)(t)\Delta(t,t') + \int_{t_{\mathrm{p}}}^{t} \mathrm{d}u\, \widehat{M}(t,u)[\Delta(t',u) - \Delta(t,u)]$$

$$+ \int_{t_{\mathrm{p}}}^{\max(t,t')} \mathrm{d}u\, M(t,u)[\widehat{\Delta}(t',u) - \widehat{\Delta}(t,u)]$$

$$\widehat{\gamma}\frac{\partial \widehat{\Delta}}{\partial t}(t,t') = -\delta(t-t') - (\nu + \delta\nu)(t)\widehat{\Delta}(t,t') + \int_{t'}^{t} \mathrm{d}u\, \widehat{M}(t,u)\widehat{\Delta}(u,t')$$

$$(3.206)$$

The last two equations are suitable to take the limit $\Delta_{\mathrm{liq}} \to \infty$: in this limit it is very likely that $\boldsymbol{M}$ and $\boldsymbol{\Delta}$ remain finite for finite times. Thus equation (3.205) can be approximated by

$$(\nu + \delta\nu)(t) \simeq \int_{t_{\mathrm{p}}}^{t} \mathrm{d}u\, \widehat{M}(t,u) \tag{3.207}$$

So that (again responses are causal):

$$\widehat{\gamma}\frac{\partial \Delta}{\partial t}(t,t') = T(t) + 2\widehat{\gamma}T(t)\widehat{\Delta}(t',t) + \int_{t_{\mathrm{p}}}^{t} \mathrm{d}u\, \widehat{M}(t,u)[\Delta(t',u) - \Delta(t,u) - \Delta(t,t')]$$

$$+ \int_{t_{\mathrm{p}}}^{\max(t,t')} \mathrm{d}u\, M(t,u)[\widehat{\Delta}(t',u) - \widehat{\Delta}(t,u)] \tag{3.208}$$

$$\widehat{\gamma}\frac{\partial \widehat{\Delta}}{\partial t}(t,t') = -\delta(t-t') + \int_{t'}^{t} \mathrm{d}u\, \widehat{M}(t,u)[\widehat{\Delta}(u,t') - \widehat{\Delta}(t,t')]$$

One has to be careful to use (3.207) only when there are no quantities that diverges when $\Delta_{\mathrm{liq}} \to \infty$.

3.10.2 Equilibrium phase

We can now make a useful check: assume we are in the equilibrium liquid phase with constant temperature T, so that, as we did in §3.7,

- t_{p} is sent to $-\infty$ and the system relaxes for long times

- time-translation invariance holds, $\tau \equiv t - t'$

- FDT holds for $\boldsymbol{\Delta}$ and $\boldsymbol{M}$, *e.g.* $\beta\dot{\Delta}(\tau) = \widehat{\Delta}(-\tau) - \widehat{\Delta}(\tau)$.

We obtain after integration by parts, from (3.198), (3.205) and (3.208),

$$\widehat{\gamma}\dot{\Delta}(\tau) = 2\widehat{\gamma}T\widehat{\Delta}(-\tau) + T - \beta\int_0^{\tau} \mathrm{d}u\, M(\tau - u)\dot{\Delta}(u)$$

$$\nu + \delta\nu = \frac{T}{\Delta_{\mathrm{liq}}} + \beta M(0)$$

$$\widehat{\gamma}\dot{\mu}(t) = -\frac{T}{\Delta_{\mathrm{liq}}}\mu(t) - \beta\int_{t_{\mathrm{p}}}^{t} \mathrm{d}u\, M(t-u)\dot{\mu}(u) + F(\mu(t) + \lambda) + \zeta(t)$$

$$\text{with} \quad \langle\zeta(t)\rangle = 0 \quad \text{and} \quad \langle\zeta(t)\zeta(t')\rangle = 2\widehat{\gamma}T\delta(t-t') + M(t-t')$$

$$(3.209)$$

the first equation being valid for finite times only. They are the same equations[39] as the ones given found in §3.7, equations (3.102), (3.100) and (3.106).

---

[39]Note that here we have taken the limit $\Delta_{\mathrm{liq}} \to \infty$ at finite time differences, so that $\Delta(\tau) \ll \Delta_{\mathrm{liq}}$; this is why this term does not appear with respect to (3.102). Besides, in (3.102) we considered only *positive* time differences $\tau > 0$ for which $\widehat{\Delta}(-\tau) = 0$ by causality.

3.10.3 Non-stationary temperature drive protocol at finite times

To specify an initial condition and remove the size of the box, we shall do the following, as in §3.7.5. We assume we start from a fixed initial condition for the microscopic system of N particles. The initial time is sent at $-\infty$ so that we can consider at $t = 0$ that we are in an equilibrium liquid state at temperature T_0 and fixed packing fraction φ. One of the simplest protocol to implement in our equations is a time-dependent temperature drive: $T(0) = T_0$ and the temperature depends upon time t for $t > 0$.

The equilibrium measure for the effective particle μ is $P_V^{\mathrm{eq}}(\mu_0) \propto e^{-H_0(\mu_0,\lambda)/T_0}$ (see (3.112)) with

$$H_0(\mu_0, \lambda) = \frac{T_0}{2\Delta_{\mathrm{liq}}}\mu_0^2 + \bar{V}(\mu_0 + \lambda) \tag{3.210}$$

Then we know from the resummation of trajectories in §3.7.3 that the dynamics becomes, from (3.198) and (3.207),

$$\begin{aligned}
&\widehat{\gamma}\dot{\mu}(t) = \int_0^t \mathrm{d}t'\, \widehat{M}(t,t')(\mu(t') - \mu(t)) + F(\mu(t) + \lambda) + \zeta(t) \\
&\text{with} \quad \langle \zeta(t) \rangle = 0 \quad \text{and} \quad \langle \zeta(t)\zeta(t') \rangle = 2\widehat{\gamma}T(t)\delta(t-t') + M(t,t') \\
&\mu(0) = \mu_0 \text{ is picked with the equilibrium measure } P_V^{\mathrm{eq}}(\mu_0)
\end{aligned} \tag{3.211}$$

Next we set $\boldsymbol{h}(a) = \boldsymbol{\mu}(a) + \lambda$ and obtain in the limit $\Delta_{\mathrm{liq}} \to \infty$:

$$M(t,t') \underset{\Delta_{\mathrm{liq}}\to\infty}{\sim} \frac{\widehat{\varphi}}{2} \int \mathrm{d}h_0\, e^{-\beta_0 w(h_0)} \left\langle F(h(t))F(h(t')) \right\rangle \quad \text{with} \quad w(h) = \bar{V}(h) - T_0 h + \underbrace{\frac{T_0}{2\Delta_{\mathrm{liq}}}h^2}_{} \tag{3.212}$$

$$\widehat{M}(t,t') \underset{\Delta_{\mathrm{liq}}\to\infty}{\sim} \frac{\widehat{\varphi}}{2} \int \mathrm{d}h_0\, e^{-\beta_0 w(h_0)} \left\langle F(h(t))\tilde{h}(t')F'(h(t')) \right\rangle$$

The underbraced term is usually negligible for finite times and represents *the box*. We defined $\beta_0 = 1/T_0$. Besides,

$$\left\langle F(h(t))\tilde{h}(t')F'(h(t')) \right\rangle = \frac{\delta \left\langle F(h(t)) \right\rangle}{\delta b(t')}\bigg|_{b=0} \tag{3.213}$$

is a response function obtained by adding a small external field $b(t)$ to the force *i.e.* $F(h(t)) \to F(h(t) + b(t))$ in the equation of motion used to compute the average, which is:

$$\begin{aligned}
&\widehat{\gamma}\dot{h}(t) = \int_0^t \mathrm{d}t'\, \widehat{M}(t,t')(h(t') - h(t)) + F(h(t)) + \zeta(t) \\
&\text{with} \quad \langle \zeta(t) \rangle = 0 \quad \text{and} \quad \langle \zeta(t)\zeta(t') \rangle = 2\widehat{\gamma}T(t)\delta(t-t') + M(t,t') \\
&h(0) = h_0 \text{ is picked with the equilibrium measure } \propto e^{-\beta_0 w(h_0)}
\end{aligned} \tag{3.214}$$

Using these equations, the correlation and response functions are derived from the equations

$$\begin{aligned}
\widehat{\gamma}\frac{\partial\Delta}{\partial t}(t,t') = &\, T(t) + 2\widehat{\gamma}T(t)\widehat{\Delta}(t',t) + \int_0^t \mathrm{d}u\, \widehat{M}(t,u)[\Delta(t',u) - \Delta(t,u) - \Delta(t,t')] \\
&+ \int_0^{\max(t,t')} \mathrm{d}u\, M(t,u)[\widehat{\Delta}(t',u) - \widehat{\Delta}(t,u)]
\end{aligned} \tag{3.215}$$

$$\widehat{\gamma}\frac{\partial\widehat{\Delta}}{\partial t}(t,t') = -\,\delta(t-t') + \int_{t'}^t \mathrm{d}u\, \widehat{M}(t,u)[\widehat{\Delta}(u,t') - \widehat{\Delta}(t,t')]$$

that follow from (3.208).

Equation (3.215) is our final equation which rules the evolution of the correlation and response of the system in contact with a non-stationary bath. Note that the response is simply $R(t,t') = -\widehat{\Delta}(t,t')$.

3.10.4 Density-driven dynamics: inflating spheres

Another protocol is to stay at constant temperature T but inflate the spheres so as to modify at will the density, à la Lubachevsky-Stillinger [257]. However, our equations were derived in a restricted setting

where instantaneous particle displacements are of order $O(1/d)$. Thus, we will start at time $t = 0$ with a particle diameter $\sigma(0) = \sigma_0$ and then a fluctuation of this diameter of order $O(1/d)$:

$$\sigma(t) = \sigma_0 \left(1 + \frac{\widehat{\sigma}(t)}{d} \right) \tag{3.216}$$

Higher orders of instantaneous displacements means a brutal exponential change in density which we do not consider. See §5.4 for some consequences of such a change.

3.10.4.1 Modifications of the dynamical equations

The derivation of the dynamical equations is the same as in the previous section, except that T is kept fixed and we have to check in the derivation of chapter 3 all steps involving the particle diameter σ. These are twofold: either due to rescaling by this relevant physical distance, or simply because it appears in the potential V.

Concerning the first issue, since the relevant typical $O(1)$ distance is given by σ_0, the rescalings are the same, with $\sigma \leftrightarrow \sigma_0$. For example one now sets, in the derivation of the interaction term:

$$\begin{aligned} \Delta_{\text{liq}} &= 2d \left(\frac{R}{\sigma_0} \right)^2 \\ [\boldsymbol{x}(a) - \boldsymbol{y}(a)]^2 &= \sigma_0^2 \left(1 + \frac{2}{d} \boldsymbol{\mu}(a) \right) \end{aligned} \tag{3.217}$$

These rescalings do not modify anything (except $\sigma \leftrightarrow \sigma_0$) to the resulting dynamical equations. To avoid confusion in the derivation term, for the normalization one takes a test Mayer function $f_0[x, \hat{x}] = \theta(\sigma_0 - |x(0)|)$ which leads to $\mathcal{S}_{\text{int}} = -\frac{\rho V_d(\sigma_0)}{2} \mathcal{F}(\boldsymbol{Q}^{\text{sp}})$. This means that $\widehat{\varphi} \leftrightarrow \widehat{\varphi}_0 \equiv \rho V_d(\sigma_0)/(2^d d)$.

However, in the potential one must insert the fluctuating $\sigma(t)$. We define as before

$$\bar{V}(h) = \lim_{d \to \infty} V \left[\sigma_0 \left(1 + \frac{h}{d} \right) \right] \tag{3.218}$$

and verify that changing the particle diameter at order $O(1/d)$ results in computing the potential in $h(t) - \widehat{\sigma}(t)$ (*i.e.* moving *the wall* by $\widehat{\sigma}(t)$). For instance:

- HS model: $V_{\text{HS}}(r) = \kappa \theta(\sigma_0 - r)$ with the limit $\kappa \to \infty$. Making the replacements $\sigma_0 \leftrightarrow \sigma(t)$ and $r = 1 + h/d$ gives $\kappa \theta(\widehat{\sigma} - h)$ which is $\bar{V}_{\text{HS}}(h - \widehat{\sigma})$.

- LJ model: $V_{\text{LJ}}(r) = \epsilon \left[(r/\sigma_0)^{-4d} - (r/\sigma_0)^{-2d} \right]$. Making these replacements yields $e^{-4(h - \widehat{\sigma})} - e^{-2(h - \widehat{\sigma})}$ which is $\bar{V}_{\text{LJ}}(h - \widehat{\sigma})$.

- *Exponential potential* class of §3.1.1: $V_{\text{exp}}(r) = e^{-dA(r)}$. We have $\bar{V}_{\text{exp}}(h) = V_{\text{exp}}(\sigma_0) e^{-\sigma_0 A'(\sigma_0) h}$ and replacing the diameter $\sigma_0 \leftrightarrow \sigma(t)$ in this expression leads to, knowing that $V_{\text{exp}}(\sigma(t)) = V_{\text{exp}}(\sigma_0) e^{-\sigma_0 A'(\sigma_0) \widehat{\sigma}(t)}$, $V_{\text{exp}}(\sigma_0) e^{\sigma_0 A'(\sigma_0) \widehat{\sigma}} e^{-\sigma_0 A'(\sigma_0) h}$ where we have neglected orders $O(1/d)$ in the exponentials when doing $\sigma_0 \leftrightarrow \sigma(t)$. Once again we recognize $\bar{V}_{\text{exp}}(h - \widehat{\sigma})$.

For a general $V(r)$ the same argument can be done by looking at the $O(1/d)$ contribution around σ_0, replacing σ_0 by $\sigma(t)$ and similarly one sees that at first order $O(1/d)$, h is replaced by $h - \widehat{\sigma}$ (which is just a change of spatial origin for the *wall*). Indeed we have at first order in $1/d$

$$\begin{aligned} \bar{V}(h) &= V(\sigma_0) + \sigma_0 \frac{h}{d} V'(\sigma_0) \\ V(\sigma) &= V(\sigma_0) + \sigma_0 \frac{\widehat{\sigma}}{d} V'(\sigma_0) \end{aligned} \tag{3.219}$$

so that the potential needed here is obtained by replacing σ_0 by $\sigma(t)$ in the first equation of (3.219), giving

$$V(\sigma) + \sigma \frac{h}{d} V'(\sigma) = V(\sigma_0) - \sigma_0 \frac{\widehat{\sigma}}{d} V'(\sigma_0) + \sigma_0 \frac{h}{d} V'(\sigma_0) + O \left(\frac{1}{d^2} \right) \tag{3.220}$$

which is equivalent to $\bar{V}(h - \widehat{\sigma})$ for $d \to \infty$.

All in all, the equations are the same as above with the only modifications of constant temperature and shift of the potential by $\widehat{\sigma}(t)$: the MSD and response are solution of

$$
\begin{aligned}
\widehat{\gamma}\frac{\partial \Delta}{\partial t}(t,t') =&\, T + 2\widehat{\gamma}T\widehat{\Delta}(t',t) + \int_0^t du\, \widehat{M}(t,u)[\Delta(t',u) - \Delta(t,u) - \Delta(t,t')] \\
&+ \int_0^{\max(t,t')} du\, M(t,u)[\widehat{\Delta}(t',u) - \widehat{\Delta}(t,u)] \\
\widehat{\gamma}\frac{\partial \widehat{\Delta}}{\partial t}(t,t') =&\, -\delta(t-t') + \int_{t'}^t du\, \widehat{M}(t,u)[\widehat{\Delta}(u,t') - \widehat{\Delta}(t,t')]
\end{aligned}
\tag{3.221}
$$

with the memory kernels:

$$
\begin{aligned}
M(t,t') &\underset{\Delta_{\mathrm{liq}}\to\infty}{\sim} \frac{\widehat{\varphi}_0}{2}\int dh_0\, e^{-\beta\widetilde{w}(h_0)} \big\langle F(h(t) - \widehat{\sigma}(t))F(h(t') - \widehat{\sigma}(t'))\big\rangle \\
&\quad\text{with}\quad \widetilde{w}(h(t)) = \bar{V}(h(t) - \widehat{\sigma}(t)) - Th(t) \\
\widehat{M}(t,t') &\underset{\Delta_{\mathrm{liq}}\to\infty}{\sim} \frac{\widehat{\varphi}_0}{2}\int dh_0\, e^{-\beta\widetilde{w}(h_0)} \Big\langle F(h(t) - \widehat{\sigma}(t))\tilde{h}(t')F'(h(t') - \widehat{\sigma}(t'))\Big\rangle
\end{aligned}
\tag{3.222}
$$

computed through the one-dimensional process for the interparticle gap:

$$
\widehat{\gamma}\dot{h}(t) = \int_0^t dt'\, \widehat{M}(t,t')(h(t') - h(t)) + F(h(t) - \widehat{\sigma}(t)) + \zeta(t)
$$

$$
\text{with}\quad \big\langle \zeta(t)\big\rangle = 0 \quad\text{and}\quad \big\langle \zeta(t)\zeta(t')\big\rangle = 2\widehat{\gamma}T\delta(t-t') + M(t,t')
$$

$h(0) = h_0$ is picked with the equilibrium measure $\propto e^{-\beta\widetilde{w}(h_0)} = e^{h_0 - \beta\bar{V}(h_0)}$ (note that $\widehat{\sigma}(0) = 0$)

$$
\tag{3.223}
$$

The dynamics of this protocol thus consists in a motion of the *wall*, governed by $\widehat{\sigma}(t)$, in the latter one-dimensional process.

3.10.4.2 A useful check: constant shift in density

So far we have taken $\widehat{\sigma}$ depending on time with $\widehat{\sigma}(0) = 0$ by convention. We may check, if now we impose it to be stationary with a non-zero value $\widehat{\sigma}$, that we get back the standard equations for a particle diameter $\sigma_0(1 + \widehat{\sigma}/d)$. Note that in this case we may assume equilibrium relations if the density is lower than the dynamical transition point, but we will not do so, in order to verify the off-equilibrium equations, even if this protocol would be at equilibrium.

We may then perform in (3.221), (3.222) and (3.223), the constant shift $\forall t$, $h(t) \longrightarrow h(t) + \widehat{\sigma}$. We then get back the same equations as in the previous section (although with a constant temperature), apart from the term[40] $\widetilde{w}(h_0) = \bar{V}(h_0 - \widehat{\sigma}) - Th_0$ in (3.222), which yields an extra factor $e^{\widehat{\sigma}}$ in both M and $\widehat{M}$. This factor renormalizes $\widehat{\varphi}_0 \longrightarrow \widehat{\varphi}_0 e^{\widehat{\sigma}}$, which indeed corresponds to a particle diameter of $\sigma_0(1 + \widehat{\sigma}/d)$. This is consistent with such a change of density.

A final remark: if the protocol starts from $\widehat{\varphi}_0 < \widehat{\varphi}_d(T)$ and goes to higher density regimes than the dynamical transition point, one expects aging dynamics at long times whereas if the long time limit of $\sigma(t)$ is stationary and remains below it, one should recover equilibrium at long times.

---

[40]Note that with the convention $\widehat{\sigma}(0) = 0$, we had $\widetilde{w}(h_0) = \bar{V}(h_0) - Th_0$.

4

THERMODYNAMICS OF THE LIQUID AND GLASS PHASES

Outline

4.1 Introduction

The purpose of this chapter is to present a parallel derivation of the thermodynamics of the system, where the analogy with the dynamical treatment of the previous chapter is explicit. The derivation is also simpler than the previously published ones [243, 242, 96, 325, 97], which were restricted to HS; here we focus on a general potential as mentioned in §3.1.1.

The *thermodynamics* we are aiming at is a partial one: we explicitly exclude, as already discussed in §3.1.2, crystalline states. These certainly dominate the equilibrium measure of the condensed phase in three dimensions, and the same might be the case in $d \to \infty$, see [386] for a discussion. The reason why it is at all possible to separate amorphous from crystalline configurations is that it is expected, and it has to be shown self-consistently, that these regions of phase space are strictly disconnected in the limit $d \to \infty$. In finite dimensions, the separation is not perfect and ultimately depends on the dynamic regime under study: the consensus is, however, that in glassy regimes the formation of crystallites may usually be neglected (see §1.1.1), especially when $d > 3$ [363, 396, 395, 386].

In the first derivation of the glassy [312, 243, 242, 96, 325, 97] statics of HS, the method followed was, as in the previous chapter, a virial expansion for the replicated liquid using the Mézard-Parisi or Monasson formalisms [288, 277, 283, 284, 276, 285, 278]: each particle is copied m times, and the copies are constrained to be close to each other, forming a *molecule* composed of m *atoms*, see §1.2.4.2. The introduction of these m replicas can be seen, in the Monasson approach, as an equivalent way of introducing a spatially random external field which will *pin* the system onto a typical configuration, which is an amorphous one in the glass phase. This random field is a quenched average (hence the introduction of replicas) that kills the crystalline minima and thus selects one of many amorphous solutions. There, the coupling is sufficient to condense these replicas in the same state: the m atoms are in the same cage of size $O(1/d)$. The problem is then to compute the entropy of this molecular liquid. Using the exact same argument as in §3.2.2, where one can view the molecule as a trajectory made of m time steps, one

can truncate the virial series accordingly and get an entropy functional [243, 242]

$$\mathcal{S}[\rho(\bar{x})] = \int \mathrm{d}\bar{x}\, \rho(\bar{x})[1 - \ln\rho(\bar{x})] + \frac{N}{2} \int \mathrm{d}\bar{x}\mathrm{d}\bar{y}\, \rho(\bar{x})\rho(\bar{y}) f(\bar{x} - \bar{y}) \tag{4.1}$$

where $\bar{x} = \{x_1, \ldots, x_m\}$ is a molecule (replicated configuration of an original particle). This is analogous to the dynamic generating functional (3.31). The precise meanings of the replicated liquid density $\rho(\bar{x})$ and the replicated Mayer function $f(\bar{x} - \bar{y})$ will be explicited in the following.

There is another useful way of imposing a similar situation, valid in any dimension. Consider a system with interaction potential

$$H_{\mathrm{normal}} = \sum_{i<j} V(|x_i - x_j|) \ , \tag{4.2}$$

in any dimension. We will refer to this as the *normal* system. Replace it now by a different system, this one with *randomly shifted* interactions

$$H_{\mathrm{MK}} = \sum_{i<j} V(|x_i - \mathcal{R}_{ij} x_j|) \ , \tag{4.3}$$

where $\mathcal{R}_{ij}$ is a *shift* chosen randomly for each pair of particles once and for all. In the spherical case, $\mathcal{R}_{ij}$ denotes a rotation on the $d+1$-dimensional hypersphere. We refer to this as the *MK* system, because it was studied extensively by Mari and Kurchan in [270]. If the size of these shifts is large, for example of the order of the box itself, the network of interactions is *tree-like*, *i.e.* if a particle 1 interacts with both particle 2 and particle 3, the probability that 2 and 3 interact is vanishingly small. Likewise, if the spatial dimension is large, from the virial argument (2.2) one concludes that the chances that particles 2 and 3, both interacting with 1, interact between themselves are negligible, see figure 4.1. This model has been studied in finite dimensions, and it is definitely much closer to mean-field behaviour than the normal system, although it is not clear what is the exact nature of its glass transition, if even there is a sharp one: we will not discuss this issue here and we refer the reader to [270, 90] for further details.

A point which is clear is that the limit $d \to \infty$ of the MK model (4.3) and the normal model (4.2) should coincide exactly (see §H for a detailed discussion) in all disordered phases -liquid and glass- but not in a possible crystalline phase, which would be suppressed in (4.3). In this chapter we use this as a trick to simplify the derivation of the equations for the thermodynamics of (4.2), and by analogy for the dynamics, as will be discussed below: the introduction of a disorder that is *a posteriori* irrelevant helps to justify and simplify the derivation. The same technique in various forms has been used in glassy systems (see §1.2.4.2, [288] and references therein). Note that here we focus on the derivation of the equations more than on the extraction of physical results from them, which have already been discussed in numerous papers [312, 243, 242, 96, 97, 325, 98]. Still, the reader can refer to §1.5 and §4.4.3.4.

The structure of this chapter is the following. In section 4.2, we recapitulate the basic definitions, and we derive the free energy as a functional of the single-particle density. We show that this functional contains only the ideal-gas term plus a mean-field density-density interaction. In section 4.3, we show that in the limit $d \to \infty$, thanks to rotational invariance, one can evaluate all integrals involving the single-particle density through a saddle point. We thus obtain the free energy as a simple function of a matrix $\hat{\Delta}$ that encodes the MSD between different replicas in the thermodynamics or, by an analogy, different times in the dynamics. In section 4.4, we consider a special choice of $\hat{\Delta}$, corresponding to Parisi's hierarchical ansatz, and we show that in this case we reproduce previous results for glassy thermodynamics [312, 243, 242, 96, 97]. In section 4.5 we write a general equation for the matrix $\hat{\Delta}$, without assuming that it is a hierarchical matrix, and we show that this equation has the form of a Mode-Coupling equation [187], controlled by a memory kernel for which we give a microscopic expression in terms of force-force or stress-stress correlations. In section 4.6 we show that (glassy) thermodynamics and (glassy) dynamics give consistent results, in compliance with the general RFOT picture. In appendix A we provide a list of the most recurrent mathematical definitions and notations.

4.2   Setting of the problem

4.2.1   Definition of the model

Let us recapitulate here the precise definition of the system we wish to investigate.
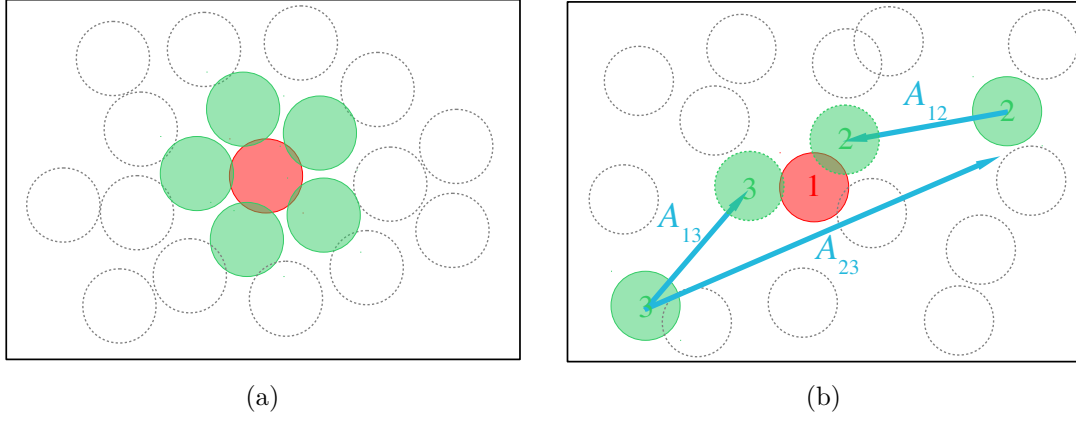
(a)   (b)

Figure 4.1: (a) A soft spheres system in $d \to \infty$ dimensions (original model *i.e.* $R \to \infty$ limit for the spherical setting, and in absence random rotations $\mathcal{R}_{ij}$). The red particle interacts with its green neighbours, which do not *see* each other (the most likely configuration is that they all are in orthogonal directions). The others (dashed gray) particles do not interact with the red one and again have a tree-like structure of contacts. (b) In the MK model in d dimensions ($R \to \infty$), random rotations become random shifts A_{ij} [270]. The red particle 1 interacts only with the green ones 2 and 3 owing to the shifts, the others (dashed gray) do not interact with particle 1. 2 and 3 may interact as well if $|A_{12} + A_{13} + A_{23}| \sim \sigma$, which is very unlikely for high d or for shifts that are of the order of the linear size of the *box*.

- The basic degrees of freedom are N point particles living on the surface of a $(d+1)$-dimensional hypersphere of radius R (noted $\mathbb{S}_d(R)$), hence it is a point $x_i \in \mathbb{R}^{d+1}$ with the constraint $x_i^2 = R^2$. The *volume* of this d-dimensional curved space is

$$\mathcal{V} = \Omega_{d+1} R^d \tag{4.4}$$

  This is discussed in §3.1.3. For $R \to \infty$ we recover a system defined on a flat (Euclidean) and infinite space $\mathbb{R}^d$.

- We wish then to consider *first* the thermodynamic limit where $R \to \infty$ with constant density $\rho = N/\mathcal{V}$, in which the model becomes equivalent to the usual definition in a d-dimensional Euclidean periodic cubic volume, and *then* the limit $d \to \infty$, where the model is exactly solvable.

- Each particle pair interacts through a potential $V(|x_i - \mathcal{R}_{ij} x_j|)$, where $\mathcal{R}x$ is a uniformly distributed random rotation of point x on the sphere. Here $|x| = \left(\sum_{\mu=1}^{d+1} x_\mu^2\right)^{1/2}$ is the modulus of the vector x in $\mathbb{R}^{d+1}$, or in other words $|x - y|$ is the Euclidean distance[1] between points x and y in $\mathbb{R}^{d+1}$. The total potential energy is thus (we drop the *MK* suffix for simplicity)

$$H = \sum_{i<j} V(|x_i - \mathcal{R}_{ij} x_j|) \ . \tag{4.5}$$

  As discussed in the introduction, the random rotations $\mathcal{R}_{ij}$ are introduced for pedagogical convenience. In the limit $d \to \infty$, they become irrelevant, and the model becomes equivalent to a standard model where all the $\mathcal{R}_{ij}$ are equal to the identity. We discuss this in more details in section 4.2.5.

- In order to have a proper limit $d \to \infty$, we consider a class of inter-particle potentials V at temperature $T = 1/\beta$ described in §3.1.1.

The main definitions are summarized in appendix A.

---

[1]For a central potential we could have defined the model with the great-circle distance (geodesic distance) on $\mathbb{S}$ instead of the Euclidean one, however in the large R limit these two coincides up to irrelevant $\mathcal{O}(1/R^2)$ corrections. For convenience we choose to work with the Euclidean distance.

4.2.2 Replicated partition function

For simplicity we focus in this section on the HS potential, but the derivation can be easily extended to a generic potential of the class §3.1.1, as mentioned in section 4.2.1, by changing the details of the function $\chi(\bar{x}, \bar{y})$ defined in (4.6) below, that are irrelevant for the truncation of the logarithm of the partition function. We denote by $\mathrm{d}\mathcal{R}$ the uniform measure over rotations, and by an overbar the average over it, i.e. over all the random rotations. To compute the average of the free energy over the random rotations, we apply the so-called replica trick by considering the n-times replicated partition function and use the relation $\overline{\ln Z} = \lim_{n \to 0} \partial_n \overline{Z^n}$ (see §2.3). We denote by $\bar{x} = (x^1, \cdots, x^n) \in \mathbb{S}_d(R)^n$ the coordinates of a replicated particle, and by $\bar{X} = (X_1, \cdots, X_n)$ a full replicated configuration of the system. Let us define

$$\chi(\bar{x}_i, \bar{x}_j) = \prod_{a=1}^n e^{-\beta V(|x_i^a - x_j^a|)} = \prod_{a=1}^n \theta(|x_i^a - x_j^a| - \sigma) \;,$$

$$\bar{\chi}(\bar{x}, \bar{y}) = \int \mathrm{d}\mathcal{R} \, \chi(\bar{x}, \mathcal{R}\bar{y}) = \int \mathrm{d}\mathcal{R} \prod_{a=1}^n \theta(|x^a - \mathcal{R}y^a| - \sigma) \;. \tag{4.6}$$

We have

$$\overline{Z^n} = \overline{\int \mathrm{d}\bar{X} \prod_{a=1}^n e^{-\beta H[X_a]}} = \int \mathrm{d}\bar{X} \, \overline{\prod_{i<j} \chi(\bar{x}_i, \mathcal{R}_{ij}\bar{x}_j)} = \int \mathrm{d}\bar{X} \prod_{i<j} \int \mathrm{d}\mathcal{R} \, \chi(\bar{x}_i, \mathcal{R}\bar{x}_j) = \int \mathrm{d}\bar{X} \, e^{\sum_{i<j} \ln \bar{\chi}(\bar{x}_i, \bar{x}_j)} \;, \tag{4.7}$$

where we recall that the overline denotes the average over the $N(N-1)/2$ independent random rotations $\mathcal{R}_{ij}$. For an arbitrary point $x \in \mathbb{S}_d(R)$, $\mathcal{V}_d(\sigma)/\mathcal{V} = \int \mathrm{d}\mathcal{R} \, \theta(\sigma - |x - \mathcal{R}x|)$ is the fraction of volume excluded by a particle of radius σ on $\mathbb{S}_d(R)$. Simple geometrical considerations allow one to bound the function $\bar{\chi}(\bar{x}, \bar{y})$ from above and below. In fact, the value of $\bar{\chi}(\bar{x}, \bar{y})$ is obtained by taking the n particles described by $\bar{y}$, rotating all of them by the same random rotation $\mathcal{R}$, and computing the probability that none of the rotated spheres overlap with the corresponding particle in $\bar{x}$. Clearly the value of $\bar{\chi}$ is maximal when $\bar{y} = \mathcal{R}_0 \bar{x}$ for some $\mathcal{R}_0$, because in this case one minimizes the number of excluded rotations. We can choose $\mathcal{R}_0$ to be the identity, in such a way that $\bar{y} = \bar{x}$, without loss of generality. In that case we have

$$\bar{\chi}(\bar{x}, \bar{y}) \leqslant \bar{\chi}(\bar{x}, \bar{x}) = \int \mathrm{d}\mathcal{R} \prod_{a=1}^n \theta(|x^a - \mathcal{R}x^a| - \sigma) = 1 - \frac{\mathcal{V}_d(\sigma)}{\mathcal{V}} \;. \tag{4.8}$$

Similarly, the value of $\bar{\chi}$ is minimal if $\bar{y}$ is chosen in such a way that, for any rotation $\mathcal{R}$, at most one of the particles in $\mathcal{R}\bar{y}$ is in overlap with the corresponding particle of $\bar{x}$. Indeed, in this way one maximizes the number of excluded rotations. Using this we have

$$\bar{\chi}(\bar{x}, \bar{y}) \geqslant 1 - n\frac{\mathcal{V}_d(\sigma)}{\mathcal{V}} \;, \tag{4.9}$$

because the integrand is 1 except in n distinct regions where the rotation brings one of the $\bar{y}$ particles in overlap with one of the $\bar{x}$. For generic configurations we thus get

$$1 - n\frac{\mathcal{V}_d(\sigma)}{\mathcal{V}} \leqslant \bar{\chi}(\bar{x}, \bar{y}) \leqslant 1 - \frac{\mathcal{V}_d(\sigma)}{\mathcal{V}} \;. \tag{4.10}$$

Hence, defining the Mayer function

$$f(\bar{x}, \bar{y}) = \chi(\bar{x}, \bar{y}) - 1 = -1 + \prod_{a=1}^n \theta(|x^a - y^a| - \sigma) \;, \qquad \bar{f}(\bar{x}, \bar{y}) = \bar{\chi}(\bar{x}, \bar{y}) - 1 = \int \mathrm{d}\mathcal{R} \, f(\bar{x}, \mathcal{R}\bar{y}) \;, \tag{4.11}$$

we deduce that $\bar{f} \propto \mathcal{V}_d(\sigma)/\mathcal{V}$ is small in the thermodynamic limit, and in equation (4.7) we can expand $\ln \bar{\chi}(\bar{x}_i, \bar{x}_j) = \ln[1 + \bar{f}(\bar{x}_i, \bar{x}_j)] \sim \bar{f}(\bar{x}_i, \bar{x}_j)$. Introducing the order parameter (density of replicated configurations)

$$\rho(\bar{x}) = \frac{1}{N} \sum_i \delta(\bar{x} - \bar{x}_i) \;, \tag{4.12}$$

we thus have

$$\sum_{i<j} \ln \bar{\chi}(\bar{x}_i, \bar{x}_j) \sim \sum_{i<j} \bar{f}(\bar{x}_i, \bar{x}_j) = \frac{N^2}{2} \int \mathrm{d}\bar{x}\mathrm{d}\bar{y} \, \rho(\bar{x})\rho(\bar{y})\bar{f}(\bar{x}, \bar{y}) - \frac{N}{2} \int \mathrm{d}\bar{x} \, \rho(\bar{x})\bar{f}(\bar{x}, \bar{x}) \;. \tag{4.13}$$

Note that from equation (4.8) we have $\bar{f}(\bar{x}, \bar{x}) = -\mathcal{V}_d(\sigma)/\mathcal{V}$ and thus $-\frac{N}{2} \int \mathrm{d}\bar{x}\,\rho(\bar{x}) \bar{f}(\bar{x}, \bar{x}) = N\mathcal{V}_d(\sigma)/(2\mathcal{V})$ is a constant. In the following, we do not keep track explicitly of all the multiplicative constants in the partition function. We will fix this at the end of the computation in section 4.2.3, so this term will be dropped. Note also that the constant is finite in the thermodynamic limit and therefore it is subdominant with respect to the extensive terms of the free energy. Inserting a delta function for $\rho(\bar{x})$ in equation (4.7) and representing it as a Fourier integral over $\widehat{\rho}(\bar{x})$, we obtain

$$\overline{Z^n} \propto \int \mathrm{d}\bar{x}_i \int_{\rho, \widehat{\rho}} e^{N \int \mathrm{d}\bar{x}\,\rho(\bar{x})\widehat{\rho}(\bar{x}) - \sum_i \widehat{\rho}(\bar{x}_i) + \frac{N^2}{2} \int \mathrm{d}\bar{x}\mathrm{d}\bar{y}\,\rho(\bar{x})\rho(\bar{y})\bar{f}(\bar{x}, \bar{y}) - \frac{N}{2} \int \mathrm{d}\bar{x}\,\rho(\bar{x})\bar{f}(\bar{x}, \bar{x})}$$

$$\propto \int_{\rho, \widehat{\rho}} e^{N\left\{ \int \mathrm{d}\bar{x}\,\rho(\bar{x})\widehat{\rho}(\bar{x}) + \ln \int \mathrm{d}\bar{x} e^{-\widehat{\rho}(\bar{x})} + \frac{N}{2} \int \mathrm{d}\bar{x}\mathrm{d}\bar{y}\,\rho(\bar{x})\rho(\bar{y})\bar{f}(\bar{x}, \bar{y}) \right\}} = \int_{\rho, \widehat{\rho}} e^{N\mathcal{S}(\rho, \widehat{\rho})} \,. \tag{4.14}$$

The last integral can be evaluated by the saddle-point method by optimizing $\mathcal{S}$, which represents the *free entropy* functional[2] at fixed $\rho, \widehat{\rho}$. We will simply refer to it as *entropy* in the following. The saddle point equations for $\widehat{\rho}$ in the thermodynamic limit $N \to \infty$ is

$$\rho(\bar{x}) = \frac{e^{-\widehat{\rho}(\bar{x})}}{\int \mathrm{d}\bar{y}\, e^{-\widehat{\rho}(\bar{y})}} \,, \tag{4.16}$$

which is very simple and is compatible with the normalization of $\rho(\bar{x})$. Note that the original integral over $\widehat{\rho}$ was on the imaginary axis, but the saddle-point lies on the real axis as shown explicitly by equation (4.16) because ρ must be real-valued. We can use this equation and substitute it in the entropy, getting:

$$\begin{aligned}
\mathcal{S}(\rho) &= -\int \mathrm{d}\bar{x}\,\rho(\bar{x}) \ln \rho(\bar{x}) + \frac{N}{2} \int \mathrm{d}\bar{x}\mathrm{d}\bar{y}\,\rho(\bar{x})\rho(\bar{y})\bar{f}(\bar{x}, \bar{y}) \\
&= -\int \mathrm{d}\bar{x}\,\rho(\bar{x}) \ln \rho(\bar{x}) + \frac{N}{2} \int \mathrm{d}\bar{x}\mathrm{d}\bar{y}\,\rho(\bar{x})\rho(\bar{y}) \int \mathrm{d}\mathcal{R}\, f(\bar{x}, \mathcal{R}\bar{y}) \\
&= -\int \mathrm{d}\bar{x}\,\rho(\bar{x}) \ln \rho(\bar{x}) + \frac{N}{2} \int \mathrm{d}\mathcal{R}\mathrm{d}\bar{x}\mathrm{d}\bar{y}\,\rho(\bar{x})\rho(\mathcal{R}^{-1}\bar{y}) f(\bar{x}, \bar{y}) \\
&= -\int \mathrm{d}\bar{x}\,\rho(\bar{x}) \ln \rho(\bar{x}) + \frac{N}{2} \int \mathrm{d}\bar{x}\mathrm{d}\bar{y}\,\rho(\bar{x})\rho(\bar{y}) f(\bar{x}, \bar{y}) \,,
\end{aligned} \tag{4.17}$$

where in the last step we assumed that $\rho(\bar{y})$ is rotationally invariant, hence $\rho(\mathcal{R}^{-1}\bar{y}) = \rho(\bar{y})$, and

$$\frac{1}{N} \ln \overline{Z^n} = \max_\rho \mathcal{S}(\rho) + C_n \,, \tag{4.18}$$

where the additive constant C_n comes from the proportionality constant in equation (4.14). We will see in next section 4.2.3 that $C_n = 0$. Let us emphasize once again that, as discussed in section 4.2.5, the last line in equation (4.17) holds also in absence of random shifts in the limit $d \to \infty$. As mentioned in the introduction §4.1, it is the usual starting point of replica computations for HS in large dimensions [312, 243]. The derivation presented in this section has the advantage that it does not require to introduce the virial expansion, so it is more compact. Note that here we normalized $\rho(\bar{x})$ to $\int \mathrm{d}\bar{x}\,\rho(\bar{x}) = 1$ while in previous works [312, 243] the standard normalization of liquid theory, $\int \mathrm{d}\bar{x}\,\rho(\bar{x}) = N$, was used.

4.2.3 Liquid phase entropy and distinguishability issues

As a first check we derive the entropy in the liquid phase of HS. This corresponds to having independent and uniformly distributed particles over the sphere, so $\rho(\bar{x}) = \mathcal{V}^{-n}$. Then we have, neglecting the constant C_n,

$$\begin{aligned}
\mathcal{S}(\rho) &= n \ln \mathcal{V} + \frac{N}{2} \int \frac{\mathrm{d}\bar{x}}{\mathcal{V}^n} \frac{\mathrm{d}\bar{y}}{\mathcal{V}^n} f(\bar{x}, \bar{y}) = n \ln \mathcal{V} + \frac{N}{2} \left[-1 + \left(\int \frac{\mathrm{d}x}{\mathcal{V}} \frac{\mathrm{d}y}{\mathcal{V}} \theta(|x - y| - \sigma) \right)^n \right] \\
&= n \ln \mathcal{V} + \frac{N}{2} \left[-1 + \left(1 - \frac{\mathcal{V}_d(\sigma)}{\mathcal{V}} \right)^n \right] \sim n \ln \mathcal{V} - \frac{Nn}{2} \frac{\mathcal{V}_d(\sigma)}{\mathcal{V}} = n s_{\mathrm{liq}} \,,
\end{aligned} \tag{4.19}$$

---

[2] *Free entropy* is the logarithm of the canonical partition function. For HS, it is the same as the entropy because the partition function is temperature-independent: the entropy reads (remember that $k_{\mathrm{B}} = 1$)

$$S = -\frac{\partial F}{\partial T} = \frac{\partial (T \ln Z)}{\partial T} = \ln Z \tag{4.15}$$

where

$$s_{\text{liq}} = \ln \mathcal{V} - \frac{N \mathcal{V}_d(\sigma)}{2\mathcal{V}} = \ln \mathcal{V} - \frac{2^d \varphi}{2} \ , \tag{4.20}$$

and $\varphi = N \mathcal{V}_d(\sigma)/(2^d \mathcal{V})$ is the packing fraction in the large R limit. We therefore recover the desired result, that the replicated entropy is given by n times the liquid entropy if replicas are decorrelated [279]. This also shows that the constant C_n in equation (4.18) is equal to zero.

Note that for the liquid entropy we obtain almost the same results that has been obtained by Frisch, Percus, Rivier and Wyler [409, 161] for standard d-dimensional HS when $d \to \infty$, which is, from (2.44) and (4.15),

$$s_{\text{liq}}^{\text{HS}} = 1 - \ln(N/\mathcal{V}) - \frac{2^d \varphi}{2} \ . \tag{4.21}$$

In fact, we have $s_{\text{liq}} = s_{\text{liq}}^{\text{HS}} - 1 + \ln N$, hence

$$Z_{\text{liq}} \sim e^{N s_{\text{liq}}} \sim Z_{\text{liq}}^{\text{HS}} e^{N \ln N - N} \sim Z_{\text{liq}}^{\text{HS}} N! \ . \tag{4.22}$$

This factor of $N!$ is due to the fact that in the MK model particles are distinguishable, while in the HS model they are not. One could correct by dividing (artificially) the MK partition function by $N!$ [270]. In any case this factor is irrelevant for the thermodynamics as it only affects the location of the Kauzmann point [270], see §1.2.4.1. A similar situation was encountered in the last chapter, where we computed the *dynamical entropy* $\mathcal{S}(\boldsymbol{Q})$ (3.68) up to an irrelevant constant (*i.e.* , which does not depend upon the saddle-point value of $\boldsymbol{Q}$).

4.2.4   Pair correlation function

Note that equation (4.7) can be written as

$$\overline{Z^n} = \overline{\int \mathrm{d}\bar{X} \, e^{-\frac{\beta}{2} \sum_{a, i \neq j} V(|x_i^a - \mathcal{R}_{ij} x_j^a|)}} = \overline{\int \mathrm{d}\bar{X} \, e^{-\frac{\beta}{2} \int \mathrm{d}\bar{x} \mathrm{d}\bar{y} \, \rho^{(2)}(\bar{x}, \bar{y}) V(\bar{x}, \bar{y})}} \tag{4.23}$$

where

$$\rho^{(2)}(\bar{x}, \bar{y}) = \sum_{i \neq j} \delta(\bar{x} - \bar{x}_i) \delta(\bar{y} - \mathcal{R}_{ij} \bar{x}_j) \ , \qquad V(\bar{x}, \bar{y}) = \sum_a V(|x^a - y^a|) \ . \tag{4.24}$$

Therefore we obtain

$$\begin{aligned} \rho(\bar{x}, \bar{y}) &= \overline{\langle \rho^{(2)}(\bar{x}, \bar{y}) \rangle} = \overline{\frac{1}{Z^n} \int \mathrm{d}\bar{X} \, e^{-\beta \sum_a H[X_a]} \rho^{(2)}(\bar{x}, \bar{y})} \\ &\sim \frac{1}{\overline{Z^n}} \overline{\int \mathrm{d}\bar{X} \, e^{-\beta \sum_a H[X_a]} \rho^{(2)}(\bar{x}, \bar{y})} = -2T \frac{\delta \ln \overline{Z^n}}{\delta V(\bar{x}, \bar{y})} = N^2 \rho(\bar{x}) \rho(\bar{y}) \chi(\bar{x}, \bar{y}) \ . \end{aligned} \tag{4.25}$$

The equality between the first and second lines in equation (5.52) holds for $n \to 0$ in which we are interested eventually, because $Z^n \to 1$ in that limit. This result (5.52) is exactly the same as keeping the leading order of the virial expansion for the two-point density [293, 342], obtained in a different way (see the similar discussion in §5.7).

From the knowledge of $\rho(\bar{x}, \bar{y})$ we can compute the averages of several interesting observables. Consider for example an observable of the non-replicated system of the form

$$\mathcal{O} = \sum_{i < j} \mathcal{O}(x_i, \mathcal{R}_{ij} x_j) \ . \tag{4.26}$$

We have

$$\begin{aligned} \frac{1}{2} \int \mathrm{d}\bar{x} \mathrm{d}\bar{y} \, \mathcal{O}(x^1, y^1) \rho(\bar{x}, \bar{y}) &= \frac{1}{2\overline{Z^n}} \overline{\int \mathrm{d}\bar{X} \, e^{-\beta \sum_a H[X_a]} \sum_{i \neq j} \mathcal{O}(x_i^1, \mathcal{R}_{ij} x_j^1)} \\ &= \frac{1}{\overline{Z^n}} \overline{Z^{n-1} \int \mathrm{d}X \, e^{-\beta H[X]} \sum_{i < j} \mathcal{O}(x_i, \mathcal{R}_{ij} x_j)} \xrightarrow[n \to 0]{} \overline{\langle \mathcal{O} \rangle} \ . \end{aligned} \tag{4.27}$$

As for the free energy, the calculation presented in this section has been done for the MK model with random rotations for simplicity; however it also holds for the normal potential without random rotations, as a result of keeping the lowest order virial expansion of two-point correlation functions [199, 293].

To conclude, let us write explicitly the result for the liquid phase where $\rho(\bar{x}) = \mathcal{V}^{-n}$, and specializing to a generic potential (of interaction range σ, see §3.1.1 for simplicity. We have

$$
\begin{aligned}
\overline{\langle \mathcal{O} \rangle} &= \frac{1}{2} \int \mathrm{d}\bar{x}\mathrm{d}\bar{y}\, \mathcal{O}(x^1, y^1) N^2 \mathcal{V}^{-2n} \chi(\bar{x}, \bar{y}) \\
&= \frac{1}{2} \left(\frac{N}{\mathcal{V}} \right)^2 \int \mathrm{d}x\mathrm{d}y\, \mathcal{O}(x, y) e^{-\beta V(|x-y|)} \left(\frac{1}{\mathcal{V}^2} \int \mathrm{d}x\mathrm{d}y\, e^{-\beta V(|x-y|)} \right)^{n-1} \\
&= \frac{N^2}{2\mathcal{V}^2} \int \mathrm{d}x\mathrm{d}y\, \mathcal{O}(x, y) e^{-\beta V(|x-y|)} O\left(\left(\frac{\mathcal{V} - \mathcal{V}_d(\sigma)}{\mathcal{V}} \right)^{n-1} \right) \xrightarrow[\mathcal{V} \to \infty]{} \frac{N^2}{2\mathcal{V}^2} \int \mathrm{d}x\mathrm{d}y\, \mathcal{O}(x, y) e^{-\beta V(|x-y|)} \ ,
\end{aligned}
$$
(4.28)

which is the correct result and corresponds to a liquid pair correlation $g(r) = e^{-\beta V(r)}$, which is the leading term in the virial expansion [199, 293] and thus gives the exact result concerning the original model in the limit $d \to \infty$, as well as for the MK model in all dimensions [270].

As an example, for HS we have $g(r) = \theta(r - \sigma)$ which amounts to say that HS cannot overlap for $r < \sigma$ due to the hard-core constraint but are non-interacting above their diameter, and this is described by the ideal gas value of $g(r > \sigma) = 1$. This is clearly an idealization of a real HS system, which still retains some physical sense. This can be interpreted as the fact that such *rather hard* potentials concentrate their details to the region defining their (effective) particle diameter when $d \to \infty$, as is clear from the analysis in §5.2. Away from this region, the behaviour is trivial when $d \to \infty$.

4.2.5 The role of random rotations

Let us comment on the choice of introducing the random rotations $\mathcal{R}_{ij}$ in the interaction potential. As we will see in the following, there are a few reasons for that choice:

1. all contributions to the free energy of the system involving three particles or more vanish, both in the statics and in the dynamics;

2. the crystalline state cannot exist in presence of random rotations, so we can focus on the amorphous liquid and glass states;

3. the presence of quenched disorder allows one to treat the thermodynamic problem by introducing replicas in a straightforward way.

The first result, when $d \to \infty$, is also true in absence of the $\mathcal{R}_{ij}$, as a result of the virial series truncation. Note also that the random shifts disappear from the two-particle virial term. The second result is not true in absence of random rotations: there might be a crystal state. However, as shown in [363, 395], crystallization is strongly suppressed in $d > 3$. Thus, the liquid and glass states are metastable but have an extremely large lifetime, that is expected to diverge when $d \to \infty$. Finally, concerning the third point, in absence of quenched disorder one can still use replicas within the Monasson [288] or Franz-Parisi [156] schemes to describe glassy states. For particle systems in $d \to \infty$ this has been done in [312, 243] and [325], respectively. This only requires minor modifications of the replica scheme (see §1.2.4.2 and §G for a discussion). We conclude that the presence of the random rotations $\mathcal{R}_{ij}$ is irrelevant in $d \to \infty$, and that the MK model with random rotations is equivalent to the normal model with $\mathcal{R}_{ij}$ equal to the identity. The equivalence between the *normal* model and MK is made more precise in appendix H. In doing so, we compute scaling forms for the interaction terms that explains the fact that computing the statics or dynamics at the scaling regime of $O(1/d)$ gap fluctuations between nearest neighbours still gives the correct results (for instance the correct liquid entropy in the statics or the diffusion regime in the dynamics) for larger distances.

The results presented in the following therefore hold also for a normal particle model without random rotations.

4.2.6 Summary of the results

Let us summarize the results obtained in this section:

1. The free energy functional has a simple form, composed by two terms, the ideal gas and a simple mean field density-density interaction:

$$\mathcal{S}(\rho) = \mathcal{S}_{\text{IG}}(\rho) + \mathcal{S}_{\text{int}}(\rho) = - \int d\bar{x}\, \rho(\bar{x}) \ln \rho(\bar{x}) + \frac{N}{2} \int d\bar{x} d\bar{y}\, \rho(\bar{x})\rho(\bar{y}) f(\bar{x}, \bar{y}) , \qquad \frac{1}{N} \ln \overline{Z^n} = \max_{\rho} \mathcal{S}(\rho) .$$
(4.29)

Here, for a generic potential, $\mathcal{S}$ is given by $-\beta$ times the free energy; it is also sometimes called *free entropy* (we nevertheless refer to it as *entropy* in the following).

2. By definition of $\rho(\bar{x})$, equation (4.12), averages of one-particle quantities can be written as

$$\mathcal{O} = \sum_i \mathcal{O}(x_i) \qquad \Rightarrow \qquad \overline{\langle \mathcal{O} \rangle} = \int d\bar{x}\, \rho(\bar{x}) \mathcal{O}(x^1) .$$
(4.30)

3. Two-particle quantities can be written as

$$\mathcal{O} = \sum_{i<j} \mathcal{O}(x_i, \mathcal{R}_{ij} x_j) \qquad \Rightarrow \qquad \overline{\langle \mathcal{O} \rangle} = \frac{1}{2} \int d\bar{x} d\bar{y}\, \rho(\bar{x}, \bar{y}) \mathcal{O}(x^1, y^1) , \qquad \rho(\bar{x}, \bar{y}) = N^2 \rho(\bar{x})\rho(\bar{y})\chi(\bar{x}, \bar{y}) .$$
(4.31)

Note that the random shifts in the definition of $\mathcal{O}$ have to be included for the MK model, while they should not be included for the normal particle system.

Correlations involving more than two particles are factorized in terms of one- and two-particle correlations, as discussed in [312, 270, 414].

4.3 Rotational invariance and large-dimensional limit

As we did in the dynamics, we can derive the static free energy through the general analogy with the SUSY formalism described in §2.4, see §2.5.2 for the p-spin case. The computation is formally the same, and we will not reproduce it here. Yet, for completeness, it is done in appendix §F.

In a few words, the strategy used in this appendix is the following, as in the dynamics. Due to rotational invariance on the hypersphere, the density of replicated configurations $\rho(\bar{x})$ can only depend on the matrix of the scalar products $q_{ab} = x_a \cdot x_b$, or more physically, on the matrix of MSDs between replicas (recall that $q_{aa} = x_a^2 = R^2$):

$$\mathsf{D}_{ab} = (x_a - x_b)^2 = 2R^2 - 2q_{ab} , \qquad q_{ab} = x_a \cdot x_b .$$
(4.32)

These definitions are summarized in appendix A.2. We can thus make a change of variables in the integration over $d\bar{x}$ to q_{ab} or D_{ab}, integrating out the irrelevant degrees of freedom. Roughly speaking[3], the change of variables gives for density averages:

$$\int d\bar{x} \; \bullet \; \rho(\bar{x}) \rightarrow \int d\hat{q} \; \bullet \; e^{\frac{d}{2} \ln \det \hat{q} + d\,\Omega(\hat{q})} ,$$
(4.33)

where the factor $e^{\frac{d}{2} \ln \det \hat{q}}$ is the Jacobian of the transformation, and one can show that $\rho(\hat{q}) = e^{d\,\Omega(\hat{q})}$ where $\Omega(\hat{q})$ is finite for large d. This is shown explicitly in [243, Eq. (65)], recalling that in the relevant regime $2^d \varphi = d\widehat{\varphi}$ with finite $\widehat{\varphi}$ and that $\mathcal{F}$, as defined in [243], is a finite function. We quickly recall here the argument, which is more easily proven in the framework of [243] than in the equivalent spherical model used here. The saddle-point condition in (4.14) gives

$$\forall \bar{x}, \; \frac{\delta \mathcal{S}}{\delta \rho(\bar{x})} = 0 \qquad \Longleftrightarrow \qquad \forall \bar{x}, \; \ln \rho(\bar{x}) = -1 + N \int d\bar{y}\, \rho(\bar{y}) f(\bar{x} - \bar{y})$$
(4.34)

where the expression of $\mathcal{S}(\rho)$ is provided by (4.17). Then, using the same argument as in §3.3.4.2 in the dynamics or §F.3.2 in the statics, the scaling of the last term of (4.34) is given by the test function $f(\bar{x} - \bar{y}) = -\theta(\sigma - |x_1 - y_1|)$ which tells us that $N \int d\bar{y}\, \rho(\bar{y}) f(\bar{x} - \bar{y}) \propto 2^d \varphi$, *i.e.* it is $O(d)$ in the regime where one might expect a glass transition to happen, see the discussion in §2.2. Hence the density scales as $\rho(\bar{x}) = e^{d\Omega(\bar{x})}$ and using rotational invariance on the sphere this becomes $\rho(\hat{q}) = e^{d\Omega(\hat{q})}$.

---

[3]This is made mathematically more precise in appendix §F.

The appearance of the dimension in the exponent leads to a narrowing of fluctuations of correlations, when $d \to \infty$, and saddle-point evaluation becomes exact [168, 169, 265]. In this way we obtain an exact expression of $\mathcal{S}(\rho)$ in terms of the matrix $\hat{\mathsf{D}}$.

Let us now summarize the main results of this appendix.

1. We have shown that for a generic function $f(\{|x_a - y_a|\})$ that is not exponential in d and constraining the replicas to be close to each other, we have, from equation (F.39):

$$\frac{N}{2} \int_V \mathrm{d}\bar{x}\mathrm{d}\bar{y}\rho(\bar{x})\rho(\bar{y})f(\bar{x}, \bar{y}) = -\frac{2^d\varphi}{2}\mathcal{F}(\hat{\Delta}) \ ,$$

$$\mathcal{F}(\hat{\Delta}) = -e^{-A/2} \int \mathcal{D}_{Avv^{\mathrm{T}} - \hat{\Delta}}\bar{\mu} \, \mathrm{d}\lambda \, e^{\lambda} f(\{\sigma(1 + \mu_a/d + \lambda/d)\}) \ , \tag{4.35}$$

where $\mathcal{D}_{Avv^{\mathrm{T}} - \hat{\Delta}}\bar{\mu}$ is a Gaussian measure with $\langle \mu_a \mu_b \rangle = A - \Delta_{ab}$, as defined in equation (F.36), and A is an arbitrary constant. Here $\hat{\Delta} = d\hat{\mathsf{D}}/\sigma^2$, since our crucial assumption is that $\hat{\mathsf{D}} = O(1/d)$ (see §3.3.2), is the saddle-point matrix defined in equation (F.14):

$$0 = \frac{d}{2}n\ln(2\pi e/d) + \frac{d}{2}\left[\ln\det(-\hat{\mathsf{D}}_{\mathrm{sp}}/2) + \ln(1 - 2R^2 v^{\mathrm{T}}\hat{\mathsf{D}}_{\mathrm{sp}}^{-1}v)\right] + d\,\Omega(\hat{\mathsf{D}}_{\mathrm{sp}}) \ . \tag{4.36}$$

Other equivalent expressions for $\mathcal{F}(\hat{\Delta})$, namely equations (F.41) and (F.44), have been derived in the special case in which f is the replicated Mayer function defined in equation (4.11). Using equation (4.31), this result can be used to compute the averages of two-particle rotationally invariant observables.

2. Our second result is an expression of the entropy in terms of the saddle-point scaled MSD matrix $\hat{\Delta} = d\hat{\mathsf{D}}/\sigma^2$ and the scaled density $\widehat{\varphi} = 2^d\varphi/d$. The ideal gas term is given by equation (F.16). For the interaction term we use equation (4.35). We obtain[4]

$$\mathcal{S}(\hat{\Delta}) = \frac{d}{2}n\ln(\pi e\sigma^2/d^2) + \frac{d}{2}\ln\det(-\hat{\Delta}) + \frac{d}{2}\ln\left(1 - \frac{2dR^2}{\sigma^2}v^{\mathrm{T}}\hat{\Delta}^{-1}v\right) - \frac{d}{2}\widehat{\varphi}\mathcal{F}(\hat{\Delta}) \ , \tag{4.37}$$

where for $\mathcal{F}(\hat{\Delta})$ we have three expressions: equations (F.41), (F.44) and (4.35).

3. The matrices $\hat{\Delta}$ or $\hat{\mathsf{D}}$ should be determined by solving the $d \to \infty$ saddle-point condition, i.e. by maximizing the terms that are exponential in d in equation (F.13). The problem is that we have never derived explicitly the form of $\Omega(\hat{\mathsf{D}})$. However, one can show that $\hat{\Delta}$ can be equivalently determined by maximizing the final result for the entropy, equation (4.37), which is quite intuitive (a formal proof can be found in [243, 242]). Indeed, the thermodynamic limit saddle-point equation is $\delta\mathcal{S}/\delta\rho = 0$. In infinite d, $\mathcal{S}$ depends on ρ only through the saddle-point value of $\Omega(\hat{\Delta}_{\mathrm{sp}})$, which is known in terms of $\hat{\Delta}_{\mathrm{sp}}$ via (F.46). Therefore $\delta\mathcal{S}/\delta\rho = 0$ is equivalent to $\mathrm{d}\mathcal{S}/\mathrm{d}\hat{\Delta}_{\mathrm{sp}} = \hat{0}$ where we have expressed $\mathcal{S}$ only in terms of the saddle-point value $\hat{\Delta}_{\mathrm{sp}}$ as in (4.37). This condition fully determines the saddle-point value $\hat{\Delta}_{\mathrm{sp}}$ and is thus equivalent to the $d \to \infty$ saddle-point equation.

Thanks to these results, we can express both the free energy and two-particle correlations in terms of the matrix $\hat{\Delta}$. Our next task is to determine explicitly this matrix.

4.4 Hierarchical matrices and replica symmetry breaking

In this section we show that equation (4.37) reproduces all the correct results in the different thermodynamic phases of the system, where the matrix $\hat{\Delta}$ is a hierarchical matrix [279]. We will focus on HS for simplicity, and to make contact with previous results [243, 242, 96]. In particular we will show that

---

[4]It may seem that this expression of the entropy is ill-defined (imaginary) because the logarithms might be evaluated at negative values. Indeed, since $\mathrm{Tr}\hat{\Delta} = 0$, $\hat{\Delta}$ has both positive and negative eigenvalues; thus, $\det(-\hat{\Delta})$ and $1 - \frac{2dR^2}{\sigma^2}v^{\mathrm{T}}\hat{\Delta}^{-1}v$ might be negative. However, remember that in the end one wishes to take the limit $n \to 0$. In this limit, these expressions are regularized: one can check from Appendix B that $\hat{\Delta}$ is negative definite. Another option, which will be used in section 4.5 and chapter 3, is to express $\mathcal{S}$ in terms of $\hat{Q} \equiv \Delta_{\mathrm{liq}}vv^{\mathrm{T}} - \hat{\Delta}$, which is positive definite.

1. For a general form of the matrix Δ_{ab}, equation (4.37) coincides with the result obtained in [243, 242, 96] through a quite different derivation. For the interaction term, this is shown in equation (F.44) of §F. For the ideal gas term, this is shown in G.

2. In the liquid phase, we expect that all replicas are uncorrelated (see §1.2.4.2 and §2.3.2). Hence[5] for $a \neq b$, $x_a \cdot x_b = 0$ and $\Delta_{ab} = d(x_a - x_b)^2/\sigma^2 = 2dR^2/\sigma^2 \equiv \Delta_{\text{liq}}$. Consistently we will show that in this phase the matrix $\hat{\Delta}$ is replica symmetric (RS) with $\Delta_{ab} = \Delta_0(1 - \delta_{ab})$ and $\Delta_0 = \Delta_{\text{liq}}$. Furthermore, $\mathcal{S} = ns_{\text{liq}}$ as expected from section 4.2.3. These results are discussed in section 4.4.1.

3. In the glass phase, where $\hat{\Delta}$ is a hierarchical replica symmetry breaking (RSB) matrix [279, 288, 278, 81], from equation (4.37) we can derive the expression of $s = \lim_{n \to 0} \mathcal{S}/n$ and again we find the same results as in [96] for the 1-RSB, 2RSB, $\cdots$, full-RSB cases. For pedagogical reasons we first discuss the 1-RSB computation (section 4.4.2) and then the general kRSB computation (section 4.4.3).

Some useful mathematical properties of hierarchical RSB matrices are discussed in Appendix B; we will also use the notations for Gaussian integrals defined in Appendix A.4.

4.4.1 Liquid (replica symmetric) phase

The liquid phase is described by a replica symmetric matrix $\hat{\Delta} = \Delta_0(vv^{\mathrm{T}} - I)$, as in the paramagnetic phase in the p-spin, §2.3.2. As an example for $n = 3$ we have

$$\hat{\Delta} = \begin{pmatrix} 0 & \Delta_0 & \Delta_0 \\ \Delta_0 & 0 & \Delta_0 \\ \Delta_0 & \Delta_0 & 0 \end{pmatrix} . \tag{4.38}$$

Using this ansatz amounts to assume that in the liquid phase (moderate density), the free energy landscape describing the system as a function of the mean-square displacement matrix $\hat{\Delta}$ has a minimum, corresponding to the stable thermodynamic phase, having the form given by equation (4.38). Dynamically, this means that the time-dependent mean-square displacement has a single plateau at long times, corresponding to Δ_0, see figure 4.2. We can compute $\mathcal{S}(\Delta_0)$ and find the stable value of Δ_0, as one would compute the magnetization of the paramagnetic phase at high temperature as the minimum of the free energy of the Curie-Weiss ferromagnet model. We define $\Delta_{\text{liq}} = 2dR^2/\sigma^2$ as in (3.39) in the last chapter. Note that $\Delta_{\text{liq}} \to \infty$ in the thermodynamic limit. We wish to show that $\Delta_0 = \Delta_{\text{liq}}$ and recover equation (4.20).

4.4.1.1 Replica symmetric entropy

We start from equation (4.37) and we plug in the RS form of $\hat{\Delta}$. Equation (B.4) implies that $1 - \frac{2dR^2}{\sigma^2}v^{\mathrm{T}}\hat{\Delta}^{-1}v = 1 - \frac{\Delta_{\text{liq}}}{\Delta_0}\frac{n}{n-1}$. Using also equation (B.5), the ideal gas term in equation (4.37) becomes

$$\mathcal{S}_{\text{IG}} = \frac{d}{2}n\ln\left(\frac{\pi e \sigma^2 \Delta_0}{d^2}\right) + \frac{d}{2}\ln(1 - n) + \frac{d}{2}\ln\left(1 - \frac{\Delta_{\text{liq}}}{\Delta_0}\frac{n}{n-1}\right) . \tag{4.39}$$

For the interaction part, using equation (F.38) and the representation in equation (F.41), we have

$$\mathcal{F}(\Delta_0 vv^{\mathrm{T}} - \Delta_0 I) = e^{-\Delta_0/2}\mathcal{F}(-\Delta_0 I) = e^{-\Delta_0/2}\int \mathrm{d}\lambda\, e^{\lambda}\left\{1 - \frac{1}{(2\pi\Delta_0)^{n/2}}\int_{-\lambda}^{\infty}\mathrm{d}\mu_a e^{-\sum_a \frac{\mu_a^2}{2\Delta_0}}\right\}$$

$$= e^{-\Delta_0/2}\int \mathrm{d}\lambda\, e^{\lambda}\left\{1 - \left(\int_{-\lambda}^{\infty}\mathcal{D}_{\Delta_0}h\right)^n\right\} = e^{-\Delta_0/2}\int \mathrm{d}\lambda\, e^{\lambda}\left\{1 - \Theta\left(\frac{\lambda}{\sqrt{2\Delta_0}}\right)^n\right\} . \tag{4.40}$$

Note that through an integration by parts and a change of variables, we obtain

$$\mathcal{F}(\Delta_0) = n\int \mathcal{D}\lambda\, \Theta\left(\frac{\sqrt{\Delta_0} - \lambda}{\sqrt{2}}\right)^{n-1} , \tag{4.41}$$

---

[5]The value of $q_{ab} = x_a \cdot x_b$ considered here is the average value of the corresponding microscopic quantity, due to saddle-point evaluation, as in §3.8.4.1.

where the function $\Theta(x)$ is defined in Appendix A. This is exactly the replica-symmetric result for $\mathcal{F}$ obtained in [242, equation (40)]. In the limit $n \to 0$ we obtain

$$s_{\mathrm{RS}}(\Delta_0) = \lim_{n \to 0} \frac{\mathcal{S}(\hat{\Delta}_{\mathrm{RS}})}{n} = \frac{d}{2} \ln \left(\frac{\pi \sigma^2 \Delta_0}{d^2} \right) + \frac{d}{2} \frac{\Delta_{\mathrm{liq}}}{\Delta_0} - \frac{d}{2} \widehat{\varphi} \int \mathcal{D}\lambda \, \Theta \left(\frac{\sqrt{\Delta_0} - \lambda}{\sqrt{2}} \right)^{-1} . \tag{4.42}$$

4.4.1.2 Saddle-point equation

The saddle-point equation for Δ_0 is obtained by taking the derivative of equation (4.42). We expect that $\Delta_0 = \Delta_{\mathrm{liq}}$ and we are thus interested in the case where Δ_0 is large. For $\Delta_0 \to \infty$, we have

$$\begin{aligned} \Theta \left(\frac{\sqrt{\Delta_0} - \lambda}{\sqrt{2}} \right) &\sim 1 - \frac{e^{-\frac{1}{2}(\sqrt{\Delta_0} - \lambda)^2}}{\sqrt{2\pi}(\sqrt{\Delta_0} - \lambda)} \,, \\ \frac{1}{n}\mathcal{F}(\Delta_0) &\sim 1 + \int \mathcal{D}\lambda \frac{e^{-\frac{1}{2}(\sqrt{\Delta_0} - \lambda)^2}}{\sqrt{2\pi}(\sqrt{\Delta_0} - \lambda)} = 1 + e^{-\Delta_0/4} \int \frac{d\lambda}{2\pi} \frac{e^{-(\sqrt{\Delta_0}/2 - \lambda)^2}}{\sqrt{\Delta_0} - \lambda} \sim 1 + \sqrt{\frac{1}{\pi\Delta_0}} e^{-\Delta_0/4} \,. \end{aligned} \tag{4.43}$$

We conclude that $\mathcal{F}(\hat{\Delta})/n \to 1$ with corrections exponentially small in Δ_0. It follows that the interaction term is a constant for large Δ_0, and its derivative vanishes exponentially. We therefore obtain

$$0 = \frac{\partial s_{\mathrm{RS}}}{\partial \Delta_0} \propto \frac{1}{\Delta_0} - \frac{\Delta_{\mathrm{liq}}}{\Delta_0^2} + \mathcal{O}(e^{-\Delta_0/4}/\sqrt{\Delta_0}) \,, \tag{4.44}$$

which is solved by $\Delta_0 = \Delta_{\mathrm{liq}}$ in the limit $R \to \infty$ where $\Delta_{\mathrm{liq}} \to \infty$.

4.4.1.3 Thermodynamic entropy

Plugging the result $\Delta_0 = \Delta_{\mathrm{liq}} = 2dR^2/\sigma^2$ in equation (4.39) we obtain

$$\mathcal{S}_{\mathrm{IG}} = \frac{d}{2} n \ln(2\pi e/d) + dn \ln R \sim n \ln(\Omega_{d+1} R^d) = n \ln \mathcal{V} \,. \tag{4.45}$$

Hence, recalling that $\mathcal{F}(\Delta_0 \to \infty) \to 1$, equation (4.37) becomes

$$\mathcal{S}_{\mathrm{RS}} = n \left(\ln \mathcal{V} - \frac{d}{2} \widehat{\varphi} \right) = n\mathcal{S}_{\mathrm{liq}} \,. \tag{4.46}$$

and we recover equation (4.20): the replicated entropy is given by n times the liquid entropy[6] if replicas are decorrelated [279], see also §2.3.

4.4.2 The 1-RSB glass phase

We now repeat the same procedure for a 1-RSB matrix that describes the glass phase in the vicinity of the liquid phase [312, 242], and we show that we recover the results of [312, 243, 242]. The properties of 1-RSB matrices [279], that are parametrized by n and by an additional integer m and by elements Δ_0 and Δ_1, as in the p-spin §2.3.3, are derived in B.2. As an example, for $m = 3$ one has (with n/m blocks):

$$\hat{\Delta} = \begin{pmatrix} \begin{pmatrix} 0 & \Delta_1 & \Delta_1 \\ \Delta_1 & 0 & \Delta_1 \\ \Delta_1 & \Delta_1 & 0 \end{pmatrix} & & \Delta_0 \\ & \ddots & \\ \Delta_0 & & \begin{pmatrix} 0 & \Delta_1 & \Delta_1 \\ \Delta_1 & 0 & \Delta_1 \\ \Delta_1 & \Delta_1 & 0 \end{pmatrix} \end{pmatrix} . \tag{4.47}$$

This amounts to assume that, at high enough density the free energy landscape develops another minimum while the liquid one becomes unstable, somewhat similarly to what happens in the low temperature

---

[6]This might seem surprising since our scaling hypotheses in the derivation of section 4.3 constrain replicas within the same configuration to be close and two particles to be almost at contact, which is not the case in the liquid phase. An explanation for this fact is given in §4.2.5.
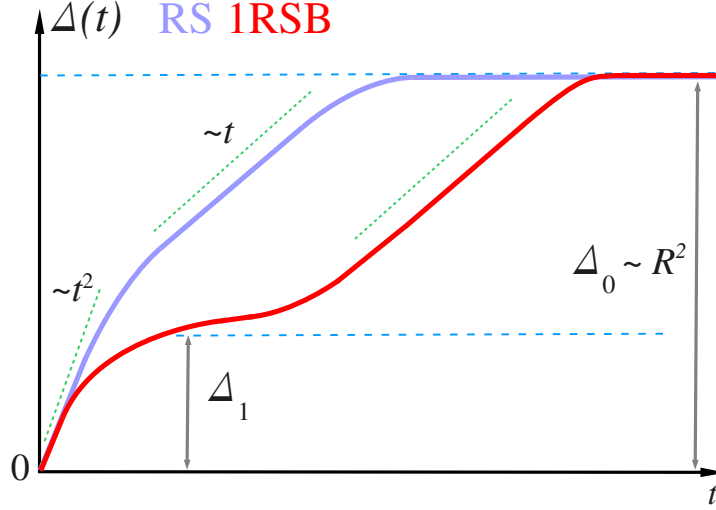
Figure 4.2: Interpretation of the replica-symmetric (RS) and one-step replica-symmetry-breaking (1-RSB) hierarchical matrices in terms of the corresponding dynamical quantity, the scaled mean-square displacement (MSD) $\Delta(t)$. In the liquid phase where the RS solution is stable, the MSD displays the usual ballistic (for inertial dynamics) then diffusive regimes, saturating at the volume of the *box* represented by $\Delta_0 = \Delta_{\text{liq}}$. In the 1-RSB glass phase, the diffusive regime is replaced by an infinite plateau measured by the parameter Δ_1, related to the size of the cage. Before reaching this liquid-glass transition, the plateau develops as a crossover between ballistic and diffusive behaviours.

phase of the Curie-Weiss model, in a *direction* given by the 1-RSB ansatz. The stability of this phase was investigated in [242]; we thus refer to it to prove that this is indeed a correct hypothesis. Dynamically, this means we assume that the time-dependent mean-square displacement has a plateau at intermediate times, corresponding to Δ_1, followed by the true long-time plateau corresponding to Δ_0, as in figure 4.2. The new parameter Δ_1 thus represents the typical size of a cage (scaled by $1/d$), *i.e.* the amplitude of particles vibrations around an amorphous lattice. It is also sometimes called *non-ergodicity factor* because it signals the breaking of ergodicity in the liquid phase: the set of liquid configurations which were previously solution of the problem is now split into many disconnected clusters of glassy configurations [81, 417], see §1.2.4 and figure 1.15.

4.4.2.1 1-RSB entropy

We start by computing $\mathcal{F}(\hat{\Delta}_{1-\text{RSB}})$. Using equations (F.38), (F.41), (B.6), (B.13) and (B.14), and defining $\Delta_{\text{B}} = [m\Delta_0 + (1-m)\Delta_1]/\Delta_1$, we have

$$
\mathcal{F}(\hat{\Delta}_{1-\text{RSB}}) = e^{-\Delta_0/2} \mathcal{F}[(\Delta_1 - \Delta_0)\hat{I}^m - \Delta_1 \hat{I}^1]
$$

$$
= e^{-\Delta_0/2} \int \mathrm{d}\lambda\, e^{\lambda}
$$

$$
\times \left\{ 1 - \frac{1}{(2\pi)^{n/2}\sqrt{\det[(\Delta_0 - \Delta_1)\hat{I}^m + \Delta_1 \hat{I}^1]}} \int_{-\lambda}^{\infty} \mathrm{d}\mu_a e^{\frac{1}{2}\left[\frac{\Delta_0 - \Delta_1}{\Delta_{\text{B}}\Delta_1^2} \sum_B \left(\sum_{a \in B} \mu_a \right)^2 - \frac{1}{\Delta_1} \sum_a \mu_a^2 \right]} \right\}
$$

$$
= e^{-\Delta_0/2} \int \mathrm{d}\lambda\, e^{\lambda} \left\{ 1 - \frac{1}{\Delta_{\text{B}}^{\frac{n}{2m}}} \int_{-\lambda}^{\infty} \mathcal{D}_{\Delta_1}\mu_a \prod_B \int \mathcal{D}z_B e^{\sqrt{\frac{\Delta_0 - \Delta_1}{\Delta_{\text{B}}\Delta_1^2}} z_B \sum_{a \in B} \mu_a} \right\} \tag{4.48}
$$

$$
= e^{-\Delta_0/2} \int \mathrm{d}\lambda\, e^{\lambda} \left\{ 1 - \left[\frac{1}{\sqrt{\Delta_{\text{B}}}} \int \mathcal{D}z \left(\int_{-\lambda}^{\infty} \mathcal{D}_{\Delta_1} h\, e^{\sqrt{\frac{\Delta_0 - \Delta_1}{\Delta_{\text{B}}\Delta_1^2}} zh} \right)^m \right]^{\frac{n}{m}} \right\}
$$

$$
= e^{-\Delta_0/2} \int \mathrm{d}\lambda\, e^{\lambda} \left\{ 1 - \left[\int \mathcal{D}_{\Delta_0 - \Delta_1} z\, \Theta\left(\frac{\lambda - z}{\sqrt{2\Delta_1}} \right)^m \right]^{\frac{n}{m}} \right\},
$$

where the last equality can be proven by a series of changes of variable on z and λ. Therefore we obtain, setting $h \equiv \lambda$ to recover the notations of previous results,

$$\lim_{n \to 0} \frac{\mathcal{F}(\hat{\Delta}_{1-\mathrm{RSB}})}{n} = -\frac{1}{m} e^{-\Delta_0/2} \int \mathrm{d}h \, e^h \ln \left[\int \mathcal{D}_{\Delta_0 - \Delta_1} z \, \Theta \left(\frac{h - z}{\sqrt{2\Delta_1}} \right)^m \right] . \tag{4.49}$$

Finally, in equation (4.37) we plug equations (B.8) and (B.12) and we obtain

$$\begin{aligned}
s_{1-\mathrm{RSB}}(\Delta_0, \Delta_1, m) = \lim_{n \to 0} \frac{\mathcal{S}(\hat{\Delta}_{1-\mathrm{RSB}})}{n} &= \frac{d}{2} \ln(\pi e \sigma^2/d^2) \\
&+ \frac{d}{2} \left[\frac{m-1}{m} \ln \Delta_1 + \frac{1}{m} \ln(m\Delta_0 + (1-m)\Delta_1) - \frac{\Delta_0}{m\Delta_0 + (1-m)\Delta_1} \right] \\
&+ \frac{d}{2} \frac{\Delta_{\mathrm{liq}}}{m\Delta_0 + (1-m)\Delta_1} + \frac{d}{2m} \widehat{\varphi} e^{-\Delta_0/2} \int \mathrm{d}h \, e^h \ln \left[\int \mathcal{D}_{\Delta_0 - \Delta_1} z \, \Theta \left(\frac{h - z}{\sqrt{2\Delta_1}} \right)^m \right] .
\end{aligned} \tag{4.50}$$

4.4.2.2 Saddle point equations

The reasoning is similar to the RS one: we conjecture that Δ_0 is very large at the saddle point level, and we thus expand the entropy for large Δ_0. We have for the interaction term

$$\begin{aligned}
-m \lim_{n \to 0} \frac{\mathcal{F}(\hat{\Delta}_{1-\mathrm{RSB}})}{n} &= e^{-\Delta_0/2} \int \mathrm{d}h \, e^h \ln \left\{ 1 + \int \mathrm{d}z \gamma_{\Delta_0 - \Delta_1}(h - z) \left[\Theta \left(\frac{z}{\sqrt{2\Delta_1}} \right)^m - 1 \right] \right\} \\
&= e^{-\Delta_0/2} \int \mathrm{d}h \, e^h \ln \left\{ 1 + \int \mathrm{d}z \gamma_{\Delta_0 - \Delta_1}(h - z) f(z) \right\} ,
\end{aligned} \tag{4.51}$$

where $f(z) = \Theta \left(\frac{z}{\sqrt{2\Delta_1}} \right)^m - 1$ decays quickly to zero for $z \to \infty$ and to -1 for $z \to -\infty$. As in the RS case, the integral over h is dominated by large values of h, where $\gamma_{\Delta_0 - \Delta_1} \star f(h)$ is small, we can thus expand the logarithm and we obtain, at the leading order for large Δ_0,

$$\begin{aligned}
-m \lim_{n \to 0} \frac{\mathcal{F}(\hat{\Delta}_{1-\mathrm{RSB}})}{n} &= \int \mathrm{d}h \, e^{h - \Delta_0/2} \int \mathrm{d}z \gamma_{\Delta_0 - \Delta_1}(h - z) f(z) \\
&\quad - \frac{1}{2} \int \mathrm{d}h \, e^{h - \Delta_0/2} \left(\int \mathrm{d}z \gamma_{\Delta_0 - \Delta_1}(h - z) f(z) \right)^2 + \cdots \\
&= e^{-\Delta_1/2} \int \mathrm{d}z \, e^z f(z) - \frac{1}{2} e^{-\Delta_0/4} \int \mathrm{d}z \mathrm{d}z' \frac{e^{-\frac{(z-z')^2}{4\Delta_0}}}{\sqrt{4\pi\Delta_0}} e^{\frac{z+z'}{2}} f(z) f(z') + \cdots \\
&= e^{-\Delta_1/2} \int \mathrm{d}z \, e^z \left[\Theta \left(\frac{z}{\sqrt{2\Delta_1}} \right)^m - 1 \right] + \mathcal{O}(e^{-\Delta_0/4}/\sqrt{\Delta_0}) ,
\end{aligned} \tag{4.52}$$

where we see that the corrections have the same scaling than in the RS case.

Combining equations (4.50) and (4.52) we obtain:

$$0 = \frac{\partial s_{1-\mathrm{RSB}}}{\partial \Delta_0} \propto \frac{\Delta_0 - \Delta_{\mathrm{liq}}}{[m\Delta_0 + (1-m)\Delta_1]^2} + \mathcal{O}(e^{-\Delta_0/4}/\sqrt{\Delta_0}) , \tag{4.53}$$

which is again solved by $\Delta_0 = \Delta_{\mathrm{liq}}$ in the limit $R \to \infty$ where $\Delta_{\mathrm{liq}} \to \infty$.

4.4.2.3 Thermodynamic entropy

Plugging the result $\Delta_0 = \Delta_{\mathrm{liq}} = 2dR^2/\sigma^2$ in equation (4.50) and using equation (4.52) we obtain

$$\begin{aligned}
s_{1-\mathrm{RSB}}(\Delta_1, m) &= \frac{d}{2} \ln(\pi e \sigma^2/d^2) + \frac{d}{2} \left[\frac{m-1}{m} \ln \Delta_1 + \frac{1}{m} \ln(m\Delta_{\mathrm{liq}}) \right] \\
&\quad + \frac{d}{2m} \widehat{\varphi} e^{-\Delta_1/2} \int \mathrm{d}z \, e^z \left[\Theta \left(\frac{z}{\sqrt{2\Delta_1}} \right)^m - 1 \right] \\
&= \frac{1}{m} \left\{ \ln V + \frac{d}{2}(m-1) \ln \left(\frac{\pi e \sigma^2 \Delta_1}{d^2} \right) + \frac{d}{2} \ln m + \frac{d}{2} \widehat{\varphi} \int \mathrm{d}z \, e^z \left[\Theta \left(\frac{z + \Delta_1/2}{\sqrt{2\Delta_1}} \right)^m - 1 \right] \right\} ,
\end{aligned} \tag{4.54}$$

which is exactly[7] the result derived in [312, equation (50)]. Taking the derivative with respect to Δ_1 and the limit $m \to 1$ one obtains the equation

$$\frac{1}{\Delta_1} = \frac{\widehat{\varphi}}{2} \int \mathcal{D}\eta \frac{e^{-\frac{1}{2}(\eta+\sqrt{\Delta_1})^2}}{\sqrt{2\pi\Delta_1}} \frac{1}{\Theta[(\eta + \sqrt{\Delta_1})/2]} \ , \tag{4.55}$$

that gives the cage parameter Δ_1 on the equilibrium line [312] and will be useful for future comparison with the dynamic result.

4.4.3   The full-RSB glass phase

It was shown in [242] that for high enough density, the 1-RSB solution is unstable, leading to consider the more general full-RSB formalism in [96]. Therefore, we consider here full-hierarchical replica matrices that describe the Gardner phase (see §4.4.3.4), and we show that in this case we obtain the same results as [96]. Full-RSB matrices are obtained by iterating the procedure that brings from RS to 1-RSB, see §2.3.4.

4.4.3.1   Full-RSB entropy

We have

$$s_{\text{fRSB}} = s_{\text{IG}} + s_{\text{int}} \ . \tag{4.56}$$

For the ideal gas term, plugging equations (B.17) and (B.18) in equation (4.37), we have

$$s_{\text{IG}} = \lim_{n\to 0} \frac{1}{n} \mathcal{S}_{\text{IG}} = \frac{d}{2}\ln(\pi e \sigma^2/d^2) + \frac{d}{2}\left[\ln(\langle\Delta\rangle) - \int_0^1 \frac{dx}{x^2}\ln\left(1 + \frac{[\Delta](x)}{\langle\Delta\rangle}\right) + \frac{\Delta_{\text{liq}} - \Delta(0)}{\langle\Delta\rangle}\right] \ . \tag{4.57}$$

For the interaction term, we start from equation (F.44), which coincides with the result of [96]. We can then follow the derivation of [96], with a slight modification. In fact here we have n replicas and we wish to take the limit $n \to 0$. The function $\Delta(x)$ is parametrized as in [96] but with non-zero $\Delta(0) = \Delta_0$ in the interval $[n, m_0] = [0, m]$. Adapting the results of [96, equation (42)-(46)] to take into account this modification, and using the same notations, we obtain

$$g(1,h) = \gamma_{\Delta_k} \star \theta(h) = \Theta\left(\frac{h}{\sqrt{2\Delta_k}}\right) \ ,$$
$$g(m_i,h) = \gamma_{\Delta_i - \Delta_{i+1}} \star g(m_{i+1},h)^{\frac{m_i}{m_{i+1}}} \ , \qquad i = 0\cdots k-1 \ , \tag{4.58}$$
$$\mathcal{F}(\hat{\Delta}) = e^{-\frac{\Delta_0}{2}} \int_{-\infty}^{\infty} dh\, e^h \left\{1 - g(m_0,h)^{\frac{n}{m_0}}\right\} \ .$$

Therefore the interaction term becomes (recall that $m_0 = m$):

$$\begin{aligned}
s_{\text{int}} &= -\frac{d}{2}\widehat{\varphi}\lim_{n\to 0}\frac{1}{n}\mathcal{F}(\hat{\Delta}) = \frac{d}{2m_0}\widehat{\varphi}e^{-\frac{\Delta_0}{2}}\int_{-\infty}^{\infty} dh\, e^h \ln g(m_0,h) \\
&= \frac{d}{2m_0}\widehat{\varphi}e^{-\frac{\Delta_0}{2}}\int_{-\infty}^{\infty} dh\, e^h \ln\left[\gamma_{\Delta_0-\Delta_1} \star g(m_1,h)^{\frac{m_0}{m_1}}\right] \\
&= \frac{d}{2m}\widehat{\varphi}e^{-\frac{\Delta_0}{2}}\int_{-\infty}^{\infty} dh\, e^h \ln\left\{1 + \int dz\, \gamma_{\Delta_0-\Delta_1}(h-z)\left[g(m_1,z)^{\frac{m}{m_1}} - 1\right]\right\} \ .
\end{aligned} \tag{4.59}$$

In the continuum limit $m_i = x - dx$ and $m_{i+1} = x$, (4.58) gives a nonlinear partial differential equation for $g(x,h)$. Remarkably enough [96], it is the same, once expressed in terms of $f(x,h) = \frac{1}{x}\ln g(x,h)$, as the Parisi equation for the free energy density derived in the full-RSB glass phase of the SK model [358, 279, 135, 307] (except for the boundary conditions).

---

[7]With two small differences. First, in [312] the entropy of m replicas was computed, while here we divided the entropy by n, hence we computed the entropy per replica. This explains the additional factor $1/m$ in front of the entropy. For a more detailed discussion, see §G. Second, we should keep in mind that to obtain the correct result in absence of random rotations we should take into account that particles are identical, which introduces an additional factor of $N!$, see §4.2.3.
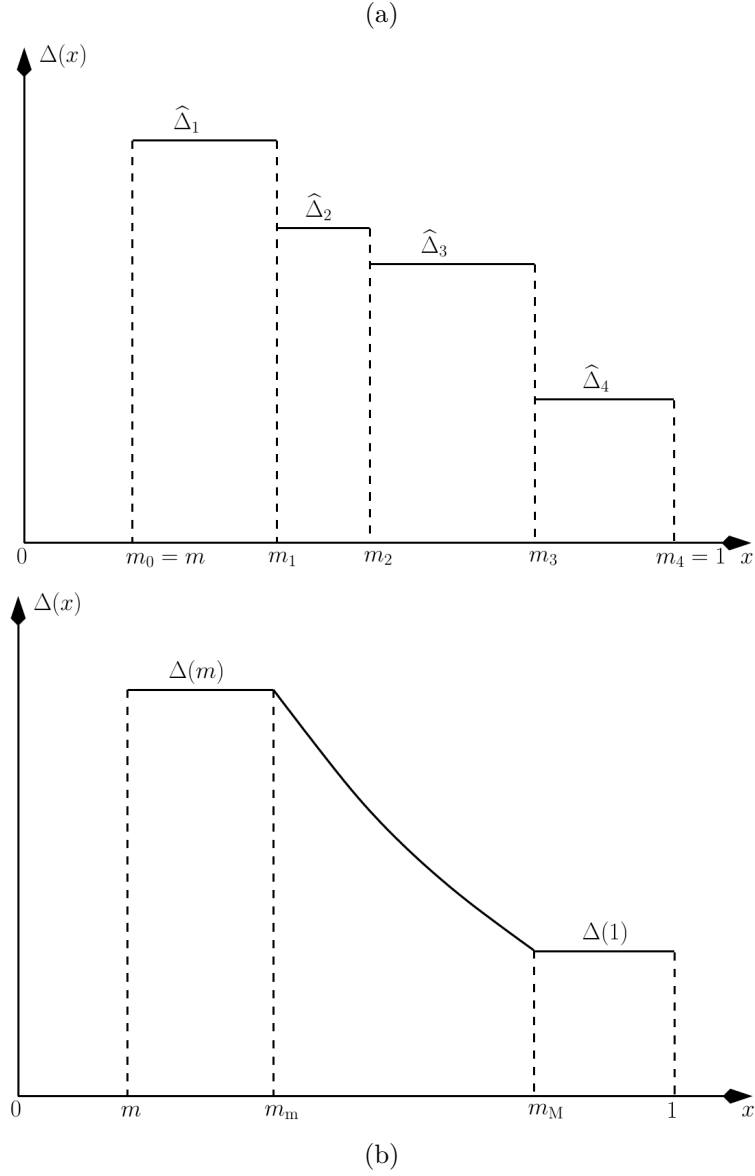
(a)

(b)

Figure 4.3: (a) An example of the parametrization of the matrix $\hat{\Delta}$ for a 4RSB case. (b) The expected form of the function $\Delta(x)$ in the ∞-RSB limit. The value on $[0, m]$ is $\Delta(0) = \Delta_0$ and corresponds to Δ_{liq}. [*Reprinted from* [96]]

4.4.3.2 Saddle point equations

Like in the previous discussions, we conjecture that at the saddle point level $\Delta(x) = \Delta(0) = \Delta_0 \to \infty$ for $0 < x < m$, while $\Delta(x)$ remains finite for $R \to \infty$ when $m < x < 1$. In the ideal gas term, we have $[\Delta](x) = 0$ for $0 < x < m$, and $\langle \Delta \rangle = m\Delta_0 + \int_m^1 \mathrm{d}x \Delta(x) = m\Delta_0 + \langle \Delta \rangle_m$. We can also write

$$\langle \Delta \rangle + [\Delta](x) = x\Delta(x) + \int_x^1 \mathrm{d}y \, \Delta(y) \, , \tag{4.60}$$

which remains therefore finite for $m < x < 1$. Then we get at the leading order for $\Delta_0 \to \infty$

$$s_{\text{IG}} = \frac{d}{2} \ln(\pi e \sigma^2/d^2) + \frac{d}{2} \left[\frac{1}{m} \ln (m\Delta_0) - \int_m^1 \frac{\mathrm{d}x}{x^2} \ln \left(x\Delta(x) + \int_x^1 \mathrm{d}y \, \Delta(y) \right) + \frac{\Delta_{\text{liq}} - \Delta_0}{m\Delta_0} \right] . \tag{4.61}$$

In the interaction term, for $\Delta_0 \to \infty$, the integral over h in equation (4.59) is dominated by large values of h. At large h, we have that $\int \mathrm{d}z \, \gamma_{\Delta_0 - \Delta_1}(h - z) \left[g(m_1, z)^{\frac{m}{m_1}} - 1 \right]$ is small so we can expand the logarithm

and we obtain

$$
\begin{aligned}
s_{\text{int}} &= \frac{d}{2m}\widehat{\varphi}e^{-\frac{\widehat{\Delta}_0}{2}} \int_{-\infty}^{\infty} \mathrm{d}h\, e^h \int \mathrm{d}z\, \gamma_{\widehat{\Delta}_0-\widehat{\Delta}_1}(h-z) \left[g(m_1,z)^{\frac{m}{m_1}} - 1 \right] \\
&= -\frac{d}{2m}\widehat{\varphi}e^{-\frac{\widehat{\Delta}_1}{2}} \int \mathrm{d}z\, e^z \left[1 - g(m_1,z)^{\frac{m}{m_1}} \right] \ .
\end{aligned}
\tag{4.62}
$$

Because the interaction term has a finite limit for $\Delta_0 \to \infty$, its derivative with respect to Δ_0 must go to zero in that limit. Then we have, at the leading order in Δ_0

$$
\frac{\partial s_{\text{fRSB}}}{\partial \Delta_0} = \frac{\partial s_{\text{IG}}}{\partial \Delta_0} = \frac{1}{m\Delta_0} - \frac{\Delta_{\text{liq}}}{m\Delta_0^2} = 0 \ ,
\tag{4.63}
$$

which implies that $\Delta_0 = \Delta_{\text{liq}} = 2dR^2/\sigma^2$.

4.4.3.3 Thermodynamic entropy

Plugging the result $\Delta_0 = \Delta_{\text{liq}} = 2dR^2/\sigma^2$ in equation (4.61), we get

$$
\begin{aligned}
s_{\text{IG}} &= \frac{d}{2}\ln(\pi e\sigma^2/d^2) + \frac{d}{2}\left[\frac{1}{m}\ln\left(2mdR^2/\sigma^2\right) - \int_m^1 \frac{\mathrm{d}x}{x^2} \ln\left(x\Delta(x) + \int_x^1 \mathrm{d}y\, \Delta(y) \right) \right] \\
&= \frac{1}{m}\left[\ln V + \frac{d}{2}(m-1)\ln(\pi e\sigma^2/d^2) + \frac{d}{2}\ln m - \frac{dm}{2}\int_m^1 \frac{\mathrm{d}x}{x^2} \ln\left(x\Delta(x) + \int_x^1 \mathrm{d}y\, \Delta(y) \right) \right] \ .
\end{aligned}
\tag{4.64}
$$

and adding the interaction term given in equation (4.62) we obtain

$$
\begin{aligned}
s_{\text{fRSB}} &= \frac{1}{m}\Bigg\{ \ln V + \frac{d}{2}(m-1)\ln(\pi e\sigma^2/d^2) + \frac{d}{2}\ln m - \frac{dm}{2}\int_m^1 \frac{\mathrm{d}x}{x^2} \ln\left(x\Delta(x) + \int_x^1 \mathrm{d}y\, \Delta(y) \right) \\
&\quad - \frac{d}{2}\widehat{\varphi}e^{-\frac{\widehat{\Delta}_1}{2}} \int \mathrm{d}z\, e^z \left[1 - g(m_1,z)^{\frac{m}{m_1}} \right] \Bigg\} \ .
\end{aligned}
\tag{4.65}
$$

This is exactly[8] the result reported in [96, section 3.4].

4.4.3.4 Physical interpretation: the Gardner phase

The transition from the 1-RSB *normal* glass phase, described by disconnected basins (pure states) of the free energy, to a full-RSB *marginal* glass phase, also called *Gardner* phase, was first described by Gardner [171] and Gross-Kanter-Sompolinsky [193] in the context of spin glasses.

At this transition, the basins of the 1-RSB glass phase become unstable and each one breaks down into a collection of sub-basins. We henceforth call the basin a *metabasin*. This means that basins form within this basin, characterized by another typical MSD $\Delta_2 < \Delta_1$, which physically measures the size of a certain type of *global* cages in the amorphous configuration (this interpretation is clearer in figure 4.4). These sub-basins themselves break into sub-sub-basins characterized by $\Delta_3 < \Delta_2$, and so on up to k-RSB sub-basins of MSD Δ_k. The full-RSB solution consists in the limit $k \to \infty$ where the spacing between two successive MSD Δ_k and Δ_{k+1} becomes infinitesimal and the structure of basins is described by the continuous Parisi function $\Delta(x)$. In the case of HS, this continuous fracturation of basins has been referred to as a *fractal* free energy landscape [97] due to this infinitely iterated structure which gives rise to a fractal dimension of the free energy (or rather entropy for HS) landscape close to the jamming transition where the innermost basin width measured by a MSD $\Delta(1)$ goes to zero as a power law with the reduced pressure $\Delta(1) \sim p^{-\kappa}$. This is measured by the growth of the typical entropy s_{typ} as a function of the MSD between configurations in the sub-basins. It is indeed found to scale as $s_{\text{typ}} \sim \sqrt{\Delta}^{2/\kappa}$ with the fractal dimension $2/\kappa = 1.41267\ldots$.

We refer to figure 4.4 and [98] for the following interpretation. In the liquid phase the system is ergodic and the whole phase space is reached by the system. Particles are not caged. At the first static glass transition to the normal glass phase (1-RSB), the phase space splits in exponentially many disconnected

---

[8]With the same small difference already noted for the 1-RSB case.

basins, ergodicity is broken so that the system remains in one of these basins forever. The particles are caged, giving rise to an infinite plateau in the MSD; the diffusive behaviour is suppressed. The size of the cage is measured by the plateau value Δ_1. The packing is an amorphous lattice but particles vibrate around their position, reaching all the many different local configurations of the basin they are in. Configurations of two different basins have a large relative MSD (measured by Δ_{ab}, $a \neq b$) given by Δ_{liq}, hence corresponding to very large rearrangement of the packing. At the Gardner transition each basin becomes a metabasin as mentioned above. By going from innermost sub-basins to innermost sub-basins the system vibrates slightly around an amorphous lattice. Then going to outer sub-basins the system slowly modifies this amorphous lattice, and is progressively able to reach similar lattices than the ones reached in the normal glass phase. The amplitudes of vibrations of spheres thus fluctuate a lot and are correlated over large regions. Considering the MSD, these events trigger a (continuous) sequence of plateaus which results in a continuous increase of the MSD as time goes by, up to Δ_1.
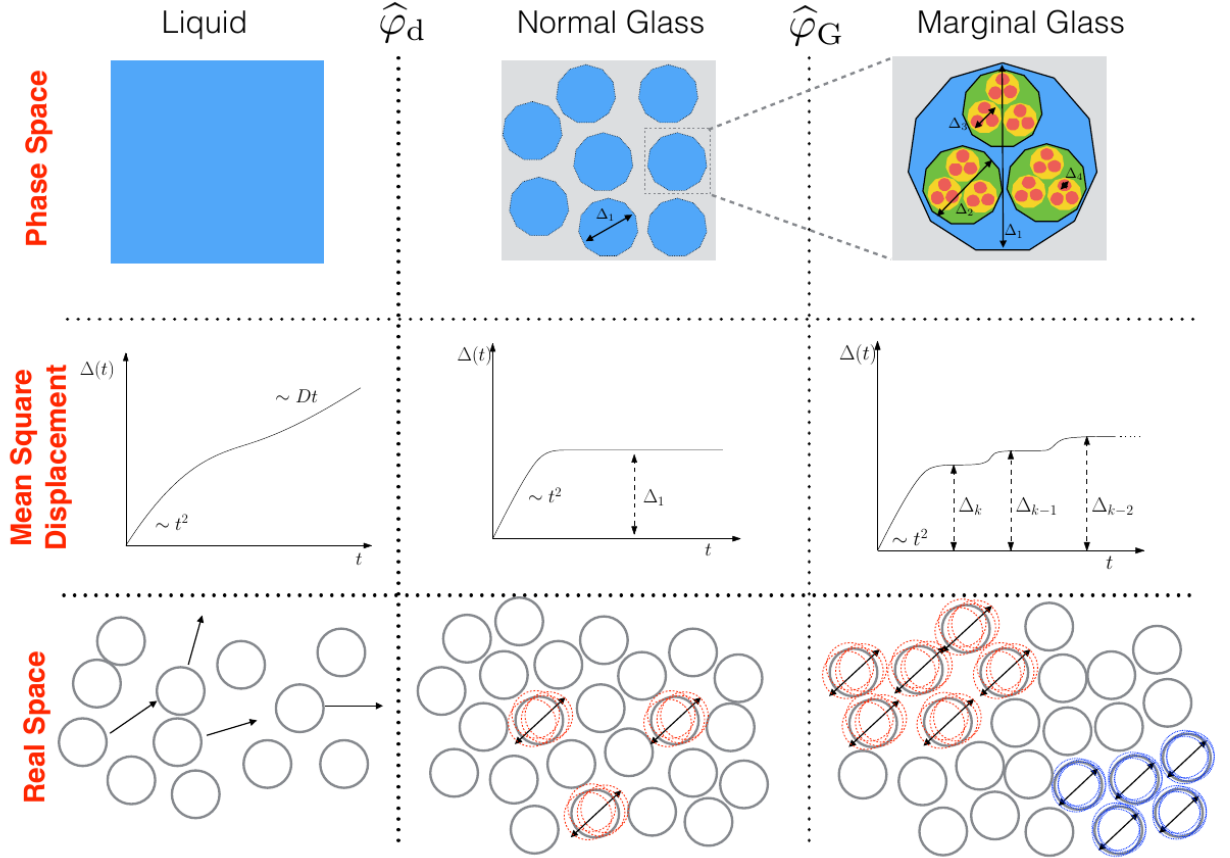

Figure 4.4: The liquid (first column), normal (second column) and marginal (third column) phases of HS and their phase space (top), dynamical (middle) and real space structural (bottom) interpretations, commented in this section. [*Reprinted from* [98]]

The Gardner phase is relevant to investigate the jamming transition, which is a crucial outcome of the theory for the HS potential, see §1.5. A phase diagram is in figure 4.5. For thermal systems, it should exist in a restricted part of the (T, ρ) phase diagram containing a $T = \infty$ half-line (with large enough density) and continuing to some extent at finite temperature [98].

More details about the physical properties of this phase can be found in [279, 242, 96, 97, 98]. It was confirmed numerically in the MK model [94], see also the investigation of the jamming transition §1.5 and [92].

4.4.4 Relation with previous works

Having explained the mathematical structure of the MSD matrix Δ_{ab} in the different phases of the system, let us give some additional comments on the relation with previous work. Note that for a dynamic calculation (see chapter 3), this is just the MSD in time of a particle, averaged over particles

(figure 4.2). For the static calculation, the formalism leads to considering distances between different replicas. As usual in the replica trick, the total number of replicas tends to zero to take the average over the disorder. In the case in which the system is solved by a 1-RSB ansatz as in equation (4.47), the replicas are grouped in *blocks*, and all the replicas of a block may be pictured as constituting a *molecule* [284, 283], albeit with non-integer number of elements. If, as it happens at the highest densities or lowest temperature, the ansatz is full-RSB, then one may see the system as being made of molecules, and molecules of molecules, and so on [96]. It must be however born in mind that this is an evocative way of picturing Parisi's ultrametric solution (see §2.3.4), and it involves no extra assumption.

In previous work that used the replica scheme [284, 283, 312, 325], the problem was simplified by using the so-called Monasson [288] or Franz-Parisi [156] approaches. In these approaches, which are particularly efficient for systems without quenched disorder, one couples the replicas to a reference system, in such a way that the replicas are always correlated. Mathematically, this corresponds to eliminating the outermost block of the ultrametric ansatz, corresponding to the element Δ_0 in equation (4.47). This decoupling is explicitly seen in appendix G, that is not inserted here for concision. The problem is simplified because then all the elements of the replicated matrix Δ_{ab} remain finite in the termodynamic limit: particles remain confined into *molecules* and one can use molecular liquid methods to solve the problem [284, 283, 312].

This approach is however not efficient if one wishes to study the dynamics in the liquid phase: in fact, the value of Δ_0 corresponds to the long-time limit of the MSD in the liquid phase (figure 4.2). Therefore, if one wishes to establish clearly the parallel between the static and dynamic treatments, one needs to keep the outermost block in the replica structure. However, this corresponds to decorrelated replicas that have therefore a diverging MSD in the thermodynamic limit. In fact, we found above that $\Delta_0 \sim \Delta_{\text{liq}} \to \infty$ in the thermodynamic limit.

The advantage of the present derivation is that it makes no assumptions about the existence of molecules, and it allows one to treat a general structure of Δ_{ab} including finite or diverging matrix elements. In this way we can at the same time reproduce previous results, and extend them to include a complete relation with long-time dynamics in the liquid phase.

4.5   Saddle-point equation for the order parameter

In this section we will derive and discuss the equation for the order parameter $\hat{\Delta}$ without making any assumption on its structure. While this is not very interesting for thermodynamics, where we already know that $\hat{\Delta}$ is a hierarchical matrix (section 4.4), it is interesting for a direct comparison with dynamics. We will obtain the following results.

1. The saddle-point equation for $\hat{\Delta}$ can be written in a form that has the same algebraic structure as a Mode-Coupling (MCT) equation, equation (4.74), and involves a memory kernel $\hat{M}$ (section 4.5.1).

2. The kernel $\hat{M}$ that enters in the MCT equation has a microscopic interpretation in terms of a force-force correlation or stress-stress correlation between replicas, as in the dynamics, and gives the shear modulus of the glass (section 4.5.2).

3. In the MCT equation we will introduce a Lagrange multiplier to enforce the spherical constraint, and we will get its expression from replicas, equation (4.91). This will be useful for comparison with dynamics.

4. We will show that the MCT equation, plugging a 1-RSB structure for $\hat{\Delta}$ and taking the limit $m \to 1$, in which Δ_1 corresponds to the equilibrium non-ergodicity factor [81], gives the same equation as the 1-RSB computation of section 4.4 (section 4.5.4).

These results will be compared with the dynamical results of chapter 3.

4.5.1   Derivation of the saddle-point equation

Before deriving the saddle-point equation we write the replicated entropy in equation (4.37) using the representation in equation (4.35) with $A = \Delta_{\text{liq}}$. We obtain, neglecting irrelevant constant terms in the

entropy

$$\mathcal{S}(\hat{\Delta}) = \frac{d}{2}\ln\det(-\hat{\Delta}) + \frac{d}{2}\ln\left(1 - \Delta_{\text{liq}}v^{\text{T}}\hat{\Delta}^{-1}v\right) - \frac{d\widehat{\varphi}}{2}\mathcal{F}(\hat{\Delta}) \ ,$$

$$\mathcal{F}(\hat{\Delta}) = -e^{-\Delta_{\text{liq}}/2}\int \mathcal{D}_{\Delta_{\text{liq}}vv^{\text{T}}-\hat{\Delta}}\,\bar{\mu}\,\Psi(\bar{\mu}) \ , \qquad \Psi(\bar{\mu}) = \int d\lambda\, e^{\lambda}\left(-1 + e^{-\beta\sum_{a=1}^{n}\bar{V}(\mu_a+\lambda)}\right) \ . \tag{4.66}$$

The advantage of this formulation is that the correlations of the μ_a are well defined. In fact, $\langle\mu_a\mu_b\rangle = \Delta_{\text{liq}} - \Delta_{ab} \geqslant 0$. For convenience we can also express the entropy in terms of an overlap matrix

$$Q_{ab} = \Delta_{\text{liq}} - \Delta_{ab} = \frac{2d}{\sigma^2}\langle x_a \cdot x_b\rangle \tag{4.67}$$

The matrix $\hat{Q}$ is determined by $\partial\mathcal{S}/\partial Q_{ab} = 0$ for $a < b$ (the matrix is symmetric and the diagonal elements are $Q_{aa} = \Delta_{\text{liq}}$). However we assume a general form for $\hat{Q}$ and add a Lagrange multiplier term $\nu\sum_a Q_{aa}$ to $\mathcal{S}$ in order to impose the constraint[9] on the diagonal elements. We obtain a very simple expression:

$$\mathcal{S}(\hat{Q}) = \frac{d}{2}\ln\det\hat{Q} - \frac{d}{2}\widehat{\varphi}\mathcal{F}(\hat{Q}) - \frac{d}{2}\beta\nu\sum_a Q_{aa} \ , \qquad \mathcal{F}(\hat{Q}) = -e^{-\Delta_{\text{liq}}/2}\int \mathcal{D}_{\hat{Q}}\bar{\mu}\,\Psi(\bar{\mu}) \ . \tag{4.68}$$

The matrix $\hat{Q}$ is now determined by $\forall(a,b)$, $\partial\mathcal{S}/\partial Q_{ab} = 0$. Using the relations $\frac{\partial}{\partial Q_{ab}}\ln\det\hat{Q} = Q_{ba}^{-1}$ and $\frac{\partial Q_{cd}^{-1}}{\partial Q_{ab}} = -Q_{ca}^{-1}Q_{bd}^{-1}$, we obtain

$$0 = Q_{ab}^{-1} - \beta\nu\delta_{ab} - \widehat{\varphi}\frac{\partial\mathcal{F}}{\partial Q_{ab}} \ , \qquad \frac{\partial\mathcal{F}}{\partial Q_{ab}} = \frac{1}{2}Q_{ab}^{-1}e^{-\Delta_{\text{liq}}/2}\int \mathcal{D}_{\hat{Q}}\bar{\mu}\,\Psi(\bar{\mu}) - \frac{1}{2}e^{-\Delta_{\text{liq}}/2}\sum_{cd}Q_{ac}^{-1}\int \mathcal{D}_{\hat{Q}}\bar{\mu}\,\Psi(\bar{\mu})\,\mu_c\mu_d\,Q_{db}^{-1} \ . \tag{4.69}$$

This equation can be simplified by observing that, by integration by parts:

$$\sum_{cd}Q_{ac}^{-1}\int \mathcal{D}_{\hat{Q}}\bar{\mu}\,\mu_c\mu_d e^{-\beta\sum_{a=1}^{n}\bar{V}(\mu_a+\lambda)}\,Q_{db}^{-1} = \int d\bar{\mu}\,\frac{e^{-\beta\sum_{a=1}^{n}\bar{V}(\mu_a+\lambda)}}{(2\pi)^{n/2}\sqrt{\det(\hat{Q})}}\left(\frac{\partial^2}{\partial\mu_a\partial\mu_b} + Q_{ab}^{-1}\right)e^{-\frac{1}{2}\bar{\mu}^T\hat{Q}^{-1}\bar{\mu}}$$

$$= \int \mathcal{D}_{\hat{Q}}\bar{\mu}\left(\frac{\partial^2}{\partial\mu_a\partial\mu_b} + Q_{ab}^{-1}\right)e^{-\beta\sum_{a=1}^{n}\bar{V}(\mu_a+\lambda)} \ . \tag{4.70}$$

Using this relation (and the same relation with $\bar{V} = 0$) we obtain[10]

$$\sum_{cd}Q_{ac}^{-1}\int \mathcal{D}_{\hat{Q}}\bar{\mu}\,\Psi(\bar{\mu})\,\mu_c\mu_d\,Q_{db}^{-1} = Q_{ab}^{-1}\int \mathcal{D}_{\hat{Q}}\bar{\mu}\,\Psi(\bar{\mu}) + \int d\lambda\, e^{\lambda}\int \mathcal{D}_{\hat{Q}}\bar{\mu}\,\frac{\partial^2}{\partial\mu_a\partial\mu_b}e^{-\beta\sum_{a=1}^{n}\bar{V}(\mu_a+\lambda)} \tag{4.71}$$

and defining $F(\mu) = -\bar{V}'(\mu)$ we get:

$$\frac{\partial\mathcal{F}}{\partial Q_{ab}} = -\frac{1}{2}\left\langle\beta^2 F(\mu_a+\lambda)F(\mu_b+\lambda) + \beta F'(\mu_a+\lambda)\delta_{ab}\right\rangle_V = \frac{1}{\widehat{\varphi}}\left[-\beta^2 M_{ab} + \beta\delta\nu_a\delta_{ab}\right] \ ,$$

$$\langle\mathcal{O}\rangle_V = \int d\lambda\, e^{\lambda-\Delta_{\text{liq}}/2}\int \mathcal{D}_{\hat{Q}}\bar{\mu}\, e^{-\beta\sum_{a=1}^{n}\bar{V}(\mu_a+\lambda)}\,\mathcal{O} \ , \tag{4.72}$$

where we defined

$$M_{ab} = \frac{\widehat{\varphi}}{2}\left\langle F(\mu_a+\lambda)F(\mu_b+\lambda)\right\rangle_V \ , \qquad \delta\nu_a = -\frac{\widehat{\varphi}}{2}\left\langle F'(\mu_a+\lambda)\right\rangle_V \ . \tag{4.73}$$

Then equation (4.69) takes the form

$$0 = Q_{ab}^{-1} + \beta^2 M_{ab}(\hat{Q}) - \beta(\nu+\delta\nu_a)\delta_{ab} \ , \qquad \Leftrightarrow \qquad 0 = \delta_{ab} + \beta^2\sum_c M_{ac}(\hat{Q})Q_{cb} - \beta(\nu+\delta\nu_a)Q_{ab} \ . \tag{4.74}$$

Written in this form, the saddle-point equation for Q is manifestly similar to the exact dynamic equations that are the basis of Mode-Coupling Theory [187]: roughly, one has $\hat{Q} \sim \hat{M}(\hat{Q})\hat{Q}$, where $\hat{M}(\hat{Q})$ is the analog of the memory kernel (this appears more clearly in §3.4.3.3). Mode-Coupling Theory amounts to a polynomial approximation $M_{ab}(\hat{Q}) \sim Q_{ab}^2$, which is exact for some spin glass models [81]; while here we obtain a more complicated form for $\hat{M}$.

---

[9]As in the dynamics, since for each replica $x_a^2 = R^2$ must be enforced, ν should depend upon the replica index and the Lagrange term should thus read $\sum_a \nu_a Q_{aa}$, but this does not matter for RS and 1-RSB computations we focus on here (and could be easily modified).

[10]This is the same computation as in the dynamical counterpart §3.4.3.1.

4.5.2 A microscopic expression of the memory kernel: force-force, stress-stress correlations, and the shear modulus

We now provide a microscopic interpretation of the memory kernel.

4.5.2.1 Force-force correlation

First, we wish to show that M_{ab} is related to the correlation of inter-particle forces. Using equation (4.31), we have:

$$
\begin{aligned}
F_{ab} &= \frac{\sigma^2}{2d^3N} \sum_{i \neq j} \left\langle \nabla V(|x_i^a - x_j^a|) \cdot \nabla V(|x_i^b - x_j^b|) \right\rangle \\
&= \frac{N\sigma^2}{2d^3} \int d\bar{x} d\bar{y}\, \rho(\bar{x})\rho(\bar{y}) \prod_c e^{-\beta V(|x^c - y^c|)} \nabla V(|x^a - y^a|) \cdot \nabla V(|x^b - y^b|) .
\end{aligned}
$$
(4.75)

For large d we have $x^a - y^a = X + \mathcal{O}(1/d)$ with $|X| = \sigma$. Also when we use equation (4.35) we have to compute the function f in $|x^a - y^a| = \sigma(1 + \mu_a/d + \lambda/d)$. Thus at leading order $\frac{(x^a - y^a)\cdot(x^b - y^b)}{|x^a - y^a||x^b - y^b|} = \frac{X\cdot X}{\sigma^2} = 1$, and $v'(|x^a - y^a|) = (d/\sigma)\bar{V}'(\lambda + \mu_a)$ according to equation (3.4). We obtain

$$
\nabla V(|x^a - y^a|) \cdot \nabla V(|x^b - y^b|) = V'(|x^a - y^a|)V'(|x^b - y^b|)\frac{(x^a - y^a)\cdot(x^b - y^b)}{|x^a - y^a||x^b - y^b|} \sim \left(\frac{d}{\sigma}\right)^2 \bar{V}'(\lambda + \mu_a)\bar{V}'(\lambda + \mu_b) .
$$
(4.76)

Finally using equation (4.35) with $A = \Delta_{\text{liq}}$ we obtain

$$
F_{ab} = \frac{\widehat{\varphi}}{2} e^{-\Delta_{\text{liq}}/2} \int \mathcal{D}_{\hat{Q}}\bar{\mu} \, d\lambda \, e^{\lambda} \prod_c e^{-\beta\bar{V}(\lambda + \mu_c)} \bar{V}'(\lambda + \mu_a)\bar{V}'(\lambda + \mu_b) = \frac{\widehat{\varphi}}{2} \left\langle F(\mu_a + \lambda)F(\mu_b + \lambda) \right\rangle_V = M_{ab} .
$$
(4.77)

Therefore the kernel that enters in equation (4.69) is also the microscopic force-force correlation.

4.5.2.2 Stress-stress correlation

We can take another step and compute the stress-stress correlation, following [413, 414]. Note that in this derivation we neglect the kinetic component of the stress tensor [199]: we do this to simplify the computations, and because this component remains small in the glass transition regime. According[11] to [413, equations (136)-(138)], we define respectively the Born term B_a, the replicated stress-stress correlation Σ_{ab} and the potential part of the stress tensor at zero wavevector σ_{ij}^a evaluated at $x = x_i^a - x_j^a$

$$
B_a = \frac{1}{dN} \sum_{i<j} \langle b_{ij}^a \rangle , \qquad b_{ij}^a = \{\hat{x}_1^2[|x|^2 v''(|x|)\hat{x}_2^2 + |x|V'(|x|)(1 - \hat{x}_2^2)]\}_{x = x_i^a - x_j^a} ,
$$
(4.78)

and

$$
\begin{aligned}
\Sigma_{ab} &= \frac{1}{dN} \sum_{i<j,k<l} [\langle \sigma_{ij}^a \sigma_{kl}^b \rangle - \langle \sigma_{ij}^a \rangle\langle \sigma_{kl}^b \rangle] = \frac{1}{dN} \sum_{i<j,k<l} \langle \sigma_{ij}^a \sigma_{kl}^b \rangle \sim \frac{1}{dN} \sum_{i<j} \langle \sigma_{ij}^a \sigma_{ij}^b \rangle , \\
\sigma_{ij}^a &= [|x|V'(|x|)\hat{x}_1\hat{x}_2]_{x = x_i^a - x_j^a} ,
\end{aligned}
$$
(4.79)

where $\hat{x} = x/|x|$, and $\hat{x}_\mu$ are its spatial components. By isotropy the stress tensor for two directions $\mu \neq \nu$ is the same as the one written here for directions 1,2. Here we used that $\langle \sigma_{ij}^a \rangle = 0$ again by isotropy and that in $d \to \infty$ only the terms with $i = j$ and $k = l$ contribute to Σ_{ab} (see [414, Appendix A] and §3.8.4.3 for a more detailed discussion). Physically it is related to the tree-like structure of the interactions as emphasized in sections 4.1 and 4.2. From B_a and Σ_{ab} we obtain the shear modulus matrix[12]

$$
\widehat{\mu}_{ab} = \frac{\mu_{ab}}{d} = B_a \delta_{ab} - \beta\Sigma_{ab} .
$$
(4.80)

The formula (4.80) is a hierarchical version of the static fluctuation formula of the rigidity [366], coming from a second-order expansion of the replicated free energy under a simple shear of the system along some direction, quantified by the shear strain γ_a (one for each replica). This expansion reads

$$
F(\{\gamma_a\}) = F(\{0\}) + \sum_a \sigma_a \gamma_a + \frac{1}{2} \sum_{a,b} \mu_{ab}\gamma_a\gamma_b + \dots
$$
(4.81)

---

[11]Note that there is a typo in the factors of N in [413]; the correct ones are given here.
[12]The name μ is standard in the literature, and is not to be confused with the $O(1/d)$ replica displacement fluctuations.

where σ_a is the replicated stress, as in standard elasticity theory [245]. Indeed, the hierarchical RFOT picture of the free energy landscape implies a hierarchy of rigidities in the system [413, 414]. The Born term [68] represents the affine response of the system against shear, which is finite even in simple liquids. The second term is the non-affine correction term due to stress relaxations. The hierarchical structure may reflect experimental data displaying a discontinuous jump of the shear modulus at the glass transition, and its critical behavior around the jamming point [414].

Following the same reasoning that leads to equation (4.76), and observing that on average, $\hat{X}_1^2 = \hat{X}_2^2 \sim 1/d$, we obtain

$$b_{ij}^a \sim \frac{1}{d}\left[\frac{\sigma^2}{d}v''(|x^a - y^a|) + \sigma V'(|x^a - y^a|)\right] = \bar{V}''(\lambda + \mu_a) + \bar{V}'(\lambda + \mu_a)$$

$$\sigma_{ij}^a \sigma_{ij}^b \sim \sigma^2 \hat{X}_1^2 \hat{X}_2^2 V'(|x^a - y^a|)V'(|x^b - y^b|) \sim \frac{\sigma^2}{d^2} V'(|x^a - y^a|)V'(|x^b - y^b|) \sim \bar{V}'(\lambda + \mu_a)\bar{V}'(\lambda + \mu_b) \ .$$

$$(4.82)$$

Then performing similar steps as in section 4.5.2.1, we arrive to

$$B_a = -\frac{\widehat{\varphi}}{2}\left\langle F(\mu_a + \lambda) + F'(\mu_a + \lambda)\right\rangle_V = \beta \sum_b M_{ab} \ ,$$

$$\Sigma_{ab} = \frac{\widehat{\varphi}}{2}\left\langle F(\mu_a + \lambda)F(\mu_b + \lambda)\right\rangle_V = M_{ab} \ ,$$

$$(4.83)$$

where the relation $B_a = \sum_b M_{ab}$ is obtained through a simple integration by parts on λ. Therefore, the stress-stress correlation coincides, in $d \to \infty$, with the force-force correlation, and both coincide with M_{ab}, as in the dynamics (§3.8.4). Finally, for the shear modulus we obtain

$$\beta\widehat{\mu}_{ab} = \delta_{ab}\sum_{c(\neq a)}\beta^2 M_{ac} - (1 - \delta_{ab})\beta^2 M_{ab} \ .$$

$$(4.84)$$

Recalling that from equation (4.69) we have for $a \neq b$ that $\beta^2 M_{ab} = \widehat{\varphi}\frac{\partial\mathcal{F}}{\partial\Delta_{ab}}$, this result coincides[13] with the one in [414, Eq.(15)]. We refer to [414] for a discussion of the physical consequences of this result.

4.5.3 Replica symmetric solution

4.5.3.1 Product measure

In the liquid phase, the solution to this equation is $Q_{ab} = \Delta_{\text{liq}}\delta_{ab} + Q_0(1 - \delta_{ab})$ where $Q_0 = \Delta_{\text{liq}} - \Delta_0$. We already know that Q_0 is exponentially small in the limit $\Delta_{\text{liq}} \to \infty$ (section 4.4.1.2), we therefore consider for simplicity a RS solution with $Q_{ab} = \Delta_{\text{liq}}\delta_{ab}$ and $Q_{ab}^{-1} = \delta_{ab}/\Delta_{\text{liq}}$. In this case the measure in equation (4.72) becomes a product measure and defining

$$H_0(\mu, \lambda) = \bar{V}(\mu + \lambda) + \frac{T\mu^2}{2\Delta_{\text{liq}}} \ , \qquad \mathcal{Z}_0(\lambda) = \int d\mu\, e^{-\beta H_0(\mu,\lambda)} \ ,$$

$$(4.85)$$

we obtain for some observable $\mathcal{O}$ when $n \to 0$:

$$\langle\mathcal{O}(\mu_a)\rangle_V = \int d\lambda\, e^{\lambda - \Delta_{\text{liq}}/2}\int d\mu\, e^{-\beta H_0}\mathcal{O}(\mu)\left(\int d\mu\, e^{-\beta H_0}\right)^{n-1}$$

$$= \int d\lambda\, e^{\lambda - \Delta_{\text{liq}}/2}\frac{1}{\mathcal{Z}_0}\int d\mu\, e^{-\beta H_0}\mathcal{O}(\mu) = \int d\lambda\, e^{\lambda - \Delta_{\text{liq}}/2}\left\langle\mathcal{O}(\mu)\right\rangle_{H_0} \ .$$

$$(4.86)$$

For later purposes, it is useful to compute some of these averages. First of all, it is easy to show through an integration by parts that

$$\left\langle\frac{d\mathcal{O}}{d\mu}\right\rangle_{H_0} = \left\langle\mathcal{O}\left(-\beta F(\mu + \lambda) + \frac{\mu}{\Delta_{\text{liq}}}\right)\right\rangle_{H_0} \ , \qquad \Rightarrow \qquad \left\langle F(\mu + \lambda)\right\rangle_{H_0} = \frac{T}{\Delta_{\text{liq}}}\left\langle\mu\right\rangle_{H_0} \ . \qquad (4.87)$$

---

[13] The factor of 2 in [414] is due to the fact that in that paper the derivatives with respect to Δ_{ab} are defined for a symmetric matrix, hence only for $a < b$ and multiplied by 2.

where the second result is obtained by choosing $\mathcal{O} = 1$. Equation (4.86) is readily generalized for $a \neq b$ by:

$$\langle \mathcal{O}(\mu_a)\mathcal{O}(\mu_b)\rangle_V = \int d\lambda\, e^{\lambda - \Delta_{\mathrm{liq}}/2}\, \langle \mathcal{O}(\mu)\rangle_{H_0}^2 \tag{4.88}$$

which will be compared to long-time limits of dynamical quantities later on, in the liquid phase. Indeed, in the replica-symmetric language, diagonal elements represent equal-time values of the corresponding dynamical observables, while off-diagonal elements represent long-time limits, see §2.3.

4.5.3.2 Averages for large Δ_{liq}

We will be particularly interested in computing averages $\langle \bullet \rangle_V$ for $\Delta_{\mathrm{liq}} \to \infty$. For an observable $\mathcal{O}(h, \lambda)$ that decays quickly to zero for large h, we have

$$
\begin{aligned}
\langle \mathcal{O}(\mu + \lambda, \lambda)\rangle_V &= \int d\lambda\, e^{\lambda - \Delta_{\mathrm{liq}}/2} \frac{\int d\mu\, e^{-\beta \bar{V}(\mu + \lambda) - \frac{\mu^2}{2\Delta_{\mathrm{liq}}}} \mathcal{O}(\mu + \lambda, \lambda)}{\int d\mu\, e^{-\beta \bar{V}(\mu + \lambda) - \frac{\mu^2}{2\Delta_{\mathrm{liq}}}}} \\
&= \Delta_{\mathrm{liq}} \int d\alpha\, e^{-\frac{\Delta_{\mathrm{liq}}}{2}(1-\alpha)^2} \frac{\int dh\, e^{-\beta \bar{V}(h) + h\alpha - \frac{h^2}{2\Delta_{\mathrm{liq}}}} \mathcal{O}(h, \alpha \Delta_{\mathrm{liq}})}{\int d\mu\, e^{-\beta \bar{V}(\mu + \alpha \Delta_{\mathrm{liq}}) - \frac{\mu^2}{2\Delta_{\mathrm{liq}}}}} \\
&\underset{\Delta_{\mathrm{liq}} \to \infty}{\sim} \int dh\, e^{-\beta \bar{V}(h) + h}\, \mathcal{O}(h, \Delta_{\mathrm{liq}}) \ .
\end{aligned}
\tag{4.89}
$$

The above chain of equalities is based on the following reasoning, identical to the one in §3.7.5:

1. since for $\Delta_{\mathrm{liq}} \to \infty$ the integral over λ is dominated by large values of λ, we set $\alpha = \lambda/\Delta_{\mathrm{liq}}$;

2. we changed variable from μ to $h = \mu + \lambda$ in the numerator; because $\mathcal{O}(h, \bullet)$ decays to zero for large h, the term $h^2/2\Delta_{\mathrm{liq}}$ is negligible for $\Delta_{\mathrm{liq}} \to \infty$;

3. we can evaluate the integral over α by a saddle-point method in $\Delta_{\mathrm{liq}} \to \infty$, dominated by $\alpha = 1$;

4. in the denominator, contrary to the numerator, there is no damping function $\mathcal{O}$, hence $\mu^2/2\Delta_{\mathrm{liq}}$ is not negligible and we use $\bar{V}(r \to \infty) = 0$ to compute it for large Δ_{liq}.

Note that the factor $dh\, e^{-\beta \bar{V}(h) + h}$ corresponds to the $d \to \infty$ limit of $dr\, r^{d-1} g(r)$ with $r = 1 + h/d$. The interpretation of this fact will be emphasized in §5.4.

From equation (4.89) we obtain several useful relations. We specialize for simplicity on the HS potential, which we consider as the limit of a soft potential, e.g. $\bar{V}(h) = -\varepsilon h\theta(-h)$ for $\varepsilon \to \infty$. We get, for example:

$$
\begin{aligned}
\frac{T}{\Delta_{\mathrm{liq}}} \langle \lambda^n \mu \rangle_V &= \langle \lambda^n F(\mu + \lambda)\rangle_V = -\Delta_{\mathrm{liq}}^n \int_{-\infty}^0 dh\, e^{-\beta \bar{V}(h) + h} \bar{V}'(h) = T\Delta_{\mathrm{liq}}^n \ , \\
\langle (\mu + \lambda)^n F(\mu + \lambda)\rangle_V &= -\int_{-\infty}^0 dh\, e^{-\beta \bar{V}(h) + h} h^n \bar{V}'(h) = 0 \ , \qquad \forall n > 0 \ , \\
\langle \mu F(\mu + \lambda)\rangle_V &= \langle (\mu + \lambda) F(\mu + \lambda)\rangle_V - \langle \lambda F(\mu + \lambda)\rangle_V = -\langle \lambda F(\mu + \lambda)\rangle_V = -T\Delta_{\mathrm{liq}} \ .
\end{aligned}
\tag{4.90}
$$

As an example, from equations (4.74) and (4.73) we obtain the expression of the Lagrange multiplier ν:

$$\nu = \frac{1}{\Delta_{\mathrm{liq}}} + \frac{\widehat{\varphi}}{2}\langle \beta^2 F(\mu + \lambda)^2 + \beta F(\mu + \lambda)\rangle_V = \frac{1}{\Delta_{\mathrm{liq}}} + \frac{\widehat{\varphi}}{2}\frac{\beta}{\Delta_{\mathrm{liq}}} \langle \mu F(\mu + \lambda)\rangle_V = \frac{1}{\Delta_{\mathrm{liq}}} - \frac{\widehat{\varphi}}{2} \ . \tag{4.91}$$

where the last equality holds for HS using equations (4.87) and (4.90).

4.5.4 1-RSB solution

We now consider the 1-RSB solution which allows us to compute the plateau value, in the exact same manner as we did in the spherical p-spin model in §2.3.3. We restrict to the case $m = 1$ for simplicity

(see §2.5.5), and once again we consider that $Q_0 = 0$. We thus have $Q_{ab} = \Delta_{\text{liq}}\delta_{ab} + Q_1(I_{ab}^m - \delta_{ab})$ with $Q_1 = \Delta_{\text{liq}} - \Delta_1$, and

$$Q_{ab}^{-1} = \frac{1}{\Delta_{\text{liq}}}\delta_{ab} + \left(\frac{1}{\Delta_{\text{liq}}} - \frac{1}{\Delta_1}\right)(I_{ab}^m - \delta_{ab}) = \frac{1}{\Delta_{\text{liq}}}I_{ab}^m - \frac{1}{\Delta_1}(I_{ab}^m - \delta_{ab}) . \tag{4.92}$$

By taking in equation (4.69) indices $a \neq b$ that belong to the same block, and using $n \to 0$, we obtain the equation (where the index $a = 1, \ldots, m$ with $m \to 1$)

$$\frac{1}{\Delta_1} - \frac{1}{\Delta_{\text{liq}}} = \frac{\widehat{\varphi}}{2}\int \mathrm{d}\lambda\, e^{\lambda - \Delta_{\text{liq}}/2}$$

$$\times \frac{\int\left(\prod_a \mathrm{d}\mu_a\, e^{-\beta\bar{V}(\mu_a+\lambda)}\right)e^{-\frac{1}{2\Delta_1}\sum_a \mu_a^2 + \frac{1}{2}\left(\frac{1}{\Delta_1}-\frac{1}{\Delta_{\text{liq}}}\right)\left(\sum_a \mu_a\right)^2}\beta F(\mu_1+\lambda)\beta F(\mu_2+\lambda)}{\int\left(\prod_a \mathrm{d}\mu_a\, e^{-\beta\bar{V}(\mu_a+\lambda)}\right)e^{-\frac{1}{2\Delta_1}\sum_a \mu_a^2 + \frac{1}{2}\left(\frac{1}{\Delta_1}-\frac{1}{\Delta_{\text{liq}}}\right)\left(\sum_a \mu_a\right)^2}}$$

$$= \frac{\widehat{\varphi}}{2}\int \mathrm{d}\lambda\, \frac{e^{\lambda-\Delta_{\text{liq}}/2}}{\int \mathrm{d}\mu\, e^{-\beta\bar{V}(\mu+\lambda)-\frac{\mu^2}{2\Delta_{\text{liq}}}}}\int \mathcal{D}\eta\, \frac{\left[\int \mathrm{d}\mu\, e^{-\beta\bar{V}(\mu+\lambda)-\frac{\mu^2}{2\Delta_1}+\eta\mu\sqrt{\frac{1}{\Delta_1}-\frac{1}{\Delta_{\text{liq}}}}}\beta F(\mu+\lambda)\right]^2}{\int \mathrm{d}\mu\, e^{-\beta\bar{V}(\mu+\lambda)-\frac{\mu^2}{2\Delta_1}+\eta\mu\sqrt{\frac{1}{\Delta_1}-\frac{1}{\Delta_{\text{liq}}}}}}$$

$$= \frac{\widehat{\varphi}}{2}\int \mathrm{d}\lambda\, e^{\lambda-\Delta_{\text{liq}}/2}\frac{1}{\mathcal{Z}_0}\int \mathcal{D}\eta\, \mathcal{Z}_1 \left\langle\beta F(\mu+\lambda)\right\rangle_{H_1}^2 ,$$

$$\tag{4.93}$$

where we defined

$$H_1(\mu, \lambda) = \bar{V}(\mu+\lambda) + \frac{T\mu^2}{2\Delta_1} - \eta\mu T\sqrt{\frac{1}{\Delta_1} - \frac{1}{\Delta_{\text{liq}}}} , \qquad \mathcal{Z}_1(\lambda) = \int \mathrm{d}\mu\, e^{-\beta H_1(\mu,\lambda)} . \tag{4.94}$$

It remains to be checked that equation (4.93) is equivalent to the one derived in section 4.4.2.3 for $\Delta_{\text{liq}} \to \infty$. From the second line of equation (4.93), shifting in all the integrals $\mu + \lambda \to \mu$ and $\eta + \lambda\sqrt{\frac{1}{\Delta_1} - \frac{1}{\Delta_{\text{liq}}}} \to \eta$, we obtain

$$\frac{1}{\Delta_1} - \frac{1}{\Delta_{\text{liq}}} = \frac{\widehat{\varphi}}{2}\int \mathrm{d}\lambda\, \frac{e^{-\frac{1}{2\Delta_{\text{liq}}}(\lambda-\Delta_{\text{liq}})^2}}{\int \mathrm{d}\mu\, e^{-\beta\bar{V}(\mu)-\frac{(\mu-\lambda)^2}{2\Delta_{\text{liq}}}}}\int \mathcal{D}\eta\, \frac{\left[\int \mathrm{d}\mu\, \left(\frac{\mathrm{d}}{\mathrm{d}\mu}e^{-\beta\bar{V}(\mu)}\right)e^{-\frac{\mu^2}{2\Delta_1}+\frac{\mu\lambda}{\Delta_{\text{liq}}}+\eta\mu\sqrt{\frac{1}{\Delta_1}-\frac{1}{\Delta_{\text{liq}}}}}\right]^2}{\int \mathrm{d}\mu\, e^{-\beta\bar{V}(\mu)-\frac{\mu^2}{2\Delta_1}+\frac{\mu\lambda}{\Delta_{\text{liq}}}+\eta\mu\sqrt{\frac{1}{\Delta_1}-\frac{1}{\Delta_{\text{liq}}}}}} ,$$

$$\tag{4.95}$$

From this form one sees as in the replica symmetric case that for large Δ_{liq} the integral over λ is strongly peaked on $\lambda = \Delta_{\text{liq}}$. With this choice at leading order in large Δ_{liq} we have

$$\frac{1}{\Delta_1} = \frac{\widehat{\varphi}}{2}\int \mathcal{D}\eta\, \frac{\left[\int \mathrm{d}\mu\, \left(\frac{\mathrm{d}}{\mathrm{d}\mu}e^{-\beta\bar{V}(\mu)}\right)e^{-\frac{\mu^2}{2\Delta_1}+\mu+\eta\mu\sqrt{\frac{1}{\Delta_1}}}\right]^2}{\int \mathrm{d}\mu\, e^{-\beta\bar{V}(\mu)-\frac{\mu^2}{2\Delta_1}+\mu+\eta\mu\sqrt{\frac{1}{\Delta_1}}}} . \tag{4.96}$$

Specializing to HS, we obtain

$$\frac{1}{\Delta_1} = \frac{\widehat{\varphi}}{2}\int \mathcal{D}\eta\, \frac{\left[\int_0^\infty \mathrm{d}\mu\, \frac{\mathrm{d}}{\mathrm{d}\mu}e^{-\frac{\mu^2}{2\Delta_1}+\mu+\eta\mu\sqrt{\frac{1}{\Delta_1}}}\right]^2}{\int_0^\infty \mathrm{d}\mu\, e^{-\frac{\mu^2}{2\Delta_1}+\mu+\eta\mu\sqrt{\frac{1}{\Delta_1}}}} = \frac{\widehat{\varphi}}{2}\int \mathcal{D}\eta\, \frac{e^{-\frac{1}{2}(\eta+\sqrt{\Delta_1})^2}}{\sqrt{2\pi\Delta_1}}\frac{1}{\Theta[(\eta+\sqrt{\Delta_1})/\sqrt{2}]} , \tag{4.97}$$

which is equivalent to equation (4.55).

4.6 Connection between statics and dynamics: the formal analogy

In this section we emphasize the formal analogy between time dependence of observables in the dynamics and replica index of the corresponding observables in the statics, as discussed in §2.5.2 and illustrated

in figure 4.2. Indeed, although dynamics is formally more difficult to handle than the statics, it is not needed to resort to replicas in order to average over the disorder, which is a conceptual and technical advantage [122, 81]. This is a consequence of the observation that the dynamic partition function is 1 by probability conservation if one considers all possible paths, hence independent of the Hamiltonian of the system.

Let us consider the same Langevin dynamics as in §3.2.1, this time with the quenched disordered Hamiltonian of the MK model. We introduced a *dynamical partition function* $\overline{Z_N}$ in (3.8) of the form

$$\overline{Z_N} = \int_{\mathbb{S}_d(R)} \prod_{i=1}^{N} \mathrm{D}x_i \int_{\partial\mathbb{S}_d(R)} \prod_{i=1}^{N} \mathrm{D}\hat{x}_i \, e^{-\int \mathrm{d}t \sum_i [T\gamma\hat{x}_i \cdot \hat{x}_i + i\hat{x}_i \cdot \gamma\dot{x}_i + i\hat{x}_i \cdot \nu_i x_i]} \, \overline{e^{-\int \mathrm{d}t \sum_i i\hat{x}_i \cdot \nabla_i H}} \tag{4.98}$$

We called $\partial\mathbb{S}_d(R)$ the tangent hyperplane to $\mathbb{S}_d(R)$, where the response fields belong (see §3.2.3). ν_i is a Lagrange multiplier for the spherical constraint, discussed in §3.2.3. Introducing the superspace notation as in §3.2.4:

$$a = (t, \theta, \bar{\theta}) \,, \qquad \boldsymbol{x}_i(a) = x_i(t) + i\hat{x}_i(t)\theta\bar{\theta} \,, \qquad \boldsymbol{X} = (\boldsymbol{x}_1, \ldots, \boldsymbol{x}_N) \tag{4.99}$$

we can write $\overline{Z_N}$ in the compact form:

$$\overline{Z_N} = \int_{\mathbb{S}_d(R)} \mathrm{D}\boldsymbol{X} \, e^{-\sum_i \Phi(\boldsymbol{x}_i)} \overline{e^{-\int \mathrm{d}a \, H[\boldsymbol{X}(a)]}} \,. \tag{4.100}$$

The formal analogy between equations (4.100) and (4.7), apart from the single-particle kinetic term which is easily dealt with as an additive contribution to the exponent, is evident:

$$\overline{Z^n} = \int \mathrm{d}\bar{X} \, \overline{e^{-\sum_a \beta H[X_a]}} \tag{4.101}$$

The replica index $a = 1, \cdots, n$ becomes the SUSY variable $a = (t, \theta, \bar{\theta})$. Except that, the structure of the dynamical partition function $\overline{Z_N}$ is identical to the one of the replicated partition function, as in §2.5.2. As a consequence, the logarithm of the partition function is analog[14] in the statics (4.68) and dynamics (3.68)

$$\mathcal{S}_{\mathrm{stat}}(\hat{Q}) = \frac{d}{2}\ln\det\hat{Q} - \frac{d}{2}\widehat{\varphi}\mathcal{F}_{\mathrm{stat}}(\hat{Q}) - \frac{d}{2}\beta\nu\sum_a Q_{aa}$$

$$\mathcal{F}_{\mathrm{stat}}(\hat{Q}) = -e^{-\Delta_{\mathrm{liq}}/2}\int \mathrm{d}\bar{\mu}\mathrm{d}\lambda \, \frac{e^{\lambda - \frac{1}{2}\bar{\mu}^T \hat{Q}^{-1}\bar{\mu}}}{(2\pi)^{n/2}\sqrt{\det\hat{Q}}}\left[e^{-\beta\sum_{a=1}^{n}\bar{V}(\mu_a + \lambda)} - 1\right]$$

$$\mathcal{S}_{\mathrm{dyn}}(\boldsymbol{Q}) = \frac{d}{2}\ln\mathrm{sdet}\,\boldsymbol{Q} - \frac{d}{2}\widehat{\varphi}\mathcal{F}_{\mathrm{dyn}}(\boldsymbol{Q}) - \frac{d}{2}\int \mathrm{d}a\,\boldsymbol{\nu}(a)\left(\boldsymbol{Q}(a,a) - \Delta_{\mathrm{liq}}\right) - d\widehat{\Phi}(\boldsymbol{Q}) \tag{4.102}$$

$$\mathcal{F}_{\mathrm{dyn}}(\boldsymbol{Q}) = -\frac{e^{-\Delta_{\mathrm{liq}}/2}}{\sqrt{\mathrm{sdet}\,\boldsymbol{Q}}}\int \mathrm{D}\boldsymbol{\mu}\mathrm{d}\lambda \, e^{\lambda - \frac{1}{2}\int \mathrm{d}a\mathrm{d}b\,\boldsymbol{\mu}(a)\boldsymbol{Q}^{-1}(a,b)\boldsymbol{\mu}(b)}\left[e^{-\int \mathrm{d}a\,\bar{V}(\boldsymbol{\mu}(a) + \lambda)} - 1\right]$$

The derivations are thus in almost one-to-one correspondence in the dynamic and static cases. Another example of the dynamic/static analogy is given in §5.7 for the virial truncation of equilibrium averages.

In the following, we mention some quantities which are obtained independently by a dynamic computation in a long-time regime and the static computation. The fact that they coincide is reassuring and is at the basis of the replica method used in the RFOT scenario, see §1.2.

- The diagonal elements of the static saddle-point equation give the value of the Lagrange multiplier in (4.91); the same is obtained in the equal-time limit of the dynamic saddle-point equation in §3.7.6.

---

[14]The temperature factor differences are discussed in §5.5. They are just notational, and due to the fact that, owing to the Boltzmann weights, βH appears naturally in the statics whereas only H appears naturally in the MSRDDJ weights. It is enough to cast the dynamics with β factors to recover the analogy, see §5.5. This only introduces a rescaling of the timescales which is natural.
Note also that the factors $\sqrt{2\pi}$ are present in the dynamical measure $\mathrm{D}\boldsymbol{\mu}$ as in the static one if we define it in a discretized version, see §3.2.1.

In the dynamics, before getting rid of the sphere with the limit $\Delta_{\text{liq}} \to \infty$, one could write (3.131) as

$$
\begin{aligned}
\nu - \frac{T}{\Delta_{\text{liq}}} = & -\delta\nu + \beta M(0) = \frac{1}{2}\widehat{\varphi}e^{-\Delta_{\text{liq}}/2} \int \mathrm{d}\lambda\, e^{\lambda} \left\langle F'(\mu + \lambda) \right\rangle_{H_0} \\
& + \frac{\beta}{2}\widehat{\varphi}e^{-\Delta_{\text{liq}}/2} \int \mathrm{d}\lambda\, e^{\lambda} \langle F(\mu + \lambda)\, F(\mu + \lambda)\rangle_{H_0}\,,
\end{aligned}
\tag{4.103}
$$

in order to make a direct comparison with (4.91).

- The long-time limit in the liquid phase in §3.7.4 coincides with equations (4.44), (4.73), (4.88) and (4.74) for $a \neq b$, which corresponds to a long-time limit in the replica-symmetric language. For instance, (3.118) can be readily compared with (4.73) for $a \neq b$ using (4.88).

- The plateau value given by the dynamical computation (3.138) and its static counterpart using a 1-RSB ansatz in (4.93) are the same. The HS case gives equations (3.140) and (4.97), with the dynamic/static correspondence $\Delta_{\text{EA}} = \Delta_1$.

- The microscopic connections in §4.5.2 are formally identical to the one derived in §3.8.4.

- The static saddle-point equation, similar to its dynamic counterpart, has been identified in §4.5.1 as being formally analog to a MCT-like equation.

- The MCT-like exponents in §3.9.1 have been computed in [78, 157, 309, 159] through this formal analogy.

Note that some purely dynamic quantities (*e.g.* the diffusion coefficient) have been obtained only through the dynamics. Replica techniques are easier to handle, and this is the reason why a lot of work has focused on static computations, and one can hope that most interesting dynamical quantities can be obtained this way. This is one of the leitmotivs of replica theory, see §1.2. However, transient regimes in the dynamical equations cannot be *guessed* by a static computation.

4.7 Conclusion

In this chapter we presented a derivation of the glassy thermodynamics of the system, using replicas, which is parallel to the dynamics, using supersymmetry.

We introduced an irrelevant quenched disorder [288] that was helpful to derive the free energy functional without having to justify a truncation of the virial expansion, as originally done in [162, 409, 161, 146] for liquids and in [312] for glasses. We discussed a derivation of the replicated thermodynamics that is simpler but equivalent to previous ones [243, 242, 96]: we recover its results concerning the different phases of the system and its characterizations, as well as results concerning static rigidity. Contrary to the previous ones, it can be easily generalised to the supersymmetric formalism. In this way one can derive the dynamical equations of chapter 3 along the same lines and straightforwardly show the equivalence of thermodynamic and dynamic results in the glassy regime.

In previous works [312, 243, 242, 96, 97, 325], focusing in particular on the HS potential, these equations have been used to derive many observables characterising the glassy regime, namely:

1. The Kauzmann transition [312], where the number of metastable states becomes sub-exponential, giving rise to an *entropy crisis* described in §1.2.4.1 and a second order equilibrium phase transition[15].

2. The Gardner transition line, that separates a region where glass basins are stable from a region where they are broken in a complex structure of metabasins [242, 96, 325]. See also §4.4.3.4.

3. The density region where jammed packings exist (also known as *jamming line* or *J-line* [312]), which is delimited by the threshold density and the glass close packing density [312], see §1.5 and figure 1.15.

---

[15]Note that in the MK model the additional term $N!$ due to particle distinguishability (see Section 4.2.3) induces an additional term $\log N$ in the entropy of metastable states, which shifts the Kauzmann transition to infinite density. In the normal system (consider e.g. HS) this factor is replaced by a $\log d$ term, which shifts the Kauzmann transition to values of $\widehat{\varphi}_{\text{K}} \sim \log d \gg \widehat{\varphi}_{\text{d}}$, where $\widehat{\varphi}_{\text{d}} \approx 4.8$ is the dynamical transition scaled density [312].

4. The equation of state of glassy states, computed by compression and decompression of equilibrium glasses [325].

5. The response of the glass state to a shear strain [414, 325].

6. The long time limit of the mean square displacement in the glass (the so-called Edwards-Anderson order parameter) [96, 97].

7. The behaviour of the radial pair distribution function $g(r)$ in the glass [312, 96, 97].

8. The probability distribution of the forces in a packing, and the average number of particle contacts [96, 97].

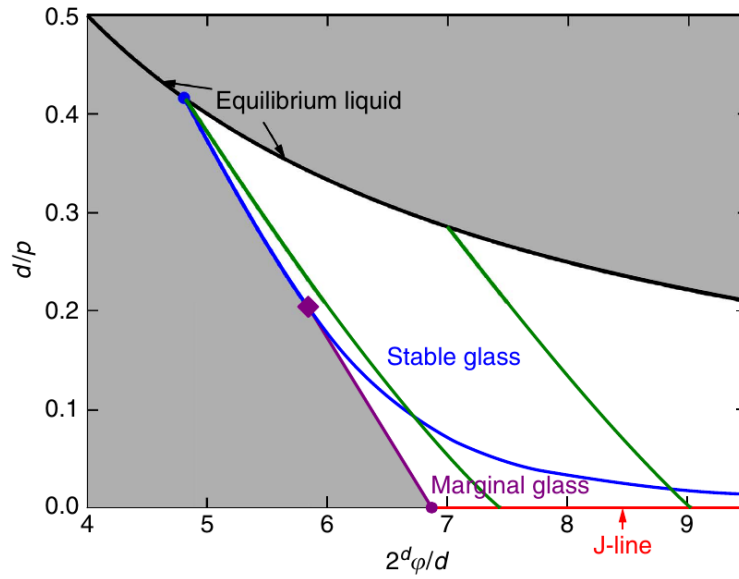In figure 4.5 we display the infinite-dimensional pressure-density phase diagram of amorphous HS.

Figure 4.5: Pressure versus packing fraction phase diagram of infinite-dimensional amorphous HS. The white region indicates the regime where the (meta)basin structure is present, either as a normal (stable) glass or as a full-RSB Gardner (marginal) glass. The line of jammed packings is found at infinite pressure, which always falls within the marginal phase. The green lines are two examples of an adiabatic following of a glass state [312, 325]. [*Reprinted from* [97]]

<div style="text-align: right;">*5*</div>

SCALE INVARIANCE IN THE PHASE DIAGRAM OF PARTICLE SYSTEMS

Outline

5.1 Introduction

In this chapter we show that the existence of isomorphs in the (T, ρ) plane actually becomes strictly true in the large-dimensional limit for a wide and well-defined class of potentials: the *rather hard* exponential potentials in the denomination of §3.1.1. This holds for the liquid as well as the glassy regions of the phase diagram. This concept of isomorphs, or more explicitly of a scale invariance in both dynamics and statics of these systems, is reviewed in the introductory chapter, §1.4. We proceed in three steps: first we show this in detail for the equilibrium properties of the liquid phase, then we show how the same manipulations allow one to prove it for the dynamics, and finally we outline a derivation for the equilibrium (*landscape*) properties within the glass phase. Then we show that, as expected from the works of the Roskilde group [19, 184, 137, 138], the virial-potential energy correlation coefficient, defined in §1.4.2, tends to one as the dimension approaches infinity. We give and study examples of potentials that do not exactly fit in this class and expose the differences. We finally compare these results with recent numerical investigations [106].

We will use, contrary to the chapters 2, 3 and 4, bold letters for d-dimensional vectors.

5.2 Mayer integral contributions

5.2.1 Liquid free energy

As in the previous chapters, we wish to focus on the large d behaviour of a system of N particles interacting via a pair potential $V(|\mathbf{r}|)$. In order to have a well-defined large-dimensional limit, we shall

assume that the potential scales as

$$V(r) = e^{-dA(r)} \tag{5.1}$$

The precise conditions on $V(r)$ will be derived below.

For large d only the first two terms of the virial expansion contribute (see §2.2); the free energy and the pressure of the liquid are respectively given by (2.45):

$$\frac{\beta F}{N} = \frac{\beta(F_{\text{IG}} + F_{\text{ex}})}{N} = \ln \rho - 1 - \frac{\rho}{2} \int d\mathbf{r} \left(e^{-\beta V(r)} - 1 \right)$$
$$\frac{\beta P}{\rho} = 1 - \frac{\rho}{2} \int d\mathbf{r} \left(e^{-\beta V(r)} - 1 \right) \tag{5.2}$$

where $\rho = N/\mathcal{V}$ is the particle density. We still denote by $\mathcal{V}$ the volume of the system[1]. The free energy has an ideal gas contribution $F_{\text{IG}} = N(\ln \rho - 1)/\beta$ and an *excess* contribution F_{ex} given by the last term, called *interaction term* in the last chapters[2] since it is zero when the potential is zero. Let us focus on the Mayer integral in the excess part:

$$\int d\mathbf{r} \left(e^{-\beta V(r)} - 1 \right) = \Omega_d \int_0^\infty dr \, r^{d-1} \left(e^{-\beta V(r)} - 1 \right) \tag{5.3}$$

by isotropy. The integrand looks as in figure 5.1, and from this picture we now deduce how to compute this excess part in the large d limit.

5.2.2   The different regimes of the Mayer function

Set an effective diameter r^* such that

$$\beta V(r^*) \equiv \widetilde{\beta} \tag{5.4}$$

with $\widetilde{\beta}$ a rescaled temperature[3] of order $O(1)$. This defines r^* up to $O(1/d)$, independently of the value of $\widetilde{\beta}$ as long as it remains of order one. We distinguish three regions for the Mayer function $f(r) = e^{-\beta V(r)} - 1$:

1. <u>$r < r^*$</u>, so that $\lim_{d \to \infty} f(r) = -1$. Then essentially the integrand is $\sim -r^d$, and in large dimensions only the right boundary $r \to r^*$ dominates.

2. $r \sim r^*$ up to $O(1/d)$, where $0 < f(r) < -1$. With our scaling of the potential in the large d limit, this region has a $O(1/d)$ extension and, setting[4] $r = r^*(1 + \tilde{r}/d)$, one may compute the contribution of this region (A), as denoted in figure 5.1, as

$$\Omega_d \int_{(A)} dr \, r^{d-1} \left(e^{-\beta V(r)} - 1 \right)$$
$$= \mathcal{V}_d(r^*) \int_{-O(d)}^{O(d)} d\tilde{r} \left(1 + \frac{\tilde{r}}{d} \right)^{d-1} \left[e^{-\beta V(r^* + \frac{r^*}{d}\tilde{r})} - 1 \right] \tag{5.5}$$
$$\sim \mathcal{V}_d(r^*) \int_{-\infty}^{\infty} d\tilde{r} \, e^{\tilde{r}} \left[e^{-\widetilde{\beta} \exp(-r^* A'(r^*)\tilde{r})} - 1 \right]$$

with $\widetilde{\beta}$ defined in (5.4). We have expanded $A(r)$ around r^* and kept non-vanishing orders when d goes to infinity. This development only makes sense if

$$A'(r^*) > \frac{1}{r^*} , \tag{5.6}$$

which ensures the convergence of the integral, and in this case only a range of values around r^* of width $O(1/d)$ contributes.

---

[1] There is no need to introduce the sphere $\mathbb{S}_d(R)$ here.

[2] We rather use the terminology *excess* here since it is the one adopted in the isomorph literature.

[3] If $\widetilde{\beta} = Be^{bd}$ and $V(r) = V_0 e^{-dA(r)}$ with B and V_0 subdominant, then r^* is given by $A(r^*) = b$ and $\widetilde{\beta} = BV_0$.

[4] $\tilde{r}$ is the same quantity as μ or h in the dynamics §3 and statics §4, but for clarity and following the notations of the isomorph literature, we keep the *reduced coordinates* [184] notation here.
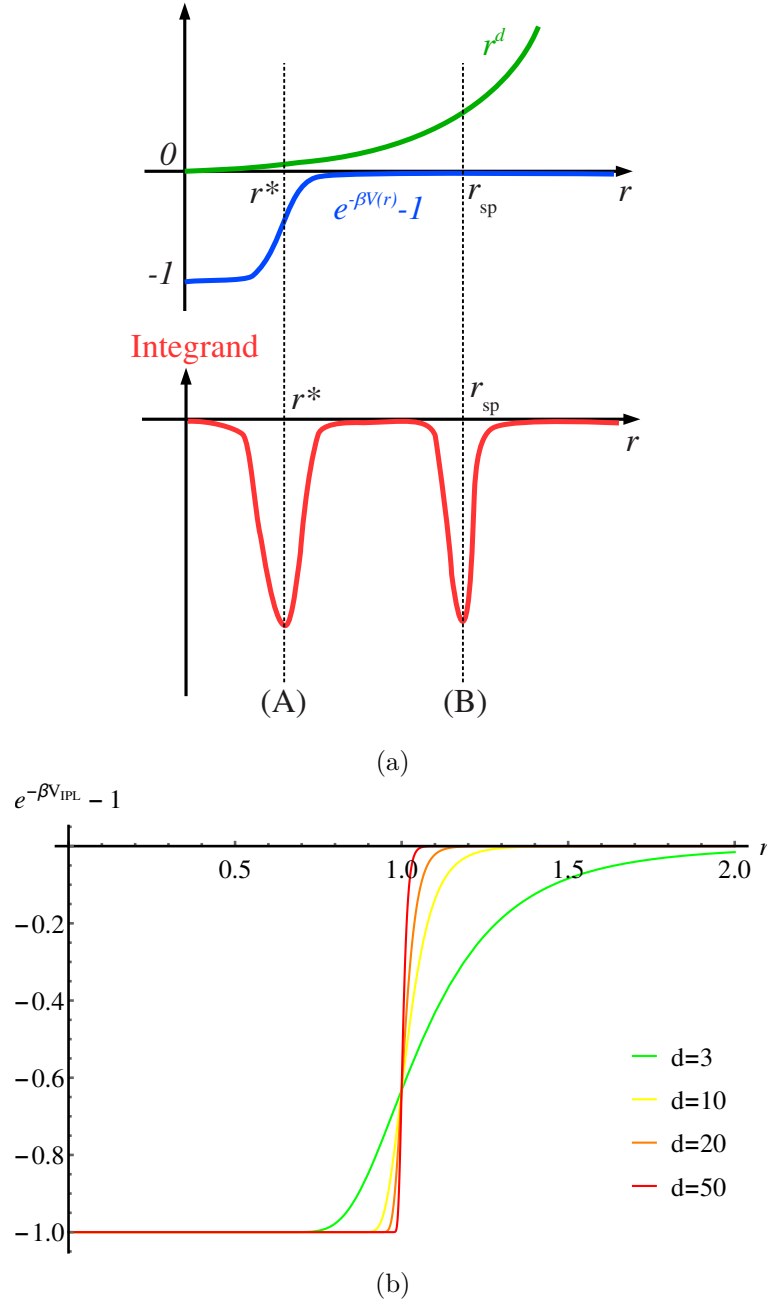
Figure 5.1: (a) The two dominant regions in the integrand of the Mayer integral for large d. At the top, the green curve is the power law r^d arising from the measure and the blue one is the Mayer function. At the bottom, the red one is the product of the two giving the integrand, which may display two peaks at r^* and at the saddle point r^{sp}. (b) The Mayer function for an IPL potential, which is in this *exponential class* of potentials (5.1) we consider, $V_{\mathrm{IPL}} = \epsilon(\sigma/r)^{d/\alpha}$ with $\beta\epsilon = 1$, $\sigma = 1$, $\alpha = 1/2$, and $d = 3, 10, 20, 50$. As d increases one clearly sees the emergence of the three distinct regions of the Mayer function: exponentially close to -1 for $r < \sigma$, $O(1)$ for r around σ with $O(1/d)$ fluctuations, and exponentially small for $r > \sigma$.

3. $\underline{r > r^*}$: these may give a further contribution. Here, we have $\lim_{d\to\infty} f(r) = 0$ and one can expand the Mayer function as $f(r) \sim -\beta V(r)$. A saddle-point evaluation of the Mayer integral in this region is possible, obtained by maximizing the exponent $\ln r - A(r)$ in a point r_{sp} given by (see region (B) in figure 5.1):

$$A'(r_{\mathrm{sp}}) = \frac{1}{r_{\mathrm{sp}}} \tag{5.7}$$

As usual, the fluctuations around this saddle point are of order $1/\sqrt{d}$ due to the vanishing of the first derivative of the exponent around it.

5.2.3   The effective diameter and the gap fluctuation scaling

Let us now comment the meanings of r^* and of the $O(1/d)$ scaling:

- r^* plays the exact same role as the *sphere diameter* σ in the last chapters. Similarly to HS, it is the typical length (here defined precisely, up to a $1/d$ correction, in the limit $d \to \infty$) above which spheres *practically* do not interact, and below which a strong repulsion occurs, leading to an excluded volume. In the case $\beta = O(1)$, r^* is precisely defined by the condition $A(r^*) = 0$. In general this effective diameter can be anywhere, and will be larger for (exponentially) lower temperatures or higher densities (§5.4).

  This also hints to the remark that a particle diameter or -more generally- a range of interaction have a meaning only in some temperature-density scaling window (in high d at least).

- The $1/d$ scaling is crucial in the last chapters and has its origin clearly identified here: it dominates, under certain conditions realized by the class of potentials studied here, the excess free energy. In the dynamics (see §3.3.2 and §3.3.4) and the glassy statics (see §4.3, §F and the scaling of the cage in [312, 243, 242, 225]), this scaling has been used and shown to lead to a well-defined high-dimensional limit.

5.2.4   Some examples

1. Purely exponential potentials $V_{\mathrm{EXP}}(r) \propto e^{-dar}$ have r^* defined only for $r^* > 1/a$. They are *soft* in the sense that below $1/a$ they are not repulsive enough to observe this regime. However they are repulsive enough at larger distance (*i.e.* at higher temperatures or lower densities). The situation is similar for a Gaussian potential $V_{\mathrm{G}}(r) = e^{-adr^2/2}$, see figure 5.2.

2. IPL potentials, where isomorphs are exact: $V_{\mathrm{IPL}}(r) \propto (\sigma/r)^{ad}$. r^* is defined if and only if $a > 1$; there is no saddle point r_{sp}. The HS potential is not within the class of *exponential potentials* analyzed here; one could try to define them in this setting with $A_{\mathrm{HS}}(r) = -\epsilon + 2\epsilon\theta(r - \sigma)$ with $\epsilon > 0$, with the convention that the Heaviside function θ is $1/2$ at zero. However this exponent A_{HS} is discontinuous and one cannot expand it around $r = \sigma$, so the conclusions presented here do not hold. Nevertheless, it is the limiting case of the previous IPL potential with $a \to \infty$; in this respect the conclusions hold but with pathological properties (for example the exponent α defined below will be zero).

3. $A(r) = -1/r + r$ has no r_{sp} defined and r^* can be defined on the whole positive real line.

4. Some other potentials will be studied in §5.8.

5.3   A second-order pseudo-transition

At each density and temperature, it may be the case that for large d the integral is dominated either by the region around r^*, the region around a saddle point r_{sp} or by $r \to \infty$. The latter case corresponds to long-range potentials, and we shall not consider it here. If condition (5.6) is satisfied, the contribution around r^* is well defined. The question remains if there exists some saddle-point value r_{sp}, i.e. if (5.7) defines an absolute maximum of the potential for $r > r^*$, that dominates. Assume that there is such a value, and let us compare the contributions

$$(r^*)^d \big(e^{-\widetilde{\beta}\exp(-r^* A'(r^*)\tilde{r})} - 1 \big) \quad \text{around } r^* \,,$$

$$r_{\mathrm{sp}}^d \left[\exp\left(-\widetilde{\beta} e^{d(A(r^*)-A(r_{\mathrm{sp}}))} \right) - 1 \right] \tag{5.8}$$

$$\sim -\widetilde{\beta} r_{\mathrm{sp}}^d e^{d(A(r^*)-A(r_{\mathrm{sp}}))} \quad \text{around } r_{\mathrm{sp}} \,.$$

We have, for large d, that the neighbourhood of r^* dominates if

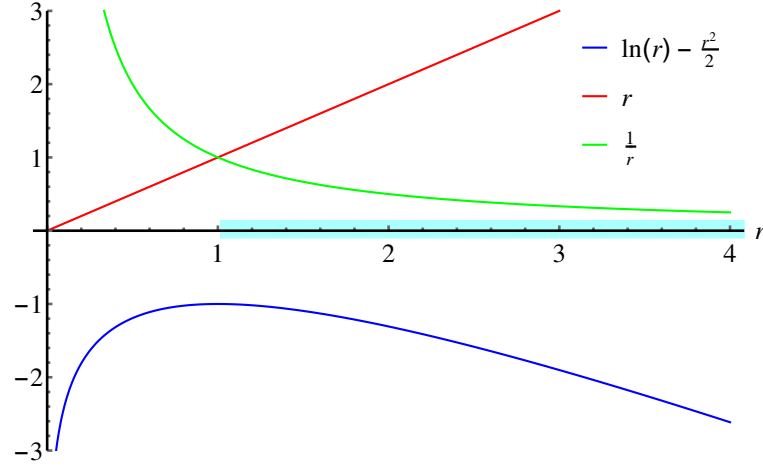$$\big[\ln r - A(r) \big]_r^{r^*} > 0 \quad \text{for } r > r^* \tag{5.9}$$

Figure 5.2: Example of the Gaussian potential $V_G(r) = e^{-adr^2/2}$, with $A_G(r) = ar^2/2$ (in this figure $a = 1$). The light blue region $r > 1/\sqrt{a}$ are values where a r^* could be defined. Here a saddle point r_{sp} could be defined in only one value $r_{\text{sp}} = 1/\sqrt{a}$. If the regime of temperature is such that a r^* is defined, the saddle point has no meaning since it is always less than r^*. Since $\ln - A_G$ is monotonically decreasing in the whole region where r^* is defined, r^* will thus dominate the Mayer integral, see §5.3. Yet, if the temperature is high enough so that $r^* < 1/\sqrt{a}$ cannot be defined anymore, the saddle point exists (and is indeed in the region where the Mayer integral is exponentially small) and dominates the integral.
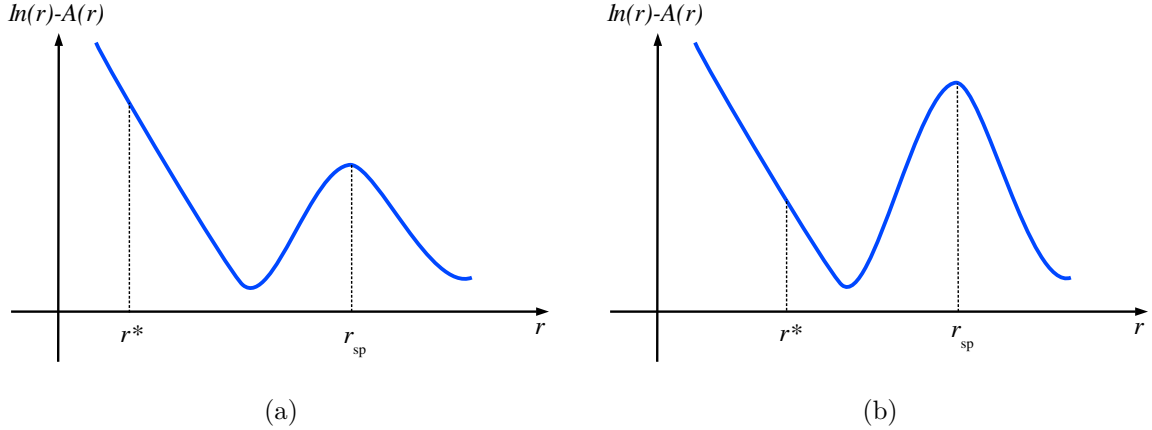

Figure 5.3: Cases where both peaks (A) and (B) could contribute to the Mayer integral: the one that prevails is (a) r^* (b) r_{sp}.

which is the case if, for example, $\ln r - A(r)$ is a monotonically decreasing function for $r \geqslant r^*$. Some potentials, such as the Gaussian one V_G or purely exponential V_{EXP} have a low-temperature *rather hard* regime where r^* dominates and a high temperature *very soft* regime where r_{sp} dominates (see §5.2.4 and figure 5.2). This is a second-order *pseudo*-transition, since one can go continuously from an effective diameter r^* to r_{sp} by increasing temperature from the *rather hard phase* to the *very soft phase* and it exists only in the limit $d \to \infty$, where this is exact. Nevertheless one may hope to observe hints of these phases in lower dimensions. This is already the case for the *rather hard phase* with the discovery of *approximate* isomorphs in a large number of three-dimensional systems [20, 21, 347, 184, 348, 19].

One can compute the energy from the canonical relation

$$\left. \frac{\partial(\beta F)}{\partial \beta} \right|_{\mathcal{V},N} = \langle H \rangle \tag{5.10}$$

In the *very soft phase*, from (5.8) we see that the main contribution to the Mayer integral is precisely given by the first order in the high-temperature expansion:

$$\int d\mathbf{r} \left(e^{-\beta V(r)} - 1 \right) \sim - \int d\mathbf{r} \, \beta V(r) \tag{5.11}$$

Thus, differentiating (5.2), we see that the *very soft phase* has constant energy:

$$\frac{\langle H \rangle}{\mathcal{V}} = \frac{1}{\rho} \frac{\partial (\beta F/N)}{\partial \beta}\bigg|_{\mathcal{V},N} = \frac{1}{2} \int d\mathbf{r}\, V(r) \tag{5.12}$$

The interpretation of equation (5.11) is clear: in this phase the high-temperature expansion is exact to first order in β, each particle strongly interacts with exponentially many others since $r_{\rm sp} > r^*$ (where r^* is for example the usual low-temperature diameter of the particles, *i.e.* a typical length which we consider as a sphere diameter), and those that are at a distance r_{sp} dominate the interactions. The transition temperature between these two *phases* is precisely the value of temperature where $\left[\ln r - A(r)\right]_{r_{sp}}^{r^*} = 0$.

We must warn about a possible flaw in this reasoning. We got the saddle-point value $r_{\rm sp}$ by *assuming* the virial truncation in (5.2) then studying the resulting excess free energy for $d \to \infty$. Yet, it is not clear if the behaviour of the potential, as dominated by this saddle point, is compatible with the HS-like assumptions used to truncate the virial series: the distance fluctuation scaling is different, and as stressed before, it is a *softer* phase. Deeper investigations are needed.

In the following we show that isomorphs exist for the *rather hard potentials phase*, we shall not consider the case in which a typical distance $r_{\rm sp} > r^*$ dominates (*very soft spheres*) - which has never been studied in the high-dimensional limit, but may be easily treated, dynamically and statically, to first order in the large-temperature expansion.

5.4   Isomorphs and effective potential

In the *rather hard* regimes where r^* dominates the Mayer integral, from (5.5) the free energy reads:

$$\frac{\beta F}{N} = \ln \rho - 1 - \frac{\widetilde{\varphi}}{2} \int_{-\infty}^{\infty} d\tilde{r}\, e^{\tilde{r}} \left[e^{-\widetilde{\beta} e^{-\tilde{r}/\alpha}} - 1 \right] \tag{5.13}$$

where

$$\widetilde{\varphi} \equiv \rho \mathcal{V}_d(r^*), \qquad 1/\alpha \equiv r^* A'(r^*) > 1 \tag{5.14}$$

The term $e^{\tilde{r}}$, related to the linear part of the effective potential in §3.7.5, is an *entropic driving force*[5], $\widetilde{\beta}$ is an effective inverse temperature and $\widetilde{\varphi}$ an effective packing fraction. We have discovered naturally that the effective potential is a pure decaying exponential

$$V_{\rm eff}(r) = V(r^*)e^{-r^* A'(r^*)\tilde{r}} = V(r^*)e^{-\tilde{r}/\alpha} \tag{5.15}$$

The value α gives its *hardness* and depends upon the value of r^* and the original potential through A'. The purely exponential decaying potential has thus a peculiar role in high d; note that however, as long as two potentials define the same *exponent* α, they have exactly the same physics. This purely repulsive potential enjoys good properties, and was used as a *building block* for liquid potentials by Dyre, Schrøder et al [19, 18].

We now show under which conditions two systems at different state points are related through a scaling transformation. If one shifts in the virial term of equation (5.13) $\tilde{r} \to \tilde{r} + c$, which corresponds to an order $1/d$ shift of r^*, one gets

$$\frac{\widetilde{\varphi}}{2} \int_{-\infty}^{\infty} d\tilde{r}\, e^{\tilde{r}} \left[e^{-\widetilde{\beta} e^{-\tilde{r}/\alpha}} - 1 \right]$$
$$= \frac{\widetilde{\varphi} e^{c}}{2} \int_{-\infty}^{\infty} d\tilde{r}\, e^{\tilde{r}} \left[e^{-\widetilde{\beta} e^{-c/\alpha} e^{-\tilde{r}/\alpha}} - 1 \right] \tag{5.16}$$

Hence, a sufficient condition for two systems at different state points 1 and 2 to be in correspondence (*i.e.* to have the same excess free energy) is that there exists c such that

$$\begin{cases} r_1^* A'(r_1^*) = r_2^* A'(r_2^*) = \dfrac{1}{\alpha} \\[2mm] \widetilde{\varphi}_1 e^{c} = \widetilde{\varphi}_2 = \widetilde{\varphi} \\[2mm] \widetilde{\beta}_1 e^{-c/\alpha} = \widetilde{\beta}_2 = \widetilde{\beta} \end{cases} \tag{5.17}$$

---

[5]It is a term that effectively lowers potential energy barriers due to the many configurations accessible owing to isotropy and translation invariance [239, Sec. 5].

These conditions mean that one may set $r_1^* = r_2^* = r^*$ (which determines $1/\alpha = r^* A'(r^*)$) and that they may be mapped by

$$\begin{cases} \rho_1 e^c = \rho_2 \\ \beta_1 e^{-c/\alpha} = \beta_2 \end{cases} \Leftrightarrow \frac{\rho_1^{\frac{1}{\alpha}}}{T_1} = \frac{\rho_2^{\frac{1}{\alpha}}}{T_2} \tag{5.18}$$

via *a value of c of sub-exponential order in d* which parametrizes the line

$$\frac{\rho^{\frac{1}{\alpha}}}{T} = \text{constant} \tag{5.19}$$

Along these lines, the partition function between two points scales changes by a purely geometric, model-independent factor:

$$\beta_2 F_2 - \beta_1 F_1 = N \ln \frac{\rho_2}{\rho_1} \tag{5.20}$$

as may be easily verified using the transformations (5.18) in (5.2). This factor is only due to ideal gas contributions; the excess free energy, which contains all potential-dependent static properties, is invariant under this transformation, explaining a number of static discoveries described in [184].

The correspondence is then valid in any phase diagram window where density and temperature are rescaled even by large factors, provided they are smaller than exponential in d (i.e. that temperatures are not rescaled exponentially in d), so that all points have the same r^*. Note that all reference to the (arbitrary) number $\widetilde{\beta}$ has disappeared; it only sets the constant that labels each line, but the lines are the same whatever the choice. Greater (exponential) changes of parameters modify the value of r^*, and through it the hardness of the potential $1/\alpha = A'(r^*)r^*$. This is the case even if one follows the same curve given by (5.19), for instance by performing an exponential compression and heating of the system, see figure 5.4. The mappings are in this case only approximate, except for the case where $1/\alpha = A'(r^*)r^* = \text{constant} \, \forall r^*$, i.e. the IPL potentials.

As an example, this is what happens for soft spheres if we compress the system way further than the jamming point of the corresponding HS system[6], such that there must be $O(1)$ overlaps (not just in the $1/d$ regime). Looking at equation (5.13), if r^* changes, α is modified as well, and if we want to have the smallest changes in the Mayer integral, we need that $\widetilde{\beta}$ and $\widetilde{\varphi}$ remain the same, meaning that we have to go to exponential changes in temperature and density according to equations (5.4) and (5.14). Conversely, introducing related exponential heating and compression of the system in this way, everything is just as if the effective diameter of the corresponding HS were decreased at order 1, and the *hardness* of the effective exponential potential were increased at order 1.

Note that, generalizing the above relations, one can map two systems at different state points 1 and 2 *and with different interaction potentials* given by their exponent A_1 and A_2. In this case only the first condition in (5.17) is modified and reads

$$r_1^* A_1'(r_1^*) = r_2^* A_2'(r_2^*) = \frac{1}{\alpha} \tag{5.21}$$

The same hardness $1/\alpha$ will generally imply different effective radii $r_1^* \neq r_2^*$, so that the two other equations become

$$\widetilde{\varphi}_1 e^c = \widetilde{\varphi}_2 = \widetilde{\varphi} = \rho_1 \mathcal{V}_d(r_1^*) e^c = \rho_2 \mathcal{V}_d(r_2^*)$$
$$\widetilde{\beta}_1 e^{-c/\alpha} = \widetilde{\beta}_2 = \widetilde{\beta} \tag{5.22}$$

The invariant curves will thus have the more general equation:

$$\widetilde{\beta}[\rho \mathcal{V}_d(r^*)]^{1/\alpha} = \text{constant} \tag{5.23}$$

5.5 Dynamics and reduced units

5.5.1 With the supersymmetric analogy

In order to discuss the dynamics in full generality, we go back to the setting of §3, confining the particles in a *box* consisting in the surface of a $d+1$-dimensional sphere of radius R, very large compared to the

---

[6]Their diameter being defined *by hand* in the HS model $V_{\text{HS}} = \epsilon\theta(\sigma - r)$, $\epsilon \to \infty$; or we can consider a potential of the exponential class and this diameter is defined by the initial regime of temperature and density once and for all.
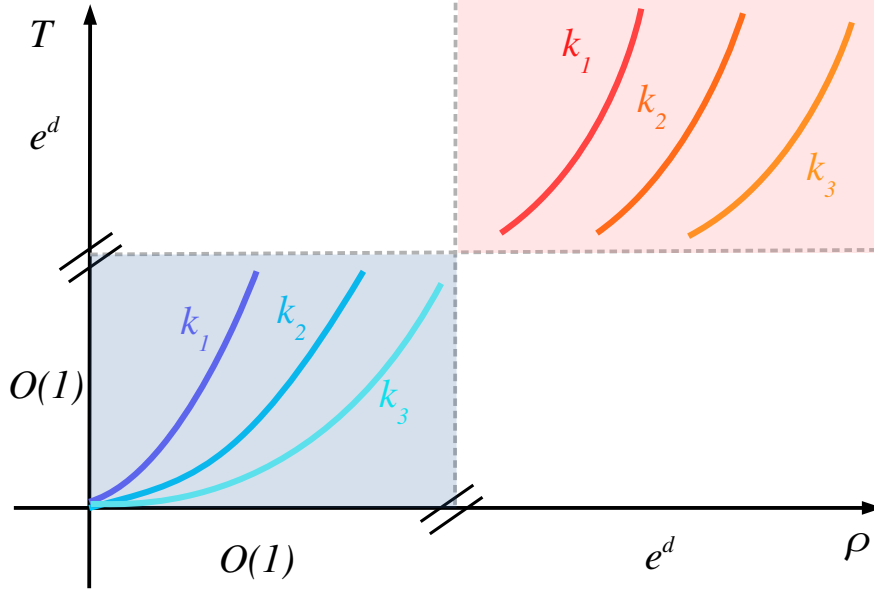
Figure 5.4: Isomorphs in the (T, ρ) phase diagram. The bottom-left quarter is a phase diagram of reference. Isomorphs are defined by $\rho^{1/\alpha}/T = k$, each isomorph corresponds to a certain value of the constant k, chosen by $\widetilde{\beta}$ (or $\widetilde{\varphi}$). One cannot extend these isomorphs for exponential changes of parameters since it would change the effective diameter r^* and thus the exponent α. In the top-right quarter, we consider an exponential change of parameters with dimension *with respect to* the phase diagram of reference in the bottom-left quarter. Isomorphs with the same constants as the previous ones exist but they are necessarily not the same, their exponent α is different: $\rho^{1/\alpha'}/T = k$.

interparticle distance. As mentioned in §5.2.2, replacing the effective hard sphere diameter σ by r^* here, the dynamical equation for correlation and responses are written in the compact SUSY form in §3.4.3.3 in terms of a superfield $\boldsymbol{Q}(a,b) = \frac{2d}{(r^*)^2} \boldsymbol{r}_a \cdot \boldsymbol{r}_b$ that encodes the correlation and response of a particle $\mathbf{r}$:

$$\beta^2 \boldsymbol{Q}^{-1}(a,b) = 2\beta^2 \boldsymbol{k}(a,b) - \beta^2 \boldsymbol{M}(a,b) + \beta^2[\boldsymbol{\nu}(a) + \boldsymbol{\delta\nu}(a)]\mathbf{1}(a,b) \tag{5.24}$$

Note that, only in this subsection, the bold letters refer to superfields.

In the next section, we will see that, owing to non-dimensionalization with appropriate units of energy, length and time, the first term $\beta^2 \boldsymbol{k}$ is independent of the control parameters (temperature and density). The last term is a Lagrange multiplier enforcing the spherical constraint $\boldsymbol{Q}(a,a) = \Delta_{\text{liq}} = 2d(R/r^*)^2$ ($\boldsymbol{\delta\nu}$ is similar to $\boldsymbol{M}$ in the sense that it has the same invariances) and thus can be expressed in terms of the other terms at equal time. In the end one needs to focus on the memory term, which will be in the correct form when multiplied by β^2, that depends explicitly on the control parameters[7]. Since $\tilde{r}$ plays the same role as μ in §3 and §4,

$$\beta^2 \boldsymbol{M}(a,b) = \frac{\widetilde{\varphi}}{2d} \int \mathrm{d}\lambda \, e^{\lambda - \Delta_{\text{liq}}/2} \left\langle \beta F(\widetilde{\boldsymbol{r}}(a) + \lambda) \beta F(\widetilde{\boldsymbol{r}}(b) + \lambda) \right\rangle$$
$$\langle \bullet \rangle = \frac{1}{\sqrt{\mathrm{sdet}\boldsymbol{Q}}} \int \mathrm{D}\widetilde{\boldsymbol{r}} \, \bullet \, e^{-\frac{1}{2} \int \mathrm{d}a \mathrm{d}b \, \widetilde{\boldsymbol{r}}(a)\beta^2 \boldsymbol{Q}^{-1}(a,b)\widetilde{\boldsymbol{r}}(b) - \int \mathrm{d}a \, \beta\bar{V}(\widetilde{\boldsymbol{r}}(a) + \lambda)} \tag{5.25}$$

we rescaled times a and b by a β factor. Then, the situation is similar to the statics' expression of §4.5.1. We have, expanding[8] again around r^*,

$$\beta^2 \boldsymbol{M}(a,b) = \frac{\widetilde{\varphi}}{2d} \int \mathrm{d}\lambda \, e^{\lambda - \Delta_{\text{liq}}/2} \left\langle \frac{\widetilde{\beta}}{\alpha} e^{-(\widetilde{\boldsymbol{r}}(a) + \lambda)/\alpha} \frac{\widetilde{\beta}}{\alpha} e^{-(\widetilde{\boldsymbol{r}}(b) + \lambda)/\alpha} \right\rangle$$
$$\langle \bullet \rangle = \frac{1}{\sqrt{\mathrm{sdet}\boldsymbol{Q}}} \int \mathrm{D}\widetilde{\boldsymbol{r}} \, \bullet \, e^{-\frac{1}{2} \int \mathrm{d}a \mathrm{d}b \, \widetilde{\boldsymbol{r}}(a)\beta^2 \boldsymbol{Q}^{-1}(a,b)\widetilde{\boldsymbol{r}}(b) - \int \mathrm{d}a \, \widetilde{\beta} e^{-(\widetilde{\boldsymbol{r}}(a) + \lambda)/\alpha}} \tag{5.26}$$

---

[7]Remember that the density scaling used was $\widehat{\varphi} = \widetilde{\varphi}/d$.

[8]Note that $F(\tilde{r}) = -\bar{V}'(\tilde{r}) = -\frac{r^*}{d} V' \left[r^* \left(1 + \tilde{r}/d \right) \right] = r^* A' \left[r^* \left(1 + \tilde{r}/d \right) \right] \exp \left\{ -dA \left[r^* \left(1 + \tilde{r}/d \right) \right] \right\}$.

We recover the same isomorphs, defined by (5.19), with the $O(1/d)$ shift of r^*, $\lambda \to \lambda + c$. This holds for equilibrium *as well as non-equilibrium* dynamics as for example in §3.10.

5.5.2 Without the supersymmetric analogy

For clarity we unveil the SUSY notation, in the simpler case of equilibrium dynamics; off-equilibrium equations can be treated in the same manner.

For equilibrium dynamics, where the initial condition at t_0 is picked with the canonical equilibrium probability, the self-consistent equations for finite times t may be written as, from §3.7.5:

$$
\begin{aligned}
\beta \widehat{m} \ddot{\tilde{r}}(t) + \beta \widehat{\gamma} \dot{\tilde{r}}(t) &= 1 - \int_{t_0}^t \mathrm{d}s\, \beta^2 M(t-s) \dot{\tilde{r}}(s) \\
&\quad - \beta \bar{V}'(\tilde{r}(t)) + \xi(t)\,, \\
\langle \xi(t) \rangle = 0\,, \quad \langle \xi(t)\xi(t') \rangle &= 2\beta \widehat{\gamma}\delta(t-t') + \beta^2 M(t-t')\,, \\
\beta^2 M(t-t') &= \frac{\widetilde{\varphi}}{2d} \int \mathrm{d}\tilde{r}_0\, e^{\tilde{r}_0 - \beta \bar{V}(\tilde{r}_0)} \langle \beta \bar{V}'(\tilde{r}(t)) \beta \bar{V}'(\tilde{r}(t')) \rangle
\end{aligned}
\tag{5.27}
$$

where $\widehat{m} = (r^*)^2 m / 2d^2$ and $\widehat{\gamma} = (r^*)^2 \gamma / 2d^2$, m being the physical mass and γ the coupling to the bath. If we set $\gamma = 0$ we have the purely Newtonian case, and with $m = 0$ the overdamped Brownian case.

5.5.2.1 Newtonian dynamics

For the purely Newtonian case, we adimensionalize these equations by setting $\tilde{t} = t/\sqrt{\widehat{m}\beta}$. We expand as before the potentials around r^* as $\beta V\left(r^*[1 + \tilde{r}(t)/d]\right) = \widetilde{\beta} e^{-\tilde{r}(t)/\alpha}$, and get:

$$
\begin{aligned}
\frac{\mathrm{d}^2 \tilde{r}}{\mathrm{d}\tilde{t}^2} &= - \int_{\tilde{t}_0}^{\tilde{t}} \mathrm{d}\tilde{s}\, \widetilde{M}(\tilde{t}-\tilde{s}) \frac{\mathrm{d}\tilde{r}}{\mathrm{d}\tilde{s}}(\tilde{s}) + \frac{\widetilde{\beta}}{\alpha} e^{-\tilde{r}(\tilde{t})/\alpha} + \widetilde{\xi}(\tilde{t}) \\
\text{with} \quad \langle \widetilde{\xi}(\tilde{t}) \rangle &= 0\,, \quad \langle \widetilde{\xi}(\tilde{t})\widetilde{\xi}(\tilde{t}') \rangle = \widetilde{M}(\tilde{t}-\tilde{t}')\,, \\
\widetilde{M}(\tilde{t}-\tilde{t}') &= \frac{\widetilde{\varphi}}{2d} \int \mathrm{d}\tilde{r}_0\, e^{\tilde{r}_0 - \beta \bar{V}(\tilde{r}_0)} \left\langle \frac{\widetilde{\beta}}{\alpha} e^{-\tilde{r}(\tilde{t})/\alpha} \frac{\widetilde{\beta}}{\alpha} e^{-\tilde{r}(\tilde{t}')/\alpha} \right\rangle
\end{aligned}
\tag{5.28}
$$

The tilde variables are rescalings in the new time units, e.g. $\widetilde{M}(\tilde{t}) = \beta^2 M(\tilde{t}\sqrt{\widehat{m}\beta})$ (nevertheless we kept the same symbol for $\tilde{r}$ to simplify the notation). Now, performing the shift $\tilde{r}(t) \to \tilde{r}(t) + c$, $\forall t$, we find exactly the same rescalings of parameters as in the static liquid phase computations, and once again the isomorphs are given by (5.19).

5.5.2.2 Brownian dynamics

For the purely Brownian case, we instead adimensionalize these equations by setting $\tilde{t} = t/\beta\widehat{\gamma}$, rescale the variables in the new time units, e.g. $\widetilde{M}(\tilde{t}) = \beta^2 M(\tilde{t}\beta\widehat{\gamma})$, and check that the translation $\tilde{r}(t) \to \tilde{r}(t) + c$ has the same effect as before:

$$
\begin{aligned}
\frac{\mathrm{d}\tilde{r}}{\mathrm{d}\tilde{t}} &= - \int_{\tilde{t}_0}^{\tilde{t}} \mathrm{d}\tilde{s}\, \widetilde{M}(\tilde{t}-\tilde{s}) \frac{\mathrm{d}\tilde{r}}{\mathrm{d}\tilde{s}}(\tilde{s}) + \frac{\widetilde{\beta}}{\alpha} e^{-\tilde{r}(\tilde{t})/\alpha} + \widetilde{\xi}(\tilde{t}) \\
\text{with} \quad \langle \widetilde{\xi}(\tilde{t}) \rangle &= 0\,, \quad \langle \widetilde{\xi}(\tilde{t})\widetilde{\xi}(\tilde{t}') \rangle = 2\delta(\tilde{t}-\tilde{t}') + \widetilde{M}(\tilde{t}-\tilde{t}')\,, \\
\widetilde{M}(\tilde{t}-\tilde{t}') &= \frac{\widetilde{\varphi}}{2d} \int \mathrm{d}\tilde{r}_0\, e^{\tilde{r}_0 - \beta \bar{V}(\tilde{r}_0)} \left\langle \frac{\widetilde{\beta}}{\alpha} e^{-\tilde{r}(\tilde{t})/\alpha} \frac{\widetilde{\beta}}{\alpha} e^{-\tilde{r}(\tilde{t}')/\alpha} \right\rangle
\end{aligned}
\tag{5.29}
$$

Interestingly, for the mixed case with friction and inertia, going from one state point to the other changes the ratio of inertial to bath intensities through an additional parameter $\widehat{\gamma}\sqrt{\beta/\widehat{m}}$. If this parameter is large (respectively small) when $d \to \infty$ then the equation of motion reduces to the Brownian (resp. purely Newtonian) case. The mixed dynamics is not fully invariant, although the correspondence is simple, and this only affects high frequency properties.

5.5.3   Reduced units

The unit of energy[9] is $1/\beta$, the unit of length is given by r^* and the unit of time is $r^*\sqrt{\beta m}$ for Newtonian dynamics and $\beta\gamma(r^*)^2$ for Brownian dynamics. This is precisely the units of [184] except that the unit of length is given there by $\rho^{-1/3}$. This is actually the same as an effective proper space per particle. If we impose an effective packing fraction $\widetilde{\varphi} = \rho\mathcal{V}_d(r^*)$ we must have $r^* \propto (\rho\Omega_d/d)^{-1/d}$; if we ignore the geometrical factor due to the sphericity of the spheres, which is a numerical constant in finite dimension, we have that $r^* \propto \rho^{-1/d}$.

All of this is not surprising because it is strictly dictated by dimensional analysis since there are very few relevant parameters.

5.6   Glassy phases of the system

Glassy phases of particle systems in the regime considered here have been studied in §4 and once again we go back to the spherical setting. The replicated free energy is given in terms of a replica matrix $Q_{ab} = \frac{2d}{(r^*)^2}\mathbf{r}_a \cdot \mathbf{r}_b$ that encodes the distance between the n replicas of a particle $\mathbf{r}$:

$$\frac{\beta F(\hat{Q})}{N} = n(\ln N - 1) - \frac{d}{2}n\ln\left(\frac{\pi e(r^*)^2}{d^2}\right) - \frac{d}{2}\ln\det\hat{Q} - \frac{\widetilde{\varphi}}{2}\int d\lambda \mathcal{D}_{\hat{Q}}\bar{\tilde{r}}\, e^{\lambda - \Delta_{\mathrm{liq}}/2}\left[e^{-\beta\sum_{a=1}^{n} V\left(r^*\left(1 + \frac{\tilde{r}_a + \lambda}{d}\right)\right)} - 1\right]$$

(5.30)

where

$$\mathcal{D}_{\hat{Q}}\bar{\tilde{r}} \equiv \frac{e^{-\frac{1}{2}\tilde{r}_a Q_{ab}^{-1}\tilde{r}_b}}{(2\pi)^{n/2}\sqrt{\det\hat{Q}}}\prod_{a=1}^{n}d\tilde{r}_a$$

(5.31)

$\Delta_{\mathrm{liq}} \equiv 2d(R/r^*)^2$ represents the size of the *box*. Even before making any ansatz for $\hat{Q}$, we may show that a mapping exists by defining $\widetilde{\beta}$ as in (5.4) and $\widetilde{\varphi}$ as in (5.14). Expanding each one of the Mayer terms around r^* as before:

$$\beta V\left(r^*\left(1 + \frac{\tilde{r}_a + \lambda}{d}\right)\right) = \widetilde{\beta}e^{-(\tilde{r}_a + \lambda)/\alpha}$$

(5.32)

we obtain the same equations as in the static case, but with the exponential potential $e^{-(\tilde{r}_a + \lambda)/\alpha}$. Using the translation $\lambda \to \lambda + c$, we conclude that condition (5.19) defines isomorphs in the glassy region of the phase diagram of the system as well.

Physical consequences of this invariance about *e.g.* aging and relaxation properties (among others) are given in [184]. Another example is that one can easily predict the dynamical transition point (or any other transition point, for example deep in the glass phase) of a system with a potential V_1 knowing the one of another potential V_2 if the regimes considered are such that their exponent α is the same, see §5.4. The result of this section in itself implies that the entire structure of metastable states is the same along points in an isomorph.

5.7   Virial-energy correlations

In [19, 184] a simple measure of the goodness of scaling relations was introduced via the virial-energy correlation coefficient (see §1.4). We recall its definition: the energy[10] and the so-called virial function [199]

$$\begin{aligned}
U &= \sum_{i<j} V(|\mathbf{r}_i - \mathbf{r}_j|) \\
W &= -\frac{1}{d}\sum_{i}\mathbf{r}_i \cdot \nabla_{\mathbf{r}_i}U
\end{aligned}$$

(5.33)

---

[9]Note that the force $F = -\bar{V}'$ has units of energy due to non-dimensionalization of $\tilde{r}$.

[10]We call the (internal) energy U here instead of H in the previous chapters since it is the standard denomination in the literature.

are used to define a virial-energy correlation coefficient $R \in [-1, 1]$ as

$$R = \frac{\langle \Delta W \Delta U \rangle}{\sqrt{\langle (\Delta W)^2 \rangle \langle (\Delta U)^2 \rangle}} \tag{5.34}$$

where $\Delta W = W - \langle W \rangle$ and brackets denote canonical equilibrium averages. A value close to unity is an indication of good scaling properties §1.4.

Here we show that $R = 1$ for large dimensions for any potential satisfying the *rather hard* condition.

5.7.1 Virial truncation

To compute R from (5.34) in high dimensions, the strategy we will use is again a virial truncation, detailed here.

One can easily show [20, Appendix B], that equilibrium fluctuations can be computed from derivatives of equilibrium averages. $Z = \sum_{\mathcal{C}} e^{-\beta U(\mathcal{C})}$ is the canonical partition function and $\mathcal{C}$ labels a microstate (configuration of the particles). We have:

$$\langle \mathcal{O} \rangle = \frac{\sum_{\mathcal{C}} \mathcal{O}(\mathcal{C}) e^{-\beta U(\mathcal{C})}}{Z}$$

$$\frac{\partial \langle \mathcal{O} \rangle}{\partial \beta} = -\frac{\sum_{\mathcal{C}} \mathcal{O}(\mathcal{C}) U(\mathcal{C}) e^{-\beta U(\mathcal{C})}}{Z} + \frac{\sum_{\mathcal{C}} \mathcal{O}(\mathcal{C}) e^{-\beta U(\mathcal{C})} \sum_{\mathcal{C}'} U(\mathcal{C}') e^{-\beta U(\mathcal{C}')}}{Z^2} \tag{5.35}$$

$$= -\langle \mathcal{O} U \rangle + \langle \mathcal{O} \rangle \langle U \rangle = -\langle \Delta \mathcal{O} \Delta U \rangle$$

hence

$$\langle \Delta W \Delta U \rangle = -\frac{\partial \langle W \rangle}{\partial \beta} \tag{5.36}$$

and similarly with $\beta F = -\ln Z$ we get the second moment

$$\left\langle (\Delta U)^2 \right\rangle = -\frac{\partial^2 (\beta F)}{\partial \beta^2} = \frac{\mathcal{V}}{2} \int d\mathbf{r} \, V(r)^2 e^{-\beta V(r)} \tag{5.37}$$

using the expression of the liquid free energy (5.2).

One can relate generically the equilibrium value of the virial function to the equation of state of the system. The argument is the following [199]. We enclose the system in a *box* whose boundaries can be used to measure the equilibrium pressure of the system. Then we define the total virial function

$$\mathcal{W}(\mathbf{r}_1, \ldots, \mathbf{r}_N) = \frac{1}{d} \sum_{i=1}^{N} \mathbf{r}_i \cdot \mathbf{F}_i \tag{5.38}$$

with $\mathbf{F}_i = \mathbf{F}_i^{\text{int}} + \mathbf{F}_i^{\text{ext}}$ the total force on particle i, consisting in the interactions between the particles $\mathbf{F}_i^{\text{int}} = -\nabla_{\mathbf{r}_i} U$ and the forces exerted by the boundaries to confine the system in the box $\mathbf{F}_i^{\text{ext}}$. From Newton's laws we find, together with an integration by parts[11],

$$\langle \mathcal{W} \rangle_t = \frac{1}{d} \lim_{\tau \to \infty} \frac{1}{\tau} \int_0^\tau dt \sum_{i=1}^{N} \mathbf{r}_i(t) \cdot \mathbf{F}_i(t) = \frac{1}{d} \lim_{\tau \to \infty} \frac{1}{\tau} \int_0^\tau dt \sum_{i=1}^{N} \mathbf{r}_i(t) \cdot m \ddot{\mathbf{r}}_i(t)$$

$$= -\frac{1}{d} \lim_{\tau \to \infty} \frac{1}{\tau} \int_0^\tau dt \sum_{i=1}^{N} m |\dot{\mathbf{r}}_i(t)|^2 = -NT \tag{5.39}$$

In the last line[12] we used the ergodic hypothesis of statistical physics to connect dynamical averages to equilibrium averages and applied the equipartition theorem. As for the forces we can separate the virial contributions between the internal part $W = \frac{1}{d} \sum_{i=1}^{N} \mathbf{r}_i \cdot \mathbf{F}_i^{\text{int}}$ and the external one $\mathcal{W}^{\text{ext}} = \frac{1}{d} \sum_{i=1}^{N} \mathbf{r}_i \cdot \mathbf{F}_i^{\text{ext}}$. The latter is related to the equilibrium pressure; for a large number of particles we can replace the discrete sum by an integral over the boundaries, where the $\mathbf{F}_i^{\text{ext}}$ have a non-zero contribution and their value on a particle at $\mathbf{r}$ is $-\mathbf{n}dS$ with dS the surface element at $\mathbf{r}$ and $\mathbf{n}$ a unit vector directed outwards. We get:

$$\langle \mathcal{W}^{\text{ext}} \rangle = -\frac{1}{d} P \int_S dS \, \mathbf{r} \cdot \mathbf{n} = -\frac{1}{d} P \int_{\mathcal{V}} d\mathcal{V} \, \nabla \cdot \mathbf{r} = -P\mathcal{V} \tag{5.40}$$

---

[11]The boundary term is not *extensive in time* and is suppressed by the factor $1/\tau$ in the $\tau \to \infty$ limit.
[12]This is akin to the virial theorem of classical mechanics [244].

from the divergence theorem. Equations (5.39) and (5.40) provide the virial equation of liquid theory [199]:

$$PV = NT + \langle W \rangle \qquad \Longleftrightarrow \qquad \frac{\beta P}{\rho} = 1 + \frac{\beta}{N} \langle W \rangle \tag{5.41}$$

Hence we use the equation of state in (5.2) and find

$$\langle W \rangle = -\frac{\mathcal{V}}{2\beta} \int d\mathbf{r} \left(e^{-\beta V(r)} - 1 \right)$$

$$\frac{\partial \langle W \rangle}{\partial \beta} = -\frac{\mathcal{V}}{2\beta^2} \int d\mathbf{r} \left(e^{-\beta V(r)} - 1 \right) - \frac{\mathcal{V}}{2\beta} \int d\mathbf{r}\, V(r) e^{-\beta V(r)} \tag{5.42}$$

We now need an expression for $\langle (\Delta W)^2 \rangle = \langle W^2 \rangle - \langle W \rangle^2$. Let us define the pair distribution function [199, 293]

$$\rho^{(2)}(\mathbf{x}, \mathbf{y}) = \sum_{i \neq j} \delta(\mathbf{x} - \mathbf{r}_i) \delta(\mathbf{y} - \mathbf{r}_j) \tag{5.43}$$

Note that

$$\sum_i \mathbf{r}_i \cdot \nabla_{\mathbf{r}_i} U = \sum_{i \neq j} \mathbf{r}_i \cdot \nabla_i V(|\mathbf{r}_i - \mathbf{r}_j|) = \frac{1}{2} \sum_{i \neq j} \mathbf{r}_i \cdot \nabla_i V(|\mathbf{r}_i - \mathbf{r}_j|) + \frac{1}{2} \sum_{i \neq j} \mathbf{r}_j \cdot \nabla_j V(|\mathbf{r}_j - \mathbf{r}_i|)$$

$$= \frac{1}{2} \sum_{i \neq j} |\mathbf{r}_i - \mathbf{r}_j| V'(|\mathbf{r}_i - \mathbf{r}_j|) \tag{5.44}$$

therefore

$$\langle W \rangle = -\frac{1}{2d} \int d\mathbf{x} d\mathbf{y} \left\langle \rho^{(2)}(\mathbf{x}, \mathbf{y}) \right\rangle |\mathbf{x} - \mathbf{y}| V'(|\mathbf{x} - \mathbf{y}|) = -\frac{N}{2d} \rho \int d\mathbf{r}\, r g(r) V'(r) \tag{5.45}$$

where $g(r)$ is the radial distribution function [199, 293]. The lowest-order virial contribution to the radial distribution function is $g(r) = e^{-\beta V(r)}$ [199, 293, 342]. This is consistent with (5.42) since with an integration by parts

$$\frac{1}{d} \int d\mathbf{r}\, r g(r) V'(r) = \frac{\Omega_d}{d} \int dr\, r^d e^{-\beta V(r)} V'(r) = -\frac{\Omega_d}{\beta d} \underbrace{\left[(e^{-\beta V(r)} - 1) r^d \right]_0^\infty}_{=0} + \frac{\Omega_d}{\beta} \int dr\, r^{d-1} \left(e^{-\beta V(r)} - 1 \right)$$

$$= \frac{1}{\beta} \int d\mathbf{r} \left(e^{-\beta V(r)} - 1 \right) \tag{5.46}$$

Similarly,

$$\left\langle W^2 \right\rangle = \frac{1}{4d^2} \int d\mathbf{x}_1 d\mathbf{x}_2 d\mathbf{x}_3 d\mathbf{x}_4 \left\langle \rho^{(2)}(\mathbf{x}_1, \mathbf{x}_2) \rho^{(2)}(\mathbf{x}_3, \mathbf{x}_4) \right\rangle |\mathbf{x}_1 - \mathbf{x}_2| |\mathbf{x}_3 - \mathbf{x}_4| V'(|\mathbf{x}_1 - \mathbf{x}_2|) V'(|\mathbf{x}_3 - \mathbf{x}_4|)$$

$$= \frac{V^2}{4d^2} \int d\mathbf{x} d\mathbf{y} \left\langle \rho^{(2)}(\mathbf{0}, \mathbf{x}) \rho^{(2)}(\mathbf{0}, \mathbf{y}) \right\rangle |\mathbf{x}| |\mathbf{y}| V'(|\mathbf{x}|) V'(|\mathbf{y}|) \tag{5.47}$$

To get $\left\langle \rho^{(2)}(\mathbf{0}, \mathbf{x}) \rho^{(2)}(\mathbf{0}, \mathbf{y}) \right\rangle$ we will use the lowest order in its virial expansion. Working with the grand-canonical partition function, we have [293]

$$\Xi = \sum_{N \geqslant 0} \frac{e^{\beta \mu N}}{N!} \int d\mathbf{r}_1 \ldots d\mathbf{r}_N \prod_{i < j} e^{-\beta V(\mathbf{r}_i, \mathbf{r}_j)} = \sum_{N \geqslant 0} \frac{e^{\beta \mu N}}{N!} \int d\mathbf{r}_1 \ldots d\mathbf{r}_N e^{-\frac{\beta}{2} \int d\mathbf{x} d\mathbf{y}\, \rho^{(2)}(\mathbf{x}, \mathbf{y}) V(\mathbf{x}, \mathbf{y})} \tag{5.48}$$

$$\ln \Xi = N(1 - \ln \rho - \beta \mu) + \frac{1}{2} \int d\mathbf{x} d\mathbf{y}\, \rho(\mathbf{x}) \rho(\mathbf{y}) \left(e^{-\beta V(\mathbf{x}, \mathbf{y})} - 1 \right)$$

where here $\rho(\mathbf{x}) = \left\langle \sum_i \delta(\mathbf{x} - \mathbf{r}_i) \right\rangle$ is the equilibrium local density as in liquid theory [199, 293]. Each line of (5.48) is respectively used to derive the corresponding lines below:

$$\frac{\delta^2 \ln \Xi}{\delta V(\mathbf{x}, \mathbf{y}) \delta V(\mathbf{r}, \mathbf{r}')} = \frac{\beta^2}{4} \left[\left\langle \rho^{(2)}(\mathbf{x}, \mathbf{y}) \rho^{(2)}(\mathbf{r}, \mathbf{r}') \right\rangle - \left\langle \rho^{(2)}(\mathbf{x}, \mathbf{y}) \right\rangle \left\langle \rho^{(2)}(\mathbf{r}, \mathbf{r}') \right\rangle \right]$$

$$= \frac{\beta^2}{2} \rho(\mathbf{x}) \rho(\mathbf{y}) \delta(\mathbf{x} - \mathbf{r}) \delta(\mathbf{y} - \mathbf{r}') e^{-\beta V(\mathbf{x}, \mathbf{y})} \tag{5.49}$$

Multiplying (5.49) by $|\mathbf{x} - \mathbf{y}||\mathbf{r} - \mathbf{r}'|V'(|\mathbf{x} - \mathbf{y}|)V'(|\mathbf{r} - \mathbf{r}'|)$ and integrating over $\mathbf{x}$, $\mathbf{y}$, $\mathbf{r}$ and $\mathbf{r}'$ we can make the connection with $\langle(\Delta W)^2\rangle$ and obtain[13]

$$\left\langle (\Delta W)^2 \right\rangle = \left\langle W^2 \right\rangle - \left\langle W \right\rangle^2 = \frac{2\rho^2}{4d^2} \int d\mathbf{x} d\mathbf{y}\, e^{-\beta V(|\mathbf{x}-\mathbf{y}|)} (\mathbf{x} - \mathbf{y})^2 V'(|\mathbf{x} - \mathbf{y}|)^2 = \frac{N\rho}{2d^2} \int d\mathbf{r}\, r^2 V'(r)^2 e^{-\beta V(r)} \tag{5.50}$$

All in all, (5.34), (5.37) and (5.50) gives for the correlation coefficient

$$R \underset{d\to\infty}{\sim} -d \frac{\int d\mathbf{r}\left(e^{-\beta V(r)} - 1\right) + \beta \int d\mathbf{r}\, V(r)e^{-\beta V(r)}}{\beta^2 \sqrt{\int d\mathbf{r}\, r^2 V'(r)^2 e^{-\beta V(r)} \int d\mathbf{r}'\, V(r')^2 e^{-\beta V(r')}}} = -\frac{\int d\mathbf{r}\,[rV'(r) + dV(r)]e^{-\beta V(r)}}{\beta \sqrt{\int d\mathbf{r}\, r^2 V'(r)^2 e^{-\beta V(r)} \int d\mathbf{r}'\, V(r')^2 e^{-\beta V(r')}}} \tag{5.51}$$

through an integration by parts.

Here we can also confirm, in the light of §4.6, that considering the MK model as in §4 leads to the same results. One has

$$\frac{\delta^2 \ln \overline{Z^n}}{\delta V(\bar{x}, \bar{y}) \delta V(\bar{r}, \bar{r}')} = \frac{\beta^2}{4} \overline{\left\langle \rho^{(2)}(\bar{x}, \bar{y}) \rho^{(2)}(\bar{r}, \bar{r}') \right\rangle} - \frac{\beta^2}{4} \overline{\left\langle \rho^{(2)}(\bar{x}, \bar{y}) \right\rangle} \, \overline{\left\langle \rho^{(2)}(\bar{r}, \bar{r}') \right\rangle}$$
$$= \frac{\beta^2}{2} \rho(\bar{x}) \rho(\bar{y}) \delta(\bar{x} - \bar{r}) \delta(\bar{y} - \bar{r}') e^{-\beta V(\bar{x}, \bar{y})} \tag{5.52}$$

Here $\rho(\bar{x}) = \overline{\left\langle \sum_i \delta(\bar{x} - \bar{x}_i) \right\rangle}$ as in liquid theory. The second line uses the $d \to \infty$ limit in which $\ln \overline{Z^n} = N\mathcal{S}(\rho)$ is given[14] by (4.17), while the first line is obtained with the definition of the averaged replicated partition function (4.7),

$$\overline{Z^n} = \int d\bar{X}\, e^{-\frac{\beta}{2} \int d\bar{x} d\bar{y}\, \rho^{(2)}(\bar{x}, \bar{y}) V(\bar{x}, \bar{y})}$$
$$\frac{\delta^2 \ln \overline{Z^n}}{\delta V(\bar{x}, \bar{y}) \delta V(\bar{r}, \bar{r}')} = \frac{1}{\overline{Z^n}} \frac{\delta^2 \overline{Z^n}}{\delta V(\bar{x}, \bar{y}) \delta V(\bar{r}, \bar{r}')} - \frac{1}{\overline{Z^n}} \frac{\delta \overline{Z^n}}{\delta V(\bar{x}, \bar{y})} \frac{1}{\overline{Z^n}} \frac{\delta \overline{Z^n}}{\delta V(\bar{r}, \bar{r}')} \tag{5.53}$$

Note that the identification

$$\overline{\left\langle \rho^{(2)}(\bar{x}, \bar{y}) \right\rangle} = \overline{\frac{1}{Z^n} \int d\bar{X}\, e^{-\beta \sum_a H[X_a]} \rho^{(2)}(\bar{x}, \bar{y})} \sim \frac{1}{\overline{Z^n}} \overline{\int d\bar{X}\, e^{-\beta \sum_a H[X_a]} \rho^{(2)}(\bar{x}, \bar{y})} \tag{5.54}$$

holds only in the $n \to 0$ limit where $Z^n \to 1$.

As in the previous derivation, multiplying (5.52) by $|\bar{x} - \bar{y}||\bar{r} - \bar{r}'|V'(|\bar{x} - \bar{y}|)V'(|\bar{r} - \bar{r}'|)$ and integrating over $\bar{x}$, $\bar{y}$, $\bar{r}$ and $\bar{r}'$ we can make the connection with $\langle(\Delta W)^2\rangle$ taking the limit $n \to 0$. We have, for example,

$$\frac{1}{2} \int d\bar{x} d\bar{y}\, |x^1 - y^1|V'(|x^1 - y^1|) \overline{\left\langle \rho^{(2)}(\bar{x}, \bar{y}) \right\rangle} = \frac{1}{2} \overline{\frac{1}{Z^n} \int d\bar{X}\, e^{-\beta \sum_a H[X_a]} \sum_{i \neq j} |x_i^1 - \mathcal{R}_{ij} x_j^1| V'(|x_i^1 - \mathcal{R}_{ij} x_j^1|)}$$
$$= \overline{\frac{1}{Z} \int dX\, e^{-\beta H[X]} \sum_{i < j} |x_i - \mathcal{R}_{ij} x_j| V'(|x_i - \mathcal{R}_{ij} x_j|)}$$
$$= \int d\mathbf{x} \overline{\left\langle \rho^{(2)}(\mathbf{0}, \mathbf{x}) \right\rangle} |\mathbf{x}| V'(|\mathbf{x}|) \ . \tag{5.55}$$

The bold letters refer to vectors, in the replicated MK model in §4 we do not use this notation for clarity, so here they are mixed. With a very similar calculation one can treat the other terms. Hence we get (5.50).

We can write (5.51) with explicit inverse temperature factors:

$$R = -\frac{\int d\mathbf{r}\,[r\beta V'(r) + d\beta V(r)]e^{-\beta V(r)}}{\sqrt{\int d\mathbf{r}\, r^2 \beta^2 V'(r)^2 e^{-\beta V(r)} \int d\mathbf{r}'\, \beta^2 V(r')^2 e^{-\beta V(r')}}} \tag{5.56}$$

---

[13] Here we considered only the first term of the virial expansion, but one may wonder if doing the second derivatives with respect to the potential used here and then using the infinite-dimensional limit affects this truncation, leading to consider higher-order diagrams. One can check, for example with the triangle term ⟁, that it does not since the factors $|\mathbf{x} - \mathbf{y}||\mathbf{r} - \mathbf{r}'|V'(|\mathbf{x} - \mathbf{y}|)V'(|\mathbf{r} - \mathbf{r}'|)$ play a similar role to reintroducing the missing Mayer functions due to derivation.

[14] Note that in (4.17) the notation is $\rho(\bar{x}) = \frac{1}{N} \left\langle \sum_i \delta(\bar{x} - \bar{x}_i) \right\rangle$.

5.7.2   The case of the exponential potentials

In the integrals of (5.56) the situation is similar to the Mayer integral in §5.2, with the potential $\beta V = \beta e^{-dA}$ playing the role of the Mayer function $e^{-\beta V} - 1$. We can make a similar analysis as in §5.2, comparing contributions of an integrand of the type $r^d \beta V(r) e^{-\beta V(r)}$:

- for $r < r^*$: $\quad r^d \beta V(r) e^{-\beta V(r)} = r^d \widetilde{\beta} e^{d(A(r^*) - A(r))} \exp[-\widetilde{\beta} e^{d(A(r^*) - A(r))}]$

- for $r \sim r^*$: $\quad (r^*)^d \widetilde{\beta} e^{-\widetilde{\beta}}$ (5.57)

- for $r > r^*$: $\quad r^d \beta V(r) e^{-\beta V(r)} \sim r^d \widetilde{\beta} e^{d(A(r^*) - A(r))}$

Still under the same hypothesis that $\left[\ln r - A(r)\right]_r^{r^*} > 0$, the first regime $r < r^*$ is strongly damped by the Boltzmann factor, and the other two regimes $r \sim r^*$ and $r > r^*$ compares exactly to the Mayer integral, where the same conditions apply. The other term in the numerator of (5.56) involves $rV'(r)$ and is treated the same way. In the denominator, the analysis is the same except that due to the power 2 we will need the condition that $\ln r - 2A(r)$ decreases instead, for the region around r^* to dominate the integral; since this means that $A'(r) > 1/2r$ it is less constraining than the previous condition $\ln r - A(r)$ decreases[15], so it is automatically fulfilled with the latter condition. Therefore we expand the integral involved in (5.56) as we did in the paper: we set $r = r^*(1 + \tilde{r}/d)$, and around $r = r^*$ we have

$$r \beta V'(r) = -dr A'(r) \beta V(r) \sim -dr^* A'(r^*) \beta V(r^*) e^{-\tilde{r}/\alpha} = -d \frac{\widetilde{\beta}}{\alpha} e^{-\tilde{r}/\alpha} \quad \text{and} \quad \beta V(r) \sim \widetilde{\beta} e^{-\tilde{r}/\alpha} \quad (5.58)$$

so that the virial-energy correlation coefficient becomes

$$R \underset{d \to \infty}{\sim} \frac{1 - \alpha}{\widetilde{\beta}} \frac{\int_{-\infty}^{\infty} \mathrm{d}\tilde{r}\, e^{\tilde{r}(1 - 1/\alpha) - \widetilde{\beta} \exp(-\tilde{r}/\alpha)}}{\int_{-\infty}^{\infty} \mathrm{d}\tilde{r}\, e^{\tilde{r}(1 - 2/\alpha) - \widetilde{\beta} \exp(-\tilde{r}/\alpha)}}$$

$$\underset{x \equiv \widetilde{\beta} e^{-\tilde{r}/\alpha}}{=} (1 - \alpha) \frac{\int_0^\infty \mathrm{d}x\, x^{-\alpha} e^{-x}}{\int_0^\infty \mathrm{d}x\, x^{1-\alpha} e^{-x}} = (1 - \alpha) \frac{\Gamma(1 - \alpha)}{\Gamma(2 - \alpha)} = 1 \quad (5.59)$$

We conclude that all liquids within the class of potentials considered here are strongly correlated in high dimension, which is expected in light of the work of Dyre, Schrøder et al., since we find the existence of exact isomorphs.

An alternative, quicker way, is to recognize that any potential may be substituted by an inverse power law potential $V(r) \propto (r^*/r)^{d/\alpha}$ once the value of r^* is fixed such that $1/\alpha = r^* A'(r^*)$, which implies $R = 1$.

Another way to see it is that in $d \to \infty$ with an exponential potential $V(r) = e^{-dA(r)}$ we have $rV'(r) = -dr A'(r) V(r)$. $dr A'(r) = O(d)$ does not play any role for saddle point considerations and will essentially be equal to $dr^* A'(r^*) = d/\alpha$, so we expect once again perfect correlation between W, linked to a sum of terms $\sim rV'(r)$ with r an interparticle distance, and U, linked to $V(r)$.

5.7.3   The slope of the isomorphs

In [184] it is argued that isomorphs are given by

$$\frac{\rho^{\gamma(\rho)}}{T} = \text{constant}, \qquad \text{where} \quad \gamma = \frac{\langle \Delta W \Delta U \rangle}{\langle (\Delta U)^2 \rangle} \quad (5.60)$$

For IPL systems with $V_{\mathrm{IPL}} \propto r^{-n}$, the equation of the isomorphs is exact with $\gamma = n/d$; since this value is also $\langle \Delta W \Delta U \rangle / \langle (\Delta U)^2 \rangle$, this has been proposed in [184] to be a good simple measure of this exponent (called *slope of isomorphs*), and is actually well verified in simulations for a wide range of strongly correlating potentials [184, 348, 19].

---

[15] Actually the condition is $\left[\ln r - A(r)\right]_r^{r^*} > 0$ which is weaker than $\ln r - A(r)$ decreases, but this is to fix ideas.

As in the previous subsections one gets in $d \to \infty$

$$
\begin{aligned}
\gamma = \frac{\langle \Delta W \Delta U \rangle}{\langle (\Delta U)^2 \rangle} &\underset{d \to \infty}{\sim} -\frac{\int d\mathbf{r} \left(e^{-\beta V(r)} - 1 \right) + \beta \int d\mathbf{r}\, V(r) e^{-\beta V(r)}}{\beta^2 \int d\mathbf{r}\, V(r)^2 e^{-\beta V(r)}} \\
&= -\frac{1}{d} \frac{\int d\mathbf{r}\, [rV'(r) + dV(r)] e^{-\beta V(r)}}{\beta \int d\mathbf{r}\, V(r)^2 e^{-\beta V(r)}} \sim \frac{1/\alpha - 1}{\widetilde{\beta}} \frac{\int_{-\infty}^{\infty} d\tilde{r}\, e^{\tilde{r}(1 - 1/\alpha) - \widetilde{\beta} \exp(-\tilde{r}/\alpha)}}{\int_{-\infty}^{\infty} d\tilde{r}\, e^{\tilde{r}(1 - 2/\alpha) - \widetilde{\beta} \exp(-\tilde{r}/\alpha)}} = \frac{R}{\alpha} = \frac{1}{\alpha}
\end{aligned}
\tag{5.61}
$$

This is exactly what we have found, see (5.19). Once again, it is no surprise if one recognizes that any potential may be substituted by an inverse power law potential $V(r) \propto (r^*/r)^n$ with $n = d/\alpha$ once the value of r^* is fixed such that $1/\alpha = r^* A'(r^*)$.

5.8 Other types of potentials

Other potentials can be considered, analyzing the Mayer integral in the same way. The case of a sum of exponential potentials (5.1) with different interaction ranges (measured by α) is straightforward: for a given temperature (thus r^*), only one of the terms will dominate. This case has been thought to be generic in [18, 19]; in high d the situation does not give further hints since the demarcation is too sharp due to the scalings. In finite d all exponentials mix their ranges and the situation is more complex, and is analog to the Lennard-Jones potential in the peculiar regime of $O(1)$ temperature analyzed below.

The situation is more entangled if we consider terms with different signs or same interaction ranges. The Lennard-Jones (LJ) potential belongs to this class[16]; its study can readily be done along the same lines and its interest also lies in the fact that it is directly relevant for three-dimensional liquids and glasses [199, 21, 348, 105, 50, 51, 52]. This potential can be generalized in d-dimensions as

$$
V_{\mathrm{LJ}}(r) = \epsilon \left[\left(\frac{r}{\sigma} \right)^{-4d} - \left(\frac{r}{\sigma} \right)^{-2d} \right]
\tag{5.62}
$$

The Mayer function is very similar: it is -1 at short distance, then there is an $O(1)$ part over a range $O(1/d)$ around σ where there is a positive bump, and it is exponentially small at large distances. For
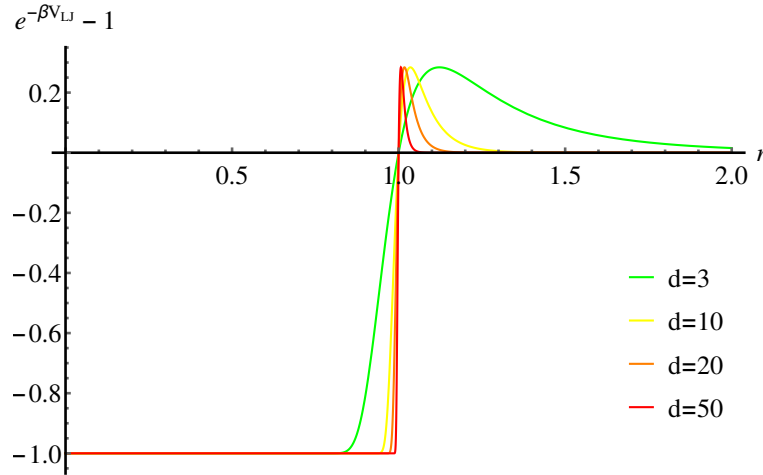

Figure 5.5: The Lennard-Jones Mayer function for $\beta\epsilon = 1$, $\sigma = 1$ and $d = 3, 10, 20, 50$.

exponentially high temperatures, one can define a $r^* < \sigma$ where only the repulsive IPL term plays a role; one thus finds trivial isomorphs. The interesting regime is when the temperature is $O(1)$. Then r^* is defined in the $O(1/d)$ region close to σ where attractive and repulsive parts compete. We can expand the potential once again setting $r = r^*(1 + \tilde{r}/d)$, giving an effective potential

$$
\beta V_{\mathrm{LJ}}(r) \sim \widetilde{\beta} \widetilde{V}_{\mathrm{LJ}}^{\mathrm{eff}}(\tilde{r}) = \widetilde{\beta}(e^{-4\tilde{r}} - e^{-2\tilde{r}})
\tag{5.63}
$$

Here the previous scaling transformations does not provide an invariance since the two exponentials have a different *exponent* α. One can still demand that the static liquid excess free energy $F_{\mathrm{ex}}(\rho, T) = \text{constant}$,

---

[16]A similar discussion can be made with the Weeks-Chandler-Anderson potential [402, 88].

defining generally lines. But these lines will not have a dynamic (respectively glassy static) counterpart, which would depend upon the times (respectively the replica *blocks*) considered. Indeed, as in §5.5.1, one could look to an invariance of the dynamic memory kernel $\boldsymbol{M}(a,b)$. If we generically demand it to be a constant, the lines in the (T,ρ) phase diagram will depend upon the time (t,t') considered; the same reasoning applies to the static memory kernel M_{ab} where these lines would depend upon the replica indices a,b, in the case of a non-replica-symmetric order parameter.

Thus in this regime there are no isomorphs. One could write the LJ potential (5.62) as an exponential potential (5.1), but the assumption which is not fulfilled here is that $A(r)$ becomes discontinuous at $r=\sigma$: one cannot expand $A(r)$ around this point and the previous analysis does not hold.

One can look to the virial-energy correlation coefficient in this regime, as in §5.7 by computing the dominant contribution (around r^*) of the formula (5.56), giving

$$R_{\mathrm{LJ}} \underset{d\to\infty}{\sim} -\frac{1}{\widetilde{\beta}} \frac{\int_{-\infty}^{\infty} d\tilde{r}\,(-3e^{-4\tilde{r}}+e^{-2\tilde{r}})e^{\tilde{r}-\widetilde{\beta}(e^{-4\tilde{r}}-e^{-2\tilde{r}})}}{\sqrt{\int_{-\infty}^{\infty} d\tilde{r}\,(-4e^{-4\tilde{r}}+2e^{-2\tilde{r}})^2 e^{\tilde{r}-\widetilde{\beta}(e^{-4\tilde{r}}-e^{-2\tilde{r}})} \int_{-\infty}^{\infty} d\tilde{r}\,(e^{-4\tilde{r}}-e^{-2\tilde{r}})^2 e^{\tilde{r}-\widetilde{\beta}(e^{-4\tilde{r}}-e^{-2\tilde{r}})}}} \tag{5.64}$$

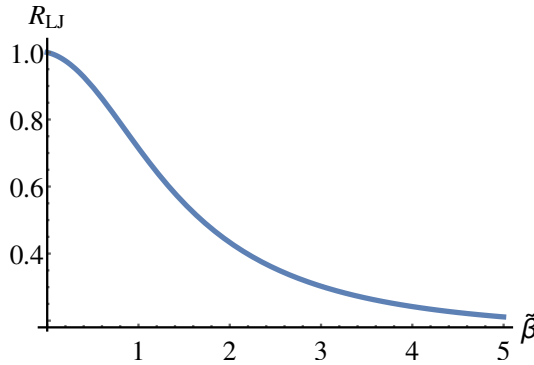We plot in figure 5.6 the virial-energy correlation coefficient in this regime. We note accordingly that the

Figure 5.6: The correlation coefficient $R_{\mathrm{LJ}}(\widetilde{\beta})$ for the peculiar regime of $O(1)$ temperature.

WU correlation coefficient is less than one, except in the *infinite* temperature limit $\widetilde{\beta}\to 0$ within this regime. Indeed at high temperature only the repulsive IPL term is felt by the system. It coincides with trying to shift r^* to lower values where only this term is relevant, and where the isomorphs are exact.

5.9   Discussion

5.9.1   Simulation results from the Roskilde group

In a very recent paper following this work [106], Costigliola, Schrøder and Dyre (CSD) showed numerical evidence that in $d=2$, 3 and 4 in Lennard-Jones systems, both the virial-energy correlation coefficient R approaches quickly 1 and scale invariances become increasingly good with increasing dimension, which is to be expected on the basis of this work. In this section we reproduce some of their results to illustrate the isomorph concept as well. The system studied is a standard Lennard-Jones liquid:

$$V_{\mathrm{LJ}}(r) = 4\varepsilon \left[\left(\frac{\sigma}{r}\right)^{12} - \left(\frac{\sigma}{r}\right)^{6} \right] \tag{5.65}$$

Our hypothesis of scaling the potential with d, as in (5.62), is not respected. However, in such low dimensions it is probably hard to see any difference: we expect that it would give even worse results since this makes the Mayer function less clear-cut than if they had scaled it with d, see figure 5.5. The entropic drive due to the increase of the space's *volume*, which is taken into account in their simulations by changing space dimensionality, is the dominant effect here. Despite this, they obtain a very good approximate scale invariance, which foretells that the behaviour of this system quickly converges to the infinite-dimensional one.

5.9.1.1 Invariance of the static structure

CSD investigated the radial pair distribution function in these dimensions, see figure 5.7. It indicates that, as expected, the structure above the first coordination shell becomes trivial, with $g(r)$ quickly approaching a steady value of 1. Direct isomorph invariance has been checked in $d = 4$, in which $g(r)$ for different state points collapses into the same curve using the rescaled distance $\tilde{\mathbf{r}} = \rho^{1/4}\mathbf{r}$. Similar results pointing at the flattening of $g(r)$ for increasing dimensions 2 to 5 had been obtained by Bishop, Whitlock and Klein and by Charbonneau's group for the HS system [65, Fig.7].
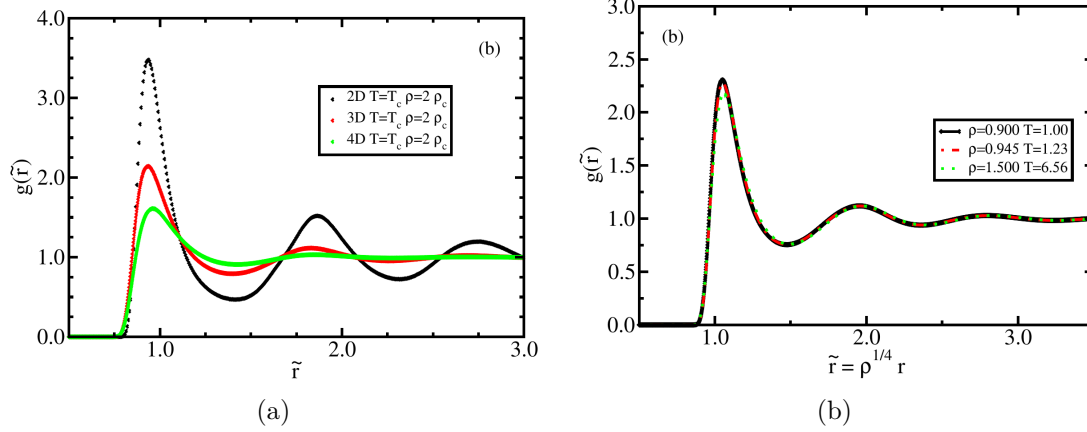

Figure 5.7: (a) Radial pair distribution function along the critical liquid-vapour isotherm in $d = 2, 3, 4$ in reduced units $\tilde{\mathbf{r}} = \rho^{1/d}\mathbf{r}$. (b) Radial pair distribution function at three isomorphic state points in four dimensions. [*Reprinted from* [106]]

5.9.1.2 *WU* correlations

This scale invariance (to a very good approximation) is verified by the computation of the virial-energy coefficient reproduced in figure 5.8, which is shown to quickly approach 1 as the dimension is increased. Notice that the LJ system is already a good strongly-correlating liquid in $d = 3$ [348], in regions of the phase diagram not too far from the melting line and in the solid phase as well.
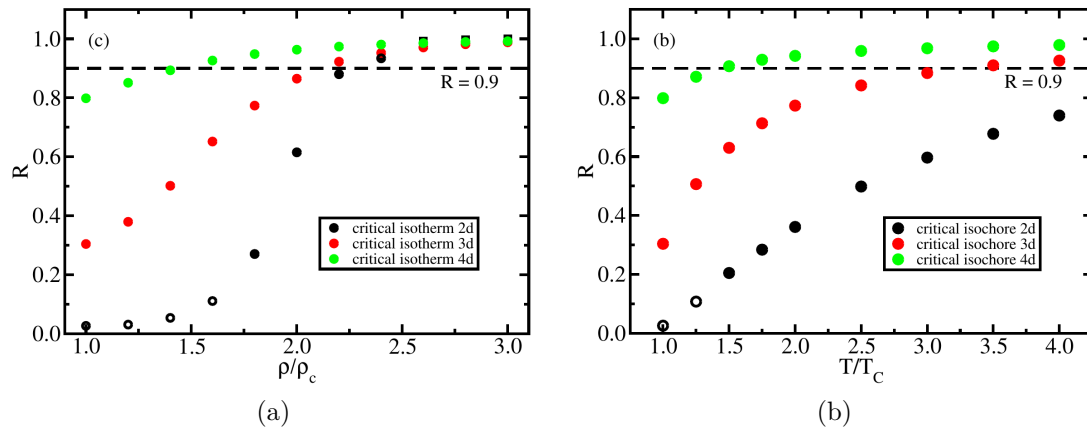

Figure 5.8: The virial potential-energy correlation coefficient R (a) along the critical liquid-vapour isotherm (b) along the critical isochore. The two-dimensional system crystallized at the highest densities $(\rho/\rho_c > 2.5)$, which is indicated by the black square symbols; the four open symbols indicate that the sample developed holes close to the critical point. The threshold $R = 0.9$ for being qualified empirically as strongly-correlating is more quickly reached by higher-dimensional systems. At each state point we have $R_{d=4} > R_{d=3} > R_{d=2}$. [*Reprinted from* [106]]

5.9.1.3   Invariance of dynamical quantities

A direct isomorph check of the MSD has been performed, see figure 5.9. The reduced-units data collapse to a master curve in $d = 4$, reflecting the fact that the invariance holds also in the dynamics.
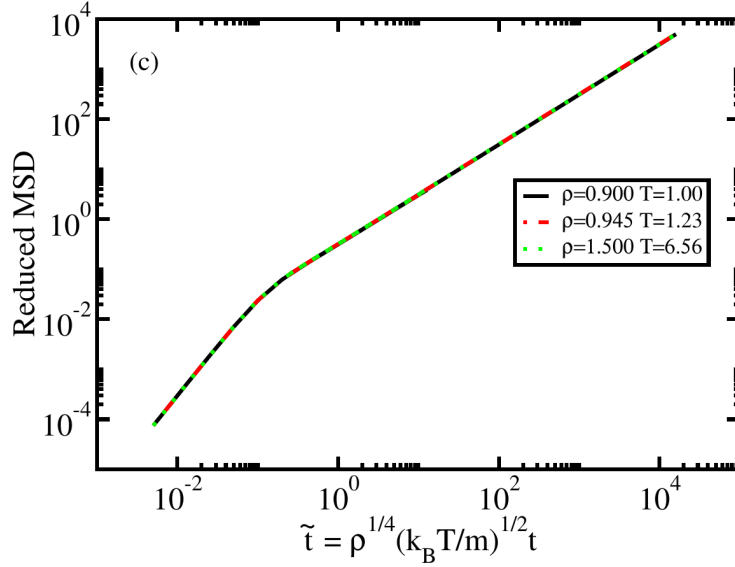

Figure 5.9: Reduced MSD as a function of reduced time for the same three isomorphic state points in four dimensions. The dynamics being Newtonian, the time rescaling is the corresponding one given in §5.5.2. [*Reprinted from* [106]]

5.9.2   Summary

We have shown that whenever the potential $V(r) = e^{-dA(r)}$ satisfies the condition that at the point r^* such that $\beta V(r^*) = O(1)$ one has $\left[\ln r - A(r)\right]_r^{r^*}$ for all $r > r^*$, then in the large-dimensional limit the parameter space (T, ρ) is foliated with lines (isomorphs), where static and dynamic properties coincide once expressed in reduced units. The simple explanation of this fact is that, in large dimensions, there is a typical interparticle distance that dominates the physics: larger distances have weak interactions, shorter distances are too rare. The arguments hold for dynamic as well as equilibrium calculations, both in the liquid and in the glass phase. Transition and dynamical crossover lines follow these isomorphs.

One may interpret the fact that in finite dimensions the scaling properties hold to a good approximation [184, 348, 19] as a symptom of the high-dimensional approximation being qualitatively good. Note that this approximation is intimately tied to the RFOT scenario for dense liquids [225, 220, 221, 223, 224, 227, 285, 69] (see the short review in §1.2), so this is another instance in which we are confronted with a unifying perspective.

6

Conclusions and outlook

And yet it flows!

Galileo Galilei, backing his viewpoint about
the glass transition at his iniquitous trial
(probably apocryphal)

6.1 Main results

Let us summarize the main outcomes drawn from this work.

We generalized the virial expansion to dynamics along the lines of [270], which provided an equivalent quenched-disordered model we studied as well. We showed that in the $d \to \infty$ limit, the dynamics is governed only by two-time correlation and response functions, and may be expressed by a single-particle effective dynamics, representing the inter-particle gap.

With this, we have derived a rather simple equation for the dynamics of liquids in the well-defined limit of large space dimension. We have not solved it exactly for all times but studied particularly interesting regimes of it. Its analytical solution would be quite involved. In spite of this, we stress that it is rather simple first because it can be easily simulated numerically, compared to a full simulation of the dN microscopic equations ruling the system, which anyway would be restricted to finite sizes and low dimensions, not to mention the issue of increasing relaxation times at low temperatures. Second, although we just stressed that an analytic solution seems very complicated, we believe simple particular cases, like the HS potential at finite times, or using a simple ansatz, might be amenable to a solution. Third, this result does not contain major surprises in itself[1] in the sense that the final equilibrium equation is a standard generalized Langevin equation for a single variable evolving in an effective potential given by the sum of the original potential and an entropic term, the latter coming from the Jacobian which arises due to isotropy in large dimension. The memory kernel is a force-force correlation over this effective process, which may also be expected. This does not mean that its outcomes are trivial. A final reason in support of simplicity is that the derivation resorts to dynamical tools that may be dealt with in a rigorous mathematical framework. Indeed we have only taken advantage of the virial truncation, translation and rotation invariances, and saddle-point techniques. We used scalings stemming from the static Mayer integral (about the scaling of the gap) and the virial series at large d (about the density scaling) which has been studied extensively, including convergence issues. No replica methods, whose analytic continuation assumptions are very problematic, are needed to make progress in the dynamics. A rigorous proof would also mean directly improving the lower bound on hyperspherical packings in $d \to \infty$.

It is also rather universal since, first, it is valid for a wide class of pair potentials: not only HS but other usual potentials well suited for the study of liquids that are affected by temperature. Second it is valid for any type of physical dynamics, be it Newtonian or Brownian (or the mixed Langevinian case). Finally we have not restricted the derivation to an equilibrium regime, and gave the out-of-equilibrium version.

---

[1]As usual, this is easy to say once the solution has been worked out...

These equations are the first exact[2] equations ruling the dynamics of classical systems in a strong-coupling regime in the thermodynamic limit, starting from first principles and obtaining the result in an exact limit, with a clear parameter under control. The terminology *strong-coupling regime* may seem somewhat elusive or even exaggerated, noticing that the virial series reduces to single term, a much welcomed property which is commonly used in the description of dilute or moderately dense gases (think of the mean-field van der Waals equation of state [86, 85, 28]), *associated with low-density behaviour.* Note here that it is *not* the case: the virial expansion parameter, related to the packing fraction $\rho \mathcal{V}_d(\sigma) = 2^d \varphi$, is not even small but diverging (it is $O(d)$ in the limit $d \to \infty$). It is instead due to purely geometrical constraints in the infinite-dimensional space. A particle interacts with a large number ($O(d)$) of nearest-neighbours. The resulting phenomenology at low temperatures exhibits clearly a complex glassy behaviour and a jammed phase, whose critical properties are strikingly close to the finite-dimensional ones in the latter case. These phenomena necessitate strong interactions.

At equilibrium, we showed that a diffusive regime takes place at long times and is already decided at small scales, *i.e.* at the $O(\sigma/d)$ gap scale, smaller than the particle radius; it is about $\sigma/5$ for real colloids [401]. The physics of diffusion originates from interactions at that small scale, while all particle motion beyond that scale consists of uncorrelated steps of displacement, and memory of what happens at distances $\gg \sigma/d$ is lost.

This diffusive regime disappears at low temperatures or high densities and the system undergoes a true non-ergodic dynamical transition. We gave Mode-Coupling-like exponents close to the plateau and discussed the relation to MCT equations by relating real space correlation functions to the intermediate scattering functions used in standard MCT. It appears that even if at the quantitative level, the predictions of MCT fail, the overall phenomenology (*e.g.* the divergence of viscosity, time-scaling laws, relations between exponents) is the same, the equations being more general soft-spin-like equations. We were able to give a microscopic expression for the memory kernel and make a prediction for the Stokes-Einstein relation, which are purely dynamic quantities.

Using the SUSY formalism as an analogy between thermodynamics and dynamics, we recovered within the same formalism the liquid and glassy thermodynamic phases of the system, in a clearer way than previous computations. We used either the disordered MK model or the original one in this thesis, showing their equivalence in high dimension for what concerns the computation of averaged quantities. We wrote the equation governing the order parameter of the system in a general way, allowing to make contact with the dynamics and revealing the global consistency of the solution. The major outcome, on the glassy side, of this $d \to \infty$ solution, is the confirmation of RFOT as the theory of glasses *in a well-defined mean-field level.*

Finally, we benefited from the derivation of both statics and dynamics to investigate the isomorph concept. In doing so we studied the simple static liquid Mayer integral at large d which gave clear hints on what type of potentials may be considered to display the type of glassy behaviour we described statically and dynamically, the *rather hard* ones, though they may not exhaust the list. We showed that isomorphs are *exact* in large dimensions and made contact with a number of features of isomorph theory, such as the virial-potential energy correlations.

6.2   An overview of perspectives

As a final note, we discuss some further questions and progresses direclty related to this work.

1. The number of metastable states can be computed directly from (4.37) using Bray and Moore's ansatz [75, 76], which later was shown to be generic by Biroli and Kurchan [63]. The study of the TAP equations for HS in $d \to \infty$ is also under way [7].

2. In the liquid phase, the thermodynamical (and dynamical) quantities becoming very simple one-dimensional expressions, one may hope to get hints and new predictions from the $d \to \infty$ regime about isomorph theory, or about comparison between standard liquid pair potentials, and clarify related issues [50, 51, 52]. Indeed, this simplicity may help accomplish some progress. The *very soft sphere* phase is intriguing and may have interesting bearings on the physics of liquids.

---

[2]For now, at the level of theoretical physics, and hopefully at a rigorous level.

3. The out-of-equilibrium equations of §3.10 may be studied numerically and analytically, in the spirit of [110]. This would allow to assess if the mean-field spin-glass timescales and effective temperatures concepts are valid for structural glasses [112], see the short review in sections 1.1.7 and 1.2.5. These may also be extended to a shear protocol, considered statically by Rainone, Urbani, Yoshino and Zamponi [413, 414, 325], see also the relation with the Gardner phase in [324, 64]. These quasi-equilibrium regimes are conjectured to be probed by a static state-following computation whose study began in [156, 24] and specifically in $d \to \infty$ structural glasses in [325, 324], see [98] for a review.

   As emphasized previously, as a first step one could study numerically and analytically further the equilibrium equations of §3.7.5 , which are easier to deal with.

4. We mentioned in §3.8.2 that one can obtain better lower bounds on hyperspherical packings by, for instance, finding a potential that maximizes the packing fraction at the dynamical transition in (3.138). A first step in this direction has been achieved by Sellitto and Zamponi in [356, 355], and work is under way along these lines.

5. The partition function of quantum systems, in a path integral formulation, is very close to the dynamical action we studied [422, 112]; thus similar methods could be followed. This might be of interest for the low-temperature properties of glasses, which manifest a linear temperature dependence of the specific heat [419, 9, 316, 259], therefore deviating from the Debye T^3 scaling due to phonons in a crystal lattice [17]. This regime remains a controversial issue [314].

6. Assessing which dynamic diagrams could be included to improve over the mean-field approximation, be it the $d \to \infty$ one or MCT, is ongoing work. See also the research effort to *go beyond MCT* in §1.3.

7. Following this last point, more generally a major issue is to get a valid theory beyond mean-field[3], that ideally would describe real supercooled liquids and glasses in $d = 2$ or 3, as pointed out in the header quote. An approximation scheme based on the $d \to \infty$ solution has been devised by Mangeat and Zamponi [267], giving reasonable quantitative results. A renormalization group analysis has yet to be fully developed, be it perturbative or non-perturbative in nature. Preliminary results have been obtained in [390, 340]. The prediction of the existence of the Gardner phase in high dimension has triggered numerical and experimental works to detect hints of it in actual systems [46, 354], which would result in novel interpretations and research directions.

---

[3]In particular one of the questions that it would address is: *Is the mean-field ideology a mythology in finite dimensions?* or: *Is $1/d$ small enough when $d = 3$?*

A
RECAP OF NOTATIONS

We collect here a few recurrent mathematical definitions and general formulas. We set the Boltzmann constant $k_{\mathrm{B}} = 1$.

A.1 Definition of basic quantities of the model

A.1.1 Basic definitions

d	Dimension of space
N	Number of particles
$\theta(x)$	Heaviside theta function
$\mathbb{S}_d(R)$	A $d+1$-dimensional hypersphere of radius R
$x \in \mathbb{S}_d(R)$	Position of a particle
$\Omega_d = \frac{2\pi^{d/2}}{\Gamma(d/2)}$	d-dimensional solid angle
$\mathcal{V} = \mathrm{vol}(\mathbb{S}_d(R)) = \Omega_{d+1} R^d$	Volume of $\mathbb{S}_d(R)$ in $\mathbb{R}^{d+1}$, and more generally volume of the system
σ or r^*	Particle effective diameter
$\mathcal{V}_d(\sigma) = \frac{\Omega_d}{d}\sigma^d$	Volume of the d-dimensional hypersphere of **radius** σ or
$\mathcal{V}_d(\sigma) = \mathcal{V}\int \mathrm{d}\mathcal{R}\,\theta(\sigma - |x - \mathcal{R}x|) = \int \mathrm{d}x\,\theta(\sigma - |x|)$	volume excluded by a particle on the surface of $\mathbb{S}_d(R)$
$\beta = 1/T$	Inverse temperature
$\rho = N/\mathcal{V}$	Average number density
$\Omega = (\ln \rho)/d$	Density exponent
$\varphi = \rho \mathcal{V}_d(\sigma)/2^d$	Packing fraction
$\widehat{\varphi} = 2^d \varphi/d$	Scaled packing fraction
$\widetilde{\varphi} = 2^d \varphi$	Scaled packing fraction
R	Radius of the spherical system

A.1.2 Static quantities

$r = \lvert x - y \rvert$	Euclidean distance between two particles x and y
$V(r)$	Interaction potential energy between two particles
$A(r)$	Exponent of the exponential potentials
$f(r) = e^{-\beta V(r)} - 1$	Mayer function
$g(r)$	Radial pair distribution function
$\rho(x)$	Local particle density
$\rho^{(2)}(x, y)$	Two-particle distribution function
$S(q)$	Static structure factor
$\mu = d(r - \sigma)$	Scaled *interparticle gap*
$\tilde{r} = d(r - r^*)$	Scaled *interparticle gap* in chapter 5
$\bar{V}(\mu) = \lim\limits_{d \to \infty} V[\sigma(1 + \mu/d)]$	Scaled interaction potential
$F(\mu) = -\frac{\mathrm{d}}{\mathrm{d}\mu}\bar{V}(\mu)$	Scaled force
$U = \sum_{i<j}^{1,N} V(\lvert x_i - x_j \rvert)$	Potential energy of the system
$W = -\frac{1}{d}\sum_{i=1}^{N} x_i \cdot \nabla_{x_i} U$	Virial function
$R = \frac{\langle \Delta W \Delta U \rangle}{\sqrt{\langle(\Delta W)^2\rangle\langle(\Delta U)^2\rangle}}$	WU correlation coefficient

A.1.3 Dynamic quantities

$x(t)$	Time-dependent particle position
$\mathrm{D}x$	Functional integration measure over $x(t)$
γ	Friction coefficient of the Langevin equation
$\widehat{\gamma} = \frac{\sigma^2}{2d^2}\gamma$	Scaled friction coefficient
m	Mass of the particles
$\widehat{m} = \frac{\sigma^2}{2d^2}m$	Scaled mass
D	Diffusion coefficient
$D_0 = T/\gamma$	Free diffusion coefficient
η	Viscosity
σ_{ij}	Stress tensor
$\phi_q(t, t')$	Intermediate scattering functions
$\phi_q^{\mathrm{s}}(t, t')$	Self-intermediate scattering functions
$C(t, t')$	Autocorrelation function
$R(t, t')$	Response function
$\Phi(\boldsymbol{x})$	Kinetic term
$\widehat{\Phi}(\boldsymbol{Q}) = \Phi/d = \mathrm{str}(\boldsymbol{kQ})$	Scaled kinetic term
ν	Lagrange multiplier
$\mathcal{S}$	Effective action

A.2 Replica coordinates

$\bar{x} = \{x_1, \cdots, x_n\}$	Coordinates of a replicated atom	
$\hat{M} = \{M_{ab}\}$	$n \times n$ replica matrix	
$\mathbb{1} = \{\delta_{ab}\}$	Identity matrix	
$q_{ab} = x_a \cdot x_b$	Matrix of scalar products, or overlaps	$q_{aa} = R^2$
$\mathrm{D}_{ab} = (x_a - x_b)^2$	Matrix of MSD	$\mathrm{D}_{aa} = 0$
$Q_{ab} = 2d\, q_{ab}/\sigma^2$	Scaled overlaps	$Q_{aa} = 2dR^2/\sigma^2 = \Delta_{\mathrm{liq}}$
$\Delta_{ab} = d\, \mathrm{D}_{ab}/\sigma^2$	Scaled MSD	$\Delta_{aa} = 0$
$\Delta_{\mathrm{liq}} = 2dR^2/\sigma^2$	Scaled MSD of the liquid phase	
$v = \{1, \cdots, 1\}$	All-ones vector in replica space	$v_a = 1, \forall a$

A.3 SUSY

$\theta_i, \bar\theta_i$	Grassmann variables
$a = (t, \theta, \bar\theta)$	SUSY time coordinates
$\boldsymbol{P}(a, b) = 1$	SUSY *projector*, playing the role of the static projector vv^{T}
$\mathbf{1}(a, b) = \delta(t - t')(\bar\theta_1\theta_1 + \bar\theta_2\theta_2)$	Identity operator for superfields
$\mathrm{str}\boldsymbol{Q} = \int \mathrm{d}a\, \boldsymbol{Q}(a, a)$	Supertrace
$\mathrm{sdet}\boldsymbol{Q}$	Superdeterminant
$\mathsf{M}(\boldsymbol{r})$	2×2 block-matricial form of a two-time superfield $\boldsymbol{r}$
$\mathrm{D}\boldsymbol{r}$	Functional integration measure over a superfield
$\mathrm{D}^{\mathrm{s}}\boldsymbol{q}$	Functional integration measure over a symmetric superfield

A.4 Gaussian integrals and special functions

$\gamma_a(x) = \dfrac{e^{-\frac{x^2}{2a}}}{\sqrt{2\pi a}}$	Gaussian kernel
$\mathcal{D}_a\lambda = \mathrm{d}\lambda\, \dfrac{e^{-\frac{\lambda^2}{2a}}}{\sqrt{2\pi a}}$	Gaussian integration measure
$\mathcal{D}\lambda = \mathrm{d}\lambda\, \dfrac{e^{-\frac{\lambda^2}{2}}}{\sqrt{2\pi}}$	Gaussian measure of unit variance
$\gamma_a \star f(x) = \int \mathrm{d}z\, \gamma_a(z) f(x - z) = \int \mathcal{D}_a z\, f(x - z)$	Convolution product
$\Theta(x) = \frac{1}{2}[1 + \mathrm{erf}(x)] = \int_{-x}^{\infty} \mathcal{D}_{1/2}\lambda = \int_{-x}^{\infty} d\lambda\, \dfrac{e^{-\lambda^2}}{\sqrt{\pi}} = \gamma_{1/2} \star \theta(x)$	Smoothed theta function
$\Theta\left(\dfrac{x}{\sqrt{a}}\right) = \int_{-x}^{\infty} \mathcal{D}_{a/2}\lambda = \gamma_{a/2} \star \theta(x)$	Smoothed theta function of width a
$\mathcal{D}_{\hat\Delta}\bar h = \dfrac{\mathrm{d}\bar h}{(2\pi)^{n/2}\sqrt{\det\hat\Delta}}\, e^{-\frac{1}{2}\bar h^T\hat\Delta^{-1}\bar h}$	Gaussian measure for replicated variables
$\mathcal{D}_{\boldsymbol{Q}}\boldsymbol{h} = \dfrac{\mathrm{D}\boldsymbol{h}}{\sqrt{\mathrm{sdet}\boldsymbol{Q}}}\, e^{-\frac{1}{2}\int \mathrm{d}a\mathrm{d}b\, \boldsymbol{h}(a)\boldsymbol{Q}^{-1}(a,b)\boldsymbol{h}(b)}$	Dynamical SUSY Gaussian measure
$\Gamma(x) = \int_0^{\infty} \mathrm{d}t\, t^{x-1}e^{-t}$ with $\mathrm{Re}\,(x) > 0$, $\quad \Gamma(x + 1) = x\Gamma(x)$	Euler Gamma function

A.5 Averages

$\langle \bullet \rangle$	Usually denotes the thermal average
$\overline{\bullet}$	Average over the disorder
$\langle \mathcal{O} \rangle_V = \int \mathrm{d}\lambda\, e^{\lambda - \Delta_{\mathrm{liq}}/2} \int \mathcal{D}_{\hat Q}\bar\mu\, e^{-\beta \sum_{a=1}^{n} \bar V(\mu_a + \lambda)}\, \mathcal{O}$	Replica average over the scaled potential
$H_0(\mu, \lambda) = \bar V(\mu + \lambda) + \dfrac{T\mu^2}{2\Delta_{\mathrm{liq}}}$	RS effective Hamiltonian
$\mathcal{Z}_0(\lambda) = \int \mathrm{d}\mu\, e^{-\beta H_0(\mu, \lambda)}$	RS partition function
$\langle \mathcal{O}(\mu) \rangle_{H_0} = \frac{1}{\mathcal{Z}_0} \int \mathrm{d}\mu\, e^{-\beta H_0}\mathcal{O}(\mu)$	RS average
$H_1(\mu, \lambda) = \bar V(\mu + \lambda) + \dfrac{T\mu^2}{2\Delta_1} - \eta\mu T\sqrt{\dfrac{1}{\Delta_1} - \dfrac{1}{\Delta_{\mathrm{liq}}}}$	1-RSB effective Hamiltonian
$\mathcal{Z}_1(\lambda) = \int \mathrm{d}\mu\, e^{-\beta H_1(\mu, \lambda)}$	1-RSB partition function
$\langle \mathcal{O}(\mu) \rangle_{H_1} = \frac{1}{\mathcal{Z}_1} \int \mathrm{d}\mu\, e^{-\beta H_1}\mathcal{O}(\mu)$	Average over H_1
$\langle \mathcal{O} \rangle_V = \int \mathrm{d}\lambda\, e^{\lambda - \Delta_{\mathrm{liq}}/2} \int \mathrm{D}\boldsymbol{\mu}\, e^{-\frac{1}{2}\int \mathrm{d}a\mathrm{d}b\, \boldsymbol{\mu}(a)\boldsymbol{Q}^{-1}(a,b)\boldsymbol{\mu}(b) - \int \mathrm{d}a\, \bar V(\boldsymbol{\mu}(a) + \lambda)}\mathcal{O}$	Dynamical SUSY average

$\mathcal{B}$
ALGEBRA OF HIERARCHICAL MATRICES

Outline

Here we discuss some general properties of hierachical replica matrices. We restrict to matrices Δ_{ab} such that $\Delta_{aa} = 0$. We often use a vector v with all components equal to 1. We also define a $n \times n$ matrix $\hat{I}^m$ which has elements $I_{ab}^m = 1$ in blocks of size m around the diagonal, and $I_{ab}^m = 0$ otherwise. Note that $\hat{I}^1 = \hat{I}$ is the identity matrix with $I_{ab} = \delta_{ab}$, and $\hat{I}^n = vv^{\mathrm{T}}$ is the matrix of all ones. Assuming that m_1 is a multiple of m_2 (hence $m_1 \geqslant m_2$), we have

$$\hat{I}^{m_1} \hat{I}^{m_2} = m_2 \hat{I}^{m_1} . \tag{B.1}$$

This relation holds in particular for $m_1 = n$ or for $m_2 = 1$.

B.1 RS matrices

For a replica symmetric matrix we have

$$
\begin{aligned}
\Delta_{ab} &= \Delta_0(1 - \delta_{ab}) & \hat{\Delta} &= \Delta_0(\hat{I}^n - \hat{I}^1) , & \text{(B.2)} \\
\Delta_{ab}^{-1} &= \frac{1}{\Delta_0}\left(\frac{1}{n-1} - \delta_{ab}\right) & \hat{\Delta}^{-1} &= \frac{1}{\Delta_0}\left(\frac{1}{n-1}\hat{I}^n - \hat{I}^1\right) , & \text{(B.3)} \\
\sum_b \Delta_{ab}^{-1} &= \frac{1}{\Delta_0}\frac{1}{n-1} , & \hat{\Delta}^{-1}v &= \frac{1}{n-1}\frac{1}{\Delta_0}v . & \text{(B.4)}
\end{aligned}
$$

The eigenvectors of $\hat{\Delta}$ are v, with eigenvalue $\Delta_0(n-1)$, and $n-1$ orthogonal vectors with eigenvalue $-\Delta_0$; hence,

$$\det \hat{\Delta} = (n-1)(\Delta_0)^n(-1)^{n-1} . \tag{B.5}$$

B.2 1-RSB matrices

A 1-RSB matrix has the form

$$\hat{\Delta} = \Delta_0 \hat{I}^n + (\Delta_1 - \Delta_0)\hat{I}^m - \Delta_1 \hat{I}^1 , \tag{B.6}$$

and using Eq. (B.1) one obtains that the inverse is

$$\hat{\Delta}^{-1} = \Delta_0^{-1}\hat{I}^n + (\Delta_1^{-1} - \Delta_0^{-1})\hat{I}^m + (\Delta_\mathrm{d}^{-1} - \Delta_1^{-1})\hat{I}^1 \ ,$$

$$\Delta_0^{-1} = -\frac{\Delta_0}{[\Delta_1(m-1) - m\Delta_0][\Delta_0(n-m) + \Delta_1(m-1)]} \ ,$$

$$\Delta_1^{-1} = \Delta_0^{-1} + \frac{\Delta_0 - \Delta_1}{\Delta_1[\Delta_1 + m(\Delta_0 - \Delta_1)]} \ ,$$

$$\Delta_\mathrm{d}^{-1} = \Delta_1^{-1} - \frac{1}{\Delta_1} \ ,$$

(B.7)

and

$$\hat{\Delta}^{-1}v = \frac{1}{\Delta_0(n-m) + \Delta_1(m-1)}v \ .$$

(B.8)

Finally, the determinant can be computed in the following way. The n-dimensional vector space can be decomposed in three subspaces:

1. The vector v of all ones. It has $\hat{I}^n v = nv$ and $\hat{I}^m v = mv$. Hence

$$\hat{\Delta}v = [\Delta_0(n-m) + \Delta_1(m-1)]v \ .$$

(B.9)

2. A set of $n/m - 1$ independent vectors w, such that w_a is constant in each block, and $\sum_a w_a = 0$. These are orthogonal to v and such that $I^n w = 0$ and $I^m w = mw$. Hence

$$\hat{\Delta}w = [-m\Delta_0 + \Delta_1(m-1)]v \ .$$

(B.10)

3. A set of $(n/m)(m-1)$ vectors x such that $\sum_{a\in B} x_a = 0$ in each block B. These are orthogonal to v and all the w, and they are such that $I^n x = I^m x = 0$. Hence

$$\hat{\Delta}x = -\Delta_1 x \ .$$

(B.11)

Therefore we obtain

$$\det\hat{\Delta} = [\Delta_0(n-m) + \Delta_1(m-1)] \times [-m\Delta_0 + \Delta_1(m-1)]^{n/m-1} \times [-\Delta_1]^{n/m(m-1)}$$

$$= \frac{\Delta_0(m-n) + \Delta_1(1-m)}{m\Delta_0 + \Delta_1(1-m)} \times \left[\frac{m\Delta_0 + \Delta_1(1-m)}{\Delta_1}\right]^{n/m} \times [-\Delta_1]^n \ .$$

(B.12)

Note that we recover the RS result for $m = 1$, as it should be.

Finally, with a similar procedure, we obtain

$$[(\Delta_1 - \Delta_0)\hat{I}^m - \Delta_1\hat{I}^1]^{-1} = \frac{\Delta_1 - \Delta_0}{\Delta_1[-m\Delta_0 + \Delta_1(m-1)]}\hat{I}^m - \frac{1}{\Delta_1}\hat{I}^1 \ ,$$

(B.13)

and

$$\det[(\Delta_0 - \Delta_1)\hat{I}^m + \Delta_1\hat{I}^1] = \left[\frac{m\Delta_0 + \Delta_1(1-m)}{\Delta_1}\right]^{n/m} \times [\Delta_1]^n \ ,$$

(B.14)

which can be derived in the same way as Eq. (B.12), but taking into account that for the matrix $(\Delta_0 - \Delta_1)\hat{I}^m + \Delta_1\hat{I}^1$ the eigenvalues associated to the vectors v and w coincide.

B.3   Full-RSB matrices

For ∞RSB matrices we restrict ourselves to the limit $n \to 0$. In the limit $n \to 0$, a hierarchical matrix $\hat{\Delta}$ is parametrized by its diagonal element Δ_d and by a continuous function $\Delta(x)$ for $0 < x < 1$, see §2.3.4. In the case of interest here, $\Delta_\mathrm{d} = (x_a - x_a)^2 = 0$. Also, replicas in the outermost block are described by $\Delta(0)$ which plays a special role.

We follow the notation of [282, Appendix II] and introduce

$$\langle\Delta\rangle = \int_0^1 \mathrm{d}x\,\Delta(x)$$

$$[\Delta](x) = x\Delta(x) - \int_0^x \mathrm{d}y\,\Delta(y)$$

(B.15)

The formula for the inverse can be deduced directly from (2.77) with $AB = C$ where $C \leftrightarrow \{c_d, c(x)\}$ is the identity *i.e.* $\{c_d, c(x)\} = \{1, 0\}$, and is given in [282, Eq. (AII.7)]. Specialized to $\Delta_\mathrm{d} = 0$, it reads

$$\Delta_\mathrm{d}^{-1} = -\frac{1}{\langle \Delta \rangle} \left[1 + \int_0^1 \frac{\mathrm{d}x}{x^2} \frac{[\Delta](x)}{\langle \Delta \rangle + [\Delta](x)} + \frac{\Delta(0)}{\langle \Delta \rangle} \right] ,$$

$$\Delta^{-1}(x) = \frac{1}{\langle \Delta \rangle} \left[-\frac{[\Delta](x)}{x(\langle \Delta \rangle + [\Delta](x))} - \int_0^x \frac{\mathrm{d}y}{y^2} \frac{[\Delta](y)}{\langle \Delta \rangle + [\Delta](y)} - \frac{\Delta(0)}{\langle \Delta \rangle} \right] .$$

(B.16)

Then, for the special case $\Delta_\mathrm{d} = 0$ which is of interest here, the determinant is given in [282, Eq. (AII.11)] and reference [281] therein:

$$\lim_{n \to 0} \frac{1}{n} \ln \det \hat{\Delta} = \ln \left(- \langle \Delta \rangle \right) - \frac{\Delta(0)}{\langle \Delta \rangle} - \int_0^1 \frac{\mathrm{d}x}{x^2} \ln \left(1 + \frac{[\Delta](x)}{\langle \Delta \rangle} \right)$$

(B.17)

Using these equations one can easily show that

$$\sum_b \Delta_{ab}^{-1} = \Delta_\mathrm{d}^{-1} - \int_0^1 \mathrm{d}x \, \Delta^{-1}(x) = -\frac{1}{\langle \Delta \rangle} , \qquad \hat{\Delta}^{-1} v = \frac{1}{\langle \Delta \rangle} v .$$

(B.18)

C

A PEDESTRIAN PRESENTATION OF THE MARTIN-SIGGIA-ROSE-DE DOMINICIS-JANSSEN GENERATING FUNCTIONAL

Outline

The aim of this appendix is to derive the Martin-Siggia-Rose-De Dominicis-Janssen (MSRDDJ) path integral formulation of the stochastic dynamics of a set of N interacting particles in contact with a thermal bath, with a *multiplicative* noise (raising interpretation issues of the corresponding Langevin equation in continuous time), in d spatial dimensions and with several choices of dynamics. This formalism is the classical equivalent of the Schwinger-Keldysh generating functional [351, 216, 115, 112, 422]. The basic idea was developed by Martin, Siggia and Rose [271] and put to work by De Dominicis, Janssen and others [317, 208, 27, 318, 124, 209, 210]. These references usually focus on more particular cases, one has to go through all of them to have a correct picture of the derivation in a quite general case. Moreover, the derivations are often a bit elusive. The main section here proposes a very pedestrian derivation[1] with very little assumptions of knowledge of more sophisticated techniques (however it is a bit tedious). A very good recent reference is [16].

C.1 The idea

We consider the Langevin equation for one particle in one dimension

$$\frac{\mathrm{d}x}{\mathrm{d}t} = A(x) + \xi \tag{C.1}$$

where $\xi(t)$ is a Gaussian centered noise of variance $G(t,t') = \langle \xi(t)\xi(t') \rangle$. By definition the average of an observable $O(x)$ is

$$\langle O(x(t)) \rangle = \frac{1}{\sqrt{\det G}} \int \mathrm{D}\xi \, e^{-\frac{1}{2}\int_{[0,t]^2} \mathrm{d}u\mathrm{d}v\, \xi(u)G^{-1}(u,v)\xi(v)} O(x[\xi](t)) \tag{C.2}$$

---

[1]I learnt this derivation in the case $N = 1$, $d = 1$ for a Brownian process thanks to Frédéric van Wijland; I thank him very much for the clear presentation he gave, as usual in his lectures. The rest is rather simple generalizations.

We want to formulate this as a path integral over the process $x(t)$. We will thus make a change of variables imposing the right paths of x through a Dirac delta function, à la Fadeev-Popov [149, 315, 422],

$$\langle O(x(t)) \rangle = \frac{1}{\sqrt{\det G}} \int \mathrm{D}\xi \, e^{-\frac{1}{2} \int_{[0,t]^2} \mathrm{d}u\mathrm{d}v\, \xi(u)G^{-1}(u,v)\xi(v)} \int \mathrm{D}x \left| \det\left(\frac{\delta\xi}{\delta x}\right) \right| \delta[\dot{x} - A(x) - \xi] O(x(t)) \quad (C.3)$$

If we assume the Jacobian is 1, we exponentiate the delta function through an auxiliary field $\hat{x}$ and integrate out the noise,

$$\langle O(x(t)) \rangle = \frac{1}{\sqrt{\det G}} \int \mathrm{D}\xi \, e^{-\frac{1}{2} \int_{[0,t]^2} \mathrm{d}u\mathrm{d}v\, \xi(u)G^{-1}(u,v)\xi(v)} \int \mathrm{D}x\mathrm{D}\hat{x} \, e^{-\int \mathrm{d}u\, i\hat{x}(u)(\dot{x}-A(x)-\xi)} O(x(t))$$

$$= \int \mathrm{D}[x,\hat{x}] \, O(x(t)) e^{-S[x,\hat{x}]} \quad (C.4)$$

$$S[x,\hat{x}] = \frac{1}{2} \int_{[0,t]^2} \mathrm{d}u\mathrm{d}v\, \hat{x}(u)G(u,v)\hat{x}(v) + \int_0^t \mathrm{d}u\, i\hat{x}(u)[\dot{x} - A(x)]$$

In the end one sums over trajectories with a certain probability weight. This permits a probabilistic interpretation not in terms of the realizations of the thermal noise but rather in terms of a real space viewpoint of trajectories of particles. This is the interest of the method, together with providing us with a field-theoretical framework and hence the affiliated techniques.

However, such a continuous formalism eludes possible problems in the interpretation of the Langevin equation (C.1), which has a clear meaning only when discretized. The action S, due to the Jacobian, actually depends on the choice of discretization for *multiplicative* noises (which is absent in (C.1)). We address this problem and further generalizations in the following.

Note that integrating away the auxiliary field $\hat{x}$ yields the Onsager-Machlup action functional [297, 262, 196], which is equivalent but we prefer to work with the auxiliary fields that decouples the quadratic term in the exponent of the Onsager-Machlup path probability, making Gaussian integrations over *e.g.* disordered couplings of the Hamiltonian or other terms arising in §3 easier.

C.2 Pedestrian way: discretization

C.2.1 Setting

We consider N interacting particles in one dimension with multiplicative noise, whose dynamics read

$$\frac{\mathrm{d}x_i}{\mathrm{d}t} = A_i(x_1,\ldots,x_N) + B_i(x_1,\ldots,x_N)\xi_i(t) \quad (C.5)$$

Indices i,j refer to labeled particles. A_i refers to the details of interactions with particle i. For a Hamiltonian evolution one considers $A_i = -\partial_i H$. B_i is a multiplicative term and $\xi(x_i,t)$ is a thermal noise term taken to be Gaussian defined by its first two moments:

$$\langle \xi_i(t) \rangle = 0 \qquad \langle \xi_i(t)\xi_j(t') \rangle = \delta_{ij}G(t,t') \quad (C.6)$$

Further generalizations will be made below for pedagogical reasons; in this respect, the case $N = 1$ is more direct and instructive but for compactness we will consider the interacting case.

Due to interpretation issues of the Langevin equation (C.5), we consider an evolution in a time window $[0,t]$ discretized in M time steps of duration $\delta = t/M$. The position of particle i at time $t_n = n\delta$ is noted $x_i(n\delta) = x_i^n$, and $\Delta x_i^n \equiv x_i^{n+1} - x_i^n$. Indices n,m refer to time dependences. All $\{x_i^0\}$ are fixed initial conditions (the dynamical system is first-order in time).

C.2.2 Time scaling of the noise term

- If $G(t,t') = \delta(t-t')$ (singular), one writes in the discrete setting $\langle \xi_i^n \xi_j^m \rangle = \delta_{ij}\frac{\delta_{nm}}{\delta}$. We then define $\eta_i^n = \sqrt{\delta}\xi_i^n$ so that $\langle \eta_i^n \eta_j^m \rangle = \delta_{ij}\delta_{nm}$. This is to cope with the discrete definition of the Dirac delta $\int \mathrm{d}t\, G(t,t') = 1 = \delta \sum_n \langle \xi_i^n \xi_i^m \rangle$.

- If G is non-singular, then $\eta_i^n \equiv \xi_i^n$.

In the end we define $\xi_i^n \equiv I(\delta)\eta_i^n$ for all cases, where $I(\delta) = \begin{cases} 1 \\ \dfrac{1}{\sqrt{\delta}} \end{cases}$. We then define $G_{nm} \equiv \langle \xi_i^n \xi_i^m \rangle$ and

$\widehat{G}_{nm} \equiv \langle \eta_i^n \eta_i^m \rangle$, hence $G_{nm} = I(\delta)^2 \widehat{G}_{nm}$.

C.2.3 α-discretization

we discretize (C.5),

$$\Delta x_i^n = \delta \underbrace{A_i(\{x_j^n + \alpha \Delta x_j^n\})}_{\equiv A_i^n} + \delta I(\delta) \underbrace{B_i(\{x_j^n + \alpha \Delta x_j^n\})}_{\equiv B_i^n} \eta_i^n \tag{C.7}$$

with $\alpha \in [0, 1]$. The results *a priori* depends upon the value of α, and corresponds to a particular interpretation of the continuous-time stochastic equation (C.5). This is discussed in [394, 170]; a more mathematically-oriented presentation is found in [296].

We change variables $\{\eta_i^n\} \to \{x_j^m\}$ where $n = 0, \ldots, M-1$ and $m = 1, \ldots, M$ with $(i, j) \in [\![1, N]\!]^2$ in the computation of the mean of an observable O at time t:

$$
\begin{aligned}
\left\langle O(x_1^M, \ldots, x_N^M) \right\rangle &= (\det \widehat{G})^{-N/2} \int \prod_{i=1}^{N} \prod_{n=0}^{M-1} \frac{d\eta_i^n}{\sqrt{2\pi}} e^{-\frac{1}{2} \sum_{i,n,m} \eta_i^n \widehat{G}_{nm}^{-1} \eta_i^m} O(x_1^M[\{\eta_1^n\}], \ldots, x_N^M[\{\eta_N^n\}]) \\
&= (\det \widehat{G})^{-N/2} \int \prod_{i=1}^{N} \prod_{n=1}^{M} \frac{dx_i^n}{\sqrt{2\pi}} \prod_{i=1}^{N} e^{-\frac{1}{2} \sum_{n,m} \left(\frac{\Delta x_i^n - \delta A_i^n}{\delta I(\delta) B_i^n} \right) \widehat{G}_{nm}^{-1} \left(\frac{\Delta x_i^m - \delta A_i^m}{\delta I(\delta) B_i^m} \right)} \\
&\quad \times \left| \det \left(\frac{\partial \eta_i^m}{\partial x_j^n} \right) \right| O(x_1^M, \ldots, x_N^M)
\end{aligned}
\tag{C.8}
$$

The Jacobian is the determinant of a $M \times M$ block matrix where each block is a $N \times N$ matrix, and reads

$$
J = \det \left(\frac{\partial \eta_i^m}{\partial x_j^n} \right) = \begin{vmatrix} \frac{\partial \eta_i^0}{\partial x_j^1} & \frac{\partial \eta_i^1}{\partial x_j^1} & \cdots & \cdots & \frac{\partial \eta_i^{M-1}}{\partial x_j^1} \\ 0 & \frac{\partial \eta_i^1}{\partial x_j^2} & \frac{\partial \eta_i^2}{\partial x_j^2} & & \vdots \\ \vdots & \ddots & \ddots & \ddots & \vdots \\ \vdots & & \ddots & \frac{\partial \eta_i^{M-2}}{\partial x_j^{M-1}} & \frac{\partial \eta_i^{M-1}}{\partial x_j^{M-1}} \\ 0 & \cdots & \cdots & 0 & \frac{\partial \eta_i^{M-1}}{\partial x_j^M} \end{vmatrix} = \prod_{n=0}^{M-1} \left| \frac{\partial \eta_i^n}{\partial x_j^{n+1}} \right| \tag{C.9}
$$

the last equality follows from the fact that the $M \times M$ block matrix is block triangular due to causality. Indeed, η_i^n cannot depend on any x_j^m when $m \geqslant n+2$ (for overdamped dynamics). For fixed (i, j, n) one has from (C.7)

$$\frac{\partial \eta_i^n}{\partial x_j^{n+1}} = \frac{\delta_{ij} - \delta \alpha \partial_j A_i^n}{\delta I(\delta) B_i^n} - \frac{\Delta x_i^n - \delta A_i^n}{\delta I(\delta)} \alpha \frac{\partial_j B_i^n}{(B_i^n)^2} \tag{C.10}$$

∂_j refers to derivation with respect to the jth variable. We use a Hubbard-Stratonovitch transform to linearize the quadratic term in the exponent, introducing additional response fields

$$
\begin{aligned}
&\frac{1}{\sqrt{\det \widehat{G}}} e^{-\frac{1}{2} \sum_{n,m} \left(\frac{\Delta x_i^n - \delta A_i^n}{\delta I(\delta) B_i^n} \right) \widehat{G}_{nm}^{-1} \left(\frac{\Delta x_i^m - \delta A_i^m}{\delta I(\delta) B_i^m} \right)} \\
&= \int \prod_{n=0}^{M-1} \left(\frac{d\hat{x}_i^n}{\sqrt{2\pi}} \delta I(\delta) |B_i^n| \right) \times e^{-\frac{1}{2} \delta^2 I(\delta)^2 \sum_{n,m} \hat{x}_i^n B_i^n \widehat{G}_{nm} \hat{B}_i^m x_i^m - \sum_n i \hat{x}_i^n (\Delta x_i^n - \delta A_i^n)}
\end{aligned}
\tag{C.11}
$$

Then in the average (F.15), the Jacobian J and terms $\delta I(\delta) |B_i^n|$ combine from the last two equations to

give

$$|J|\left(\prod_{i=1}^{N}\prod_{n=0}^{M-1}\delta I(\delta)|B_i^n|\right) = \prod_{n=0}^{M-1}\left|\delta_{ij} - \delta\alpha\partial_j A_i^n - \underbrace{(\Delta x_i^n - \delta A_i^n)\alpha\frac{\partial_j B_i^n}{B_i^n}}\right|$$

$$= \prod_{n=0}^{M-1}|\det(\mathbb{1} - \mathcal{M}_n)| \underset{\delta\to 0}{=} \prod_{n=0}^{M-1}(1 - \text{Tr}\mathcal{M}_n) + O(\delta^2)$$

(C.12)

since, from (C.7), the matrix $\mathcal{M}_n$ is small in the limit $\delta \to 0$. Now, imagine we expand the last product. The diagonal elements (only needed for the trace) of the underbraced matrix in (C.12) can be rewritten as

$$\alpha\frac{\partial_i B_i^n}{B_i^n}\left(\underbrace{\Delta x_i^n - \delta A_i^n - \sum_m i\hat{x}_i^m \widehat{G}_{nm}B_i^n B_i^m \delta^2 I(\delta)^2}_{\equiv\lambda_i^n} + \sum_m i\hat{x}_i^m \widehat{G}_{nm}B_i^n B_i^m \delta^2 I(\delta)^2\right)$$

(C.13)

then the term λ_i^n will be in factor of quantities independent of $\hat{x}_i^n$ except the exponential weight from (C.11), resulting in a term

$$\propto \lambda_i^n e^{-\frac{1}{2}\delta^2 I(\delta)^2 \sum_{n,m}\hat{x}_i^n B_i^n \widehat{G}_{nm}\hat{B}_i^m x_i^m - \sum_n i\hat{x}_i^n(\Delta x_i^n - \delta A_i^n)}$$

$$= -\frac{\partial}{\partial(i\hat{x}_i^n)}e^{-\frac{1}{2}\delta^2 I(\delta)^2 \sum_{n,m}\hat{x}_i^n B_i^n \widehat{G}_{nm}\hat{B}_i^m x_i^m - \sum_n i\hat{x}_i^n(\Delta x_i^n - \delta A_i^n)}$$

(C.14)

Then when we integrate over $\hat{x}_i^n$, this term gives no contribution since the limits of the last exponential when $\hat{x}_i^n \to \pm\infty$ are zero, therefore in (C.12) we can forget about all the λ_i^n terms, and retain only the non-underbraced term in (C.13). We wish to write everything as an exponential weight so we exponentiate $1 - \text{Tr}\mathcal{M}_n \underset{\delta\to 0}{\sim} e^{-\text{Tr}\mathcal{M}_n}$.

All in all,

$$\left\langle O(x_1^M, \ldots, x_N^M)\right\rangle = \int\left(\prod_{i=1}^{N}\prod_{n=0}^{M-1}\frac{\mathrm{d}x_i^{n+1}}{\sqrt{2\pi}}\frac{\mathrm{d}\hat{x}_i^n}{\sqrt{2\pi}}\right)O(x_1^M, \ldots, x_N^M)\prod_{i=1}^{N}e^{-\frac{1}{2}\delta^2 I(\delta)^2\sum_{n,m}\hat{x}_i^n B_i^n \widehat{G}_{nm}\hat{B}_i^m x_i^m}$$

$$\times \prod_{i=1}^{N}e^{-\sum_n[i\hat{x}_i^n(\Delta x_i^n - \delta A_i^n) + \delta\alpha\partial_i A_i^n + \delta^2 I(\delta)^2\alpha\partial_i B_i^n \sum_m i\hat{x}_i^m B_i^m \widehat{G}_{nm}]}$$

(C.15)

Taking the continuous limit $\delta \to 0$ gives, noting $x^N \equiv \{x_1, \ldots, x_N\}$,

$$\left\langle O(x^N(t))\right\rangle = \int\prod_{i=1}^{N}\mathrm{D}x_i\mathrm{D}\hat{x}_i\, O(x^N(t))e^{-S[\{x_i,\hat{x}_i\}]}$$

$$S[\{x_i, \hat{x}_i\}] = \sum_{i=1}^{N}\frac{1}{2}\int_{[0,t]^2}\mathrm{d}u\mathrm{d}v\,\hat{x}_i(u)B_i(x^N(u))G(u,v)B_i(x^N(v))\hat{x}_i(v)$$

$$+ i\int_0^t\mathrm{d}u\,\hat{x}_i(u)\left[\dot{x}_i(u) - A_i(x^N(u))\right] + \alpha\int_0^t\mathrm{d}u\,\partial_i A_i(x^N(u))$$

$$+ \alpha\int_{[0,t]^2}\mathrm{d}u\mathrm{d}v\,\partial_i B_i(x^N(u))G(u,v)i\hat{x}_i(v)B_i(x^N(v))$$

(C.16)

C.2.4 The action in d dimensions

Formally, generalizing (C.5) to d dimensions amounts to replace indices i by (i, μ) where $\mu \in [\![1, d]\!]$ denotes a spatial component, except for the multiplicative functions B_i. This gives immediately

$$\left\langle O(\mathbf{x}^N(t)) \right\rangle = \int \mathrm{D}[\mathbf{x}^N, \hat{\mathbf{x}}^N] \, O(\mathbf{x}^N(t)) e^{-S[\mathbf{x}^N, \hat{\mathbf{x}}^N]}$$

$$\begin{aligned}
S[\mathbf{x}^N, \hat{\mathbf{x}}^N] = & \sum_{i=1}^N \frac{1}{2} \int_{[0,t]^2} \mathrm{d}u \mathrm{d}v \, B_i(\mathbf{x}^N(u)) G(u,v) B_i(\mathbf{x}^N(v)) \hat{\mathbf{x}}_i(u) \cdot \hat{\mathbf{x}}_i(v) \\
& + i \int_0^t \mathrm{d}u \, \hat{\mathbf{x}}_i(u) \cdot \left[\frac{\mathrm{d}\mathbf{x}_i}{\mathrm{d}u}(u) - \mathbf{A}_i(\mathbf{x}^N(u)) \right] + \alpha \int_0^t \mathrm{d}u \, \nabla_{\mathbf{x}_i} \cdot \mathbf{A}_i(\mathbf{x}^N(u)) \\
& + \alpha \int_{[0,t]^2} \mathrm{d}u \mathrm{d}v \, B_i(\mathbf{x}^N(v)) G(u,v) i \hat{\mathbf{x}}_i(v) \cdot \nabla_{\mathbf{x}_i} B_i(\mathbf{x}^N(u))
\end{aligned} \tag{C.17}$$

C.3 Additional remarks

- $\alpha = 1/2$ is the right choice if one wishes to use differential calculus on the action [210, Eq. (18)], while $\alpha = 0$ is usually more convenient since some additional terms are suppressed. For non-multiplicative processes the value of α is irrelevant.

- The weight e^{-S} is a transition probability density and probability conservation (summing on all the final positions) ensures the causality of the path integral: one does not need to introduce later times than the ones stepping in the correlation function we wish to compute.

- Non-Gaussian and non-Markovian processes can be included with higher order terms of the response field and multiple-time integrals in the action S [209, 210].

- The MSRDDJ formalism can be extended to other types of dynamics, *e.g.* Newtonian or with causal generalized friction terms [16].

C.4 À la Feynman

Another derivation can be found in Zinn-Justin's book [422], and is akin to the Onsager-Machlup generating functional: the idea is the same as Feynman's path integral in quantum mechanics [131, 152, 315, 422], using a master equation of the Fokker-Planck type (for a homogeneous Markov process) for the transition probability $P(\{p_i, x_i\}, t | \{p_i^0, x_i^0\}, t_0)$ analogous to the unitary dynamics of the evolution operator given by the Schrödinger equation,

$$\dot{P} = -H_{\mathrm{FP}} P \tag{C.18}$$

The path integral is constructed by propagating the transition amplitudes $\left\langle \{p_i, x_i\} \right| e^{-H_{\mathrm{FP}}(t-t')} \left| \{p_i', x_i'\} \right\rangle$ for each (infinitesimal) time steps using the Chapman-Kolmogorov relation [150].

Derivation of the dynamic generating functional through the Mari-Kurchan model

The MK model [270] is a mean field model (equivalent to the original one in infinite dimension) in which the particles are submitted to a quenched disorder induced by random shifts $\{A_{ij}\}$ of the relative positions of each pair. The energy is

$$H_{\text{MK}}(\{A_{ij}\}) = \sum_{i=1}^{N} \frac{p_i^2}{2m} + \sum_{i<j}^{1,N} V(x_i - x_j - A_{ij}) \tag{D.1}$$

For the dynamics, we define as in section 3.2.1

$$\begin{aligned}
\Phi_i &= \Phi[x_i, \tilde{x}_i] \\
W_{ij}(A) &= W[x_i - x_j - A, \tilde{x}_i - \tilde{x}_j] \\
\bar{\chi}_{ij} &= \int \frac{\mathrm{d}A}{V} e^{-W_{ij}(A)}
\end{aligned} \tag{D.2}$$

We denote by an overline the average over all the random shifts, whose distributions are taken as independent and uniform. We have

$$\begin{aligned}
\overline{Z_N} &= \int \prod_{i=1}^{N} \mathrm{D}[x_i, \tilde{x}_i] e^{-\Phi_i} \prod_{i<j}^{1,N} \int \frac{\mathrm{d}A_{ij}}{V} e^{-W_{ij}(A_{ij})} \\
&= \int \prod_{i=1}^{N} \mathrm{D}[x_i, \tilde{x}_i] e^{-\Phi_i} \prod_{i<j}^{1,N} \bar{\chi}_{ij} = \int \prod_{i=1}^{N} \mathrm{D}[x_i, \tilde{x}_i] e^{-\sum_i \Phi_i - \frac{1}{2} \sum_{ij} \ln \bar{\chi}_{ij}} \\
&= \int \prod_{i=1}^{N} \mathrm{D}[x_i, \tilde{x}_i] \int \mathrm{D}\rho \mathrm{D}\hat{\rho} \, e^{N \int \mathrm{D}[x,\tilde{x}]\rho[x,\tilde{x}](\hat{\rho}[x,\tilde{x}]-\Phi[x,\tilde{x}])-\sum_i \hat{\rho}[x_i,\tilde{x}_i] + \frac{N^2}{2} \int \mathrm{D}[x,\tilde{x}]\mathrm{D}[y,\tilde{y}]\rho[x,\tilde{x}]\rho[y,\tilde{y}] \ln \bar{\chi}[x-y,\tilde{x}-\tilde{y}]} \\
&= \int \mathrm{D}\rho \mathrm{D}\hat{\rho} \, e^{N\left\{ \int \mathrm{D}[x,\tilde{x}]\rho[x,\tilde{x}](\hat{\rho}[x,\tilde{x}]-\Phi[x,\tilde{x}])+\ln \int \mathrm{D}[x,\tilde{x}]e^{-\hat{\rho}[x,\tilde{x}]} + \frac{N}{2} \int \mathrm{D}[x,\tilde{x}]\mathrm{D}[y,\tilde{y}]\rho[x,\tilde{x}]\rho[y,\tilde{y}] \ln \bar{\chi}[x-y,\tilde{x}-\tilde{y}] \right\}} \\
&= \int \mathrm{D}\rho \mathrm{D}\hat{\rho} \, e^{N\mathcal{S}(\rho,\hat{\rho})}
\end{aligned} \tag{D.3}$$

This is obtained by inserting a delta function for the field $\rho[x, \tilde{x}]$ and representing it as a Fourier integral over the imaginary field $\hat{\rho}[x, \tilde{x}]$.

In the thermodynamic limit we must maximize $\mathcal{S}$. The saddle point equation for $\hat{\rho}$ is

$$\rho[x, \tilde{x}] = \frac{e^{-\hat{\rho}[x,\tilde{x}]}}{\int \mathrm{D}[y, \tilde{y}] e^{-\hat{\rho}[y,\tilde{y}]}} \tag{D.4}$$

which is compatible with the normalization of $\rho[x, \tilde{x}]$.

We can use this equation and substitute it in the new action, then we get:

$$\mathcal{S}(\rho) = - \int \mathrm{D}[x, \tilde{x}]\rho[x, \tilde{x}](\ln \rho[x, \tilde{x}] + \Phi[x, \tilde{x}]) + \frac{N}{2} \int \mathrm{D}[x, \tilde{x}]\mathrm{D}[y, \tilde{y}]\rho[x, \tilde{x}]\rho[y, \tilde{y}] \ln \bar{\chi}[x - y, \tilde{x} - \tilde{y}] \tag{D.5}$$

As we only want to keep $\mathcal{O}(N^0)$ contributions of the interaction term, let us focus on the term $\ln \bar{\chi}$:

$$\bar{\chi}[x-y, \tilde{x}-\tilde{y}] = \int \frac{\mathrm{d}A}{V} e^{-i \int \mathrm{d}t \, (\tilde{x}-\tilde{y}) \cdot \nabla V(x-y-A)} \tag{D.6}$$

which is 1 except in a region where the shift A brings the two trajectories closer. This region is of order Γ/V where Γ is the typical volume spanned by a trajectory during the time considered. If we do not consider times much longer than the relaxation time τ_α, $\Gamma \ll V$ is finite and we can expand the logarithm. Note that we get the same restrictions at long times than in the previous virial method. Defining, as in the previous section,

$$f = e^{-W} - 1 \tag{D.7}$$

such that $\int \frac{\mathrm{d}A}{V} f[x-y-A, \tilde{x}-\tilde{y}] = \bar{\chi}[x-y, \tilde{x}-\tilde{y}] - 1 \simeq \Gamma/V$, hence

$$
\begin{aligned}
\mathcal{S}(\rho) &= -\int \mathrm{D}[x,\tilde{x}] \rho[x,\tilde{x}] (\ln \rho[x,\tilde{x}] + \Phi[x,\tilde{x}]) + \frac{N}{2} \int \mathrm{D}[x,\tilde{x}] \mathrm{D}[y,\tilde{y}] \rho[x,\tilde{x}] \rho[y,\tilde{y}] \int \frac{\mathrm{d}A}{V} f[x-y-A, \tilde{x}-\tilde{y}] \\
&= -\int \mathrm{D}[x,\tilde{x}] \rho[x,\tilde{x}] (\ln \rho[x,\tilde{x}] + \Phi[x,\tilde{x}]) + \frac{N}{2} \int \frac{\mathrm{d}A}{V} \mathrm{D}[x,\tilde{x}] \mathrm{D}[y,\tilde{y}] \rho[x,\tilde{x}] \rho[y+A, \tilde{y}] f[x-y, \tilde{x}-\tilde{y}] \\
&= -\int \mathrm{D}[x,\tilde{x}] \rho[x,\tilde{x}] (\ln \rho[x,\tilde{x}] + \Phi[x,\tilde{x}]) + \frac{N}{2} \int \mathrm{D}[x,\tilde{x}] \mathrm{D}[y,\tilde{y}] \rho[x,\tilde{x}] \rho[y,\tilde{y}] f[x-y, \tilde{x}-\tilde{y}]
\end{aligned}
\tag{D.8}
$$

In the last step we assumed that $\rho[y,\tilde{y}]$ is translation invariant (only on the physical positions, not on the response field), hence $\rho[y+A, \tilde{y}] = \rho[y,\tilde{y}]$.

The last line in this equation is the dynamic analog of the usual starting point of replica computations for hard spheres in large dimensions [312, 243], with the saddle point condition for the thermodynamic limit $\delta\mathcal{S}/\delta\rho[x,\tilde{x}] = 0$.

DYNAMICS FROM AN EQUILIBRIUM INITIAL CONDITION

Here we give a simple argument to neglect the past history when one starts from equilibrium in a Langevin equation with memory. This discussion applies to exponentially decaying memory kernels only. In this special case, only by adding one additional degree of freedom, one can consider an explicit Markovian evolution of the two-body system. For more general memory kernels one has to resort to a coupling with a bath containing many degrees of freedom. The corresponding discussion can be found in §3.7.3.

Consider the following Langevin equation:

$$
\begin{aligned}
\gamma \dot{x} &= -\frac{\mathrm{d}U}{\mathrm{d}x} + \xi(t) - x(t) + \eta_1(t) \ , \\
\gamma \dot{\xi} &= -\xi(t) + x(t) + \eta_2(t) \ , \\
\langle \eta_1(t)\eta_1(t') \rangle &= \langle \eta_2(t)\eta_2(t') \rangle = 2T\gamma\delta(t-t') \ .
\end{aligned}
\tag{E.1}
$$

This equation is Markovian and it admits a Boltzmann stationary distribution

$$
P_{\mathrm{eq}}(x,\xi) = \frac{1}{Z}e^{-\beta\left[U(x)+\frac{1}{2}(x-\xi)^2\right]} \ ,
\tag{E.2}
$$

moreover the marginal distribution of x is the Boltzmann one with potential $U(x)$:

$$
P_{\mathrm{eq,x}}(x) = \int \mathrm{d}\xi \, P_{\mathrm{eq}}(x,\xi) = \frac{1}{Z}e^{-\beta U(x)} \ .
\tag{E.3}
$$

We show in the following that these two correlation functions are identical:

1. Starting with any initial condition at $t = t_0 \to -\infty$, we compute $C(t-t') = \langle x(t)x(t') \rangle$ for $t, t' > 0$.

2. Starting at $t = t_0 = 0$ with an initial condition x_0, ξ_0 drawn from $P_{\mathrm{eq}}(x_0, \xi_0)$, we compute $C(t-t') = \langle x(t)x(t') \rangle$ for $t, t' > 0$.

To proceed, we write the effective Langevin equation for x integrating out ξ. We have

$$
\xi(t) = \xi_0 e^{-(t-t_0)/\gamma} + \frac{1}{\gamma}\int_{t_0}^{t} \mathrm{d}s \, e^{-(t-s)/\gamma}[x(s)+\eta_2(s)] \ .
\tag{E.4}
$$

Substituting in the equation for x we obtain

$$
\begin{aligned}
\gamma \dot{x} &= -\frac{\mathrm{d}U}{\mathrm{d}x} + \xi_0 e^{-(t-t_0)/\gamma} + \frac{1}{\gamma}\int_{t_0}^{t} \mathrm{d}s \, e^{-(t-s)/\gamma}[x(s)+\eta_2(s)] - x(t) + \eta_1(t) \\
&= -\frac{\mathrm{d}U}{\mathrm{d}x} - \int_{t_0}^{t} \mathrm{d}s \, e^{-(t-s)/\gamma}\dot{x}(s) + (\xi_0 - x_0)e^{-(t-t_0)/\gamma} + \frac{1}{\gamma}\int_{t_0}^{t} \mathrm{d}s \, e^{-(t-s)/\gamma}\eta_2(s) + \eta_1(t)
\end{aligned}
\tag{E.5}
$$

We define $\rho(t,x_0) = (\xi_0 - x_0)e^{-(t-t_0)/\gamma} + \frac{1}{\gamma}\int_{t_0}^{t} \mathrm{d}s \, e^{-(t-s)/\gamma}\eta(s) + \eta_1(t)$ and we note that for fixed x_0 it is a random Gaussian variable (because it is a linear combination of Gaussian variables), which depends on $\eta_1(t)$, $\eta_2(t)$ and ξ_0. We have

$$
\gamma \dot{x} = -\frac{\mathrm{d}U}{\mathrm{d}x} - \int_{t_0}^{t} \mathrm{d}s \, e^{-(t-s)/\gamma}\dot{x}(s) + \rho(t,x_0) \ ,
\tag{E.6}
$$

$$
\langle \rho(t,x_0)\rho(t',x_0) \rangle = 2T\gamma\delta(t-t') + Te^{-(t-t')/\gamma} + [\langle(\xi_0-x_0)^2\rangle - T]e^{-(t-t_0)/\gamma}e^{-(t'-t_0)/\gamma}
$$

where here $\langle \bullet \rangle$ is an average over $\eta_1(t)$, $\eta_2(t)$ and ξ_0 at fixed x_0.

Now, in the two cases outlined above, we obtain:

1. In case (1), the dependence on the inital condition is lost when $t_0 \to -\infty$. Therefore we obtain

$$\gamma \dot{x} = -\frac{dU}{dx} - \int_{-\infty}^{t} ds\, e^{-(t-s)/\gamma} \dot{x}(s) + \rho(t) \,,$$
$$\langle \rho(t)\rho(t') \rangle = 2T\gamma\delta(t-t') + Te^{-(t-t')/\gamma} \,.$$
(E.7)

2. In case (2), we have $\langle (\xi_0 - x_0)^2 \rangle = T$ due to the form[1] of $P_{\text{eq}}(x,\xi)$. Then the dependence on x_0 in ρ again disappears, and we obtain

$$\gamma \dot{x} = -\frac{dU}{dx} - \int_{0}^{t} ds\, e^{-(t-s)/\gamma} \dot{x}(s) + \rho(t) \,,$$
$$\langle \rho(t)\rho(t') \rangle = 2T\gamma\delta(t-t') + Te^{-(t-t')/\gamma}$$
(E.8)

We conclude therefore that equations (E.7) and (E.8) give rise to the same correlation $C(t - t') = \langle x(t)x(t') \rangle$ at positive times.

Note that this is a particular instance of a memory kernel $M_C(t) = Te^{-t/\gamma}$, with corresponding reponse kernel $M_R(t) = -\beta\theta(t)\dot{M}_C(t) = \theta(t)e^{-t/\gamma}/\gamma$. The corresponding equation is

$$\gamma \dot{x} = -\frac{dU}{dx} - \beta \int_{t_0}^{t} ds\, M_C(t-s)\dot{x}(s) + \rho(t) \,,$$
$$\langle \rho(t)\rho(t') \rangle = 2T\gamma\delta(t-t') + M_C(t-t') \,.$$
(E.9)

and this argument shows that starting with any initial condition at $t_0 = -\infty$ is equivalent to starting in equilibrium at $t_0 = 0$ for the purpose of computing correlations at positive times.

---

[1] Note that this result is completely independent on the form of the distribution of x_0. It is enough that $P_{\text{init}}(x_0, \xi_0) \propto p(x_0)e^{-\frac{\beta}{2}(x_0-\xi_0)^2}$. However, we need to assume that ξ_0 is in equilibrium, and therefore also x_0 must be in equilibrium.

$\mathcal{F}$

DERIVATION OF THE STATIC FREE ENERGY

Outline

In this appendix we reproduce a derivation of the statics analog to the dynamical one §3.3, taking into account rotational invariance in order to solve exactly the limit $d \to \infty$ of the free entropy (4.29):

$$\mathcal{S}(\rho) = \mathcal{S}_{\text{IG}}(\rho) + \mathcal{S}_{\text{int}}(\rho) = -\int d\bar{x}\, \rho(\bar{x}) \ln \rho(\bar{x}) + \frac{N}{2} \int d\bar{x} d\bar{y}\, \rho(\bar{x}) \rho(\bar{y}) f(\bar{x}, \bar{y})\ , \qquad \frac{1}{N} \ln \overline{Z^n} = \max_\rho \mathcal{S}(\rho)\ . \tag{F.1}$$

Before proceeding, let us recall that we also wish to take the thermodynamic limit $R \to \infty$. In some cases the order of the two limits is irrelevant, but when relevant, according to section 4.2.1, we should take the $R \to \infty$ limit first. In other words, we should consider that R/d is a large quantity.

Due to rotational invariance on the hypersphere, the density of replicated configurations $\rho(\bar{x})$ can only depend on the matrix of the scalar products $q_{ab} = x_a \cdot x_b$, or more physically, on the matrix of mean square displacements between replicas (recall that $q_{aa} = x_a^2 = R^2$):

$$\mathsf{D}_{ab} = (x_a - x_b)^2 = 2R^2 - 2q_{ab}\ , \qquad q_{ab} = x_a \cdot x_b\ . \tag{F.2}$$

These definitions are summarized in appendix A.2.

F.1   Integrals for rotationally invariant functions

Here we prove the following useful equation, valid for a rotationally invariant function $f(\bar{x})$:

$$\int_{\mathbb{R}^{d+1}} D\bar{x}\, f(\bar{x}) = C_{n+1}^{d+1} \int \prod_{a<b}^{1,n} dq_{ab}\, (\det \hat{q})^{\frac{d-n}{2}} f(\hat{q})$$

$$= C_{n+1}^{d+1} (-2)^{\frac{-n(n-1)}{2}} \int \prod_{a<b}^{1,n} d\,\mathsf{D}_{ab}\, e^{\frac{d-n}{2}\left[\ln \det(-\hat{\mathsf{D}}/2) + \ln(1 - 2R^2 v^{\mathrm{T}} \hat{\mathsf{D}}^{-1} v)\right]} f(\hat{\mathsf{D}})\ , \tag{F.3}$$

where $v = (1, \cdots, 1)$, by definition $q_{aa} = R^2$ and $\mathsf{D}_{aa} = 0$, and

$$C_{n+1}^{d+1} = 2^{-n} \Omega_{d+1} \Omega_d \cdots \Omega_{d-n+2} \sim e^{\frac{d}{2} n \ln(2\pi e/d)}\ . \tag{F.4}$$

We consider a rotationally invariant function $f(x_1, \cdots, x_n)$ and, setting $q_{aa} = R^2$ and $\hat{q}$ symmetric[1],

---

[1] $q_{aa} = R^2$ due to the constraint $\delta(x_a^2 - R^2)$ in the left hand side. We take $\hat{q}$ symmetric in order to integrate only on its independent variables $a < b$.

we write

$$\int_{\mathbb{R}^{d+1}} \prod_{a=1}^n \left[\mathrm{d}x_a \delta(x_a^2 - R^2) \right] f(x_1, \cdots, x_n) = \int_{\mathbb{R}^{d+1}} \prod_{a=1}^n \mathrm{d}x_a \int \prod_{a<b}^{1,n} \left[\mathrm{d}q_{ab}\, \delta(x_a \cdot x_b - q_{ab}) \right] f(\hat{q}) \qquad \text{(F.5)}$$

In [242, Appendix A] it is shown that

$$\int_{\mathbb{R}^{d+1}} \prod_{a=1}^n \mathrm{d}x_a \prod_{a<b}^{1,n} \delta(x_a \cdot x_b - q_{ab}) = 2^{-n}\Omega_{d+1}\cdots\Omega_{d-n+2}[\det \hat{q}]^{(d-n)/2} \ , \qquad \text{(F.6)}$$

which proves the first equality in equation (F.3):

$$\int_{\mathbb{R}^{d+1}} \prod_{a=1}^n \left[\mathrm{d}x_a\, \delta(x_a^2 - R^2) \right] f(x_1, \cdots, x_n) = 2^{-n}\Omega_{d+1}\cdots\Omega_{d-n+2} \int \prod_{a<b}^{1,n} \mathrm{d}q_{ab}\, [\det \hat{q}]^{(d-n)/2} f(\hat{q}) \ . \qquad \text{(F.7)}$$

To obtain the second equality we change variables from q_{ab} to $\mathsf{D}_{ab} = (x_a - x_b)^2 = 2R^2 - 2q_{ab}$, or $\hat{\mathsf{D}} = 2(R^2 vv^{\mathrm{T}} - \hat{q})$. Then we have

$$\hat{q} = -\frac{\hat{\mathsf{D}}}{2}(I - 2R^2\hat{\mathsf{D}}^{-1} vv^{\mathrm{T}}) \ . \qquad \text{(F.8)}$$

and

$$\ln \det \hat{q} = \ln\det(-\hat{\mathsf{D}}/2) + \mathrm{Tr}\ln(I - 2R^2\hat{\mathsf{D}}^{-1}vv^{\mathrm{T}}) = \ln\det(-\hat{\mathsf{D}}/2) + \ln(1 - 2R^2 v^{\mathrm{T}}\hat{\mathsf{D}}^{-1} v) \ . \qquad \text{(F.9)}$$

Note that for $a = b$ we have $\mathsf{D}_{aa} = 0$, and we do not integrate over these variables. For $a < b$, going from q_{ab} to D_{ab} is a simple linear change of variables, so we have

$$\int \prod_{a<b}^{1,n} \mathrm{d}q_{ab}\, [\det \hat{q}]^{(d-n)/2} f(\hat{q}) = (-2)^{-n(n-1)/2} \int \prod_{a<b}^{1,n} \mathrm{d}\,\mathsf{D}_{ab}\, e^{\frac{d-n}{2}\left[\ln\det(-\hat{\mathsf{D}}/2)+\ln(1-2R^2 v^{\mathrm{T}}\hat{\mathsf{D}}^{-1} v) \right]} f(\hat{\mathsf{D}}) \ , \qquad \text{(F.10)}$$

which proves the second equality.

F.2 One-particle integrals: normalization of the density and ideal gas term

As a preliminary remark, $\mathcal{V} = \Omega_{d+1} R^d$ being the surface of the $d + 1$-dimensional hypersphere, we have:

$$\int_{\mathbb{R}^{d+1}} \mathrm{d}\bar{x} \prod_{a=1}^n \delta(x_a^2 - R^2) = \left[\Omega_{d+1} \int_0^\infty \mathrm{d}r\, r^d \delta(r^2 - R^2) \right]^n = \left[\Omega_{d+1}\frac{R^d}{2R} \right]^n = \left[\frac{\mathcal{V}}{2R} \right]^n = \frac{1}{(2R)^n}\int_{\mathcal{V}} \mathrm{d}\bar{x} \ , \qquad \text{(F.11)}$$

and therefore, defining $D\bar{x} = \mathrm{d}\bar{x} \prod_{a=1}^n \delta(x_a^2 - R^2)$, we have

$$\mathcal{S}(\rho) = -(2R)^n \int_{\mathbb{R}^{d+1}} D\bar{x}\, \rho(\bar{x}) \ln\rho(\bar{x}) + \frac{N}{2}(2R)^{2n} \int_{\mathbb{R}^{d+1}} D\bar{x}D\bar{y}\, \rho(\bar{x})\rho(\bar{y}) f(\bar{x}, \bar{y}) \ . \qquad \text{(F.12)}$$

We now use rotational invariance to deduce that the density $\rho(\bar{x})$ must depend only on $q_{ab} = x_a \cdot x_b$, or equivalently on $\mathsf{D}_{ab} = (x_a - x_b)^2$. The density is normalized as

$$1 = \int_{\mathcal{V}} \mathrm{d}\bar{x}\, \rho(\bar{x}) = (2R)^n C_{n+1}^{d+1} \int \prod_{a<b}^{1,n} \mathrm{d}q_{ab}\, (\det \hat{q})^{\frac{d-n}{2}} \rho(\hat{q})$$

$$= (2R)^n C_{n+1}^{d+1}(-2)^{\frac{n(n-1)}{2}} \int \prod_{a<b}^{1,n} \mathrm{d}\,\mathsf{D}_{ab}\, e^{\frac{d-n}{2}\left[\ln\det(-\hat{\mathsf{D}}/2)+\ln(1-2R^2 v^{\mathrm{T}}\hat{\mathsf{D}}^{-1} v) \right]} \rho(\hat{\mathsf{D}}) \ . \qquad \text{(F.13)}$$

We write $\rho(\hat{\mathsf{D}}) = e^{d\,\Omega(\hat{\mathsf{D}})}$, and we take a saddle point in d assuming that Ω is finite for large d. Taking the logarithm of the equation (F.13), at leading order for $d \to \infty$, using equation (F.4), we have

$$0 = \frac{d}{2}n\ln(2\pi e/d) + \frac{d}{2}\left[\ln\det(-\hat{\mathsf{D}}_{\mathrm{sp}}/2) + \ln(1 - 2R^2 v^{\mathrm{T}}\hat{\mathsf{D}}_{\mathrm{sp}}^{-1} v) \right] + d\,\Omega(\hat{\mathsf{D}}_{\mathrm{sp}}) \ . \qquad \text{(F.14)}$$

Note that equation (F.14) holds only for the matrix $\hat{D}_{sp}$ that maximizes the exponent in equation (F.13), and not for generic values of $\hat{D}$: in other words, equation (F.14) does not give the full shape of $\Omega(\hat{D})$ but only its value at $\hat{D} = \hat{D}_{sp}$. For a rotationally invariant observable $\mathcal{O}(\hat{D})$ that is not exponential in d, the average over $\rho(\bar{x})$ is dominated by the same value $\hat{D}_{sp}$ and we have

$$\int_{\mathcal{V}} \mathrm{d}\bar{x}\, \rho(\bar{x})\mathcal{O}(\bar{x}) = \mathcal{O}(\hat{D}_{sp}) \ . \tag{F.15}$$

In particular, the first term in equation (F.12) (the ideal gas term) is the average of $\ln \rho(\bar{x})$, which by hypothesis is not exponential in d. Thus we can apply equation (F.15) and we obtain

$$\mathcal{S}_{IG} = -\ln \rho(\hat{D}_{sp}) = -d\Omega(\hat{D}_{sp}) = \frac{d}{2} n \ln(2\pi e/d) + \frac{d}{2}\left[\ln\det(-\hat{D}_{sp}/2) + \ln(1 - 2R^2 v^{\mathrm{T}}\hat{D}_{sp}^{-1}v)\right] \ . \tag{F.16}$$

F.3 Two-particle integrals: the interaction term

For two-particle integrals, the exact calculation of the Jacobian of the change of variables is more difficult, so we will use a slightly different procedure where we compute the Jacobian by a saddle point in d. This procedure is simpler but the price to pay is that we cannot keep track easily of all the normalization constants[2]. We will compute the normalization constant only at the end, and for the moment all the proportionality factors will be neglected.

F.3.1 Change of variables

We consider a generic function f that depends only on the distances between pairs of atoms in two replicas, $|x_a - y_a|$, and a two-particle integral of the form

$$\begin{aligned}
I_f &= \frac{N}{2} \int_{\mathcal{V}} \mathrm{d}\bar{x}\mathrm{d}\bar{y}\, \rho(\bar{x})\rho(\bar{y})f(\bar{x},\bar{y}) \propto \int_{\mathbb{R}^{d+1}} D\bar{x}D\bar{y}\, \rho(\bar{x})\rho(\bar{y})f(\{|x_a - y_a|\}) \\
&= \int \mathrm{d}\hat{q}^x\mathrm{d}\hat{q}^y\mathrm{d}\bar{\omega}\, \rho(\hat{q}^x)\rho(\hat{q}^y)f(\sqrt{\bar{\omega}})K(\hat{q}^x, \hat{q}^y, \bar{\omega}) \ .
\end{aligned} \tag{F.17}$$

Here $q_{ab}^x = x_a \cdot x_b$ and $q_{ab}^y = y_a \cdot y_b$ are symmetric matrices such that $q_{aa}^x = q_{aa}^y = R^2$, hence $\mathrm{d}\hat{q}^{x,y} = \prod_{a<b} \mathrm{d}q_{ab}^{x,y}$, while $\bar{\omega} = (\omega_1, \cdots, \omega_n)$ with $\omega_a = (x_a - y_a)^2$. With an abuse of notation we defined $\sqrt{\bar{\omega}} = (\sqrt{\omega_1}, \cdots, \sqrt{\omega_n})$. Therefore

$$\begin{aligned}
K(\hat{q}^x, \hat{q}^y, \bar{\omega}) &= \int \mathrm{d}\bar{x}\mathrm{d}\bar{y} \prod_{a\leqslant b}^{1,n} \delta(x_a \cdot x_b - q_{ab}^x)\delta(y_a \cdot y_b - q_{ab}^y) \prod_{a=1}^{n} \delta(\omega_a - (x_a - y_a)^2) \\
&\propto \int \mathrm{d}\bar{x}\mathrm{d}\bar{y}\mathrm{d}\hat{\lambda}^x\mathrm{d}\hat{\lambda}^y\mathrm{d}\bar{\omega}'\, e^{\sum_{ab}^{1,n}(\lambda_{ab}^x q_{ab}^x - \lambda_{ab}^x x_a \cdot x_b + \lambda_{ab}^y q_{ab}^y - \lambda_{ab}^y y_a \cdot y_b) + \sum_{a=1}^{n}(\omega_a' \omega_a - \omega_a'(x_a - y_a)^2)} \\
&\propto \int \mathrm{d}\hat{\lambda}^x\mathrm{d}\hat{\lambda}^y\mathrm{d}\bar{\omega}' \exp\left\{\mathrm{Tr}(\hat{\lambda}^x\hat{q}^x + \hat{\lambda}^y\hat{q}^y) + \bar{\omega}'^T\bar{\omega} - \frac{d}{2}\ln\det\begin{pmatrix} \hat{\lambda}^x + \hat{\omega}' & -\hat{\omega}' \\ -\hat{\omega}' & \hat{\lambda}^y + \hat{\omega}' \end{pmatrix}\right\} \ ,
\end{aligned} \tag{F.18}$$

where $\bar{\omega}'$ has been written for convenience as a diagonal $n \times n$ matrix $\hat{\omega}'$ with $\omega_{ab}' = \omega_a'\delta_{ab}$. In the above derivation we performed the following steps:

1. In the second line, we introduced a Fourier representation of the delta functions by integrating over $\hat{\lambda}^x, \hat{\lambda}^y, \bar{\omega}'$. Note that because the delta functions are introduced for $a \leqslant b$, the matrix $\hat{\lambda}^x$ (and similarly $\hat{\lambda}^y$) has as independent elements the ones for $a \leqslant b$ only. Correspondingly $\mathrm{d}\hat{\lambda}^x = \prod_{a\leqslant b} \mathrm{d}\lambda_{ab}^x$, differently from the matrices $\hat{q}^x$.

2. The integrals over $\hat{\lambda}^x, \hat{\lambda}^y, \bar{\omega}'$ should be done on the imaginary axis. However, we are going to compute K by a saddle point and we anticipate that the saddle point is on the real axis, so we can equivalently treat them as real variables [81]. Then the integral over $\bar{x}, \bar{y}$ is a simple Gaussian integral and gives the determinant term.

---

[2]This is why we did not use this procedure for the ideal gas term, where the normalization is crucial.

In equations (F.17) and (F.18) there is clearly a symmetry $x \leftrightarrow y$ and it is very unreasonable that this symmetry is broken at the saddle point. Hence we assume that $\hat{q}^x = \hat{q}^y = \hat{q}$ and $\hat{\lambda}^x = \hat{\lambda}^y = \hat{\lambda}$ at the saddle point. Using

$$\det \begin{pmatrix} \hat{\lambda} + \hat{\omega}' & -\hat{\omega}' \\ -\hat{\omega}' & \hat{\lambda} + \hat{\omega}' \end{pmatrix} = \det(\hat{\lambda})\det(\hat{\lambda} + 2\hat{\omega}') = \det(\hat{\lambda})^2 \det(1 + 2\hat{\lambda}^{-1}\hat{\omega}') , \tag{F.19}$$

we have

$$K(\hat{q}, \hat{q}, \bar{\omega}) \propto \int d\bar{\omega}' \exp\left\{ 2\text{Tr}(\hat{q}\hat{\lambda}) + \bar{\omega}'^T \bar{\omega} - d\ln\det\hat{\lambda} - \frac{d}{2}\ln\det(1 + 2\hat{\lambda}^{-1}\hat{\omega}') \right\} , \tag{F.20}$$

where $\hat{\lambda}$ (and $\bar{\omega}'$, but we postpone its saddle-point evaluation) are determined by maximizing the exponent. We now make a simplifying assumption[3] (to be checked *a posteriori*), namely that the last term in the expression above is not proportional to d and therefore does not affect the saddle point on $\hat{\lambda}$. Maximizing the exponent with respect to $\hat{\lambda}$ we obtain the relation

$$\hat{q} - \frac{d}{2}\hat{\lambda}^{-1} = 0 , \tag{F.21}$$

and therefore

$$K(\hat{q}, \hat{q}, \bar{\omega}) \propto \int d\bar{\omega}' \exp\left\{ \bar{\omega}'^T \bar{\omega} + d\ln\det\hat{q} - \frac{d}{2}\ln\det\left(1 + \frac{4}{d}\hat{q}\hat{\omega}'\right) \right\} , \tag{F.22}$$

and

$$I_f \propto \int d\hat{q}d\bar{\omega}d\bar{\omega}' \, \rho(\hat{q})^2 f(\sqrt{\bar{\omega}}) \, e^{\bar{\omega}'^T \bar{\omega} + d\ln\det\hat{q} - \frac{d}{2}\ln\det\left(1 + \frac{4}{d}\hat{q}\hat{\omega}'\right)} . \tag{F.23}$$

Under the assumption that the last term is not exponential in d, $\hat{q}$ is determined by maximizing $\left(\rho(\hat{q})e^{\frac{d}{2}\ln\det\hat{q}}\right)^2$, which is exactly the same factor that determines the saddle point value of $\hat{q}$ in the ideal gas term, see equation (F.13). We therefore assume from now on that $\hat{q}$ is equal to this saddle point value (without adding explicitly the *sp* suffix to $\hat{q}$ for notational convenience). We know from equation (F.13) that at this saddle point value $\rho(\hat{q})e^{\frac{d}{2}\ln\det\hat{q}}$ is a constant. We obtain

$$I_f \propto \int d\bar{\omega}d\bar{\omega}' \, f(\sqrt{\bar{\omega}}) \, e^{\bar{\omega}'^T \bar{\omega} - \frac{d}{2}\ln\det\left(1 + \frac{4}{d}\hat{q}\hat{\omega}'\right)} . \tag{F.24}$$

F.3.2 Scaling of the mean square displacement

We now change variables by introducing the mean square displacement D_{ab}, equation (F.2), with $q_{ab} = R^2 - D_{ab}/2$. Our crucial assumption is that $D_{ab} = \sigma^2 \Delta_{ab}/d$, with Δ_{ab} remaining finite for $d \to \infty$. This assumption is based on the scaling that has been already found in [312, 243, 96, 225] and in §5.2, and we will check *a posteriori* that it is the only possible choice to obtain a meaningful scaling for $d \to \infty$. In matrix form we have

$$\hat{q} = R^2 vv^T - \frac{1}{2}\hat{D} = R^2 vv^T - \frac{\sigma^2}{2d}\hat{\Delta} . \tag{F.25}$$

In equation (F.24) we have

$$\ln\det\left(1 + \frac{4}{d}\hat{q}\hat{\omega}'\right) = \ln\det\left(1 + \frac{4R^2}{d}vv^T\hat{\omega}' - \frac{2\sigma^2}{d^2}\hat{\Delta}\hat{\omega}'\right)$$
$$= \ln\det\left(1 + \frac{4R^2}{d}vv^T\hat{\omega}'\right) + \ln\det\left[1 - \frac{1}{1 + \frac{4R^2}{d}vv^T\hat{\omega}'}\frac{2\sigma^2}{d^2}\hat{\Delta}\hat{\omega}'\right] . \tag{F.26}$$

Using the cyclic properties of the trace we have

$$\ln\det\left(1 + \frac{4R^2}{d}vv^T\hat{\omega}'\right) = \text{Tr}\ln\left(1 + \frac{4R^2}{d}vv^T\hat{\omega}'\right) = \ln\left(1 + \frac{4R^2}{d}v^T\hat{\omega}'v\right) . \tag{F.27}$$

---

[3]This assumption is not necessary, see the analog dynamic derivation in §3.3.4, but it simplifies the derivation.

Similarly, we have

$$\frac{1}{1 + \frac{4R^2}{d} vv^{\mathrm{T}}\hat{\omega}'} = 1 + \sum_{n=1}^{\infty}\left(-\frac{4R^2}{d}\right)^n (vv^{\mathrm{T}}\hat{\omega}')^n = 1 - \frac{4R^2}{d} vv^{\mathrm{T}}\hat{\omega}' \sum_{n=0}^{\infty}\left(-\frac{4R^2}{d}\right)^n (v^{\mathrm{T}}\hat{\omega}'v)^n$$

$$= 1 - \frac{4R^2/d}{1 + (4R^2/d)v^{\mathrm{T}}\hat{\omega}'v} vv^{\mathrm{T}}\hat{\omega}' \to 1 - \frac{vv^{\mathrm{T}}\hat{\omega}'}{v^{\mathrm{T}}\hat{\omega}'v}\,, \tag{F.28}$$

where the last result holds for R^2/d large. Using these results we obtain for large R^2/d

$$I_f \propto \int \mathrm{d}\bar{\omega}\mathrm{d}\bar{\omega}'\, f(\sqrt{\bar{\omega}})\, e^{\bar{\omega}'^{\mathrm{T}}\bar{\omega} - \frac{d}{2}\ln\left(v^{\mathrm{T}}\hat{\omega}'v\right) - \frac{d}{2}\mathrm{Tr}\ln\left[1 - \left(1 - \frac{vv^{\mathrm{T}}\hat{\omega}'}{v^{\mathrm{T}}\hat{\omega}'v}\right)\frac{2\sigma^2}{d^2}\hat{\Delta}\hat{\omega}'\right]}. \tag{F.29}$$

The last term can be expanded for large d, we have

$$\frac{d}{2}\mathrm{Tr}\ln\left[1 - \left(1 - \frac{vv^{\mathrm{T}}\hat{\omega}'}{v^{\mathrm{T}}\hat{\omega}'v}\right)\frac{2\sigma^2}{d^2}\hat{\Delta}\hat{\omega}'\right] \sim -\frac{\sigma^2}{d}\mathrm{Tr}\left[\left(1 - \frac{vv^{\mathrm{T}}\hat{\omega}'}{v^{\mathrm{T}}\hat{\omega}'v}\right)\hat{\Delta}\hat{\omega}'\right]$$

$$= \frac{\sigma^2}{d}\frac{\mathrm{Tr}(vv^{\mathrm{T}}\hat{\omega}'\hat{\Delta}\hat{\omega}')}{v^{\mathrm{T}}\hat{\omega}'v} = \frac{\sigma^2}{d}\frac{v^{\mathrm{T}}\hat{\omega}'\hat{\Delta}\hat{\omega}'v}{v^{\mathrm{T}}\hat{\omega}'v}\,, \tag{F.30}$$

where we used that $\mathrm{Tr}(\hat{\Delta}\hat{\omega}') = \sum_{a=1}^{n}\omega_a'\Delta_{aa} = 0$ because $\Delta_{aa} = 0$. Finally we obtain

$$I_f \propto \int \mathrm{d}\bar{\omega}\,\mathrm{d}\bar{\omega}'\, f(\sqrt{\bar{\omega}})\, e^{\sum_a \omega_a'\omega_a - \frac{d}{2}\ln\left(\sum_a \omega_a'\right) - \frac{\sigma^2}{d}\frac{\sum_{ab}\omega_a'\Delta_{ab}\omega_b'}{\sum_a \omega_a'}}. \tag{F.31}$$

We now make a change of variable, $\omega_a = \sigma^2(1 + 2\mu_a/d)$ and $\omega_a' = d\mu_a'/\sigma^2$. We have $\sqrt{\omega_a} \sim \sigma(1 + \mu_a/d)$ and we get

$$I_f \propto -\int \mathrm{d}\bar{\mu}\,\mathrm{d}\bar{\mu}'\, f(\{\sigma(1 + \mu_a/d)\})\, e^{d\sum_a \mu_a' + 2\sum_a \mu_a\mu_a' - \frac{d}{2}\ln\left(\sum_a \mu_a'\right) - \frac{\sum_{ab}\mu_a'\Delta_{ab}\mu_b'}{\sum_a \mu_a'}}$$

$$\propto -\int \mathrm{d}\bar{\mu}\,\mathrm{d}\bar{\mu}'\,\mathrm{d}x\,\mathrm{d}\lambda\, f(\{\sigma(1 + \mu_a/d)\})\, e^{\lambda\left(x - \sum_a \mu_a'\right) + d\,x + 2\sum_a \mu_a\mu_a' - \frac{d}{2}\ln x - \frac{1}{x}\sum_{ab}\mu_a'\Delta_{ab}\mu_b'}\,, \tag{F.32}$$

where we introduced a delta function of $x = \sum_a \mu_a'$ through the integral representation (rotated on the real axis). The integral over x can be done via a saddle point because of the presence of a factor d in front of the exponential. For the saddle point over x we can neglect the last term, and we obtain $1 = 1/(2x)$ hence $x = 1/2$. The integral over μ_a' is Gaussian, giving

$$I_f = -\frac{\mathcal{C}}{2}\int \mathrm{d}\bar{\mu}\,\mathrm{d}\lambda\, f(\{\sigma(1 + \mu_a/d)\})\, e^{\frac{1}{2}\lambda + \frac{1}{2}\sum_{ab}(\mu_a - \lambda/2)(\Delta^{-1})_{ab}(\mu_b - \lambda/2)}$$

$$= -\mathcal{C}\int \mathrm{d}\bar{\mu}\,\mathrm{d}\lambda\, f(\{\sigma(1 + \mu_a/d + \lambda/d)\})\, e^{\lambda + \frac{1}{2}\bar{\mu}^T\hat{\Delta}^{-1}\bar{\mu}}\,. \tag{F.33}$$

Note that the crucial assumption made for the saddle point in equation (F.20) has now been checked self-consistently: the terms that were neglected are not exponential[4] in d.

The proportionality constant $\mathcal{C}$ does not depend upon the choice of f. Hence we can choose a test function[5] $f(\{|x_a - y_a|\}) = \theta(\sigma - |x_1 - y_1|)$. Recall that $\int \mathrm{d}\bar{x}\rho(\bar{x}) = 1$, and $\int \mathrm{d}x_2\cdots\mathrm{d}x_m\rho(\bar{x}) = 1/\mathcal{V}$ because it must be a constant due to translational invariance. With the test function f we obtain

$$I_f = \frac{N}{2}\int \mathrm{d}\bar{x}\mathrm{d}\bar{y}\rho(\bar{x})\rho(\bar{y})\theta(\sigma - |x_1 - y_1|) = \frac{N}{2\mathcal{V}^2}\int \mathrm{d}x_1 dy_1\theta(\sigma - |x_1 - y_1|) = \frac{N\mathcal{V}_d(\sigma)}{2\mathcal{V}} = \frac{2^d\varphi}{2}\,. \tag{F.34}$$

From equation (F.33) we obtain instead (recalling that $\Delta_{11} = 0$)

$$I_f = -\mathcal{C}\int \mathrm{d}\bar{\mu}\,\mathrm{d}\lambda\,\theta(-\mu_1 - \lambda)\, e^{\lambda + \frac{1}{2}\bar{\mu}^T\hat{\Delta}^{-1}\bar{\mu}} = -\mathcal{C}\int \mathrm{d}\bar{\mu}\, e^{-\mu_1 + \frac{1}{2}\bar{\mu}^T\hat{\Delta}^{-1}\bar{\mu}} = -\mathcal{C}(2\pi)^{n/2}\sqrt{\det(-\hat{\Delta})} \tag{F.35}$$

---

[4]Only multiplicative constants resulting from these terms are exponential in d. They are computed in the following in an easier way.

[5] Note that the choice of the test function is not completely arbitrary. In particular it should satisfy the properties of the Mayer function f, that we used to derive the entropy, such as $\bar{f} \sim \mathcal{V}_d(\sigma)/\mathcal{V}$. Making a choice that does not respect these properties would lead to absurd results.

Comparing these two expressions we obtain $\mathcal{C} = -\frac{2^d \varphi}{2} \frac{1}{(2\pi)^{n/2}\sqrt{\det(-\hat{\Delta})}}$ which leads to the result:

$$I_f = \frac{2^d \varphi}{2} \int \mathcal{D}_{-\hat{\Delta}} \bar{\mu} \, d\lambda \, e^\lambda f(\{\sigma(1 + \mu_a/d + \lambda/d)\}) \,, \qquad \mathcal{D}_{\hat{\Delta}} \bar{\mu} = d\bar{\mu} \frac{1}{(2\pi)^{n/2}\sqrt{\det(\hat{\Delta})}} e^{-\frac{1}{2}\bar{\mu}^T \hat{\Delta}^{-1} \bar{\mu}} \,.$$

(F.36)

An important remark is that the measure $\mathcal{D}_{-\hat{\Delta}} \bar{\mu}$ defined in equation (F.36) cannot really be considered as a Gaussian measure over the μ_a. In fact, one has $\langle \mu_a \mu_b \rangle = -\Delta_{ab}$ which clearly makes no sense, because $\langle \mu_a^2 \rangle = -\Delta_{aa} = 0$ which implies that actually all the $\mu_a = 0$. A related problem is that $\mathrm{Tr}\hat{\Delta} = \sum_a \Delta_{aa} = 0$, hence $\hat{\Delta}$ has both positive and negative eigenvalues, which makes the Gaussian integral ill-defined. However, these problems can bypassed by considering $\mathcal{D}_{-\hat{\Delta}} \bar{\mu}$ as an abstract measure, and the prescription to compute integrals of functions of μ_a is that $\langle \mu_a \rangle = 0$, $\langle \mu_a \mu_b \rangle = -\Delta_{ab}$, and higher moments are computed using the Wick rule for Gaussian integrals.

The problem can be fixed by a change of variables[6]. Let us define the function

$$\mathcal{F}(\hat{\Delta}) = -\int \mathcal{D}_{-\hat{\Delta}} \bar{\mu} \, d\lambda \, e^\lambda f(\{\sigma(1 + \mu_a/d + \lambda/d)\}) \,.$$

(F.37)

Here $\hat{\Delta}$ is (minus) the matrix of correlations of the Gaussian measure of the μ_a. Then, if we wish to compute $\mathcal{F}(-Avv^T + \hat{\Delta})$, we have $\langle \mu_a \mu_b \rangle = A - \Delta_{ab}$. Equivalently, we can write $\mu_a = g_a + H$, where μ_a and H are uncorrelated Gaussian variables with zero mean, such that $\langle H^2 \rangle = A$ and $\langle g_a g_b \rangle = -\Delta_{ab}$. We thus have

$$\mathcal{F}(-Avv^T + \hat{\Delta}) = -\int \mathcal{D}_{-\hat{\Delta}} \bar{g} \, dH \frac{e^{-\frac{H^2}{2A}}}{\sqrt{2\pi A}} \, d\lambda \, e^\lambda f(\{\sigma(1 + g_a/d + H/d + \lambda/d)\})$$

$$= -\int \mathcal{D}_{-\hat{\Delta}} \bar{\mu} \, dH \frac{e^{-\frac{H^2}{2A}}}{\sqrt{2\pi A}} \, d\lambda \, e^{\lambda - H} f(\{\sigma(1 + \mu_a/d + \lambda/d)\})$$

$$= -e^{A/2} \int \mathcal{D}_{-\hat{\Delta}} \bar{\mu} \, d\lambda \, e^\lambda f(\{\sigma(1 + \mu_a/d + \lambda/d)\}) = e^{A/2} \mathcal{F}(\hat{\Delta}) \,.$$

(F.38)

This shows that $\mathcal{F}(\hat{\Delta}) = e^{-A/2} \mathcal{F}(-Avv^T + \hat{\Delta})$ for arbitrary A and leads to our final result:

$$I_f = -\frac{2^d \varphi}{2} \mathcal{F}(\hat{\Delta}) \,, \qquad \mathcal{F}(\hat{\Delta}) = -e^{-A/2} \int \mathcal{D}_{Avv^T - \hat{\Delta}} \bar{\mu} \, d\lambda \, e^\lambda f(\{\sigma(1 + \mu_a/d + \lambda/d)\}) \,.$$

(F.39)

We will see that A can be chosen conveniently to have a well defined Gaussian measure, and simplify these expressions in concrete cases.

F.3.3 Mayer function

Let us now specialize to the case in which f is the replicated Mayer function defined in equation (4.11) and make contact with previous results [96]. Then using equation (3.4) we get

$$f(\{\sigma(1 + \mu_a/d + \lambda/d)\}) = -1 + \prod_{a=1}^n e^{-\beta v[\sigma(1 + \mu_a/d + \lambda/d)]} = -1 + \prod_{a=1}^n e^{-\beta \bar{V}(\mu_a + \lambda)} \,.$$

(F.40)

and thus

$$\mathcal{F}(\hat{\Delta}) = e^{-A/2} \int d\lambda \, e^\lambda \left\{ 1 - \int \mathcal{D}_{Avv^T - \hat{\Delta}} \bar{\mu} \prod_{a=1}^n e^{-\beta \bar{V}(\mu_a + \lambda)} \right\} \,,$$

(F.41)

---

[6] This discussion could have been hidden by introducing the shift $\hat{\Delta} \to \hat{\Delta} - Avv^T$ directly in (F.32). However equations like (F.38) and (F.39) will be needed in the following to simplify computations. The important point is that there exist well-chosen values of A that makes the expression of $\mathcal{F}$ in equation (F.39) well defined; equation (F.37) can be seen as an analytic continuation to $A = 0$.

One can show that for any function $f(\{\mu_a\})$ the following relation holds[7] (here we choose $A = 0$ for simplicity):

$$\int \mathcal{D}_{-\hat{\Delta}} \bar{\mu} \, f(\{\mu_a\}) = \exp\left(-\frac{1}{2}\sum_{ab}^{1,n} \Delta_{ab} \frac{\partial^2}{\partial \mu_a \partial \mu_b}\right) f(\{\mu_a\})\Bigg|_{\{\mu_a=0\}} . \tag{F.43}$$

Using this we obtain

$$
\begin{aligned}
\mathcal{F}(\hat{\Delta}) &= \int \mathrm{d}\lambda\, e^\lambda \left\{ 1 - \exp\left(-\frac{1}{2}\sum_{ab}^{1,n} \Delta_{ab} \frac{\partial^2}{\partial \mu_a \partial \mu_b}\right) \prod_{a=1}^{n} e^{-\beta\bar{V}(\mu_a+\lambda)}\Bigg|_{\{\mu_a=0\}} \right\} \\
&= \int \mathrm{d}h\, e^h \left\{ 1 - \exp\left(-\frac{1}{2}\sum_{ab}^{1,n} \Delta_{ab} \frac{\partial^2}{\partial h_a \partial h_b}\right) \prod_{a=1}^{n} e^{-\beta\bar{V}(h_a)}\Bigg|_{\{h_a=h\}} \right\} \\
&= \int \mathrm{d}h\, e^h \frac{\mathrm{d}}{\mathrm{d}h} \left\{ \exp\left(-\frac{1}{2}\sum_{ab}^{1,n} \Delta_{ab} \frac{\partial^2}{\partial h_a \partial h_b}\right) \prod_{a=1}^{n} e^{-\beta\bar{V}(h_a)}\Bigg|_{\{h_a=h\}} \right\} .
\end{aligned}
\tag{F.44}
$$

which coincides with the result obtained in [96, equation (15)] (the last line is obtained by an integration by parts).

F.4 Final result

Let us now summarize the main results of this appendix.

1. We have shown that for a generic function $f(\{|x_a - y_a|\})$ that is not exponential in d and constraining the replicas to be close to each other, we have, from equation (F.39):

$$
\begin{aligned}
\frac{N}{2} \int_V \mathrm{d}\bar{x}\mathrm{d}\bar{y}\rho(\bar{x})\rho(\bar{y})f(\bar{x},\bar{y}) &= -\frac{2^d\varphi}{2}\mathcal{F}(\hat{\Delta}) , \\
\mathcal{F}(\hat{\Delta}) &= -e^{-A/2} \int \mathcal{D}_{Avv^{\mathrm{T}}-\hat{\Delta}}\bar{\mu}\, \mathrm{d}\lambda\, e^\lambda f(\{\sigma(1+\mu_a/d+\lambda/d)\}) ,
\end{aligned}
\tag{F.45}
$$

where $\mathcal{D}_{Avv^{\mathrm{T}}-\hat{\Delta}}\bar{\mu}$ is a Gaussian measure with $\langle\mu_a\mu_b\rangle = A - \Delta_{ab}$, as defined in equation (F.36), and A is an arbitrary constant. Here $\hat{\Delta} = d\hat{\mathsf{D}}/\sigma^2$, since our crucial assumption is that $\hat{\mathsf{D}} = O(1/d)$ (see §3.3.2), is the saddle-point matrix defined in equation (F.14):

$$0 = \frac{d}{2}n\ln(2\pi e/d) + \frac{d}{2}\left[\ln\det(-\hat{\mathsf{D}}_{\mathrm{sp}}/2) + \ln(1 - 2R^2 v^{\mathrm{T}}\hat{\mathsf{D}}_{\mathrm{sp}}^{-1}v)\right] - d\,\Omega(\hat{\mathsf{D}}_{\mathrm{sp}}) . \tag{F.46}$$

Other equivalent expressions for $\mathcal{F}(\hat{\Delta})$, namely equations (F.41) and (F.44), have been derived in the special case in which f is the HS replicated Mayer function. Equation (F.44) reproduces the previous result of [96].

2. Our second result is an expression of the entropy in terms of the saddle-point scaled mean square displacement matrix $\hat{\Delta} = d\hat{\mathsf{D}}/\sigma^2$ and the scaled density $\hat{\varphi} = 2^d\varphi/d$. The ideal gas term is given by equation (F.16). For the interaction term we use equation (F.45). We obtain[8]

$$\mathcal{S}(\hat{\Delta}) = \frac{d}{2}n\ln(\pi e\sigma^2/d^2) + \frac{d}{2}\ln\det(-\hat{\Delta}) + \frac{d}{2}\ln\left(1 - \frac{2dR^2}{\sigma^2}v^{\mathrm{T}}\hat{\Delta}^{-1}v\right) - \frac{d}{2}\hat{\varphi}\mathcal{F}(\hat{\Delta}) , \tag{F.47}$$

---

[7] The proof is obtained by performing, on the left hand side, a Taylor expansion of the function $f(\{\mu_a\})$ and using the Wick rule, while on the right hand side expanding the exponential [135]. For example, at the lowest order, one obtains

$$\int \mathcal{D}_{-\hat{\Delta}}\bar{\mu}\, f(\{\mu_a\}) = f(\{0\}) - \frac{1}{2}\sum_{ab}^{1,n} \Delta_{ab}\frac{\partial^2 f}{\partial\mu_a\partial\mu_b}(\{0\}) + \cdots = \exp\left(-\frac{1}{2}\sum_{ab}^{1,n}\Delta_{ab}\frac{\partial^2}{\partial\mu_a\partial\mu_b}\right)f(\{\mu_a\})\Bigg|_{\{\mu_a=0\}} . \tag{F.42}$$

[8]It may seem that this expression of the entropy is ill-defined (imaginary) because the logarithms might be evaluated at negative values. Indeed, since $\mathrm{Tr}\hat{\Delta} = 0$, $\hat{\Delta}$ has both positive and negative eigenvalues; thus, $\det(-\hat{\Delta})$ and $1 - \frac{2dR^2}{\sigma^2}v^{\mathrm{T}}\hat{\Delta}^{-1}v$ might be negative. However, remember that in the end one wishes to take the limit $n \to 0$. In this limit, these expressions are regularized: one can check from Appendix B that $\hat{\Delta}$ is negative definite. Another option, which is used in sections 4.5 and in chapter 3, is to express $\mathcal{S}$ in terms of $\hat{Q} \equiv \Delta_{\mathrm{liq}}vv^{\mathrm{T}} - \hat{\Delta}$, which is positive definite.

where for $\mathcal{F}(\hat{\Delta})$ we have three expressions: equations (F.41), (F.44) and (F.45).

3. The matrices $\hat{\Delta}$ or $\hat{D}$ should be determined by solving the $d \to \infty$ saddle-point condition, i.e. by maximizing the terms that are exponential in d in equation (F.13). The problem is that we have never derived explicitly the form of $\Omega(\hat{D})$. However, one can show that $\hat{\Delta}$ can be equivalently determined by maximizing the final result for the entropy, equation (F.47), which is quite intuitive (a formal proof can be found in [243, 242]). Indeed, the thermodynamic limit saddle-point equation is $\delta\mathcal{S}/\delta\rho = 0$. In infinite d, $\mathcal{S}$ depends on ρ only through the saddle-point value of $\Omega(\hat{\Delta}_{\mathrm{sp}})$, which is known in terms of $\hat{\Delta}_{\mathrm{sp}}$ via (F.46). Therefore $\delta\mathcal{S}/\delta\rho = 0$ is equivalent to $\mathrm{d}\mathcal{S}/\mathrm{d}\hat{\Delta}_{\mathrm{sp}} = \hat{0}$ where we have expressed $\mathcal{S}$ only in terms of the saddle-point value $\hat{\Delta}_{\mathrm{sp}}$ as in (F.47). This condition fully determines the saddle-point value $\hat{\Delta}_{\mathrm{sp}}$ and is thus equivalent to the $d \to \infty$ saddle-point equation.

EQUIVALENCE WITH PREVIOUS STATIC COMPUTATIONS

Outline

G.1 The ideal gas term

We show here that the ideal gas term in equation (4.37) is equivalent to the results derived in [243, 242, 96] for the replicated entropy, e.g. [96, Eq.(1)], for a general order parameter $\hat{\Delta}$ (mean-square displacements matrix). There is a subtlety because in [243, 242, 96] the calculation was restricted to a block of m replicas, following *e.g.* [288], hence it was assumed that the matrix elements of $\hat{\Delta}$ are finite. In equation (4.37) we instead considered the more general case where some matrix elements can be $O(R^2)$ (*e.g.* in the liquid phase). The two methods are equivalent; this can be seen on the ideal gas term as an example we focus on here. The interaction term can be treated by a similar calculation than the one presented in section 4.4.2.1. As shown in section 4.5, it can be written as

$$\mathcal{S}_{\text{IG}} = \frac{d}{2} n \ln(\pi e \sigma^2 / d^2) + \frac{d}{2} \ln \det \hat{Q} \tag{G.1}$$

where $\hat{Q} = \Delta_{\text{liq}} v v^{\text{T}} - \hat{\Delta}$ reads:

$$\hat{Q} = \begin{pmatrix} \begin{pmatrix} & & \\ & \hat{Q}_m & \\ & & \end{pmatrix} & & \Delta_{\text{liq}} - \Delta_0 \\ & \ddots & \\ \Delta_{\text{liq}} - \Delta_0 & & \begin{pmatrix} & & \\ & \hat{Q}_m & \\ & & \end{pmatrix} \end{pmatrix},$$

where the suffix m denotes the restriction to the first block, $\hat{Q}_m = \Delta_{\text{liq}} \hat{v} \hat{v}^{\text{T}} - \hat{\Delta}_m$ can be any $m \times m$ matrix ($\hat{v}$ is the m-dimensional vector of all ones). As shown in section 4.4, we have $\Delta_{\text{liq}} - \Delta_0 = \mathcal{O}(\Delta_0^{3/2} e^{-\Delta_0/4})$ which tends exponentially to zero in the large R limit. As a consequence, the entropy of the n replicas breaks into n/m times the entropy of the $m \times m$ blocks:

$$\mathcal{S}_{\text{IG}} = \frac{n}{m} \mathcal{S}_{\text{IG}}^{(m)} = \frac{n}{m} \left[\frac{d}{2} m \ln(\pi e \sigma^2 / d^2) + \frac{d}{2} \ln \det(-\hat{\Delta}_m) + \frac{d}{2} \ln \left(1 - \frac{2 d R^2}{\sigma^2} \hat{v}^{\text{T}} \hat{\Delta}_m^{-1} \hat{v} \right) \right] \tag{G.2}$$

Therefore, we can go back to the setting of [243, 242, 96]. We thus focus on $\mathcal{S}_{\text{IG}}^{(m)}$ and drop the hat on $\hat{v}$ and the suffix m on matrices, restricting on a $m \times m$ block. In this setting, $\hat{\Delta}$ is finite (as an example, for a 1-RSB glass phase, it is a replica symmetric matrix with parameter Δ_1 which is finite, as shown in section 4.4.2 and 4.5.4). Then, for large R we can approximate $\ln\left(1 - \frac{2dR^2}{\sigma^2} v^{\text{T}} \hat{\Delta}^{-1} v\right) \sim \ln\left(-\frac{2dR^2}{\sigma^2} v^{\text{T}} \hat{\Delta}^{-1} v\right)$ and the ideal gas term of equation (4.37) becomes, recalling equation (4.39),

$$
\begin{aligned}
\mathcal{S}_{\text{IG}}^{(m)} &= \frac{d}{2} m \ln(2\pi e \sigma^2/d^2) + \frac{d}{2} \ln[\det(-\hat{\Delta}/2)(-v^{\text{T}} \hat{\Delta}^{-1} v)] - \frac{d}{2} \ln\left(\frac{\sigma^2}{2d}\right) + d \ln R \\
&= \frac{d}{2}(m-1) \ln(2\pi e \sigma^2/d^2) + \frac{d}{2} \ln[2 \det(-\hat{\Delta}/2)(-v^{\text{T}} \hat{\Delta}^{-1} v)] + \ln \mathcal{V} \ ,
\end{aligned}
\tag{G.3}
$$

which, recalling that to compare with HS we should replace $\ln \mathcal{V} \to 1 - \ln \rho$, coincides with the results of [243, 242, 96] (see e.g. [96, Eqs.(1) and (2)]) provided

$$
\ln[2 \det(-\hat{\Delta}/2)(-v^{\text{T}} \hat{\Delta}^{-1} v)] = \ln \det \hat{\alpha}^{m,m} + 2 \ln m \ ,
\tag{G.4}
$$

where $\alpha_{ab} = d(x_a \cdot x_b)/\sigma^2$ is a symmetric and Laplacian matrix ($\sum_b \alpha_{ab} = 0$) that is related to $\hat{\Delta}$ by the relation $\Delta_{ab} = \alpha_{aa} + \alpha_{bb} - 2\alpha_{ab}$, and $\hat{\alpha}^{a,a}$ is the (a,a)-cofactor of $\hat{\alpha}$. The task is then to prove equation (G.4).

G.2 The cofactor

To prove equation (G.4), we note first that for Laplacian matrices $\det \hat{\alpha} = 0$ and $\det \hat{\alpha}^{a,a}$ is independent of a (Kirchhoff's matrix-tree theorem). Then

$$
\det(\epsilon I + \hat{\alpha}) = \epsilon \sum_a \det \hat{\alpha}^{a,a} + O(\epsilon^2) = \epsilon m \det \hat{\alpha}^{m,m} + O(\epsilon^2) \quad \Rightarrow \quad \det \hat{\alpha}^{m,m} = \lim_{\epsilon \to 0} \frac{1}{\epsilon m} \det(\epsilon I + \hat{\alpha}) \ . \tag{G.5}
$$

Then we note that defining $\chi_a = \alpha_{aa}$, we have

$$
\Delta_{ab} = \alpha_{aa} + \alpha_{bb} - 2\alpha_{ab} = \chi_a + \chi_b - 2\alpha_{ab} \quad \Rightarrow \quad \alpha_{ab} = \frac{1}{2}\left[\chi_a + \chi_b - \Delta_{ab}\right] \ , \tag{G.6}
$$

which is written in matrix notation as $\hat{\alpha} = \frac{1}{2}[\chi v^{\text{T}} + v\chi^T - \hat{\Delta}]$. To determine χ we impose the Laplacian condition, $\hat{\alpha} v = 0$,

$$
0 = 2\hat{\alpha} v = m\chi + v(\chi \cdot v) - \hat{\Delta} v \quad \Rightarrow \quad \chi = \frac{1}{m}\left[\hat{\Delta} v - v(\chi \cdot v)\right] \ . \tag{G.7}
$$

Multiplying the last equation by v^{T} we get

$$
2m(\chi \cdot v) - v^{\text{T}} \hat{\Delta} v = 0 \quad \Rightarrow \quad \chi \cdot v = \frac{v^{\text{T}} \hat{\Delta} v}{2m} \quad \Rightarrow \quad \chi = \frac{1}{m}\left[\hat{\Delta} v - v\frac{v^{\text{T}} \hat{\Delta} v}{2m}\right] \ . \tag{G.8}
$$

Finally, defining $u = v/\sqrt{m}$ which is normalized to $u^T u = 1$, we get

$$
\hat{\alpha} = \frac{1}{2}\left[-(u^T \hat{\Delta} u)uu^T + \hat{\Delta} uu^T + uu^T \hat{\Delta} - \hat{\Delta}\right] \ . \tag{G.9}
$$

Therefore the matrices $\hat{\alpha}$ and $\hat{\Delta}$ differ by a projector on a vector space spanned by u and $\hat{\Delta} u$. The proof can be done in general, but let us focus here on the case (of interest for us) in which α_{aa} is a constant independent on a, or equivalently $\sum_b \Delta_{ab}$ does not depend on a. In this case u is an eigenvector of $\hat{\Delta}$, and $\hat{\Delta} u = \lambda u$ with $\lambda = u^T \hat{\Delta} u$. Also, $\hat{\Delta}^{-1} u = u/\lambda$ and therefore $u^T \hat{\Delta}^{-1} u = 1/\lambda$. We have $\hat{\alpha} = (\lambda uu^T - \hat{\Delta})/2$ and

$$
\det(\epsilon I + \hat{\alpha}) = \det(\epsilon I - \hat{\Delta}/2) \det\left(1 + \frac{\lambda}{2}\frac{1}{\epsilon - \hat{\Delta}/2}uu^T\right) = \det(\epsilon I - \hat{\Delta}/2)\left[1 + \frac{1}{2}\frac{\lambda}{\epsilon - \lambda/2}\right] = \det(\epsilon I - \hat{\Delta}/2)\frac{2\epsilon}{2\epsilon - \lambda} \ , \tag{G.10}
$$

where we used the relations $\frac{1}{\epsilon - \hat{\Delta}/2} u = \frac{1}{\epsilon - \lambda/2} u$ and $\det(1 + Auu^T) = 1 + A$. Finally,

$$
\begin{aligned}
\det \hat{\alpha}^{m,m} &= \lim_{\epsilon \to 0} \frac{1}{\epsilon m} \det(\epsilon I + \hat{\alpha}) = -\frac{2}{m u^T \hat{\Delta} u} \det(-\hat{\Delta}/2) = -\frac{2}{m} (u^T \hat{\Delta}^{-1} u) \det(-\hat{\Delta}/2) \\
&= -\frac{2}{m^2} (v^{\mathrm{T}} \hat{\Delta}^{-1} v) \det(-\hat{\Delta}/2) ,
\end{aligned}
\tag{G.11}
$$

which completes the proof of equation (G.4) and therefore of the equivalence of our results with those of [243, 242, 96].

G.3 Cayler-Menger determinant: rotation and translation invariances

Finally we mention a relationship with the Cayley-Menger determinant. It could be used to derive our expressions of the static or dynamic actions (via a suitable generalization for the dynamics), without resorting to introduce the sphere $\mathbb{S}_d(R)$ since it directly deals with rotation and translation invariance on the same footing, as the MSD does.

The (squared) volume of a $m - 1$-dimensional simplex, with m points $x_1, \ldots, x_m$ can be expressed through the relative distances between pair of points $d_{ab} = d_{ba}$ only:

$$
V^2(x_1, \ldots, x_m) = \frac{(-1)^m}{2^{m-1}[(m-1)!]^2}
\begin{vmatrix}
0 & 1 & \ldots & \ldots & \ldots & 1 \\
1 & 0 & d_{12}^2 & \ldots & \ldots & d_{1m}^2 \\
\vdots & d_{21}^2 & \ddots & \ddots & \ldots & \vdots \\
\vdots & \vdots & \ddots & \ddots & \ddots & \vdots \\
\vdots & \vdots & \ldots & \ddots & \ddots & d_{m-1\,m}^2 \\
1 & d_{m1}^2 & \ldots & \ldots & d_{m\,m-1}^2 & 0
\end{vmatrix}
\tag{G.12}
$$

The fact that a *true* $m-1$-dimensional simplex (consisting of m points *embeddable* in $\mathbb{R}^{m-1}$) is completely characterized, modulo translations and rotations of it, *only* by the relative distances of its compounding points is a consequence of translation and rotation invariance. This is analogous to stating that a set of linearly independent vectors are characterized, modulo rotations of the whole set, by the scalar products between vectors.

The lower-right block in (G.12) is the same as the MSD matrix $\hat{\mathsf{D}}$ for m replicas. We note $\det(\mathrm{CM})$ this determinant[1], called Cayler-Menger determinant [362]. Let us show that the volume of the simplex formed by our m replicas (if non-singular) appears in the expressions (*e.g.* the free energy) which use a similar quotienting by the translations and rotations. We may relate CM to $\hat{\mathsf{D}}$ by computing the determinant (x_0 is supplemented to take care of the first line and column):

$$
\begin{aligned}
\det(\mathrm{CM})^{-\frac{1}{2}} &= \int \frac{dx_0}{\sqrt{2\pi}} \prod_{a=1}^m \frac{dx_a}{\sqrt{2\pi}} e^{-\frac{1}{2} \sum_{i,j}^{0,m} x_i (\mathrm{CM})_{ij} x_j} = \int \frac{dx_0}{\sqrt{2\pi}} \prod_{a=1}^m \frac{dx_a}{\sqrt{2\pi}} e^{-\frac{1}{2} \left[2x_0 \sum_{a=1}^m x_a + \sum_{a,b}^{1,m} x_a \mathsf{D}_{ab} x_b \right]} \\
&= (-1)^{\frac{m}{2}} \det(-\hat{\mathsf{D}})^{-\frac{1}{2}} \int \frac{dx_0}{\sqrt{2\pi}} e^{-\frac{1}{2} x_0^2 \left(-\sum_{a,b}^{1,m} \mathsf{D}_{ab}^{-1} \right)} = (-1)^{\frac{m}{2}} \det(-\hat{\mathsf{D}})^{-\frac{1}{2}} (-v^{\mathrm{T}} \hat{\mathsf{D}}^{-1} v)^{-\frac{1}{2}} \\
&\implies \quad \det(\mathrm{CM}) = (-1)^m \det(-\hat{\mathsf{D}})(-v^{\mathrm{T}} \hat{\mathsf{D}}^{-1} v)
\end{aligned}
\tag{G.13}
$$

Then from (G.12) we get

$$
V(x_1, \ldots, x_m) = \frac{1}{(m-1)!} \sqrt{2 \det(-\hat{\mathsf{D}}/2)(-v^{\mathrm{T}} \hat{\mathsf{D}}^{-1} v)}
\tag{G.14}
$$

The ideal gas replicated entropy of equations (G.3) becomes

$$
\mathcal{S}_{\mathrm{IG}}^{(m)} = \frac{dm}{2} \ln\left(\frac{2\pi e}{d} \right) + d \ln\left[(m-1)! \frac{\Delta_{\mathrm{liq}}}{2} V(x_1, \ldots, x_m) \right]
\tag{G.15}
$$

---

[1]To avoid divergent integrals in (G.13), depending on the parity of m one should rather use *minus* this Cayley-Menger matrix.

We conclude that the ideal gas term enjoys a very simple expression in terms of the volume of the simplex defined by the MSD matrix $\hat{D}$, modulo translations and rotations of it. This gives an intuitive interpretation of the expression in the right-hand side of (G.14) that appears everywhere when *integrating away rotations and translations*, and points at the Cayley-Menger determinant as being the right quantity to consider in quotienting by rotations and translations. It would be useful to generalize it to continuous variables.

$\mathcal{H}$

<div style="background:purple">

Equivalence between the Mari-Kurchan model and Hard Spheres without random shifts

</div>

Outline

We consider the original MK model [270] in d dimensions. It is the $R \to \infty$ version of the spherical model presented in the statics §4; introducing the hypersphere is an irrelevant complication for the purpose of this subsection. The rotations $\mathcal{R}_{ij}$ are thus replaced by d-dimensional shifts A_{ij}. Though these random rotations were picked with an infinite variance, here we go back to the original model with a variance λ^2 of the distribution of the shifts, which is taken to be Gaussian centered. We show that this model is described by the entropy functional in equation (4.17) when

- one fixes $\lambda \in \mathbb{R}^+$ and takes the limit $d \to \infty$

- or one fixes d and takes the limit $\lambda \to \infty$

except for the additive constant due to discernability in the MK model, see §4.2.3. We only focus on the HS potential; any generic potential of the class in §3.1.1 can be treated similarly, the conclusions with respect to the scalings are not changed. This implies, quoting [270], that the limits $\lambda \to \infty$ and $d \to \infty$ are of the same nature.

When computing the replicated entropy, we introduced in section 4.2.2 the functions

$$\bar{\chi}(\bar{x}, \bar{y}) = \int \mathcal{D}_{\lambda^2} A \prod_{a=1}^n \theta(|x^a - y^a + A| - \sigma) = \int \mathcal{D}_{\lambda^2} A \, \theta(\min_a |x^a - y^a + A| - \sigma) = 1 + \bar{f}(\bar{x}, \bar{y}) \; ,$$

$$\bar{f}(\bar{x}, \bar{y}) = \bar{f}(\bar{u} \equiv \bar{x} - \bar{y}) = - \int \mathcal{D}_{\lambda^2} A \, \theta(\sigma^2 - \min_a |u^a + A|^2) \; ,$$

(H.1)

where $\bar{f}$ is the replicated Mayer function. To show the equivalence, following the derivation in section 4.2.2 one sees that we only need to prove that it vanishes in these limits. Indeed, if so, the leading order of the entropy functional is obtained by keeping the first term in the expansion of $\ln(1 + \bar{f}) \sim \bar{f}$, the other terms giving vanishingly small contributions.

H.1   With the random shifts

1. $\underline{\lambda > 0 \text{ case:}}$ Following [243], let us compute the replicated Mayer function when all u^a are zero. With a few changes of variables, we have

$$\bar{f}(\bar{0}) = -\int \mathcal{D}_{\lambda^2} A \, \theta(\sigma^2 - A^2) = -\frac{\Omega_d}{(2\pi\lambda^2)^{d/2}} \int \mathrm{d}A \, A^{d-1} e^{-A^2/2\lambda^2} = -\frac{\Omega_d \lambda^d}{(2\pi\lambda^2)^{d/2}} 2^{d/2-1} \gamma\left(\frac{d}{2}, \frac{1}{2(\lambda/\sigma)^2}\right) \tag{H.2}$$

where the incomplete Gamma function is $\gamma(a, z) = \int_0^z \mathrm{d}t \, t^{a-1} e^{-t}$ defined for $\mathrm{Re}(a) > 0$. For $\mathrm{Re}(z) > 0$, we have the relation $\gamma(a, z) = \frac{1}{a} z^a e^{-z} F_1(1, a+1, z)$, where F_1 is Kummer's function of the first kind which can be given by a hypergeometric series[1]

$$F_1(1, a+1, z) = 1 + \sum_{p=1}^{\infty} \frac{z^p}{\prod_{j=1}^{p}(a+j)} \tag{H.4}$$

whose radius of convergence is infinite. Then,

$$\bar{f}(\bar{0}) = -e^{-\frac{\sigma^2}{2\lambda^2}} V_d(\sigma/\lambda\sqrt{2\pi})\left[1 + O\left(\frac{1}{d(\lambda/\sigma)^2}\right)\right] \tag{H.5}$$

2. For $\lambda > 0$, we look at the general case. However, we assume that the n vectors in $\bar{u}$ are linearly independent. If they are not[2], it suffices to reduce the number of components of $A_\parallel$ introduced below to the rank of the vectors in $\bar{u}$ instead of n. Using the fact that the Gaussian measure is rotation invariant, we can build an orthonormal basis for $A = A_\parallel + A_\perp$ where $A_\parallel \in \mathrm{Span}(u^1, \ldots, u^n)$ and $A_\perp$ lies in the orthogonal subspace. Then, doing the same kind of change of variables, and using the relation between γ and F_1, we get

$$\begin{aligned}
\bar{f}(\bar{u}) &= -\int \mathcal{D}^n A_\parallel \mathcal{D}^{d-n} A_\perp \, \theta(\sigma^2 - \min_a |u^a + A_\parallel|^2 - A_\perp^2) \\
&= -\frac{\Omega_{d-n}}{2(2\pi\lambda^2)^{\frac{d-n}{2}}} \int \mathcal{D}^n A_\parallel \, \theta(\sigma^2 - \min_a |u^a + A_\parallel|^2) \int_0^{\sigma^2 - \min_a |u^a + A_\parallel|^2} \mathrm{d}r \, r^{\frac{d-n}{2}+1} e^{-r/2\lambda^2} \\
&= -\frac{\Omega_{d-n}}{2(2\pi\lambda^2)^{\frac{d-n}{2}}} \int \mathcal{D}^n A_\parallel \, \theta(\sigma^2 - \min_a |u^a + A_\parallel|^2)(2\lambda^2)^{\frac{d-n}{2}} \gamma\left(\frac{d-n}{2}, \frac{\sigma^2 - \min_a |u^a + A_\parallel|^2}{2\lambda^2}\right) \\
&= -e^{-\frac{\sigma^2}{2\lambda^2}} V_{d-n}(\sigma/\lambda\sqrt{2\pi}) \\
&\quad \times \int \mathcal{D}^n A_\parallel \, \mathcal{G}_{d-n}\left(1 - \min_a \left|\frac{u^a + A_\parallel}{\sigma}\right|^2\right) e^{-\min_a |u^a + A_\parallel|^2/2\lambda^2}\left[1 + O\left(\frac{1}{d(\lambda/\sigma)^2}\right)\right]
\end{aligned} \tag{H.6}$$

where $\mathcal{G}_\alpha(x) = x^{\alpha/2}\theta(x)$. A very rough bound on the leading order of the integrand is 1, which gives

$$\boxed{|\bar{f}(\bar{u})| \leqslant e^{-\frac{\sigma^2}{2\lambda^2}} V_{d-n}(\sigma/\lambda\sqrt{2\pi})} \tag{H.7}$$

So $\bar{f}$ tends to zero when either d goes to infinity at fixed $\lambda > 0$ or conversely, when λ goes to infinity at finite $d > n$.

3. One can obtain a simplified expression when $\forall a \neq b, |u^a - u^b| > \sigma$ and $d \to \infty$. Indeed, in this limit, the integral over $A_\parallel$ is dominated by the points where $\epsilon^a = u^a + A = 0$. Since the integrand is very peaked at these points, we can assume that the integral splits in each of the n regions where the

---

[1] For the generic case ($b \notin \mathbb{Z}^-$), one has

$$F_1(a, b, z) = 1 + \sum_{p=1}^{\infty} \frac{\prod_{j=0}^{p-1}(a+j)}{\prod_{j=0}^{p-1}(b+j)} z^p \tag{H.3}$$

[2] In high dimension, the likeliest configuration is that all the vectors in $\bar{u}$ are orthogonal to each other, see the comment of (2.26) in §2.2.

vectors in $\bar{\epsilon}$ are small, and by the assumption $\forall a \neq b$, $|u^a - u^b| > \sigma$, there holds $\min_b |u^b + A_{/\!/}| = |\epsilon^a|$ in a region where ϵ^a is small.

$$
\begin{aligned}
\bar{f}(\bar{u}) &\simeq -e^{-\frac{\sigma^2}{2\lambda^2}} V_{d-n}(\sigma/\lambda\sqrt{2\pi}) \sum_{a=1}^{n} \int \frac{\mathrm{d}^n\epsilon^a}{(2\pi\lambda^2)^{n/2}} e^{-\frac{(\epsilon^a-u^a)^2}{2\lambda^2}-\frac{(\epsilon^a)^2}{2\lambda^2}} \mathcal{G}_{d-n}\left(1-(\epsilon^a/\sigma)^2\right) \\
&= -e^{-\frac{\sigma^2}{2\lambda^2}} V_{d-n}(\sigma/\lambda\sqrt{2\pi}) \frac{\Omega_{n-1}\sigma^n}{(2\pi\lambda^2)^{n/2}} \sum_{a=1}^{n} e^{-\frac{(u^a)^2}{2\lambda^2}} \int_0^1 \mathrm{d}\epsilon\, \epsilon^{n-1}(1-\epsilon^2)^{\frac{d-n}{2}} e^{-\frac{\epsilon^2}{(\lambda/\sigma)^2}} \\
&\qquad \times \underbrace{\int_0^\pi \mathrm{d}\theta\, \sin^{n-2}\theta\, e^{-\frac{\epsilon|u^a/\sigma|}{(\lambda/\sigma)^2}\cos\theta}}_{\simeq \Omega_n/\Omega_{n-1}} \\
&\simeq -e^{-\frac{\sigma^2}{2\lambda^2}} V_d(\sigma/\lambda\sqrt{2\pi}) F_1\left(\frac{n}{2},\frac{d}{2}+1,-\frac{\sigma^2}{\lambda^2}\right) \sum_{a=1}^{n} e^{-\frac{(u^a)^2}{2\lambda^2}}
\end{aligned}
\tag{H.8}
$$

We introduced $\epsilon = |\epsilon^a|/\sigma$ and θ the angle between ϵ^a and u^a, using hyperspherical coordinates (see §2.2) and the definition of the solid angle (2.27) in the second line. The integral over ϵ, for high d, is peaked around $\epsilon = 0$, so that the exponential in the integral over the angle is close to 1, and thus its dependence over u^a can be overlooked. We also neglected the $O(1/[d(\lambda/\sigma)]^2)$ contribution to $\bar{f}(\bar{u})$ given in the original formula (H.6), since we are interested either in the limits of infinite variance or dimension. From (H.3) we know that again

$$
F_1\left(\frac{n}{2},\frac{d}{2}+1,-\frac{\sigma^2}{\lambda^2}\right) = 1 + O\left(\frac{1}{d(\lambda/\sigma)^2}\right)
\tag{H.9}
$$

We conclude:

- For fixed $\lambda > 0$ and $d \to \infty$,

$$
\bar{f}(\bar{u}) \sim -e^{-\frac{\sigma^2}{2\lambda^2}} V_d(\sigma/\lambda\sqrt{2\pi}) \sum_{a=1}^{n} e^{-\frac{(u^a)^2}{2\lambda^2}}
\tag{H.10}
$$

- For high d and λ it does not depend upon $\bar{u}$ anymore

$$
\bar{f}(\bar{u}) \sim -nV_d(\sigma/\lambda\sqrt{2\pi})
\tag{H.11}
$$

H.2 Without the random shifts

$\underline{\lambda = 0 \text{ case:}}$ The HS model without random shifts has been analyzed in [243]. The function $\bar{f}_{\mathrm{HS}}(\bar{u}) = \int \mathrm{d}X\, f(X + \bar{u})$ in [243] ($X + \bar{u}$ means that we add X to each u^a) is different than the one defined here with $\lambda = 0$ (and thus $\mathcal{D}_{\lambda^2}A = \delta(A)\mathrm{d}A$), but plays a similar role, in the sense that *the average over the center of mass X has a similar effect to the Gaussian average over the quenched disorder here*. Indeed such a function is exactly the same function $\bar{f}$ than the one considered here (H.1) in the limit $\lambda \to \infty$ in which the Gaussian average becomes flat $\mathcal{D}_{\lambda^2}A \sim \mathrm{d}A/\lambda\sqrt{2\pi}$.

A very similar computation than above, [243] gives the following conclusions in $d \to \infty$:

$$
\begin{aligned}
\bar{f}_{\mathrm{HS}}(\bar{u}) &= -V_d(\sigma)\mathcal{F}\left(\frac{\sqrt{d-n}}{\sigma}\bar{u}\right) \\
\mathcal{F}(\bar{x}) &= \int \frac{\mathrm{d}^n\epsilon}{(2\pi)^{n/2}} e^{-\frac{1}{2}\min_a|x^a+\epsilon|^2}
\end{aligned}
\tag{H.12}
$$

Note that

$$
1 \leqslant \mathcal{F}(\bar{x}) \leqslant \sum_{a=1}^{n} \int \frac{\mathrm{d}^n\epsilon}{(2\pi)^{n/2}} e^{-\frac{1}{2}|x^a+\epsilon|^2} = n
\tag{H.13}
$$

The minimum 1 is obtained when all x^a are equal and the integrand is a Gaussian centered at this position; as soon as they differ, several Gaussians peaked at the different positions contribute to the integral, giving additional contributions. Therefore the prefactor $V_d(\sigma)$ makes $\bar{f}_{\mathrm{HS}}$ tend exponentially to zero when $d \to \infty$.

For further comparison we have the following properties of the function $\bar{f}_{\mathrm{HS}}$ at $\lambda = 0$:

- If all u^a are zero,
$$\bar{f}_{\mathrm{HS}}(\bar{0}) = -V_d(\sigma) \tag{H.14}$$

  This is analog to (H.5) with the correspondence $\sigma \leftrightarrow \sigma/\lambda\sqrt{2\pi}$ and $\lambda \gg \sigma$.

- If $\forall a \neq b$, $|u^a - u^b| > \sigma$,
$$\bar{f}_{\mathrm{HS}}(\bar{u}) = -nV_d(\sigma) \tag{H.15}$$

  independent of $\bar{u}$. This is analog to (H.11) with the correspondence $\sigma \leftrightarrow \sigma/\lambda\sqrt{2\pi}$.

- The critical region is where $\bar{u} = O(\sigma/\sqrt{d})$, where the dependence of $\mathcal{F}$ upon $\bar{u}$ is non-trivial.

  The u_a are seen as n independent vectors (so effectively n-dimensional). This crucial scaling means that the overlaps defined in [243]

$$q_{ab}^{\mathrm{HS}} = u^a \cdot u^b = \sum_{\mu=1}^{n} u_\mu^a u_\mu^b = O\left(\frac{1}{d}\right) ,$$
$$\text{thus} \quad (u^a - u^b)^2 = q_{aa}^{\mathrm{HS}} + q_{bb}^{\mathrm{HS}} - 2q_{ab}^{\mathrm{HS}} = O\left(\frac{1}{d}\right) \tag{H.16}$$

  This is precisely the same situation as in §4 with the mean-squared displacement D_{ab}, and is linked to the $O(1/d)$ fluctuations discussed in §5.4.

  All these results are of course compatible with the reasoning that for an infinite range of shifts, $\bar{f} = O\left(V_d(\sigma)/\mathcal{V}\right)$ where $\mathcal{V} \sim \lambda^d$ is the volume of the system (§4.2.2).

H.3   The Mayer function and scalings in $d \to \infty$

From these observations, one concludes that the averaged Mayer function $\bar{f}(\bar{u})$ has a trivial behaviour close to zero and as soon as the different replicas (respectively different trajectories for the dynamics) wander away from more than a particle diameter, its value is essentially a constant. The critical regime where $\bar{f}$ has a non-trivial behaviour is when $\bar{u} = \bar{x} - \bar{y}$, the relative positions of two replicated configurations (respectively relative trajectories of two particles in the dynamics) is of the order the particle diameter (and fluctuations of order $1/d$) [243], see also §5.2. This critical scaling regime where replicas (respectively trajectories) are close reproduces, for large distances within this scaling, the behaviour of the regime where they are not constrained to remain close to contact, *i.e.* the liquid phase. Indeed, the entropy of the liquid phase is recovered in the statics, see equation (4.19), and respectively diffusive behaviour is recovered in the dynamics at large times, see §3.8.3. The fact that the Mayer function (equivalently $\mathcal{F}(\bar{x})$ of equation (H.12), or $\mathcal{F}(\boldsymbol{Q})$ in the dynamics (3.67), or $\mathcal{F}(\hat{\Delta})$ of the glassy statics (4.35), which are all related) becomes a constant for distances larger than the particle diameter elucidates these paradoxes.

GROUP PROPERTY OF FDT SUPERFIELDS

We quickly prove that superfields in equilibrium form satisfying FDT enjoy a multiplicative group property (FDT holds trivially for **1**). The following two statements are used in chapter 3.

I.1   Product

Let us prove that FDT holds for a product of superfields satisfying FDT.

If $\boldsymbol{AB} = \boldsymbol{C}$ with

$$
\mathsf{M}(\boldsymbol{A}) = \begin{pmatrix} A_C & A_R \\ A_R^{\mathrm{T}} & 0 \end{pmatrix} \qquad \mathsf{M}(\boldsymbol{B}) = \begin{pmatrix} B_C & B_R \\ B_R^{\mathrm{T}} & 0 \end{pmatrix}
$$

$$
\text{thus}\quad \mathsf{M}(\boldsymbol{C}) = \begin{pmatrix} C_C & C_R \\ C_R^{\mathrm{T}} & 0 \end{pmatrix} = \begin{pmatrix} A_R B_C + A_C B_R^{\mathrm{T}} & A_R B_R \\ A_R^{\mathrm{T}} B_R^{\mathrm{T}} & 0 \end{pmatrix}
$$

(I.1)

assuming both $\boldsymbol{A}$ and $\boldsymbol{B}$ satisfy FDT then

$$
\begin{aligned}
-\beta \frac{\mathrm{d}C_C}{\mathrm{d}\tau}(\tau) &= -\beta \frac{\mathrm{d}}{\mathrm{d}\tau} \int_{-\infty}^{\infty} \mathrm{d}u \, \left[A_R(u) B_C(\tau - u) + A_C(\tau + u) B_R(u) \right] \\
&= \int_{-\infty}^{\infty} \mathrm{d}u \, \left\{ A_R(u) \left[B_R(\tau - u) - B_R(u - \tau) \right] + \left[A_R(\tau + u) - A_R(-\tau - u) \right] B_R(u) \right\} \\
&= \int_{-\infty}^{\infty} \mathrm{d}u \, \left[A_R(u) B_R(\tau - u) - A_R(-\tau - u) B_R(u) \right] = C_R(\tau) - C_R(-\tau)
\end{aligned}
$$

(I.2)

I.2   Inverse

Let us now show that FDT holds for the inverse of a superfield satisfying FDT.

The inverse $\boldsymbol{Q}^{-1}$ reads from §2.4.3.2:

$$
\boldsymbol{Q}^{-1}(a,b) = \widetilde{C}(t - t') + \bar{\theta}_1 \theta_1 \widetilde{R}(t' - t) + \bar{\theta}_2 \theta_2 \widetilde{R}(t - t') \quad \text{with} \quad \widetilde{C} = -R^{-\mathrm{T}} C R^{-1} \quad \text{and} \quad \widetilde{R} = R^{-1}
$$

(I.3)

where C and R obey FDT.

Then, using $\tau = t - t'$ by TTI,

$$
\begin{aligned}
-\beta \frac{\mathrm{d}\widetilde{C}}{\mathrm{d}\tau}(\tau) &= \beta \frac{\mathrm{d}}{\mathrm{d}\tau} \int_{-\infty}^{\infty} \mathrm{d}u\mathrm{d}v \, R^{-1}(u - \tau) C(u - v) R^{-1}(v) \\
&= -\beta \int_{-\infty}^{\infty} \mathrm{d}u\mathrm{d}v \, \left[\frac{\partial}{\partial u} R^{-1}(u - \tau) \right] C(u - v) R^{-1}(v) \\
&= \int_{-\infty}^{\infty} \mathrm{d}u\mathrm{d}v \, R^{-1}(u - \tau)[R(v - u) - R(u - v)] R^{-1}(v) \\
&= R^{-1}(\tau) - R^{-1}(-\tau) = \widetilde{R}(\tau) - \widetilde{R}(-\tau)
\end{aligned}
$$

(I.4)

where we used an integration by part and the fact that correlations vanish at $\pm\infty$, in the ergodic regime before the dynamical transition (see §3.8.1).

Bibliography

[1] David J Acheson. *Elementary fluid dynamics*. Oxford University Press, 1990. 10, 11, 26, 42

[2] Gerold Adam and Julian H Gibbs. On the temperature dependence of cooperative relaxation properties in glass-forming liquids. *The journal of chemical physics*, 43(1):139–146, 1965. 28, 35, 40

[3] C Alba-Simionesco, A Cailliaux, A Alegria, and G Tarjus. Scaling out the density dependence of the α relaxation in glass-forming polymers. *EPL (Europhysics Letters)*, 68(1):58, 2004. 43

[4] Christiane Alba-Simionesco, Daniel Kivelson, and Gilles Tarjus. Temperature, density, and pressure dependence of relaxation times in supercooled liquids. *Journal of Chemical Physics*, 116:5033–5038, 2002. 43

[5] Christiane Alba-Simionesco and Gilles Tarjus. Temperature versus density effects in glassforming liquids and polymers: A scaling hypothesis and its consequences. *Journal of non-crystalline solids*, 352(42):4888–4894, 2006. 43

[6] Mike P Allen and Dominic J Tildesley. *Computer simulation of liquids*. Oxford university press, 1989. 6, 21

[7] Ada Altieri, Silvio Franz, and Giorgio Parisi. The jamming transition in high dimension: an analytical study of the tap equations and the effective thermodynamic potential. *arXiv preprint arXiv:1607.00966*, 2016. 57, 172

[8] Hans C Andersen. Molecular dynamics studies of heterogeneous dynamics and dynamic crossover in supercooled atomic liquids. *Proceedings of the National Academy of Sciences of the United States of America*, 102(19):6686–6691, 2005. 3, 19

[9] P W Anderson, BI Halperin, and C M Varma. Anomalous low-temperature thermal properties of glasses and spin glasses. *Philosophical Magazine*, 25(1):1–9, 1972. 173

[10] EN da C Andrade. Xli. a theory of the viscosity of liquids.—part i. *The London, Edinburgh, and Dublin Philosophical Magazine and Journal of Science*, 17(112):497–511, 1934. 45

[11] A Andreanov, G Biroli, and J-P Bouchaud. Mode coupling as a landau theory of the glass transition. *EPL (Europhysics Letters)*, 88(1):16001, 2009. 31, 43, 120

[12] A Andreanov, G Biroli, and A Lefevre. Dynamical field theory for glass-forming liquids, self-consistent resummations and time-reversal symmetry. *Journal of Statistical Mechanics: Theory and Experiment*, 2006(07):P07008, 2006. 43

[13] L. Angelani, R. Di Leonardo, G. Ruocco, A. Scala, and F. Sciortino. Saddles in the energy landscape probed by supercooled liquids. *Phys. Rev. Lett.*, 85:5356–5359, Dec 2000. 34

[14] C Austen Angell. Formation of glasses from liquids and biopolymers. *Science*, 267(5206):1924, 1995. 3, 4, 19, 20

[15] CA Angell. Relaxation in liquids, polymers and plastic crystals—strong/fragile patterns and problems. *Journal of Non-Crystalline Solids*, 131:13–31, 1991. 3, 19

[16] Camille Aron, Giulio Biroli, and Leticia F Cugliandolo. Symmetries of generating functionals of langevin processes with colored multiplicative noise. *Journal of Statistical Mechanics: Theory and Experiment*, 2010(11):P11018, 2010. 65, 74, 76, 183, 187

[17] Neil W Ashcroft and N David Mermin. Solid state physics. 1976. 1, 6, 17, 22, 173

[18] Andreas K Bacher and Jeppe C Dyre. The mother of all pair potentials. *Colloid and Polymer Science*, 292(8):1971–1975, 2014. 158, 167

[19] Andreas K Bacher, Thomas B Schrøder, and Jeppe C Dyre. Explaining why simple liquids are quasi-universal. *Nature communications*, 5:5424, 2014. 44, 45, 153, 157, 158, 162, 166, 167, 170

[20] Nicholas P Bailey, Ulf R Pedersen, Nicoletta Gnan, Thomas B Schrøder, and Jeppe C Dyre. Pressure-energy correlations in liquids. i. results from computer simulations. *The Journal of chemical physics*, 129(18):184507, 2008. 44, 157, 163

[21] Nicholas P Bailey, Ulf R Pedersen, Nicoletta Gnan, Thomas B Schrøder, and Jeppe C Dyre. Pressure-energy correlations in liquids. ii. analysis and consequences. *The Journal of chemical physics*, 129(18):184508, 2008. 44, 157, 167

[22] Keith Ball. A lower bound for the optimal density of lattice packings. *International Mathematics Research Notices*, 1992(10):217–221, 1992. 109, 110

[23] A Barrat. The p-spin spherical spin glass model. *arXiv preprint cond-mat/9701031*, 1997. 62, 78

[24] A Barrat, R Burioni, and M Mézard. Dynamics within metastable states in a mean-field spin glass. *Journal of Physics A: Mathematical and General*, 29(5):L81, 1996. 39, 173

[25] Heinz Bässler. Viscous flow in supercooled liquids analyzed in terms of transport theory for random media with energetic disorder. *Physical review letters*, 58(8):767, 1987. 4, 20

[26] Marc Baus. The modern theory of crystallization and the hansen-verlet rule. *Molecular Physics*, 50(3):543–565, 1983. 45

[27] R Bausch, Hans-Karl Janssen, and Ho Wagner. Renormalized field theory of critical dynamics. *Zeitschrift für Physik B Condensed Matter*, 24(1):113–127, 1976. 183

[28] Rodney J Baxter. *Exactly solved models in statistical mechanics*. Courier Corporation, 2007. 58, 172

[29] Carlo Becchi. Introduction to brs symmetry. *arXiv preprint hep-th/9607181*, 1996. 76

[30] Carlo Becchi, Alain Rouet, and Raymond Stora. Renormalization of gauge theories. *Annals of Physics*, 98(2):287–321, 1976. 76

[31] G. Ben Arous, Amir Dembo, and Alice Guionnet. Aging of spherical spin glasses. *Probability Theory and Related Fields*, 120(1):1–67, 2001. 38, 109

[32] Gerard Ben Arous, Amir Dembo, and Alice Guionnet. Cugliandolo-kurchan equations for dynamics of spin-glasses. *Probability theory and related fields*, 136(4):619–660, 2006. 38, 109

[33] U. Bengtzelius, W. Götze, and A. Sjölander. Dynamics of supercooled liquids and the glass transition. *Journal of Physics C: Solid State Physics*, 17(33):5915–5934, 1984. 28, 31, 77

[34] T. H. Berlin and M. Kac. The spherical model of a ferromagnet. *Phys. Rev.*, 86:821–835, Jun 1952. 58

[35] Etienne P. Bernard and Werner Krauth. Two-step melting in two dimensions: First-order liquid-hexatic transition. *Phys. Rev. Lett.*, 107:155704, Oct 2011. 2, 18

[36] D. S. Bernstein. *Matrix Mathematics.* Princeton University Press, 2009. 67, 68, 69

[37] L. Berthier, G. Biroli, J-P Bouchaud, L. Cipelletti, and W. van Saarloos. *Dynamical Heterogeneities and Glasses, Colloids and Granular Media.* Oxford University Press, 2011. 8, 10, 24, 26

[38] L. Berthier, G. Biroli, J.P. Bouchaud, L. Cipelletti, D. El Masri, D. L'Hôte, F. Ladieu, and M. Pierno. Direct experimental evidence of a growing length scale accompanying the glass transition. *Science*, 310(5755):1797–1800, 2005. 9, 25

[39] L. Berthier, G. Biroli, J.P. Bouchaud, W. Kob, K. Miyazaki, and DR Reichman. Spontaneous and induced dynamic fluctuations in glass formers. I. General results and dependence on ensemble and dynamics. *The Journal of chemical physics*, 126:184503, 2007. 107

[40] L Berthier, V Viasnoff, O White, V Orlyanchik, and F Krzakala. *Slow Relaxations and Nonequilibrium Dynamics in Condensed Matter ed JL Barrat, J Dalibard, M Feigelman and J Kurchan.* Springer Berlin Heidelberg, 2003. 12, 27, 121

[41] Ludovic Berthier. Revisiting the slow dynamics of a silica melt using monte carlo simulations. *Physical Review E*, 76(1):011507, 2007. 107

[42] Ludovic Berthier and Jean-Louis Barrat. Shearing a glassy material: numerical tests of nonequilibrium mode-coupling approaches and experimental proposals. *Physical review letters*, 89(9):095702, 2002. 39

[43] Ludovic Berthier and Giulio Biroli. Theoretical perspective on the glass transition and amorphous materials. *Rev. Mod. Phys.*, 83:587–645, Jun 2011. 8, 10, 12, 13, 24, 26, 27, 28, 32, 38, 39, 41

[44] Ludovic Berthier, Giulio Biroli, J-P Bouchaud, Walter Kob, Kunimasa Miyazaki, and David R Reichman. Spontaneous and induced dynamic correlations in glass formers. ii. model calculations and comparison to numerical simulations. *The Journal of chemical physics*, 126(18):184504, 2007. 107

[45] Ludovic Berthier, Giulio Biroli, Jean-Philippe Bouchaud, and Robert L Jack. Overview of different characterisations of dynamic heterogeneity. In L. Berthier, G. Biroli, J-P Bouchaud, L. Cipelletti, and W. van Saarloos, editors, *Dynamical Heterogeneities in Glasses, Colloids, and Granular Media.* Oxford University Press, 2011. 7, 9, 10, 23, 25

[46] Ludovic Berthier, Patrick Charbonneau, Yuliang Jin, Giorgio Parisi, Beatriz Seoane, and Francesco Zamponi. Growing timescales and lengthscales characterizing vibrations of amorphous solids. *Proceedings of the National Academy of Sciences*, 2016. 173

[47] Ludovic Berthier, Patrick Charbonneau, and Francesco Zamponi. La théorie du verre de plus en plus solide. *La Recherche*, 510:68–72, 2016. v

[48] Ludovic Berthier, Daniele Coslovich, Andrea Ninarello, and Misaki Ozawa. Equilibrium sampling of hard spheres up to the jamming density and beyond. *Physical Review Letters*, 116(23):238002, 2016. 3, 19

[49] Ludovic Berthier and Walter Kob. The monte carlo dynamics of a binary lennard-jones glass-forming mixture. *Journal of Physics: Condensed Matter*, 19(20):205130, 2007. 107

[50] Ludovic Berthier and Gilles Tarjus. Nonperturbative effect of attractive forces in viscous liquids. *Phys. Rev. Lett.*, 103:170601, Oct 2009. 31, 167, 172

[51] Ludovic Berthier and Gilles Tarjus. Critical test of the mode-coupling theory of the glass transition. *Phys. Rev. E*, 82:031502, Sep 2010. 31, 167, 172

[52] Ludovic Berthier and Gilles Tarjus. The role of attractive forces in viscous liquids. *The Journal of Chemical Physics*, 134(21):214503, 2011. 31, 167, 172

[53] Ludovic Berthier and Thomas A. Witten. Glass transition of dense fluids of hard and compressible spheres. *Phys. Rev. E*, 80(2):021502, Aug 2009. 4, 14, 20, 47

[54] Sarika Maitra Bhattacharyya, Biman Bagchi, and Peter G Wolynes. Facilitation, complexity growth, mode coupling, and activated dynamics in supercooled liquids. *Proceedings of the National Academy of Sciences*, 105(42):16077–16082, 2008. 42

[55] K. Binder and W. Kob. *Glassy materials and disordered solids: An introduction to their statistical mechanics.* World Scientific, 2005. 3, 19

[56] K. Binder and A. P. Young. Spin glasses: Experimental facts, theoretical concepts, and open questions. *Rev. Mod. Phys.*, 58:801–976, Oct 1986. 31, 63

[57] G. Biroli and J.P. Bouchaud. Critical fluctuations and breakdown of the Stokes-Einstein relation in the mode-coupling theory of glasses. *J. Phys.: Cond. Matt.*, 19:205101, 2007. 12, 27

[58] G. Biroli and J.P. Bouchaud. The Random First-Order Transition Theory of Glasses: a critical assessment. In P.G.Wolynes and V.Lubchenko, editors, *Structural Glasses and Supercooled Liquids: Theory, Experiment and Applications.* Wiley & Sons, 2012. 39

[59] G. Biroli, J.P. Bouchaud, A. Cavagna, TS Grigera, and P. Verrocchio. Thermodynamic signature of growing amorphous order in glass-forming liquids. *Nature Physics*, 4(10):771–775, 2008. 10, 26

[60] G. Biroli and R. Monasson. From inherent structures to pure states: Some simple remarks and examples. *Europhysics Letters*, 50(2):155–161, 2000. 33

[61] Giulio Biroli. A crash course on ageing. *Journal of Statistical Mechanics: Theory and Experiment*, 2005(05):P05014, 2005. 12, 27

[62] Giulio Biroli. *Glass and Jamming Transitions*, pages 41–76. Springer Basel, Basel, 2011. 3, 18

[63] Giulio Biroli and Jorge Kurchan. Metastable states in glassy systems. *Physical Review E*, 64(1):016101, 2001. 33, 172

[64] Giulio Biroli and Pierfrancesco Urbani. Breakdown of elasticity in amorphous solids. *arXiv preprint arXiv:1601.06724*, 2016. 173

[65] Marvin Bishop, Paula A. Whitlock, and Dino Klein. The structure of hyperspherical fluids in various dimensions. *The Journal of Chemical Physics*, 122(7):074508,, 2005. 169

[66] A Blandin. Theories versus experiments in the spin glass systems. *Le Journal de Physique Colloques*, 39(C6):C6–1499, 1978. 60

[67] André Blandin, Marc Gabay, and Thomas Garel. On the mean-field theory of spin glasses. *Journal of Physics C: Solid State Physics*, 13(3):403, 1980. 60

[68] M Born and K Huang. *Dynamical theories of crystal lattices*, volume 265. 1954. 147

[69] J. P. Bouchaud and G. Biroli. On the Adam-Gibbs-Kirkpatrick-Thirumalai-Wolynes scenario for the viscosity increase in glasses. *J. Chem. Phys.*, 121:7347, 2004. 9, 25, 28, 39, 40, 170

[70] Jean-Philippe Bouchaud. Weak ergodicity breaking and aging in disordered systems. *Journal de Physique I*, 2(9):1705–1713, 1992. 41

[71] Jean-Philippe Bouchaud, Leticia Cugliandolo, Jorge Kurchan, and Marc Mézard. Mode-coupling approximations, glass theory and disordered systems. *Physica A: Statistical Mechanics and its Applications*, 226(3):243–273, 1996. 28, 29, 65, 74, 100, 119

[72] Jean-Philippe Bouchaud, Leticia F Cugliandolo, Jorge Kurchan, and Marc Mézard. Out of equilibrium dynamics in spin-glasses and other glassy systems. *in Spin Glasses And Random Fields, Edited by A.P. Young*, World Scientific, 1997. 28, 29, 119

[73] JP Bouchaud. The mode-coupling theory of supercooled liquids: Does it wear any clothes? *Commentary for Journal Club for Condensed Matter Physics, http://www. condmatjournalclub. org*, 2010. 31

[74] G. Brambilla, D. El Masri, M. Pierno, L. Berthier, L. Cipelletti, G. Petekidis, and A. B. Schofield. Probing the equilibrium dynamics of colloidal hard spheres above the mode-coupling glass transition. *Phys. Rev. Lett.*, 102:085703, Feb 2009. 31

[75] AJ Bray and MA Moore. Replica-symmetry breaking in spin-glass theories. *Physical Review Letters*, 41(15):1068, 1978. 60, 172

[76] AJ Bray and MA Moore. Metastable states in spin glasses. *Journal of Physics C: Solid State Physics*, 13(19):L469, 1980. 172

[77] Kurt Broderix, Kamal K. Bhattacharya, Andrea Cavagna, Annette Zippelius, and Irene Giardina. Energy landscape of a lennard-jones liquid: Statistics of stationary points. *Phys. Rev. Lett.*, 85:5360–5363, Dec 2000. 34

[78] F. Caltagirone, U. Ferrari, L. Leuzzi, G. Parisi, F. Ricci-Tersenghi, and T. Rizzo. Critical slowing down exponents of mode coupling theory. *Phys. Rev. Lett.*, 108:085702, Feb 2012. 117, 151

[79] R. Casalini and C. M. Roland. Thermodynamical scaling of the glass transition dynamics. *Phys. Rev. E*, 69:062501, Jun 2004. 44

[80] H. B. G. Casimir. On onsager's principle of microscopic reversibility. *Rev. Mod. Phys.*, 17:343–350, Apr 1945. 76

[81] Tommaso Castellani and Andrea Cavagna. Spin glass theory for pedestrians. *Journal of Statistical Mechanics: Theory and Experiment*, 2005:P05012, 2005. 31, 32, 33, 35, 36, 38, 58, 59, 60, 61, 73, 77, 89, 99, 105, 108, 119, 136, 138, 144, 145, 150, 195

[82] M. E. Cates. *Course 3: Structural Relaxation and Rheology of Soft Condensed Matter*, pages 75–129. Springer Berlin Heidelberg, Berlin, Heidelberg, 2003. 3, 19, 33

[83] A. Cavagna. Supercooled liquids for pedestrians. *Physics Reports*, 476(4-6):51–124, 2009. 3, 5, 10, 18, 19, 21, 26, 33, 35, 40, 41

[84] Andrea Cavagna, Irene Giardina, and Giorgio Parisi. Role of saddles in mean-field dynamics above the glass transition. *Journal of Physics A: Mathematical and General*, 34(26):5317, 2001. 33

[85] Paul M Chaikin and Tom C Lubensky. *Principles of condensed matter physics*, volume 1. Cambridge Univ Press, 2000. 1, 2, 17, 18, 32, 172

[86] David Chandler. *Introduction to modern statistical mechanics*. Oxford University Press, 1987. 37, 40, 51, 172

[87] David Chandler and Juan P. Garrahan. Dynamics on the way to forming glass: Bubbles in space-time. *Annual Review of Physical Chemistry*, 61(1):191–217, 2010. 41

[88] David Chandler, Juan P. Garrahan, Robert L. Jack, Lutz Maibaum, and Albert C. Pan. Lengthscale dependence of dynamic four-point susceptibilities in glass formers. *Phys. Rev. E*, 74:051501, Nov 2006. 83, 167

[89] I Chang, F Fujara, B Geil, G Heuberger, T Mangel, and H Sillescu. Translational and rotational molecular motion in supercooled liquids studied by nmr and forced rayleigh scattering. *Journal of non-crystalline solids*, 172:248–255, 1994. 11, 26

[90] Benoit Charbonneau, Patrick Charbonneau, Yuliang Jin, Giorgio Parisi, and Francesco Zamponi. Dimensional dependence of the stokes–einstein relation and its violation. *The Journal of chemical physics*, 139(16):164502, 2013. 116, 128

[91] P. Charbonneau, A. Ikeda, G. Parisi, and F. Zamponi. Dimensional study of the caging order parameter at the glass transition. *Proceedings of the National Academy of Sciences*, 109(35):13939–13943, 2012. 110, 111, 117

[92] Patrick Charbonneau, Eric I. Corwin, Giorgio Parisi, and Francesco Zamponi. Jamming criticality revealed by removing localized buckling excitations. *Phys. Rev. Lett.*, 114:125504, Mar 2015. 14, 47, 143

[93] Patrick Charbonneau, Atsushi Ikeda, Giorgio Parisi, and Francesco Zamponi. Glass transition and random close packing above three dimensions. *Phys. Rev. Lett.*, 107:185702, Oct 2011. 116

[94] Patrick Charbonneau, Yuliang Jin, Giorgio Parisi, Corrado Rainone, Beatriz Seoane, and Francesco Zamponi. Numerical detection of the gardner transition in a mean-field glass former. *Phys. Rev. E*, 92:012316, Jul 2015. 143

[95] Patrick Charbonneau, Yuliang Jin, Giorgio Parisi, and Francesco Zamponi. Hopping and the stokes-einstein relation breakdown in simple glass formers. *Proceedings of the National Academy of Sciences*, 111(42):15025, 2014. 116, 117

[96] Patrick Charbonneau, Jorge Kurchan, Giorgio Parisi, Pierfrancesco Urbani, and Francesco Zamponi. Exact theory of dense amorphous hard spheres in high dimension. iii. the full replica symmetry breaking solution. *Journal of Statistical Mechanics: Theory and Experiment*, 2014(10):P10009, 2014. 12, 13, 14, 45, 46, 47, 127, 128, 135, 136, 140, 141, 142, 143, 144, 151, 152, 196, 198, 199, 201, 202, 203

[97] Patrick Charbonneau, Jorge Kurchan, Giorgio Parisi, Pierfrancesco Urbani, and Francesco Zamponi. Fractal free energies in structural glasses. *Nature Communications*, 5:3725, 2014. 13, 14, 46, 47, 83, 127, 128, 142, 143, 151, 152

[98] Patrick Charbonneau, Jorge Kurchan, Giorgio Parisi, Pierfrancesco Urbani, and Francesco Zamponi. Glass and jamming transitions: From exact results to finite-dimensional descriptions. *arXiv preprint arXiv:1605.03008*, 2016. 12, 45, 111, 116, 117, 128, 142, 143, 173

[99] Song-Ho Chong. Connections of activated hopping processes with the breakdown of the stokes-einstein relation and with aspects of dynamical heterogeneities. *Physical Review E*, 78(4):041501, 2008. 42

[100] Marcus T Cicerone and MD Ediger. Enhanced translation of probe molecules in supercooled o-terphenyl: Signature of spatially heterogeneous dynamics? *The Journal of chemical physics*, 104(18):7210–7218, 1996. 11, 26, 27

[101] Henry Cohn and Noam Elkies. New upper bounds on sphere packings i. *Annals of Mathematics*, pages 689–714, 2003. 110

[102] Henry Cohn, Abhinav Kumar, Stephen D Miller, Danylo Radchenko, and Maryna Viazovska. The sphere packing problem in dimension 24. *arXiv preprint arXiv:1603.06518*, 2016. 109

[103] Barbara Coluzzi, Giorgio Parisi, and Paolo Verrocchio. Thermodynamical liquid-glass transition in a lennard-jones binary mixture. *Phys. Rev. Lett.*, 84:306–309, Jan 2000. 33

[104] Fred Cooper, Avinash Khare, and Uday Sukhatme. Supersymmetry and quantum mechanics. *Physics Reports*, 251(5):267–385, 1995. 65

[105] D. Coslovich and C. M. Roland. Density scaling in viscous liquids: From relaxation times to four-point susceptibilities. *The Journal of Chemical Physics*, 131(15), 2009. 167

[106] Lorenzo Costigliola, Thomas B. Schrøder, and Jeppe C. Dyre. Studies of the lennard-jones fluid in 2, 3, and 4 dimensions highlight the need for a liquid-state 1/d expansion. *The Journal of Chemical Physics*, 144(23):231101, 2016. 153, 168, 169, 170

[107] A Crisanti, H Horner, and H-J Sommers. The sphericalp-spin interaction spin-glass model. *Zeitschrift für Physik B Condensed Matter*, 92(2):257–271, 1993. 31, 38, 77

[108] A Crisanti and F Ritort. Potential energy landscape of finite-size mean-field models for glasses. *EPL (Europhysics Letters)*, 51(2):147, 2000. 33

[109] Andrea Crisanti and H-J Sommers. The spherical p-spin interaction spin glass model: the statics. *Zeitschrift für Physik B Condensed Matter*, 87(3):341–354, 1992. 31, 35, 58, 60, 62

[110] L. F. Cugliandolo and J. Kurchan. Analytical solution of the off-equilibrium dynamics of a long-range spin-glass model. *Phys. Rev. Lett.*, 71(1):173–176, Jul 1993. 39, 173

[111] Leticia Cugliandolo and Jorge Kurchan. A scenario for the dynamics in the small entropy production limit (frontiers in magnetism). *Journal of the Physical Society of Japan*, 69:247–256, 2000. 108

[112] Leticia F Cugliandolo. Dynamics of glassy systems. In *Slow Relaxations and nonequilibrium dynamics in condensed matter*, pages 367–521. Springer, 2003. 12, 27, 29, 33, 38, 39, 59, 65, 73, 74, 76, 119, 173, 183

[113] Leticia F Cugliandolo, Jorge Kurchan, and Luca Peliti. Energy flow, partial equilibration, and effective temperatures in systems with slow dynamics. *Physical Review E*, 55(4):3898, 1997. 39

[114] LF Cugliandolo and J Kurchan. On the out-of-equilibrium relaxation of the sherrington-kirkpatrick model. *Journal of Physics A: Mathematical and General*, 27(17):5749, 1994. 100, 119

[115] Pawel Danielewicz. Quantum theory of nonequilibrium processes, i. *Annals of Physics*, 152(2):239–304, 1984. 183

[116] Shankar P. Das. Mode-coupling theory and the glass transition in supercooled liquids. *Rev. Mod. Phys.*, 76:785–851, Oct 2004. 28

[117] Shankar P Das and Gene F Mazenko. Fluctuating nonlinear hydrodynamics and the liquid-glass transition. *Physical Review A*, 34(3):2265, 1986. 43

[118] Shankar P Das and Gene F Mazenko. Field theoretic formulation of kinetic theory: basic development. *Journal of Statistical Physics*, 149(4):643–675, 2012. 43

[119] Shankar P Das and Gene F Mazenko. Newtonian kinetic theory and the ergodic-nonergodic transition. *Journal of Statistical Physics*, 152(1):159–194, 2013. 43

[120] Shankar P. Das, Gene F. Mazenko, Sriram Ramaswamy, and John J. Toner. Hydrodynamic theory of the glass transition. *Phys. Rev. Lett.*, 54:118–121, Jan 1985. 29, 43

[121] JRL De Almeida and David J Thouless. Stability of the sherrington-kirkpatrick solution of a spin glass model. *Journal of Physics A: Mathematical and General*, 11(5):983, 1978. 60, 63

[122] C De Dominicis. Dynamics as a substitute for replicas in systems with quenched random impurities. *Physical Review B*, 18(9):4913, 1978. 73, 150

[123] C De Dominicis and T Garel. A solution of sherrington kirkpatrick model for ising spin glass with physically acceptable entropy. *Journal de Physique Lettres*, 40(22):575–578, 1979. 60

[124] C De Dominicis and L Peliti. Field-theory renormalization and critical dynamics above t c: Helium, antiferromagnets, and liquid-gas systems. *Physical Review B*, 18(1):353, 1978. 183

[125] Cirano De Dominicis and Irene Giardina. *Random fields and spin glasses: a field theory approach*. Cambridge University Press, 2006. 63

[126] Pablo G Debenedetti and Frank H Stillinger. Supercooled liquids and the glass transition. *Nature*, 410(6825):259–267, 2001. 41

[127] P.G. Debenedetti. *Metastable liquids: concepts and principles*. Princeton Univ Press, 1996. 29, 43

[128] Eric DeGiuli, Edan Lerner, Carolina Brito, and Matthieu Wyart. Force distribution affects vibrational properties in hard-sphere glasses. *Proceedings of the National Academy of Sciences*, 111(48):17054–17059, 2014. 14, 47

[129] Bernard Derrida. Random-energy model: Limit of a family of disordered models. *Physical Review Letters*, 45(2):79, 1980. 31, 58

[130] Bernard Derrida. Random-energy model: An exactly solvable model of disordered systems. *Physical Review B*, 24(5):2613, 1981. 31, 58

[131] PAM Dirac. The lagrangian in quantum mechanics. 3(1):64–72, 1933. 187

[132] Bernard Diu, Claudine Guthmann, Danielle Lederer, and Bernard Roulet. *Physique statistique*. Hermann, Paris, 1989. 51

[133] C. Dreyfus, A. Aouadi, J. Gapinski, M. Matos-Lopes, W. Steffen, A. Patkowski, and R. M. Pick. Temperature and pressure study of brillouin transverse modes in the organic glass-forming liquid orthoterphenyl. *Phys. Rev. E*, 68:011204, Jul 2003. 44

[134] J-M Drouffe, G Parisi, and N Sourlas. Strong coupling phase in lattice gauge theories at large dimension. *Nuclear Physics B*, 161(2):397–416, 1979. 1, 17

[135] B Duplantier. Comment on parisi's equation for the sk model for spin glasses. *Journal of Physics A: Mathematical and General*, 14(1):283, 1981. 140, 199

[136] Jeppe C Dyre. Colloquium: The glass transition and elastic models of glass-forming liquids. *Reviews of modern physics*, 78(3):953, 2006. 3, 19, 41

[137] Jeppe C Dyre. Isomorphs, hidden scale invariance, and quasiuniversality. *Physical Review E*, 88(4):042139, 2013. 45, 153

[138] Jeppe C Dyre. Simple liquids' quasiuniversality and the hard-sphere paradigm. *Journal of Physics: Condensed Matter*, 28(32):323001, 2016. 43, 44, 153

[139] R Edgeworth, BJ Dalton, and T Parnell. The pitch drop experiment. *European Journal of Physics*, 5(4):198, 1984. 3, 19

[140] Mi D Ediger. Spatially heterogeneous dynamics in supercooled liquids. *Annual review of physical chemistry*, 51(1):99–128, 2000. 8, 10, 24, 26

[141] Samuel Frederick Edwards and Phil W Anderson. Theory of spin glasses. *Journal of Physics F: Metal Physics*, 5(5):965, 1975. 29, 63

[142] SF Edwards and PW Anderson. Theory of spin glasses. ii. *Journal of Physics F: Metal Physics*, 6(10):1927, 1976. 29, 63

[143] Konstantin Efetov. *Supersymmetry in disorder and chaos*. Cambridge University Press, 1997. 65, 67

[144] Albert Einstein. Investigations on the theory of brownian motion. 1905. 10, 26

[145] Yael S Elmatad, David Chandler, and Juan P Garrahan. Corresponding states of structural glass formers. *The Journal of Physical Chemistry B*, 113(16):5563–5567, 2009. 5, 20

[146] Yves Elskens and Harry L Frisch. Kinetic theory of hard spheres in infinite dimensions. *Physical Review A*, 37(11):4351, 1988. 42, 151

[147] D Enskog. Kinetic theory of heat conductivity, viscosity and diffusion in certain condensed gases and liquids. *Kungl. Svenska Vetenskap. Handl*, 63:1–44, 1922. 42

[148] Thomas E Faber. *Introduction to the theory of liquid metals*. Cambridge University Press, 1972. 2, 18

[149] Ludvig D Faddeev and Victor N Popov. Feynman diagrams for the yang-mills field. *Physics Letters B*, 25(1):29–30, 1967. 59, 184

[150] William Feller. *An introduction to probability theory and its applications*. 1971. 109, 187

[151] Julián R. Fernández and Peter Harrowell. Crystal phases of a glass-forming lennard-jones mixture. *Phys. Rev. E*, 67:011403, Jan 2003. 2, 18

[152] Richard P Feynman, Albert R Hibbs, and Daniel Styer. *Quantum mechanics and path integrals*. Dover Publications, 2010. 187

[153] Richard P Feynman, Robert B Leighton, Matthew Sands, and EM Hafner. *The Feynman lectures on physics*, volume 33. American Association of Physics Teachers, 1965. 2, 18

[154] Paul J Flory. Phase equilibria in solutions of rod-like particles. In *Proceedings of the Royal Society of London A: Mathematical, Physical and Engineering Sciences*, volume 234, pages 73–89. The Royal Society, 1956. 28, 35, 40

[155] Daniel Fragiadakis and C Michael Roland. On the density scaling of liquid dynamics. *The Journal of chemical physics*, 134(4):044504, 2011. 44

[156] S. Franz and G. Parisi. Recipes for metastable states in spin glasses. *Journal de Physique I*, 5(11):1401–1415, 1995. 37, 133, 144, 173

[157] S. Franz, G. Parisi, F. Ricci-Tersenghi, and T. Rizzo. Field theory of fluctuations in glasses. *The European Physical Journal E: Soft Matter and Biological Physics*, 34(9):1–17, 2011. 117, 151

[158] Silvio Franz, Claudio Donati, Giorgio Parisi, and Sharon C Glotzer. On dynamical correlations in supercooled liquids. *Philosophical Magazine B*, 79(11-12):1827–1831, 1999. 9, 25

[159] Silvio Franz, Hugo Jacquin, Giorgio Parisi, Pierfrancesco Urbani, and Francesco Zamponi. Static replica approach to critical correlations in glassy systems. *J. Chem. Phys.*, 138(12):12A540, 2013. 117, 151

[160] Luc Frappat, Antonino Sciarrino, and Paul Sorba. *Dictionary on Lie algebras and superalgebras*, volume 10. Academic Press USA, 2000. 67

[161] H. L. Frisch and J. K. Percus. High dimensionality as an organizing device for classical fluids. *Phys. Rev. E*, 60(3):2942–2948, Sep 1999. 2, 13, 18, 46, 53, 54, 57, 87, 89, 132, 151

[162] H. L. Frisch, N. Rivier, and D. Wyler. Classical hard-sphere fluid in infinitely many dimensions. *Phys. Rev. Lett.*, 54:2061–2063, May 1985. 2, 13, 18, 46, 53, 54, 57, 89, 151

[163] HL Frisch and JK Percus. Nonuniform classical fluid at high dimensionality. *Physical Review A*, 35(11):4696, 1987. 2, 13, 18, 46, 53, 58

[164] HL Frisch, N Rivier, and D Wyler. Frisch, rivier, and wyler respond. *Physical review letters*, 56(21):2331, 1986. 2, 13, 18, 46, 53

[165] M Fuchs. The kohlrausch law as a limit solution to mode coupling equations. *Journal of non-crystalline solids*, 172:241–247, 1994. 30

[166] F Fujara, B Geil, H Sillescu, and G Fleischer. Translational and rotational diffusion in supercooled orthoterphenyl close to the glass transition. *Zeitschrift für Physik B Condensed Matter*, 88(2):195–204, 1992. 11, 26

[167] Gordon S Fulcher. Analysis of recent measurements of the viscosity of glasses. *Journal of the American Ceramic Society*, 8(6):339–355, 1925. 4, 20

[168] Yan V Fyodorov. Negative moments of characteristic polynomials of random matrices: Ingham–siegel integral as an alternative to hubbard–stratonovich transformation. *Nuclear Physics B*, 621(3):643–674, 2002. 135

[169] Yan V Fyodorov and H-J Sommers. Classical particle in a box with random potential: exploiting rotational symmetry of replicated hamiltonian. *Nuclear Physics B*, 764(3):128–167, 2007. 135

[170] Crispin W Gardiner. *Handbook of stochastic methods*, volume 3. Springer Berlin, 1985. 185

[171] Ed Gardner. Spin glasses with p-spin interactions. *Nuclear Physics B*, 257:747–765, 1985. 142

[172] J.P. Garrahan, P. Sollich, and C. Toninelli. Kinetically constrained models. In L. Berthier, G. Biroli, J-P Bouchaud, L. Cipelletti, and W. van Saarloos, editors, *Dynamical Heterogeneities and Glasses, Colloids and Granular Media*. Oxford University Press, 2011. 41

[173] Stanley J Gates, Warren Siegel, Martin Rocek, and Marc T Grisaru. *Superspace*. Number hep-th/0108200. Benjamin-Cummings, 1983. 65, 67

[174] Bernard Gaveau, Annick Lesne, and LS Schulman. Spectral signatures of hierarchical relaxation. *Physics Letters A*, 258(4):222–228, 1999. 33

[175] Bernard Gaveau and LS Schulman. Master equation based formulation of nonequilibrium statistical mechanics. *Journal of Mathematical Physics*, 37(8):3897–3932, 1996. 33

[176] Bernard Gaveau and LS Schulman. A general framework for non-equilibrium phenomena: The master equation and its formal consequences. *Physics Letters A*, 229(6):347–353, 1997. 33

[177] Bernard Gaveau and LS Schulman. Theory of nonequilibrium first-order phase transitions for stochastic dynamics. *Journal of Mathematical Physics*, 39(3):1517–1533, 1998. 33

[178] A. Georges and JS Yedidia. How to expand around mean-field theory using high-temperature expansions. *Journal of Physics A: Mathematical and General*, 24:2173, 1991. 53, 83

[179] Antoine Georges, Gabriel Kotliar, Werner Krauth, and Marcelo J Rozenberg. Dynamical mean-field theory of strongly correlated fermion systems and the limit of infinite dimensions. *Reviews of Modern Physics*, 68(1):13, 1996. 1, 17, 53

[180] Julian H Gibbs. Nature of the glass transition in polymers. *The Journal of Chemical Physics*, 25(1):185–186, 1956. 28, 35, 40

[181] Julian H Gibbs and Edmund A DiMarzio. Nature of the glass transition and the glassy state. *The Journal of Chemical Physics*, 28(3):373–383, 1958. 28, 35, 40

[182] Tobias Gleim, Walter Kob, and Kurt Binder. How does the relaxation of a supercooled liquid depend on its microscopic dynamics? *Physical review letters*, 81(20):4404, 1998. 107

[183] Sharon C Glotzer. Spatially heterogeneous dynamics in liquids: insights from simulation. *Journal of Non-Crystalline Solids*, 274(1):342–355, 2000. 8, 10, 24, 26

[184] Nicoletta Gnan, Thomas B Schrøder, Ulf R Pedersen, Nicholas P Bailey, and Jeppe C Dyre. Pressure-energy correlations in liquids. iv.“isomorphs” in liquid phase diagrams. *The Journal of chemical physics*, 131(23):234504, 2009. 44, 45, 153, 154, 157, 159, 162, 166, 170

[185] Martin Goldstein. Viscous liquids and the glass transition: A potential energy barrier picture. *The Journal of Chemical Physics*, 51(9):3728–3739, 1969. 28, 33

[186] W Götze. The essentials of the mode-coupling theory for glassy dynamics. *Condens. Matter Phys.*, 1:873–904, 1998. 28, 30, 103, 110, 117, 118, 119, 120

[187] W. Götze. *Complex dynamics of glass-forming liquids: A mode-coupling theory*, volume 143. Oxford University Press, USA, 2009. 28, 29, 30, 43, 45, 74, 103, 108, 110, 117, 118, 119, 120, 128, 145

[188] Wolfgang Götze. Recent tests of the mode-coupling theory for glassy dynamics. *Journal of Physics: Condensed Matter*, 11(10A):A1–A45, 1999. 28

[189] E Gozzi. Onsager principle of microscopic reversibility and supersymmetry. *Physical Review D*, 30(6):1218, 1984. 65, 74

[190] Ennio Gozzi. Stochastic and non-stochastic supersymmetry. *Progress of Theoretical Physics Supplement*, 111:115–150, 1993. 65, 74

[191] Tomás S. Grigera, Andrea Cavagna, Irene Giardina, and Giorgio Parisi. Geometric approach to the dynamic glass transition. *Phys. Rev. Lett.*, 88:055502, Jan 2002. 34

[192] D. J. Gross and M. Mézard. The simplest spin glass. *Nucl. Phys. B*, 240:431, 1984. 31, 58

[193] DJ Gross, I Kanter, and Haim Sompolinsky. Mean-field theory of the potts glass. *Physical review letters*, 55(3):304, 1985. 142

[194] Francesco Guerra. Broken replica symmetry bounds in the mean field spin glass model. *Communications in mathematical physics*, 233(1):1–12, 2003. 64

[195] F de J Guevara-Rodriguez and Magdaleno Medina-Noyola. Dynamic equivalence between soft-and hard-core brownian fluids. *Physical Review E*, 68(1):011405, 2003. 43

[196] H Haken. Generalized onsager-machlup function and classes of path integral solutions of the fokker-planck equation and the master equation. *Zeitschrift für Physik B Condensed Matter*, 24(3):321–326, 1976. 184

[197] Peter Hänggi. Generalized langevin equations: A useful tool for the perplexed modeller of nonequilibrium fluctuations? In *Stochastic dynamics*, pages 15–22. Springer, 1997. 10, 26, 102, 103

[198] Peter Hänggi, Peter Talkner, and Michal Borkovec. Reaction-rate theory: fifty years after kramers. *Rev. Mod. Phys.*, 62:251–341, Apr 1990. 4, 19, 33

[199] J.-P. Hansen and I. R. McDonald. *Theory of simple liquids.* Academic Press, London, 1986. 1, 2, 5, 6, 10, 11, 17, 18, 21, 26, 28, 29, 33, 42, 44, 49, 51, 52, 85, 89, 113, 115, 118, 120, 132, 133, 146, 162, 163, 164, 167

[200] Jean-Pierre Hansen and Loup Verlet. Phase transitions of the lennard-jones system. *physical Review*, 184(1):151, 1969. 45

[201] Tina Hecksher, Albena I Nielsen, Niels Boye Olsen, and Jeppe C Dyre. Little evidence for dynamic divergences in ultraviscous molecular liquids. *Nature Physics*, 4(9):737–741, 2008. 5, 20

[202] Matthias Heinrich, Mohammad-Ali Miri, Simon Stützer, Ramy El-Ganainy, Stefan Nolte, Alexander Szameit, and Demetrios N Christodoulides. Supersymmetric mode converters. *Nature communications*, 5, 2014. 65

[203] Atsushi Ikeda and Kunimasa Miyazaki. Mode-coupling theory as a mean-field description of the glass transition. *Phys. Rev. Lett.*, 104(25):255704, Jun 2010. 116, 120

[204] Atsushi Ikeda and Kunimasa Miyazaki. Ikeda and miyazaki reply:. *Phys. Rev. Lett.*, 106:049602, Jan 2011. 116, 120

[205] Robert L Jack and Juan P Garrahan. Phase transition for quenched coupled replicas in a plaquette spin model of glasses. *Physical review letters*, 116(5):055702, 2016. 35, 41

[206] Hugo Jacquin. Glass and jamming transition of simple liquids: static and dynamic theory. *arXiv:1307.3997*, 2013. 14, 38, 43, 46, 49

[207] Hugo Jacquin and Frédéric van Wijland. Field-theoretic formulation of a mode-coupling equation for colloids. *Phys. Rev. Lett.*, 106:210602, May 2011. 43, 116

[208] Hans-Karl Janssen. On a lagrangean for classical field dynamics and renormalization group calculations of dynamical critical properties. *Zeitschrift für Physik B Condensed Matter*, 23(4):377–380, 1976. 183

[209] HK Janssen. Field-theoretic method applied to critical dynamics. In *Dynamical critical phenomena and related topics*, pages 25–47. Springer, 1979. 183, 187

[210] HK Janssen. On the renormalized field theory of nonlinear critical relaxation. *From Phase Transitions to Chaos-Topics in Modern Statistical Physics*, 1992. 183, 187

[211] Liesbeth M. C. Janssen, Peter Mayer, and David R. Reichman. Relaxation patterns in supercooled liquids from generalized mode-coupling theory. *Phys. Rev. E*, 90:052306, Nov 2014. 42, 43

[212] Liesbeth MC Janssen, Peter Mayer, and David R Reichman. Generalized mode-coupling theory of the glass transition: schematic results at finite and infinite order. *Journal of Statistical Mechanics: Theory and Experiment*, 2016(5):054049, 2016. 42, 43

[213] Liesbeth MC Janssen and David R Reichman. Microscopic dynamics of supercooled liquids from first principles. *Physical review letters*, 115(20):205701, 2015. 42, 43

[214] YounJoon Jung, Juan P Garrahan, and David Chandler. Excitation lines and the breakdown of stokes-einstein relations in supercooled liquids. *Physical Review E*, 69(6):061205, 2004. 12, 27

[215] Walter Kauzmann. The nature of the glassy state and the behavior of liquids at low temperatures. *Chemical Reviews*, 43(2):219–256, 1948. 35

[216] Leonid V Keldysh. Diagram technique for nonequilibrium processes. *Sov. Phys. JETP*, 20(4):1018–1026, 1965. 183

[217] Ken Kelton and Alan Lindsay Greer. *Nucleation in condensed matter: applications in materials and biology*, volume 15. Elsevier, 2010. 2, 18

[218] Sergey A Khrapak, Manis Chaudhuri, and Gregor E Morfill. Communication: Universality of the melting curves for a wide range of interaction potentials. *The Journal of chemical physics*, 134(24):241101, 2011. 45

[219] Bongsoo Kim and Kyozi Kawasaki. A fluctuation-dissipation relationship-preserving field theory for interacting brownian particles: one-loop theory and mode coupling theory. *Journal of Statistical Mechanics: Theory and Experiment*, 2008(02):P02004, 2008. 43

[220] T. R. Kirkpatrick and D. Thirumalai. Dynamics of the structural glass transition and the *p*-spin-interaction spin-glass model. *Phys. Rev. Lett.*, 58(20):2091–2094, May 1987. 28, 31, 100, 119, 170

[221] T. R. Kirkpatrick and D. Thirumalai. *p*-spin-interaction spin-glass models: Connections with the structural glass problem. *Phys. Rev. B*, 36:5388–5397, Oct 1987. 28, 100, 119, 170

[222] T. R. Kirkpatrick and D. Thirumalai. Comparison between dynamical theories and metastable states in regular and glassy mean-field spin models with underlying first-order-like phase transitions. *Phys. Rev. A*, 37:4439–4448, Jun 1988. 28

[223] T R Kirkpatrick and D Thirumalai. Random solutions from a regular density functional hamiltonian: a static and dynamical theory for the structural glass transition. *Journal of Physics A: Mathematical and General*, 22(5):L149, 1989. 28, 170

[224] T. R. Kirkpatrick, D. Thirumalai, and P. G. Wolynes. Scaling concepts for the dynamics of viscous liquids near an ideal glassy state. *Phys. Rev. A*, 40(2):1045–1054, Jul 1989. 28, 39, 40, 170

[225] T. R. Kirkpatrick and P. G. Wolynes. Connections between some kinetic and equilibrium theories of the glass transition. *Phys. Rev. A*, 35(7):3072–3080, Apr 1987. 13, 28, 46, 57, 91, 116, 156, 170, 196

[226] T. R. Kirkpatrick and P. G. Wolynes. Stable and metastable states in mean-field Potts and structural glasses. *Phys. Rev. B*, 36(16):8552–8564, Dec 1987. 28

[227] TR Kirkpatrick and D Thirumalai. The cavity approach for metastable glassy states near random first order phase transitions. *Journal de Physique I*, 5(7):777–786, 1995. 170

[228] John G Kirkwood and Elizabeth Monroe. Statistical mechanics of fusion. *The Journal of Chemical Physics*, 9(7):514–526, 1941. 58

[229] W. Kob. *Course 5: Supercooled Liquids, the Glass Transition, and Computer Simulations*, pages 199–269. Springer Berlin Heidelberg, Berlin, Heidelberg, 2003. 3, 19, 28

[230] W Kob and R Schilling. Ergodicity of a system with second-order phase transition: applicability of mode coupling theory. *Journal of Physics: Condensed Matter*, 3(46):9195, 1991. 116

[231] Walter Kob and Hans C. Andersen. Scaling behavior in the β-relaxation regime of a supercooled lennard-jones mixture. *Phys. Rev. Lett.*, 73:1376–1379, Sep 1994. 3, 4, 19, 20

[232] Walter Kob and Hans C. Andersen. Testing mode-coupling theory for a supercooled binary Lennard-Jones mixture I: The van Hove correlation function. *Phys. Rev. E*, 51(5):4626–4641, May 1995. 7, 8, 22, 23, 28, 31, 119, 120

[233] Walter Kob and Hans C. Andersen. Testing mode-coupling theory for a supercooled binary Lennard-Jones mixture. II. intermediate scattering function and dynamic susceptibility. *Phys. Rev. E*, 52(4):4134–4153, Oct 1995. 8, 23, 28, 31, 119, 120

[234] Walter Kob, Markus Nauroth, and Francesco Sciortino. Quantitative tests of mode-coupling theory for fragile and strong glass formers. *Journal of non-crystalline solids*, 307:181–187, 2002. 28

[235] R Kohlrausch. Nachtrag uber die elastiche nachwirkung beim cocon und glasladen. *Ann. Phys.(Leipzig)*, 72:393, 1847. 7, 23, 30

[236] J Kurchan. Supersymmetry in spin glass dynamics. *Journal de Physique I*, 2(7):1333–1352, 1992. 65, 73, 74

[237] J Kurchan, G Parisi, and Miguel Angel Virasoro. Barriers and metastable states as saddle points in the replica approach. *Journal de Physique I*, 3(8):1819–1838, 1993. 33, 62

[238] Jorge Kurchan. Supersymmetry, replica and dynamic treatments of disordered systems: a parallel presentation. *Markov Processes and Related Fields*, 9(2):243–260, 2003. 65, 73, 74

[239] Jorge Kurchan. Glasses. In *Glasses and Grains*, pages 1–24. Springer, 2011. 3, 4, 18, 20, 158

[240] Jorge Kurchan and Laurent Laloux. Phase space geometry and slow dynamics. *Journal of Physics A: Mathematical and General*, 29(9):1929, 1996. 39

[241] Jorge Kurchan, Thibaud Maimbourg, and Francesco Zamponi. Statics and dynamics of infinite-dimensional liquids and glasses: a parallel and compact derivation. *Journal of Statistical Mechanics: Theory and Experiment*, 2016(3):033210, 2016. v

[242] Jorge Kurchan, Giorgio Parisi, Pierfrancesco Urbani, and Francesco Zamponi. Exact theory of dense amorphous hard spheres in high dimension. II. The high density regime and the gardner transition. *J. Phys. Chem. B*, 117:12979–12994, 2013. 12, 13, 45, 46, 57, 84, 91, 117, 127, 128, 135, 136, 137, 138, 140, 143, 151, 156, 194, 200, 201, 202, 203

[243] Jorge Kurchan, Giorgio Parisi, and Francesco Zamponi. Exact theory of dense amorphous hard spheres in high dimension i. the free energy. *Journal of Statistical Mechanics: Theory and Experiment*, 2012(10):P10012, 2012. 12, 13, 45, 46, 57, 84, 91, 92, 127, 128, 131, 133, 134, 135, 136, 137, 151, 156, 190, 196, 200, 201, 202, 203, 206, 207, 208

[244] Lev D Landau and EM Lifshitz. *Classical mechanics*, volume 6 of *Course of Theoretical Physics*. Pergamon Press, Oxford, 1960. 29, 163

[245] Lev D Landau and EM Lifshitz. *Theory of Elasticity*, volume 7 of *Course of Theoretical Physics*. Elsevier, New York, 1986. 3, 19, 147

[246] Lev D Landau and EM Lifshitz. *Fluid mechanics*, volume 6 of *Course of Theoretical Physics*. Pergamon Press, New York, 1987. 10, 26, 42

[247] Lev Davidovich Landau. On the theory of phase transitions. i. *Zh. Eksp. Teor. Fiz.*, 11:19, 1937. 2, 18, 32, 43

[248] Lev Davidovich Landau and EM Lifshitz. *Statistical physics, part I*, volume 5 of *Course of Theoretical Physics*. Pergamon, Oxford, 1980. 2, 18, 32, 43

[249] Tsung-Dao Lee and Chen-Ning Yang. Statistical theory of equations of state and phase transitions. ii. lattice gas and ising model. *Physical Review*, 87(3):410, 1952. 2, 18, 32

[250] Anthony J. Leggett. Amorphous materials at low temperatures: why are they so similar? *Physica B: Condensed Matter*, 169(1):322 – 327, 1991. 2, 18

[251] Edan Lerner, Nicholas P Bailey, and Jeppe C Dyre. Density scaling and quasiuniversality of flow-event statistics for athermal plastic flows. *Physical Review E*, 90(5):052304, 2014. 45

[252] E Leutheusser. Dynamical model of the liquid-glass transition. *Physical Review A*, 29(5):2765, 1984. 28, 31, 77

[253] L. Leuzzi and T.M. Nieuwenhuizen. *Thermodynamics of the glassy state*. Taylor & Francis, 2007. 39

[254] Laurent J Lewis and Göran Wahnström. Molecular-dynamics study of supercooled ortho-terphenyl. *Physical Review E*, 50(5):3865, 1994. 4, 20

[255] Leticia López-Flores, Honorina Ruíz-Estrada, Martín Chávez-Páez, and Magdaleno Medina-Noyola. Dynamic equivalences in the hard-sphere dynamic universality class. *Physical Review E*, 88(4):042301, 2013. 43

[256] Peter J Lu, Emanuela Zaccarelli, Fabio Ciulla, Andrew B Schofield, Francesco Sciortino, and David A Weitz. Gelation of particles with short-range attraction. *Nature*, 453(7194):499–503, 2008. 2, 18

[257] Boris D. Lubachevsky and Frank H. Stillinger. Geometric properties of random disk packings. *J. Stat. Phys.*, 60:561–583, 1990. 109, 121, 124

[258] Marshall Luban. Comment on "classical hard-sphere fluid in infinitely many dimensions". *Physical review letters*, 56(21):2330, 1986. 2, 13, 18, 46, 53

[259] Vassiliy Lubchenko and Peter G. Wolynes. Intrinsic quantum excitations of low temperature glasses. *Phys. Rev. Lett.*, 87:195901, Oct 2001. 173

[260] Vassiliy Lubchenko and Peter G. Wolynes. Theory of structural glasses and supercooled liquids. *Annual Review of Physical Chemistry*, 58(1):235–266, 2007. 39

[261] Ivan Lyubimov, Mark D Ediger, and Juan J de Pablo. Model vapor-deposited glasses: Growth front and composition effects. *The Journal of chemical physics*, 139(14):144505, 2013. 3, 18

[262] S. Machlup and L. Onsager. Fluctuations and irreversible process. ii. systems with kinetic energy. *Phys. Rev.*, 91:1512–1515, Sep 1953. 184

[263] Thibaud Maimbourg and Jorge Kurchan. Approximate scale invariance in particle systems: A large-dimensional justification. *EPL (Europhysics Letters)*, 114(6):60002, 2016. v

[264] Thibaud Maimbourg, Jorge Kurchan, and Francesco Zamponi. Solution of the dynamics of liquids in the large-dimensional limit. *Physical Review Letters*, 116(1):015902, 2016. v

[265] Satya N. Majumdar and Massimo Vergassola. Large deviations of the maximum eigenvalue for wishart and gaussian random matrices. *Phys. Rev. Lett.*, 102:060601, Feb 2009. 135

[266] Kirone Mallick, Moshe Moshe, and Henri Orland. A field-theoretic approach to non-equilibrium work identities. *Journal of Physics A: Mathematical and Theoretical*, 44(9):095002, 2011. 74, 76

[267] Matthieu Mangeat and Francesco Zamponi. Quantitative approximation schemes for glasses. *Physical Review E*, 93(1):012609, 2016. 173

[268] Marie K Mapes, Stephen F Swallen, and MD Ediger. Self-diffusion of supercooled o-terphenyl near the glass transition temperature. *The Journal of Physical Chemistry B*, 110(1):507–511, 2006. 11, 26

[269] Norman Henry March. *Liquid metals: concepts and theory*. Cambridge University Press, 1990. 2, 18

[270] R. Mari and J. Kurchan. Dynamical transition of glasses: From exact to approximate. *J. Chem. Phys.*, 135:124504, 2011. 36, 58, 81, 85, 89, 105, 111, 112, 114, 115, 128, 129, 132, 133, 134, 171, 189, 205

[271] P. C. Martin, E. D. Siggia, and H. A. Rose. Statistical dynamics of classical systems. *Phys. Rev. A*, 8:423–437, Jul 1973. 183

[272] D El Masri, G Brambilla, M Pierno, G Petekidis, A B Schofield, L Berthier, and L Cipelletti. Dynamic light scattering measurements in the activated regime of dense colloidal hard spheres. *Journal of Statistical Mechanics: Theory and Experiment*, 2009(07):P07015, 2009. 31

[273] J Clerk Maxwell. On the calculation of the equilibrium and stiffness of frames. *The London, Edinburgh, and Dublin Philosophical Magazine and Journal of Science*, 27(182):294–299, 1864. 14, 47, 83

[274] JE Mayer and MG Mayer. *Statistical Mechanics*. John Wiley & Sons, New York, 1940. 50

[275] Peter Mayer, Kunimasa Miyazaki, and David R Reichman. Cooperativity beyond caging: Generalized mode-coupling theory. *Physical review letters*, 97(9):095702, 2006. 42

[276] M. Mézard. How to compute the thermodynamics of a glass using a cloned liquid. *Physica A*, 265(3):352–369, 1999. 36, 37, 127

[277] M. Mézard and G. Parisi. A tentative replica study of the glass transition. *Journal of Physics A: Mathematical and General*, 29:6515, 1996. 36, 37, 127

[278] M. Mezard and G. Parisi. Glasses and replicas. In P.G.Wolynes and V.Lubchenko, editors, *Structural Glasses and Supercooled Liquids: Theory, Experiment and Applications*. Wiley & Sons, 2012. 36, 37, 127, 136

[279] M. Mézard, G. Parisi, and M. A. Virasoro. *Spin glass theory and beyond*. World Scientific, Singapore, 1987. 28, 32, 35, 58, 59, 60, 61, 63, 64, 132, 135, 136, 137, 140, 143

[280] Marc Mézard and Andrea Montanari. Reconstruction on trees and spin glass transition. *Journal of statistical physics*, 124(6):1317–1350, 2006. 9, 25

[281] Marc Mézard and Giorgio Parisi. Replicas and optimization. *Journal de Physique Lettres*, 46(17):771–778, 1985. 181

[282] Marc Mézard and Giorgio Parisi. Replica field theory for random manifolds. *Journal de Physique I*, 1(6):809–836, 1991. 180, 181

[283] Marc Mézard and Giorgio Parisi. A first-principle computation of the thermodynamics of glasses. *The Journal of Chemical Physics*, 111(3):1076–1095, 1999. 33, 36, 37, 38, 127, 144

[284] Marc Mézard and Giorgio Parisi. Thermodynamics of glasses: A first principles computation. *Physical review letters*, 82(4):747, 1999. 33, 36, 37, 127, 144

[285] Marc Mézard and Giorgio Parisi. Statistical physics of structural glasses. *Journal of Physics: Condensed Matter*, 12(29):6655–6673, 2000. 36, 37, 127, 170

[286] Mohammad-Ali Miri, Matthias Heinrich, Ramy El-Ganainy, and Demetrios N Christodoulides. Supersymmetric optical structures. *Physical review letters*, 110(23):233902, 2013. 65

[287] Kunimasa Miyazaki and David R Reichman. Mode-coupling theory and the fluctuation–dissipation theorem for nonlinear langevin equations with multiplicative noise. *Journal of Physics A: Mathematical and General*, 38(20):L343, 2005. 43

[288] Rémi Monasson. Structural glass transition and the entropy of the metastable states. *Phys. Rev. Lett.*, 75(15):2847–2850, Oct 1995. 36, 127, 128, 133, 136, 144, 151, 201

[289] A. Montanari and G. Semerjian. Rigorous inequalities between length and time scales in glassy systems. *J.Stat.Phys.*, 125:23–54, 2006. 10, 26, 109

[290] Cécile Monthus and Jean-Philippe Bouchaud. Models of traps and glass phenomenology. *Journal of Physics A: Mathematical and General*, 29(14):3847, 1996. 41

[291] Hazime Mori. A continued-fraction representation of the time-correlation functions. *Progress of Theoretical Physics*, 34(3):399–416, 1965. 29

[292] Hazime Mori. Transport, collective motion, and brownian motion. *Progress of theoretical physics*, 33(3):423–455, 1965. 29

[293] T. Morita and K. Hiroike. A new approach to the theory of classical fluids. III. *Progr. Theor. Phys.*, 25:537, 1961. 49, 52, 113, 132, 133, 164

[294] G Mussardo. *Statistical Field Theory: An Introduction to Exactly Solved Models in Statistical Physics.* Oxford Graduate TextsOUP Oxford, 2009. 58, 59

[295] Markus Nauroth and Walter Kob. Quantitative test of the mode-coupling theory of the ideal glass transition for a binary lennard-jones system. *Physical Review E*, 55(1):657, 1997. 28

[296] Bernt Oksendal. *Stochastic differential equations: an introduction with applications.* Springer Science & Business Media, 2013. 185

[297] L. Onsager and S. Machlup. Fluctuations and irreversible processes. *Phys. Rev.*, 91:1505–1512, Sep 1953. 184

[298] Lars Onsager. Reciprocal relations in irreversible processes. i. *Phys. Rev.*, 37:405–426, Feb 1931. 76

[299] Lars Onsager. Reciprocal relations in irreversible processes. ii. *Phys. Rev.*, 38:2265–2279, Dec 1931. 76

[300] Hirofumi Osada. Positivity of the self-diffusion matrix of interacting brownian particles with hard core. *Probability theory and related fields*, 112(1):53–90, 1998. 30

[301] G Parisi. The magnetic properties of the sherrington-kirkpatrick model for spin glasses: Theory versus monte carlo simulations. *Philosophical Magazine B*, 41(6):677–680, 1980. 61

[302] G. Parisi and N. Sourlas. Random magnetic fields, supersymmetry, and negative dimensions. *Phys. Rev. Lett.*, 43:744–745, Sep 1979. 65

[303] Giorgio Parisi. Infinite number of order parameters for spin-glasses. *Physical Review Letters*, 43(23):1754, 1979. 61

[304] Giorgio Parisi. Magnetic properties of spin glasses in a new mean field theory. *Journal of Physics A: Mathematical and General*, 13(5):1887, 1980. 61, 65

[305] Giorgio Parisi. Mean field theory for spin glasses. *Physics Reports*, 67(1):25–28, 1980. 61

[306] Giorgio Parisi. The order parameter for spin glasses: A function on the interval 0-1. *Journal of Physics A: Mathematical and General*, 13(3):1101, 1980. 61

[307] Giorgio Parisi. A sequence of approximated solutions to the sk model for spin glasses. *Journal of Physics A: Mathematical and General*, 13(4):L115, 1980. 61, 140

[308] Giorgio Parisi. *Statistical field theory.* Addison-Wesley, 1988. 32

[309] Giorgio Parisi and Tommaso Rizzo. Critical dynamics in glassy systems. *Physical Review E*, 87(1):012101, 2013. 73, 117, 151

[310] Giorgio Parisi and Francesco Sciortino. Structural glasses: Flying to the bottom. *Nature materials*, 12(2):94–95, 2013. 3, 18

[311] Giorgio Parisi and Nucl Sourlas. Supersymmetric field theories and stochastic differential equations. *Nuclear Physics B*, 206(2):321–332, 1982. 65

[312] Giorgio Parisi and Francesco Zamponi. Mean-field theory of hard sphere glasses and jamming. *Rev. Mod. Phys.*, 82(1):789–845, Mar 2010. 12, 13, 15, 37, 45, 46, 48, 84, 89, 91, 110, 127, 128, 131, 133, 134, 137, 140, 144, 151, 152, 156, 190, 196

[313] Jerome K Percus and George J Yevick. Analysis of classical statistical mechanics by means of collective coordinates. *Physical Review*, 110(1):1, 1958. 6, 21

[314] Tomás Pérez-Castañeda, Cristian Rodríguez-Tinoco, Javier Rodríguez-Viejo, and Miguel A Ramos. Suppression of tunneling two-level systems in ultrastable glasses of indomethacin. *Proceedings of the National Academy of Sciences*, 111(31):11275–11280, 2014. 173

[315] Michael Peskin and Dan Schroeder. *An introduction to quantum field theory.* Addison-Wesley Publishing Company, 1995. 29, 59, 65, 74, 76, 97, 184, 187

[316] WA Phillips. Tunneling states in amorphous solids. *Journal of Low Temperature Physics*, 7(3-4):351–360, 1972. 173

[317] R Phythian. The operator formalism of classical statistical dynamics. *Journal of Physics A: Mathematical and General*, 8(9):1423, 1975. 183

[318] R Phythian. The functional formalism of classical statistical dynamics. *Journal of Physics A: Mathematical and General*, 10(5):777, 1977. 183

[319] Eva Arianna Aurelia Pogna, Cristian Rodríguez-Tinoco, Giulio Cerullo, Carino Ferrante, Javier Rodríguez-Viejo, and Tullio Scopigno. Probing equilibrium glass flow up to exapoise viscosities. *Proceedings of the National Academy of Sciences*, 112(8):2331–2336, 2015. 5, 20

[320] Robert O. Pohl, Xiao Liu, and EunJoo Thompson. Low-temperature thermal conductivity and acoustic attenuation in amorphous solids. *Rev. Mod. Phys.*, 74:991–1013, Oct 2002. 2, 18

[321] Mark J Pond, Jeffrey R Errington, and Thomas M Truskett. Communication: Generalizing rosenfeld's excess-entropy scaling to predict long-time diffusivity in dense fluids of brownian particles: From hard to ultrasoft interactions. *The Journal of chemical physics*, 134(8):081101, 2011. 45

[322] Noëlle Pottier. *Nonequilibrium statistical physics: linear irreversible processes.* Oxford University Press, 2009. 74, 76

[323] Corrado Rainone. Following the evolution of metastable glassy states under external perturbations: compression and shear-strain. *arXiv preprint arXiv:1601.01713*, 2016. 3, 19, 33, 39

[324] Corrado Rainone and Pierfrancesco Urbani. Following the evolution of glassy states under external perturbations: the full replica symmetry breaking solution. *Journal of Statistical Mechanics: Theory and Experiment*, 2016(5):053302, 2016. 173

[325] Corrado Rainone, Pierfrancesco Urbani, Hajime Yoshino, and Francesco Zamponi. Following the evolution of hard sphere glasses in infinite dimensions under external perturbations: Compression and shear strain. *Phys. Rev. Lett.*, 114(1):015701, 2015. 13, 39, 46, 127, 128, 133, 144, 151, 152, 173

[326] David R Reichman and Patrick Charbonneau. Mode-coupling theory. *Journal of Statistical Mechanics: Theory and Experiment*, 2005(05):P05013, 2005. 28, 117, 120

[327] Pierre MV Résibois and Michel De Leener. *Classical kinetic theory of fluids.* John Wiley & Sons, 1977. 42

[328] Ranko Richert and Charles Angell. Dynamics of glass-forming liquids. v. on the link between molecular dynamics and configurational entropy. *Journal of Chemical Physics*, 108(21):9016–9026, 1998. 35

[329] Tommaso Rizzo. Long-wavelength fluctuations lead to a model of the glass crossover. *EPL (Europhysics Letters)*, 106(5):56003, 2014. 43

[330] Tommaso Rizzo. Dynamical landau theory of the glass crossover. *Phys. Rev. B*, 94:014202, Jul 2016. 43

[331] Tommaso Rizzo. The glass crossover from mean-field spin-glasses to supercooled liquids. *Philosophical Magazine*, 96(7-9):636–647, 2016. 43

[332] Tommaso Rizzo and Thomas Voigtmann. Qualitative features at the glass crossover. *EPL (Europhysics Letters)*, 111(5):56008, 2015. 43

[333] Carl A Rogers. The packing of equal spheres. *Proceedings of the London Mathematical Society*, 3(4):609–620, 1958. 110

[334] C M Roland, S Hensel-Bielowka, M Paluch, and R Casalini. Supercooled dynamics of glass-forming liquids and polymers under hydrostatic pressure. *Reports on Progress in Physics*, 68(6):1405, 2005. 44

[335] Yaakov Rosenfeld. Relation between the transport coefficients and the internal entropy of simple systems. *Physical Review A*, 15(6):2545, 1977. 43, 45

[336] Ernst Rössler. Indications for a change of diffusion mechanism in supercooled liquids. *Physical review letters*, 65(13):1595, 1990. 11, 26

[337] JS Rowlinson. The equation of state of dense systems. *Reports on Progress in Physics*, 28(1):169, 1965. 6, 21

[338] C Patrick Royall and Stephen R Williams. The role of local structure in dynamical arrest. *Physics Reports*, 560:1–75, 2015. 3, 4, 19, 20, 34, 41

[339] David Ruelle and Statistical Mechanics. *Rigorous results.* World Scientific, 1969. 32

[340] Charlotte Rulquin, Pierfrancesco Urbani, Giulio Biroli, Gilles Tarjus, and Marco Tarzia. Nonperturbative fluctuations and metastability in a simple model: from observables to microscopic theory and back. *Journal of Statistical Mechanics: Theory and Experiment*, 2016(2):023209, 2016. 173

[341] Barbara Ruzicka, Emanuela Zaccarelli, Laura Zulian, Roberta Angelini, Michael Sztucki, Abdellatif Moussaïd, Theyencheri Narayanan, and Francesco Sciortino. Observation of empty liquids and equilibrium gels in a colloidal clay. *Nature materials*, 10(1):56–60, 2011. 2, 18

[342] Edwin E Salpeter. On mayer's theory of cluster expansions. *Annals of Physics*, 5(3):183–223, 1958. 113, 132, 164

[343] F Sausset, G Biroli, and J Kurchan. Do solids flow? *Journal of Statistical Physics*, 140(4):718–727, 2010. 3, 19

[344] Rolf Schilling and Bernhard Schmid. Comment on "mode-coupling theory as a mean-field description of the glass transition". *Phys. Rev. Lett.*, 106:049601, Jan 2011. 116, 120

[345] Bernhard Schmid and Rolf Schilling. Glass transition of hard spheres in high dimensions. *Phys. Rev. E*, 81(4):041502, Apr 2010. 116, 120

[346] Michael Schmiedeberg, Thomas K Haxton, Sidney R Nagel, and Andrea J Liu. Mapping the glassy dynamics of soft spheres onto hard-sphere behavior. *EPL (Europhysics Letters)*, 96(3):36010, 2011. 43

[347] Thomas B Schrøder, Nicholas P Bailey, Ulf R Pedersen, Nicoletta Gnan, and Jeppe C Dyre. Pressure-energy correlations in liquids. iii. statistical mechanics and thermodynamics of liquids with hidden scale invariance. *The Journal of chemical physics*, 131(23):234503, 2009. 44, 157

[348] Thomas B Schrøder, Nicoletta Gnan, Ulf R Pedersen, Nicholas P Bailey, and Jeppe C Dyre. Pressure-energy correlations in liquids. v. isomorphs in generalized lennard-jones systems. *The Journal of chemical physics*, 134(16):164505, 2011. 44, 45, 157, 166, 167, 169, 170

[349] Thomas B Schrøder, Srikanth Sastry, Jeppe C Dyre, and Sharon C Glotzer. Crossover to potential energy landscape dominated dynamics in a model glass-forming liquid. *The Journal of Chemical Physics*, 112(22):9834–9840, 2000. 33

[350] Kenneth S Schweizer. Derivation of a microscopic theory of barriers and activated hopping transport in glassy liquids and suspensions. *The Journal of chemical physics*, 123(24):244501, 2005. 42

[351] Julian Schwinger. Brownian motion of a quantum oscillator. *Journal of Mathematical Physics*, 2(3):407–432, 1961. 183

[352] Francesco Sciortino and Walter Kob. Debye-waller factor of liquid silica: Theory and simulation. *Physical review letters*, 86(4):648, 2001. 28

[353] Richard P Sear. The non-classical nucleation of crystals: microscopic mechanisms and applications to molecular crystals, ice and calcium carbonate. *International Materials Reviews*, 57(6):328–356, 2012. 2, 18

[354] Antoine Seguin and Olivier Dauchot. Experimental evidences of the gardner phase in a granular glass. *arXiv preprint arXiv:1605.00827*, 2016. 173

[355] Mauro Sellitto and Francesco Zamponi. Packing hard spheres with short-range attraction in infinite dimension: phase structure and algorithmic implications. In *Journal of Physics: Conference Series*, volume 473, page 012020. IOP Publishing, 2013. 109, 173

[356] Mauro Sellitto and Francesco Zamponi. A thermodynamic description of colloidal glasses. *EPL (Europhysics Letters)*, 103(4):46005, 2013. 109, 173

[357] A Sepúlveda, M Tylinski, Anthony Guiseppi-Elie, Ranko Richert, and MD Ediger. Role of fragility in the formation of highly stable organic glasses. *Physical review letters*, 113(4):045901, 2014. 3, 18

[358] David Sherrington and Scott Kirkpatrick. Solvable model of a spin-glass. *Physical review letters*, 35(26):1792, 1975. 32, 59, 60, 63, 140

[359] Hans Sillescu. Heterogeneity at the glass transition: a review. *Journal of Non-Crystalline Solids*, 243(2):81–108, 1999. 8, 10, 24, 26

[360] Sadanand Singh, MD Ediger, and Juan J de Pablo. Ultrastable glasses from in silico vapour deposition. *Nature materials*, 12(2):139–144, 2013. 3, 18

[361] Sadanand Singh, MD Ediger, and Juan J de Pablo. Corrigendum: Ultrastable glasses from in silico vapour deposition. *Nature materials*, 13(6):662–662, 2014. 3, 18

[362] Manfred J Sippl and Harold A Scheraga. Cayley-menger coordinates. *Proceedings of the National Academy of Sciences*, 83(8):2283–2287, 1986. 203

[363] Monica Skoge, Aleksandar Donev, Frank H. Stillinger, and Salvatore Torquato. Packing hyperspheres in high-dimensional Euclidean spaces. *Physical Review E (Statistical, Nonlinear, and Soft Matter Physics)*, 74(4):041127, 2006. 83, 127, 133

[364] AP Sokolov. The glass transition: general scenario and crossover temperature. *Journal of non-crystalline solids*, 235:190–195, 1998. 33

[365] Haim Sompolinsky and Annette Zippelius. Relaxational dynamics of the edwards-anderson model and the mean-field theory of spin-glasses. *Physical Review B*, 25(11):6860, 1982. 59, 77, 100, 119

[366] DR Squire, AC Holt, and WG Hoover. Isothermal elastic constants for argon. theory and monte carlo calculations. *Physica*, 42(3):388–397, 1969. 146

[367] F Stickel, Erhard W Fischer, and Ranko Richert. Dynamics of glass-forming liquids. i. temperature-derivative analysis of dielectric relaxation data. *The Journal of chemical physics*, 102(15):6251–6257, 1995. 5, 20

[368] Frank H Stillinger and Jennifer A Hodgdon. Translation-rotation paradox for diffusion in fragile glass-forming liquids. *Physical review E*, 50(3):2064, 1994. 12, 27

[369] Frank H Stillinger and Thomas A Weber. Packing structures and transitions in liquids and solids. *Science(Washington, DC)*, 225(4666):983–9, 1984. 33

[370] GG Stokes. On the theories of internal friction of fluids in motion. *Camb. Phil. Trans*, 8, 1845. 10, 26

[371] Leendert Cornelis Elisa Struik. *Physical aging in amorphous polymers and other materials.* PhD thesis, TU Delft, Delft University of Technology, 1977. 12, 27

[372] Anatoly Svidzinsky, Marlan Scully, and Dudley Herschbach. Bohr's molecular model, a century later. *Physics Today*, 67(1), 2014. 1, 17

[373] Stephen F Swallen, Kenneth L Kearns, Marie K Mapes, Yong Seol Kim, Robert J McMahon, Mark D Ediger, Tian Wu, Lian Yu, and Sushil Satija. Organic glasses with exceptional thermodynamic and kinetic stability. *Science*, 315(5810):353–356, 2007. 3, 18, 19

[374] Grzegorz Szamel. Colloidal glass transition: beyond mode-coupling theory. *Physical review letters*, 90(22):228301, 2003. 42

[375] Grzegorz Szamel. Mode-coupling theory and beyond: A diagrammatic approach. *Progress of Theoretical and Experimental Physics*, 2013(1):012J01, 2013. 42

[376] Grzegorz Szamel and Elijah Flenner. Independence of the relaxation of a supercooled fluid from its microscopic dynamics: Need for yet another extension of the mode-coupling theory. *EPL (Europhysics Letters)*, 67(5):779, 2004. 107

[377] Grzegorz Szamel, Elijah Flenner, and Hisao Hayakawa. Breakdown of a renormalized perturbation expansion around mode-coupling theory of the glass transition. *EPL (Europhysics Letters)*, 103(5):56003, 2013. 42

[378] Michel Talagrand. *Spin glasses: a challenge for mathematicians: cavity and mean field models*, volume 46. Springer Science & Business Media, 2003. 60, 62

[379] Michel Talagrand. The parisi formula. *Annals of Mathematics*, pages 221–263, 2006. 64

[380] G. Tammann and W. Hesse. Die abhängigkeit der viscosität von der temperatur bie unterkühlten flüssigkeiten. *Zeitschrift für anorganische und allgemeine Chemie*, 156(1):245–257, 1926. 4, 20

[381] G. Tarjus. An overview of the theories of the glass transition. In L. Berthier, G. Biroli, J-P Bouchaud, L. Cipelletti, and W. van Saarloos, editors, *Dynamical Heterogeneities and Glasses, Colloids and Granular Media*. Oxford University Press, 2011. 41

[382] Gilles Tarjus and Daniel Kivelson. Breakdown of the stokes–einstein relation in supercooled liquids. *The Journal of chemical physics*, 103(8):3071–3073, 1995. 12, 27

[383] Gilles Tarjus, Steven A Kivelson, Z Nussinov, and Pascal Viot. The frustration-based approach of supercooled liquids and the glass transition: a review and critical assessment. *Journal of Physics: Condensed Matter*, 17(50):R1143, 2005. 41

[384] DJ Thouless, PW Anderson, and RG Palmer. Solution of 'Solvable model of a spin glass'. *Philosophical Magazine*, 35(3):593–601, 1977. 32

[385] Cristina Toninelli, Matthieu Wyart, Ludovic Berthier, Giulio Biroli, and Jean-Philippe Bouchaud. Dynamical susceptibility of glass formers: Contrasting the predictions of theoretical scenarios. *Physical Review E*, 71(4):041505, 2005. 9, 25

[386] S. Torquato and F. H. Stillinger. Jammed hard-particle packings: From Kepler to Bernal and beyond. *Rev. Mod. Phys.*, 82(3):2633–2672, Sep 2010. 83, 109, 127

[387] Søren Toxvaerd, Ulf R Pedersen, Thomas B Schrøder, and Jeppe C Dyre. Stability of supercooled binary liquid mixtures. *The Journal of chemical physics*, 130(22):224501, 2009. 2, 18

[388] Alfred René Ubbelohde. *Melting and Crystal Structures.* Oxford University Press, 1965. 45

[389] Pierfrancesco Urbani. Theory of fluctuations in disordered systems. *PhD thesis*, 2013. 36

[390] Pierfrancesco Urbani and Giulio Biroli. Gardner transition in finite dimensions. *Physical Review B*, 91(10):100202, 2015. 173

[391] A. Vaknin, Z. Ovadyahu, and M. Pollak. Aging effects in an anderson insulator. *Phys. Rev. Lett.*, 84:3402–3405, Apr 2000. 2, 18

[392] H Van Beijeren and MH Ernst. Kinetic theory of hard spheres. *Journal of Statistical Physics*, 21(2):125–167, 1979. 42

[393] Henk Van Beijeren and Matthieu H Ernst. The modified enskog equation. *Physica*, 68(3):437–456, 1973. 42

[394] Nicolaas Godfried Van Kampen. *Stochastic processes in physics and chemistry*, volume 1. Elsevier, 1992. 185

[395] J. A. van Meel, B. Charbonneau, A. Fortini, and P. Charbonneau. Hard-sphere crystallization gets rarer with increasing dimension. *Phys. Rev. E*, 80(6):061110, 2009. 83, 127, 133

[396] J. A. van Meel, D. Frenkel, and P. Charbonneau. Geometrical frustration: A study of four-dimensional hard spheres. *Physical Review E (Statistical, Nonlinear, and Soft Matter Physics)*, 79(3):030201, 2009. 83, 127

[397] Stephanie Vance. Improved sphere packing lower bounds from hurwitz lattices. *Advances in Mathematics*, 227(5):2144 – 2156, 2011. 109, 110

[398] Carlos Vega, Carl McBride, Eduardo Sanz, and Jose L. F. Abascal. Radial distribution functions and densities for the spc/e, tip4p and tip5p models for liquid water and ices ih, ic, ii, iii, iv, v, vi, vii, viii, ix, xi and xii. *Phys. Chem. Chem. Phys.*, 7:1450–1456, 2005. 6, 22

[399] Maryna Viazovska. The sphere packing problem in dimension 8. *arXiv preprint arXiv:1603.04246*, 2016. 109

[400] H Vogel. Das temperaturabhängigkeitsgesetz der viskosität von flüssigkeiten. *Phys. Z.*, 22:645–646, 1921. 4, 20

[401] Eric R Weeks and DA Weitz. Subdiffusion and the cage effect studied near the colloidal glass transition. *Chemical Physics*, 284(1):361–367, 2002. 7, 22, 172

[402] John D. Weeks, David Chandler, and Hans C. Andersen. Role of repulsive forces in determining the equilibrium structure of simple liquids. *The Journal of Chemical Physics*, 54(12):5237–5247, 1971. 83, 167

[403] Graham Williams and David C Watts. Non-symmetrical dielectric relaxation behaviour arising from a simple empirical decay function. *Transactions of the Faraday Society*, 66:80–85, 1970. 7, 23, 30

[404] Edward Witten. Quarks, atoms, and the $1/n$ expansion. *Physics Today*, 33:38, 1980. 1, 17

[405] P. Wolynes and V. Lubchenko. Structural glasses and supercooled liquids: Theory, experiment, and applications. Wiley, 2012. 39

[406] Jianlan Wu and Jianshu Cao. High-order mode-coupling theory for the colloidal glass transition. *Physical review letters*, 95(7):078301, 2005. 42

[407] Wenhao Wu, B. Ellman, T. F. Rosenbaum, G. Aeppli, and D. H. Reich. From classical to quantum glass. *Phys. Rev. Lett.*, 67:2076–2079, Oct 1991. 2, 18

[408] Matthieu Wyart. Marginal stability constrains force and pair distributions at random close packing. *Physical review letters*, 109(12):125502, 2012. 14, 47

[409] D. Wyler, N. Rivier, and H. L. Frisch. Hard-sphere fluid in infinite dimensions. *Phys. Rev. A*, 36:2422–2431, Sep 1987. 2, 13, 18, 46, 53, 54, 55, 56, 87, 89, 132, 151

[410] Wence Xiao, Jon Tofteskov, Troels V Christensen, Jeppe C Dyre, and Kristine Niss. Isomorph theory prediction for the dielectric loss variation along an isochrone. *Journal of Non-Crystalline Solids*, 407:190–195, 2015. 45

[411] Limei Xu, Francesco Mallamace, Zhenyu Yan, Francis W Starr, Sergey V Buldyrev, and H Eugene Stanley. Appearance of a fractional stokes–einstein relation in water and a structural interpretation of its onset. *Nature Physics*, 5(8):565–569, 2009. 11, 26

[412] Chen-Ning Yang and Tsung-Dao Lee. Statistical theory of equations of state and phase transitions. i. theory of condensation. *Physical Review*, 87(3):404, 1952. 2, 18, 32

[413] Hajime Yoshino. Replica theory of the rigidity of structural glasses. *The Journal of Chemical Physics*, 136:214108, 2012. 113, 115, 146, 147, 173

[414] Hajime Yoshino and Francesco Zamponi. Shear modulus of glasses: Results from the full replica-symmetry-breaking solution. *Physical Review E*, 90(2):022302, 2014. 134, 146, 147, 152, 173

[415] Thomas Young and Hans C Andersen. A scaling principle for the dynamics of density fluctuations in atomic liquids. *The Journal of chemical physics*, 118(8):3447–3450, 2003. 45

[416] Emanuela Zaccarelli. Colloidal gels: equilibrium and non-equilibrium routes. *Journal of Physics: Condensed Matter*, 19(32):323101, 2007. 2, 18

[417] Francesco Zamponi. Mean field theory of spin glasses. `arXiv:1008.4844`, 2010. 31, 35, 36, 37, 38, 58, 59, 63, 138

[418] Edgar Dutra Zanotto. Do cathedral glasses flow? *American Journal of Physics*, 66(5):392–395, 1998. 3, 19

[419] RC Zeller and RO Pohl. Thermal conductivity and specific heat of noncrystalline solids. *Physical Review B*, 4(6):2029, 1971. 173

[420] Jing Zhao, Sindee L Simon, and Gregory B McKenna. Using 20-million-year-old amber to test the super-arrhenius behaviour of glass-forming systems. *Nature communications*, 4:1783, 2013. 3, 19

[421] Royce KP Zia, Edward F Redish, and Susan R McKay. Making sense of the legendre transform. *American Journal of Physics*, 77(7):614–622, 2009. 51

[422] Jean Zinn-Justin. *Quantum field theory and critical phenomena*. Oxford University Press, 2002. 5, 20, 29, 51, 59, 65, 74, 76, 97, 173, 183, 184, 187

[423] R Zwanzig. Statistical mechanics of irreversibility. *Lectures in theoretical physics*, 3:106–141, 1961. 29

[424] Robert Zwanzig. Nonlinear generalized langevin equations. *Journal of Statistical Physics*, 9(3):215–220, 1973. 10, 26, 102

Thibaud MAIMBOURG	5 octobre 2016

Sujet : Théorie des liquides et verres en dimension infinie

Résumé : La dynamique des liquides, considérés comme des systèmes de particules classiques fortement couplées, reste un domaine où les descriptions théoriques sont limitées. Pour l'instant, il n'existe pas de théorie microscopique partant des premiers principes et recourant à des approximations contrôlées. Thermodynamiquement, les propriétés statiques d'équilibre sont bien comprises dans les liquides simples, *à condition* d'être loin du régime vitreux. Dans cette thèse, nous résolvons, en partant des équations microscopiques du mouvement, la dynamique des liquides et verres en exploitant la limite de dimension spatiale infinie, qui fournit une approximation de champ moyen bien définie. En parallèle, nous retrouvons leur thermodynamique à travers une analogie entre la dynamique et la statique. Cela donne un point de vue à la fois unificateur et cohérent du diagramme de phase de ces systèmes. Nous montrons que cette solution de champ moyen au problème de la transition vitreuse est un exemple du scénario de transition de premier ordre aléatoire (RFOT), comme conjecturé il y a maintenant trente ans, sur la base des solutions des modèles de verres de spin en champ moyen. Ces résultats nous permettent de montrer qu'une invariance d'échelle approchée du système, pertinente pour les expériences et les simulations en dimension finie, devient exacte dans cette limite.

Mots clés : Physique statistique des systèmes désordonnés, Théorie de champ moyen, Dynamique hors d'équilibre, Transition vitreuse, Théorie des liquides, Invariance d'échelle

Subject : Theory of high-dimensional liquids and glasses

Abstract : The dynamics of liquids, regarded as strongly-interacting classical particle systems, remains a field where theoretical descriptions are limited. So far, there is no microscopic theory starting from first principles and using controlled approximations. At the thermodynamic level, static equilibrium properties are well understood in simple liquids *only* far from glassy regimes. Here we derive, from first principles, the dynamics of liquids and glasses using the limit of large spatial dimension, which provides a well-defined mean-field approximation with a clear small parameter. In parallel, we recover their thermodynamics through an analogy between dynamics and statics. This gives a unifying and consistent view of the phase diagram of these systems. We show that this mean-field solution to the structural glass problem is an example of the Random First-Order Transition scenario, as conjectured thirty years ago, based on the solution of mean-field spin glasses. These results allow to show that an approximate scale invariance of the system, relevant to finite-dimensional experiments and simulations, becomes exact in this limit.

Keywords : Statistical physics of disordered systems, Mean-field theory, Out-of-equilibrium dynamics, Glass transition, Liquid theory, Scale invariance

Résumé

La dynamique des liquides, considérés comme des systèmes de particules classiques fortement couplées, reste un domaine où les descriptions théoriques sont limitées. Pour l'instant, il n'existe pas de théorie microscopique partant des premiers principes et recourant à des approximations contrôlées. Thermodynamiquement, les propriétés statiques d'équilibre sont bien comprises dans les liquides simples, *à condition* d'être loin du régime vitreux.

Dans cette thèse, nous résolvons, en partant des équations microscopiques du mouvement, la dynamique des liquides et verres en exploitant la limite de dimension spatiale infinie, qui fournit une approximation de champ moyen bien définie. En parallèle, nous retrouvons leur thermodynamique à travers une analogie entre la dynamique et la statique. Cela donne un point de vue à la fois unificateur et cohérent du diagramme de phase de ces systèmes. Nous montrons que cette solution de champ moyen au problème de la transition vitreuse est un exemple du scénario de transition de premier ordre aléatoire (RFOT), comme conjecturé il y a maintenant trente ans, sur la base des solutions des modèles de verres de spin en champ moyen. Ces résultats nous permettent de montrer qu'une invariance d'échelle approchée du système, pertinente pour les expériences et les simulations en dimension finie, devient exacte dans cette limite.

Abstract

The dynamics of liquids, regarded as strongly-interacting classical particle systems, remains a field where theoretical descriptions are limited. So far, there is no microscopic theory starting from first principles and using controlled approximations. At the thermodynamic level, static equilibrium properties are well understood in simple liquids *only* far from glassy regimes.

Here we derive, from first principles, the dynamics of liquids and glasses using the limit of large spatial dimension, which provides a well-defined mean-field approximation with a clear small parameter. In parallel, we recover their thermodynamics through an analogy between dynamics and statics. This gives a unifying and consistent view of the phase diagram of these systems. We show that this mean-field solution to the structural glass problem is an example of the Random First-Order Transition scenario, as conjectured thirty years ago, based on the solution of mean-field spin glasses. These results allow to show that an approximate scale invariance of the system, relevant to finite-dimensional experiments and simulations, becomes exact in this limit.

Mots Clés

Keywords